Title
Enantioselective Construction of C-N and C-C Bonds via Chiral Anion Phase-Transfer Catalysis

Author
Patel, Jigar

Publication Date
2016

Peer reviewed|Thesis/dissertation

Enantioselective Construction of C-N and C-C Bonds *via* Chiral Anion Phase-Transfer Catalysis

By Jigar Patel

A dissertation submitted in partial satisfaction of

requirements for the degree of

Doctor of Philosophy

in

Chemistry

in the

Graduate Division

of the

University of California, Berkeley

Committee in charge:

Professor F. Dean Toste, Chair
Professor John Hartwig
Professor Joseph Napoli

Spring 2016

Abstract

Enantioselective Construction of C-N and C-C Bonds *via* Chiral Anion Phase-Transfer Catalysis

by

Jigar Patel

Doctor of Philosophy in Chemistry

University of California, Berkeley

Professor F. Dean Toste, Chair

The ability to control absolute stereochemistry is a powerful tool in organic synthesis. Given the utility of enantiopure molecules in a number of industries, the pharmaceutical perhaps most prominent, many research efforts have focused on asymmetric catalysis. Recently, the Toste Group has developed and implemented a chiral anion phase-transfer strategy to achieve high enantioselectivity in a number of transformations. This thesis describes new reactivity discovered within this manifold and also discusses the design and synthesis of new phase-transfer catalysts to improve enantioinduction.

Chapter 1 details an asymmetric aminocyclization reaction of tryptamine derivatives enabled by chiral anion phase-transfer of aryldiazonium salts. The immediate products, C3-diazenated pyrroloindolines, can be converted directly to cyclotryptamine natural product derivatives, providing an efficient entryway into a complex scaffold that has been previously accessed by much longer synthetic sequences.

Chapter 2 is a natural extension of the work presented in Chapter 1 and describes an enantioselective α-amination of activated ketone derivatives, again employing aryldiazonium salts as aminating reagents. Obtaining high enantioselectivity initially proves to be very difficult, as use of our traditional library of BINOL-derived chiral phosphoric acids leads to poor enantioinduction. Eventually, we overcome this challenge through the design and synthesis of a new library of chiral phosphoric acids, specifically those derived from a 1,1′-binaphthyl-2,2′-diamine (BINAM) backbone. Chapter 2 also presents potential advantages of our methodology over more commonly used α-amination reactions that utilize dialkyl azodicarboxylates.

Chapter 3 discusses the use of aryldiazonium salts in a more traditional role as cross coupling electrophiles. By merging chiral anion phase-transfer and palladium catalysis, we report an enantioselective Heck-Matsuda arylation of cyclic olefins. Through the process of reaction optimization, we observe counterion dependent reactivity and are ultimately able to avoid the formation of undesired olefin isomers by judicious choice of phosphate. While chiral anions have almost exclusively been used to optimize enantioselectivity, this result indicates that counterions can also be used to modulate chemical reactivity in transitional metal catalyzed processes.

Table of Contents

Acknowledgements

There are numerous individuals whom I would like to thank, individuals who have provided me great guidance, friendship, and support. While this PhD is in part a reflection of my hard work, I believe it is more of a testament to the tremendous opportunities I have been given and the generosity of those who have helped me along the way.

First and foremost, I would like to dedicate this degree to my parents, Hema and Shailesh. They worked harder than I will ever know to give their two children opportunities they never had. They supported me in every decision that I made and allowed me the freedom to pursue my own interests. I would also like to thank Neha for being a great sister to grow up with and for putting up with my occasionally annoying behavior.

I thank Professor Richard B. Silverman for being the only professor at Northwestern who responded to a young undergraduate inquiring about research opportunities. He was, and still is, an extraordinary teacher. I thank Kristin Jansen Labby and Stephanie Choing for helping me get through my first year in the lab. Safe to say I needed all the help I could get. I thank Mike Luzung for his mentorship during my time at Merck, for giving me invaluable training, and for pointing me towards Berkeley as a place to pursue my PhD.

I would like to thank my advisor, Dean Toste, for giving me an incredible research opportunity and for being a great PI. He has cultivated a tremendous atmosphere in his laboratory, one that fosters creativity and values collaboration. I thank him especially for allowing his students to be self-motivated and pursue their own ideas. I'm extremely proud to have been part of his group and to have had the opportunity to learn from him.

Within the lab there are numerous individuals with whom I have become close friends and shared great experiences. I came into the group with Andrew Neel, William Wolf, Dimitri Khrakovsky and Dillon Miles, and I could not have asked for a better group of classmates. We shared many laughs together and came out of grad school with some great stories, and I will always be thankful for that. I would like to thank the rest of the Toste Group, especially my coworkers Hosea Nelson, Hunter Shunatona and Carolina Avila, for being great scientists to work with and for being great friends outside of lab. I will remember a lot about my time at Berkeley, but I will mostly remember the people who made the Toste Group such a great place to work.

I would like to thank Cathy for being my best friend. I thank her for being interested in even the most mundane aspects of my life and for always being there when I needed her. I thank her for her commitment, a commitment that could easily have succumbed to outside influences and 3,000 miles of separation. Most of all, I thank her for teaching me about love, a subject a high school junior knew very little about at the time.

Lastly, I would like to thank the rest of my family and friends (a special shout out to my friends back at home in Edison!). I have been fortunate enough to have been surrounded by great people and appreciate all the positive influence and motivation that I have received. I hope to return the favor one day.

Chapter 1. Enantioselective Synthesis of C3-Diazenated Pyrroloindolines *via* Chiral Ion Phase-Transfer of Aryl Diazonium Cations

We report a catalytic, asymmetric pyrroloindolinization reaction of tryptamine derivatives and aryldiazonium tetrafluoroborate salts. This transformation affords C3-diazenated pyrroloindolines that may subsequently be converted to cyclotryptamine natural product derivatives. High yields (up to 99%) and enantioselectivities (up to 96%) are achieved using a SPINOL-derived phosphoric acid catalyst. Control experiments indicate that a phase-transfer mechanism is operative. The air- and water-tolerant reaction conditions allow for substitution of the tryptamine core and the aryldiazonium salt with a variety of functional groups at multiple positions.

Portions of this chapter are based on work done in collaboration with Hosea Nelson, Hunter Shunatona, and Solomon Reisberg and appear in: *Angew. Chem. Int. Ed.* **2014**, 53, 5600. H.N. was responsible for initial discovery, and H.S. and S.R. contributed to reaction optimization and determination of substrate scope.

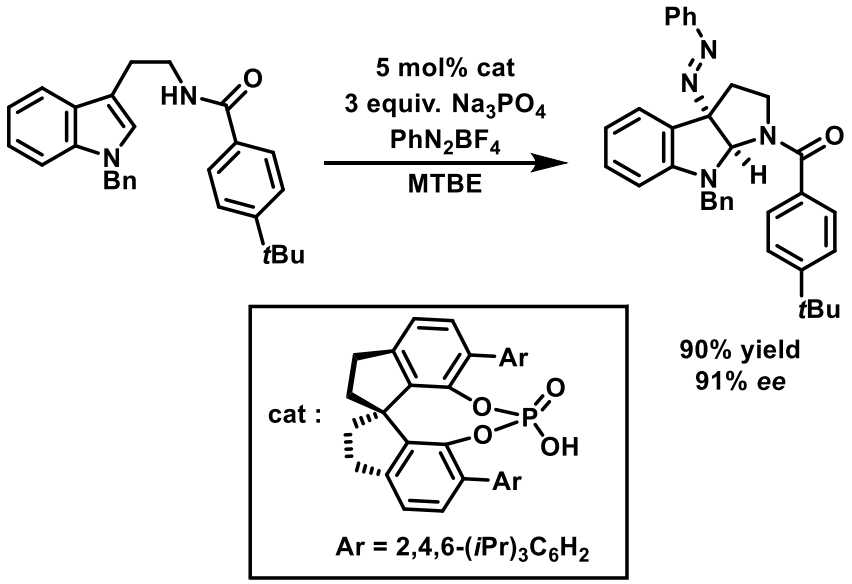

Introduction

Chiral ion phase-transfer catalysis has emerged as a powerful tool in enantioselective methodology.[1] This strategy relies on phase-separation of reactive components and a chiral catalyst that brings one reactant into bulk organic phase where the desired reaction occurs. Traditionally, chiral lipophilic cations have been used to solubilize anionic nucleophiles. In the seminal report by the Merck research group, a cinchona alkaloid-derived ammonium salt was used to catalyze alkylations of enolates (Scheme 1).[2] The chiral cation was presumed to extract a water-soluble enolate into organic solution *via* ion exchange at the interface of the organic and aqueous phase.[3] High enantioselectivities were achieved in solvents with low dielectric constants, where the catalyst and substrate were hypothesized to exist as a contact ion pair, thus maximizing enantioinduction.[2]

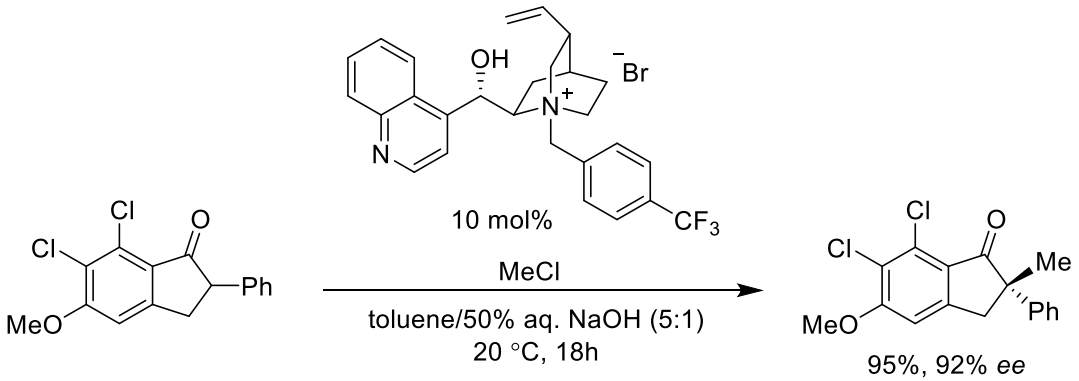

Scheme 1. First highly enantioselective phase-transfer catalyzed alkylation (ref. 2).

Similar cinchona alkaloid-derived catalysts were later employed in a variety of alkylation reactions. The groups of O'Donnel[4], Corey[5], and Lygo[6] developed enantioselective alkylations of glycine derivatives and found that enantioinduction was highly dependent on catalyst structure (Scheme 2).

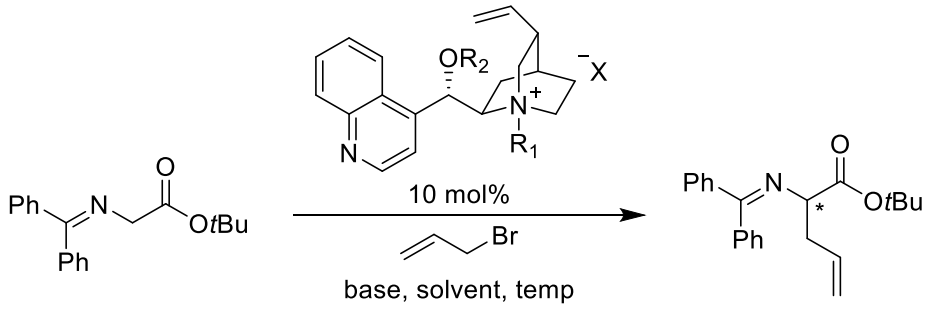

Ref	R_1	R_2	X	% yield	% ee
4	Ph	H	Br	75	66
5	9-anthracenyl	allyl	Br	89	97
6	9-anthracenyl	H	Cl	62	88

Scheme 2. Enantioselective allylation of glycine derivatives catalyzed by various cinchona alkaloid-derived ammonium salts (ref. 4-6).

Subsequent to the early contributions described herein, a variety of ammonium and phosphonium phase-transfer salts were developed for enantioselective catalysis. For instance, Maruoka and co-workers developed a catalytic asymmetric amination of indanone-derived *β*-keto esters using a tetraalkyl phosphonium bromide salt (Scheme 3).[7]

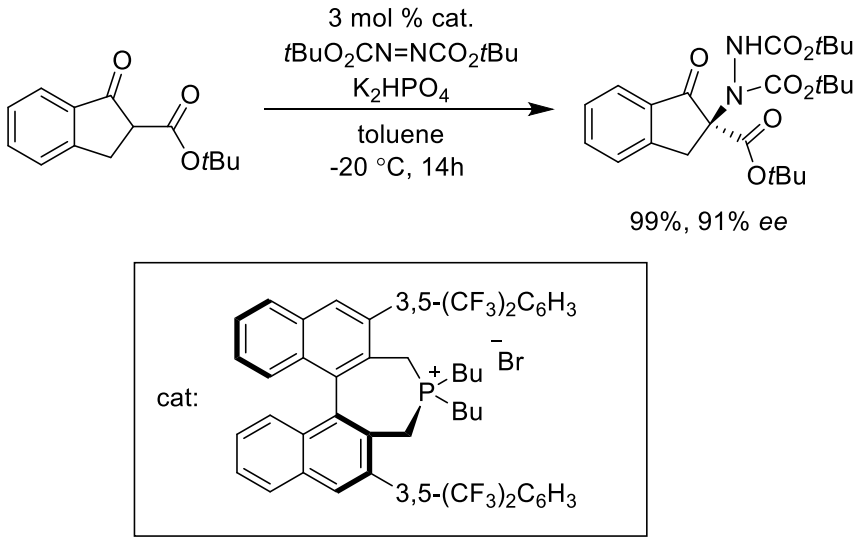

Scheme 3. Enantioselective amination of β-keto esters catalyzed by a tetraalkyl phosphonium salt (ref. 7).

While phase-transfer of anionic reactants with chiral cations has been well studied, the analogous charge-inverted process, chiral anion phase-transfer, had not been extensively investigated until contributions from our group. In an early precedent published in 2003, Nelson and co-workers reported some enantioselectivity (<15%) using chiral borate anions in the ring-opening of prochiral aziridinium intermediates.[8] Using the same reaction manifold, we became interested in developing chiral anion phase-transfer catalysis, ultimately reporting its first precedent in 2008 (Scheme 4).[9] A binapthol-derived chiral phosphate anion (TRIP),[10,11] generated *in situ via* deprotonation by Ag_2CO_3, serves as a phase-transfer catalyst for Ag^+ (as Ag_2CO_3 is insoluble in nonpolar organic solvents). The resultant soluble Ag^+ source abstracts chloride from the trans-β-chloroamine substrate (precipitating AgCl), a process that forms a *meso*-aziridinium ion paired to a chiral phosphate. This chiral phosphate then directs an enantioselective ring opening *via* attack of an alcohol, affording an enantioenriched β-alkoxyamine.

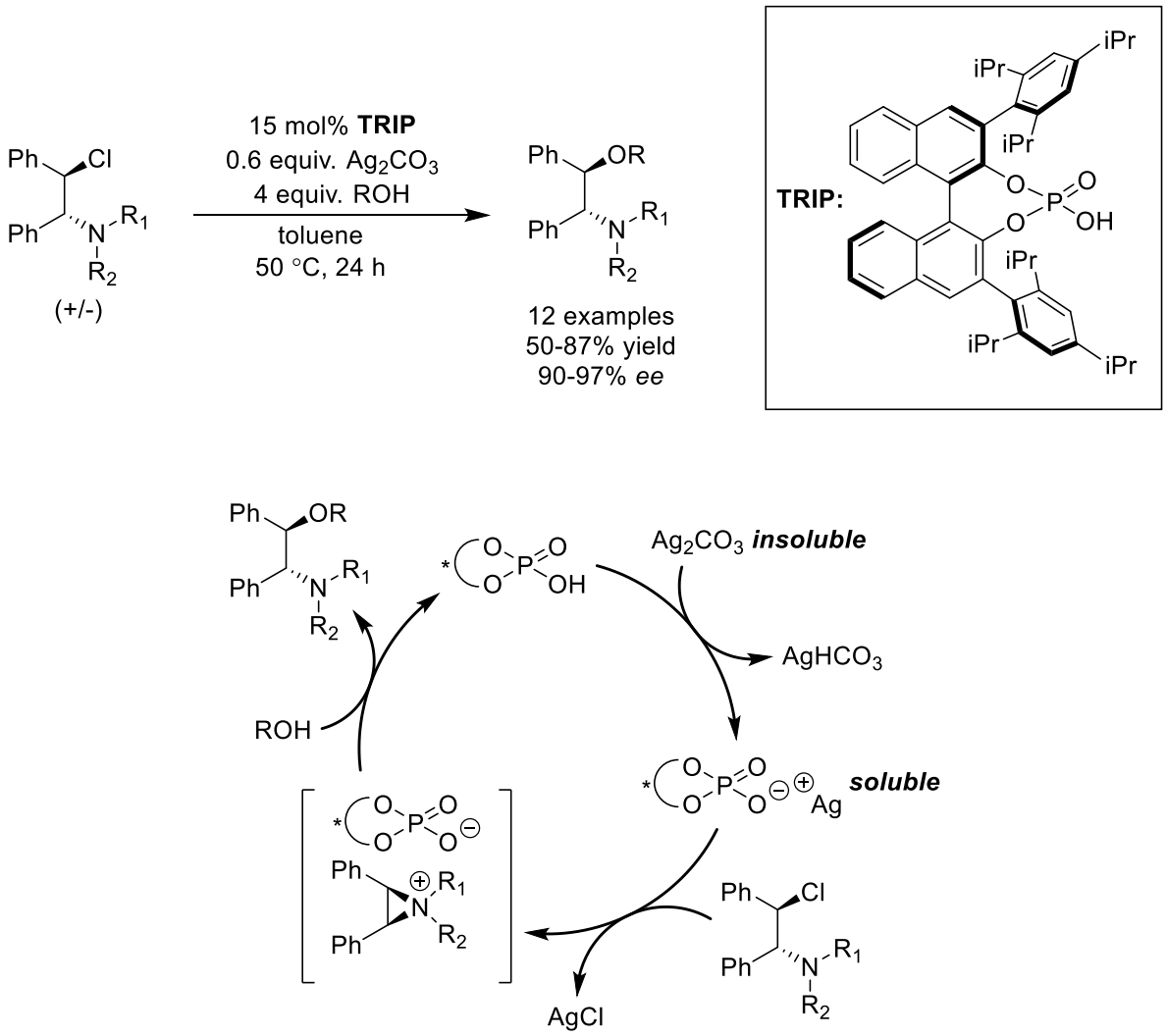

Scheme 4. Enantioselective ring opening of *meso*-aziridinium ions *via* chiral ion phase-transfer of Ag^+ (ref. 9).

In the example above, phase-transfer occurs by acid-base reaction between insoluble silver carbonate and a chiral phosphoric acid. Analogously, our group proposed phase-transfer of other reactive electrophiles *via* anion exchange with chiral lipophilic phosphates (Scheme 5). Reaction with a substrate in the organic phase would occur only when the reactive cation was paired to a solubilizing chiral anion, thereby inhibiting an unselective background reaction.

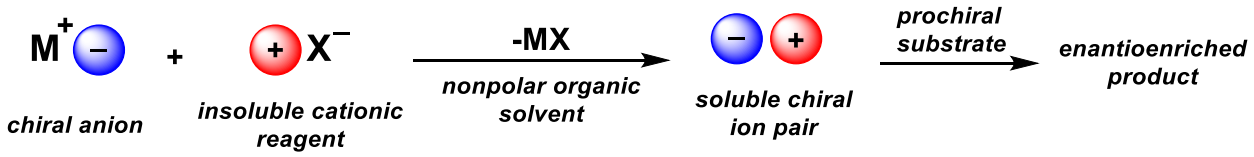

Scheme 5. Chiral anion phase-transfer strategy.

Using this strategy, our group has applied chiral anion phase-transfer catalysis to other cationic electrophiles, including Selectfluor,[12] an analogously designed brominating reagent,[13] and oxopiperidinium salts[14] (Scheme 6). Using a variety of chiral phosphates, we have achieved

excellent levels of enantioselectivity in a number of transformations, such as halocyclizations (Scheme 6a-b) and oxidative couplings (Scheme 6c).

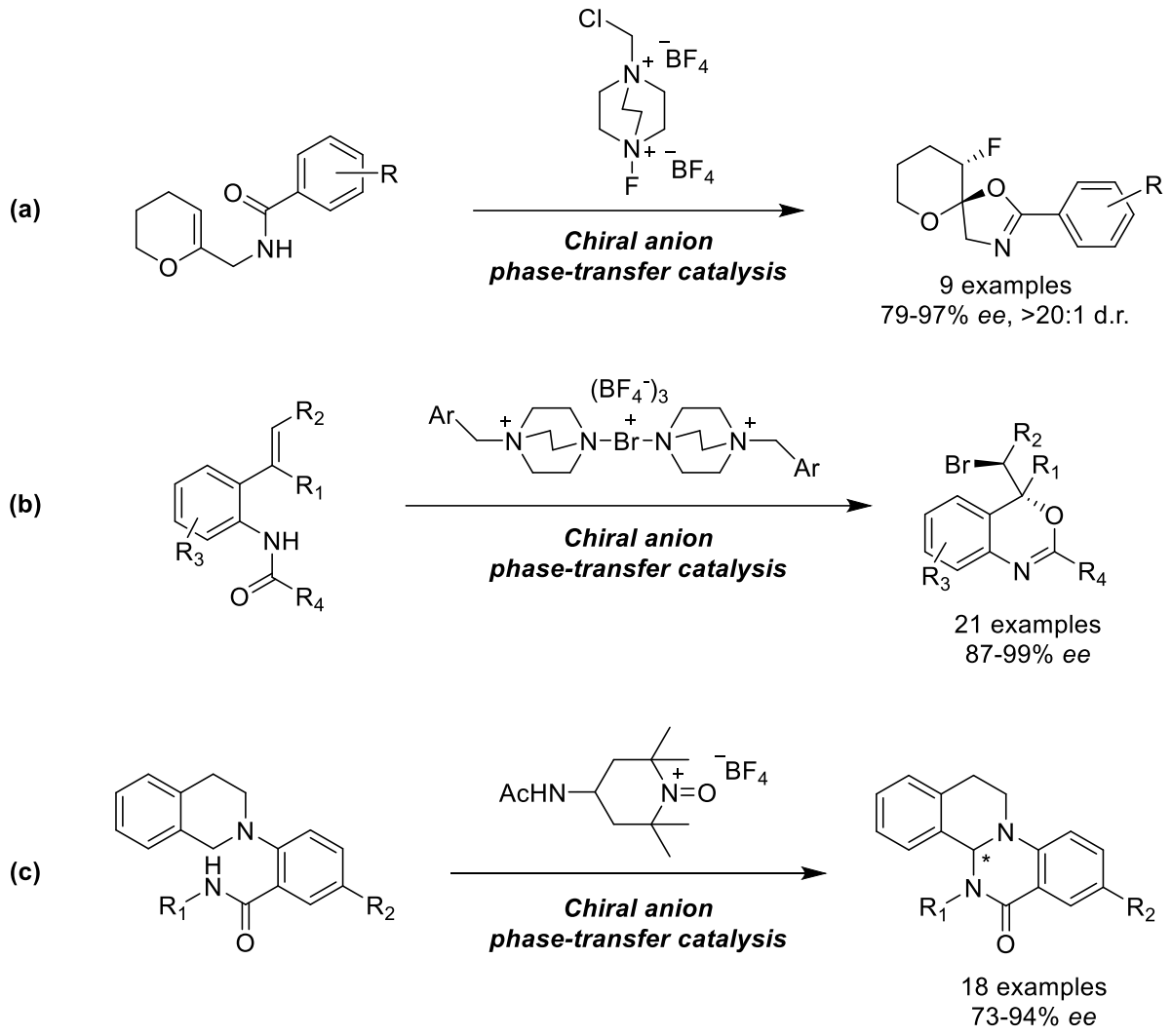

Scheme 6. Chiral anion phase-transfer of cationic oxidants (ref. 12-14).

By extension, we envisioned aryldiazonium salts as viable cationic electrophiles within this manifold, and were encouraged by reports of azo-coupling reactions that utilized aryldiazonium salts under phase-transfer conditions.[15,16] When exploring additional reactivity, we noted a Japp-Klingemann-type[17] reaction between ketene silyl acetals and phenyldiazonium tetrafluoroborate reported by Tanaka (Scheme 7).[18] The α-azo ester intermediates were subsequently hydrogenated to the corresponding α-amino esters. Notably, this was one of the first reports that utilized diazonium salts as electrophilic aminating reagents.[19]

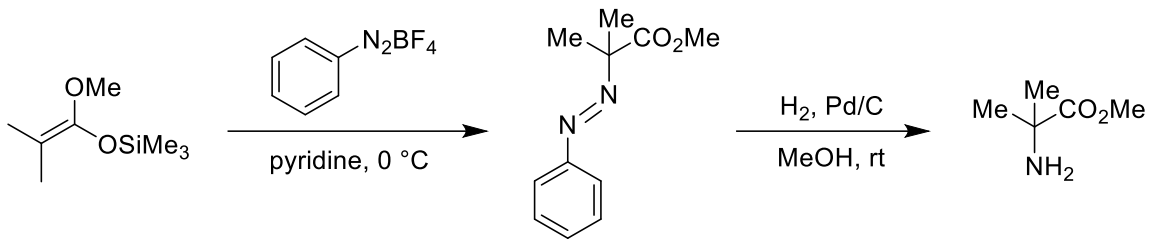

Scheme 7. Electrophilic amination of silyl ketene acetals using phenyldiazonium tetrafluoroborate (ref. 18).

In light of this mode of reactivity, we became interested in the enantioselective synthesis of azo compounds *via* chiral anion phase-transfer. We drew additional inspiration from recent work by Movassaghi and coworkers detailing the synthesis of C3-diazenated pyrroloindolines as precursors to a variety of cyclotryptamine natural products and natural product derivatives.[20,21] Photolysis of these diazenes, which were ultimately prepared in 7 or more steps from tryptophan, afforded the desired carbon-carbon bond with loss of dinitrogen (Scheme 8).

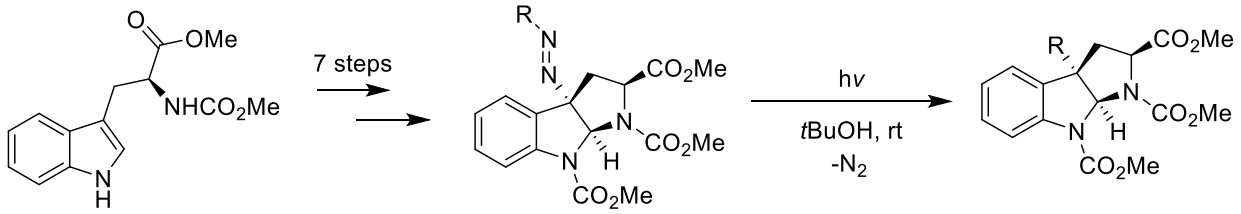

Scheme 8. Synthesis and photolysis of C-3 diazenated pyrroloindolines (ref. 20, 21).

By exploiting the π-electrophilicity of aryldiazonium salts (as initially described by Tanaka), we envisioned accessing a similar class of compounds enantioselectively in a single step *via* pyrroloindolization. We hypothesized that a tryptamine derivative would undergo enantioselective C-3 diazenation upon treatment with an aryldiazonium chiral ion pair. The subsequent iminium intermediate could then be quenched by attack of a pendant nucleophile, furnishing the desired pyrroloindoline (Scheme 9).

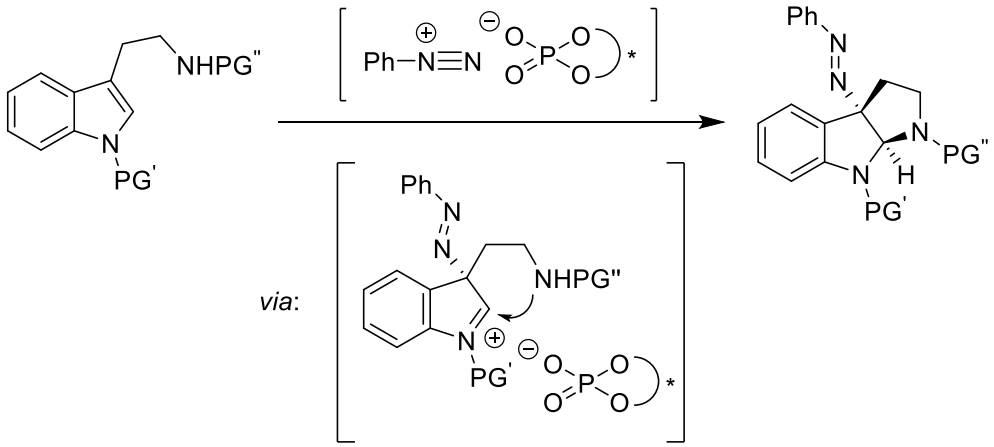

Scheme 9. Proposed enantioselective pyrroloindolization.

Results and Discussion

We began our investigation with **1.1a**, a benzamide-protected tryptamine derivative. We chose **1.1a** as a model substrate as the presence of a benzamide was crucial for high enantioselectivity in many of our previously developed phase-transfer reactions.[12-14] We were pleased to find that treatment of **1.1a** with phenyldiazonium tetrafluoroborate, 5 mol% (*R*)-TRIP (**1.3a**), 3 equivalents of Na_3PO_4 in hexane solvent led to the formation of the desired cyclized product **1.2a** in quantitative yield and in 63% ee (Scheme 10). The structure and absolute configuration of **1.2a** was confirmed by X-ray crystallographic analysis.

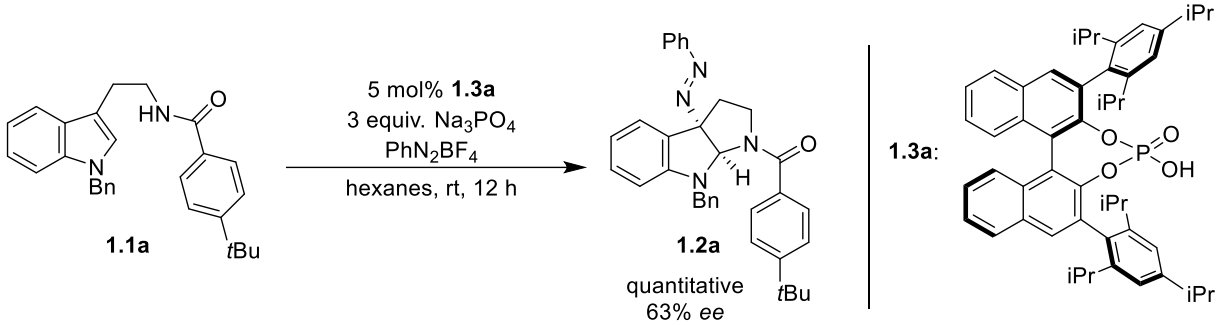

Scheme 10. Enantioselective pyrroloindolization of **1.1a**.

The proposed mechanism begins with deprotonation of the chiral phosphoric acid precatalyst to form the active phosphate. The lipophilic phosphate then undergoes anion metathesis (with precipitation of $NaBF_4$), to bring the aryldiazonium cation into organic solution. The resulting chiral ion pair reacts with the substrate which undergoes enantioselective pyrroloindolization, presumably *via* an iminium intermediate. This process regenerates the phase-transfer catalyst in the protonated form (Scheme 11).

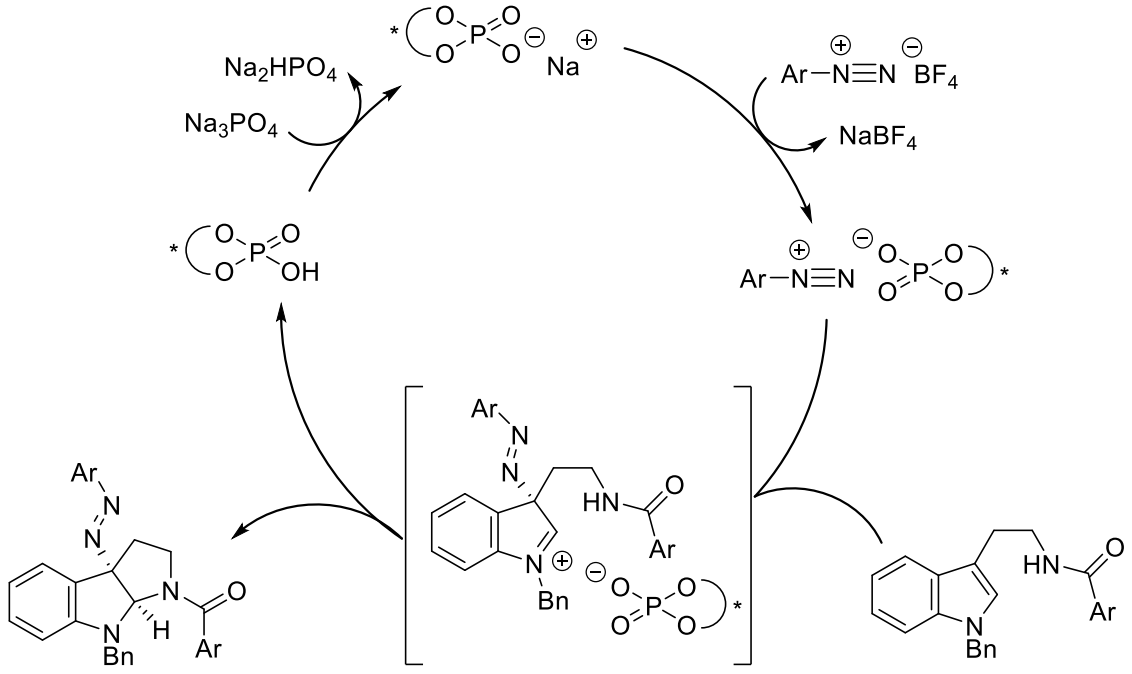

Scheme 11. Proposed mechanism of enantioselective pyrroloindolization.

Having observed the desired reactivity, we sought to optimize reaction conditions to improve enantioselectivity (Table 1), and started by investigating our library of chiral phosphoric acids. Initial work focusing on BINOL-derived catalysts revealed that **1.3a** gave the highest ee (entries 1-3). We next examined catalysts with different backbones, specifically **1.3d** derived from H_8-BINOL and **1.3e** derived from SPINOL, and found that use of **1.3e** increased enantioselectivity up to 81% (entry 5). A further increase to 91% ee was achieved by using methyl *tert*-butyl ether as solvent (entry 7). Notably, employing similar conditions in acetone solvent led to significant decomposition of starting material along with erosion of enantioselectivity (entry 8). Presumably the lack of a phase-separation between the substrate and aryldiazonium salt (which is soluble in acetone), results in a significant background reaction that produces racemic product. When exploring various bases, we found that use of most inorganic bases produced similar conversions and enantioselectivities (entries 9-10). Use of triethylamine led to no reaction, likely due to decomposition of the diazonium salt as evidenced by a strong color change (entry 11). Lastly, minimal conversion was observed in the absence of phase-transfer catalyst or base (entries 12-13). These results, along with reduced enantioselectivity under homogeneous conditions (entry 8), support a phase-transfer mechanism. Full conversion was seen under catalytic conditions (2-8 hours) with isolated yields up to 97% (entry 7).

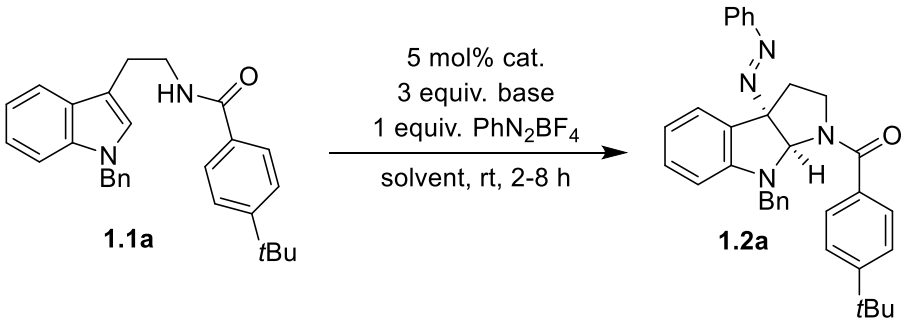

Entry	Cat.	Solvent	Base	Conv. (%)	*ee* (%)
1	**1.3a**	hexanes	Na_3PO_4	> 95	62
2	**1.3b**	hexanes	Na_3PO_4	> 95	35
3	**1.3c**	hexanes	Na_3PO_4	> 95	4
4	**1.3d**	hexanes	Na_3PO_4	> 95	44
5	**1.3e**	hexanes	Na_3PO_4	> 95	81
6	**1.3e**	pentane	Na_3PO_4	> 95	82
7	**1.3e**	MTBE	Na_3PO_4	97[a]	91
8	**1.3e**	acetone	Na_3PO_4	> 95 (21[b])	51
9	**1.3e**	MTBE	K_2CO_3	> 95	90
10	**1.3e**	MTBE	K_3PO_4	> 95	91
11	**1.3e**	MTBE	NEt_3	< 10	-
12	-	MTBE	Na_3PO_4	< 5	-
13	**1.3e**	MTBE	-	< 5	-

[b]isolated yield

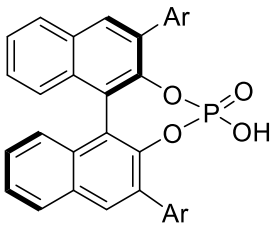

1.3a, Ar = 2,4,6-(*i*Pr)$_3$C$_6$H$_2$
1.3b, Ar = 2,4,6-(Cy)$_3$C$_6$H$_2$
1.3c, Ar = 3,5-(CF$_3$)$_2$C$_6$H$_3$

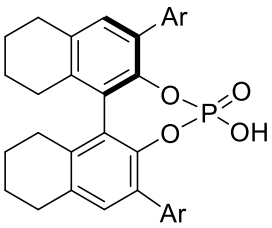

1.3d, Ar = 2,4,6-(*i*Pr)$_3$C$_6$H$_2$

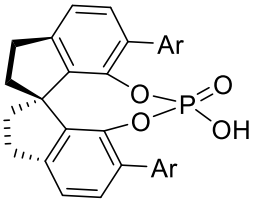

1.3e, Ar = 2,4,6-(*i*Pr)$_3$C$_6$H$_2$

Table 1. Reaction optimization.

With an optimized set of reaction conditions established, we next examined the scope of the aryldiazonium salt (Figure 1). We found that substitution at the *ortho*-, *meta*-, and *para*-positions was well tolerated with both electron-donating (**1.2b-1.2f**) and electron-withdrawing (**1.2g-1.2m**) substituents. Di-substitution of the aryldiazonium salt was also tolerated (**1.2k**). Yields ranged from 52-95%, with enantioselectivities up to 94%.

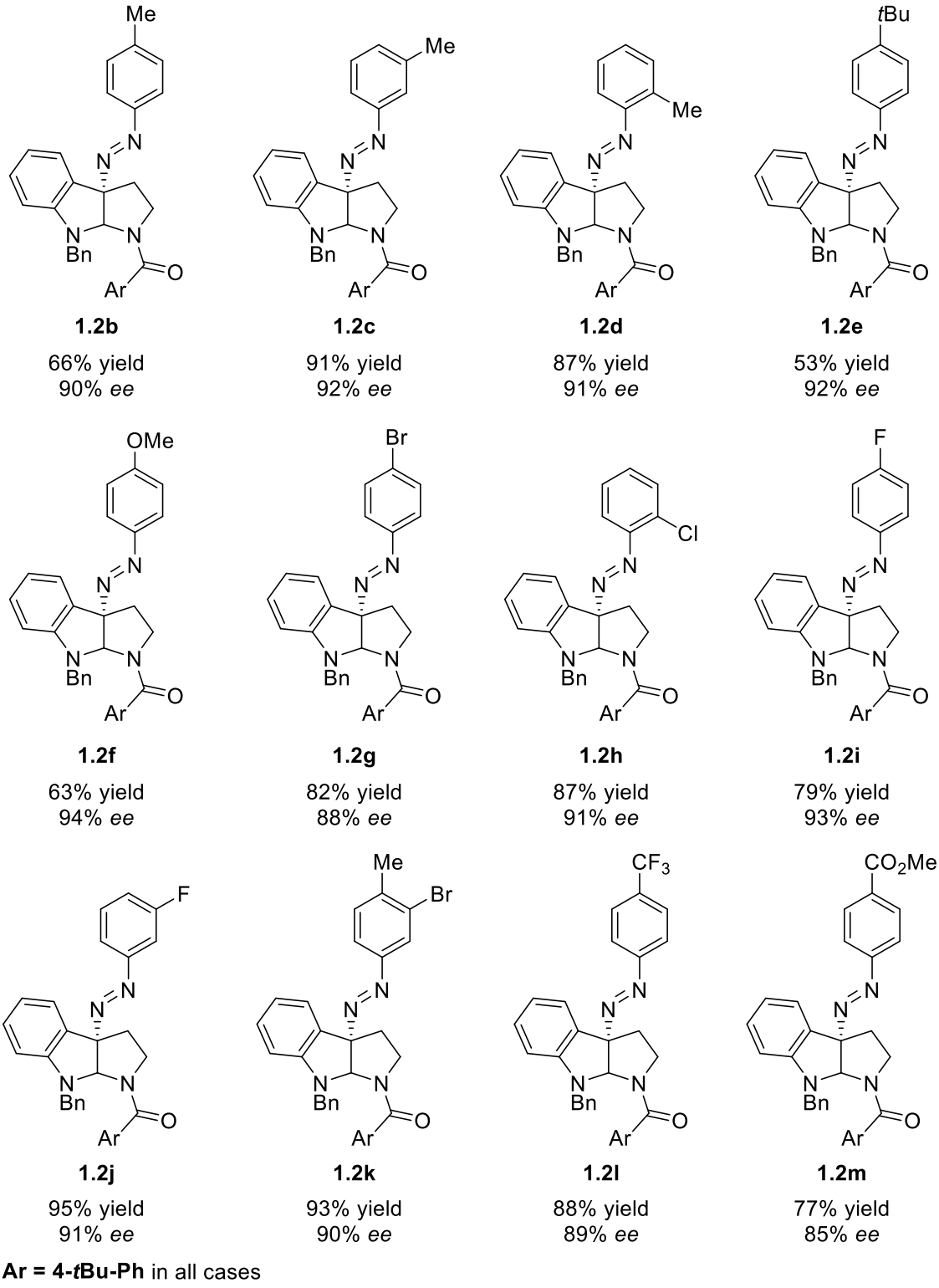

Figure 1. Aryldiazonium scope.

We next examined various derivatives of tryptamine **1.1a**. Substitution of the indole backbone at the 5-, 6- and 7-positions with both electron-donating (**1.2q-1.2r**) and electron-withdrawing groups

(**1.2n-1.2p**) led to product formation in high yield and enantioselectivity. Substrates with bromine substitution displayed diminished reactivity, thus requiring the use of more reactive electron-poor diazonium salts (**1.2n, 1.2o**). Replacement of the benzyl protecting group with a more labile p-methoxybenzyl (PMB) group did not negatively impact yield or ee (**1.2s**), nor did removal of the *tert*-butyl group from the benzamide moiety (**1.2t**). As with previously developed chiral phosphate phase-transfer reactions, the presence of a benzamide protecting group was crucial for high enantioinduction. Replacement of the benzamide with a carbamate led to a sharp decrease in ee (**1.2v**), as did replacement of indole-N benzyl group with an allyl group (**1.2u**).

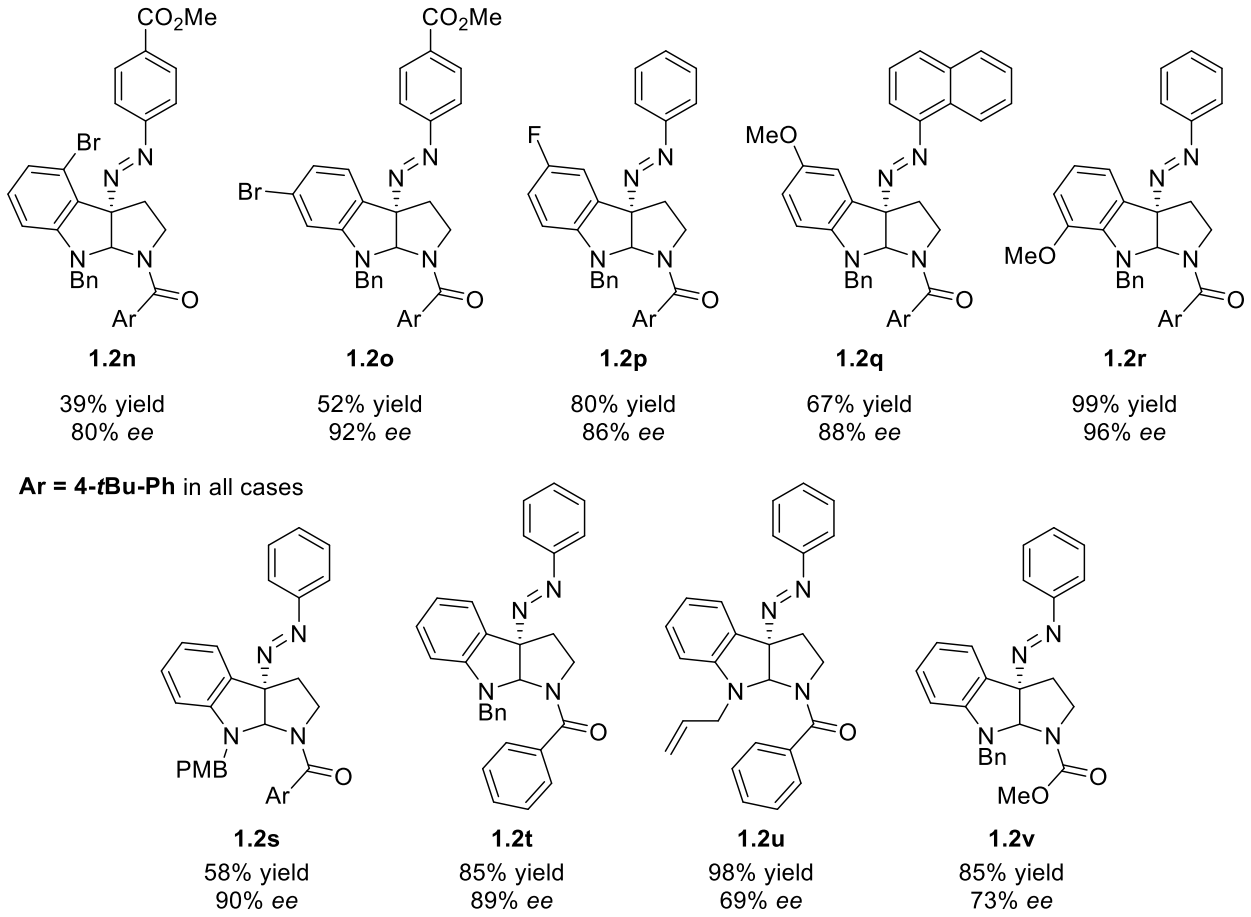

Figure 2. Indole and protecting group scope.

Lastly, we subjected diazene **1.2a** to photolytic conditions and were able to isolate the corresponding arylated product **1.3a** in modest yield and with complete retention of enantioenrichment (Scheme 13). Optimal conditions included use of a UVA light source (>300 nm) and cyclohexane as solvent.

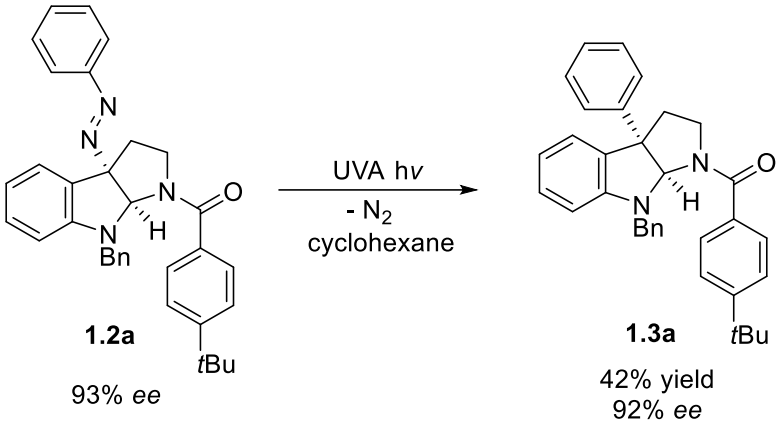

Scheme 13. Photolysis of **1.2a**.

Conclusions

Aryldiazonium salts have been utilized as insoluble electrophiles in chiral anion phase-transfer chemistry. By exploiting the π-electrophilicity of aryldiazonium salts and the specific reactivity of tryptamine derivatives, we have developed a highly enantioselective pyrroloindolization reaction. Reactions can be performed at room temperature and are tolerant to a variety of aryldiazonium salts and substituted tryptamine substrates. Control experiments indicate that a phase-transfer mechanism is operative. Photolysis of diazenated products affords the corresponding C-3 arylated compounds with complete retention of enantioselectivity.

Experimental details

General. Unless otherwise noted, all reagents were purchased from commercial suppliers and used without further purification. Chiral anion phase-transfer (CAPT) pyrroloindolization reactions were performed in 2-dram (15 X 60 mm) vials equipped with a screw cap and stirred using a magnetic Teflon stir bar (1/2" X 5/16") on the surface of a magnetic stir plate. Due to the heterogeneous nature of these reactions, fast and efficient stirring was maintained over the course of the reaction for optimal and reproducible results. Methyl *tert*-butyl ether (MTBE) was used as purchased from Fischer Scientific. Thin-layer chromatography (TLC) analysis of reaction mixtures was performed using Merck silica gel 60 F254 TLC plates, and visualized under UV or by staining with ceric ammonium molybdate or $KMnO_4$. Column chromatography was performed on Merck Silica Gel 60 Å, 230 X 400 mesh. Nuclear magnetic resonance (NMR) spectra were recorded using Bruker AV-600, AV-500, DRX-500, AVQ-400, AVB-400 and AV-300 spectrometers. ^{1}H and ^{13}C chemical shifts are reported in ppm downfield of tetramethylsilane and referenced to residual solvent peak ($CHCl_3$, δH = 7.26 ppm and δC = 77.0 ppm; DMSO, δH = 2.50 and δC = 39.5 ppm; CH_2Cl_2, δH = 5.32 and δC = 53.8 ppm).[22] Multiplicities are reported using the following abbreviations: s = singlet, d = doublet, t = triplet, q = quartet, app t = apparent triplet, m = multiplet, br = broad resonance. Solvent abbreviations are reported as follows: MTBE = Methyl *tert*-butyl ether, EtOAc = ethyl acetate, hex = hexanes, DCM = dichloromethane, Et_2O = diethyl ether, MeOH = methanol, *i*PrOH = isopropanol, THF = tetrahydrofuran, DMF = N,N-dimethylformamide, Et_3N = triethylamine. Mass spectral data were obtained from the Micro-Mass/Analytical Facility operated by the College of Chemistry, University of California, Berkeley

or by usage of an Agilent Time of Flight (Q-TOF) mass spectrometer in ESI mode. Enantiomeric excesses were measured on a Shimadzu VP Series Chiral HPLC using Chiralpak IA, IB, or IC columns.

The syntheses of TRIP (**1.3a**),[23] TCYP (**1.3b**),[24] H8-TRIP (**1.3d**),[25] and STRIP (**1.3e**)[26] have been previously reported. Racemic CAPT pyrroloindolinization products were synthesized utilizing racemic TRIP or under homogeneous conditions in the absence of phase-transfer catalyst with acetone as a solvent.

Substrate synthesis

General procedure for synthesis of tryptamine derivatives ***S1.1-S1.15***

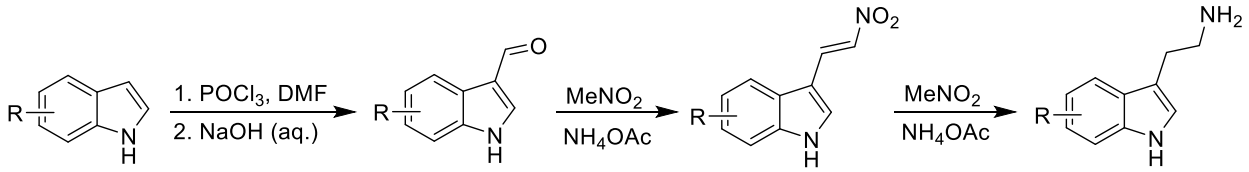

The synthesis of substituted tryptamines was adapted from the procedure of Dixon, *et al*.[27] To an oven-dried 250-mL round bottom flask was added dry DMF (20 mL) and a stir bar. The flask was cooled to 0 ˚C and $POCl_3$ (2.80 mL, 30 mmol, 1.5 equiv.) was added dropwise. The solution was stirred for 15 min at this temperature before the addition of the substituted indole (2.70 g, 20 mmol, 1.0 equiv.) dissolved DMF (20 mL). The solution was subsequently heated at 38 ˚C for 1 hour, then cooled to rt at which point ice water (40 mL) was carefully added, followed by aqueous 1 N NaOH (20 mL), with vigorous stirring. Additional 1 N NaOH was added until the reaction mixture maintained a yellow color. The reaction was then heated at 170 ˚C and refluxed for 5 minutes before being allowed to cool to rt and stirred overnight. The mixture was then extracted with EtOAc (3 x 50 mL), and the combined organic layers were washed with water (2 x 75 mL), brine (2 x 70 mL), dried over $MgSO_4$, filtered, and concentrated to yield the aldehyde as a solid which required no further purification.

To an oven-dried 250-mL round bottom flask was added the crude aldehyde (14.6 mmol, 1.0 equiv.), nitromethane (50 mL), and ammonium acetate (3.38 g, 43.9 mmol, 3.0 equiv.). The reaction was then refluxed for 90 min with vigorous stirring. After this time, the reaction was concentrated to dryness *via* rotary evaporation and subsequently dissolved in EtOAc (60 mL). The organic layer was washed with water (50 mL), brine (50 mL), dried over $MgSO_4$, filtered and concentrated. The crude material was purified by flash column chromatography (1:1 EtOAc/hex) to afford the nitro alkene.

To an oven-dried 1-L round bottom flask containing a stir-bar was added solid LAH pellets (3.33 g, 87.84 mmol, 6.0 equiv.) followed by dry THF (145 mL). The mixture was stirred in an ice bath to cool to 0 ˚C. The nitro alkene (14.6 mmol, 1.0 equiv.) was dissolved in THF (145 mL) and transferred to the cool LAH mixture *via* cannula over a period of 20 min. The mixture was allowed to slowly warm to rt and stir for 40 h. After this time, the reaction was cooled back to 0 ˚C before the slow addition of water (15 mL) until the cessation of bubbles. Then the mixture was diluted with Et_2O (150 mL) followed by addition of saturated Rochelle's salt solution (200 mL). This mixture was then vigorously stirred for 24 hours. The layers were then separated and the aqueous layer was extracted with Et_2O (1 x 100 mL) and the collected organic layers extracted with 2 N HCl (3 x 75 mL). The aqueous layer was then cooled in an ice bath and basified with 3M KOH

until pH ~ 10. This basic mixture was then extracted with Et_2O (3 x 75 mL), dried over $MgSO_4$, filtered, and concentrated to afford the pure tryptamine derivatives.

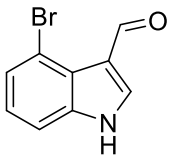

S1.1. Following the first step of the general procedure for the synthesis of tryptamine derivatives, compound **S1.1** was isolated as a pale yellow solid (52% yield). Spectral data are in accordance with literature.[28]

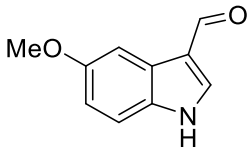

S1.2. Following the first step of the general procedure for the synthesis of tryptamine derivatives, compound **S1.2** was isolated as a pale yellow solid (79% yield). Spectral data are in accordance with literature.[29]

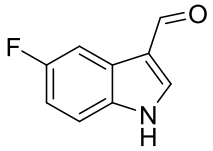

S1.3. Following the first step of the general procedure for the synthesis of tryptamine derivatives, compound **S1.3** was isolated as a pale yellow solid (73% yield). Spectral data are in accordance with literature.[27]

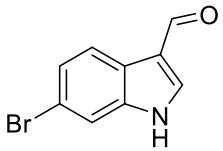

S1.4. Following the first step of the general procedure for the synthesis of tryptamine derivatives, compound **S1.4** was isolated as a pale brown solid (82% yield). Spectral data are in accordance with literature.[30]

S1.5. Following the first step of the general procedure for the synthesis of tryptamine derivatives (10 minute reflux), compound **S1.5** was isolated as a pale yellow powder (88% yield). Spectral data are in accordance with literature.[31]

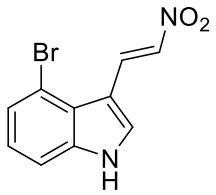

S1.6. Following the second step of the general procedure for the synthesis of tryptamine derivatives, compound **S1.6** was isolated as a brown oil (47% yield). Spectral data are in accordance with literature.[28]

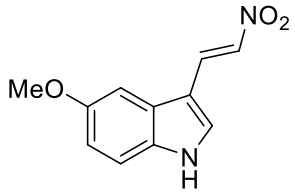

S1.7. Following the second step of the general procedure for the synthesis of tryptamine derivatives, compound **S1.7** was isolated as a solid (98% yield). Spectral data are in accordance with literature.[29]

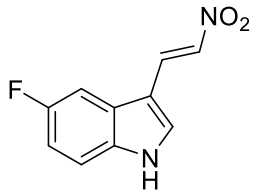

S1.8. Following the second step of the general procedure for the synthesis of tryptamine derivatives, compound **S1.8** was isolated as a solid (71% yield). Spectral data are in accordance with literature.[27]

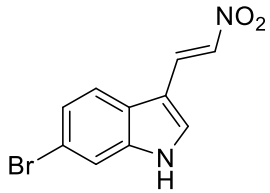

S1.9. Following the second step of the general procedure for the synthesis of tryptamine derivatives, compound **S1.9** was isolated as a solid (95% yield). Spectral data are in accordance with literature.[30]

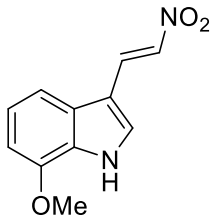

S1.10. Following the second step of the general procedure for the synthesis of tryptamine derivatives, compound **S1.10** was isolated as a solid (88% yield). Spectral data are in accordance with literature.[31]

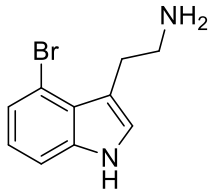

S1.11. Following the third step of the general procedure for the synthesis of tryptamine derivatives, compound **S.11** was isolated as a brown oil (54% yield). Spectral data are in accordance with literature.[28]

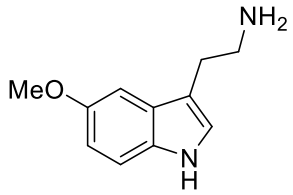

S1.12. Following the third step of the general procedure for the synthesis of tryptamine derivatives, compound **S1.12** was isolated as a brown oil (73% yield). Spectral data are in accordance with literature.[29]

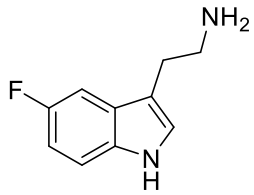

S1.13. Following the third step of the general procedure for the synthesis of tryptamine derivatives, compound **S1.13** was isolated as a brown oil (92% yield). Spectral data are in accordance with literature.[27]

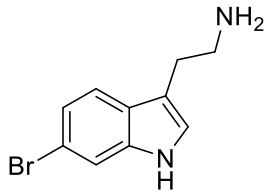

S1.14. Following the third step of the general procedure for the synthesis of tryptamine derivatives, compound **S1.14** was isolated as a brown oil (77% yield). Spectral data are in accordance with literature.[30]

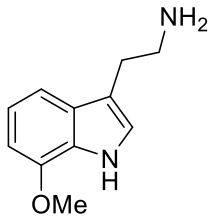

S1.15. Following the third step of the general procedure for the synthesis of tryptamine derivatives, compound **S1.15** was isolated as a brown oil (73% yield). Spectral data are in accordance with literature.[31]

General amidation and benzylation procedures for the synthesis of substrates

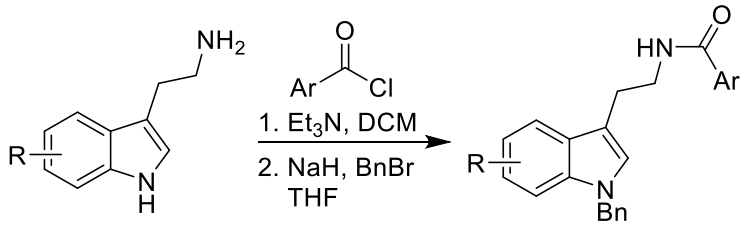

To an oven-dried 250 mL round bottom flask was added a stir-bar and the appropriate tryptamine (4.6 mmol, 1.0 equiv.), Et_3N (1.3 mL, 9.2 mmol, 2.0 equiv.), and dry DCM (20 mL). The solution was cooled to 0 ˚C before the dropwise addition of the 4-*t*butylbenzoyl chloride (0.99 mL, 5.06 mmol, 1.1 equiv.). The reaction was then stirred at room temperature for 3 h or until TLC showed complete consumption of starting material. The reaction was then concentrated *via* rotary evaporation and the crude material was purified by flash column chromatography (1:1 EtOAc:hex). This material was then taken directly into the next step. The protected tryptamine (3.41 mmol, 1.0 equiv.) was transferred to an oven-dried flask, dissolved in dry DMF (10 mL), and cooled to 0 ˚C. Sodium hydride (60 % dispersion in oil, 164 mg, 4.9 mmol, 1.2 equiv.) was added slowly to the stirred solution. The reaction was then stirred at rt for 15 min before cooling back down to 0 ˚C, followed by dropwise addition of benzyl bromide (0.43 mL, 3.58 mmol, 1.05 equiv.). The reaction was stirred cold for 5 minutes, before removal from the ice bath and then stirred at rt for 16 h. The reaction was quenched at 0 ˚C by the addition of aqueous ammonium chloride (10 mL) and water (10 mL). The mixture was extracted with EtOAc (3 x 25 mL) and the combined organic layers were washed with water (30 mL) and brine (30 mL), dried over $MgSO_4$, filtered, and concentrated. The crude reside was purified by flash column chromatography (1:4 to 1:1 EtOAc:hex) to afford the corresponding amide.

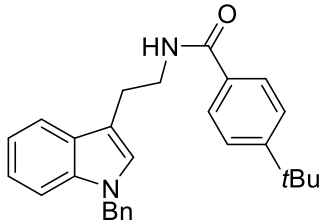

1.1a. Following the general procedure for amidation and benzylation, compound **1.1a** was isolated as a white solid (73% yield over two steps). ^{1}H NMR (500 MHz, $CDCl_3$) δ 7.67 (d, *J* = 7.9 Hz, 1H), 7.60 (d, *J* = 8.5 Hz, 2H), 7.37 (d, *J* = 8.4 Hz, 2H), 7.32-7.20 (m, 5H), 7.15-7.09 (m, 3H), 7.00 (s, 1H), 6.29 (s, 1H), 5.27 (s, 2H), 3.79 (q, *J* = 6.3 Hz, 2H), 3.09 (t, *J* = 6.6 Hz, 2H), 1.33 (s, 9H); ^{13}C NMR (126 MHz, $CDCl_3$) δ 167.3, 154.8, 137.7, 136.9, 131.9, 128.9, 128.0, 127.7, 126.9, 126.76, 126.3, 125.5, 122.1, 119.4, 119.1, 112.4, 109.9, 50.0, 40.2, 35.0, 31.3, 25.4 ppm; HRMS (+ESI) calcd. for [$C_{28}H_{31}N_2O$] ([M+H$^+$]): 411.2431, found: 411.2425.

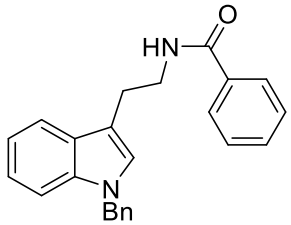

S1.16. Following the general procedure for amidation (using benzoyl chloride) and benzylation, compound **S1.16** was isolated as a white solid (70 % yield over two steps). ^{1}H NMR (500 MHz, $CDCl_3$) δ 7.67-7.64 (m, 3H), 7.48-7.44 (m, 1H), 7.37-7.34 (m, 2H), 7.30 (d, *J* = 8.2 Hz, 1H), 7.28-7.25 (m, 3H), 7.21 (td, *J* = 7.6, 1.0 Hz, 1H), 7.15-7.09 (m, 3H), 6.99 (s, 1H), 6.30 (s, 1H), 5.27 (s, 2H), 3.79 (q, *J* = 6.3 Hz, 2H), 3.10 (t, *J* = 6.7 Hz, 2H); ^{13}C NMR (126 MHz, $CDCl_3$) δ 167.5, 137.6, 136.9, 134.8, 131.4, 128.9, 128.6, 128.0, 127.7, 127.2, 126.9, 126.3, 122.2, 119.4, 119.1, 112.3, 109.9, 50.0, 40.3, 25.4; HRMS (+ESI) calcd. for [$C_{24}H_{23}N_2O$] ([M+H$^+$]): 355.1805, found: 355.1811.

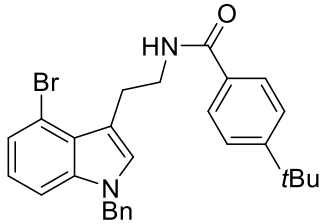

S1.17. Following the general procedure for amidation and benzylation, compound **S1.17** was isolated as a white solid (54% yield over two steps). ^{1}H NMR (400 MHz, CD_2Cl_2) δ 7.73-7.62 (m, 2H), 7.55-7.41 (m, 2H), 7.32 (m, 5H), 7.21-7.10 (m, 3H), 7.06 (t, *J* = 7.9 Hz, 1H), 5.27(s, 2H), 3.83 (dq, *J* = 21.9, 6.5 Hz, 2H), 3.39 (t, *J* = 6.8 Hz, 2H), 1.39 (s, 9H); ^{13}C NMR (101 MHz, CD_2Cl_2) δ 167.4, 155.2, 138.6, 137.7, 132.6, 129.3, 128.2, 127.3, 127.3, 127.1, 126.5, 125.9, 124.2, 123.1, 114.8, 113.5, 109.8, 50.6, 41.7, 35.3, 31.5, 26.5; HRMS (+ESI) calcd. for [$C_{24}H_{23}N_2O$] ([M+H$^+$]): 489.1536, found: 489.1542.

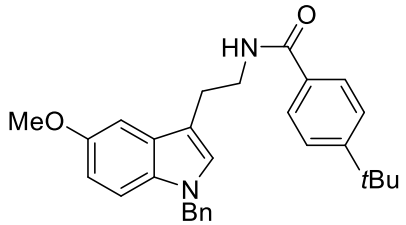

S1.18. Following the general procedure for amidation) and benzylation, compound **S1.18** was isolated as a white solid (70% yield over two steps). ^{1}H NMR (500 MHz, CD_2Cl_2) δ 7.66 – 7.53 (m, 2H), 7.46 – 7.35 (m, 2H), 7.34 – 7.21 (m, 3H), 7.16 (d, *J* = 8.9 Hz, 1H), 7.14 – 7.08 (m, 2H), 7.06 (d, *J* = 2.4 Hz, 1H), 7.03 (s, 1H), 6.80 (dd, *J* = 8.9, 2.4 Hz, 1H), 6.27 (t, *J* = 5.6 Hz, 1H), 5.25 (s, 2H), 3.74 (d, *J* = 14.3 Hz, 5H), 3.03 (t, *J* = 6.7 Hz, 2H), 1.32 (s, 9H). ^{13}C NMR (126 MHz, CD_2Cl_2) δ 167.3, 155.2, 154.5, 138.5, 132.5, 129.2, 128.9, 128.0, 128.0, 127.5, 127.3, 127.0, 125.9, 112.5, 112.4, 111.1, 101.1, 56.1, 50.6, 40.6, 35.3, 31.4, 25.8; HRMS (+ESI) calcd. for [$C_{29}H_{32}N_2O_2$] ([M+H$^+$]): 441.2537, found: 441.2540.

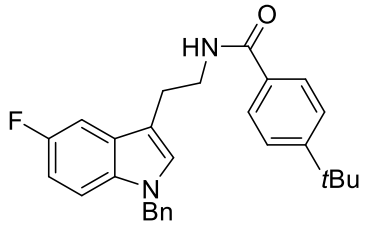

S1.19. Following the general procedure for amidation and benzylation compound, **S1.19** was isolated as an off-white solid (60% yield over two steps). ^{1}H NMR (500 MHz, $CDCl_3$) δ 7.70 – 7.48 (m, 2H), 7.45 – 7.33 (m, 2H), 7.33 – 7.22 (m, 5H), 7.17 (dd, *J* = 9.0, 4.3 Hz, 1H), 7.06 (dd, *J* = 6.4, 2.9 Hz, 2H), 6.23 (t, *J* = 5.6 Hz, 1H), 5.24 (s, 2H), 3.75 (q, *J* = 6.5 Hz, 2H), 3.02 (t, *J* = 6.8 Hz, 2H), 1.31 (s, 9H); ^{13}C NMR (126 MHz, $CDCl_3$) δ 167.7, 159.0, 157.2, 155.2, 137.6, 132.1, 128.3, 127.1, 127.0, 125.8, 112.5, 112.5, 110.9, 110.9, 110.7, 104.4, 104.2, 50.6, 40.3, 35.3, 31.5, 25.7; HRMS (+ESI) calcd. for [$C_{28}H_{30}N_2OF$] ([M+H$^+$]): 429.2337, found: 429.2338.

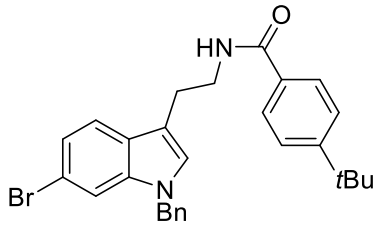

S1.20. Following the general procedure for amidation and benzylation, compound **S1.20** was isolated as a white solid (63% yield over two steps). ^{1}H NMR (500 MHz, $CDCl_3$) δ 7.58 (d, *J* = 8.1 Hz, 2H), 7.50 (d, *J* = 8.4 Hz, 1H), 7.44 (d, *J* = 1.7 Hz, 1H), 7.37 (d, *J* = 8.2 Hz, 2H), 7.33 – 7.24 (m, 3H), 7.21 (dd, *J* = 8.5, 1.7 Hz, 1H), 7.06 (dd, *J* = 6.6, 3.0 Hz, 2H), 6.95 (s, 1H), 6.28 – 6.12 (m, 1H), 5.21 (s, 2H), 3.75 (q, *J* = 6.5 Hz, 2H), 3.04 (t, *J* = 6.8 Hz, 2H), 1.32 (s, 9H); ^{13}C NMR (126 MHz, $CDCl_3$) δ 167.4, 154.9, 137.7, 137.1, 131.8, 129.0, 127.9, 126.9, 126.9, 126.8, 126.7, 125.6, 122.7, 120.5, 115.9, 112.9, 112.8, 50.0, 40.2, 35.0, 31.3, 25.4; HRMS (+ESI) calcd. for [$C_{28}H_{30}N_2OBr$] ([M+H$^+$]): 489.1536, found: 489.1535.

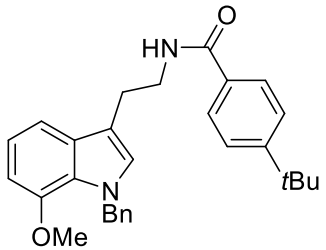

S1.21. Following the general procedure for amidation and benzylation compound, **S1.21** was isolated as an off-white solid (44% yield over two steps) and was further purified by recrystallization from hot EtOAc. ^{1}H NMR (500 MHz, $CDCl_3$) δ 7.66 –7.49 (m, 2H), 7.46 – 7.33 (m, 2H), 7.33 – 7.20 (m, 4H), 7.12 (dd, *J* = 7.2, 2.2 Hz, 2H), 7.06 (t, *J* = 7.8 Hz, 1H), 6.92 (s, 1H), 6.69 (d, *J* = 7.7 Hz, 1H), 6.21 (t, *J* = 5.3 Hz, 1H), 5.62 (s, 2H), 3.88 (s, 3H), 3.78 (q, *J* = 6.3 Hz, 2H), 3.06 (t, *J* = 6.6 Hz, 2H), 1.35 (s, 9H); ^{13}C NMR (126 MHz, $CDCl_3$) δ 167.3, 154.7, 147.8, 139.8, 131.9, 130.2, 128.6, 127.3, 127.2, 126.8, 126.7, 126.6, 125.5, 119.9, 112.6, 111.9, 103.2, 55.5, 52.4, 40.0, 35.0, 31.3, 25.4; HRMS (+ESI) calcd. for [$C_{29}H_{32}N_2O_2$] ([M+H$^+$]): 441.2537, found: 441.2541.

Synthesis of ***S1.22***

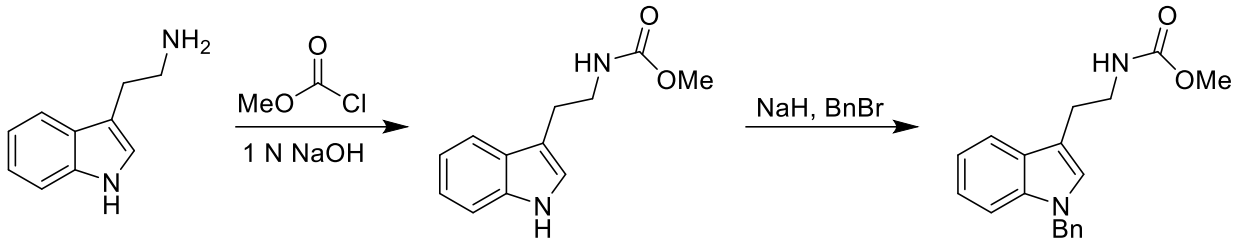

S1.22. The *Moc*-tryptamine intermediate was prepared in 90% yield following the procedure described by Skylar and Heathcock.[32] This carbamate was subsequently subjected to the general benzylation conditions and purified by flash chromatography (1:2 EtOAc:hex) to afford **S1.22** as a colorless oil (83% yield). ^{1}H NMR (500 MHz, $CDCl_3$) δ 7.63 (d, *J* = 7.9 Hz, 1H), 7.34 – 7.27 (m, 4H), 7.20 (ddd, *J* = 8.2, 7.0, 1.2 Hz, 1H), 7.17 – 7.08 (m, 3H), 6.97 (s, 1H), 5.29 (s, 2H), 4.79 (s, 1H), 3.67 (s, 3H), 3.53 (q, J = 6.6 Hz, 2H), 2.99 (t, *J* = 6.9 Hz, 2H); ^{13}C NMR (126 MHz, $CDCl_3$) δ 164.6, 157.1, 137.6, 128.9, 127.7, 126.3, 119.3, 112.2, 109.9, 77.4, 77.4, 77.2, 76.9, 52.1, 50.0, 41.5, 25.9; HRMS (+ESI) calcd. for [$C_{19}H_{20}N_2O_2$] ([M+H$^+$]): 309.1958, found: 309.1961.

Synthesis of ***S1.24***

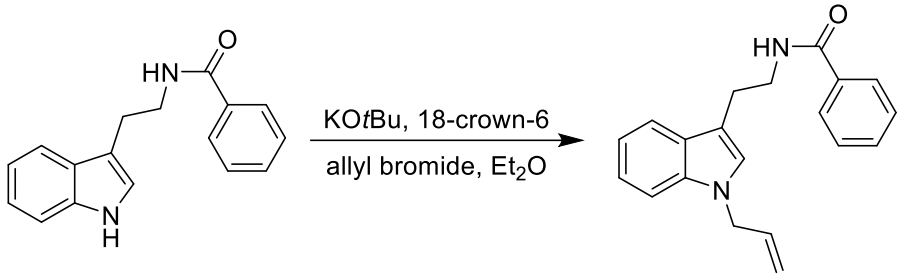

S1.24. Tryptamine **S1.23** (1.0 g, 3.8 mmol) was added to a mixture of 18-crown-6 (0.1 mg, 0.38 mmol), KO*t*Bu (508 mg, 4,5 mmol) in Et_2O (7.5 mL). The reaction mixture was cooled to 0 °C, at which time the allyl bromide (400 uL, 4.5 mmol) was added dropwise. The reaction was stirred at room temperature for 3 h, quenched with water, extracted in Et_2O and purified by flash chromatography (1:1 EtOAc:hex) to yield an orange powder. ^{1}H NMR (400 MHz, CD_2Cl_2) δ 7.77 – 7.67 (m, 2H), 7.65 (dt, *J* = 8.0, 1.0 Hz, 1H), 7.54 – 7.45 (m, 1H), 7.40 (tt, *J* = 6.6, 1.6 Hz, 2H), 7.36 – 7.28 (m, 1H), 7.21 (ddd, *J* = 8.3, 6.9, 1.3 Hz, 1H), 7.10 (ddd, *J* = 8.0, 6.9, 1.1 Hz, 1H), 7.00 (s, 1H), 6.46 (s, 1H), 6.00 (ddt, *J* = 17.1, 10.5, 5.4 Hz, 1H), 5.18 (dq, *J* = 10.2, 1.5 Hz, 1H), 5.06 (dq, *J* = 17.1, 1.6 Hz, 1H), 4.70 (dt, *J* = 5.4, 1.7 Hz, 2H), 3.75 (td, *J* = 6.9, 5.6 Hz, 2H), 3.08 (t, *J* = 6.9 Hz, 2H); ^{13}C NMR (101 MHz, CD_2Cl_2) δ 167.5, 137.1, 135.5, 134.3, 131.7, 128.9, 128.5, 127.3, 126.4, 122.2, 119.5, 119.4, 117.3, 112.5, 110.2, 49.1, 40.9, 25.8; HRMS (+ESI) calcd. for [$C_{20}H_{20}N_2O$] ([M+H$^+$]): 305.1648, found: 305.1653.

*Synthesis of **S1.25***

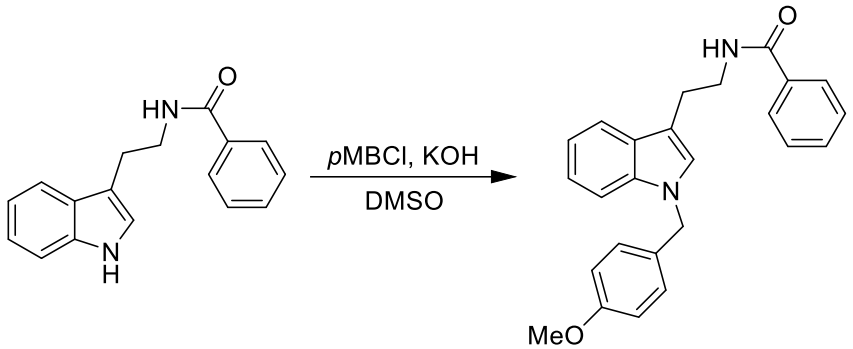

S1.25. Tryptamine **S1.23** (1.0 g, 3.8 mmol) and KOH (420 mg, 7.54 mmol) were stirred in DMSO (15 mL) for 1 hour. To the reaction mixture, *p*MBCl (1 mL, 7.54 mmol) was added dropwise. The reaction was stirred at rt overnight, quenched with water, extracted in EtOAc and purified by flash chromatography (1:1 EtOAc:hex) to yield an orange powder. ^{1}H NMR (400 MHz, CD_2Cl_2) δ 7.77 – 7.57 (m, 3H), 7.55 – 7.44 (m, 1H), 7.44 –7.35 (m, 2H), 7.35 – 7.27 (m, 1H), 7.19 (ddd, *J* = 8.3, 6.9, 1.3 Hz, 1H), 7.15 – 7.05 (m, 3H), 7.03 (s, 1H), 6.85 – 6.73 (m, 2H), 6.45 (s, 1H), 5.20 (s, 2H), 3.75 (d, *J* = 2.8 Hz, 5H), 3.08 (t, *J* = 6.8 Hz, 2H); ^{13}C NMR (101 MHz, CD_2Cl_2) δ 167.5, 159.6, 137.2, 135.4, 131.7, 130.3, 128.9, 128.8, 128.7, 127.3, 126.7, 122.3, 119.5, 119.5, 114.5, 112.6, 110.3, 55.7, 49.9, 40.8, 25.8. HRMS (+ESI) calcd. for [$C_{25}H_{24}N_2O2$] ([M+H$^+$]): 385.1911, found: 385.1897.

Synthesis of aryldiazonium salts

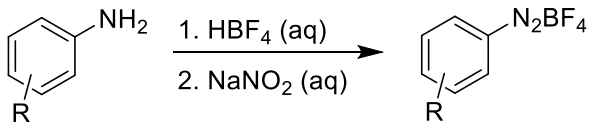

The aniline (10 mmol) was dissolved in a mixture of 50% (V/V) fluoroboric acid (3.5 mL) and water (4.0 mL). After cooling to 0° C, an aqueous solution of sodium nitrite (700 mg, 10.1 mmol, in 1.5 mL H_2O) was added in 0.25 mL portions. The mixture was stirred for 30 min and the thick precipitate was collected and dissolved in acetone. The diazonium tetrafluoroborate was then precipitated by the addition of Et_2O. The product was dried under high vacuum for several hours. Utilization of this procedure provided diazonium salts and yields comparable to those previously reported, and all spectral data that matched the data found in the literature; see the references below.

1. 4-Bromobenzenediazonium tetrafluoroborate, 4-fluorobenzenediazonium tetrafluoroborate, 4-*tert*-butylbenzenediazonium tetrafluoroborate, and 4-methoxycarbonylbenzenediazonium tetrafluoroborate.[33]

2. Benzenediazonium tetrafluoroborate, 4-methylcarbonylbenzenediazonium tetrafluoroborate, 4-methoxybenzenediazonium tetrafluoroborate, naphthalen-1-yl-diazonium tetrafluoroborate.[34]

3. 2-Chlorobenzenediazonium tetrafluoroborate.[35]

4. 2-Methylbenzenediazonium tetrafluoroborate, 3-methylbenzenediazonium tetrafluoroborate.[36]

5. 4-Trifluoromethylbenzenediazonium tetrafluoroborate.[37]

6. 3-Fluorobenzenediazonium tetrafluoroborate.[38]

7. 3-Bromo-4-methylbenzenediazonium tetrafluoroborate.[39]

General procedure for phase-transfer diazenation

A suspension of the tryptamine (0.05 mmol), Na_3PO_4 (24 mg, 0.15 mmol, 3 equiv.), and (*R*)-STRIP (1.8 mg, 0.0025 mmol, 5 mol%) in MTBE (0.5 mL) was stirred vigorously at rt for 15 minutes. To this suspension the aryldiazonium salt (0.05 mmol, 1 equiv.) was added rapidly in one portion. The reactions were stirred until TLC analysis indicated completion (1-12 h). The bright yellow reaction mixtures were filtered through cotton wool and the volatiles were removed by rotary evaporation. The crude product was dissolved in benzene and loaded onto a 1 cm column and eluted in 5:95 EtOAc:hex to yield yellow foams. The products were stable for several months at -20 °C neat, in protic solvents, or in pyridine. However, decomposition of some of the products occurred in halogenated solvents or aprotic polar solvents.

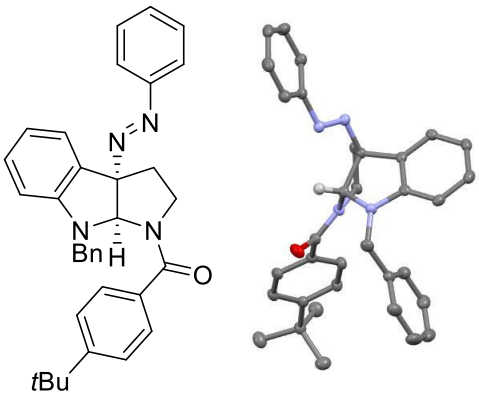

1.2a. Following the general procedure for phase-transfer diazenation, compound **1.2a** was isolated as a yellow solid (99% yield). ^{1}H NMR (500 MHz; CD_2Cl_2) δ 7.69 (dd, *J* = 7.5, 1.8 Hz, 2H), 7.45 (d, *J* = 5.9 Hz, 3H), 7.37 (t, *J* = 9.4 Hz, 4H), 7.31 (d, *J* = 8.3 Hz, 2H), 7.27 (t, *J* = 7.3 Hz, 2H), 7.21 (t, *J* = 7.0 Hz, 2H), 7.10 (t, *J* = 7.5 Hz, 1H), 6.81 (s, 1H), 6.67 (t, *J* = 7.2 Hz, 1H), 6.37 (d, *J* = 7.8 Hz, 1H), 4.83 (s, 2H), 3.79 (t, *J* = 8.9 Hz, 1H), 3.58 (td, *J* = 11.5, 5.5 Hz, 1H), 2.59-2.47 (m, 2H), 1.30 (s, 9H); ^{13}C NMR (126 MHz, CD_2Cl_2) δ 170.1, 153.8, 151.8, 151.5, 139.5, 133.0, 131.1, 130.2, 129.1, 128.4, 127.5, 127.3, 127.0, 126.8, 125.12 125.1, 122.5, 117.5, 106.3, 88.7, 80.9, 49.9, 48.7, 36.6, 34.8, 31.0 ppm; HRMS (+ESI) calcd. for [$C_{34}H_{35}N_4O$] ([M+H$^+$]): 515.2805, found: 515.2797; HPLC (ChiralPak IB column) 98:02 (hex/*i*PrOH) 1mL/min; t_{major} (21.2 min), t_{minor} (26.7 min); 91% ee.

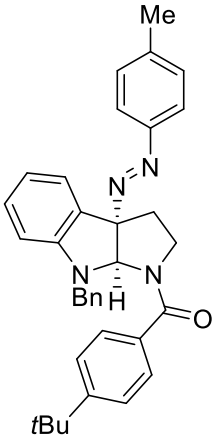

1.2b. Following the general procedure for phase-transfer diazenation, compound **1.2b** was isolated as a yellow solid (66% yield). ^{1}H NMR (300 MHz; CD_2Cl_2) δ 7.63 (d, *J* = 8.4 Hz, 2H), 7.43-7.23 (m, 11H), 7.12 (t, *J* = 7.3 Hz, 2H), 6.83 (s, 1H), 6.70 (t, *J* = 7.3 Hz, 1H), 6.39 (d, *J* = 7.8 Hz, 1H), 4.86 (s, 2H), 3.85-3.77 (m, 1H), 3.66-3.59 (m, 1H), 2.58-2.51 (m, 2H), 2.41 (s, 3H), 1.33 (s, 9H); ^{13}C NMR (126 MHz, CD_2Cl_2) δ 170.0, 164.6, 153.7, 151.4, 149.8, 141.7, 139.4, 133.0, 130.1, 129.6, 128.3, 127.3, 127.0, 126.9, 126.7, 125.0, 122.5, 117.4, 106.2, 88.3, 80.9, 49.8, 48.7, 36.6, 34.7, 30.9, 21.2 ppm; HRMS (+ESI) calcd. for [$C_{35}H_{37}N_4O$] ([M+H$^+$]): 529.2962, found: 529.2980; HPLC (ChiralPak IB column) 98:02 (hex/*i*PrOH) 1mL/min; t_{major} (11.7 min), t_{minor} (14.5 min); 90% ee.

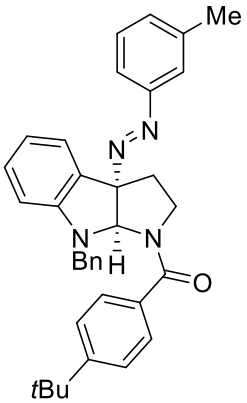

1.2c. Following the general procedure for phase-transfer diazenation, compound **1.2c** was isolated as a yellow solid (91% yield). ^{1}H NMR (500 MHz; CD_2Cl_2) δ 7.51-7.50 (m, 2H), 7.40-7.32 (m, 7H), 7.28 (t, *J* = 7.4 Hz, 3H), 7.22 (d, *J* = 7.4 Hz, 2H), 7.12 (t, *J* = 7.8 Hz, 1H), 6.81 (s, 1H), 6.69 (t, *J* = 7.4 Hz, 1H), 6.39 (d, *J* = 7.9 Hz, 1H), 4.84 (s, 2H), 3.81 (dd, *J* = 10.5, 7.9 Hz, 1H), 3.60 (td, *J* = 11.4, 5.5 Hz, 1H), 2.60-2.49 (m, 2H), 2.41 (s, 3H), 1.31 (s, 9H); ^{13}C NMR (126 MHz, CD_2Cl_2) δ 170.5, 154.2, 152.3, 151.9, 139.9, 139.7, 133.5, 132.3, 130.7, 129.3, 128.9, 127.8, 127.4, 127.2, 125.6, 125.6, 123.2, 120.5, 117.9, 106.8, 89.1, 81.4, 50.3, 49.2, 37.0, 35.3, 31.5, 21.6 ppm; HRMS (+ESI) calcd. for [$C_{35}H_{37}N_4O$] ([M+H$^+$]): 529.2967, found: 529.2979; HPLC (ChiralPak IB column) 98:02 (hex/*i*PrOH) 1mL/min; t_{major} (11.0 min), t_{minor} (14.1 min); 93% ee.

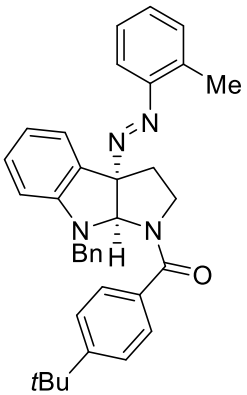

1.2d. Following the general procedure for phase-transfer diazenation, compound **1.2d** was isolated as a yellow solid (87% yield). ^{1}H NMR (500 MHz; CD_2Cl_2) δ; 7.41-7.28 (m, 11H), 7.22-7.19 (m, 2H), 7.12 (t, *J* = 7.8 Hz, 2H), 6.84 (s, 1H), 6.70 (t, *J* = 7.5 Hz, 1H), 6.39 (d, *J* = 8.0 Hz, 1H), 4.88-4.81 (m, 2H), 3.82 (dd, *J* = 9.9, 7.9 Hz, 1H), 3.62 (td, *J* = 11.3, 5.8 Hz, 1H), 2.57-2.49 (m, 5H), 1.32 (s, 9H); ^{13}C NMR (126 MHz, CD_2Cl_2) δ 170.6, 154.2, 151.9, 150.3, 140.0, 137.9, 131.6, 131.4, 130.6, 128.9, 127.8, 127.7, 127.4, 127.3, 127.2, 126.8, 125.6, 118.3, 116.1, 107.0, 89.8, 82.0, 50.4, 48.7, 37.1, 35.3, 31.4, 30.1, 18.0 ppm; HRMS (+ESI) calcd. for [$C_{35}H_{37}N_4O$] ([M+H$^+$]): 529.2962, found: 529.2980; HPLC (ChiralPak IB column) 98:02 (hex/*i*PrOH) 1mL/min; t_{major} (21.2 min), t_{minor} (26.7 min); 91% ee.

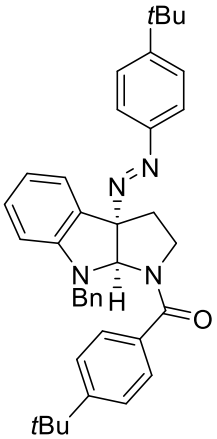

1.2e. Following the general procedure for phase-transfer diazenation, compound **1.2e** was isolated as a yellow solid (53% yield). ^{1}H NMR (500 MHz; C_6D_6) δ 7.96 (d, *J* = 8.3 Hz, 2H), 7.66 (d, *J* = 6.9 Hz, 2H), 7.60 (d, *J* = 7.5 Hz, 2H), 7.53 (d, *J* = 6.2 Hz, 2H), 7.44 (d, *J* = 8.4 Hz, 2H), 7.38-7.32 (m, 4H), 7.25 (t, *J* = 7.3 Hz, 2H), 6.92 (t, *J* = 7.4 Hz, 1H), 6.57 (d, *J* = 7.7 Hz, 1H), 5.16 (q, *J* = 21.3 Hz, 2H), 3.62-3.59 (m, 1H), 3.47-3.42 (m, 1H), 2.54-2.51 (m, 1H), 2.41 (q, *J* = 10.2 Hz, 1H), 1.36 (s, 9H), 1.35 (s, 9H); ^{13}C NMR (126 MHz, CD_2Cl_2) δ 170.0, 154.7, 153.7, 151.4, 149.6, 139.5, 133.0, 130.1, 128.3, 127.3, 127.0, 126.9, 126.7, 126.0, 125.1, 125.0, 122.2, 117.4, 106.2, 88.4, 80.9, 49.8, 48.7, 36.6, 34.9, 34.8, 31.0, 31.0; HRMS (+ESI) calcd. for [$C_{38}H_{43}N_4O$] ([M+H$^+$]): 571.3437, found: 571.3448; HPLC (ChiralPak IB column) 99:01 (hex/*i*PrOH) 1mL/min; t_{major} (13.6 min), t_{minor} (23.0 min); 93% ee.

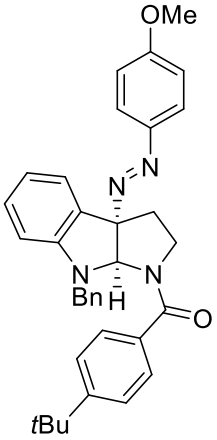

1.2f. Following the general procedure for phase-transfer diazenation, compound **1.2f** was isolated as a yellow solid (63% yield). ^{1}H NMR (500 MHz; CD_2Cl_2) δ 7.72 (d, *J* = 8.9 Hz, 2H), 7.41-7.37 (m, 3H), 7.34-7.28 (m, 3H), 7.23 (d, *J* = 7.0 Hz, 4H), 7.11 (t, *J* = 7.7 Hz, 1H), 6.97 (d, *J* = 8.7 Hz, 2H), 6.80 (s, 1H), 6.69 (t, *J* = 7.3 Hz, 1H), 6.38 (d, *J* = 7.8 Hz, 1H), 4.85 (s, 2H), 3.86 (s, 3H), 3.82-3.79 (m, 1H), 3.60 (td, *J* = 11.4, 5.4 Hz, 1H), 2.59-2.48 (m, 2H), 1.32 (s, 9H); ^{13}C NMR (126 MHz, CD_2Cl_2) δ 170.5, 162.6, 154.2, 151.9, 146.4, 140.0, 133.5, 130.5, 128.8, 127.8, 127.4, 127.2, 125.6, 125.5, 124.9, 117.9, 114.5, 106.7, 88.5, 81.5, 56.1, 50.3, 49.2, 37.2, 35.3, 31.5, 30.3 ppm; HRMS (+ESI) calcd. for [$C_{35}H_{37}N_4O_2$] ([M+H$^+$]): 545.2911, found: 545.2928; HPLC (ChiralPak IB column) 97:03 (hex/*i*PrOH) 1mL/min; t_{major} (18.3 min), t_{minor} (16.9 min); 94% ee.

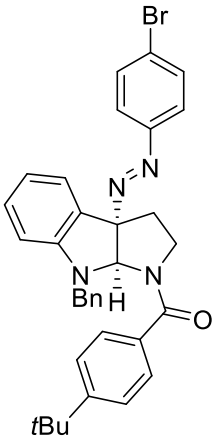

1.2g. Following the general procedure for phase-transfer diazenation, compound **1.2g** was isolated as a yellow solid (82% yield). ^{1}H NMR (500 MHz; CD_2Cl_2) δ 7.63-7.59 (m, 4H), 7.42-7.33 (m, 6H), 7.29 (t, *J* = 7.4 Hz, 2H), 7.23 (d, *J* = 7.2 Hz, 2H), 7.15-7.12 (m, 1H), 6.82 (s, 1H), 6.71 (d, *J* = 7.2 Hz, 1H), 6.41 (d, *J* = 7.9 Hz, 1H), 4.85 (s, 2H), 3.82 (dd, *J* = 10.6, 8.3 Hz, 1H), 3.61 (td, *J* = 11.5, 5.2 Hz, 1H), 2.60 (dd, *J* = 12.4, 5.1 Hz, 1H), 2.51 (td, *J* = 12.2, 7.8 Hz, 1H), 1.32 (s, 9H); ^{13}C NMR (126 MHz, CD_2Cl_2) δ 170.1, 153.8, 151.5, 150.5, 139.4, 132.9, 132.3, 130.3, 128.4, 127.3, 127.0, 126.8, 126.5, 125.4, 125.2, 125.1, 124.2, 117.5, 106.4, 88.8, 80.7, 49.8, 48.7, 36.6, 34.8, 31.0 ppm; HRMS (+ESI) calcd. for [$C_{34}H_{34}N_4OBr$] ([M+H$^+$]): 593.1910, found: 593.1903; HPLC (ChiralPak IB column) 98:02 (hex/*i*PrOH) 1mL/min; t_{major} (12.1 min), t_{minor} (14.5 min); 88% ee.

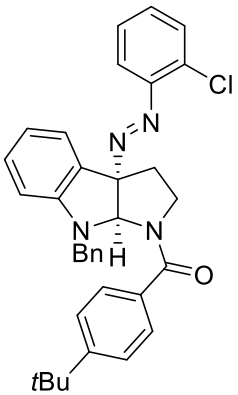

1.2h. Following the general procedure for phase-transfer diazenation, compound **1.2h** was isolated as a yellow solid (87% yield). ^{1}H NMR (500 MHz; CD_2Cl_2) δ 7.53 (d, *J* = 8.0 Hz, 1H), 7.43–7.13 (m, 13H), 6.88 (s, 1H), 6.70 (t, *J* = 7.4 Hz, 1H), 6.40 (d, *J* = 7.9 Hz, 1H), 5.32 (s, 1H), 4.85 (s, 2H), 3.87 – 3.79 (m, 1H), 3.63 (td, *J* = 11.2, 6.0 Hz, 1H), 2.61–2.51 (m, 2H), 1.32 (s, 9H); ^{13}C NMR (126 MHz, $CDCl_3$) δ 170.8, 165.3, 154.5, 152.2, 140.1, 134.9, 133.6, 132.5, 131.2, 129.1, 128.1, 128.0, 127.6, 127.5, 127.4, 126.9, 126.0, 125.9, 118.6, 118.3, 107.1, 90.2, 82.1, 50.6, 49.5, 37.3, 35.5, 31.7; HRMS (+ESI) calcd. For [$C_{34}H_{33}FN_4O$] ([M+H$^+$]): 549.2416, found: 549.2421; HPLC (ChiralPak IB column) 99:01 (hex/*i*PrOH) 1mL/min; t_{major} (22.3 min), t_{minor} (52.3 min); 91% ee.

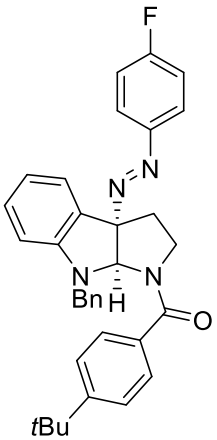

1.2i. Following the general procedure for phase-transfer diazenation, compound **1.2i** was isolated as a yellow solid (79% yield). ^{1}H NMR (500 MHz; CD_2Cl_2) δ 7.83–7.75 (m, 2H), 7.48–7.12 (m, 13H), 6.86 (s, 1H), 6.74 (t, *J* = 7.4 Hz, 1H), 6.45 (d, *J* = 8.0 Hz, 1H), 4.89 (s, 2H), 3.86 (dd, *J* = 11.1, 7.7 Hz, 1H), 3.65 (td, *J* = 11.6, 5.5 Hz, 1H), 2.60 (ddd, *J* = 36.1, 12.4, 6.6 Hz, 2H), 1.37 (s, 9H); ^{13}C NMR (126 MHz, CD_2Cl_2) δ 170.5, 165.9, 163.9, 154.2, 151.9, 148.8, 139.9, 133.4, 130.7, 128.9, 127.8, 127.4, 127.3, 125.5, 125.2, 125.1, 118.0, 116.4, 106.8, 89.0, 81.3, 50.3, 49.2, 37.1, 35.3, 31.5; HRMS (+ESI) calcd. for [$C_{34}H_{33}FN_4O$] ([M+H$^+$]): 533.2711, found: 533.2714; HPLC (ChiralPak IB column) 99:01 (hex/*i*PrOH) 1mL/min; t_{major} (16.6 min), t_{minor} (25.9 min); 93% ee.

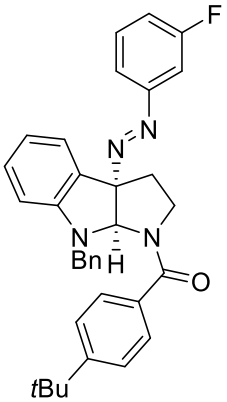

1.2j. Following the general procedure for phase-transfer diazenation, compound **1.2j** was isolated as a yellow solid (95% yield). ^{1}H NMR (500 MHz; CD_2Cl_2) δ 7.59 (dt, *J* = 8.0, 1.3 Hz, 1H), 7.52–7.11 (m, 14H), 6.84 (s, 1H), 6.71 (t, *J* = 7.4 Hz, 1H), 6.42 (d, *J* = 7.9 Hz, 1H), 4.86 (s, 2H), 3.83 (dd, *J* = 11.2, 7.5 Hz, 1H), 3.62 (td, *J* = 11.6, 5.4 Hz, 1H), 2.62 (dd, *J* = 12.5, 5.4 Hz, 1H), 2.52 (td, *J* = 12.3, 7.7 Hz, 1H), 1.33 (s, 9H); ^{13}C NMR (126 MHz, CD_2Cl_2) δ 170.5, 164.6, 162.7, 154.3, 153.7, 153.7, 151.9, 139.8, 133.4, 130.9, 128.9, 127.8, 127.5, 127.3, 127.0, 125.6, 120.7, 118.4, 118.2, 108.5, 106.9, 89.3, 81.1, 50.3, 49.1, 37.0, 35.3, 31.5; HRMS (+ESI) calcd. for [$C_{34}H_{33}FN_4O$] ([M+H$^+$]): 533.2711, found: 533.2713; HPLC (ChiralPak IB column) 99:01 (hex/*i*PrOH) 1mL/min; t_{major} (16.7 min), t_{minor} (23.1 min); 91% ee.

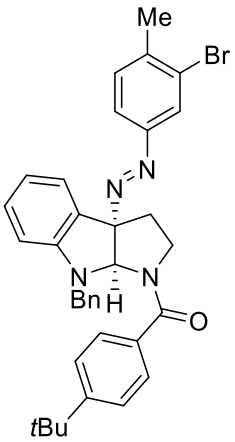

1.2k. Following the general procedure for phase-transfer diazenation, compound **1.2k** was isolated as a yellow solid (93% yield). ^{1}H NMR (500 MHz; CD_2Cl_2) δ 7.88 (d, *J* = 2.1 Hz, 1H), 7.61 (dd, *J* = 8.1, 1.9 Hz, 1H), 7.43 –7.08 (m, 12H), 6.79 (s, 1H), 6.70 (t, *J* = 7.4 Hz, 1H), 6.41 (d, *J* = 8.0 Hz, 1H), 4.84 (s, 2H), 3.82 (dd, *J* = 11.1, 7.6 Hz, 1H), 3.60 (td, *J* = 11.5, 5.4 Hz, 1H), 2.55 (ddd, *J* = 36.2, 12.4, 6.6 Hz, 2H), 2.45 (s, 3H), 1.32 (s, 9H); ^{13}C NMR (126 MHz, $CDCl_3$) δ 170.5, 154.2, 151.9, 151.1, 141.6, 139.9, 133.4, 131.6, 130.7, 128.8, 127.8, 127.5, 127.1, 125.9, 125.7, 125.6, 125.6, 123.0, 118.0, 106.9, 100.5, 89.1, 81.2, 50.3, 49.2, 37.0, 35.3, 31.5, 23.2; HRMS (+ESI) calcd. for [$C_{30}H_{27}N_4O$] ([M+H$^+$]): 607.2067, found: 607.2071; HPLC (ChiralPak IB column) 99:01 (hex/*i*PrOH) 1mL/min; t_{major} (17.8 min), t_{minor} (27.8 min); 90% ee.

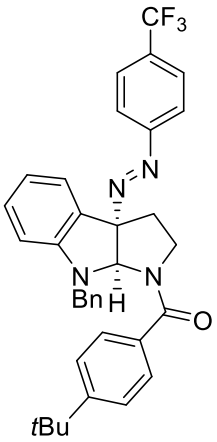

1.2l. Following the general procedure for phase-transfer diazenation, compound **1.2l** was isolated as a yellow solid (88% yield). ^{1}H NMR (400 MHz; pyridine-d_5) δ 10.18 (s, 1H), 9.24 (s, 4H), 9.05-9.03 (m, 2H), 8.94 (t, *J* = 8.9 Hz, 3H), 8.80-8.66 (m, 6H), 8.34 (t, *J* = 7.3 Hz, 1H), 8.07 (d, *J* = 7.9 Hz, 1H), 6.55 (s, 2H), 5.30 (t, *J* = 8.9 Hz, 1H), 5.10 (td, *J* = 11.0, 4.7 Hz, 1H), 4.14 (dd, *J* = 12.3, 5.2 Hz, 1H), 4.02 (td, *J* = 12.0, 8.0 Hz, 1H), 2.73 (s, 9H); ^{13}C NMR (126 MHz, pyridine-d_5) δ 171.2, 154.8, 152.8, 151.2, 140.7, 136.7, 134.6, 133.0 (q, *J* = 32.1 Hz), 131.9, 129.8, 129.1, 128.5, 128.2, 127.8, 127.6, 126.6, 126.5, 124.7, 119.2, 108.2, 90.7, 81.9, 51.1, 49.8, 37.6, 35.8, 32.1; ^{19}F NMR (376 MHz, pyridine-d_5) δ -59.7 ppm; HRMS (+ESI) calcd. for [$C_{35}H_{34}N_4OF_3$] ([M+H$^+$]): 583.2679, found: 583.2668; HPLC (ChiralPak IB column) 98:02 (hex/*i*PrOH) 1mL/min; t_{major} (10.2 min), t_{minor} (13.3 min); 89% ee.

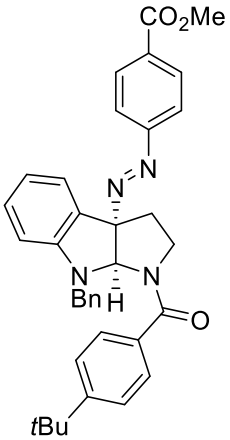

1.2m. Following the general procedure for phase-transfer diazenation, compound **1.2m** was isolated as a yellow solid (77% yield). ^{1}H NMR (500 MHz; CD_2Cl_2) δ 8.16 (d, *J* = 7.8 Hz, 2H), 7.78 (d, *J* = 7.8 Hz, 2H), 7.45-7.26 (m, 10H), 7.17 (q, *J* = 6.5 Hz, 1H), 6.87 (s, 1H), 6.74 (t, *J* = 5.0 Hz, 1H), 6.45 (d, *J* = 7.8 Hz, 1H), 4.88 (s, 2H), 3.96 (s, 3H), 3.87 (t, *J* = 7.8 Hz, 1H), 3.68-3.63 (m, 1H), 2.67-2.53 (m, 2H), 1.35 (s, 9H); ^{13}C NMR (126 MHz, CD_2Cl_2) δ 170.0, 166.2, 164.6, 154.2, 153.7, 151.4, 139.3, 132.8, 132.1, 130.4, 130.3, 128.3, 127.3, 126.9, 126.8, 125.1, 122.4, 117.5, 106.4, 89.2, 80.6, 52.2, 49.8, 48.6, 36.5, 34.8, 30.9; HRMS (+ESI) calcd. for [$C_{36}H_{37}N_4O_3$] ([M+H$^+$]): 573.2866, found: 573.2870; HPLC (ChiralPak IB column) 98:02 (hex/*i*PrOH) 1mL/min; t_{major} (23.8 min), t_{minor} (27.3 min); 87% ee.

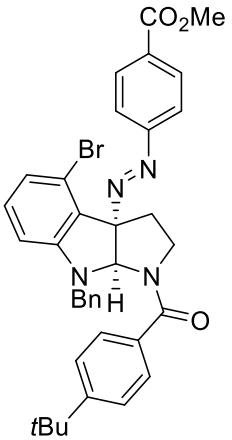

1.2n. Following the general procedure for phase-transfer diazenation, compound **1.2n** was isolated as a yellow solid (39% yield). ^{1}H NMR (500 MHz; CD_2Cl_2) δ 8.13 (d, *J* = 8.4 Hz, 2H), 7.72 (d, *J* = 8.5 Hz, 2H) 7.50-7.09 (m, 9H), 7.01 (t, *J* = 8.1 Hz, 1H), 6.82 (d, *J* = 7.9 Hz, 1H), 6.48 (s, 1H), 6.38 (d, *J* = 8.1 Hz, 1H), 4.81 (s, 2H), 3.91 (app. s, 4H), 3.69 (m, 1H), 3.09 (dd, *J* = 13.0, 5.2 Hz, 1H), 2.91(td, *J* = 12.7, 8.4 Hz, 1H), 1.31 (s, 9H); ^{13}C NMR (126 MHz, CD_2Cl_2) δ 170.2, 166.5, 154.6, 154.2, 153.8, 138.9, 132.9, 132.5, 132.0, 130.8, 130.7, 128.7, 127.6, 127.1, 125.8, 125.5, 122.7, 121.6, 105.7, 90.1, 81.5, 52.6, 49.9, 49.3, 35.1, 34.7, 31.2, 30.0; HRMS (+ESI) calcd. for [$C_{36}H_{35}N_4O_3Br$] ([M+H$^+$]): 651.1971, found: 651.1974; HPLC (ChiralPak IB column) 99:01 (hex/*i*PrOH) 1mL/min; t_{major} (23.3 min), t_{minor} (27.9 min); 89% ee.

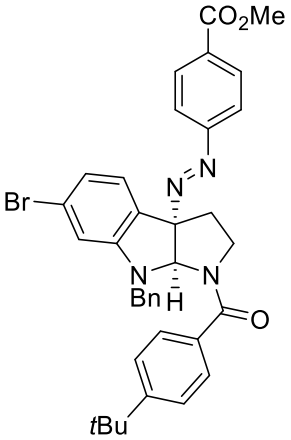

1.2o. Following the general procedure for phase-transfer diazenation, compound **1.2o** was isolated as a yellow solid (52% yield). ^{1}H NMR (500 MHz; CD_2Cl_2) δ 8.16 (d, *J* = 8.1 Hz, 2H), 7.84 – 7.70 (m, 2H), 7.51 – 7.23 (m, 9H), 7.14 (d, *J* = 7.8 Hz, 1H), 6.87 (s, 2H), 6.65 – 6.49 (m, 1H), 5.09 (s, 2H), 4.84 (d, *J* = 5.7 Hz, 1H), 4.07 – 3.78 (m, 4H), 3.66 (s, 1H), 2.57 (ddd, *J* = 24.4, 12.4, 7.0 Hz, 1H), 1.35 (s, 9H); ^{13}C NMR (126 MHz, CD_2Cl_2) δ 168.40, 166.15, 164.54, 130.43, 128.42, 127.26, 126.75, 122.36, 80.72, 53.89, 53.68, 53.46, 53.25, 53.03, 52.25, 49.47, 48.64, 34.75, 30.89; HRMS (+ESI) calcd. for [$C_{36}H_{35}BrN_4O_3$] ([M+H$^+$]): 459.2179, found: 459.2187; HPLC (ChiralPak IB column) 98:02 (hex/*i*PrOH) 1mL/min; t_{major} (36.1 min), t_{minor} (46.8 min); 92% ee.

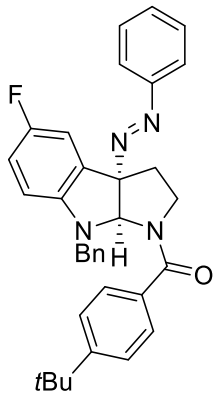

1.2p. Following the general procedure for phase-transfer diazenation, compound **1.2p** was isolated as a yellow solid (80% yield). ^{1}H NMR (500 MHz, CD_2Cl_2) δ 7.72 (dd, *J* = 6.5, 3.0 Hz, 2H), 7.52 – 7.08 (m, 12H), 7.01 (d, *J* = 7.9 Hz, 1H), 6.90 – 6.72 (m, 2H), 6.28 (dd, *J* = 8.7, 4.0 Hz, 1H), 4.82 (s, 2H), 3.84 (t, *J* = 9.7 Hz, 1H), 3.63 (dt, *J* = 17.5, 7.8 Hz, 1H), 2.54 (dt, *J* = 13.1, 5.6 Hz, 2H), 1.32 (d, *J* = 2.7 Hz, 9H); ^{13}C NMR (126 MHz, $CDCl_3$) δ 170.5, 165.1, 152.1, 148.3, 139.7, 131.7, 129.6, 128.7, 127.5, 127.3, 126.7, 125.7, 123.1, 117.2, 116.7, 116.5, 113.1, 112.9, 107.1, 88.7, 82.1, 51.0, 49.2, 37.2, 35.3, 31.5; HRMS (+ESI) calcd. for [$C_{34}H_{33}FN_4O$] ([M+H$^+$]): 533.2711, found: 533.2716; HPLC (ChiralPak IB column) 99:01 (hex/*i*PrOH) 1mL/min; t_{major} (46.4 min), t_{minor} (56.0 min); 86% ee.

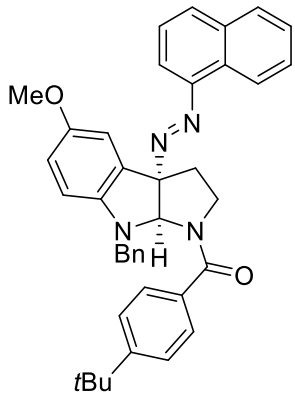

1.2q. Following the general procedure for phase-transfer diazenation, compound **1.2q** was isolated as a yellow solid (67% yield). ^{1}H NMR (500 MHz, Pyridine-d_5) δ 8.92 (d, *J* = 7.9 Hz, 1H), 8.00 (dd, *J* = 23.6, 8.0 Hz, 3H), 7.73 (m, 5H), 7.56 – 7.47 (m, 4H), 7.42 (s, 1H), 7.37 (s, 1H), 7.31 (q, *J* = 6.7, 5.9 Hz, 3H), 6.94 (d, *J* = 8.8 Hz, 1H), 6.58 (d, *J* = 8.6 Hz, 1H), 5.22 (s, 2H), 3.91 (t, *J* = 9.4 Hz, 1H), 3.72 (m, 4H), 2.87 – 2.74 (m, 1H), 2.68 (d, *J* = 9.9 Hz, 1H), 1.28 (s, 9H);^{13}C NMR (126 MHz, Pyridine-d_5) δ 171.1, 154.5, 154.3, 147.7, 147.0, 140.8, 136.8, 135.8, 135.3, 134.6, 132.5, 131.8, 130.1, 129.7, 129.5, 129.4, 129.4, 129.1, 127.9, 127.7, 126.7, 126.4, 116.7, 113.5, 113.3, 108.7, 90.7, 83.1, 51.9, 49.8, 37.8, 35.6, 32.8, 30.3; HRMS (+ESI) calcd. for [$C_{39}H_{38}N_4O_2$] ([M+H$^+$]): 595.3068, found: 595.3059; HPLC (ChiralPak IB column) 99:01 (hex/*i*PrOH) 1mL/min; t_{major} (35.3 min), t_{minor} (53.6 min); 88% ee.

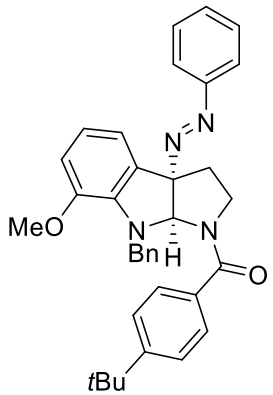

1.2r. Following the general procedure for phase-transfer diazenation, compound **1.2r** was isolated as a yellow solid (99% yield). ^{1}H NMR (500 MHz, pyridine-d_5) δ 8.26 (d, J = 8.2 Hz, 2H), 7.80 (d, J = 8.0 Hz, 2H), 7.71 (d, J = 7.6 Hz, 2H), 7.57 – 7.47 (m, 4H), 7.29 (m, 6H), 7.04 (d, J = 8.6 Hz, 1H), 6.92 (s, 1H), 5.08 (s, 2H) 3.84 (d, J = 2.4 Hz, 5H), 2.65 (s, 2H), 1.28 (d, J = 2.8 Hz, 9H); ^{13}C NMR (126 MHz, Pyridine-d_5) δ 171.0, 166.9, 155.0, 154.7, 153.8, 139.8, 134.2, 133.4, 131.6, 129.6, 128.8, 128.1, 128.1, 127.9, 126.9, 126.3, 123.6, 121.4, 110.6, 89.8, 81.8, 50.4, 49.6, 37.4, 35.6, 31.8, 30.7; HRMS (+ESI) calcd. for [$C_{35}H_{36}N_4O_2$] ([M+H$^+$]): 545.2911, found: 545.2922; HPLC (ChiralPak IB column) 98:02 (hex/*i*PrOH) 1mL/min; t_{major} (88.1 min), t_{minor} (114.9 min); 96% ee.

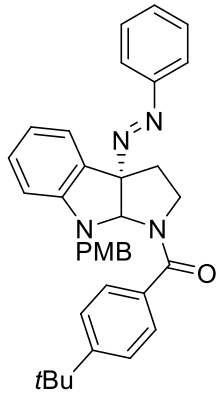

1.2s. Following the general procedure for phase-transfer diazenation, compound **1.2s** was isolated as a yellow solid (58% yield). ^{1}H NMR (500 MHz; CD_2Cl_2) δ 7.87 – 7.62 (m, 2H), 7.62 – 7.09 (m, 12H), 6.89 – 6.80 (m, 3H), 6.73 (t, J = 7.4 Hz, 1H), 6.50 (d, J = 7.9 Hz, 1H), 4.82 (d, J = 4.1 Hz, 2H), 3.78 (s, 4H), 3.61 (td, J = 11.5, 5.2 Hz, 1H), 2.71 – 2.46 (m, 2H); ^{13}C NMR (126 MHz, CD_2Cl_2) δ 170.4, 165.1, 159.2, 152.2, 151.9, 136.5, 131.8, 131.5, 130.7, 129.5, 128.8, 127.9, 127.3, 125.6, 123.0, 118.0, 114.2, 107.0, 89.1, 81.1, 55.7, 49.8, 49.1, 37.1, 30.2; HRMS (+ESI) calcd. for [$C_{31}H_{28}N_4O2$] ([M+H$^+$]): 489.2285, found: 489.2287; HPLC (ChiralPak IB column) 98:02 (hex/*i*PrOH) 1mL/min; t_{major} (22.0 min), t_{minor} (18.2 min); 90% ee.

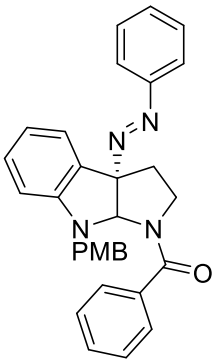

1.2t. Following the general procedure for phase-transfer diazenation, compound **1.2t** was isolated as a yellow solid (85% yield). ^{1}H NMR (500 MHz; CD_2Cl_2) δ 7.71 (d, *J* = 5.7 Hz, 2H), 7.50-7.30 (m, 10H), 7.29 (t, *J* = 7.1 Hz, 2H), 7.23 (t, *J* = 6.9 Hz, 2H), 7.13 (t, *J* = 7.0 Hz, 1H), 6.83 (s, 1H), 6.70 (t, *J* = 7.0 Hz, 1H), 6.41 (d, *J* = 7.5 Hz, 1H), 4.86-4.84 (m, 2H), 3.77-3.73 (m, 1H), 3.62-3.56 (m, 1H), 2.62-2.50 (m, 2H); ^{13}C NMR (126 MHz, CD_2Cl_2) δ 170.4, 165.1, 152.3, 151.9, 140.0, 136.5, 131.6, 130.7, 129.6, 129.5, 128.9, 128.7, 127.8, 127.4, 127.3, 125.6, 123.0, 118.0, 106.8, 89.1, 81.3, 50.3, 49.1, 37.1; HRMS (+ESI) calcd. for [$C_{30}H_{27}N_4O$] ([M+H$^+$]): 459.2179, found: 459.2187; HPLC (ChiralPak IB column) 98:02 (hex/*i*PrOH) 1mL/min; t_{major} (20.0 min), t_{minor} (17.3 min); 89% ee.

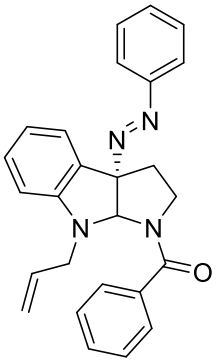

1.2u. Following the general procedure for phase-transfer diazenation, compound **1.2u** was isolated as a yellow film (98% yield). ^{1}H NMR (500 MHz; CD_2Cl_2) δ 7.73 (dd, *J* = 7.2, 2.4 Hz, 2H), 7.45 (ddt, *J* = 34.2, 13.5, 6.1 Hz, 8H), 7.18 (ddd, *J* = 20.0, 11.9, 7.3 Hz, 2H), 6.73 (s, 1H), 6.70 (t, *J* = 7.4 Hz, 1H), 6.50 (d, *J* = 7.9 Hz, 1H), 6.05 – 5.89 (m, 1H), 5.28 (dd, *J* = 17.2, 2.2 Hz, 1H), 5.14 (d, *J* = 10.2 Hz, 1H), 4.37 – 4.15 (m, 2H), 3.81 – 3.67 (m, 1H), 3.55 (td, *J* = 11.3, 6.1 Hz, 1H), 2.54 (qd, *J* = 11.7, 6.5 Hz, 2H); ^{13}C NMR (126 MHz, CD_2Cl_2) δ 170.4, 165.1, 152.3, 136.6, 130.8, 129.5, 128.8, 128.5, 127.9, 127.8, 125.4, 123.0, 117.9, 115.9, 107.1, 89.0, 81.3, 66.2, 49.2, 42.2, 36.9, 30.2; HRMS (+ESI) calcd. for [$C_{30}H_{27}N_4O$] ([M+H$^+$]): 409.2023, found: 409.2027; HPLC (ChiralPak IB column) 99:01 (hex/*i*PrOH) 1mL/min; t_{major} (13.2 min), t_{minor} (14.9 min); 69% ee.

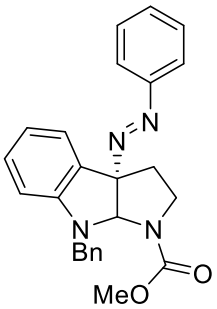

1.2v. Following the general procedure for the diazenation, compound **1.2v** was isolated as a yellow solid (85% yield). ^{1}H NMR (500 MHz; CD_2Cl_2): δ 7.72 (dd, *J* = 6.5, 3.0 Hz, 2H), 7.66-7.11 (m, 15H), 7.01 (d, *J* = 7.9 Hz, 1H), 6.92-6.77 (m, 2H), 6.41 (d, *J* = 7.5 Hz, 1H), 4.86-4.84 (m, 2H), 3.77-3.73 (m, 1H), 3.62-3.56 (m, 1H), 2.62-2.50 (m, 2H); ^{13}C NMR (126 MHz, CD_2Cl_2): δ 170.4, 165.1, 152.3, 151.9, 140.0, 136.5, 131.6, 130.7, 129.6, 128.9, 128.71, 127.8, 127.4, 127.3, 125.6, 123.0, 118.0, 106.8, 89.1, 81.3, 50.3, 49.1, 37.1 ppm; HRMS (+ESI) calcd. for [$C_{25}H_{24}N_4O_2$] ([M+H$^+$]): 413.1972, found: 413.1976; HPLC (ChiralPak IB column) 99:01 (hexane/*i*PrOH) 1mL/min; t_{major} (9.0 min), t_{minor} (8.0 min); 73% ee.

Procedure for photolysis reaction

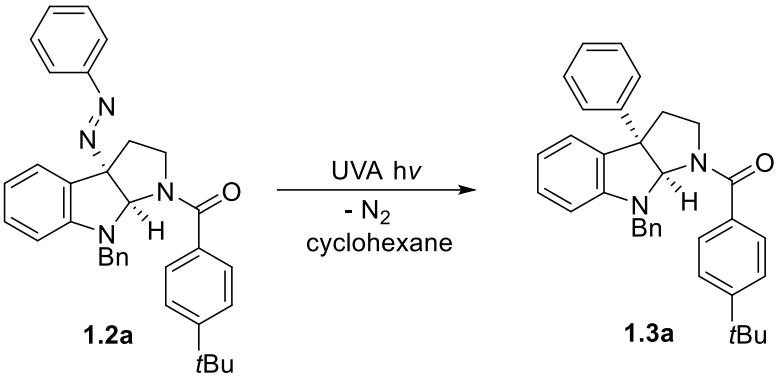

1.3a. **1.2a** (93% ee) (10 mg, 0.02 mmol) was dissolved cyclohexane (5 mL) in a 20 mL pyrex round-bottom flask, and sparged with nitrogen for 1 hour. The solvent was removed by rotary evaporation at elevated temperature (ca. 35 °C) to avoid freezing the cyclohexane. It is imperative that rapid rotation is maintained, as a widely-distributed, thin film is desired. The flask was backfilled with nitrogen and placed in a Rayonet photobox equiped with UVB spectrum bulbs for 12 h. NMR analysis using Toluene as an internal standard in CD_2Cl_2 indicated 78% conversion of starting material and 42% yield of the product. The product (**1.3a**) was difficult to separate from the starting diazene in good yield. Extension of the reaction times, followed by preparatory TLC, allowed for isolation of the product in 36% yield. ^{1}H NMR (400 MHz, CD_2Cl_2) δ 7.49 – 7.24 (m, 14H), 7.09 (td, *J* = 7.6, 1.3 Hz, 1H), 7.06 – 6.99 (d, 1H), 6.69 (t, *J* = 7.4 Hz, 1H), 6.50 – 6.37 (m, 2H), 5.00 – 4.63 (m, 2H), 3.90 – 3.73 (m, 1H), 3.59 – 3.37 (m, 1H), 2.69 – 2.52 (m, 2H), 1.36 (s, 9H); ^{13}C NMR (101 MHz, CD_2Cl_2) δ 170.09, 153.72, 150.12, 145.05, 139.38, 133.08, 132.96, 129.47, 128.59, 128.51, 128.33, 127.37, 127.00, 126.75, 125.61, 125.04, 123.85, 117.61, 115.20, 106.39, 85.35, 59.42, 49.43, 38.40, 34.72, 30.91; HRMS (+ESI) calcd. for [$C_{34}H_{34}N_2O$] ([M+H$^+$]): 487.2744, found: 287.2750; HPLC (ChiralPak IB column) 99.5:0.05 (hex/*i*PrOH) 0.5mL/min; t_{major} (9.0 min), t_{minor} (8.0 min); 93% ee.

Notes and references

(1) Ooi, T.; Maruoka, K. *Angew. Chem. Int. Ed.* **2007**, *46* (23), 4222.
(2) Dolling, U. H.; Davis, P.; Grabowski, E. J. J. *J. Am. Chem. Soc.* **1984**, *106* (2), 446.
(3) Hughes, D. L.; Dolling, U. H.; Ryan, K. M.; Schoenewaldt, E. F.; Grabowski, E. J. J. *J. Org. Chem.* **1987**, *52* (21), 4745.
(4) O'Donnell, M. J.; Bennett, W. D.; Wu, S. *J. Am. Chem. Soc.* **1989**, *111* (6), 2353.
(5) Corey, E. J.; Xu, F.; Noe, M. C. *J. Am. Chem. Soc.* **1997**, *119* (50), 12414.
(6) Lygo, B.; Wainwright, P. G. *Tetrahedron Lett.* **1997**, *38* (49), 8595.
(7) He, R.; Wang, X.; Hashimoto, T.; Maruoka, K. *Angew. Chem.* **2008**, *120* (49), 9608.
(8) Carter, C.; Fletcher, S.; Nelson, A. *Tetrahedron Asymmetry* **2003**, *14* (14), 1995.
(9) Hamilton, G. L.; Kanai, T.; Toste, F. D. *J. Am. Chem. Soc.* **2008**, *130* (45), 14984.
(10) Akiyama, T. WO2004096753, **2004**; *Chem. Abstr.* **2004**, *141*, 411087.
(11) Hoffmann, S.; Seayad, A. M.; List, B. *Angew. Chem. Int. Ed.* **2005**, *44* (45), 7424.
(12) Rauniyar, V.; Lackner, A. D.; Hamilton, G. L.; Toste, F. D. *Science* **2011**, *334* (6063), 1681.
(13) Wang, Y.-M.; Wu, J.; Hoong, C.; Rauniyar, V.; Toste, F. D. *J. Am. Chem. Soc.* **2012**, *134* (31), 12928.
(14) Neel, A. J.; Hehn, J. P.; Tripet, P. F.; Toste, F. D. *J. Am. Chem. Soc.* **2013**, *135* (38), 14044.
(15) Bredereck, K.; Karaca, S. *Tetrahedron Lett.* **1979**, *20* (39), 3711.
(16) Ellwood, M.; Griffiths, J.; Gregory, P. *J. Chem. Soc. Chem. Commun.* **1980**, No. 4, 181.
(17) Japp, F. R.; Klingemann, F. *Berichte Dtsch. Chem. Ges.* **1887**, *20* (2), 2942.
(18) Sakakura, T.; Tanaka, M. *J. Chem. Soc. Chem. Commun.* **1985**, No. 19, 1309.
(19) Garst, M. E.; Lukton, D. *Synth. Commun.* **1980**, *10* (2), 155.
(20) Movassaghi, M.; Ahmad, O. K.; Lathrop, S. P. *J. Am. Chem. Soc.* **2011**, *133* (33), 13002.
(21) Lathrop, S. P.; Movassaghi, M. *Chem. Sci.* **2013**, *5* (1), 333.
(22) Gottlieb, H. E.; Kotlyar, V.; Nudelman, A. *J. Org. Chem.* **1997**, *62* (21), 7512.
(23) Seayad, J.; Seayad, A. M.; List, B. *J. Am. Chem. Soc.* **2006**, *128* (4), 1086.
(24) Rauniyar, V.; Wang, Z. J.; Burks, H. E.; Toste, F. D. *J. Am. Chem. Soc.* **2011**, *133* (22), 8486.
(25) Romanov-Michailidis, F.; Romanova-Michaelides, M.; Pupier, M.; Alexakis, A. *Chem. – Eur. J.* **2015**, *21* (14), 5561.
(26) Čorić, I.; Müller, S.; List, B. *J. Am. Chem. Soc.* **2010**, *132* (49), 17370.
(27) Muratore, M. E.; Holloway, C. A.; Pilling, A. W.; Storer, R. I.; Trevitt, G.; Dixon, D. J. *J. Am. Chem. Soc.* **2009**, *131* (31), 10796.
(28) Kalinin, A. V.; Chauder, B. A.; Rakhit, S.; Snieckus, V. *Org. Lett.* **2003**, *5* (19), 3519.
(29) Zhang, P. Y.; Wan, S. B.; Ren, S. M.; Jiang, T. *Chin. Chem. Lett.* **2010**, *21* (11), 1307.
(30) Jin, H.; Zhang, P.; Bijian, K.; Ren, S.; Wan, S.; Alaoui-Jamali, M. A.; Jiang, T. *Mar. Drugs* **2013**, *11* (5), 1427.
(31) Somei, M.; Yamada, F.; Saida, Y. *HETEROCYCLES* **1986**, *24* (9), 2619.
(32) Skyler, D.; Heathcock, C. H. *Org. Lett.* **2001**, *3* (26), 4323.
(33) Bahr, J. L.; Yang, J.; Kosynkin, D. V.; Bronikowski, M. J.; Smalley, R. E.; Tour, J. M. *J. Am. Chem. Soc.* **2001**, *123* (27), 6536.
(34) Tang, Z.; Zhang, Y.; Wang, T.; Wang, W. *Synlett* **2010**, *2010* (05), 804.
(35) Bunnett, J. F.; Takayama, H. *J. Org. Chem.* **1968**, *33* (5), 1924.

(36) Masllorens, J.; Moreno-Mañas, M.; Pla-Quintana, A.; Roglans, A. *Org. Lett.* **2003**, *5* (9), 1559.
(37) Yang, H.-H.; McCreery, R. L. *Anal. Chem.* **1999**, *71* (18), 4081.
(38) Korzeniowski, S. H.; Leopold, A.; Beadle, J. R.; Ahern, M. F.; Sheppard, W. A.; Khanna, R. K.; Gokel, G. W. *J. Org. Chem.* **1981**, *46* (10), 2153.
(39) Gosselin, F.; Lau, S.; Nadeau, C.; Trinh, T.; O'Shea, P. D.; Davies, I. W. *J. Org. Chem.* **2009**, *74* (20), 7790.

NMR Spectra

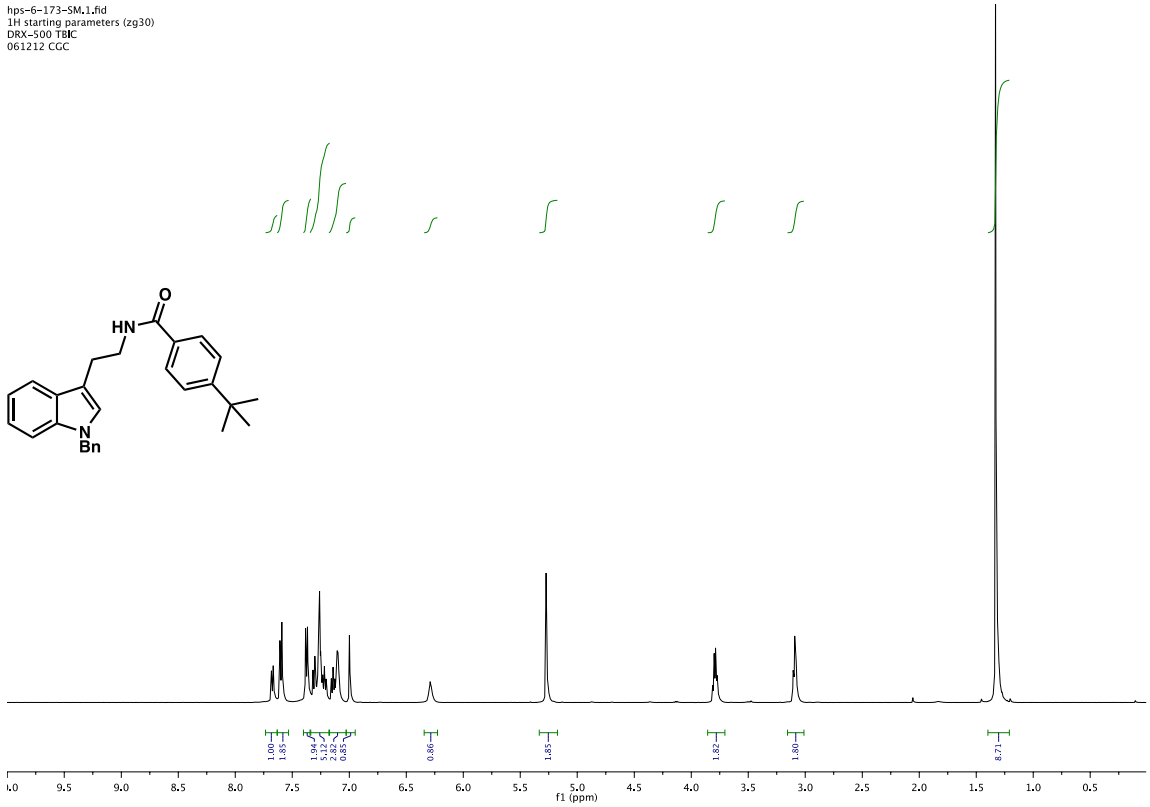

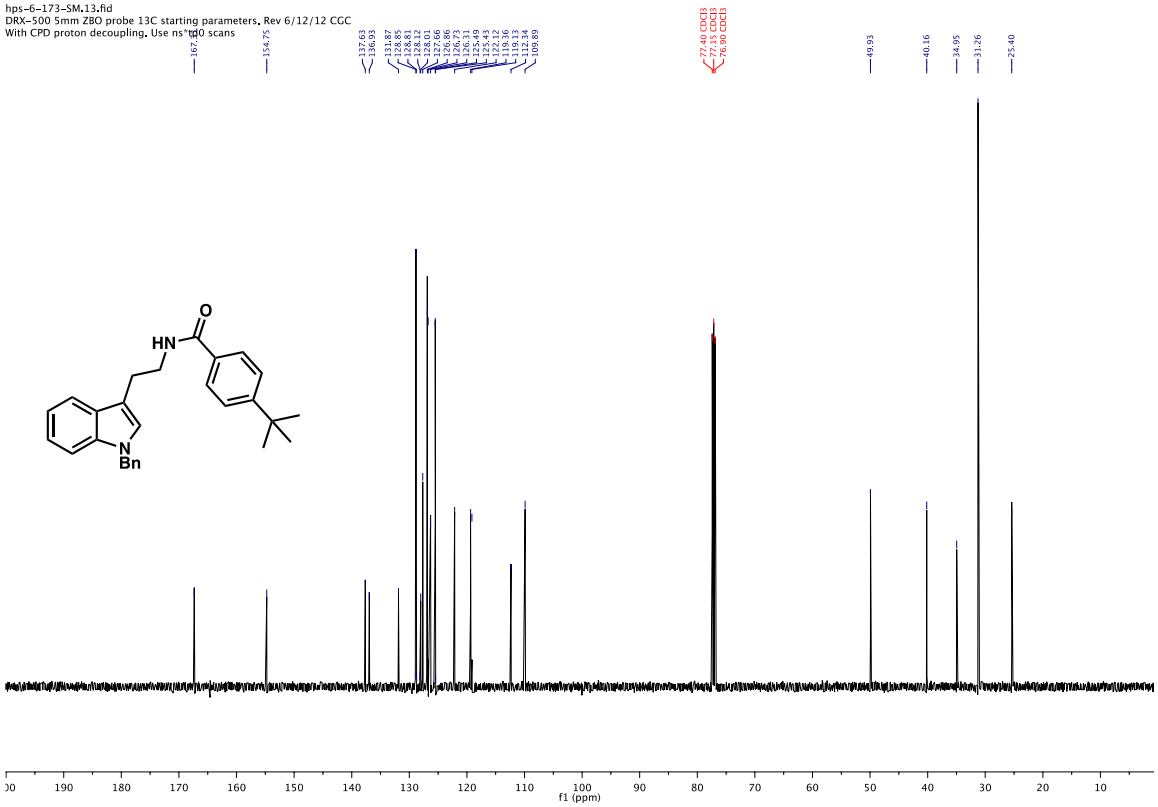
hps-6-173-SM.13.fid
DRX-500 5mm ZBO probe 13C starting parameters, Rev 6/12/12 CGC
With CPD proton decoupling. Use ns*td0 scans
167.42
154.75
137.63
136.93
131.87
128.85
128.83
128.12
128.01
127.66
127.60
126.73
126.31
125.49
125.43
122.12
119.66
119.13
112.34
109.89
77.40 CDCl3
77.15 CDCl3
76.90 CDCl3
49.93
40.16
34.95
31.26
25.40
HN
O
N
Bn
f1 (ppm)

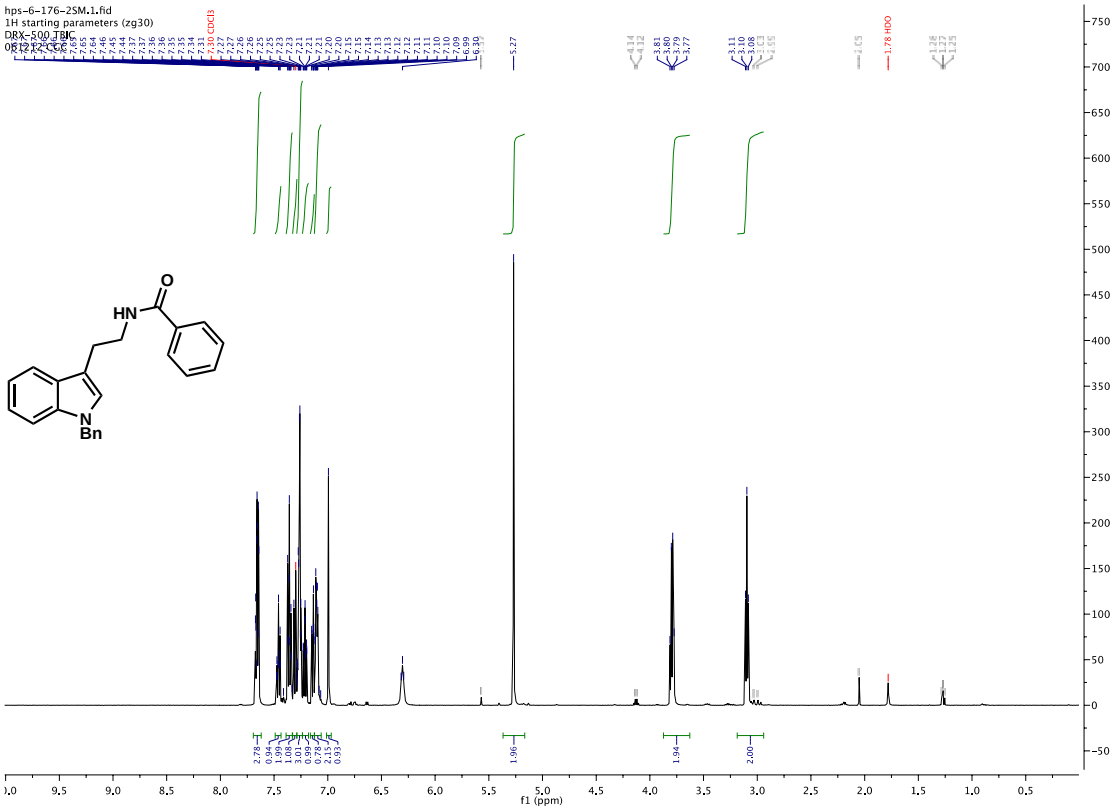
hps-6-176-2SM.1.fid
1H starting parameters (zg30)
DRX-500 TBIC
08/12/12 CGC
HN
O
N
Bn
f1 (ppm)

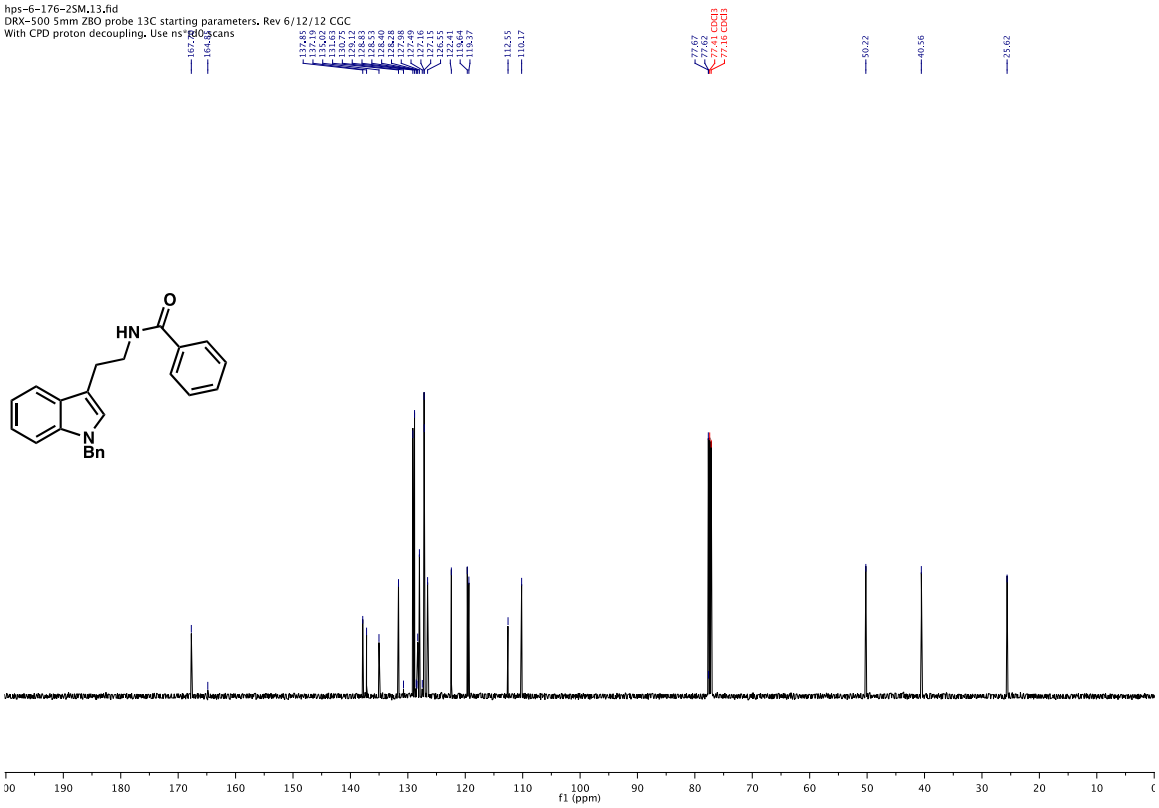
hps-6-176-2SM.13.fid
DRX-500 5mm ZBO probe 13C starting parameters. Rev 6/12/12 CGC
With CPD proton decoupling. Use ns* for scans
HN
O
N
Bn
f1 (ppm)

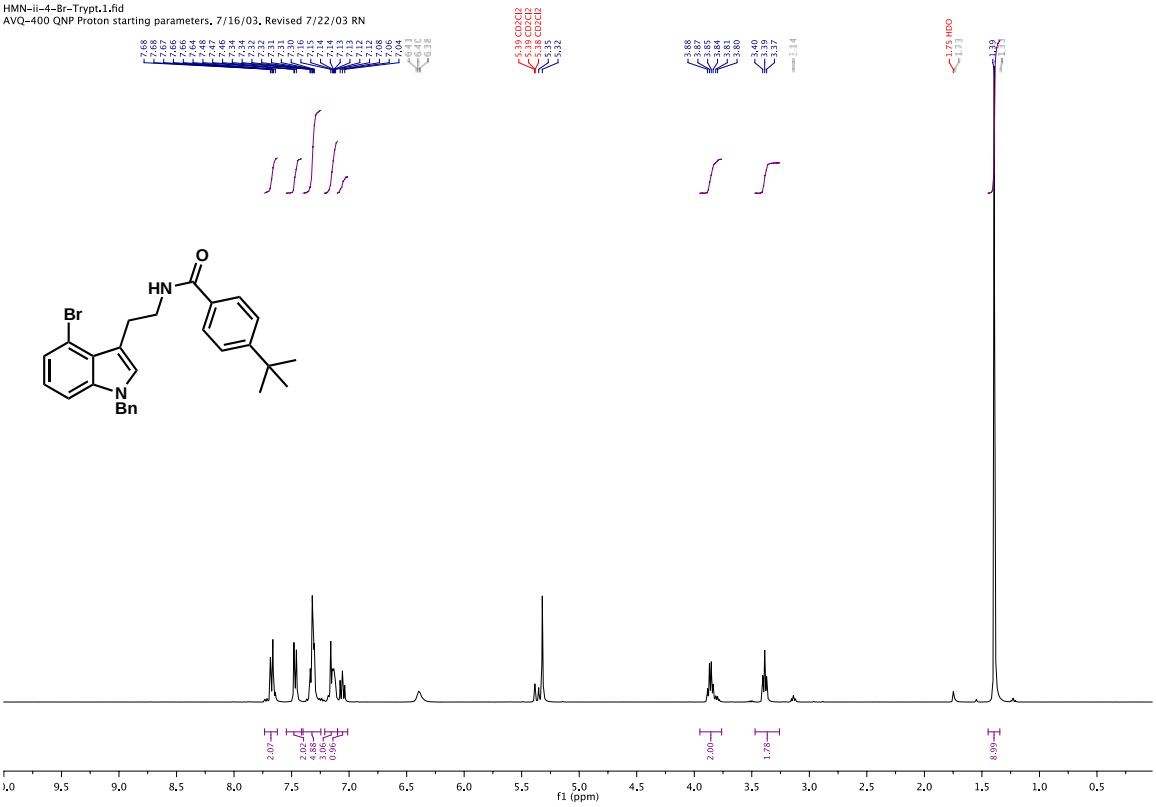
HMN-ii-4-Br-Trypt.1.fid
AVQ-400 QNP Proton starting parameters. 7/16/03. Revised 7/22/03 RN
f1 (ppm)

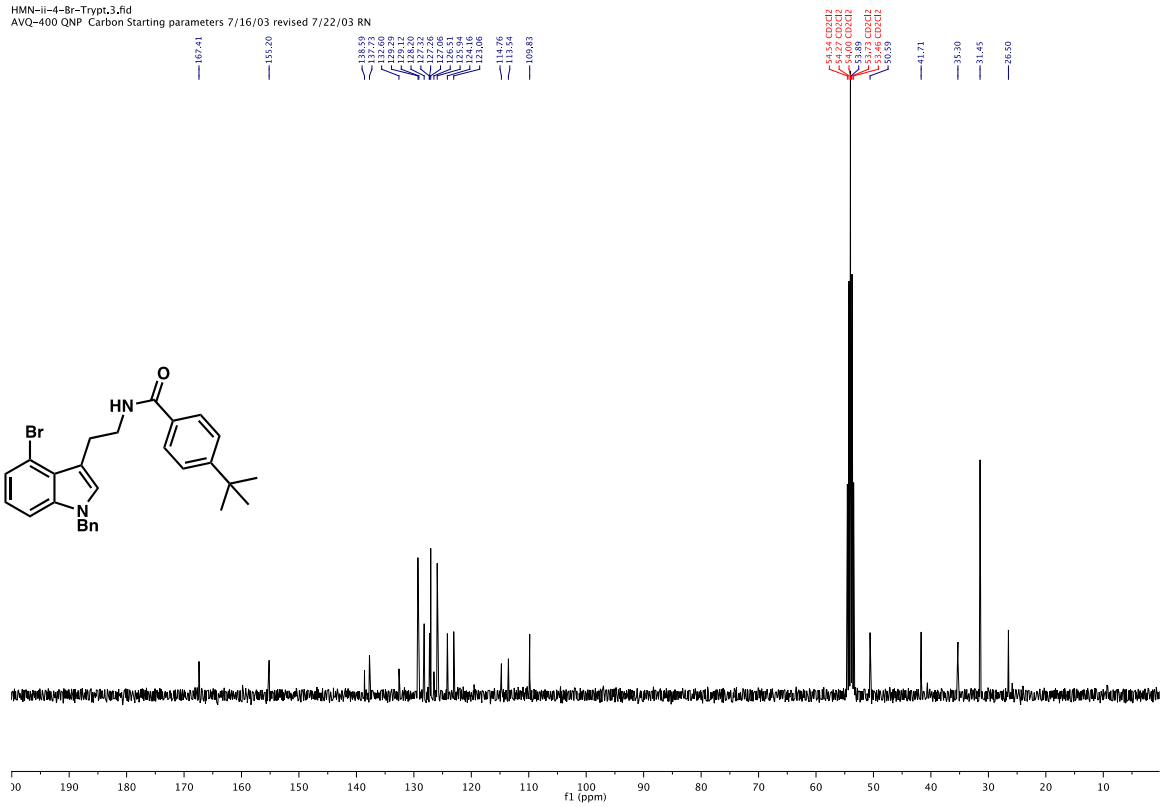
HMN-ii-4-Br-Trypt.3.fid
AVQ-400 QNP Carbon Starting parameters 7/16/03 revised 7/22/03 RN
f1 (ppm)

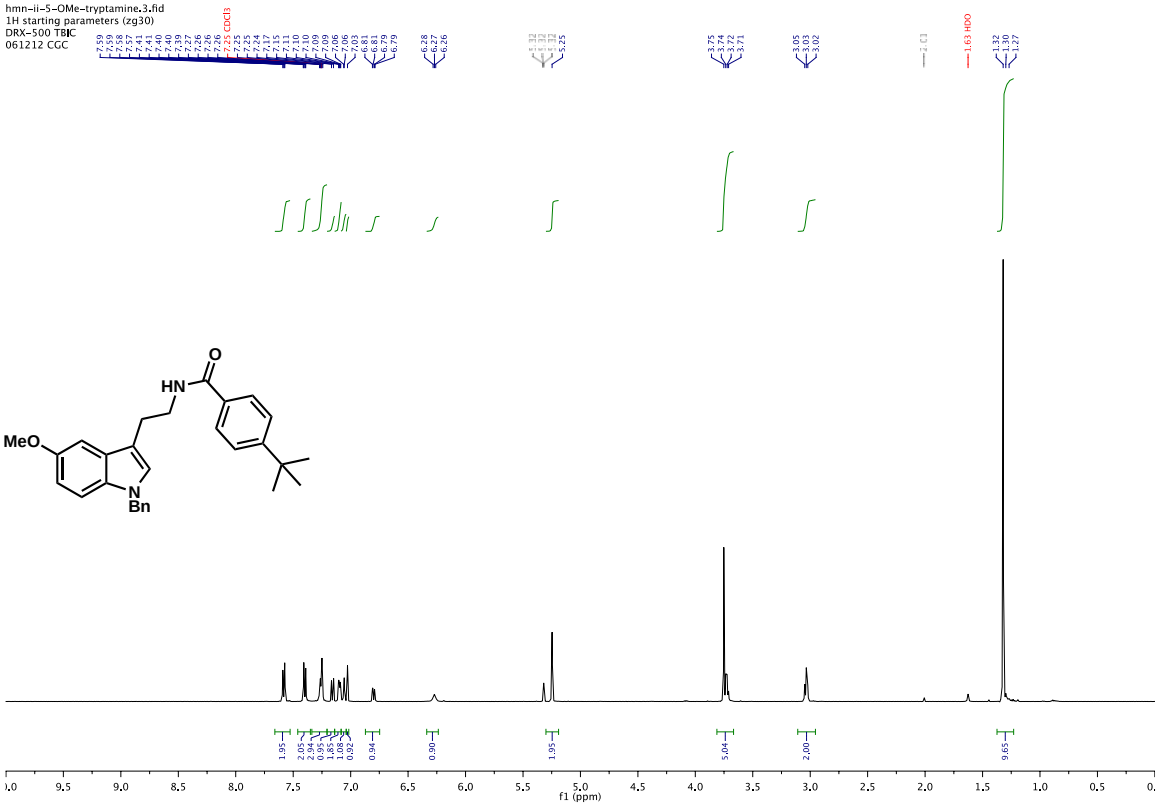
hmn-ii-5-OMe-tryptamine.3.fid
1H starting parameters (zg30)
DRX-500 TBIC
061212 CGC
7.26 CDCl3
1.63 H2O
2 C1
MeO
HN
O
N
Bn
f1 (ppm)

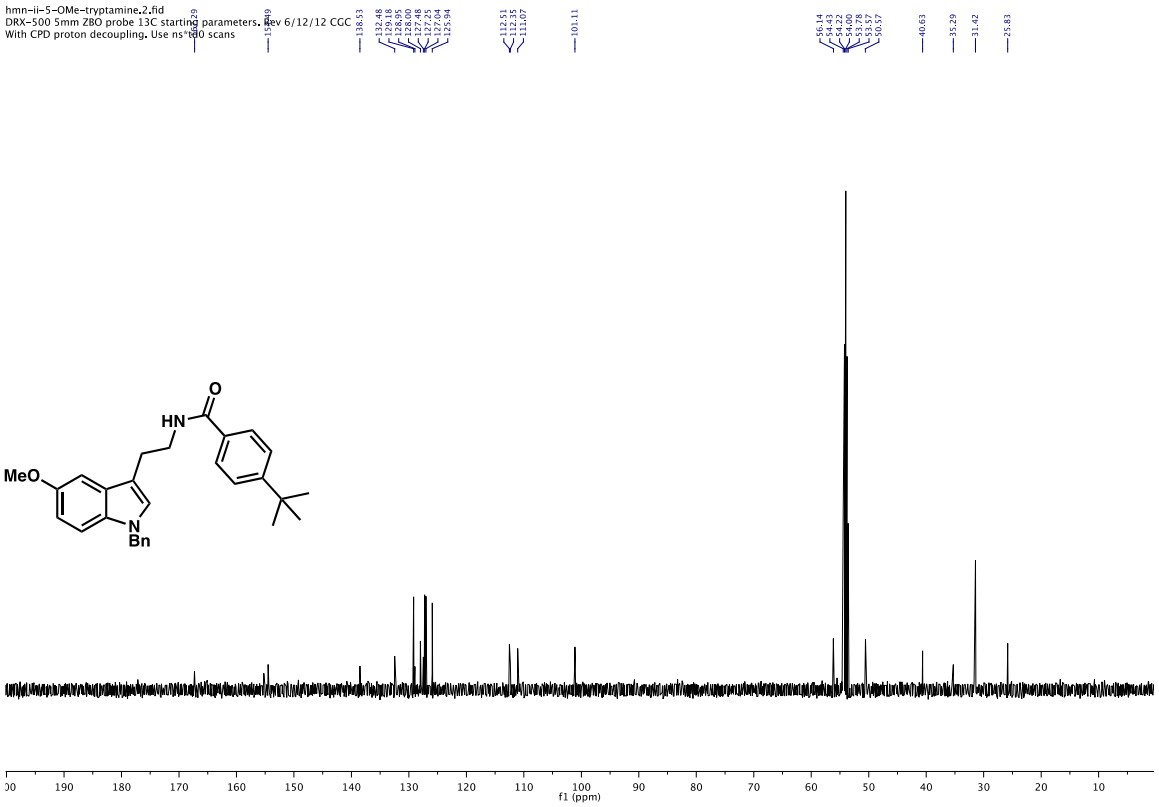
hmn-ii-5-OMe-tryptamine.2.fid
DRX-500 5mm ZBO probe 13C starting parameters. Rev 6/12/12 CGC
With CPD proton decoupling. Use ns*fid0 scans
MeO
HN
O
N
Bn
f1 (ppm)

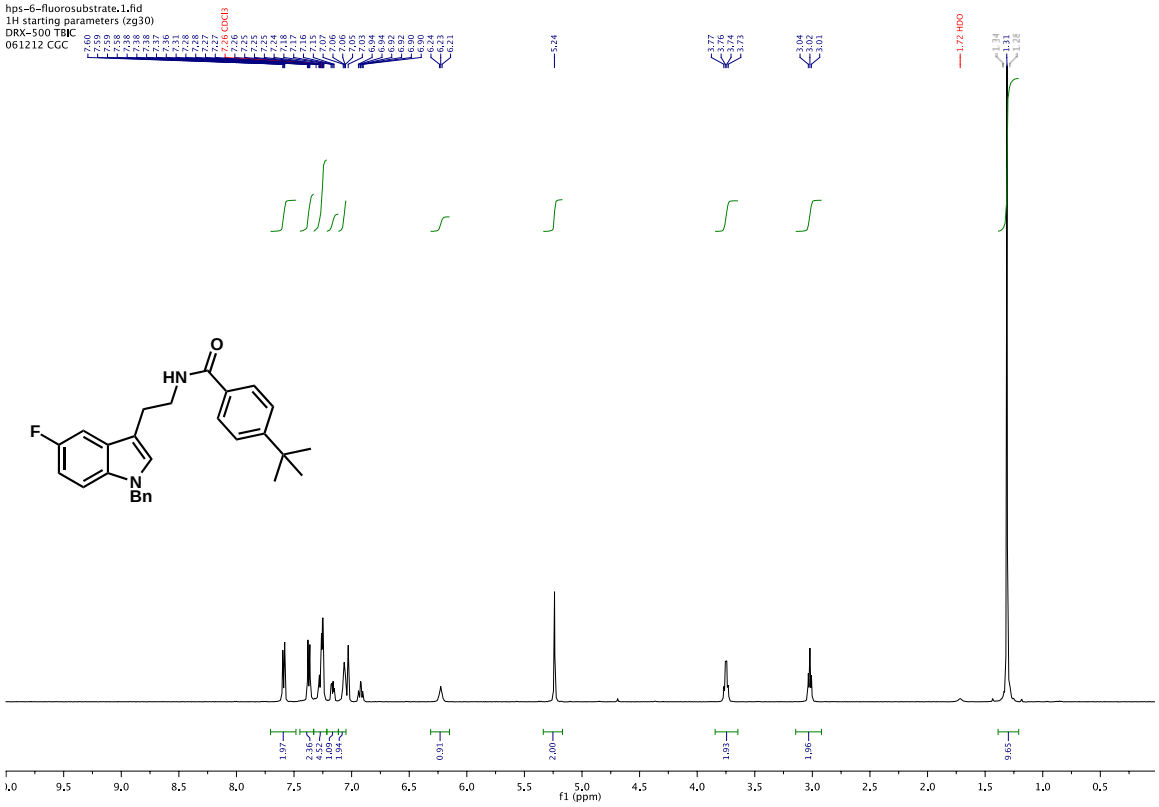
hps-6-fluorosubstrate.1.fid
1H starting parameters (zg30)
DRX-500 TBIC
061212 CGC
7.26 CDCl3
5.24
3.77
3.76
3.74
3.73
3.04
3.02
3.01
1.72 HDO
1.34
1.31
1.28
1.97
2.36
4.52
1.09
1.94
0.91
2.00
1.93
1.96
9.65
f1 (ppm)

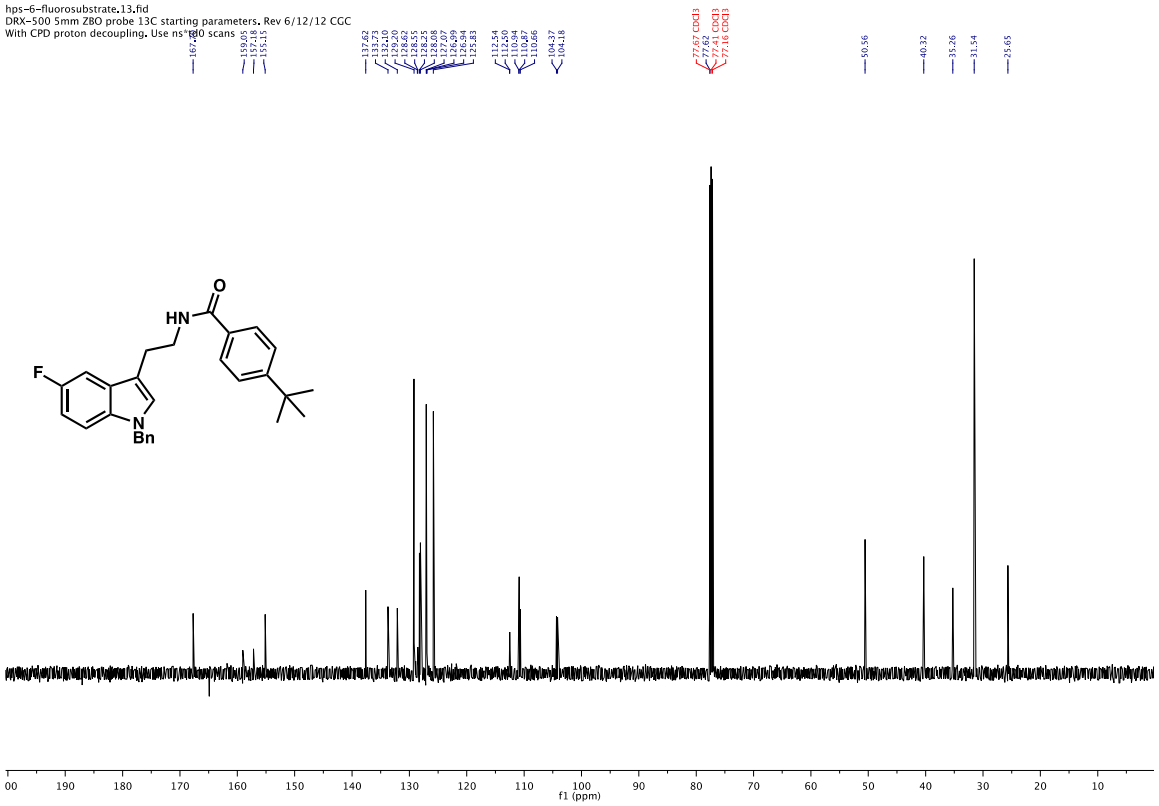
hps-6-fluorosubstrate.13.fid
DRX-500 5mm ZBO probe 13C starting parameters. Rev 6/12/12 CGC
With CPD proton decoupling. Use ns*80 scans
167.40
159.05
157.14
155.15
137.62
133.73
132.10
132.20
129.62
128.55
128.25
126.08
127.07
126.49
126.04
125.83
112.54
112.05
110.94
110.87
110.66
104.37
104.18
77.67 CDCl3
77.62
77.41 CDCl3
77.16 CDCl3
50.56
40.32
35.26
31.54
25.65
f1 (ppm)

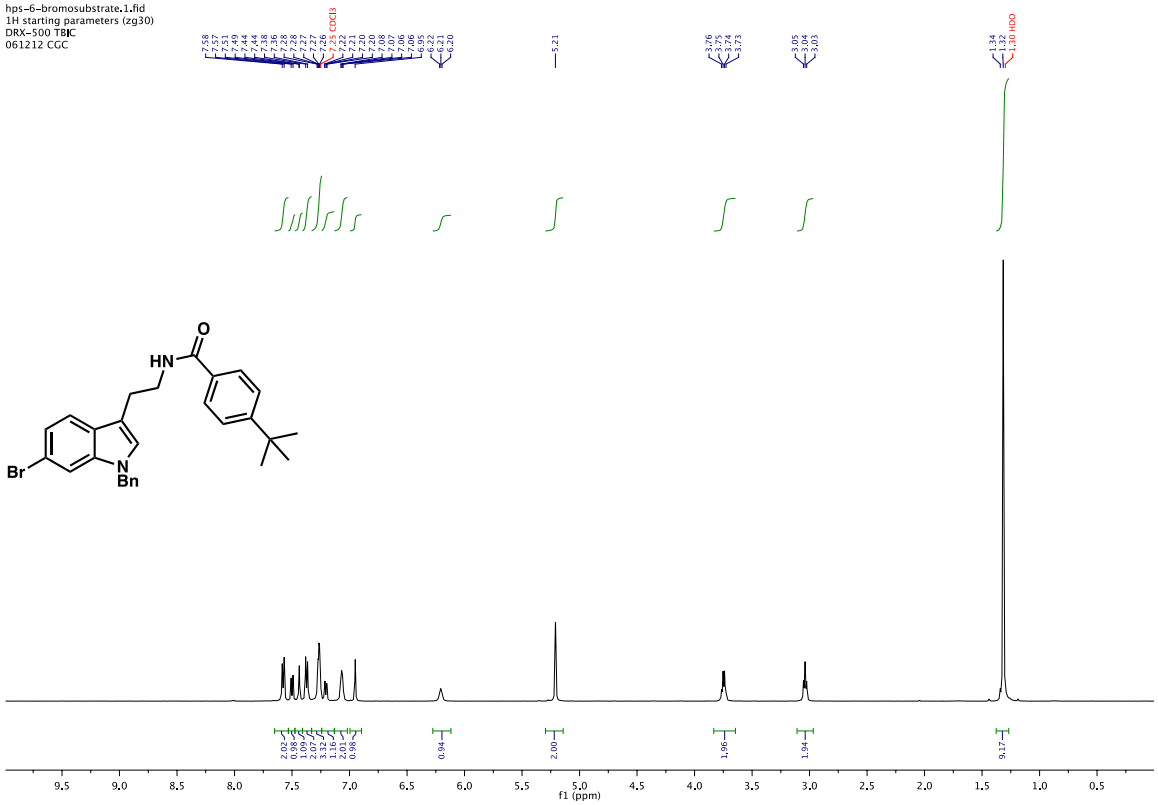
hps-6-bromosubstrate.1.fid
1H starting parameters (zg30)
DRX-500 TBIC
061212 CGC
7.25 CDCl3
1.30 H2O
f1 (ppm)

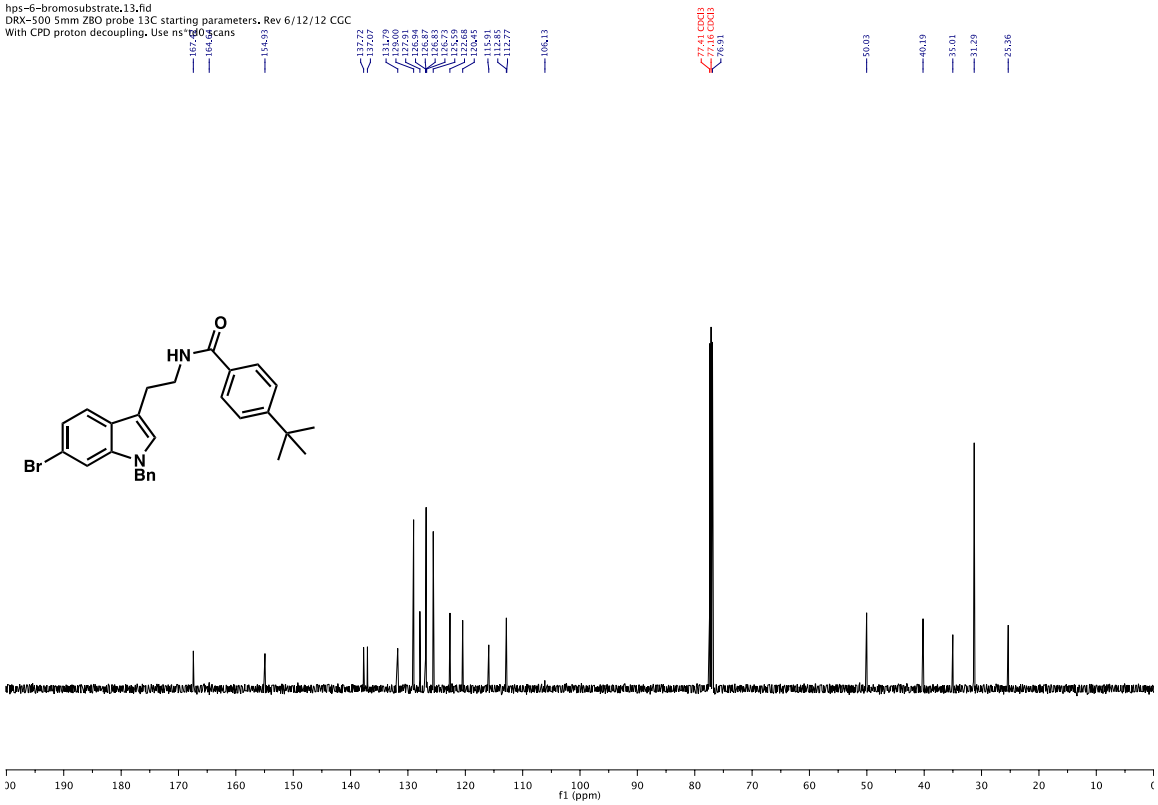
hps-6-bromosubstrate.13.fid
DRX-500 5mm ZBO probe 13C starting parameters. Rev 6/12/12 CGC
With CPD proton decoupling. Use ns*td0 scans
77.41 CDCl3
77.16 CDCl3
f1 (ppm)

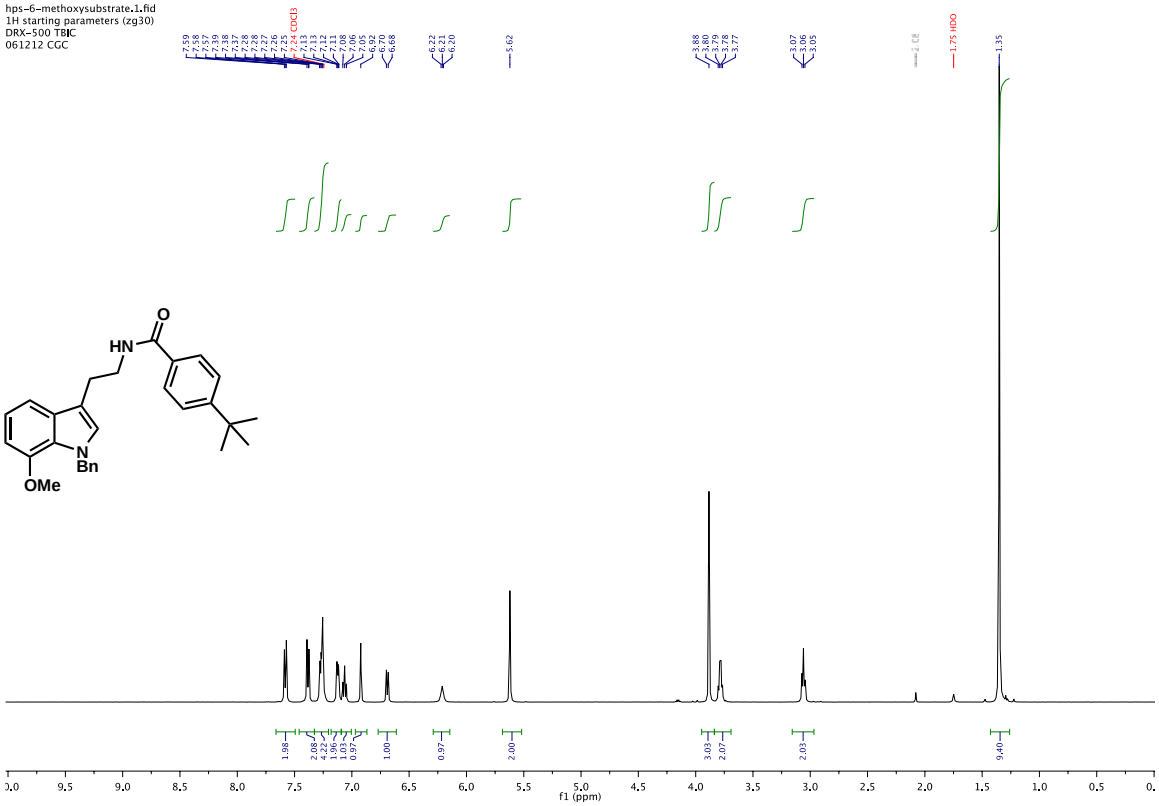
hps-6-methoxysubstrate.1.fid
1H starting parameters (zg30)
DRX-500 TBIC
061212 CGC
7.59
7.58
7.57
7.39
7.38
7.37
7.28
7.27
7.26
7.25
7.24 CDCl3
7.13
7.12
7.11
7.08
7.06
7.05
6.92
6.70
6.68
6.22
6.21
6.20
5.62
3.88
3.80
3.79
3.78
3.77
3.07
3.06
3.05
2.07
1.75 H2O
1.35
HN
O
N
Bn
OMe
1.98
2.08
4.22
1.96
1.03
0.97
1.00
0.97
2.00
3.03
2.07
2.03
9.40
f1 (ppm)

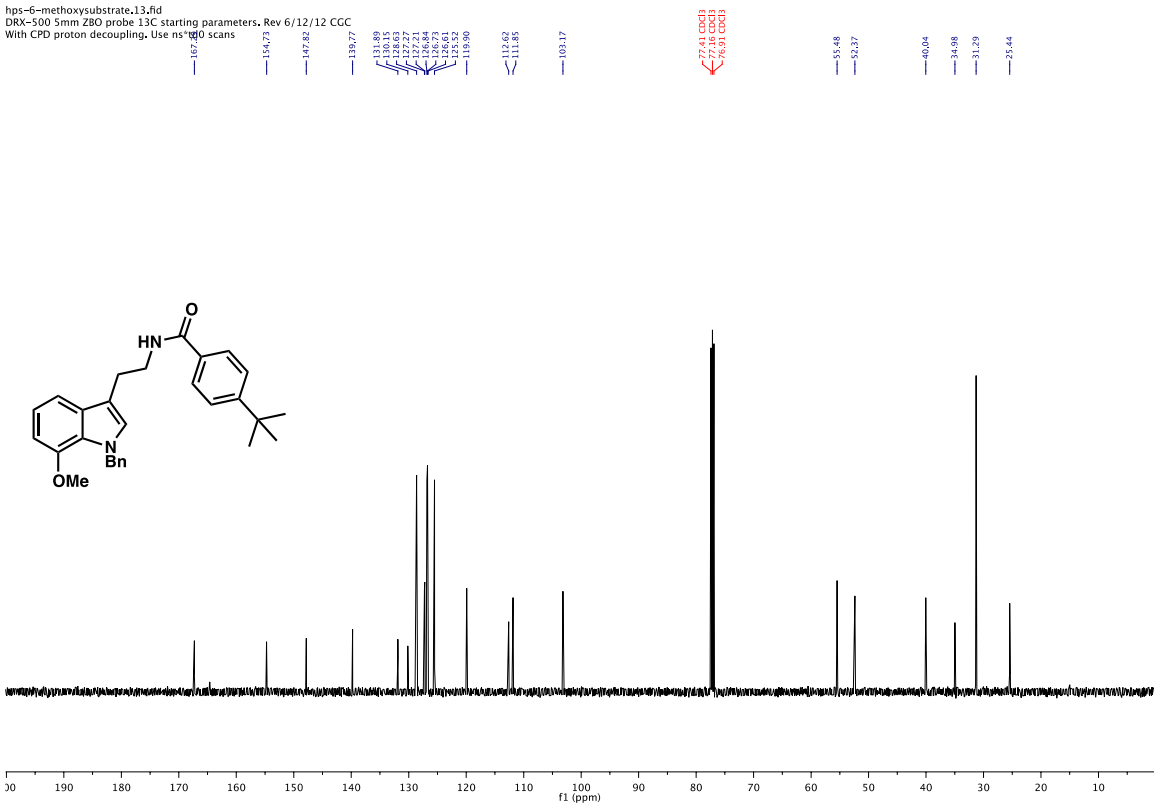
hps-6-methoxysubstrate.13.fid
DRX-500 5mm ZBO probe 13C starting parameters. Rev 6/12/12 CGC
With CPD proton decoupling. Use ns=800 scans
167.88
154.73
147.82
139.77
131.89
130.15
128.63
127.27
127.21
126.84
126.79
126.61
125.52
119.90
112.62
111.85
103.17
77.41 CDCl3
77.16 CDCl3
76.91 CDCl3
55.48
52.37
40.04
34.98
31.29
25.44
HN
O
N
Bn
OMe
f1 (ppm)

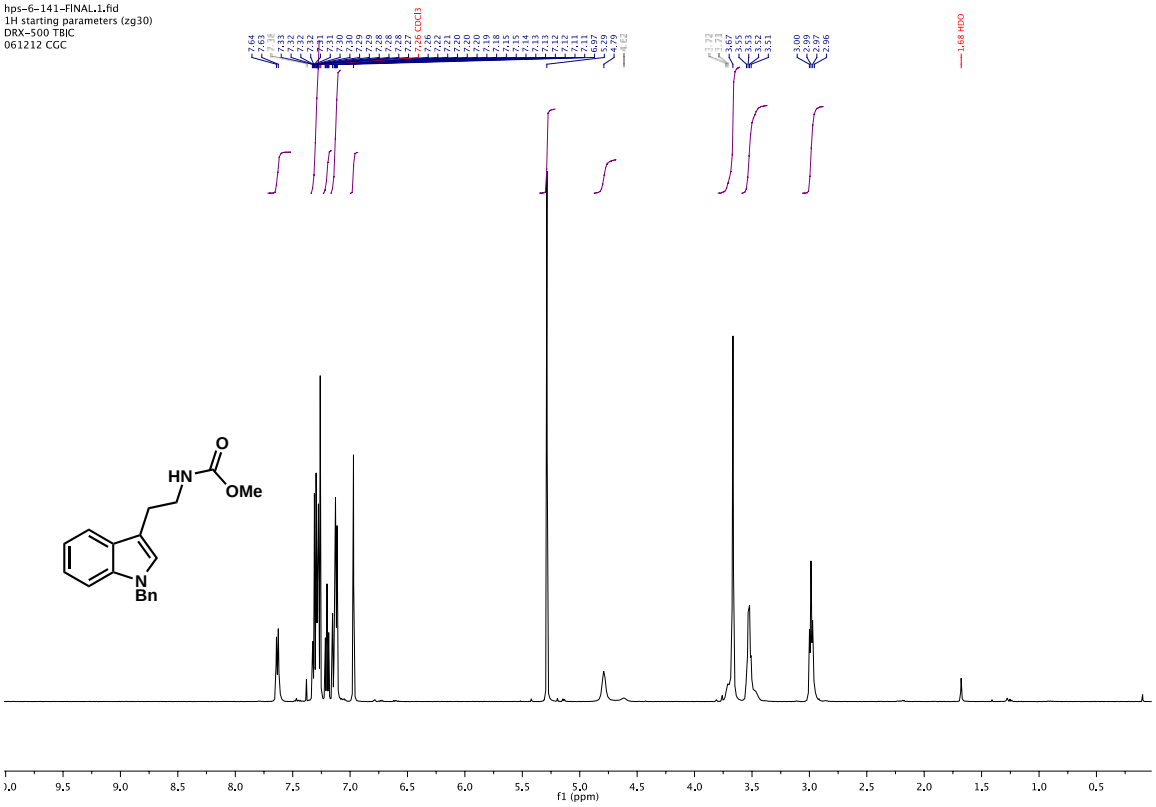
hps-6-141-FINAL.1.fid
1H starting parameters (zg30)
DRX-500 TBIC
061212 CGC
7.26 CDCl3
1.68 H2O
HN
O
OMe
N
Bn
f1 (ppm)

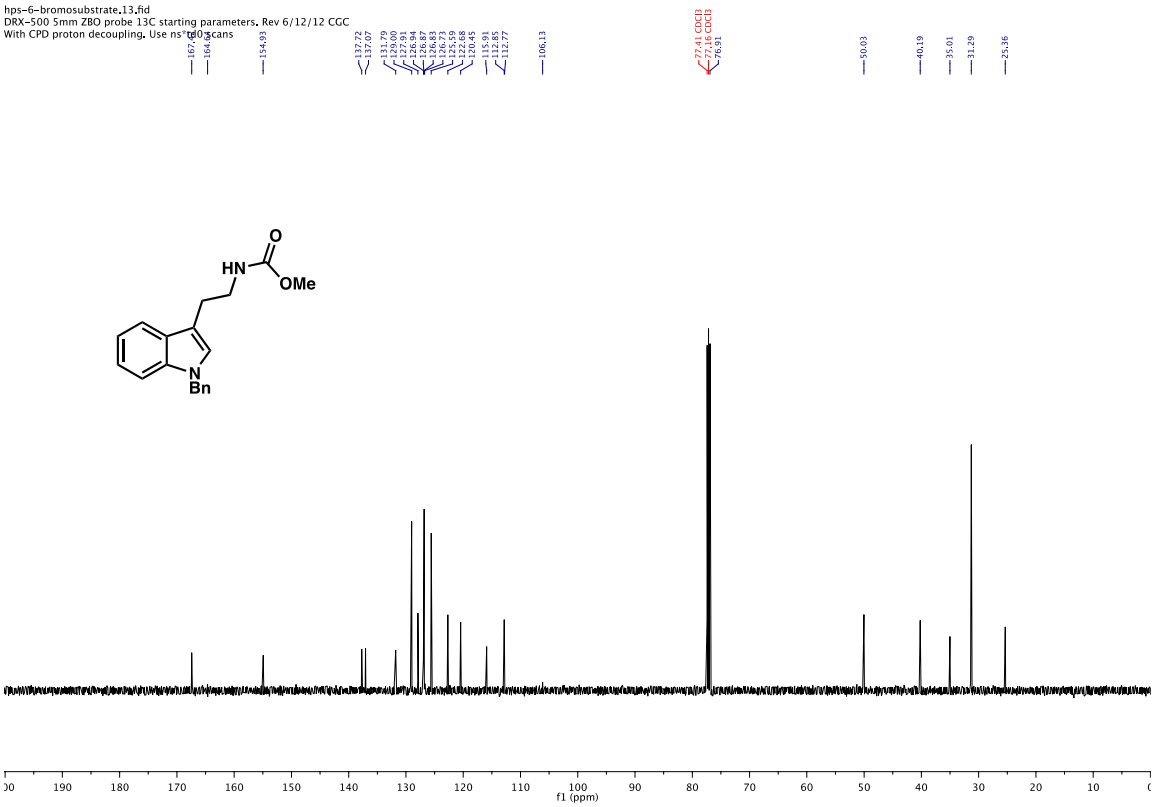
hps-6-bromosubstrate.13.fid
DRX-500 5mm ZBO probe 13C starting parameters. Rev 6/12/12 CGC
With CPD proton decoupling. Use ns*td0 scans
77.41 CDCl3
77.16 CDCl3
76.91
HN
O
OMe
N
Bn
f1 (ppm)

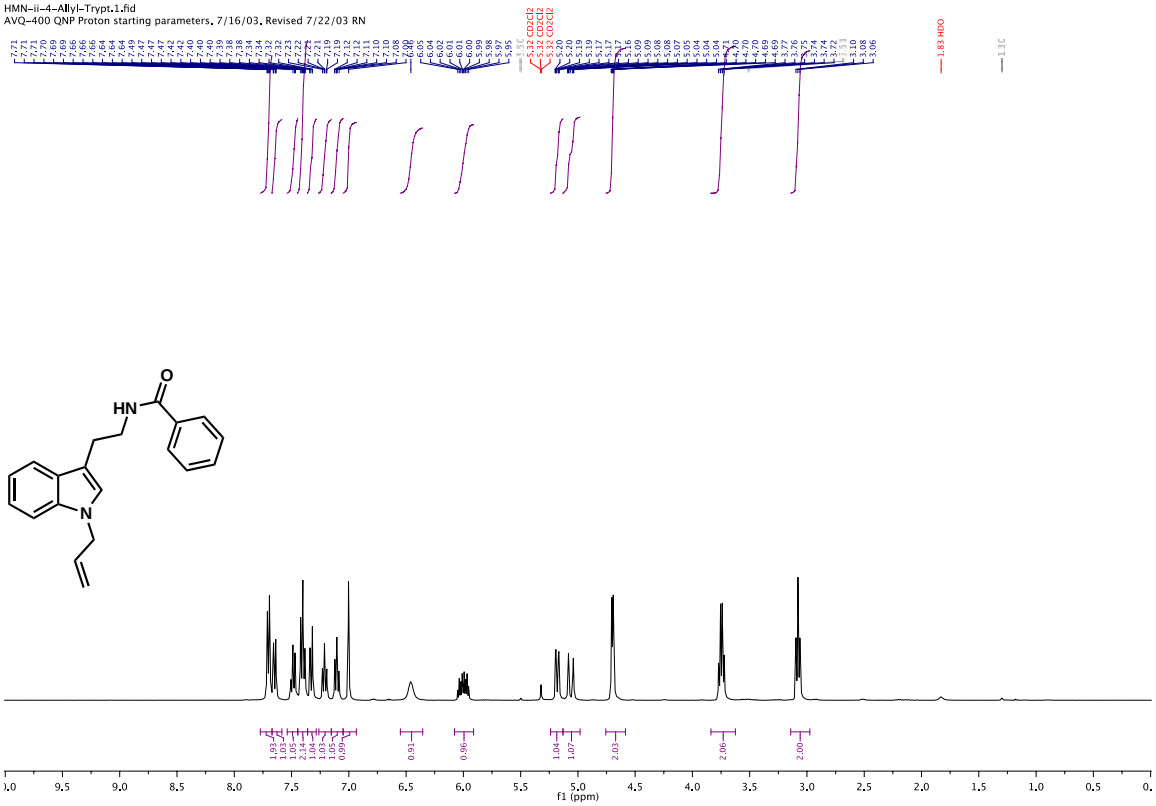
HMN-ii-4-Allyl-Trypt.1.fid
AVQ-400 QNP Proton starting parameters. 7/16/03. Revised 7/22/03 RN
1.83 HDO
f1 (ppm)

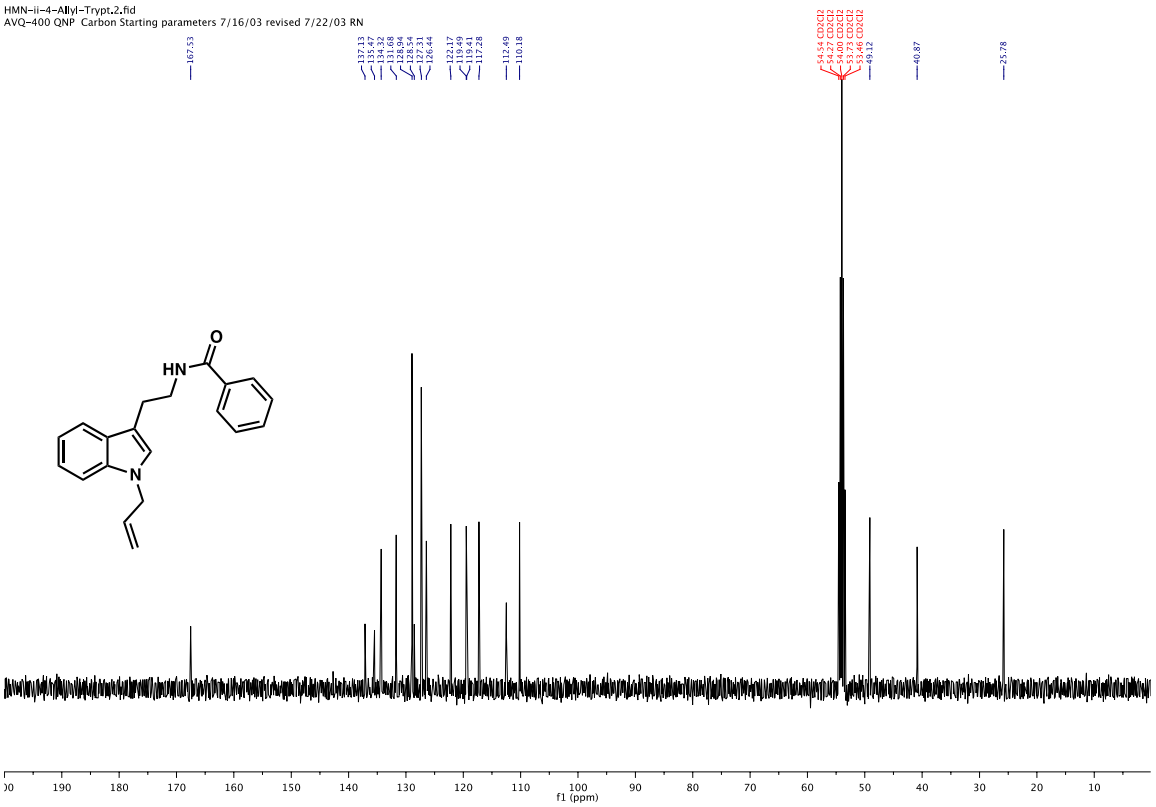
HMN-ii-4-Allyl-Trypt.2.fid
AVQ-400 QNP Carbon Starting parameters 7/16/03 revised 7/22/03 RN
167.53
137.13
135.47
134.32
131.68
128.94
128.54
127.31
126.44
122.17
119.49
119.41
117.28
112.49
110.18
54.54 CD2Cl2
54.27 CD2Cl2
54.00 CD2Cl2
53.73 CD2Cl2
53.46 CD2Cl2
49.12
40.87
25.78
f1 (ppm)

HMN-ii-4-PMB-Trypt.1.fid
AVQ-400 QNP Proton starting parameters. 7/16/03. Revised 7/22/03 RN

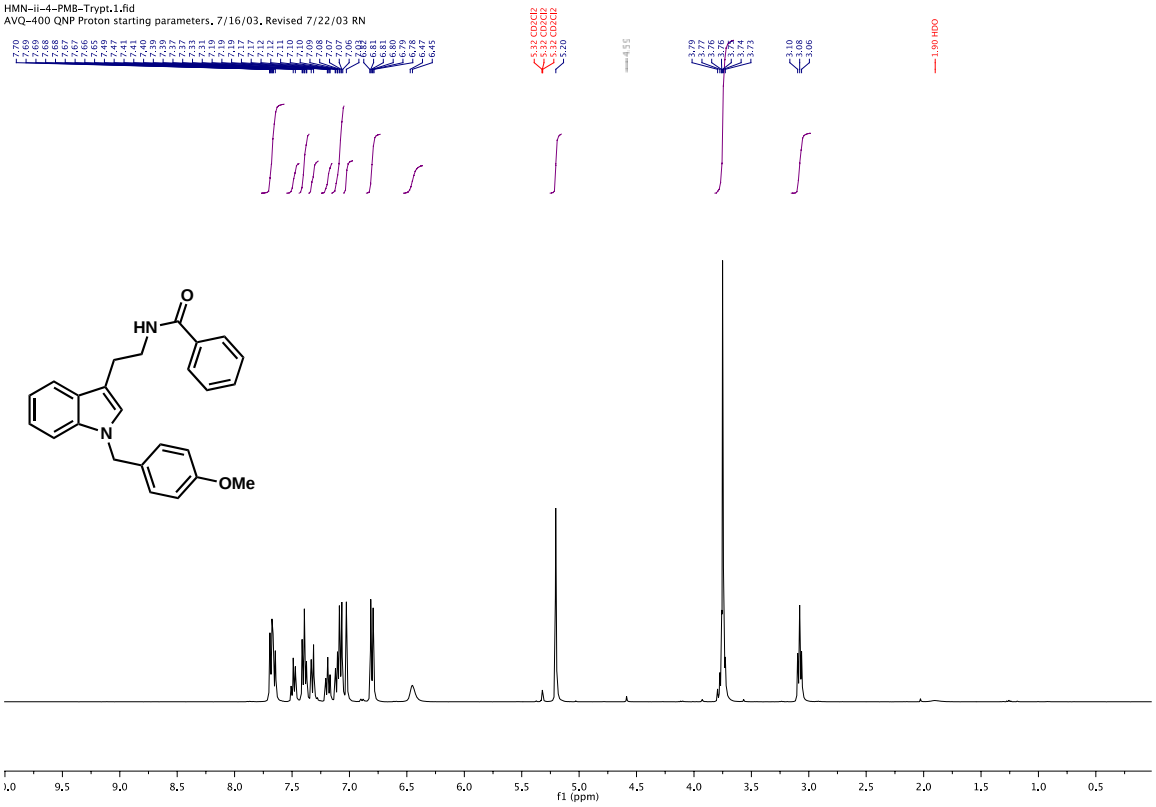

HMN-ii-4-PMB-Trypt.2.fid
AVQ-400 QNP Carbon Starting parameters 7/16/03 revised 7/22/03 RN

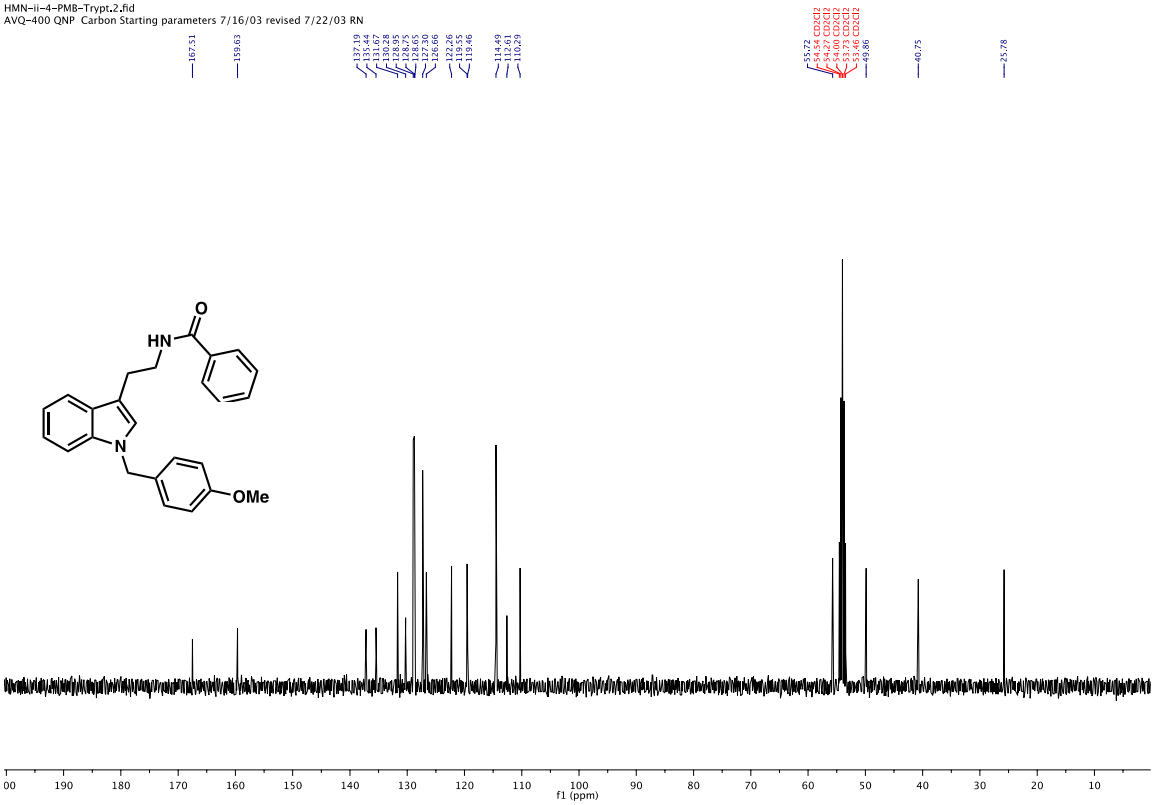

hps-6-183-3.1.fid
1H starting parameters (zg30)
DRX-500 TBIC
061212 CGC

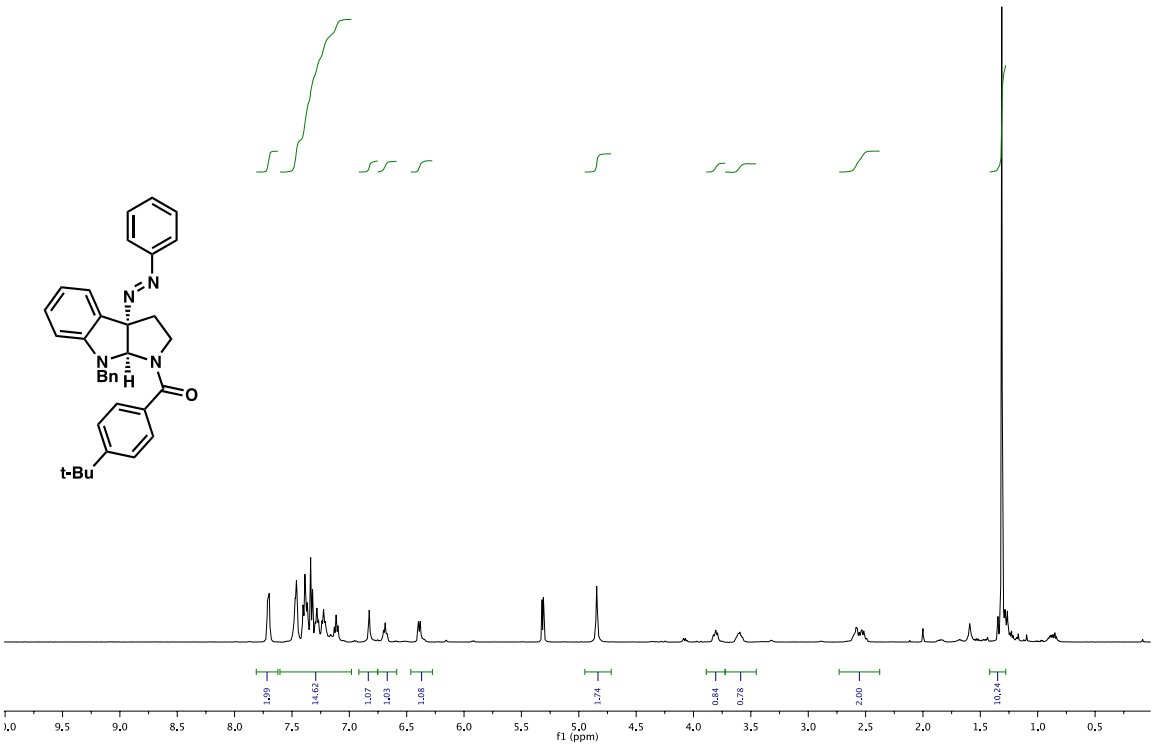

hps-6-183-3.13.fid
DRX-500 5mm ZBO probe 13C starting parameters. Rev 6/12/12 CGC
With CPD proton decoupling. Use ns*td0 scans

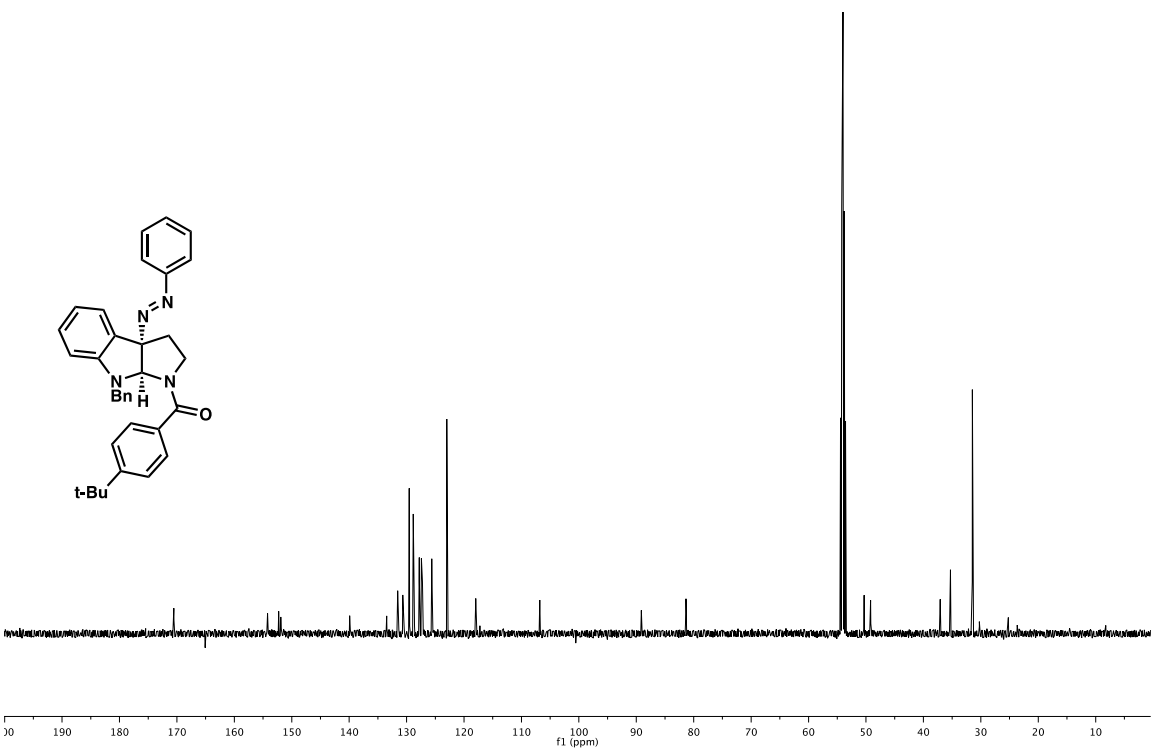

hps-6-183-2.1.fid
1H starting parameters (zg30)
DRX-500 TBIC
061212 CGC

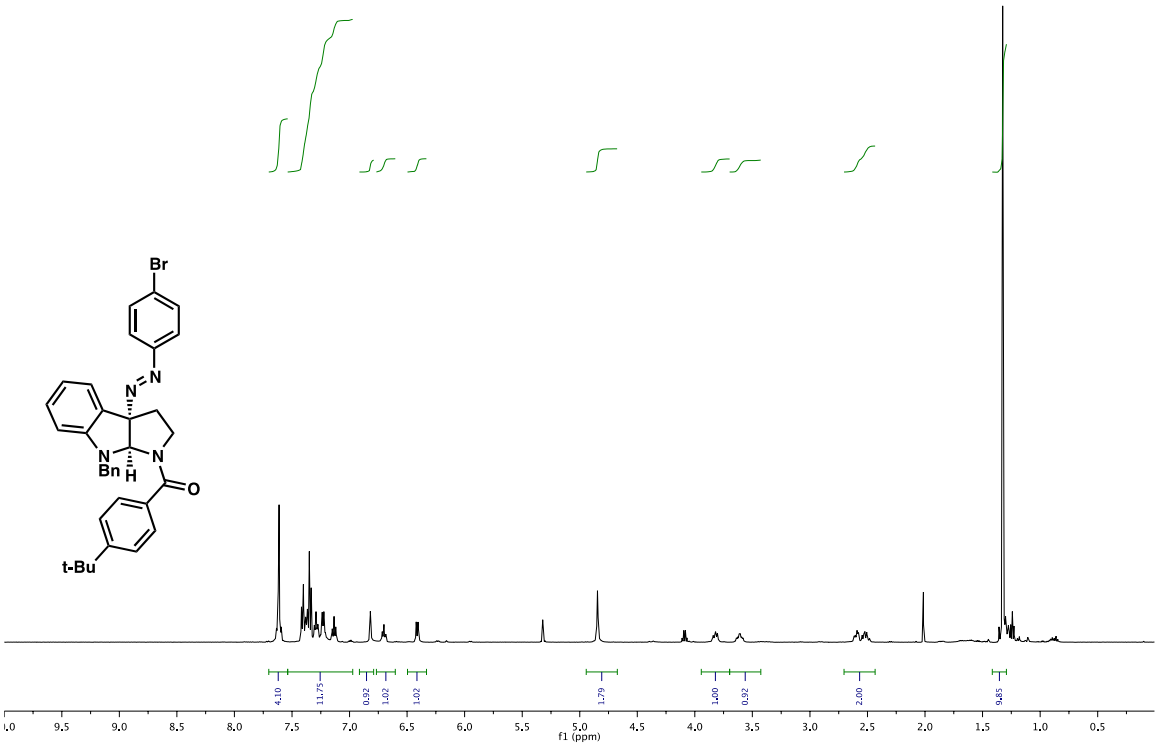

hps-6-183-2.13.fid
DRX-500 5mm ZBO probe 13C starting parameters, RG 2/12/12 CGC
With CPD proton decoupling. Use zgpg*td0 scans

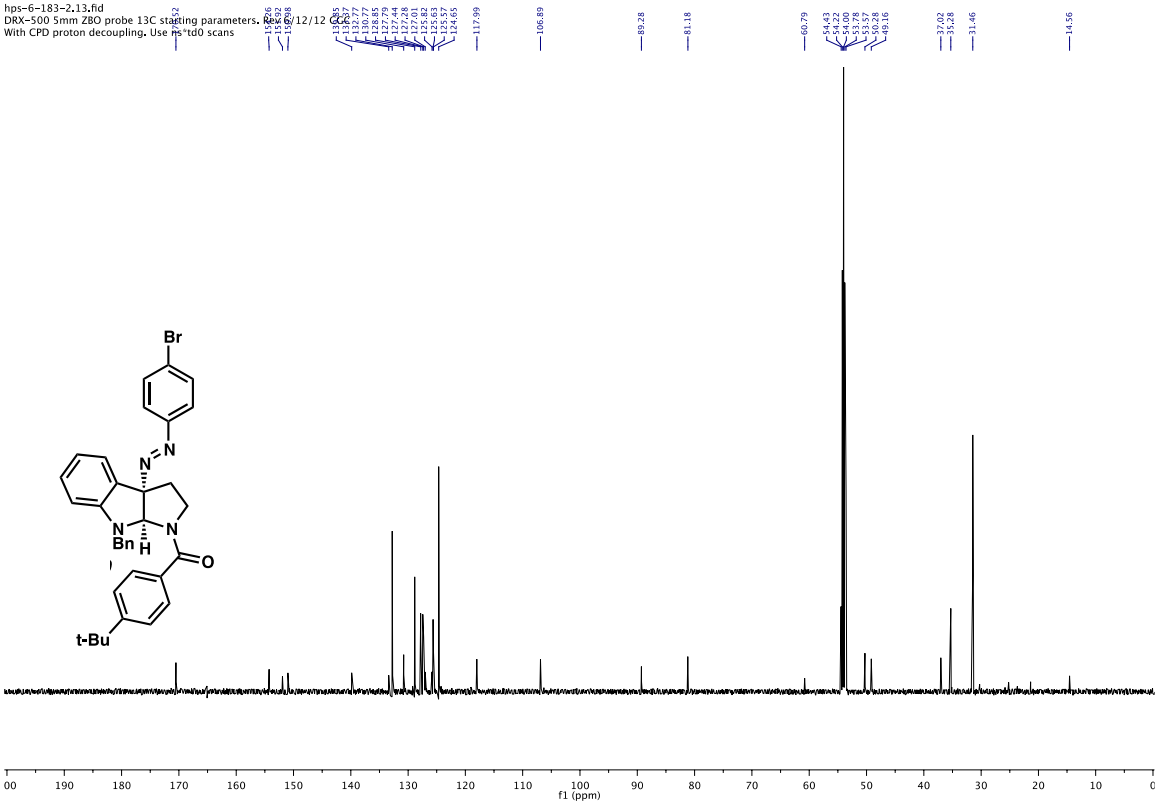

hps-6-183-1-2.1.fid
AVQ-400 QNP Proton starting parameters. 7/16/03. Revised 7/22/03 RN

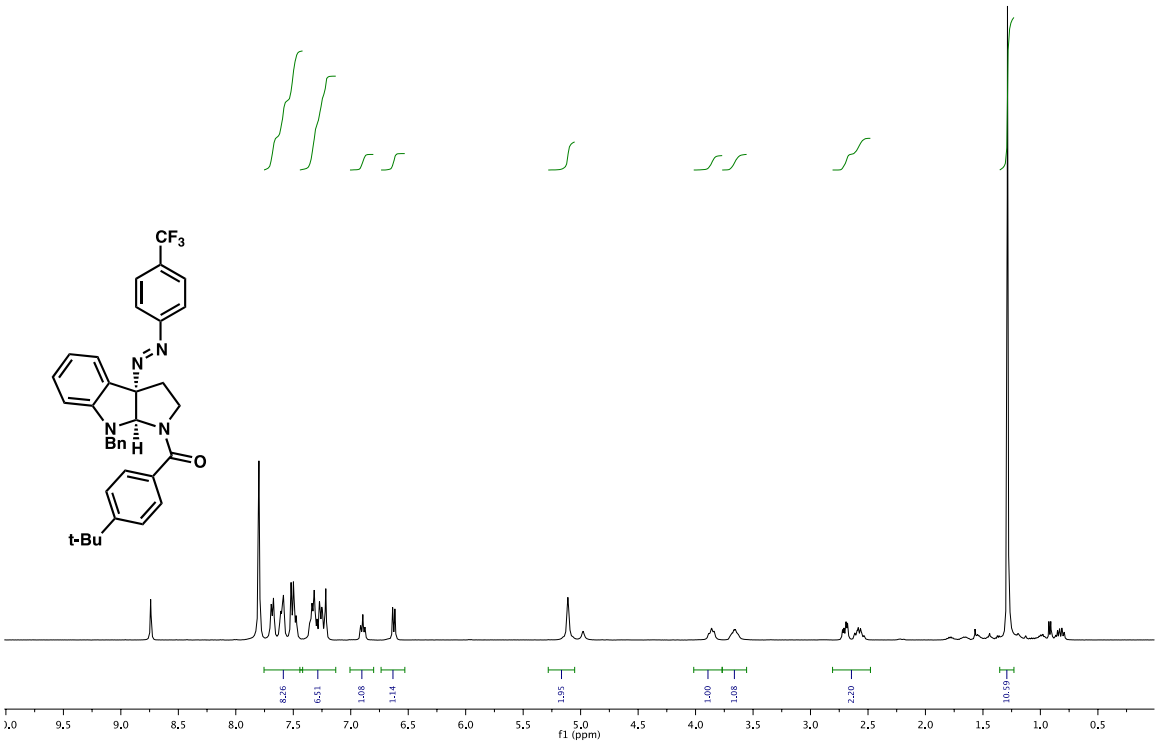

hps-6-183-1-2.13.fid
DRX-500 5mm ZBO probe 13C starting parameters. Rev 6/12/12 CGC
With CPD proton decoupling. Use ns*td0 scans

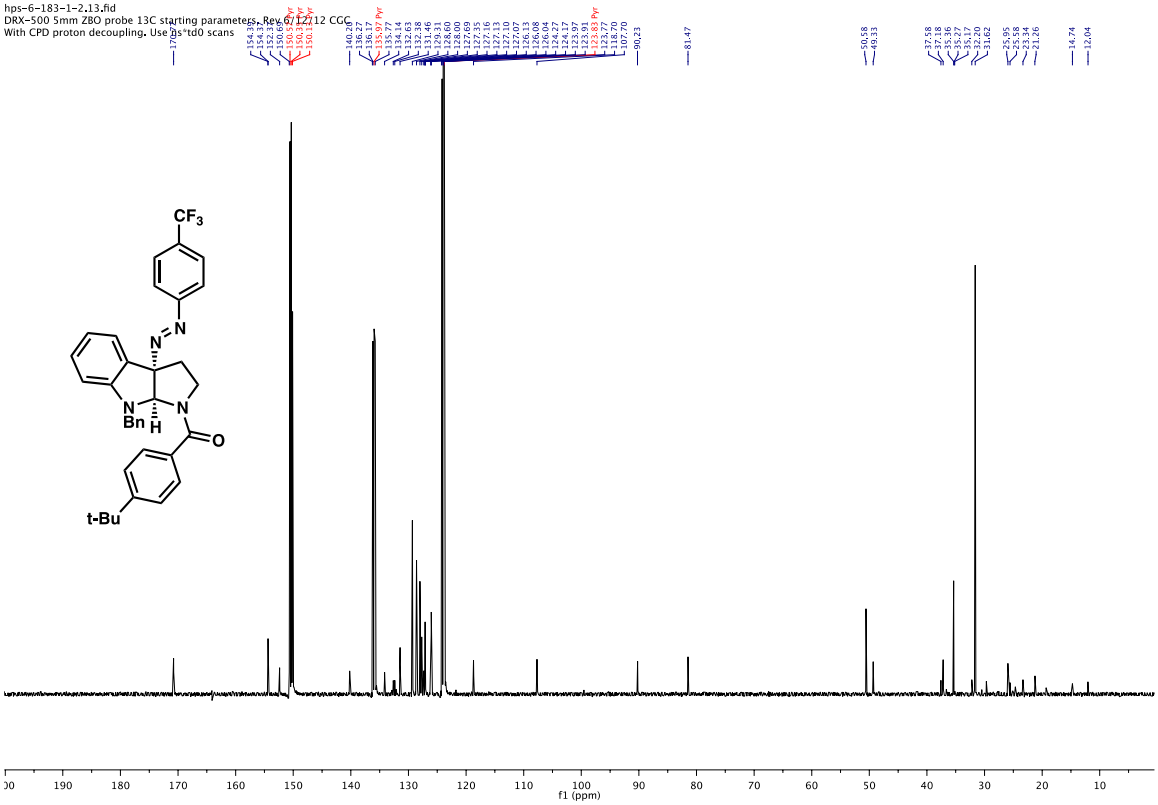

hps-6-173-1.1.fid
1H starting parameters (zg30)
DRX-500 TBIC
061212 CGC

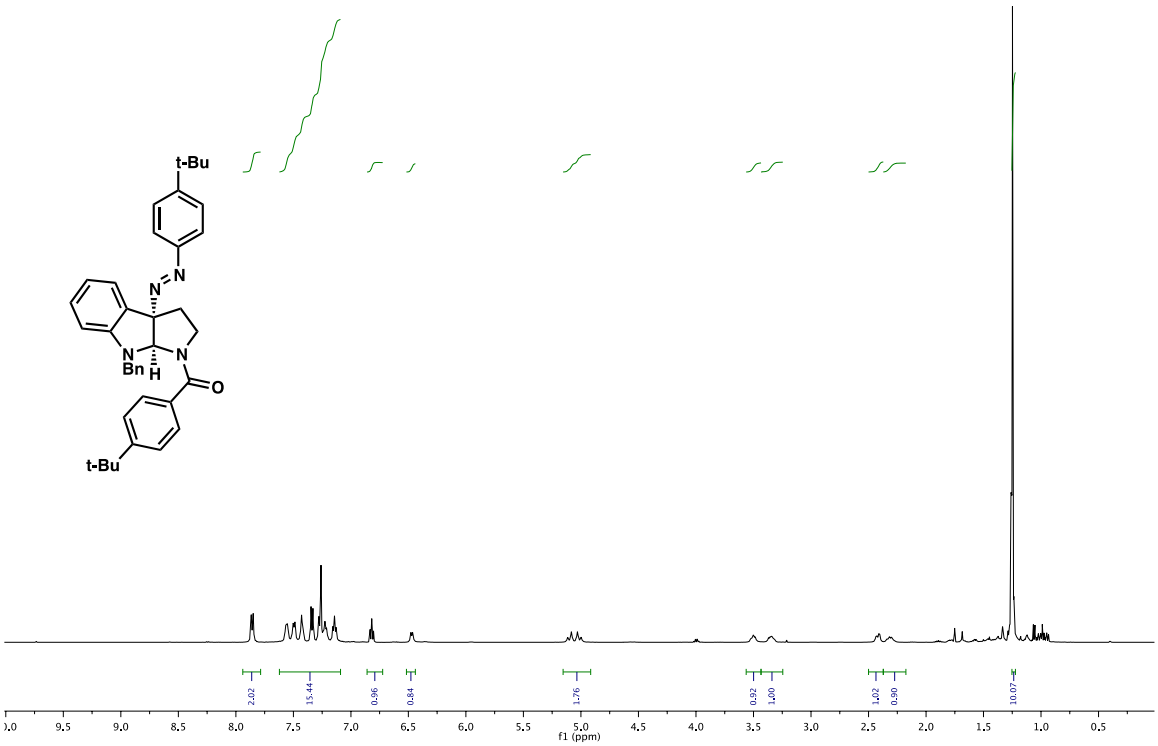

hps-6-173-1.13.fid
DRX-500 5mm ZBO probe 13C starting parameters, 061212/12 CGC
With CPD proton decoupling. Use ns*td0 scans

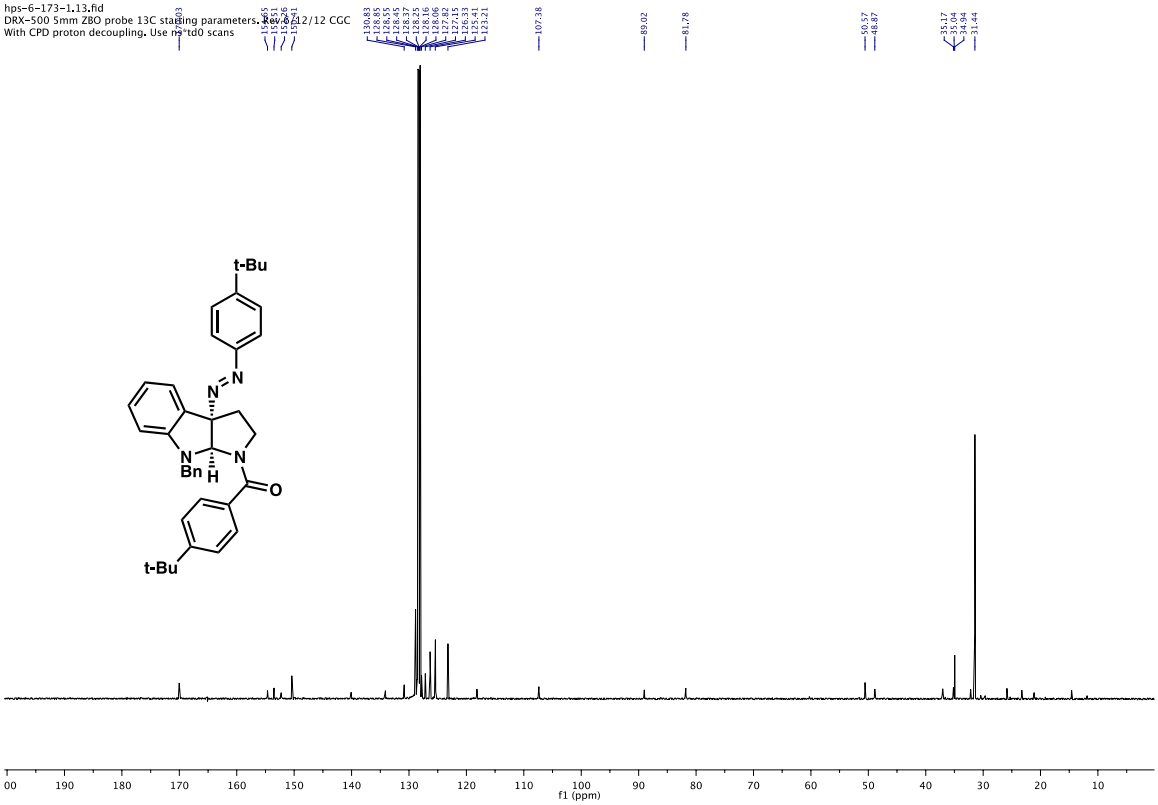

SR-i-38b.1.fid
AV-300 Dual C-H probe proton starting parameters 7/23/03 RN.

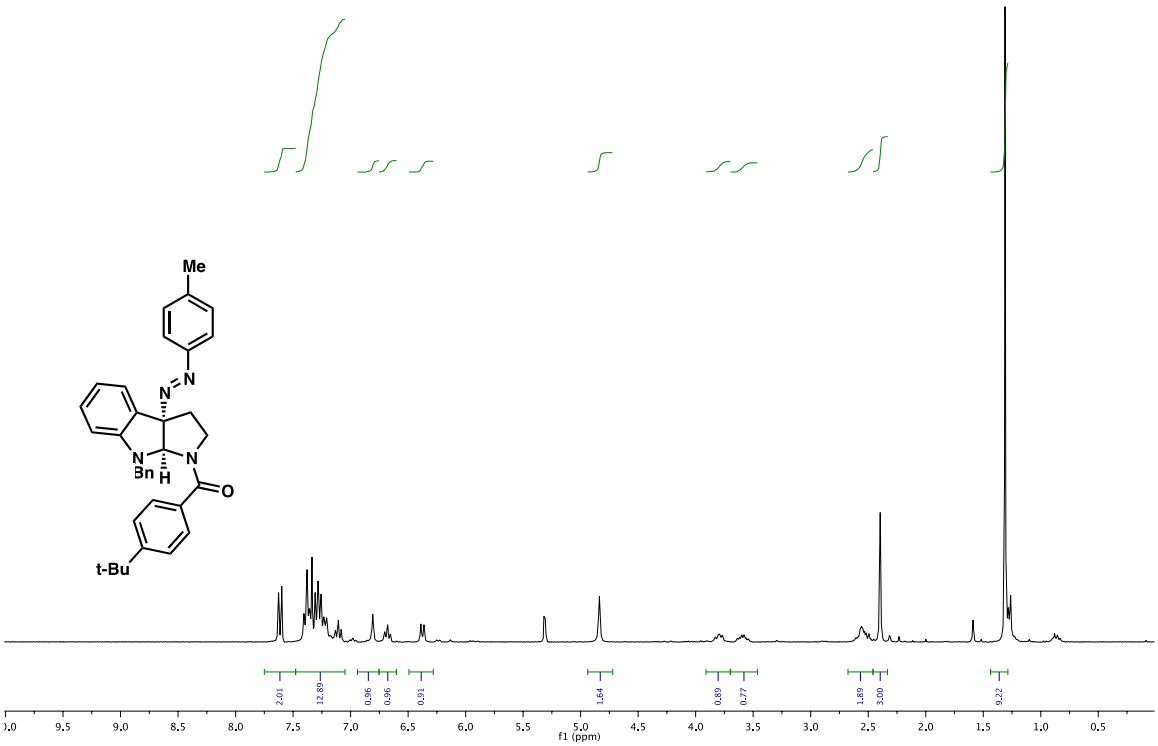

SR-i-38b.3.fid
DRX-500 5mm ZBO probe 13C starting parameters. Rev 6/12/12 CGC
With CPD proton decoupling. Use ns*td0 scans

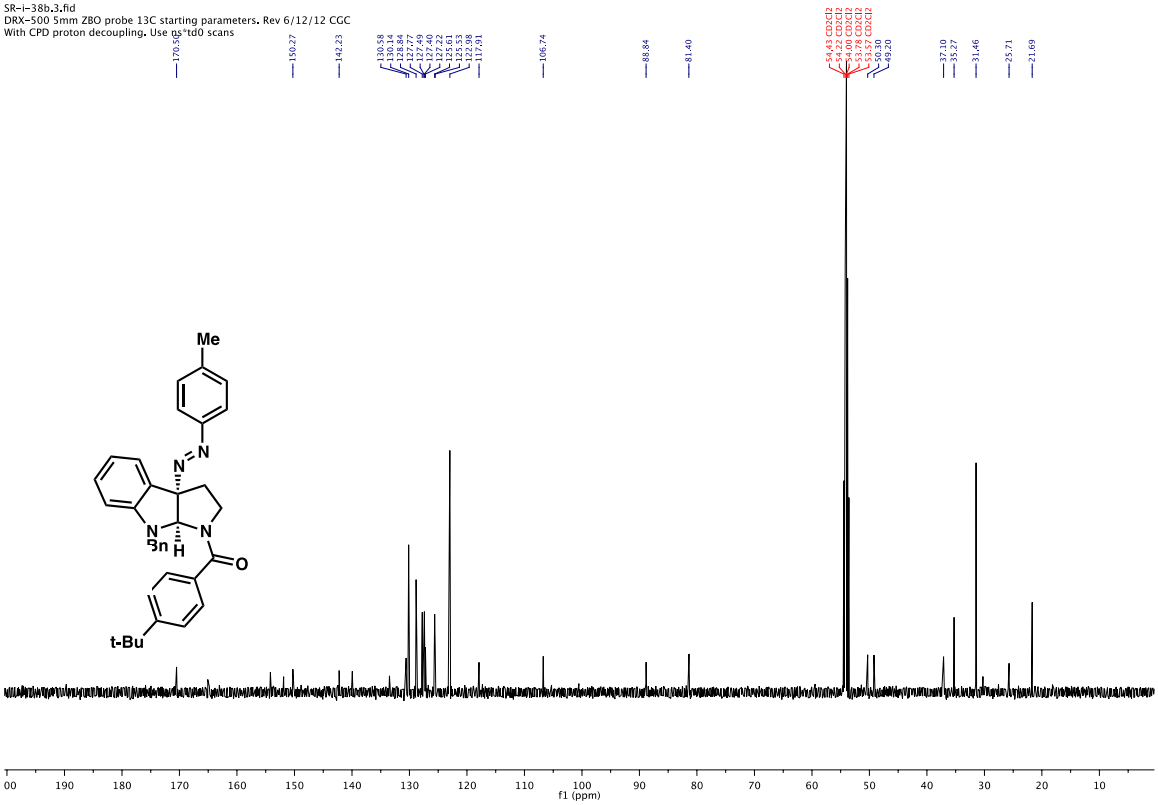

hps-6-173-2-2.1.fid
1H starting parameters (zg30)
DRX-500 TBIC
061212 CGC

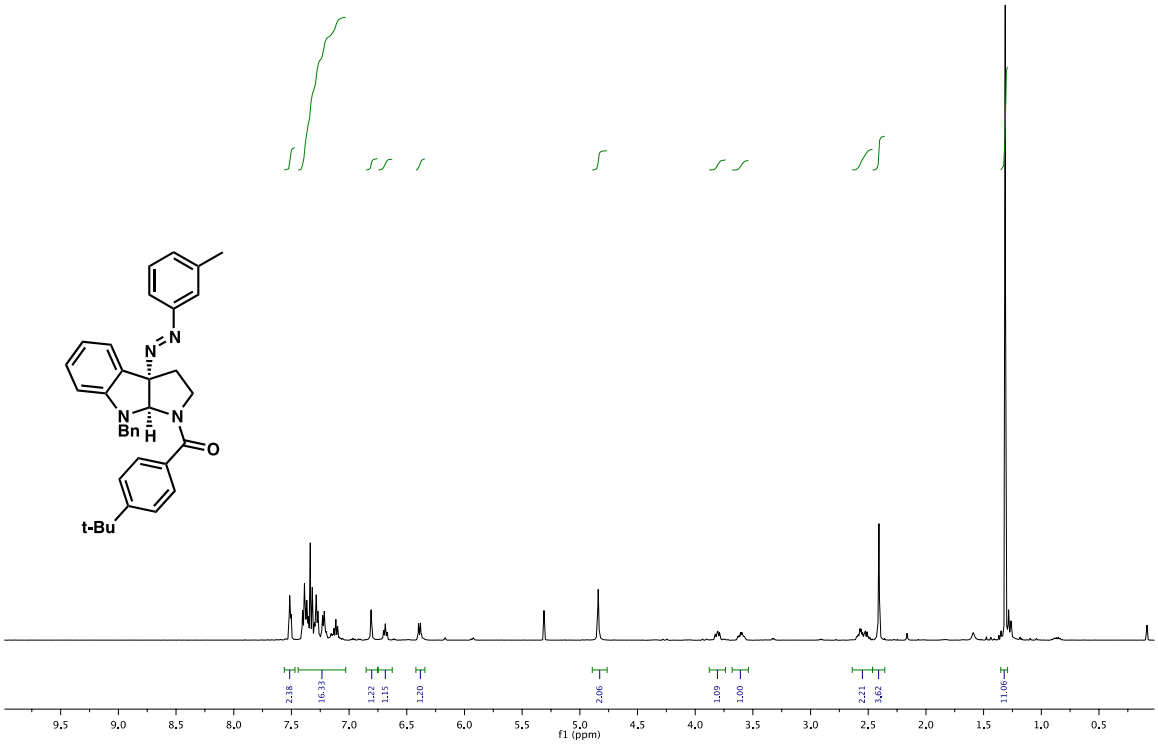

hps-6-173-2-2.13.fid
DRX-500 5mm ZBO probe 13C starting parameters, Rev. 6/12/12 CGC
With CPD proton decoupling. Use ns*td0 scans

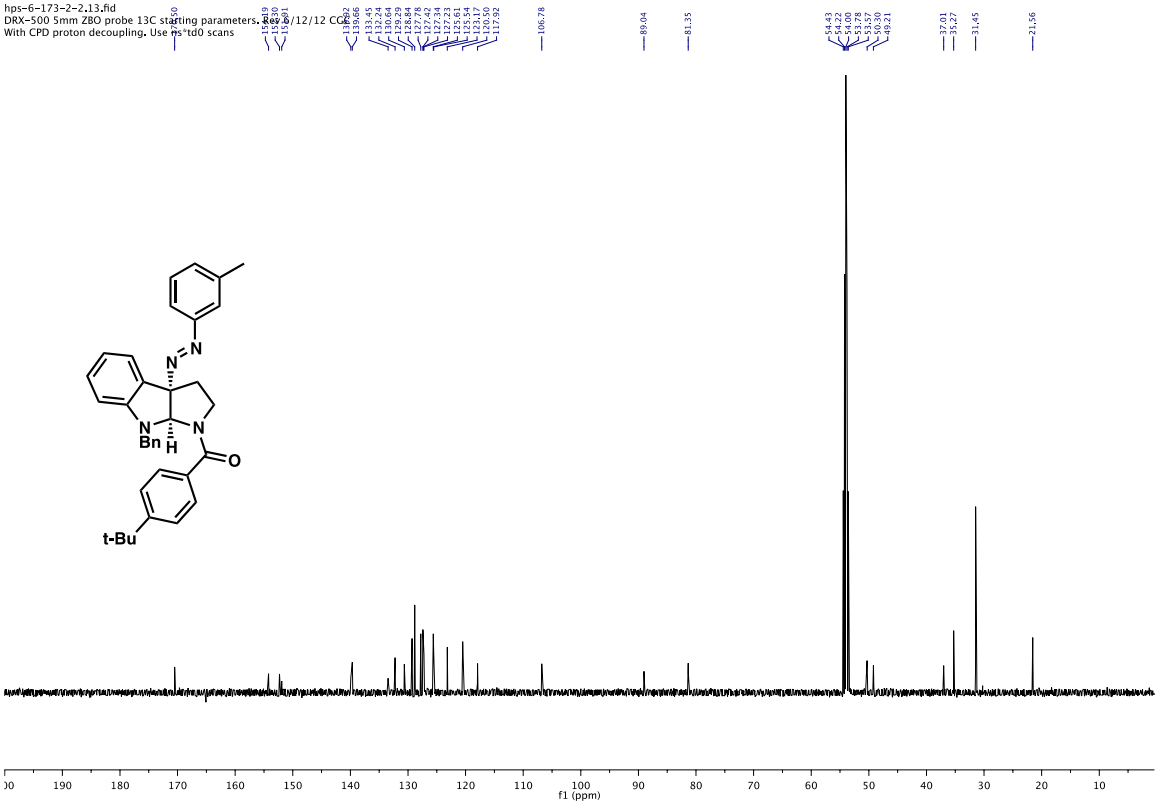

hps-6-173-3.1.fid
1H starting parameters (zg30)
DRX-500 TBIC
061212 CGC

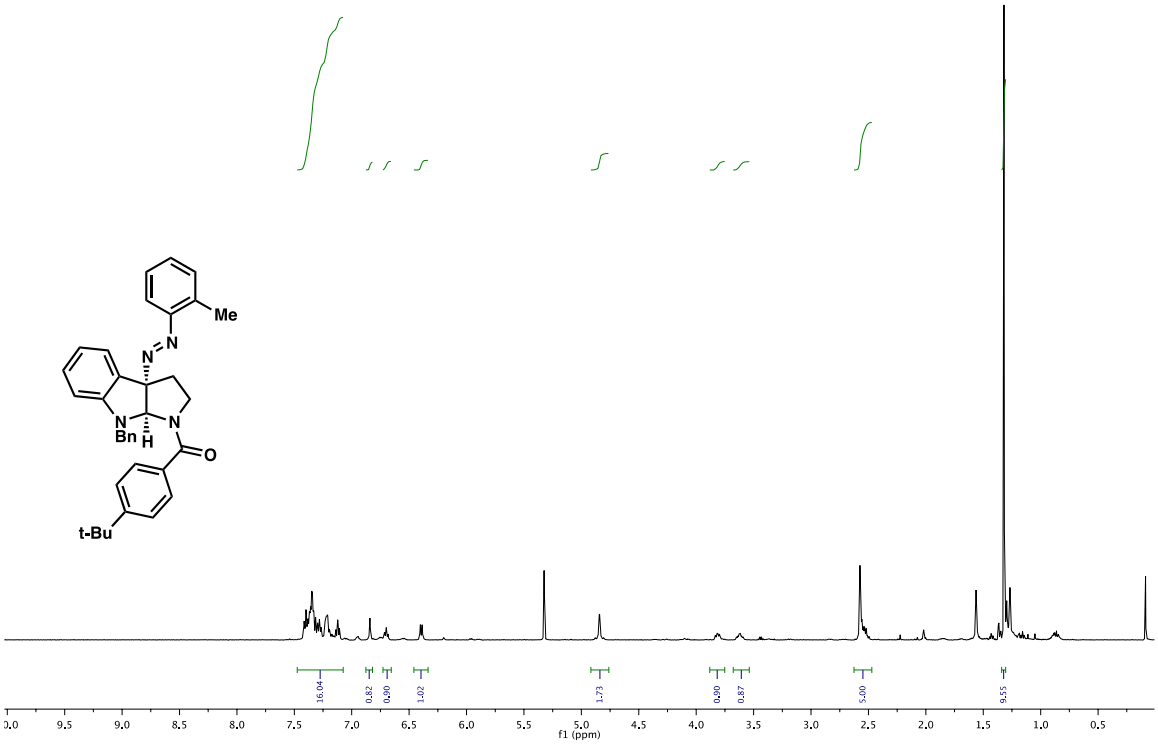

hps-6-173-3.13.fid
DRX-500 5mm ZBO probe 13C starting parameters. Revised 12/12 CGC
With CPD proton decoupling. Use ns*td0 scans

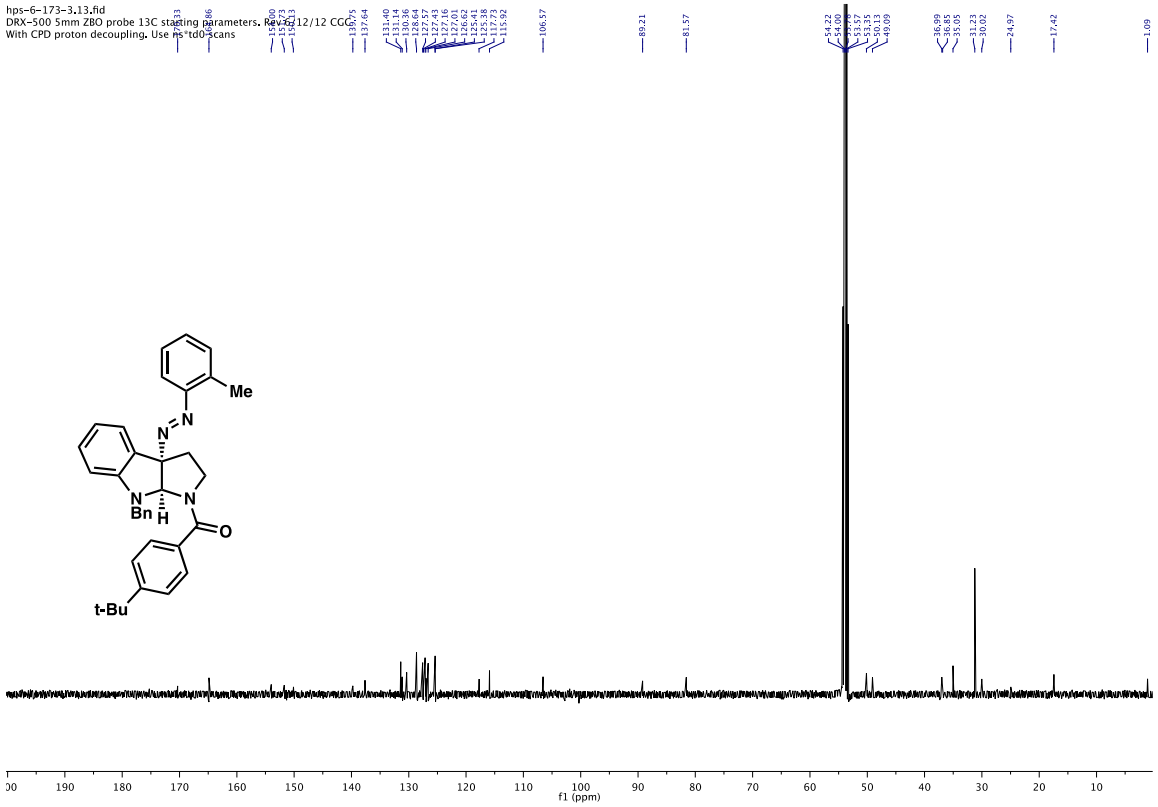

SR-i-38a.1.fid
1H starting parameters (zg30)
DRX-500 TBIC
061212 CGC

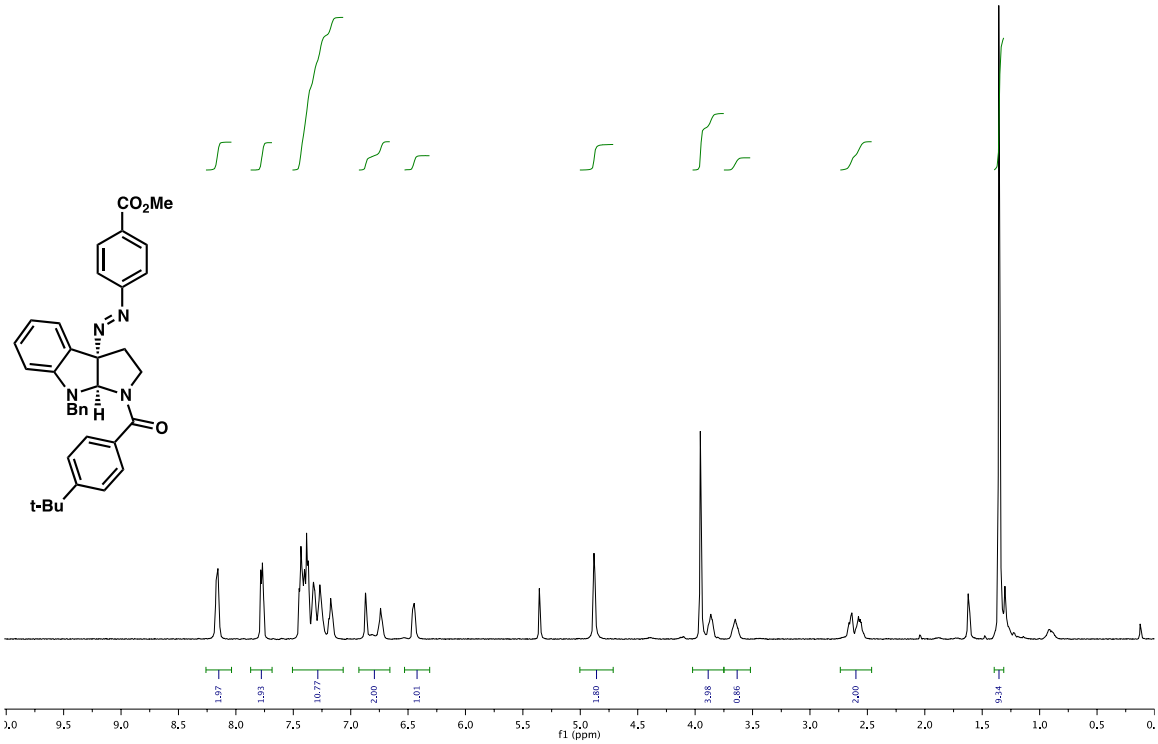

SR-i-38a.2.fid
DRX-500 5mm ZBO probe 13C starting parameters rev 6/12/12 CGC
With CPD proton decoupling. Use ns 160 scans

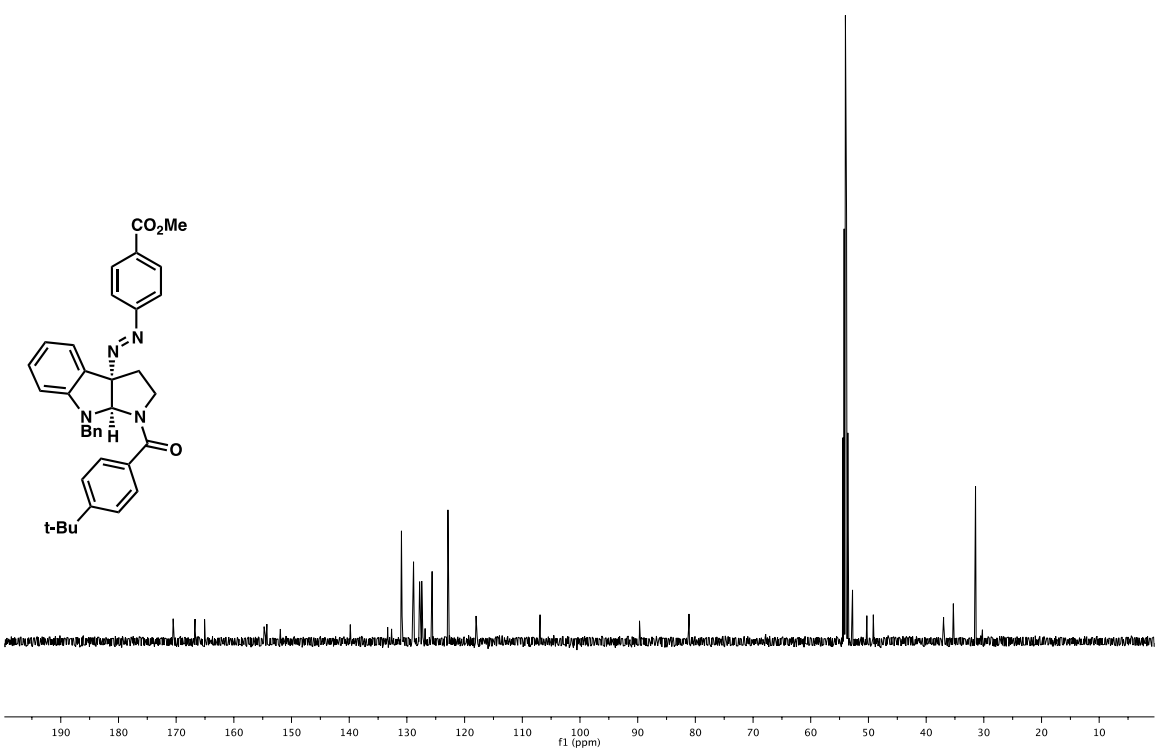

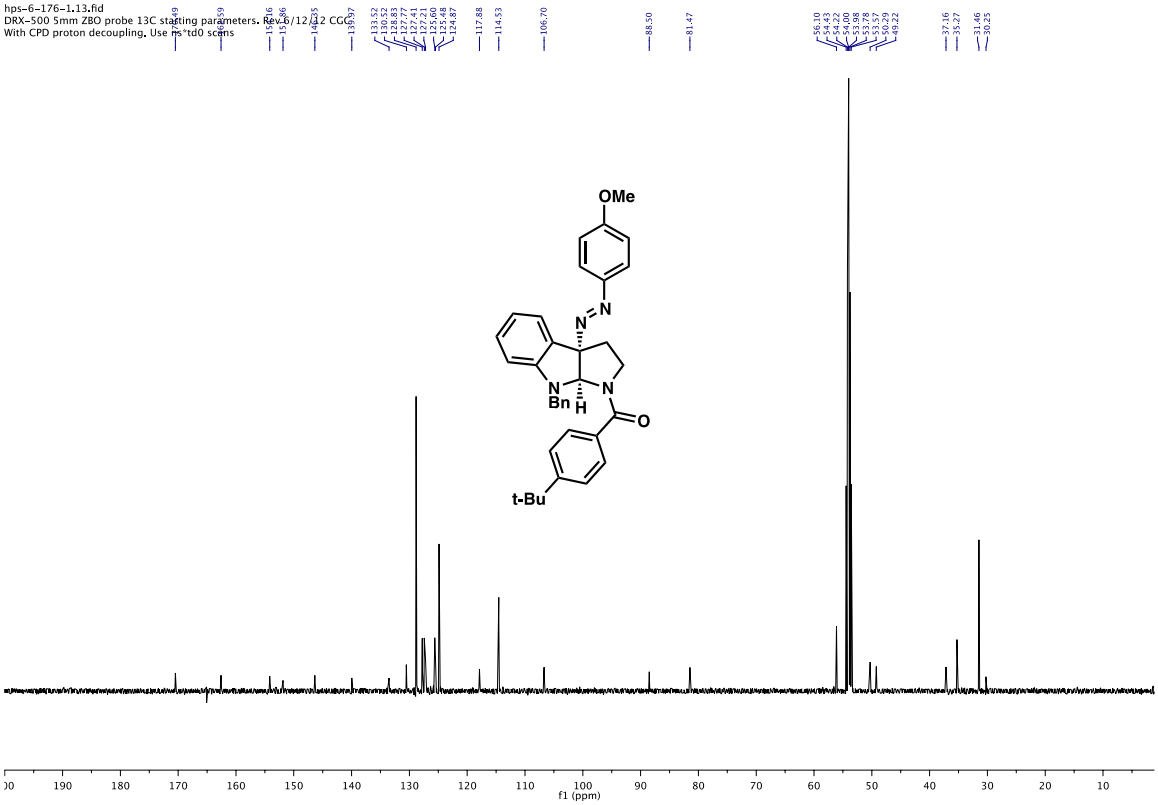
hps-6-176-1.13.fid
DRX-500 5mm ZBO probe 13C starting parameters. Rev 6/12/12 CGC
With CPD proton decoupling. Use ns*td0 scans
OMe
N
N
N
Bn
H
N
O
t-Bu
f1 (ppm)

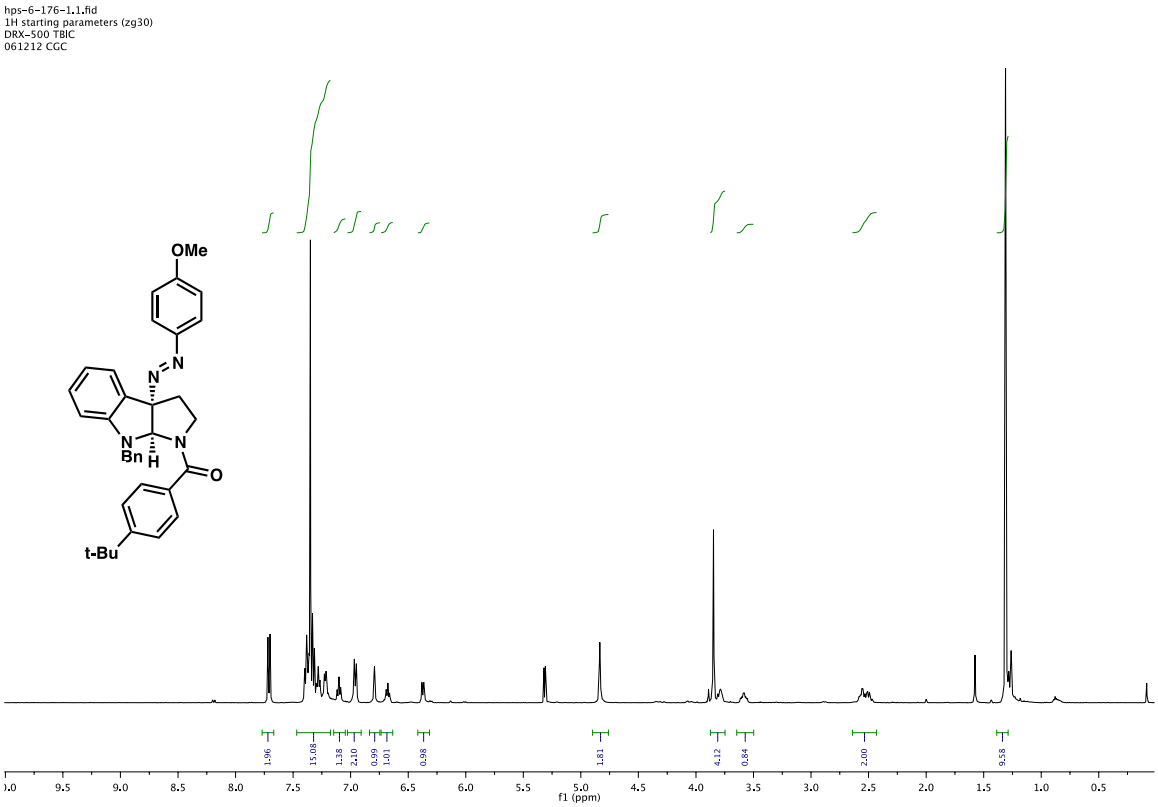
hps-6-176-1.1.fid
1H starting parameters (zg30)
DRX-500 TBIC
061212 CGC
OMe
N
N
N
Bn
H
N
O
t-Bu
1.96
15.08
1.38
2.10
0.99
1.01
0.98
1.81
4.12
0.84
2.00
9.58
f1 (ppm)

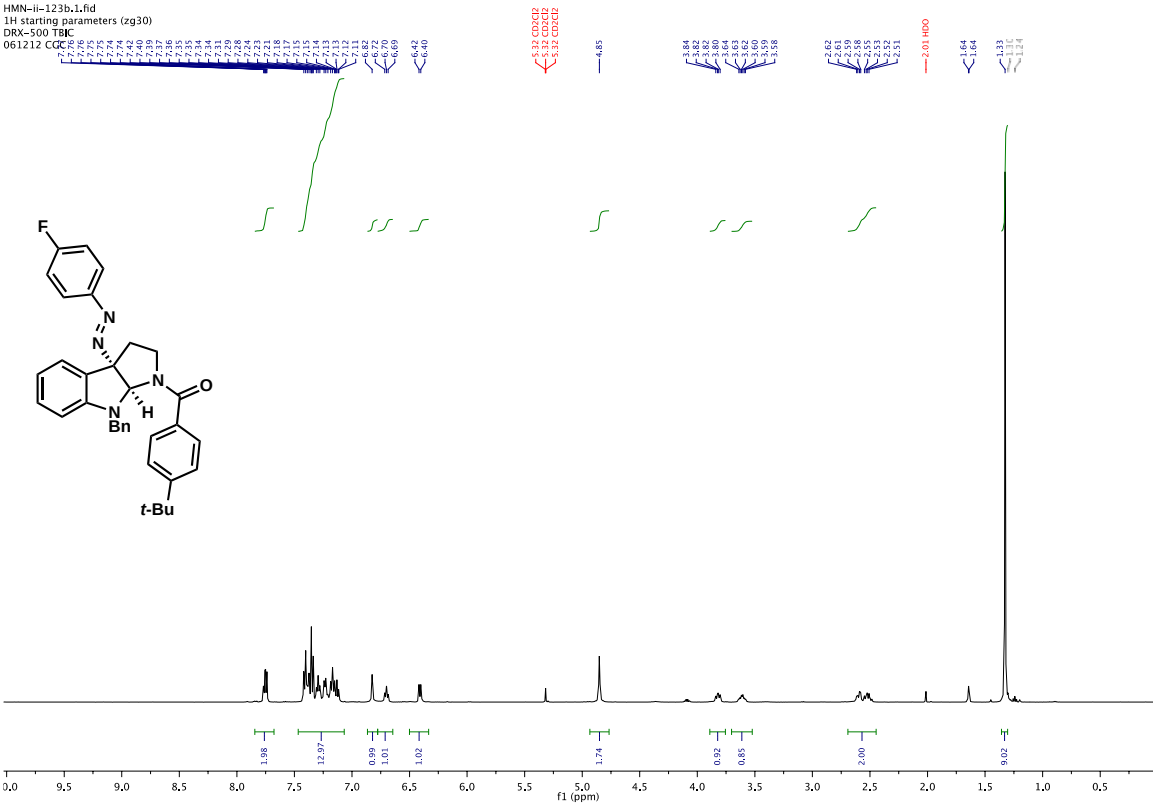
HMN-ii-123b.1.fid
1H starting parameters (zg30)
DRX-500 TBIC
061212 CDCl3
5.32 CDCl2
5.32 CDCl2
5.32 CDCl2
2.01 HDO
F
N
N
N
O
N
Bn
H
t-Bu
f1 (ppm)

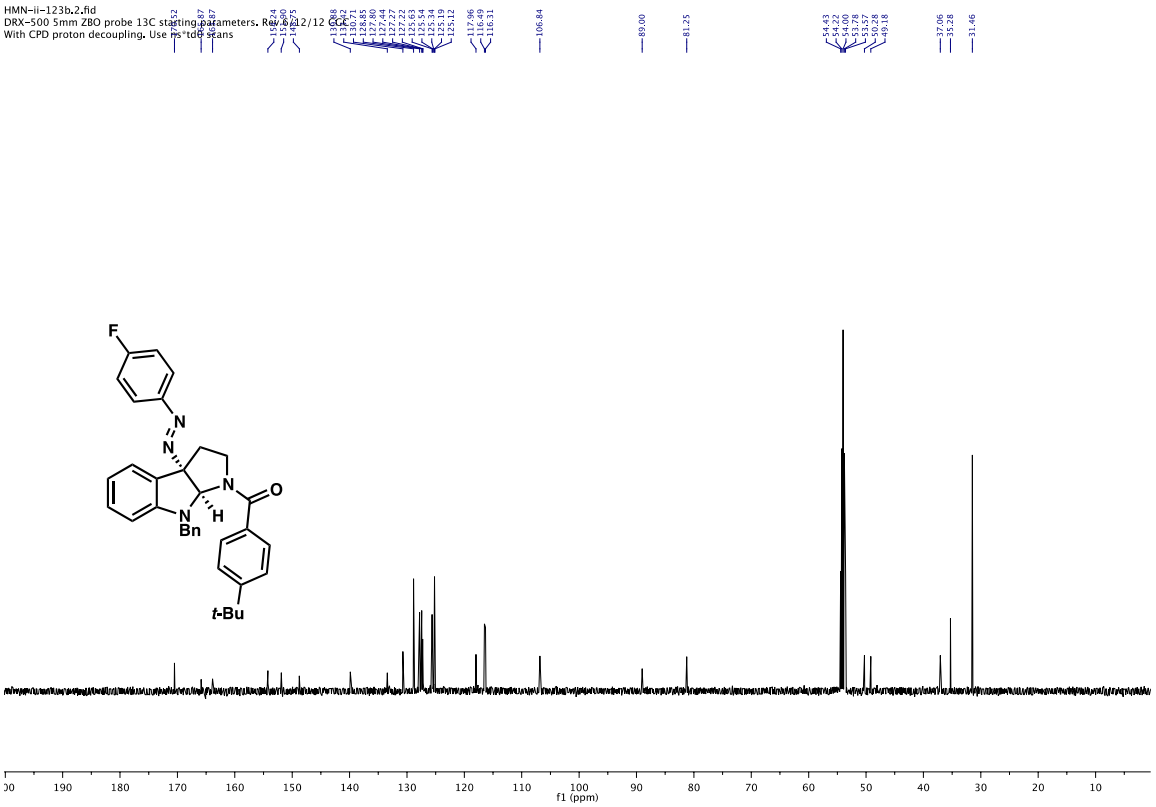
HMN-ii-123b.2.fid
DRX-500 5mm ZBO probe 13C starting parameters. Rev. 6/12/12 CCC
With CPD proton decoupling. Use zs*tdc scans
F
N
N
N
O
N
Bn
H
t-Bu
f1 (ppm)

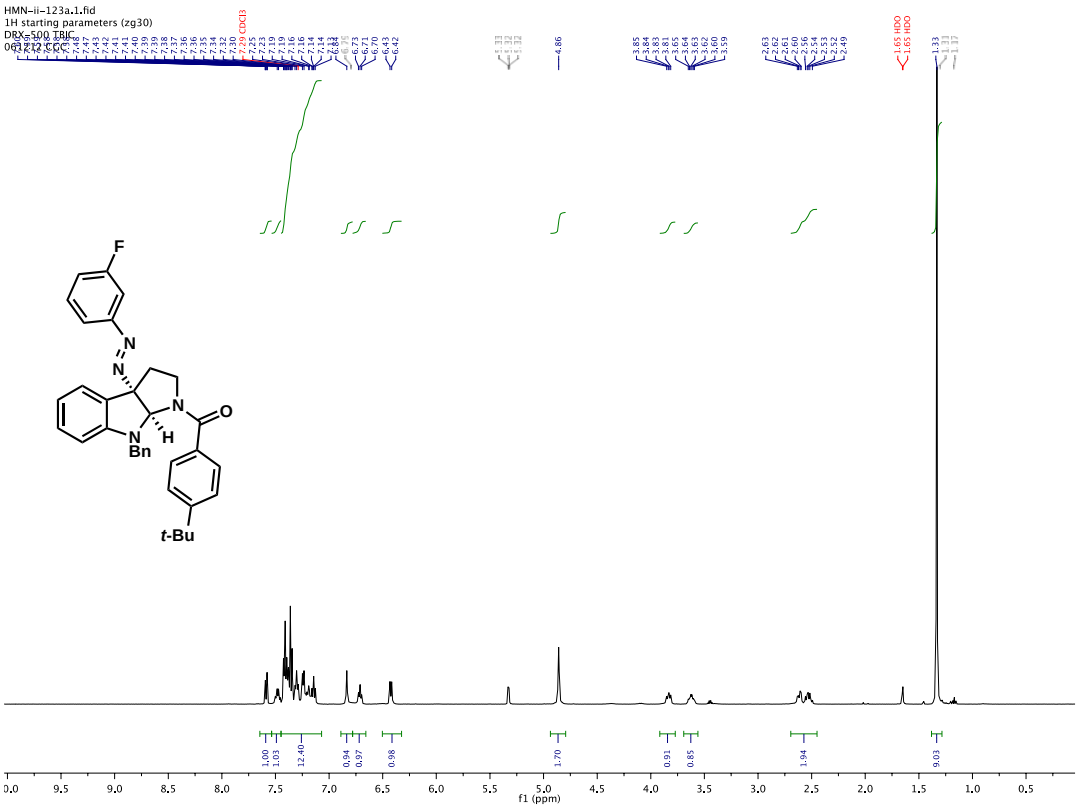
HMN-ii-123a.1.fid
1H starting parameters (zg30)
DRX-500 TRIC
061212 CCC
F
N
N
N
O
N
H
Bn
t-Bu
f1 (ppm)

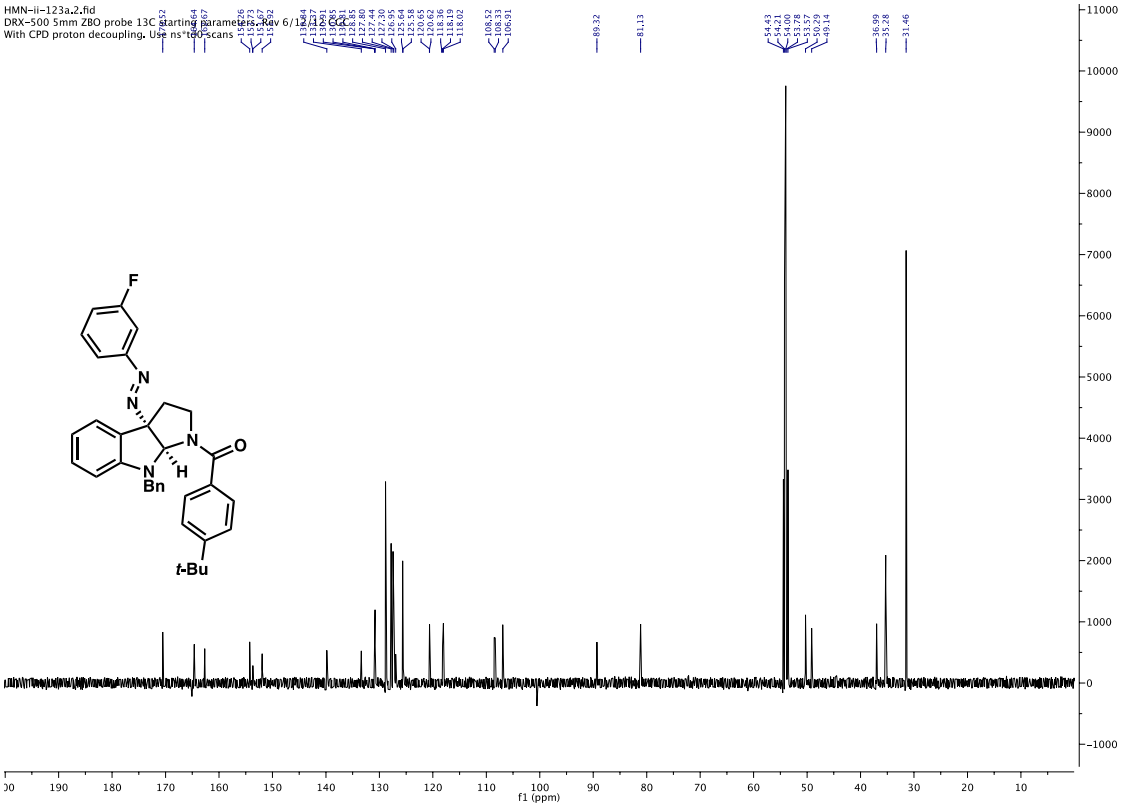
HMN-ii-123a.2.fid
DRX-500 5mm ZBO probe 13C starting parameters
With CPD proton decoupling. Use ns=100 scans
F
N
N
N
O
N
H
Bn
t-Bu
f1 (ppm)

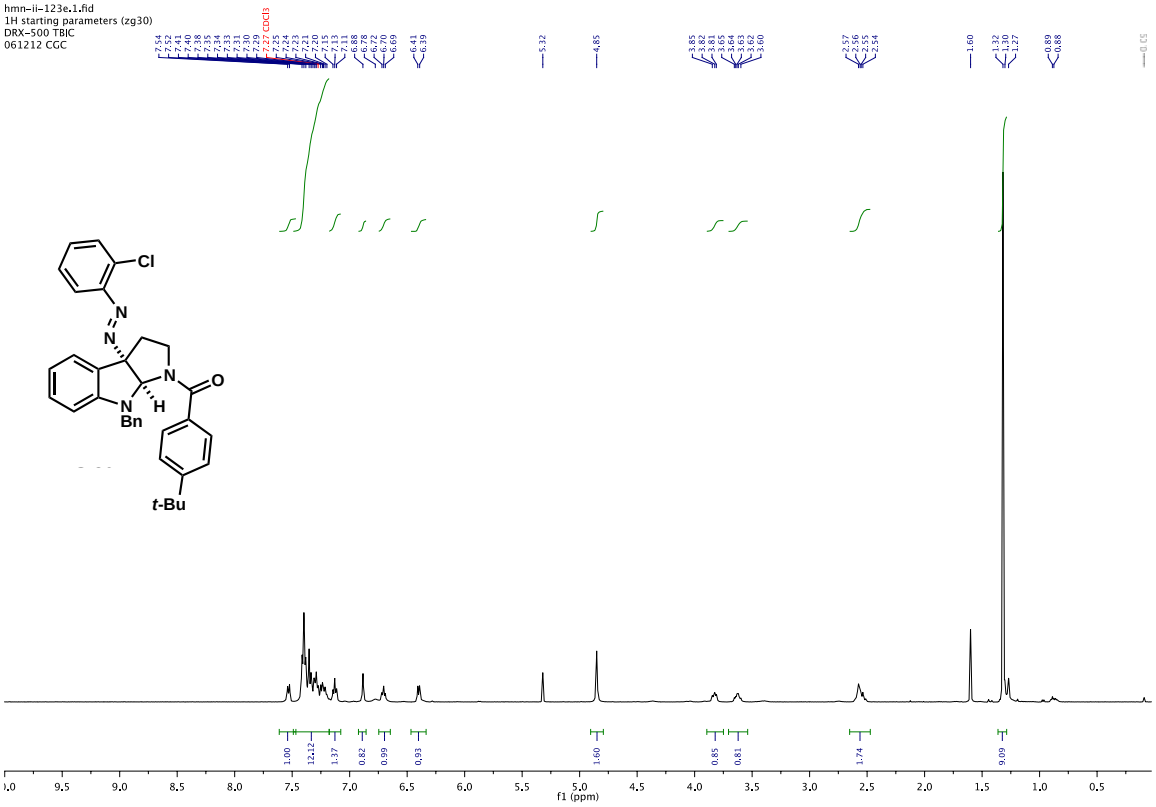
hmn-ii-123e.1.fid
1H starting parameters (zg30)
DRX-500 TBIC
061212 CGC
f1 (ppm)

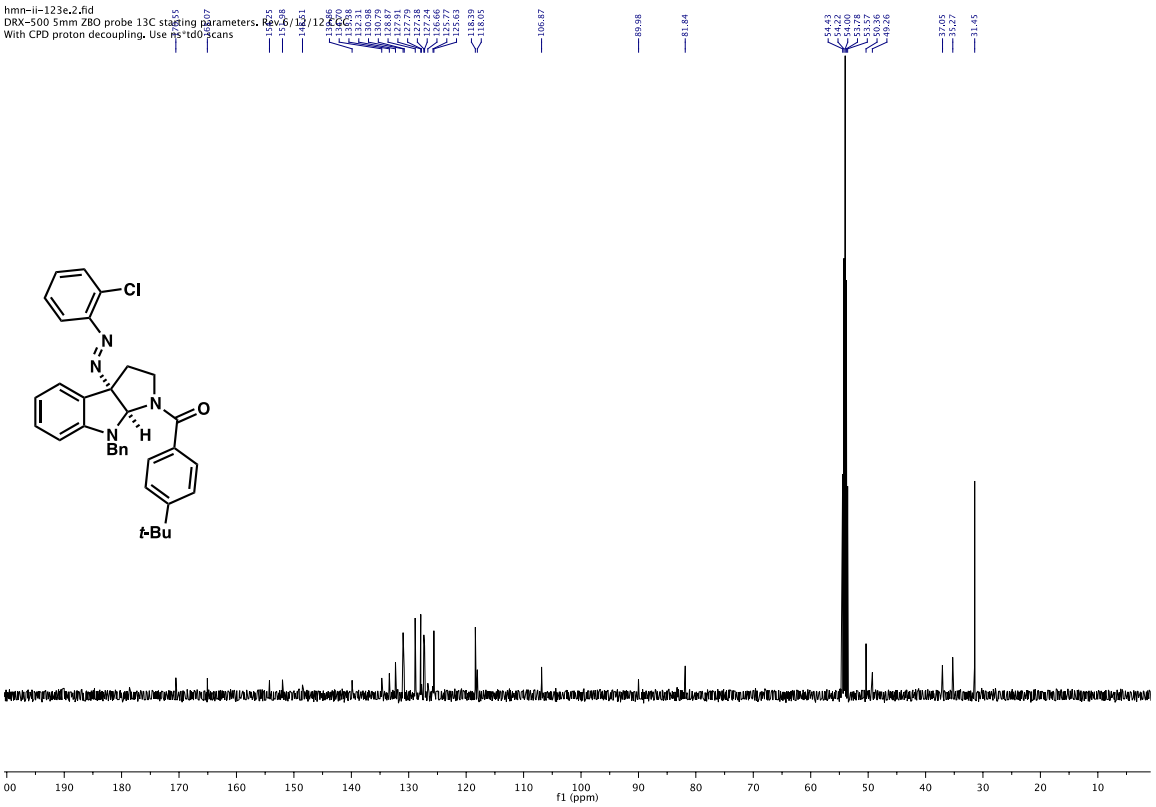
hmn-ii-123e.2.fid
DRX-500 5mm ZBO probe 13C starting parameters. Rev.6/12/12 CGC
With CPD proton decoupling. Use ns*tdd scans
f1 (ppm)

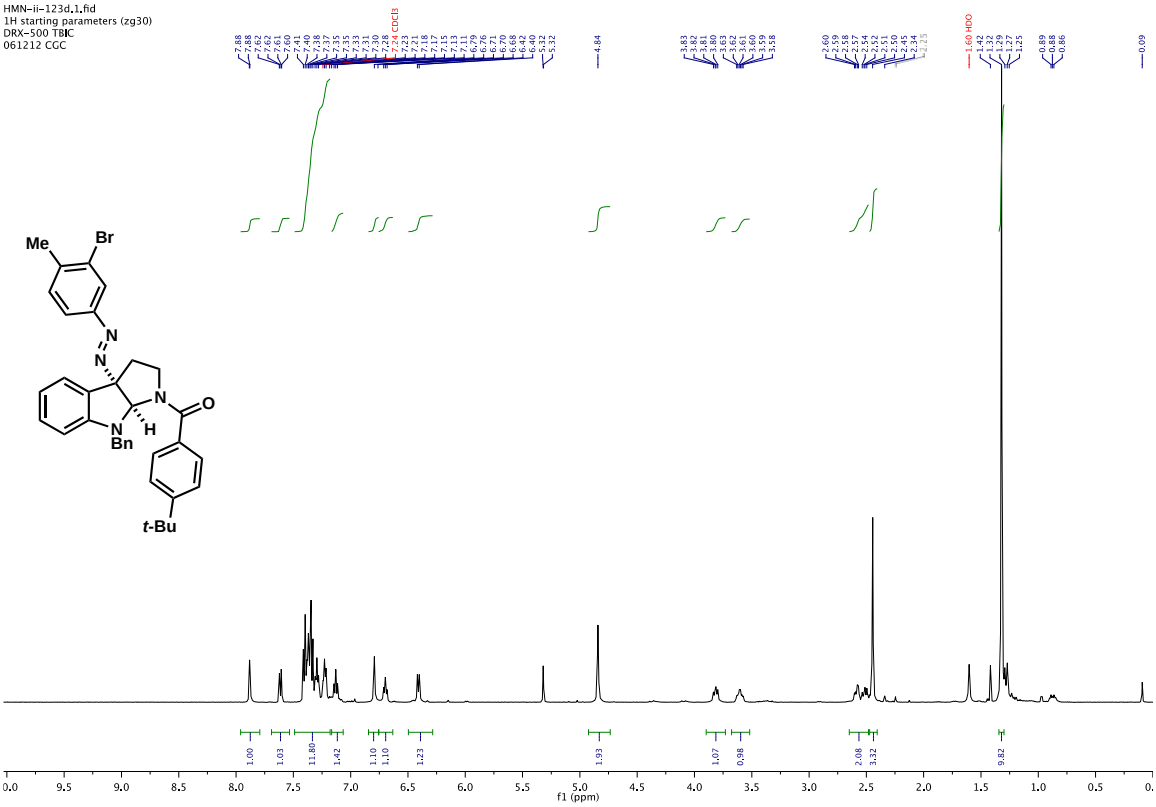
HMN-ii-123d.1.fid
1H starting parameters (zg30)
DRX-500 TBIC
061212 CGC
Me
Br
N
N
N
O
N
H
Bn
t-Bu
f1 (ppm)

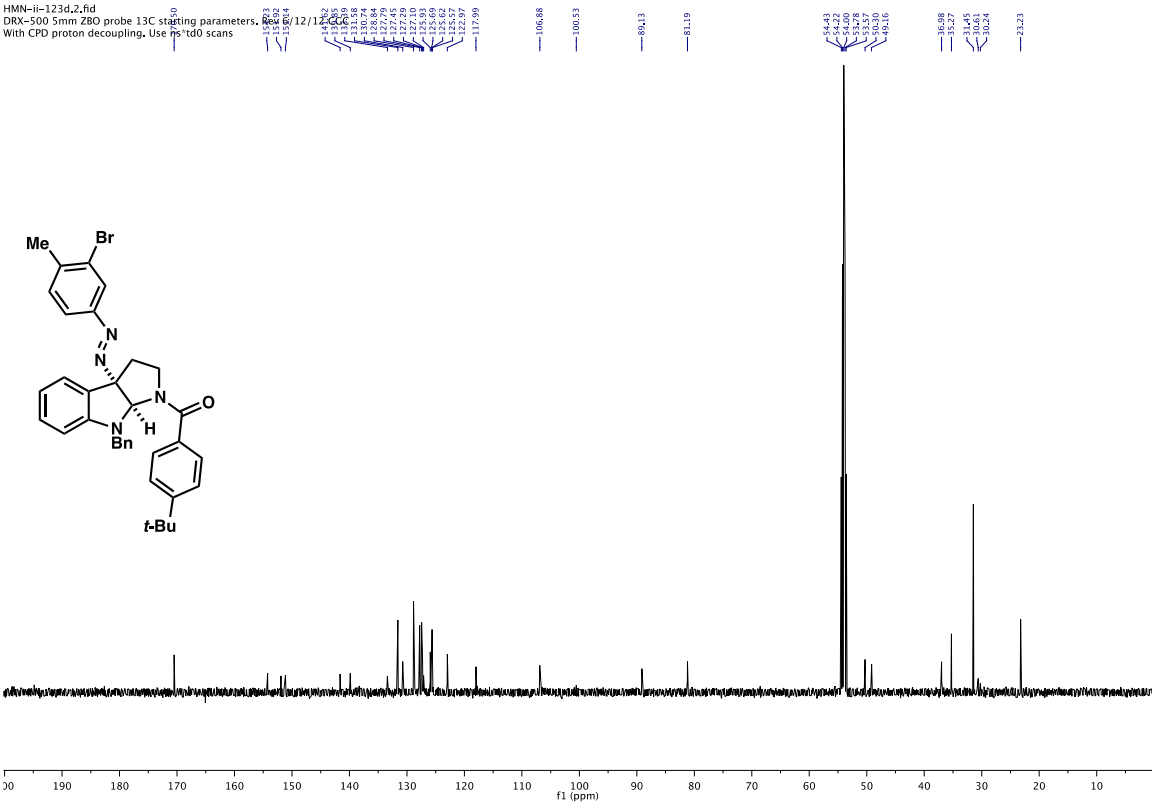
HMN-ii-123d.2.fid
DRX-500 5mm ZBO probe 13C starting parameters. Rev 6/12/12 CGC
With CPD proton decoupling. Use zgpg30 or zgdc30 or zgdc30 scans
Me
Br
N
N
N
O
N
H
Bn
t-Bu
f1 (ppm)

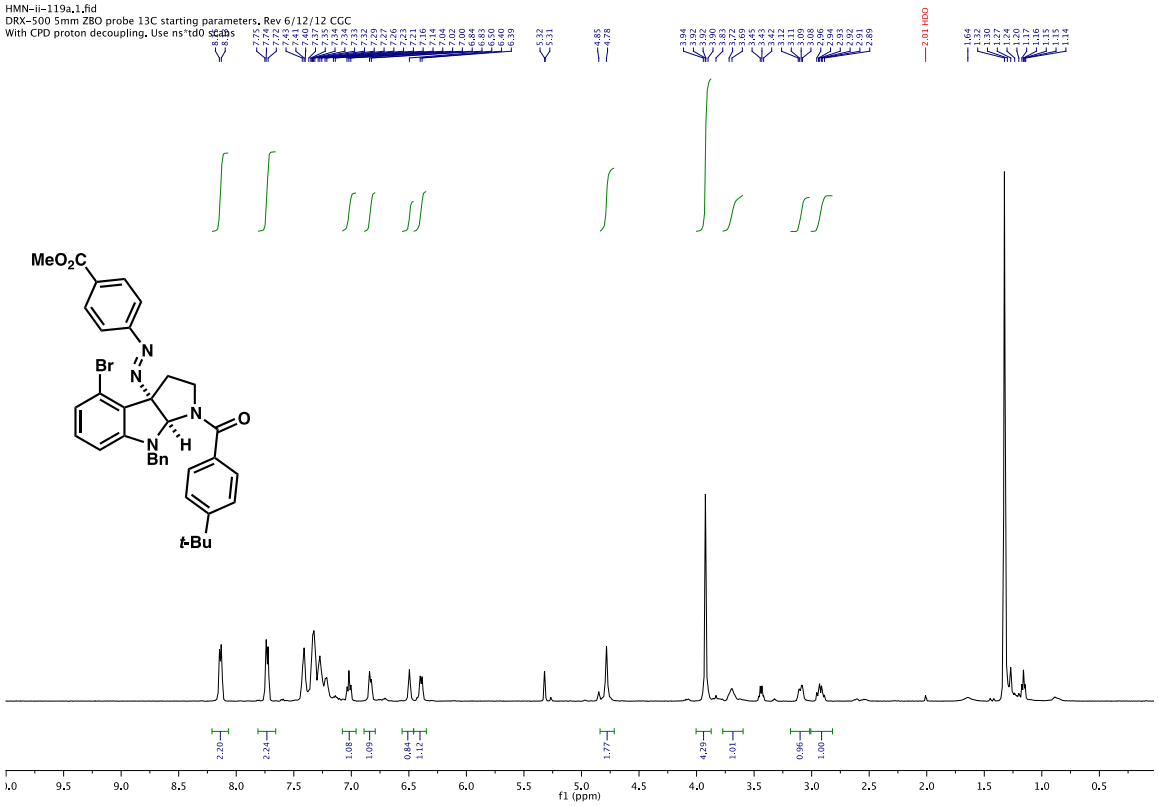
HMN-ii-119a.1.fid
DRX-500 5mm ZBO probe 13C starting parameters. Rev 6/12/12 CGC
With CPD proton decoupling. Use ns*td0 scans
2.01 HDO
MeO2C
Br
N
N
N
O
N
H
Bn
t-Bu
f1 (ppm)

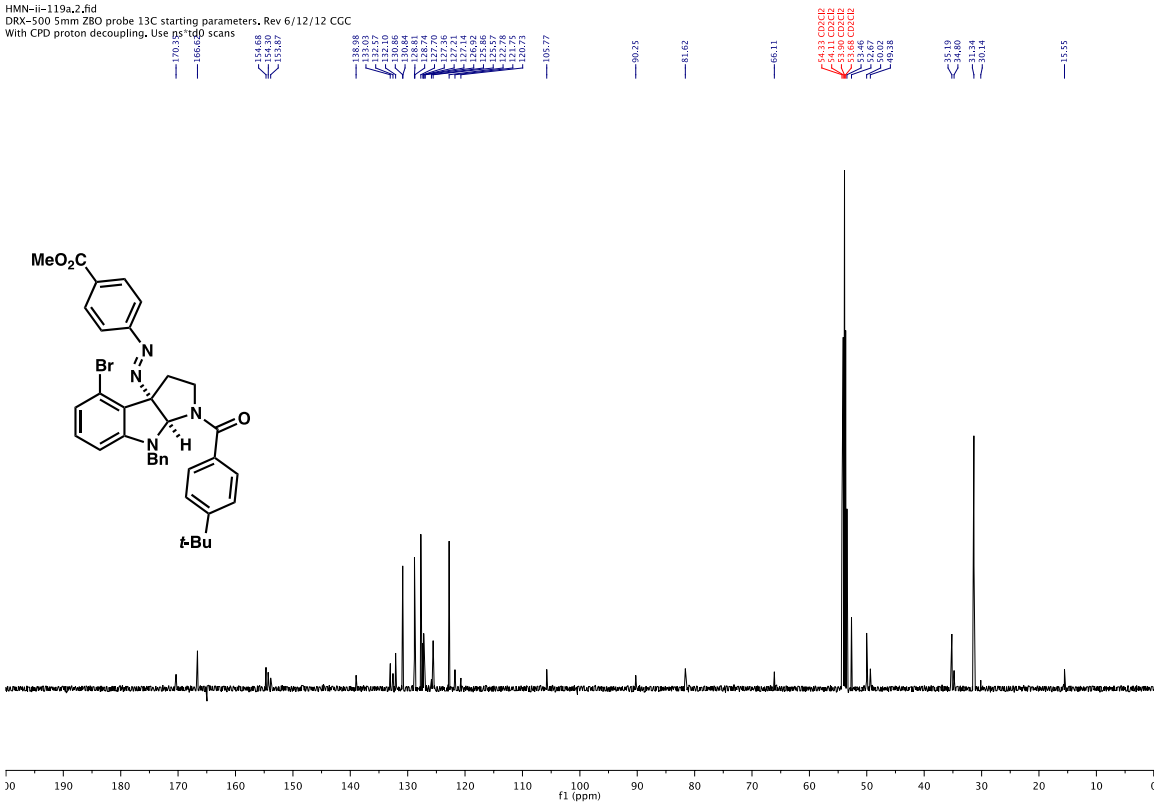
HMN-ii-119a.2.fid
DRX-500 5mm ZBO probe 13C starting parameters. Rev 6/12/12 CGC
With CPD proton decoupling. Use ns*td0 scans
MeO2C
Br
N
N
N
O
N
H
Bn
t-Bu
f1 (ppm)

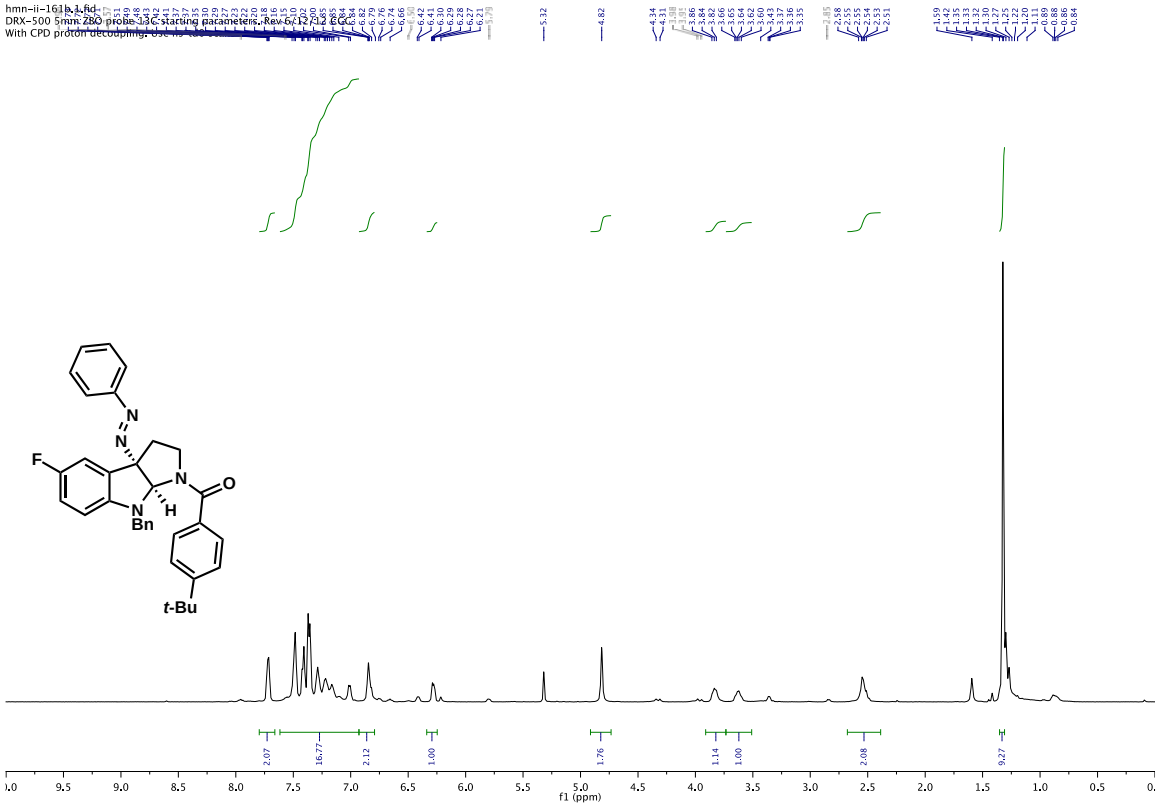
hmn-ii-161b.1.fid
DRX-500 5mm ZBO probe 13C starting parameters. Rev 6/12/12 CGC
With CPD proton decoupling. Use ns*td0 scans
f1 (ppm)

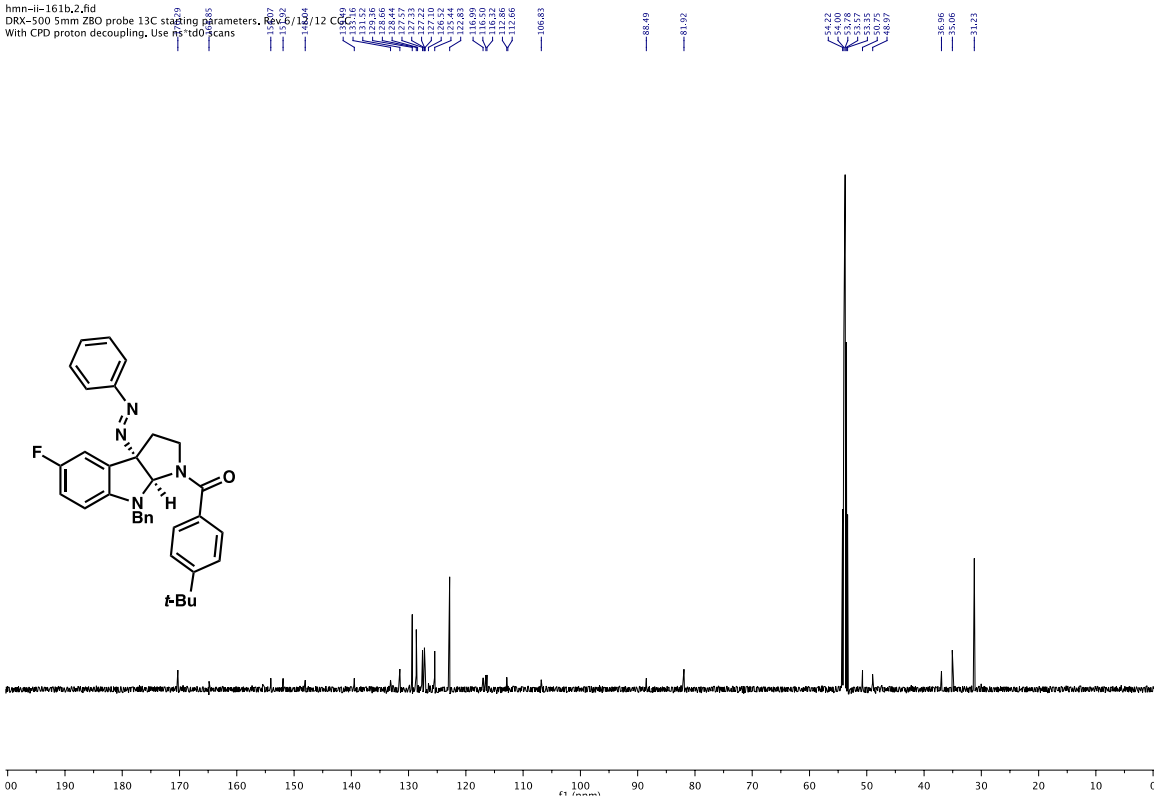
hmn-ii-161b.2.fid
DRX-500 5mm ZBO probe 13C starting parameters. Rev 6/12/12 CGC
With CPD proton decoupling. Use ns*td0 scans
f1 (ppm)

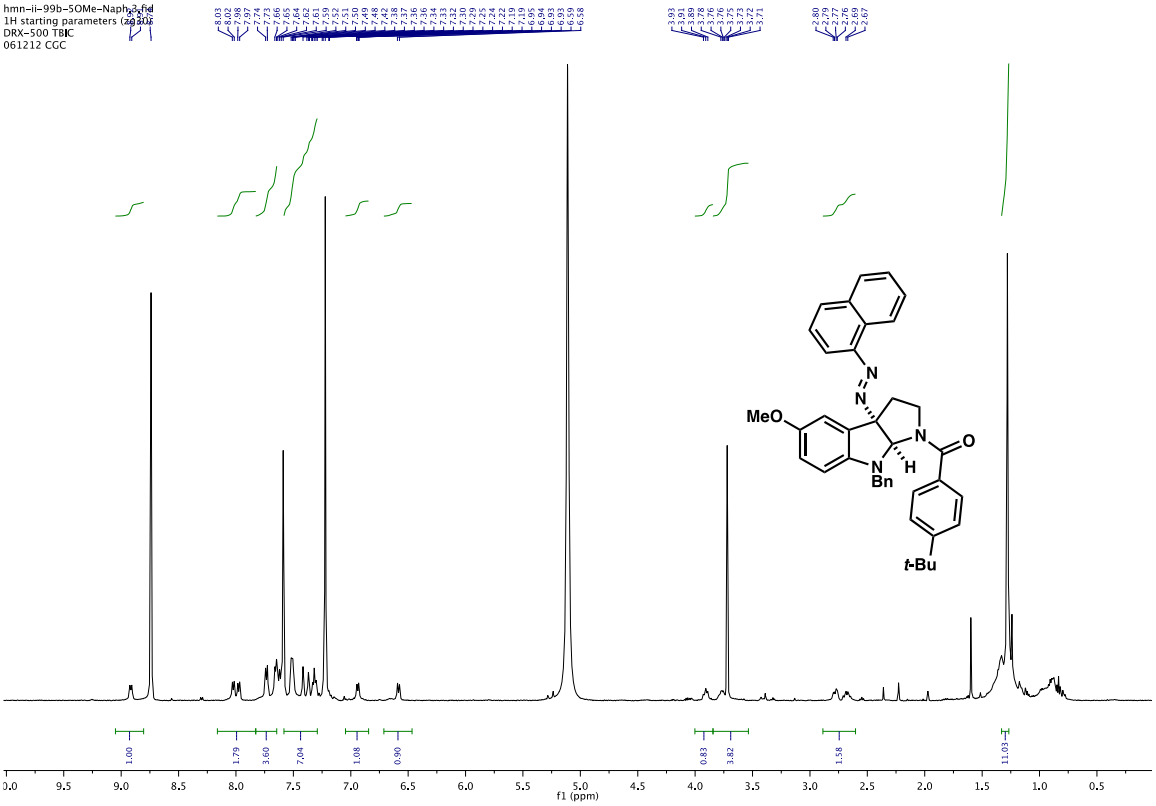
hmn-ii-99b-5OMe-Naph.3.fid
1H starting parameters (zg30)
DRX-500 TBIC
061212 CGC
MeO
N
N
N
O
N
H
Bn
t-Bu
f1 (ppm)

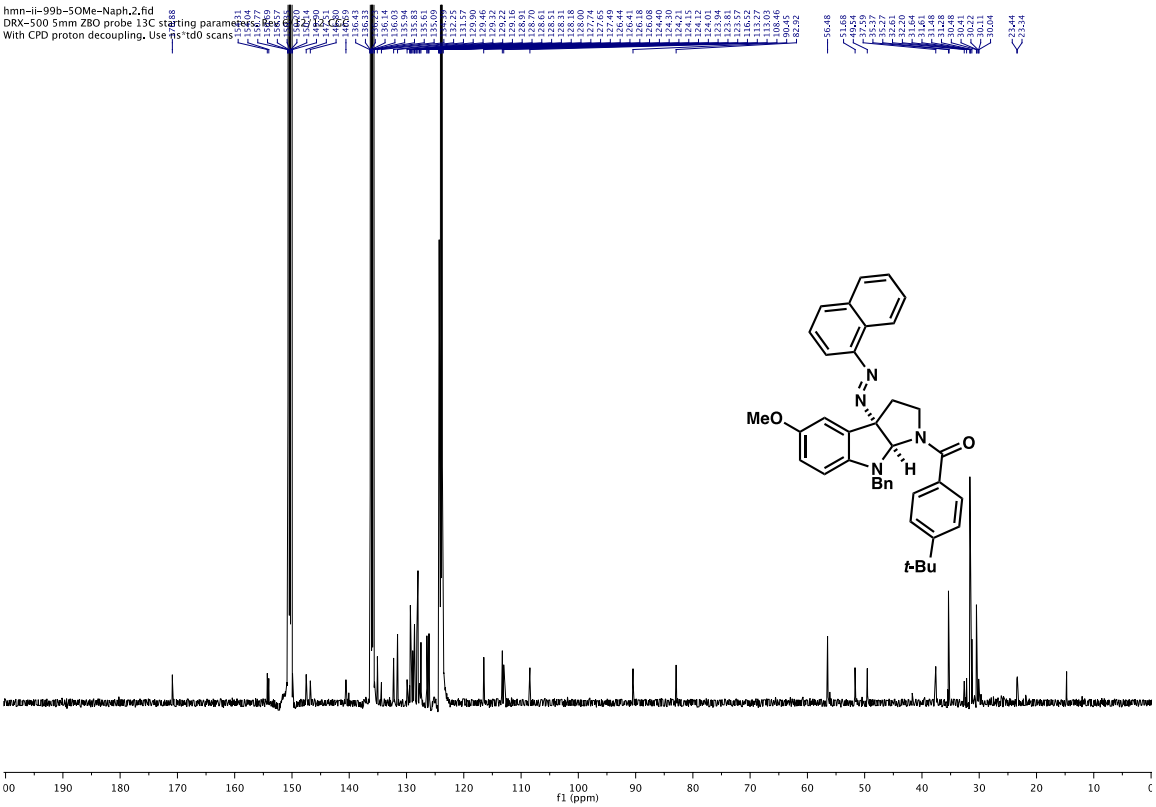
hmn-ii-99b-5OMe-Naph.2.fid
DRX-500 5mm ZBO probe 13C starting parameters (zgdc)
With CPD proton decoupling. Use ns*td0 scans
MeO
N
N
N
O
N
H
Bn
t-Bu
f1 (ppm)

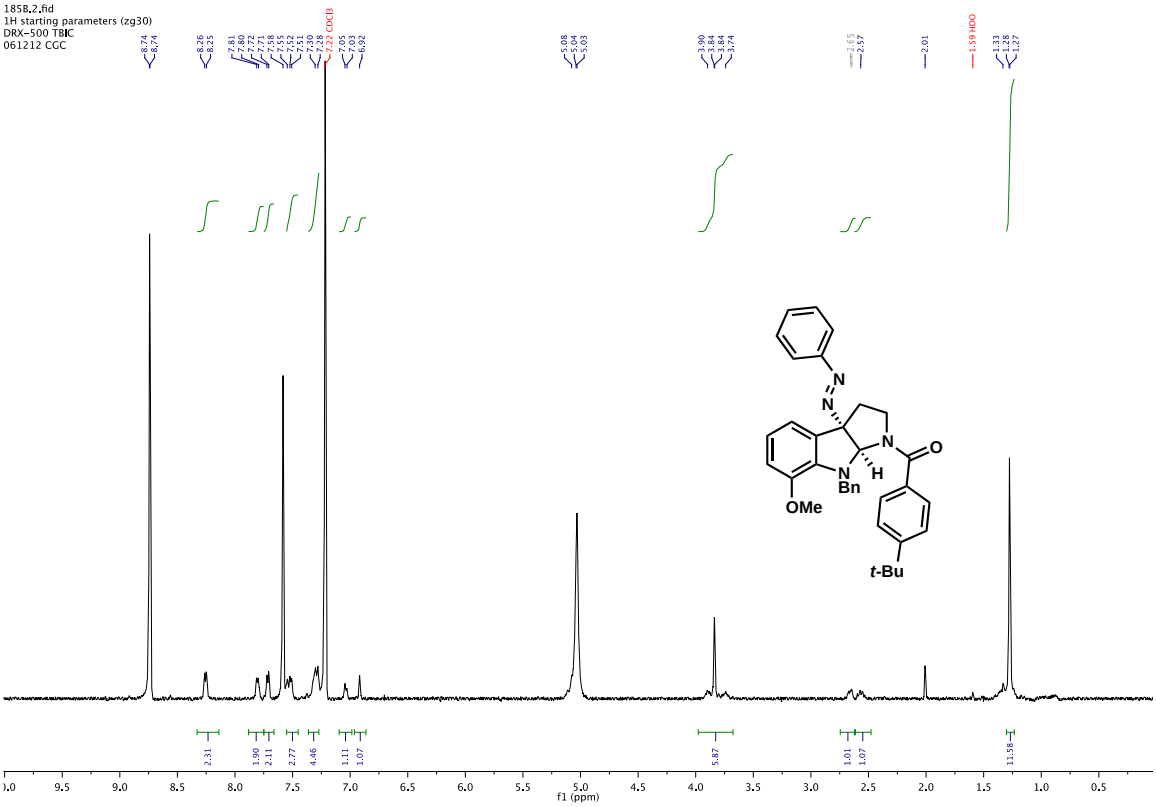
185B.2.fid
1H starting parameters (zg30)
DRX-500 TBIC
061212 CGC
8.74
8.74
8.26
8.25
7.81
7.80
7.77
7.77
7.72
7.58
7.55
7.52
7.51
7.30
7.28
7.22 CDCl3
7.05
7.03
6.92
5.08
5.04
5.03
3.90
3.88
3.84
3.74
2.65
2.57
2.01
1.59 H2O
1.33
1.28
1.27
2.31
1.90
2.11
2.77
4.46
1.11
1.07
5.87
1.01
1.07
11.58
f1 (ppm)
N
N
N
O
N
H
Bn
OMe
t-Bu

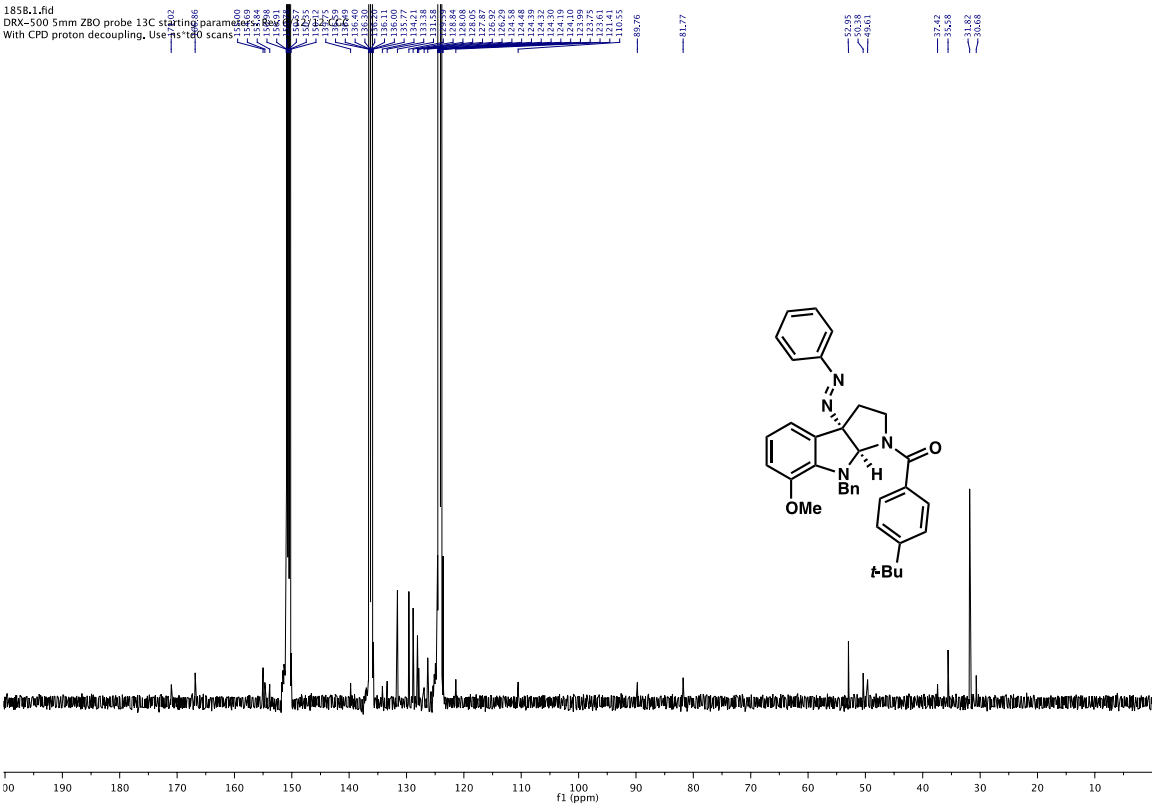
185B.1.fid
DRX-500 5mm ZBO probe 13C starting parameters (zgpg30)
With CPD proton decoupling. Use ns*ta0 scans
89.76
81.77
52.95
50.38
49.01
37.42
35.58
31.82
30.48
f1 (ppm)
N
N
N
O
N
H
Bn
OMe
t-Bu

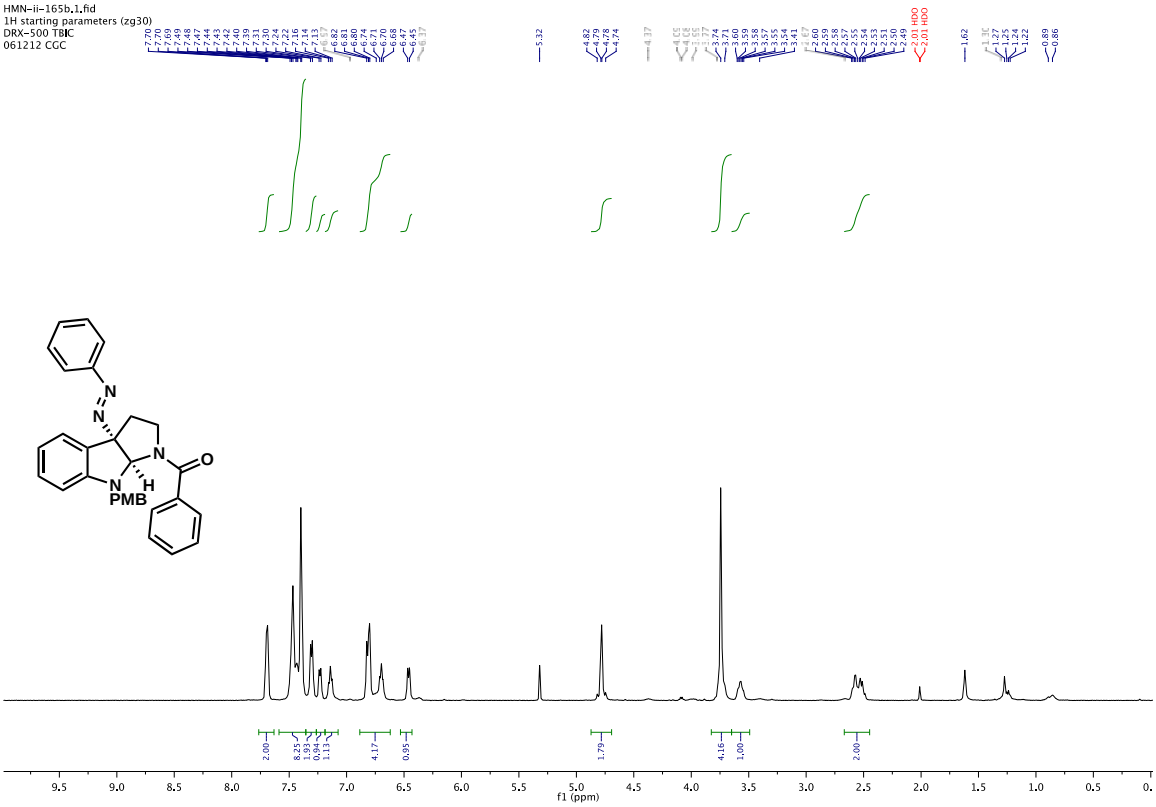
HMN-ii-165b.1.fid
1H starting parameters (zg30)
DRX-500 TBIC
061212 CGC
f1 (ppm)

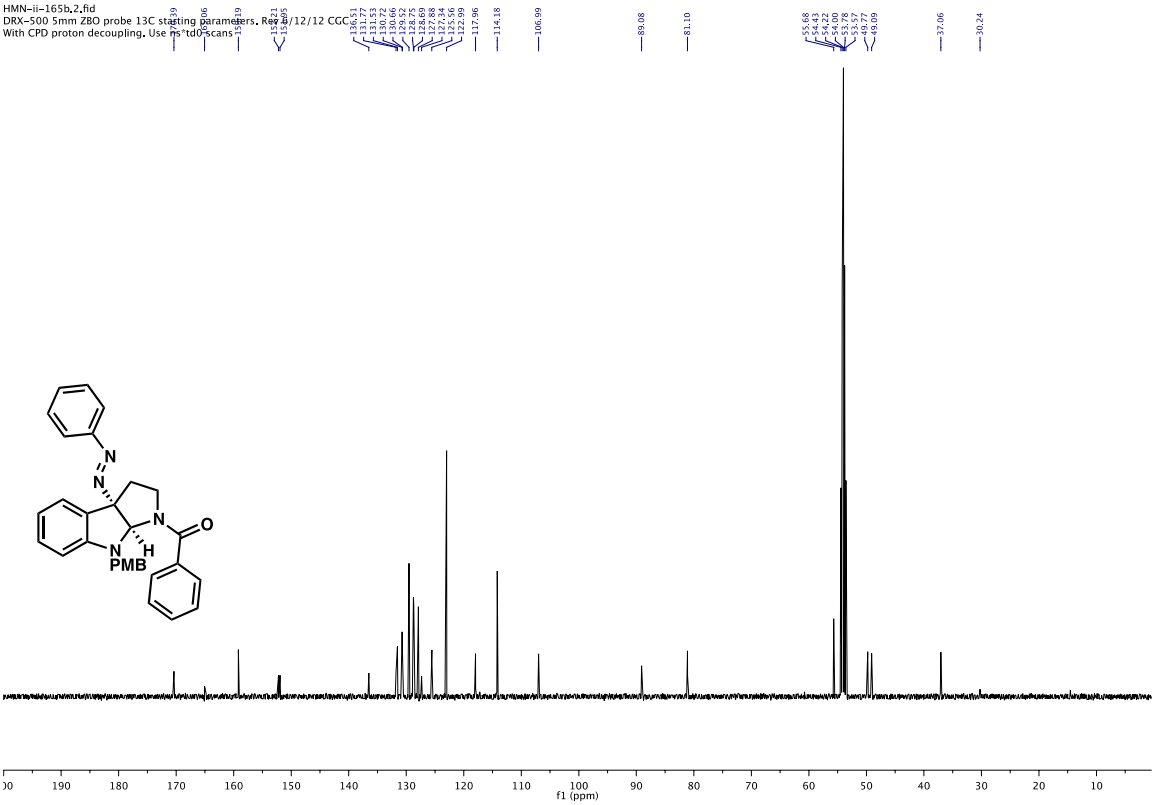
HMN-ii-165b.2.fid
DRX-500 5mm ZBO probe 13C starting parameters. Rev. 061212 CGC
With CPD proton decoupling. Use ns*td0 scans
f1 (ppm)

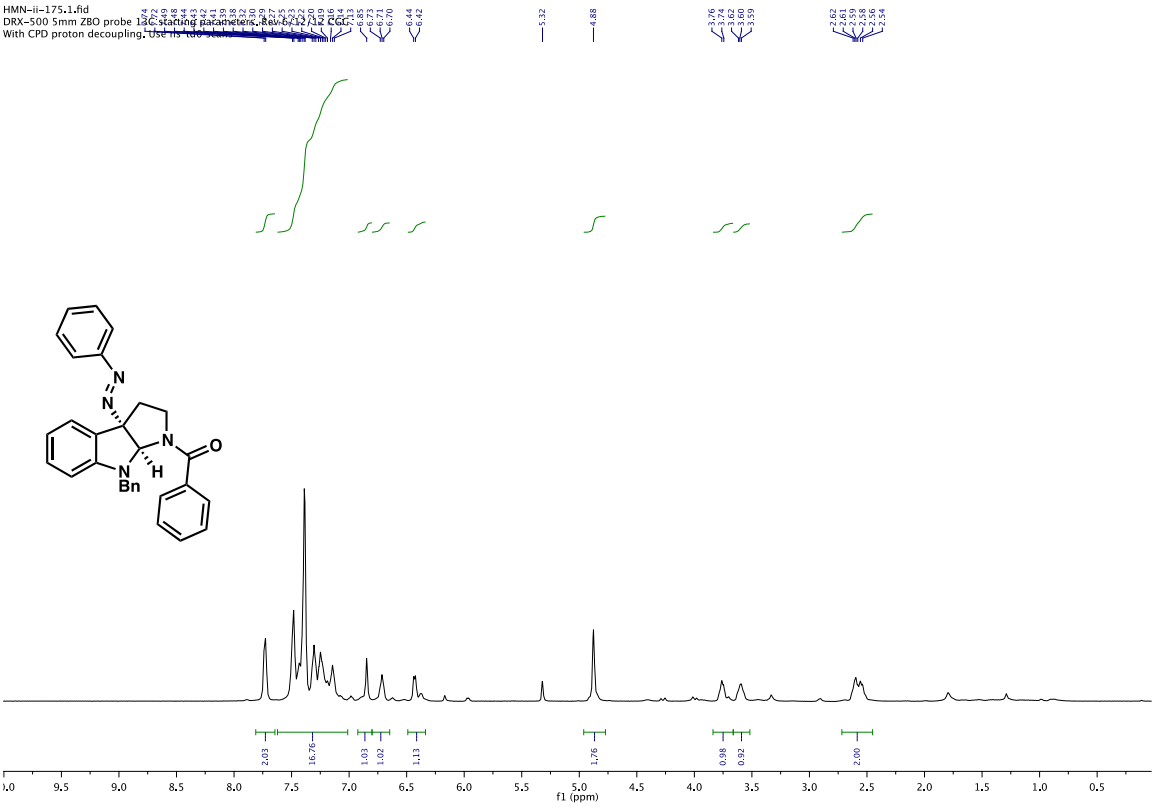
HMN-ii-175.1.fid
DRX-500 5mm ZBO probe 13C starting parameters. Rev 6/12/12 CGC
With CPD proton decoupling. Use ns*td0 scans
f1 (ppm)

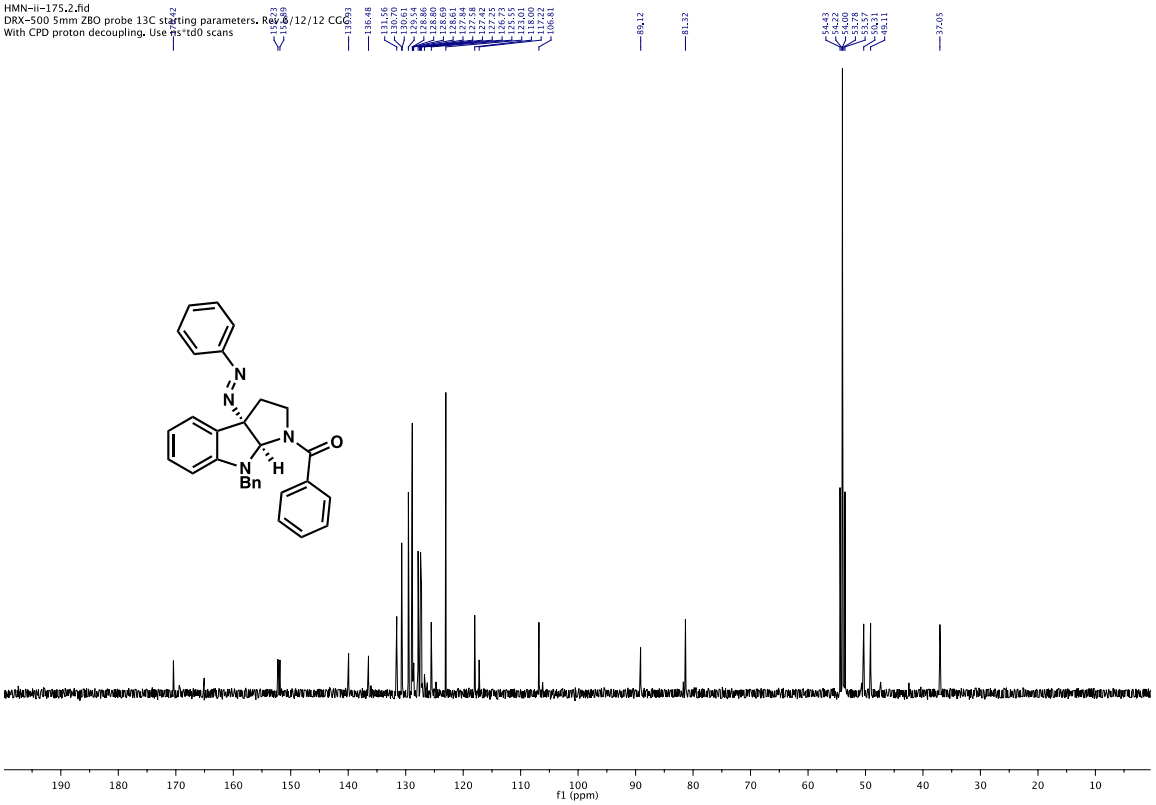
HMN-ii-175.2.fid
DRX-500 5mm ZBO probe 13C starting parameters. Rev 6/12/12 CGC
With CPD proton decoupling. Use ns*td0 scans
f1 (ppm)

HMN-ii-119b.1.fid
1H starting parameters (zg30)
DRX-500 TBIC
061212 CGC

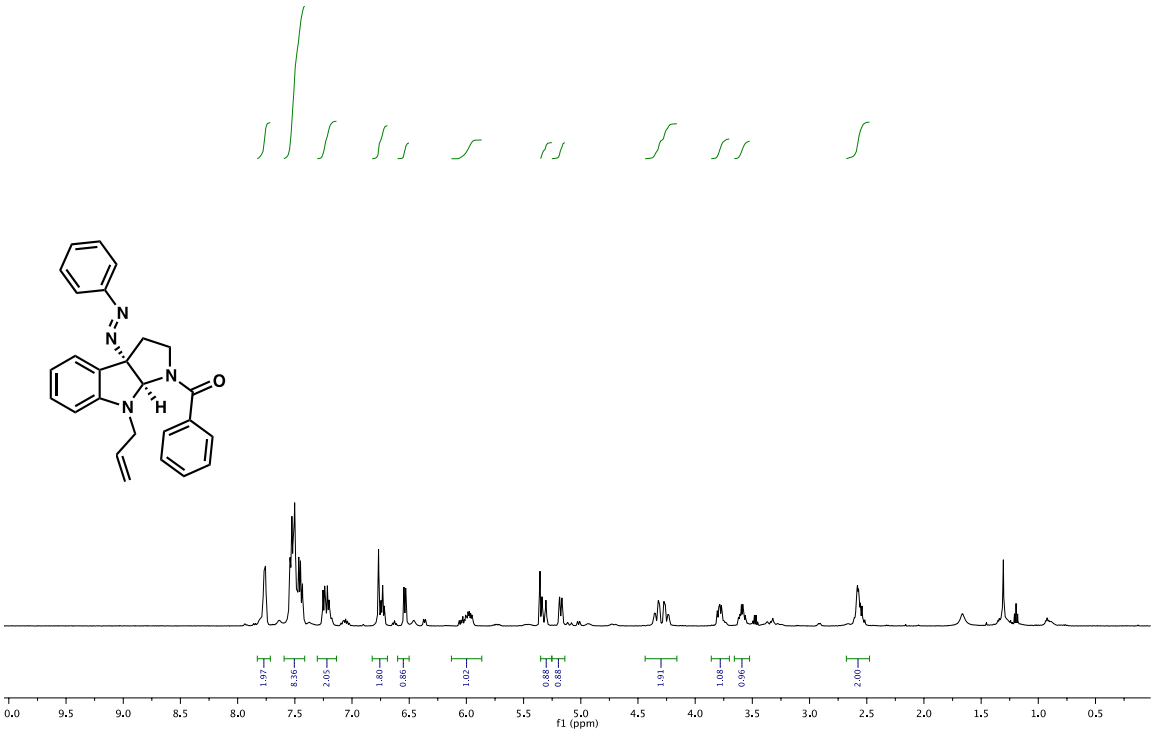

HMN-ii-119b.2.fid
DRX-500 5mm ZBO probe 13C starting parameters. Rev. 2/12/12 CGC
With CPD proton decoupling. Use ns *tdo scans

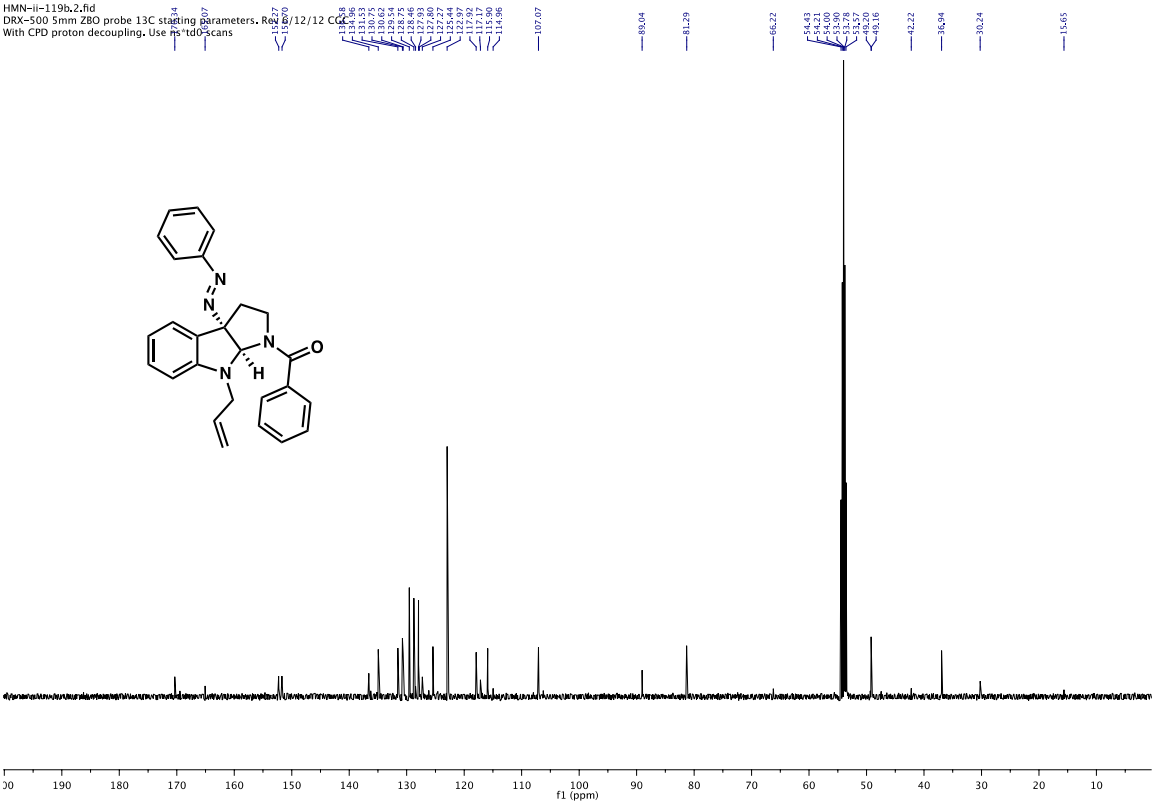

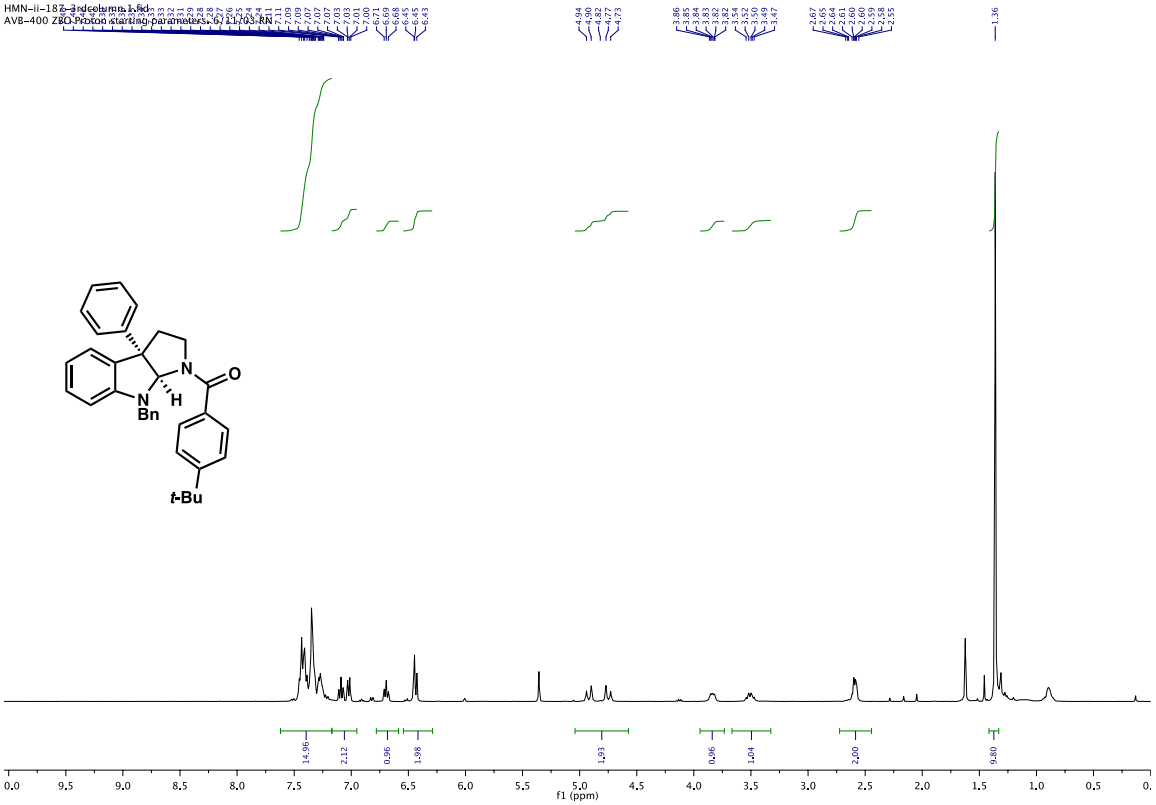
HMN-ii-187-3rdcolumn.1.fid
AVB-400 ZBO Proton starting parameters 6/11/03 RN
1.36
14.96
2.12
0.96
0.96
1.98
1.93
0.96
1.04
2.00
9.80
f1 (ppm)
N
O
N
H
Bn
t-Bu

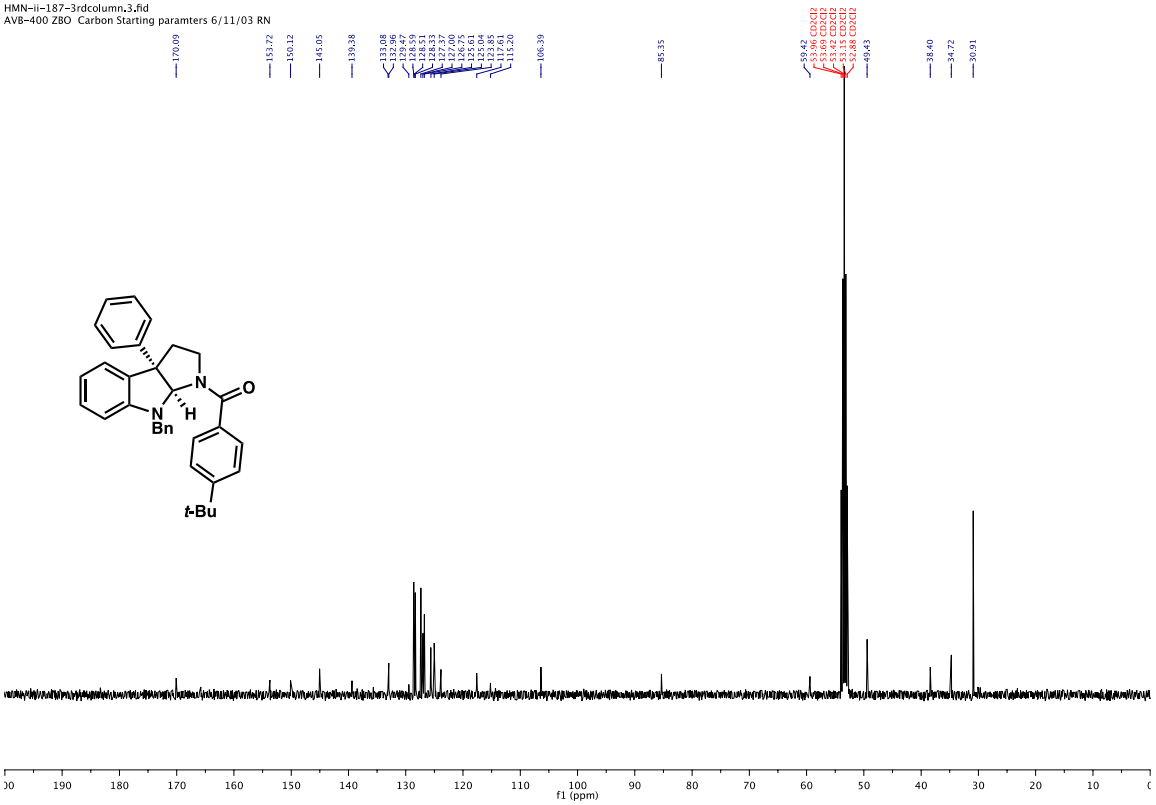
HMN-ii-187-3rdcolumn.3.fid
AVB-400 ZBO Carbon Starting paramters 6/11/03 RN
170.09
153.72
150.12
145.05
139.38
133.08
130.96
129.47
128.59
128.51
128.33
127.37
127.00
126.75
125.61
125.04
123.85
117.81
115.20
106.39
85.35
59.42
53.96 CDCl2
53.69 CDCl2
53.42 CDCl2
53.15 CDCl2
52.88 CDCl2
49.43
38.40
34.72
30.91
f1 (ppm)
N
O
N
H
Bn
t-Bu

HPLC traces

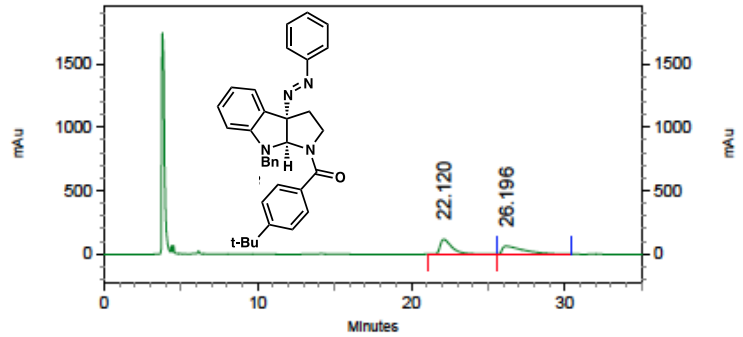

2: 260 nm, 4 nm Results

Retention Time	Area	Area Percent	Lambda Max
22.120	6316275	50.544	204
26.196	6180277	49.456	204

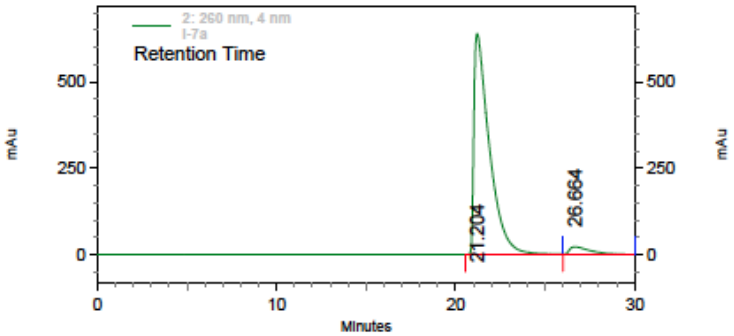

2: 260 nm, 4 nm Results

Retention Time	Area	Area Percent	Lambda Max
21.204	38505911	95.502	206
26.664	1813385	4.498	205

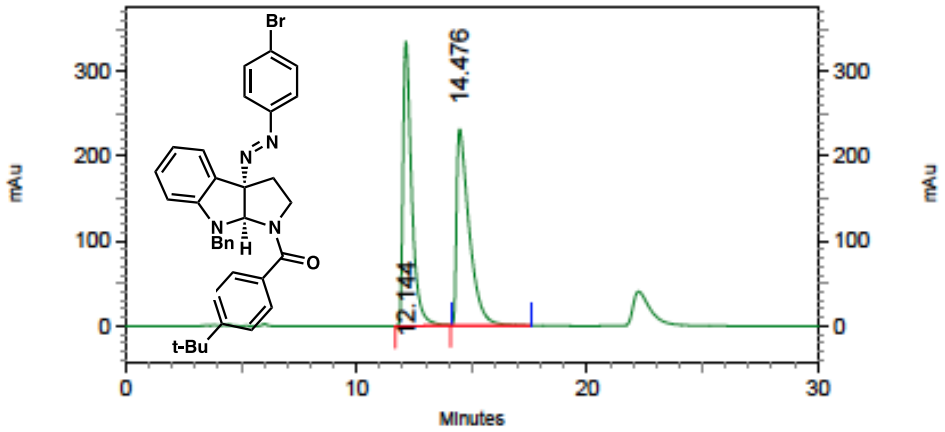

2: 260 nm, 4 nm Results

Retention Time	Area	Area Percent	Lambda Max
12.144	8807005	50.020	206
14.476	8799787	49.980	206

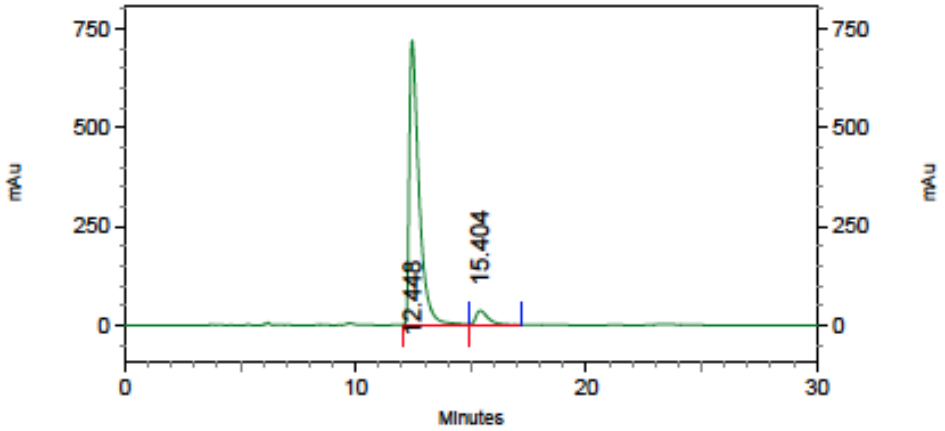

2: 260 nm, 4 nm Results

Retention Time	Area	Area Percent	Lambda Max
12.448	21091116	94.110	207
15.404	1320011	5.890	206

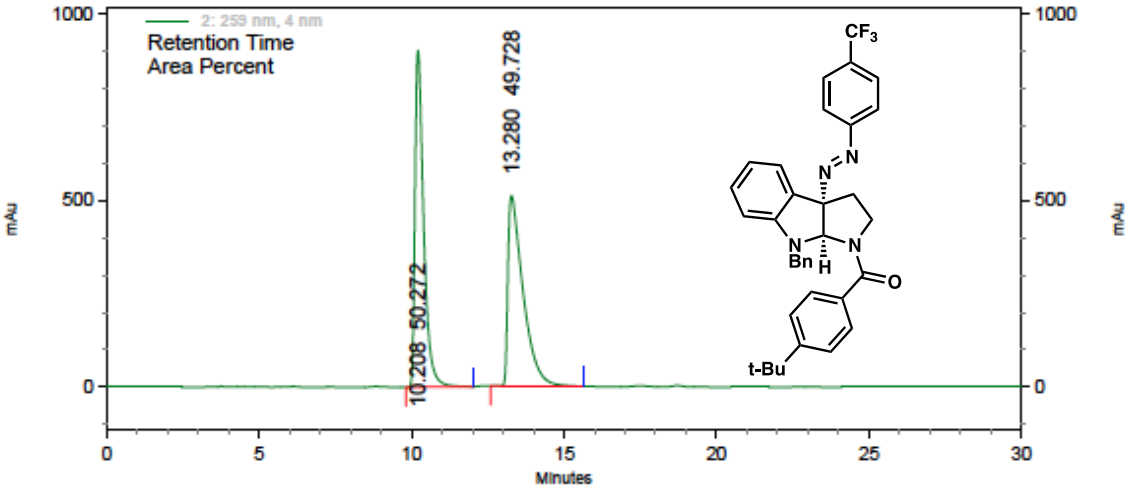

2: 259
nm, 4
nm
Results

Pk #	Retention Time	Area	Area Percent	Lambda Max
1	10.208	17855081	50.272	207
2	13.280	17661687	49.728	207

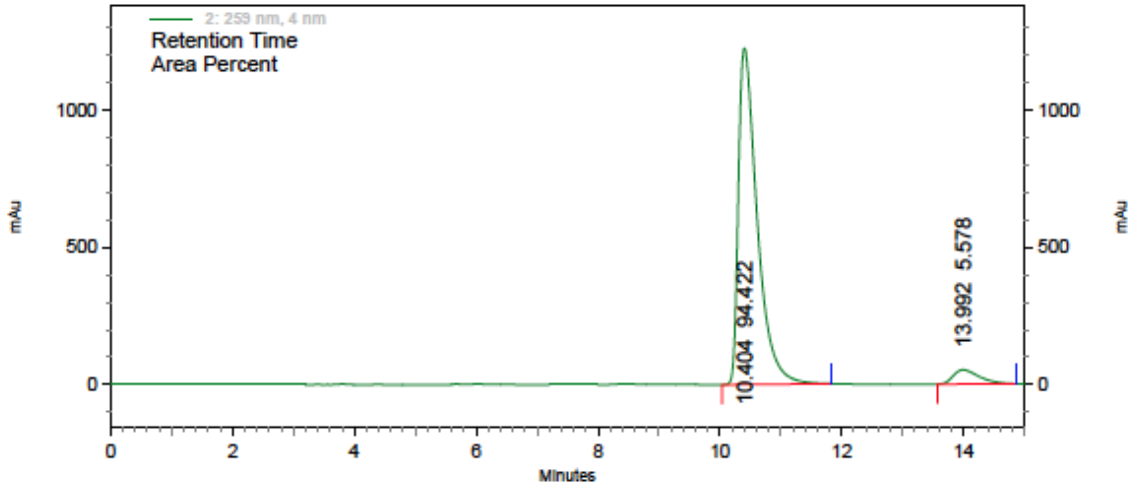

2: 259
nm, 4
nm
Results

Pk #	Retention Time	Area	Area Percent	Lambda Max
1	10.404	26176166	94.422	209
2	13.992	1546483	5.578	206

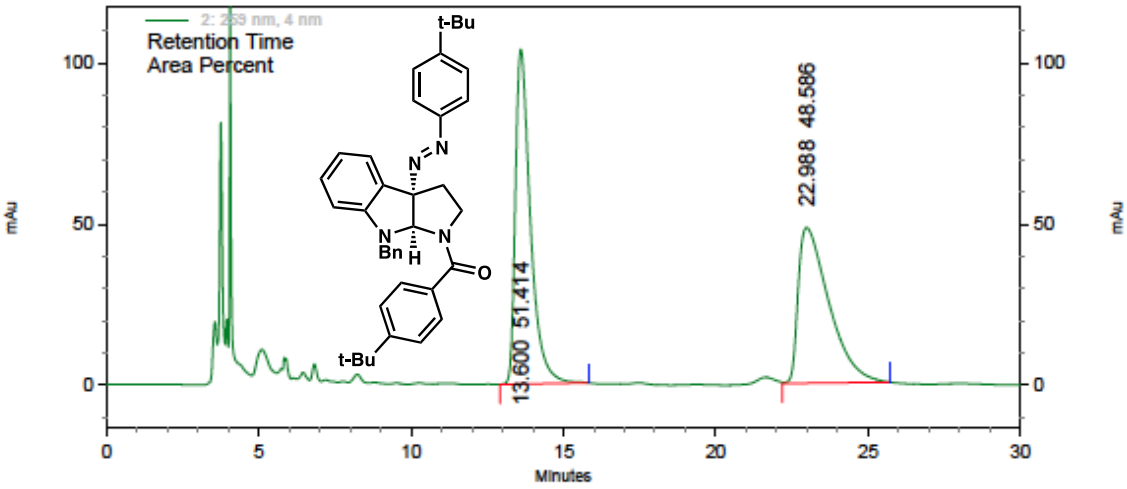

2: 259
nm, 4
nm
Results

Pk #	Retention Time	Area	Area Percent	Lambda Max
1	13.600	3584506	51.414	205
2	22.988	3387369	48.586	205

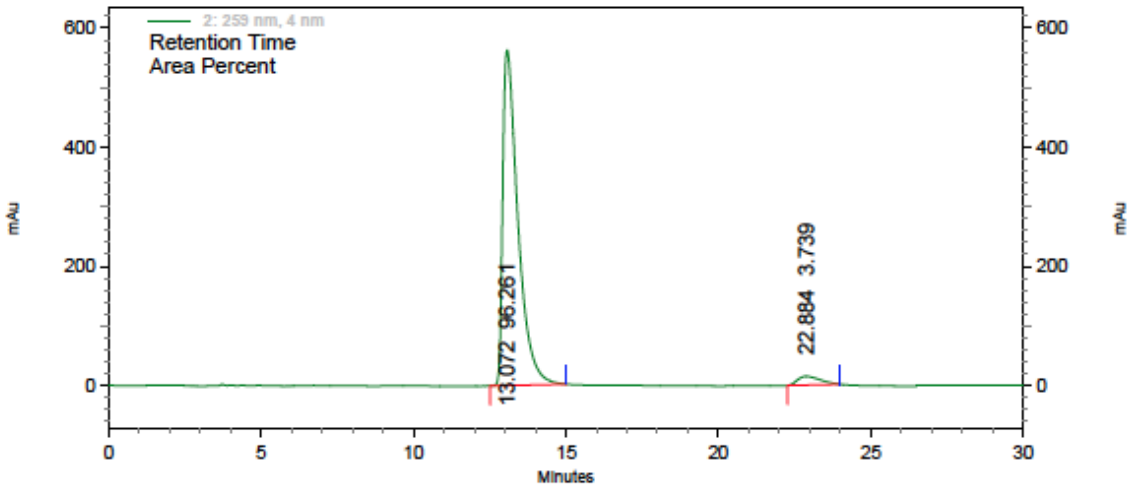

2: 259
nm, 4
nm
Results

Pk #	Retention Time	Area	Area Percent	Lambda Max
1	13.072	19496513	96.261	206
2	22.884	757254	3.739	205

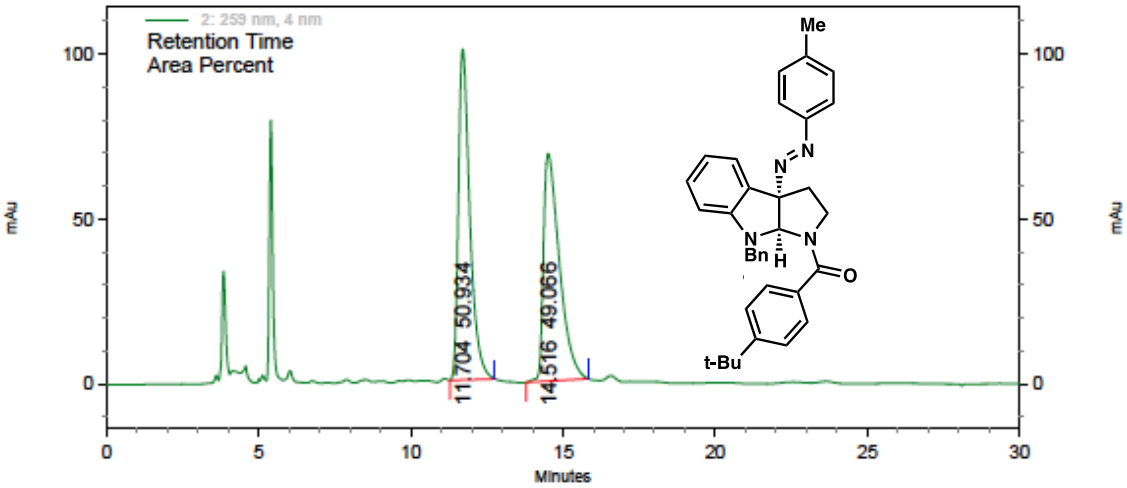

2: 259
nm, 4
nm
Results

Pk #	Retention Time	Area	Area Percent	Lambda Max
1	11.704	2614780	50.934	206
2	14.516	2518871	49.066	206

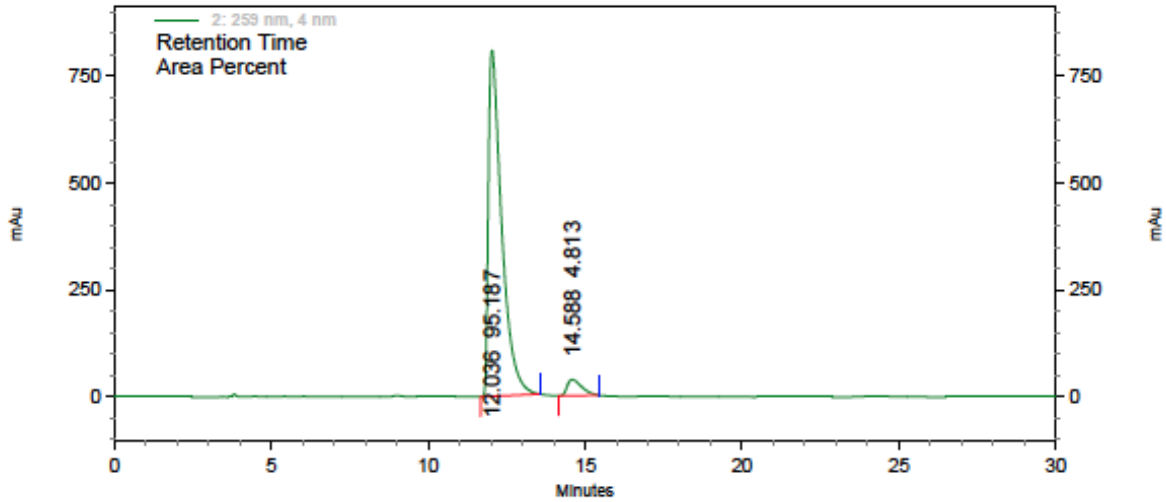

2: 259
nm, 4
nm
Results

Pk #	Retention Time	Area	Area Percent	Lambda Max
1	12.036	23835140	95.187	207
2	14.588	1205244	4.813	206

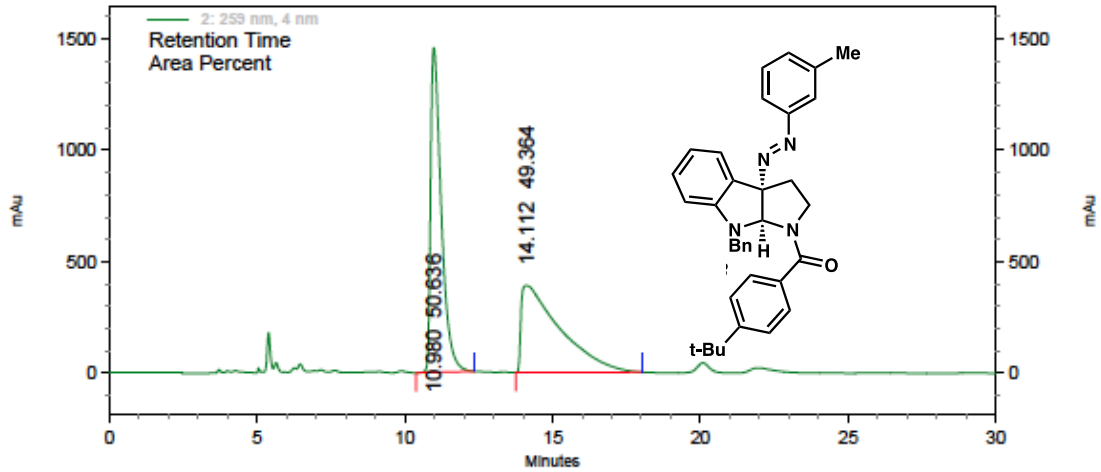

2: 259
nm, 4
nm
Results

Pk #	Retention Time	Area	Area Percent	Lambda Max
1	10.980	36542873	50.636	208
2	14.112	35625010	49.364	207

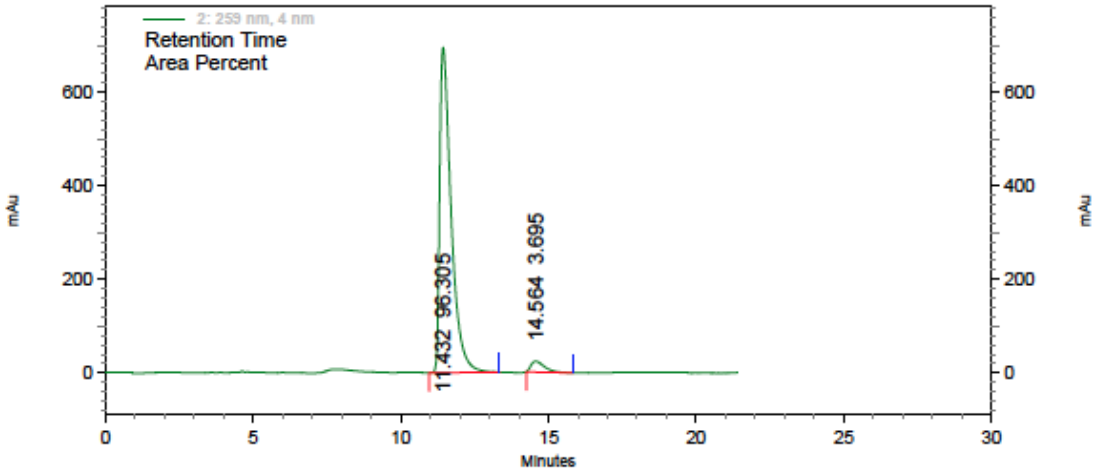

2: 259
nm, 4
nm
Results

Pk #	Retention Time	Area	Area Percent	Lambda Max
1	11.432	18801723	96.305	207
2	14.564	721339	3.695	206

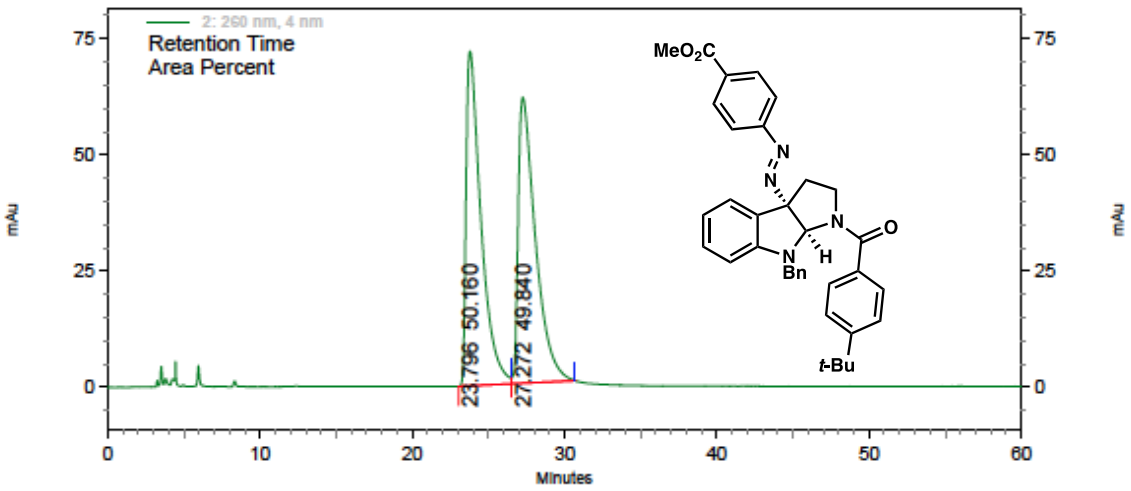

2: 260
nm, 4
nm

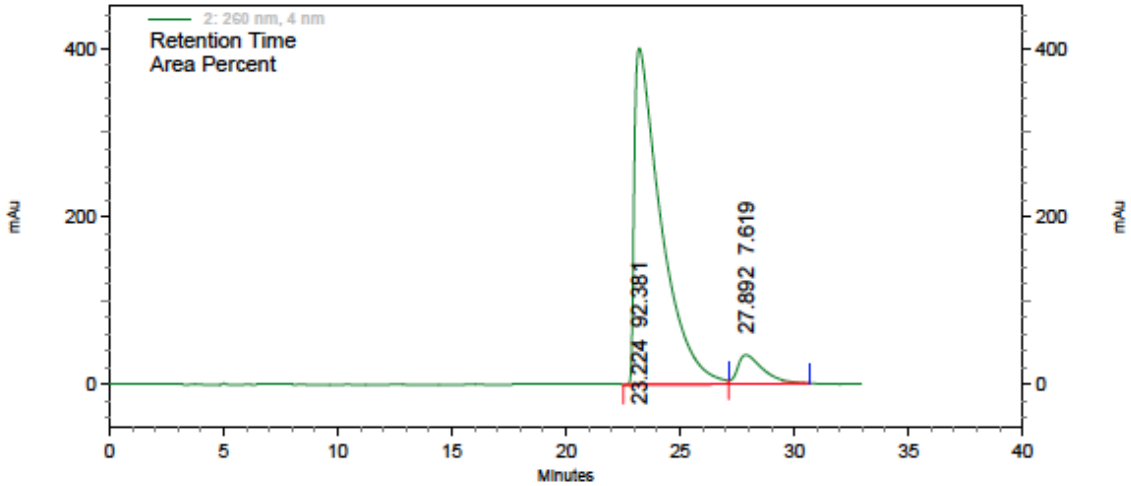

2: 260
nm, 4
nm
Results

Pk #	Retention Time	Area	Area Percent	Lambda Max
1	23.224	32537856	92.381	207
2	27.892	2683649	7.619	206

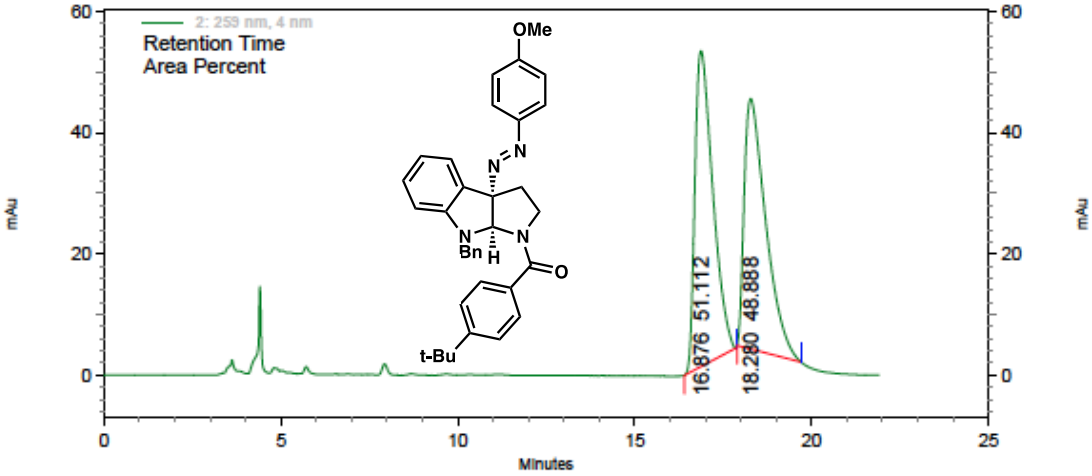

2: 259
nm, 4
nm
Results

Pk #	Retention Time	Area	Area Percent	Lambda Max
1	16.876	1833504	51.112	206
2	18.280	1753709	48.888	206

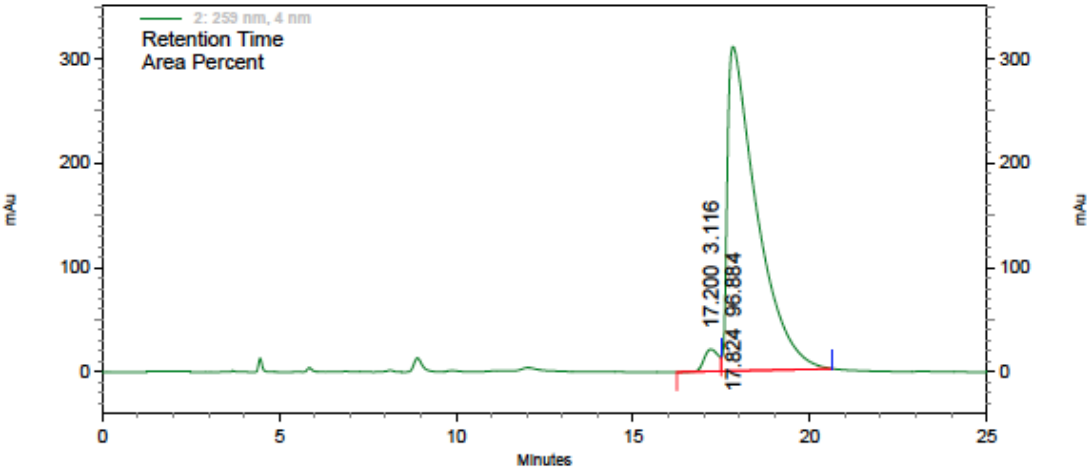

2: 259
nm, 4
nm
Results

Pk #	Retention Time	Area	Area Percent	Lambda Max
1	17.200	578774	3.116	206
2	17.824	17993450	96.884	207

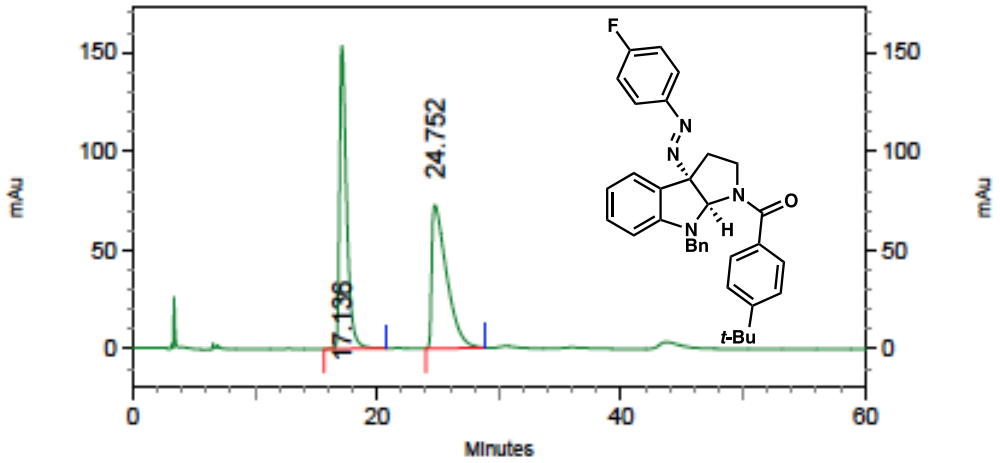

1: 260 nm, 4 nm Results

Retention Time	Area	Area Percent	Lambda Max
17.136	6184611	50.148	200
24.752	6148019	49.852	200

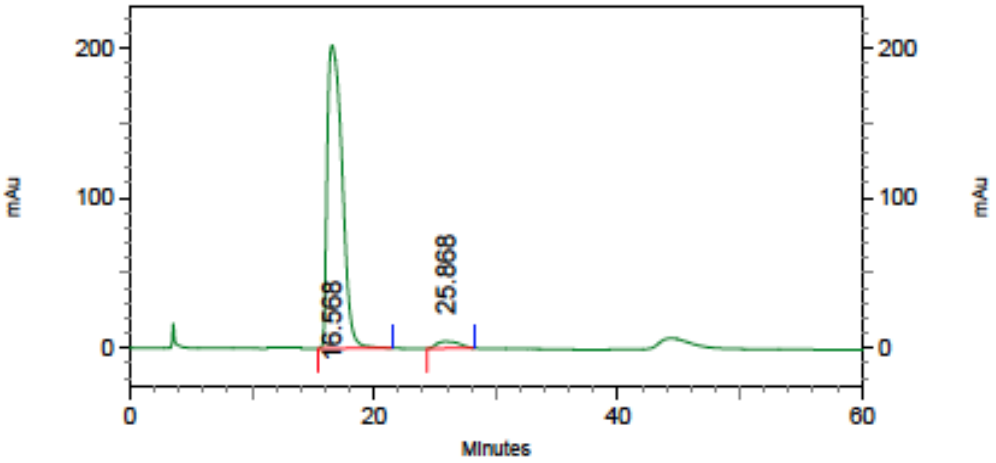

1: 260 nm, 4 nm Results

Retention Time	Area	Area Percent	Lambda Max
16.568	17162412	96.646	200
25.868	595653	3.354	205

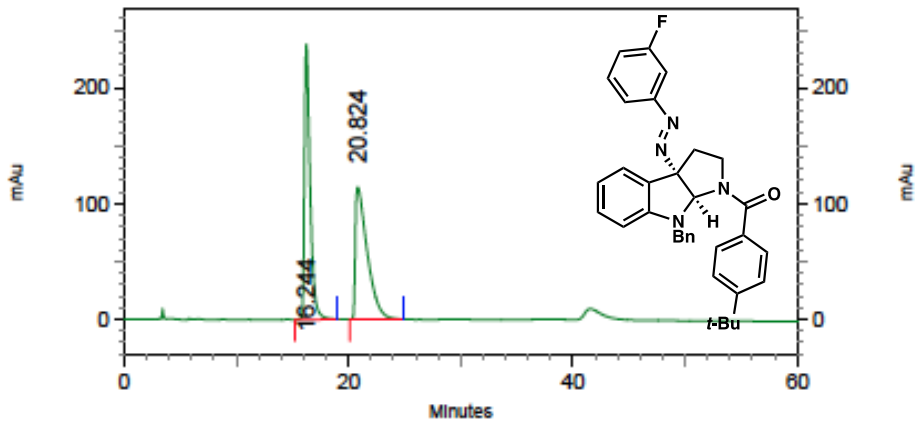

1: 260 nm, 4 nm Results

Retention Time	Area	Area Percent	Lambda Max
16.244	8402440	49.809	201
20.824	8466894	50.191	201

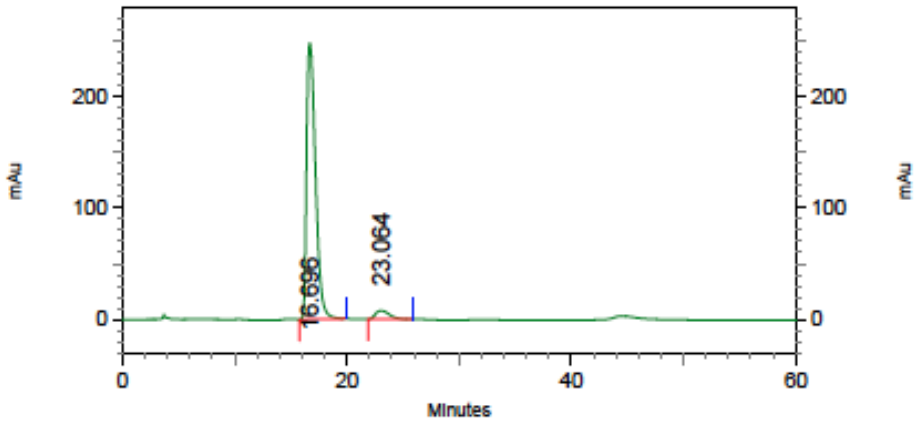

1: 260 nm, 4 nm Results

Retention Time	Area	Area Percent	Lambda Max
16.696	13653398	95.417	200
23.064	655849	4.583	200

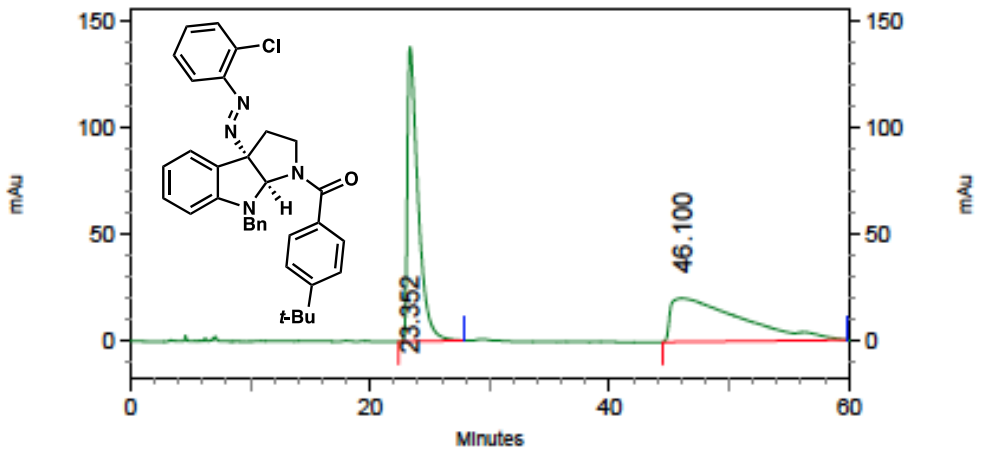

3: 288 nm, 4 nm Results

Retention Time	Area	Area Percent	Lambda Max
23.352	8545996	50.401	201
46.100	8410104	49.599	201

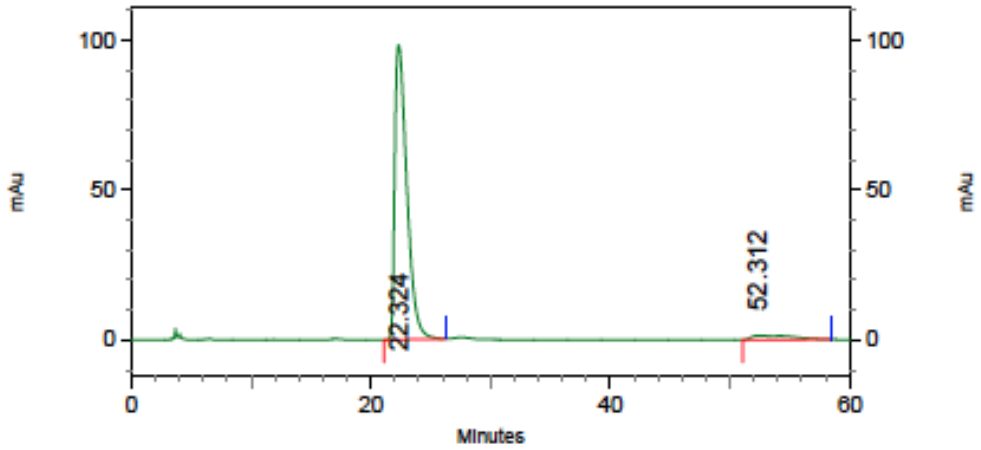

3: 288 nm, 4 nm Results

Retention Time	Area	Area Percent	Lambda Max
22.324	6876351	95.530	201
52.312	321723	4.470	200

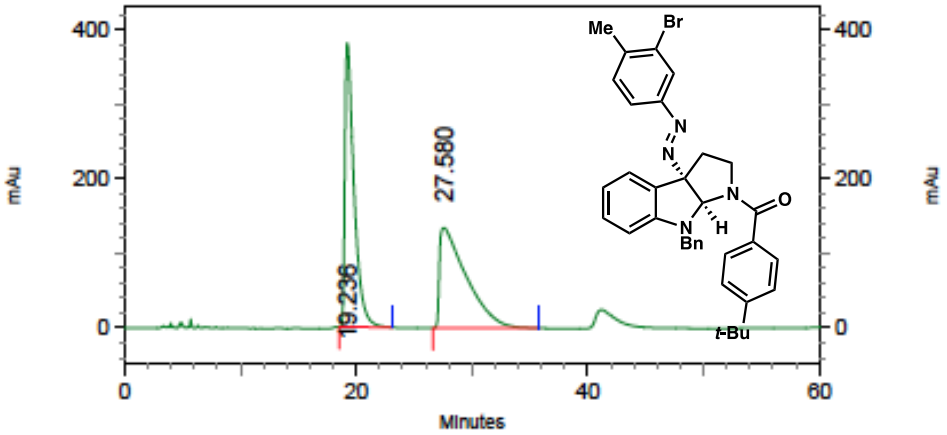

1: 260 nm, 4 nm Results

Retention Time	Area	Area Percent	Lambda Max
19.236	20944168	49.212	200
27.580	21614974	50.788	200

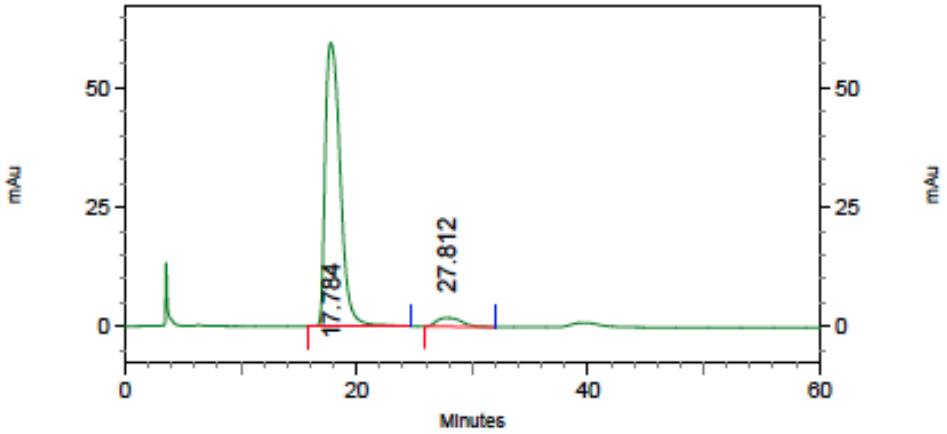

1: 260 nm, 4 nm Results

Retention Time	Area	Area Percent	Lambda Max
17.784	5355126	95.164	201
27.812	272149	4.836	206

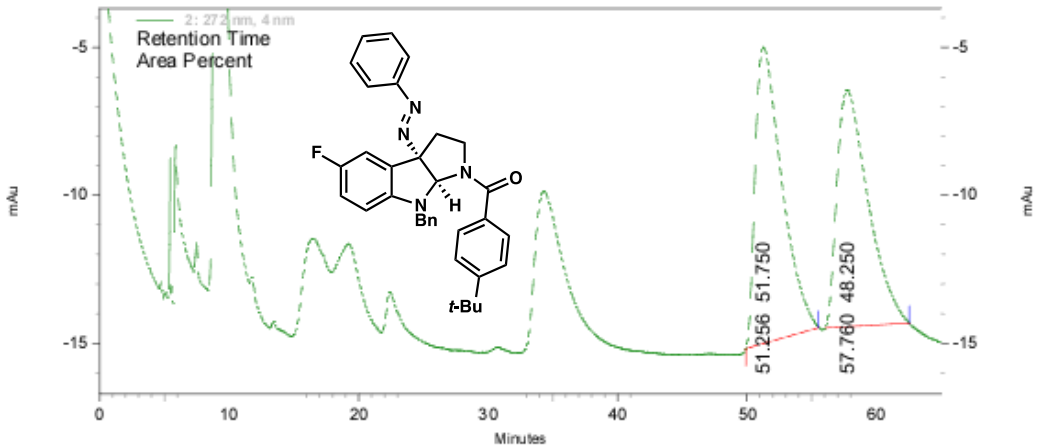

2: 272 nm, 4 nm
Results

Pk #	Retention Time	Area Percent	Lambda Max
1	51.256	51.750	202
2	57.760	48.250	202

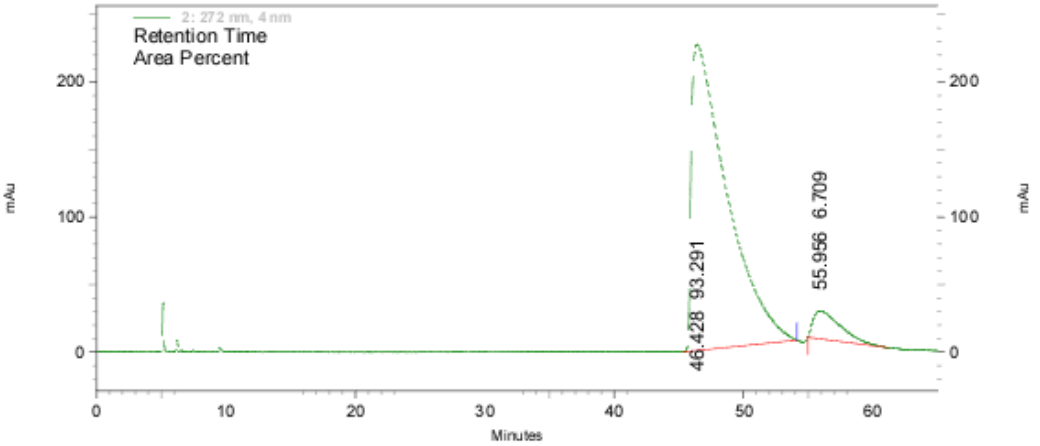

2: 272 nm, 4 nm
Results

Pk #	Retention Time	Area Percent	Lambda Max
1	46.428	93.291	249
2	55.956	6.709	203

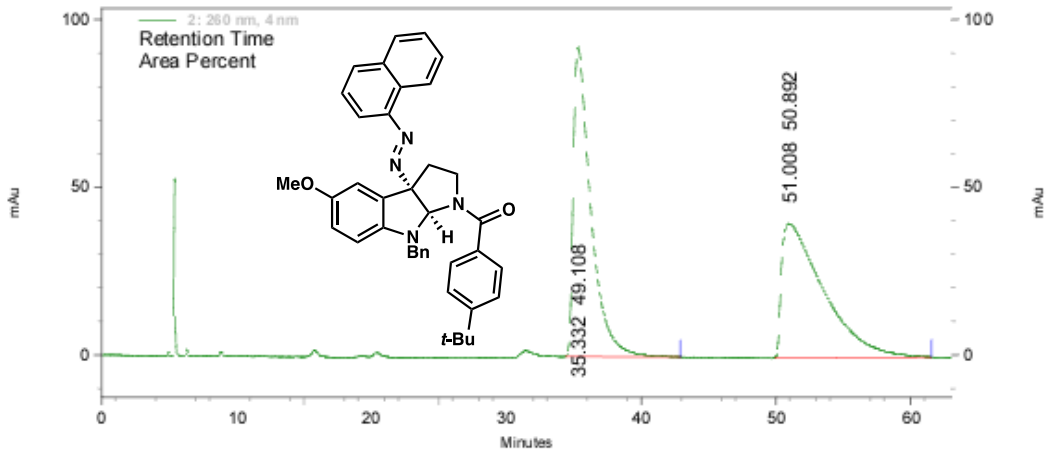

2: 260 nm, 4 nm
Results

Pk #	Retention Time	Area Percent	Lambda Max
1	35.332	49.108	243
2	51.008	50.892	213

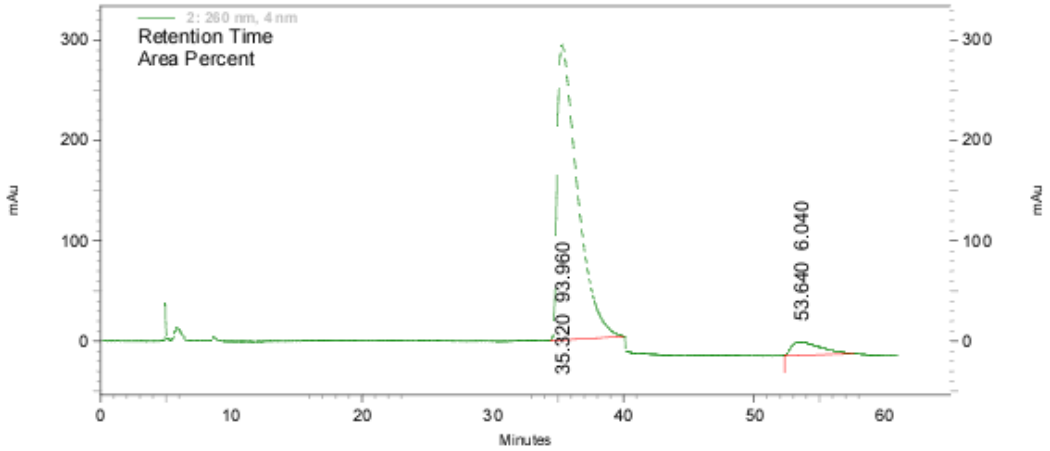

2: 260 nm, 4 nm
Results

Pk #	Retention Time	Area Percent	Lambda Max
1	35.320	93.960	199
2	53.640	6.040	212

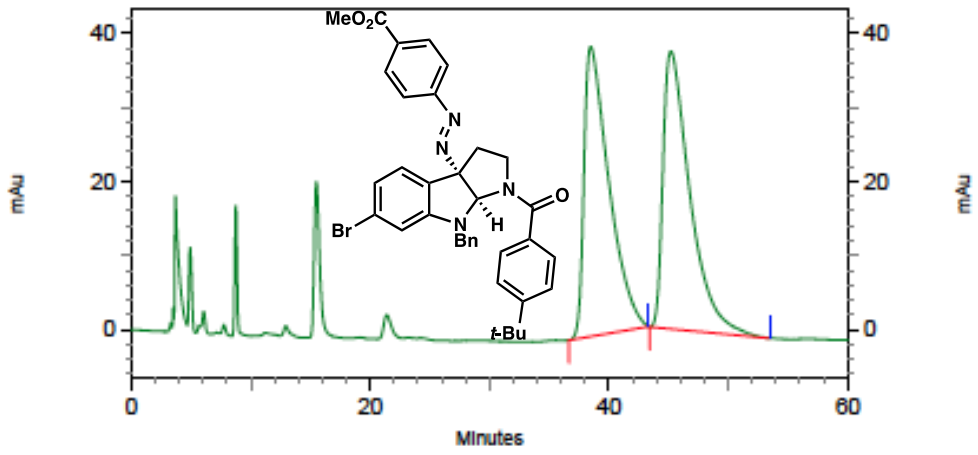

1: 260 nm, 4 nm Results

Retention Time	Area	Area Percent	Lambda Max
38.468	5670283	49.090	198
45.196	5880573	50.910	199

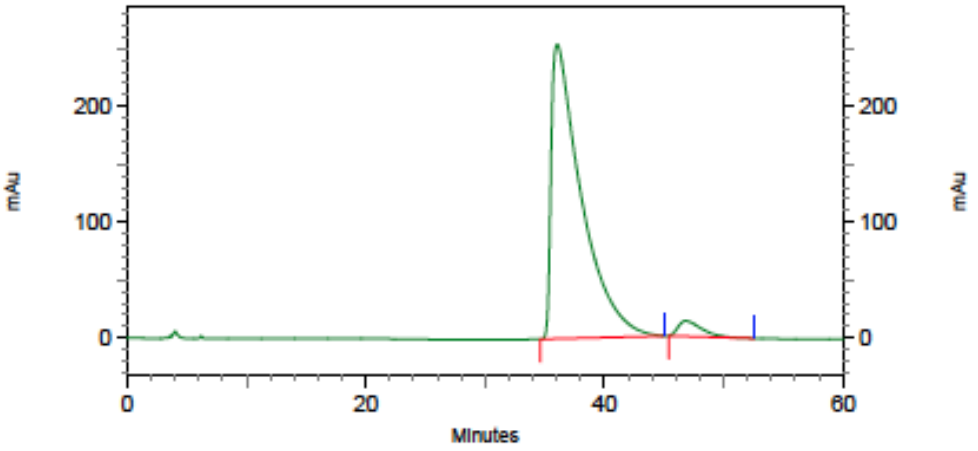

1: 260 nm, 4 nm Results

Retention Time	Area	Area Percent	Lambda Max
36.052	44456874	96.048	199
46.848	1829156	3.952	205

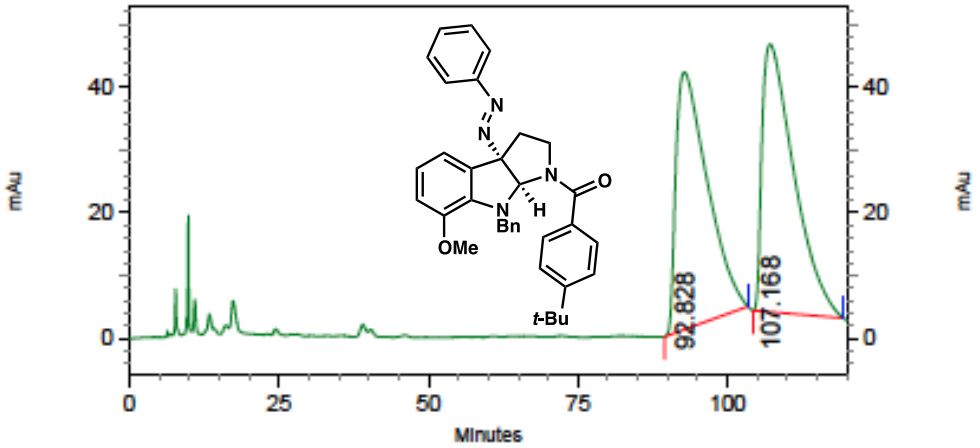

1: 259 nm, 4 nm Results

Retention Time	Area	Area Percent	Lambda Max
92.828	14998304	48.685	197
107.168	15808275	51.315	197

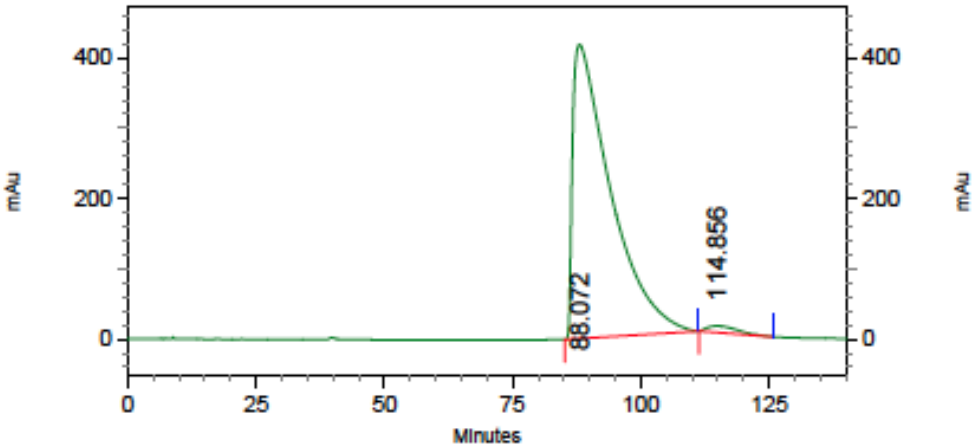

1: 259 nm, 4 nm Results

Retention Time	Area	Area Percent	Lambda Max
88.072	216051561	98.245	197
114.856	3858445	1.755	196

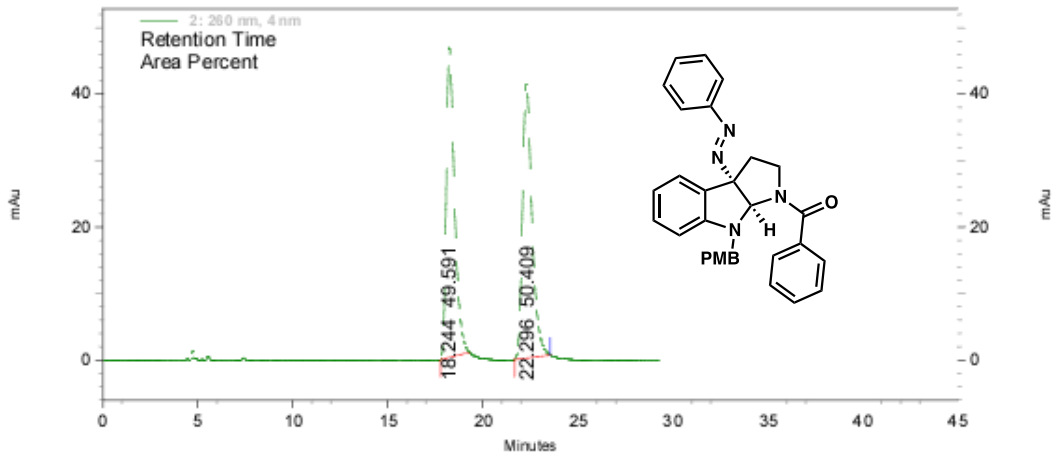

2: 260 nm, 4 nm
Results

Pk #	Retention Time	Area Percent	Lambda Max
1	18.244	49.591	203
2	22.296	50.409	203

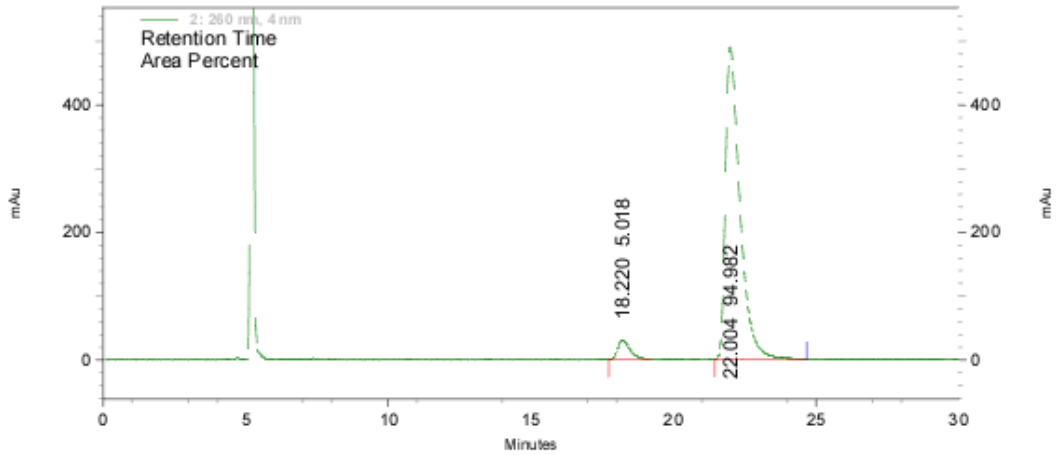

2: 260 nm, 4 nm
Results

Pk #	Retention Time	Area Percent	Lambda Max
1	18.220	5.018	204
2	22.004	94.982	198

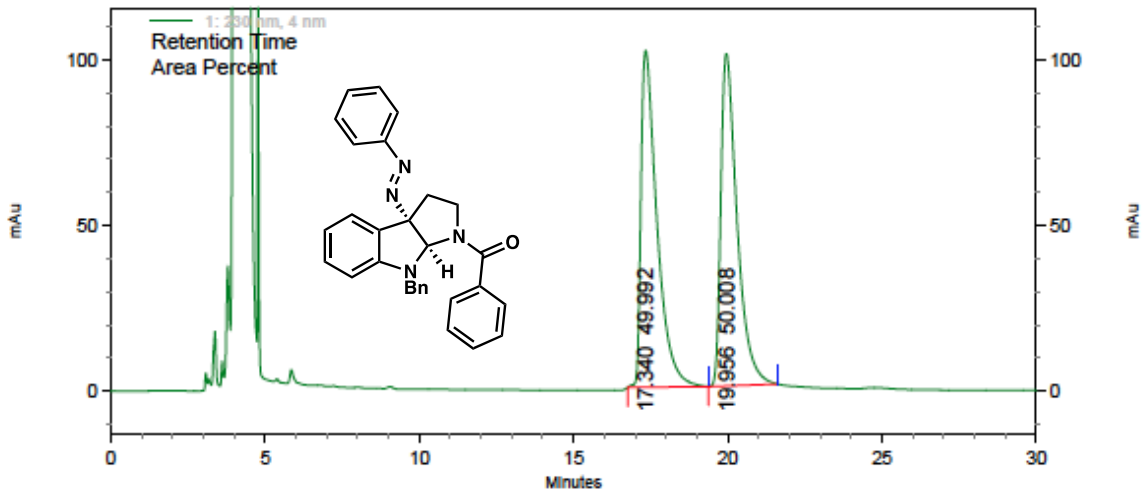

1: 230 nm,
4 nm Results

Pk #	Retention Time	Area	Area Percent	Lambda Max
1	17.340	3666526	49.992	203
2	19.956	3667705	50.008	203

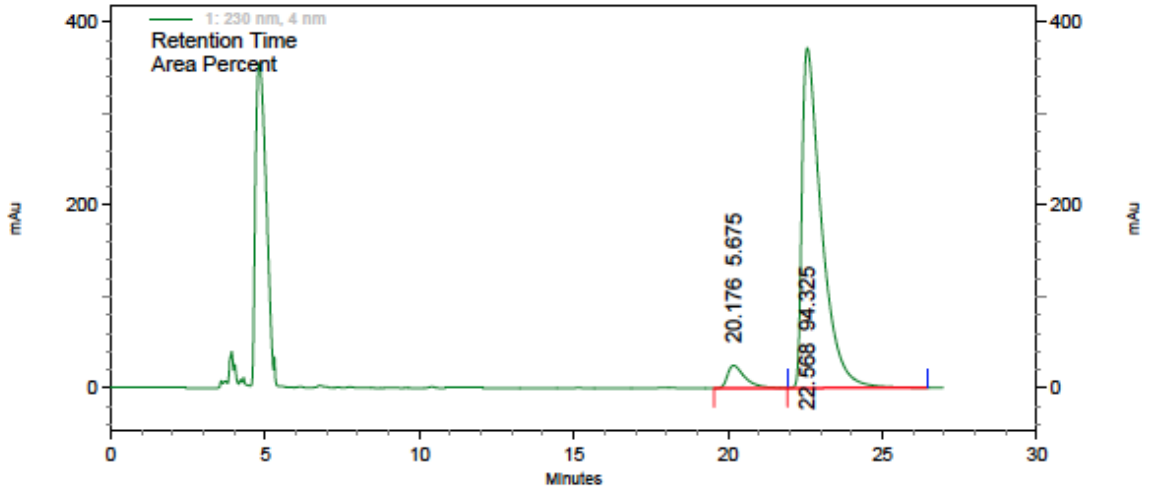

1: 230
nm, 4
nm
Results

Pk #	Retention Time	Area	Area Percent	Lambda Max
1	20.176	980710	5.675	205
2	22.568	16299679	94.325	197

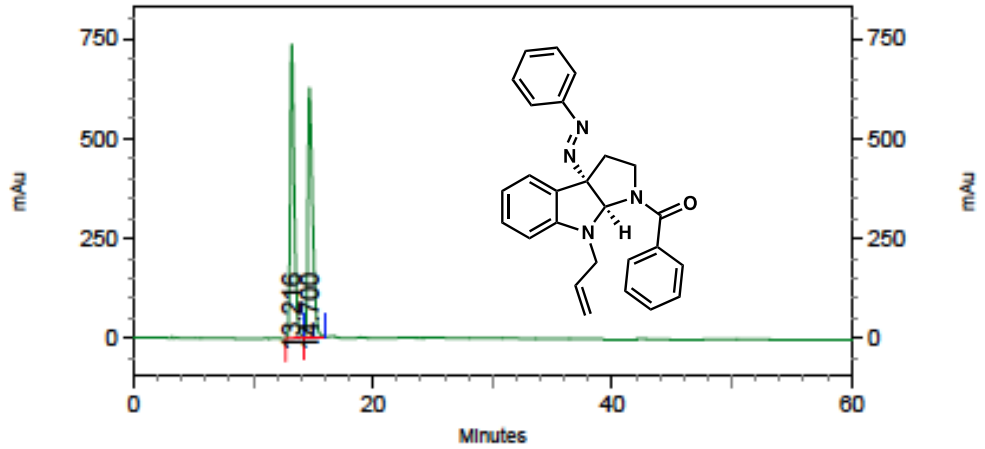

3: 260 nm, 4 nm Results

Retention Time	Area	Area Percent	Lambda Max
13.216	17196333	49.994	193
14.700	17200271	50.006	249

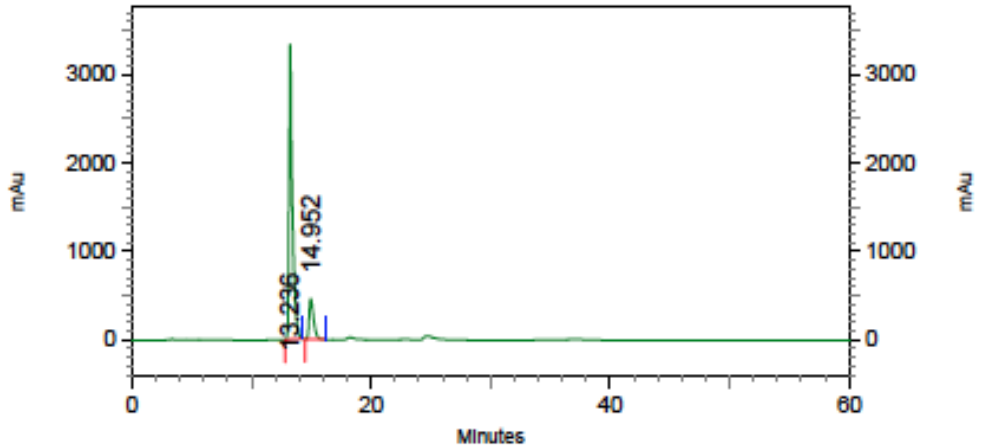

1: 260 nm, 4 nm Results

Retention Time	Area	Area Percent	Lambda Max
13.236	64271854	84.475	255
14.952	11811680	15.525	201

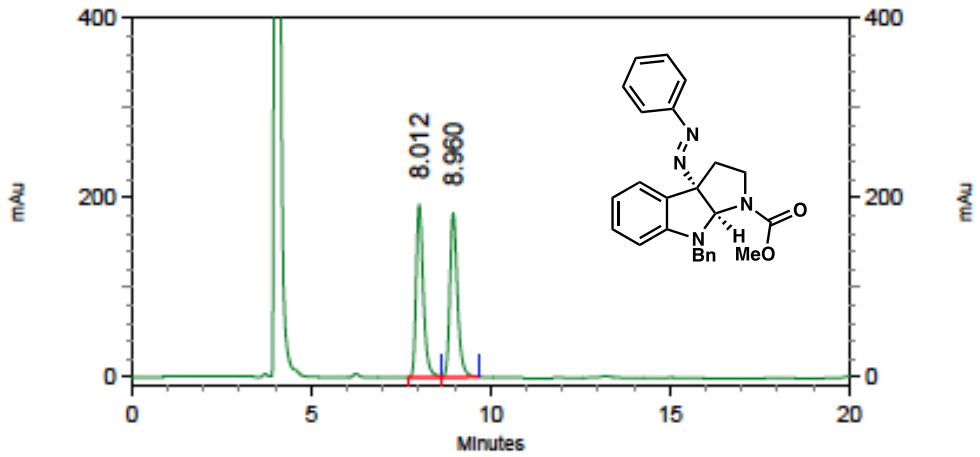

2: 260 nm, 4 nm Results

Pk #	Retention Time	Area	Area Percent	Lambda Max
1	8.012	2668090	49.807	207
2	8.960	2688785	50.193	207

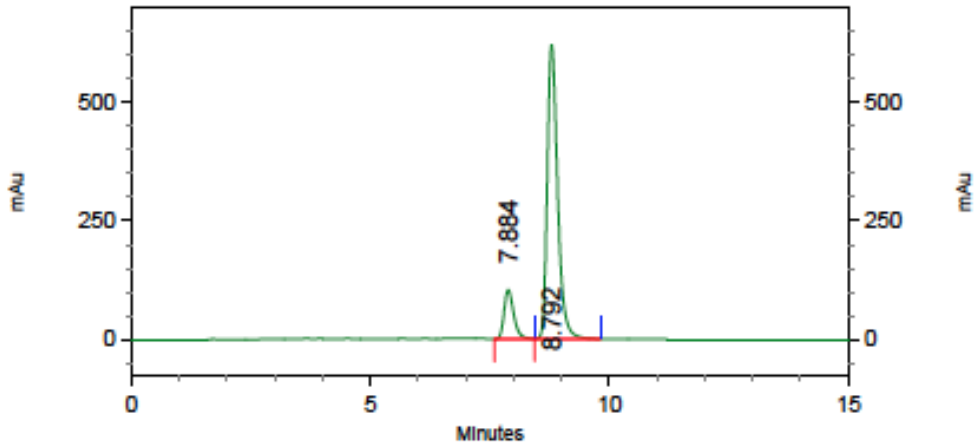

2: 260 nm, 4 nm Results

Pk #	Retention Time	Area	Area Percent	Lambda Max
1	7.884	1461730	13.546	207
2	8.792	9328984	86.454	207

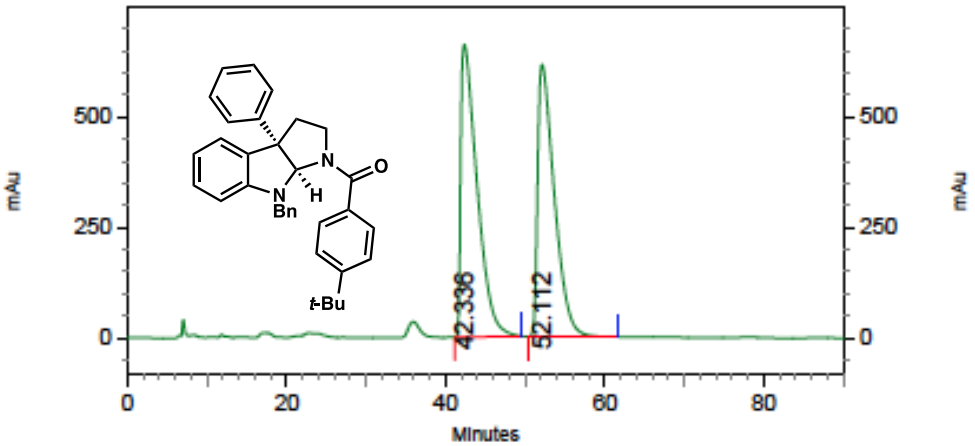

1: 220 nm, 4 nm Results

Retention Time	Area	Area Percent	Lambda Max
42.336	94401467	51.184	200
52.112	90033468	48.816	200

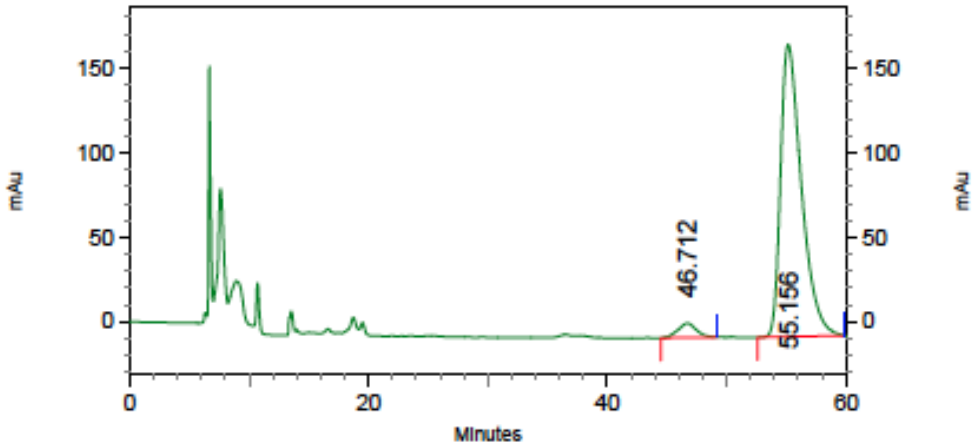

1: 220 nm, 4 nm Results

Retention Time	Area	Area Percent	Lambda Max
46.712	908713	4.151	653
55.156	20983573	95.849	200

Chapter 2. Enantioselective alpha-Amination Enabled by a BINAM-derived Phase-Transfer Catalyst

Chiral amines have notable applications as bioactive compounds, catalysts and ligands,[1] making their enantioselective synthesis a target for synthetic chemists. In this chapter, we report the asymmetric amination of ketone derivatives via chiral anion phase-transfer of aryldiazonium salts. These reactions provide high yields and enantioselectivities of the corresponding α-diazene compounds, which are easily reduced to afford enantioenriched β-hydroxy amino acid derivatives. Key to obtaining high levels of enantioinduction is the application of a new class of phase-transfer catalysts derived from 1,1'-binaphthalene-2,2'-diamine (BINAM). These catalysts were superior to our traditional library of BINOL-derived phosphoric acids. The scope of this transformation includes a variety of indanone-derived β-keto esters, benzosuberone-derived β-keto esters and β-keto amides.

Portions of this chapter are based on work done in collaboration with Hosea Nelson and Hunter Shunatona and appear in: *Chem. Sci*. **2014**, 6, 170. H.N. made key intellectual contributions and assisted with initial optimization experiments. H.S. contributed to substrate synthesis.

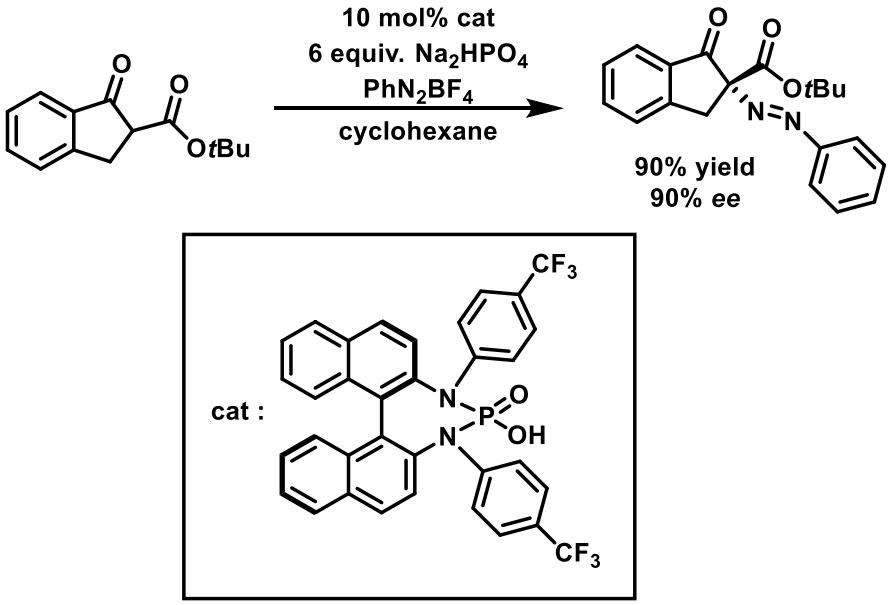

Introduction

Many synthetic efforts have focused on the enantioselective construction of C-N bonds, particularly towards the synthesis of enantiopure α-amino acids, which are prominently represented in pharmaceuticals, natural products, and agrochemicals.[2,3] The α-amination of ketone derivatives, typically employing dialkyl azodicarboxylates, is a commonly utilized method to access this scaffold.[4] This mode of reactivity was first discovered in 1954, when Huisgen and coworkers found that treatment of cyclohexanone with DEAD and catalytic amounts of potassium acetate or sulfuric acid afforded the corresponding α-hydrazinyl product (Scheme 1).[5]

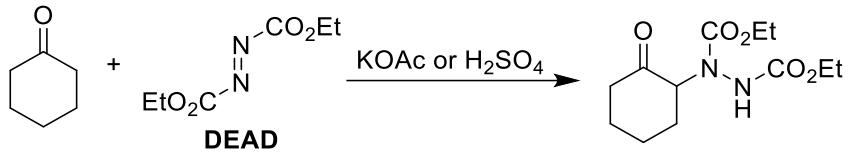

Scheme 1. Electrophilic α-amination of cyclohexanone using DEAD (ref. 5).

In recent years, asymmetric variants of this reaction have been developed. These methods primarily employ chiral organometallic complexes or organocatalysts to achieve enantioinduction. In an early precedent, the Evans group reported a highly enantioselective α-amination of *N*-acyl oxazolidinones using a magnesium bis(sulfonamide) complex and catalytic acid (Scheme 2).[6]

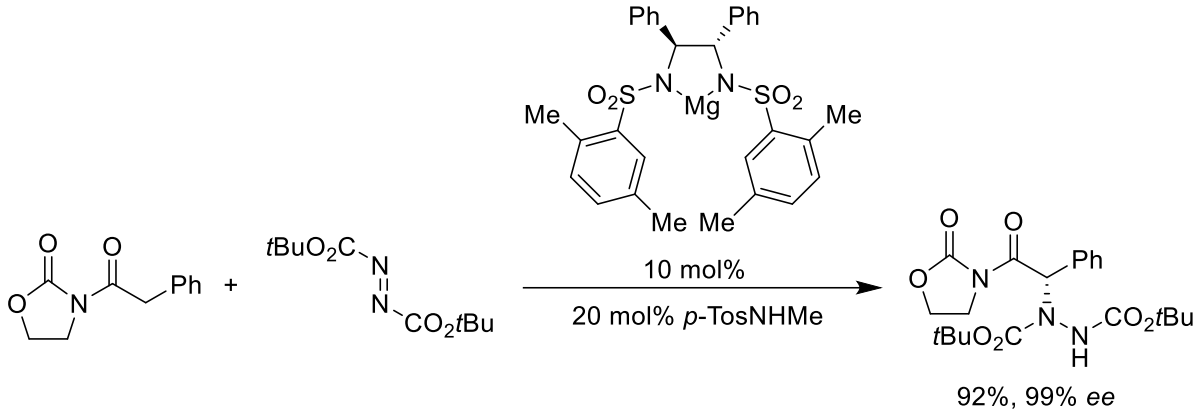

Scheme 2. Enantioselective α-amination of *N*-acyl oxazolidinones using a chiral magnesium bis(sulfonamide) complex (ref. 6).

The groups of Jørgensen[7] and List[8] have reported enantioselective organocatalytic aminations of aldehydes using proline and dialkyl azodicarboxylates. These transformations afford the corresponding *N*-amino oxazolidinones (Scheme 3a, after basic reduction) and α-amino alcohols (Scheme 3b), respectively.

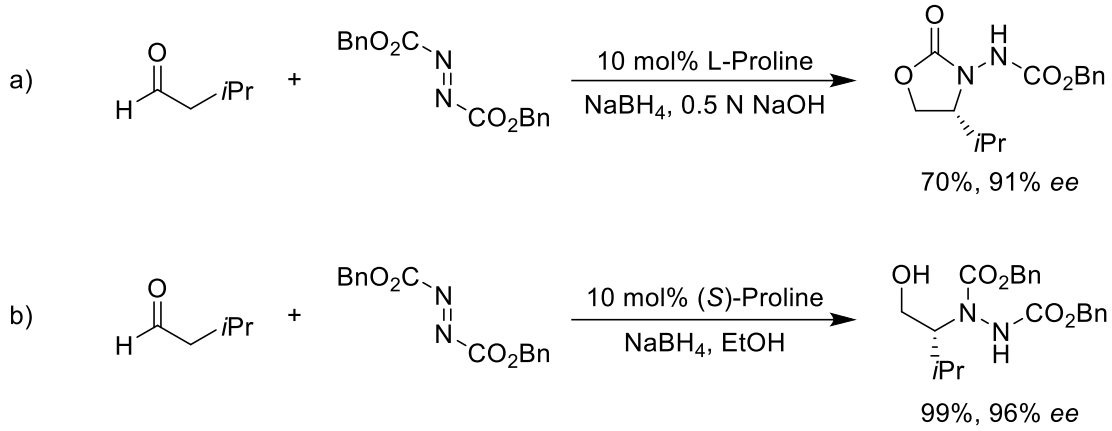

Scheme 3. Enantioselective organocatalytic α-aminations of aldehydes (ref. 7, 8).

In 2002, Jørgensen and coworkers expanded the same reactivity to ketone substrates (Scheme 4). The α-hydrazino ketone products were subsequently deprotected through a 3-step sequence.[9]

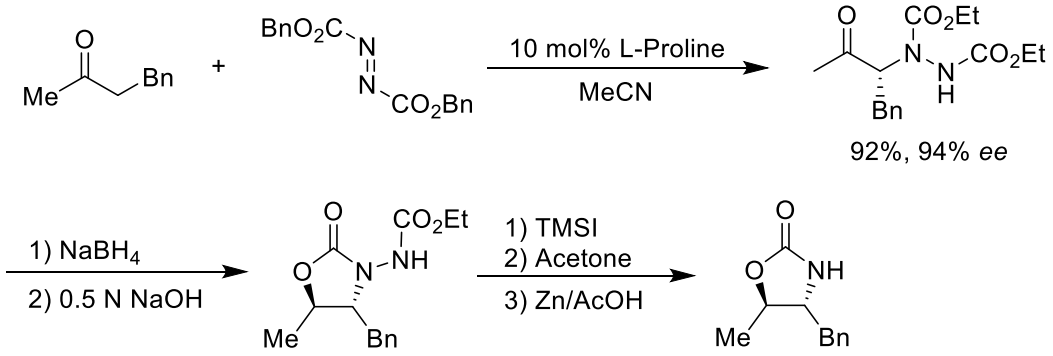

Scheme 4. Enantioselective organocatalytic α-aminations of ketones using dialkyl azodicarboxylates and subsequent deprotection sequence (ref. 9).

Although enantioselective α-amination reactions using azodicarboxylates have been fairly well developed, the α-hydrazinyl compounds they afford require multiple deprotection steps to obtain the free amine. Furthermore, deprotection conditions often involve the stoichiometric use of metal reductants and strong acids, leading to poor functional group tolerance.[4]

Given these limitations, we became interested in α-azo compounds as more viable precursors to α-amino derivatives, as they can be directly hydrogenated to the primary amines in a single step (Chapter 1, Scheme 8). More importantly, we believed that such compounds could be accessed enantioselectivity using a chiral anion phase-transfer strategy. As we had already demonstrated that diazonium salts could be employed as chiral aminating reagents,[10] application of this methodology to activated ketone compounds would allow us to develop an asymmetric α-amination reaction (Scheme 5).

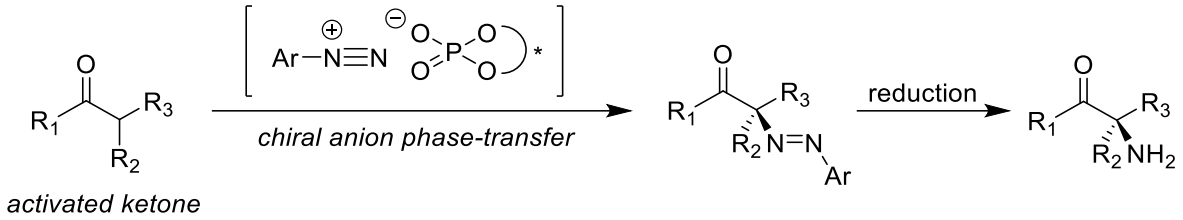

Scheme 5. Enantioselective α-amination *via* chiral anion phase-transfer of diazonium salts.

The proposed transformation would not only provide α-azo compounds that could be easily reduced to primary amines, but would also furnish nitrogen containing quaternary stereocenters. This motif is found in a number of bioactive compounds, such as ketamine and tiletamine, both of which display anesthetic properties (Figure 1).

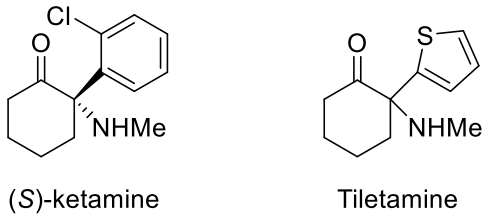

Figure 1. Bioactive compounds with nitrogen-containing quaternary stereocenters.

Results and Discussion

As an initial experiment, indanone-derived silyl enol ether **2.1a** was subjected to phase-transfer amination conditions: 1.2 equivalents of phenyldiazonium tetrafluoroborate, 10 mol% (*R*)-TRIP, 3 equivalents of Na_3PO_4, TBAT as a fluoride source, and hexane solvent. The desired diazenated product **2.2a** was isolated in 40% yield, but no enantioselectivity was observed (0% ee).

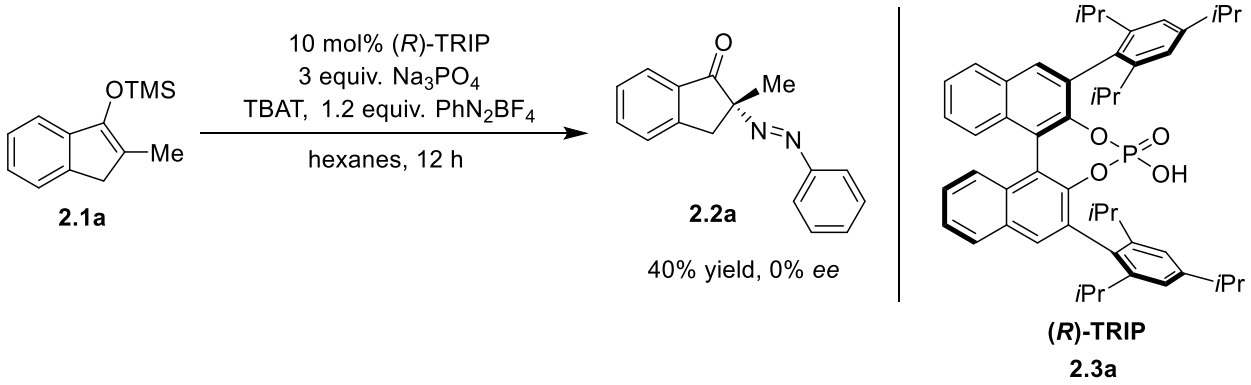

Scheme 6. Phase-transfer diazenation of **2.1a**.

In an effort to achieve favorable substrate-catalyst interactions (and higher ee), we chose to examine β-keto esters, a class of compounds that can serve as hydrogen bond donors (in enol form). Cyclopentatone derived β-keto ester **2.4a** and indanone-derived β-keto ester **2.6a** were subjected to phase-transfer amination conditions which led to formation of the desired products **2.5a** and **2.7a** respectively (Scheme 7). However, only **2.7a** was isolated in good yield (90%) and

with any enantioenrichment (7% ee). Given our diverse library of chiral phosphoric acids, we saw the potential to optimize enantioselectivity and chose **2.6a** as a model substrate.

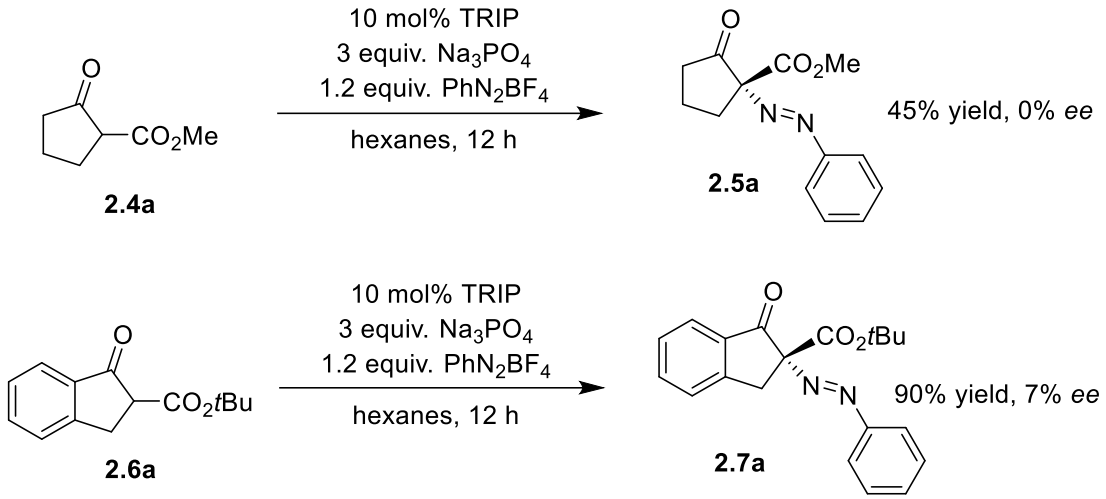

Scheme 7. Phase-transfer diazenation of β-keto esters **2.4a** and **2.6a**.

Unfortunately, initial examination of various phase-transfer catalysts led to minimal improvements in ee (Table 1). Use of BINOL-derived phosphoric acids (entries 1-2), H_8-BINOL-derived phosphoric acids (entries 3-4), and a SPINOL-derived phosphoric acid (entry 5) all led to poor enantioinduction (<10% ee), though the desired reactivity was observed in all cases (>95% conversion of **2.6a**).

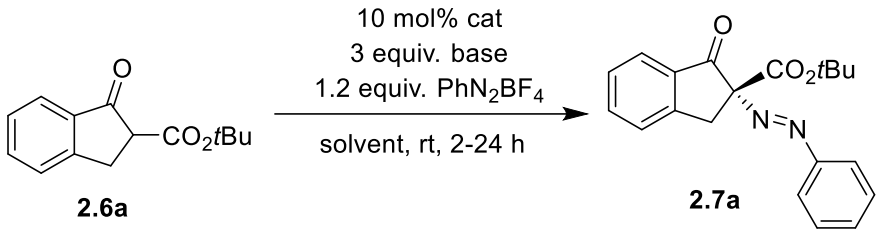

Entry	Cat.	Solvent	Base	Conv. (%)	*ee* (%)
1	**2.3a**	hexanes	Na_3PO_4	> 95	5
2	**2.3b**	hexanes	Na_3PO_4	> 95	9
3	**2.3c**	hexanes	Na_3PO_4	> 95	4
4	**2.3d**	hexanes	Na_3PO_4	> 95	7
5	**2.3e**	hexanes	Na_3PO_4	> 95	4

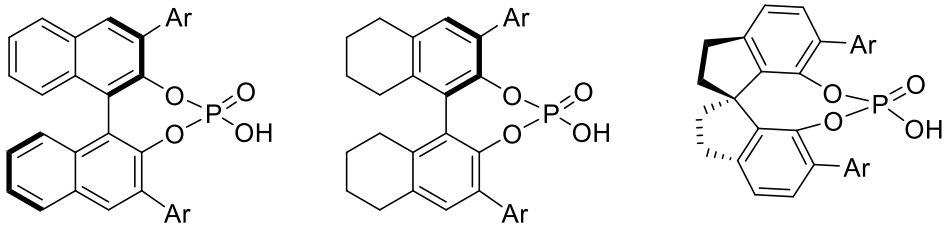

2.3a, Ar = 2,4,6-(*i*Pr)$_3$C$_6$H$_2$ **2.3c,** Ar = 2,4,6-(*i*Pr)$_3$C$_6$H$_2$ **2.3e**, Ar = 2,4,6-(*i*Pr)$_3$C$_6$H$_2$
2.3b, Ar = 2,4,6-(Cy)$_3$C$_6$H$_2$ **2.3d,** Ar = 2,4,6-(*i*Pr)$_3$C$_6$H$_2$

Table 1. Survey of phase-transfer catalysts.

We next investigated the relationship between ee and identity of base (Table 2). We found that use of a weaker bases, such as Na_2HPO_4 (entry 2) and $NaHCO_3$ (entry 3), improved enantioselectivities slightly. Presumably, weaker bases do not deprotonate the substrate, a process that would lead to an unselective background reaction between the enolate of **2.6a** and phenyldiazonium cation. Use of organic bases such as triethylamine (entry 5) and benzylamine (entry 6) led to minimal conversion, likely due to a direct reaction with the diazonium salt as evidenced by strong color change.

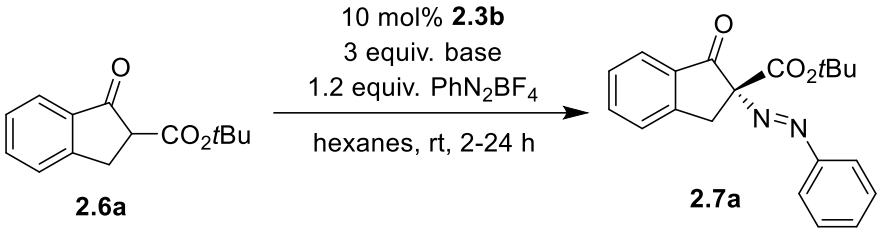

Entry	Base	Conv. (%)	*ee* (%)
1	Na_3PO_4	> 95	9
2	Na_2HPO_4	> 95	34
3	$NaHCO_3$	> 95	21
4	NaOAc	> 95	-7
5	Et_3N	< 30	0
6	$BnNH_2$	< 20	-

Table 2. Optimization of base.

Though enantioselectivities had improved slightly through the use of Na_2HPO_4, we were still far removed from our desired levels of enantioinduction (>90% ee). We believed this goal would ultimately require the design and implementation of a new class of chiral phosphates. Much of our previously developed phase-transfer chemistry had relied on substrate design. In particular, the incorporation of a hydrogen bonding benzamide moiety proved crucial for obtaining high ee.[11,12] While this particular substrate-phosphate combination was exploited in the development of a number of asymmetric transformations, a major drawback was substrate specificity and lack of scope. This limitation became increasingly apparent in our diazenation of β-keto esters.

Thus, we hypothesized that changing the electronic properties of the catalyst, rather the structure of the substrate, could provide a powerful solution. Specifically, we became interested in BINAM-derived chiral phosphoric acids, first described by Ishihara and coworkers (Figure 2).[13] As nitrogen is less inductively withdrawing and more π-donating than oxygen, the corresponding conjugate base should have greater anionic character, potentially leading to improved ion-pairing with the aryldiazonium salt and improved hydrogen bonding with the substrate.

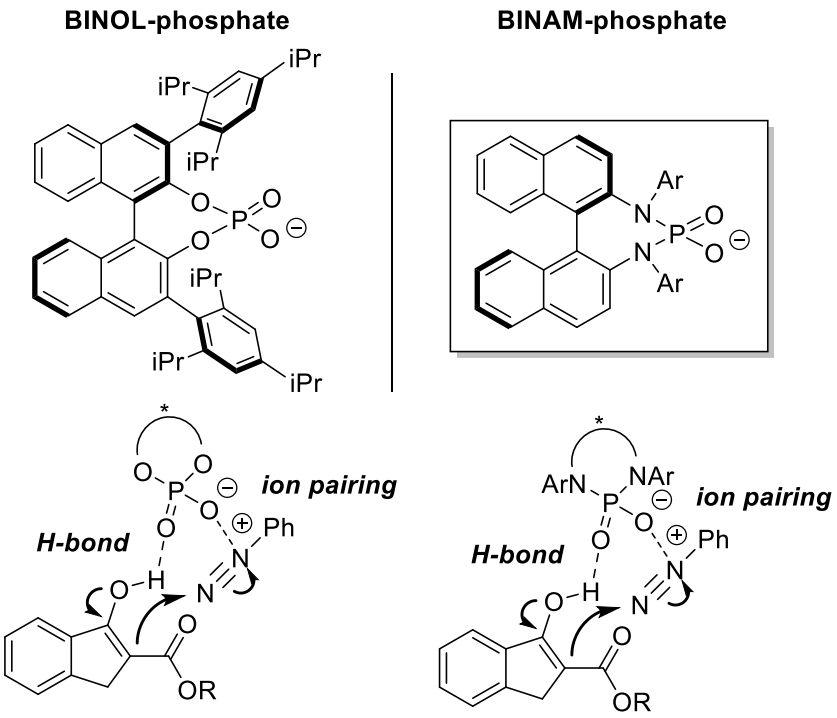

Figure 2. BINAM-derived phosphate versus BINOL-derived phosphate.

The parent compound (Ar = Ph) had been prepared previously,[13] and a similar procedure was adapted to synthesize a variety of BINAM-derived phosphoric acids (Scheme 8). The first step in the sequence, a Buchwald-Hartwig coupling of (*R*)-BINAM and various aryl bromides, introduced the element of steric and electronic diversity. The bis-arylated diamine was then phosphorylated with $POCl_3$, and the acid chloride intermediate subsequently hydrolyzed with LiOH.

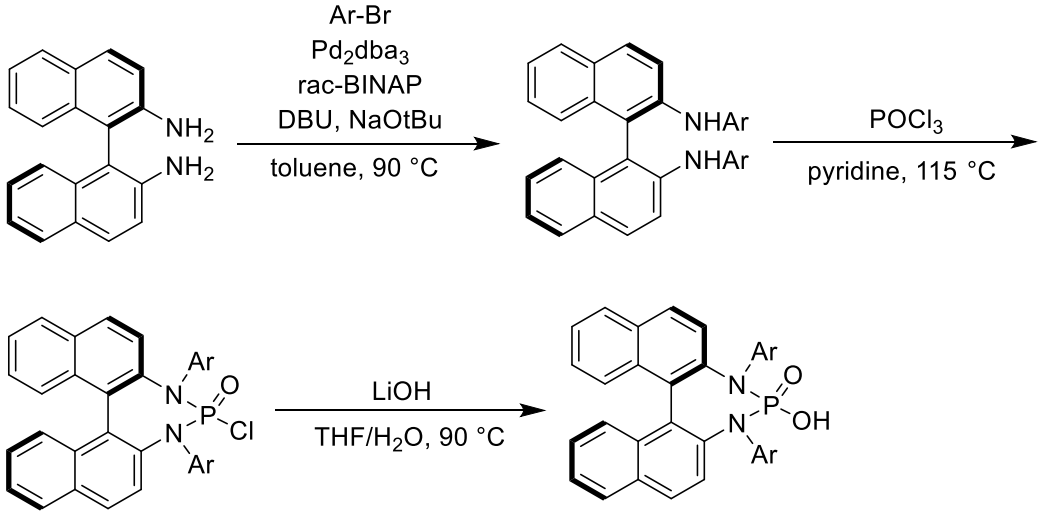

Scheme 8. Synthesis of BINAM-derived phosphoric acids.

Using this sequence, a library of new catalysts was generated (Figure 3). A variety of substituents were installed at the 3- and 4-positions of the *N*-aryl group. Substitution at the 2-position was

challenging with respect to both the initial cross-coupling reaction and the subsequent phosphorylation (low yields in both cases).

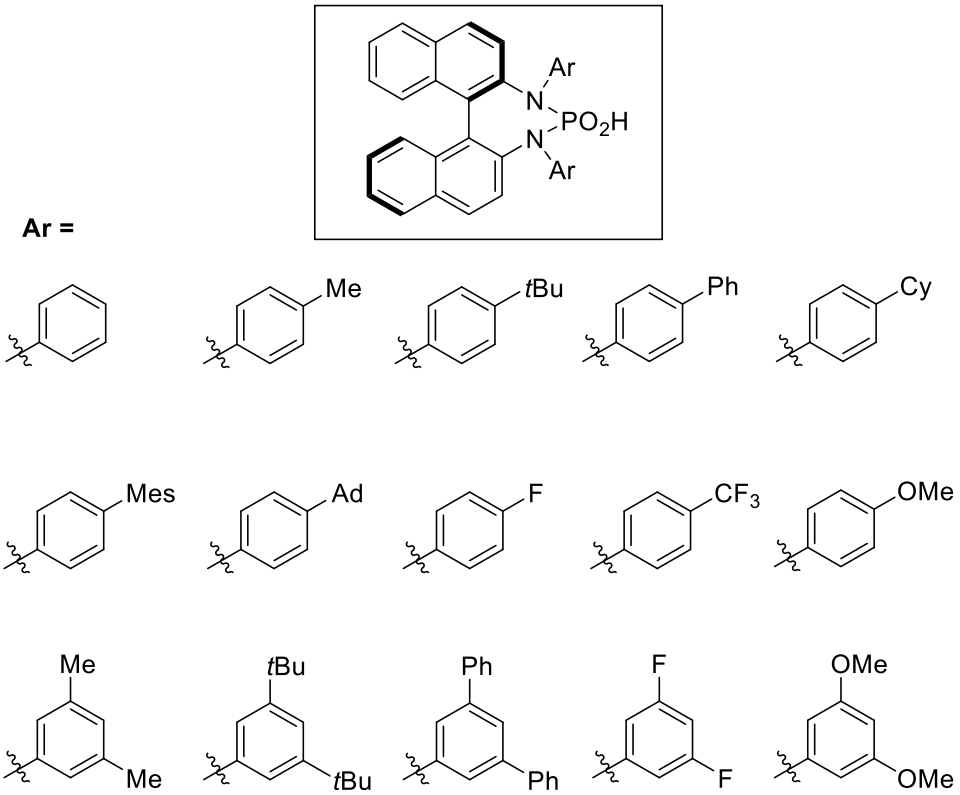

Figure 3. Library of BINAM-derived phosphoric acids.

We next examined this catalyst scaffold in the α-amination of **2.6a** (Table 3). While most of the newly synthesized catalysts performed poorly (entries 2-4, 6), use of catalyst **2.3i** resulted in formation of our desired product **2.7a** in 87% ee (entry 5), with absolute stereochemical configuration determined by X-ray crystallographic analysis. Somewhat surprisingly, electron poor **2.3i** gave a drastic improvement in enantioinduction, calling into question our initial hypothesis of the relationship between catalyst electronics and ion-pairing and hydrogen bonding interactions. Nonetheless, we attributed the increased ee associated with **2.3i** to an electronic effect, as use of sterically similar **2.3j** provided product in only 5% ee. It is possible that the conjugate base of **2.3i** falls within a narrow, optimal pK_b window, with a delicate balance between hydrogen bonding with the substrate and ion-pairing with the aryldiazonium cation. Catalysts with weaker conjugate bases, such as **2.3g**, may ion-pair strongly to the aryldiazonium cation and exhibit minimal interactions with the substrate, leading to poor enantioinduction (entry 3).

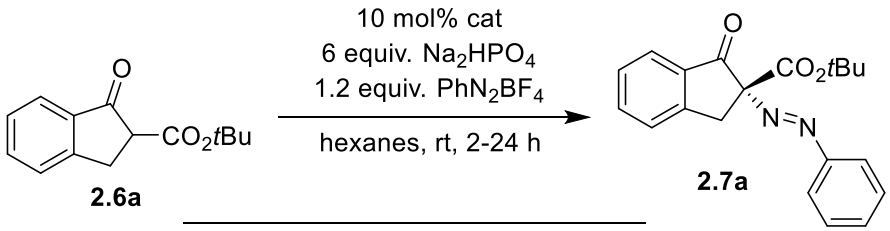

Entry	Cat.	Conv. (%)	*ee* (%)
1	**2.3b**	> 95	34
2	**2.3f**	> 95	-7
3	**2.3g**	> 95	4
4	**2.3h**	> 95	5
5	**2.3i**	> 95	87
6	**2.3j**	> 95	5

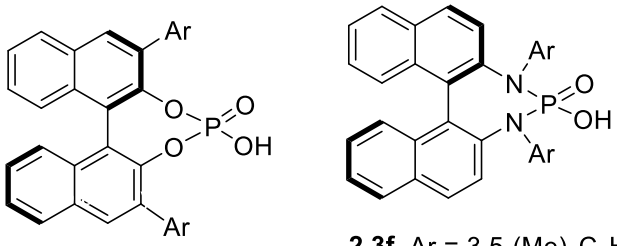

2.3b, Ar = 2,4,6-$(Cy)_3C_6H_2$

2.3f, Ar = 3,5-$(Me)_2C_6H_3$
2.3g, Ar = 3,5-$(OMe)_2C_6H_3$
2.3h, Ar = 3,5-$(Ph)_2C_6H_3$
2.3i, Ar = 4-CF_3-C_6H_4
2.3j, Ar = 4-Me-C_6H_4

Table 3. Evaluation of BINAM-derived phosphoric acids.

With optimal catalyst **2.3i**, we aimed to further increase ee through judicious choice of solvent (Table 4). Ultimately, use of cyclohexane resulted in product formation in 90% isolated yield and 90% ee, our best result (entry 2). Use of more polar solvents significantly reduced enantioselectivity (entries 3-5), likely due to an increased background reaction. For example, in 2-methyl THF, full conversion to the desired product was seen in 24 hours in the absence of any phase-transfer catalyst (entry 5). Conversely, in cyclohexane solvent, only 25% conversion was observed with omitted catalyst (entry 6).

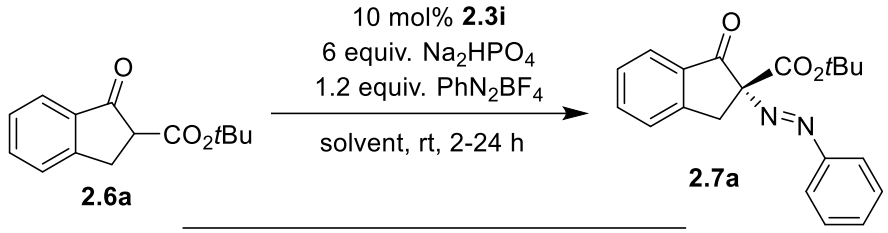

Entry	Solvent	Conv. (%)[b]	*ee* (%)
1	hexanes	> 95	87
2	cyclohexane	90[b]	90
3	MTBE	> 95	78
4	1,4-dioxane	> 95	10
5[c]	2-MeTHF	> 95	10
6[c]	cyclohexane	25	0

[b]isolated yield
[c]No catalyst

Table 4. Solvent optimization.

With an optimized set of reaction conditions established, we evaluated the scope of indanone-derived β-keto esters (Figure 4). We found that substitution at the 4-, 5- and 6-positions was well tolerated with both electron-withdrawing (**2.7b**-**2.7d**) and electron-donating groups (**2.7e**-**2.7g**), affording the corresponding diazene compounds in high yield and enantioselectivity.

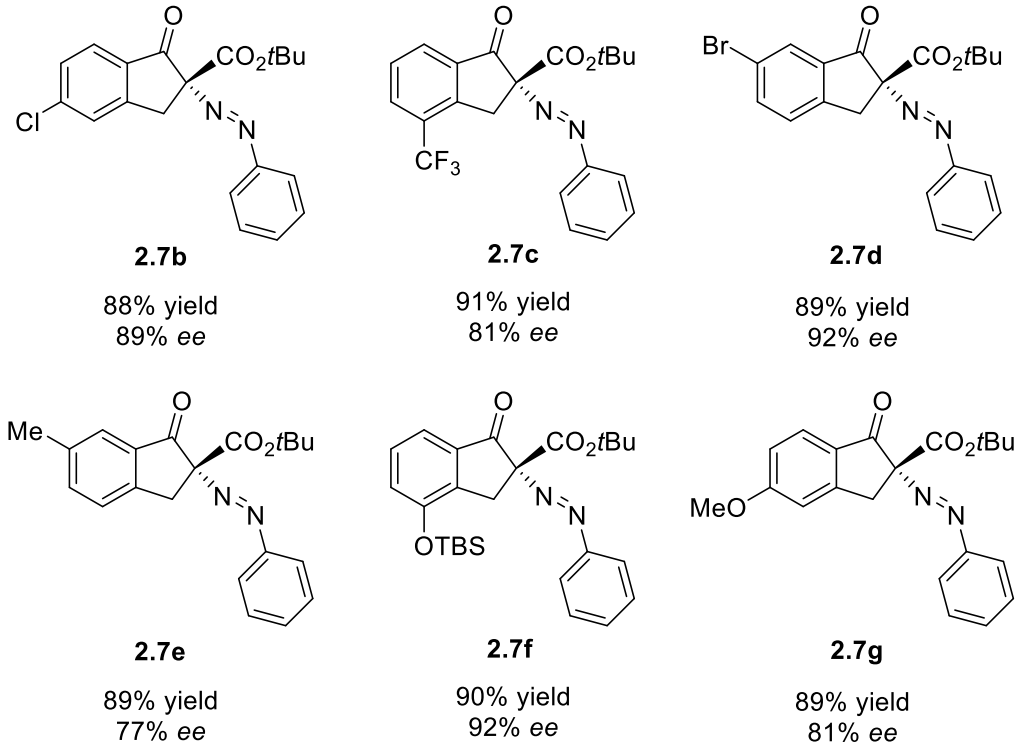

Figure 4. Scope of indanone-derived β-keto esters.

Substitution at the 7-position (substrate **2.8a**) dramatically decreased ee (Table 5). Low enantioselectivities were observed using both BINOL-derived phosphoric acids (entries 1,2) and BINAM-derived phosphoric acids (entries 3-4). A substituent at the 7-position may sterically clash with the catalyst, one rationale for the observed low ee. Alternatively, the presence of an amide may draw the catalyst away from the site of nucleophilic attack through competitive hydrogen bonding.

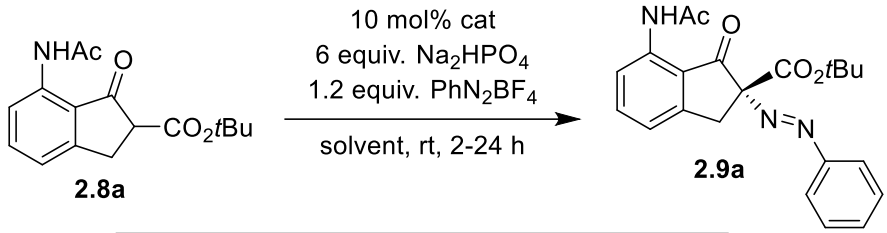

Entry	Cat.	Solvent	Conv. (%)	*ee* (%)
1	**2.3a**	toluene	> 95	35
2	**2.3b**	toluene	> 95	40
3	**2.3i**	cyclohexane	~ 50	1
4	**2.3i**	MTBE	> 95	12

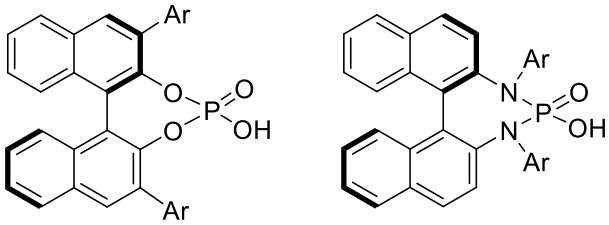

2.3a, Ar = 2,4,6-(*i*Pr)$_3$C$_6$H$_2$ **2.3i**, Ar = 4-CF$_3$-C$_6$H$_4$
2.3b, Ar = 2,4,6-(Cy)$_3$C$_6$H$_2$

Table 5. Diazenation of **2.8a**.

Installation of basic functional groups into the indanone backbone (substrate **2.10a**) also resulted in low enantioselectivity, in addition to poor yield (Table 6). Direct deprotonation of the phosphoric acid precatalyst by **2.10a**, rather than by the inorganic base, likely reduces the amount of active phosphate in solution, leading to both low ee and conversion. The tertiary amine substituent may also react directly with the aryldiazonium cation, resulting in decomposition of both reactants.

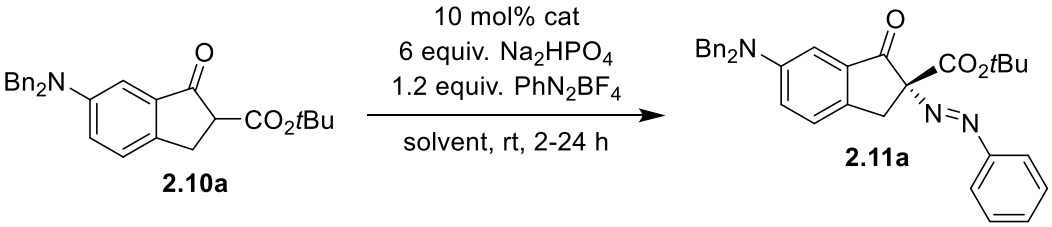

Entry	Cat.	Solvent	Conv. (%)	*ee* (%)
1	**2.3b**	toluene	< 50	5
2	**2.3i**	toluene	< 50	23

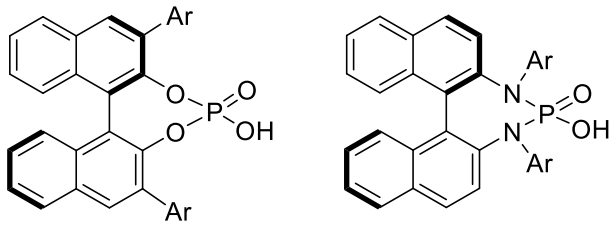

2.3b, Ar = 2,4,6-$(Cy)_3C_6H_2$ **2.3i**, Ar = 4-CF_3-C_6H_4

Table 6. Diazenation of **2.10a**.

In addition to β-keto esters derived from indanone, we also investigated other ring systems. When subjected to similar conditions, tetralone-derived β-keto ester **2.12a** was fully converted to the desired product, but in extremely low levels of enantioselectivity (Table 7). Use of both BINOL (entry 1) and BINAM (entry 2) phosphates resulted in poor enantioinduction.

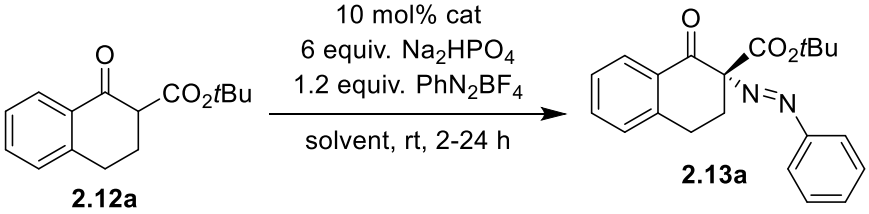

Entry	Cat.	Solvent	Conv. (%)	*ee* (%)
1	**2.3b**	hexanes	> 95	8
2	**2.3i**	hexanes	> 95	6

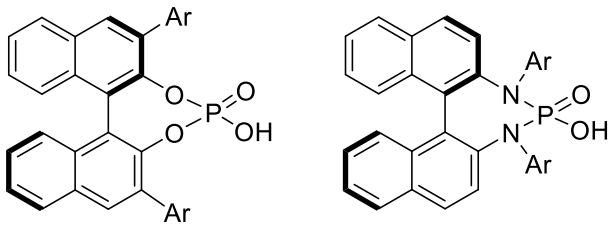

2.3b, Ar = 2,4,6-$(Cy)_3C_6H_2$ **2.3i**, Ar = 4-CF_3-C_6H_4

Table 7. Diazenation of tetralone-derived β-keto ester **2.12a**.

Use of benzosuberone-derived β-keto esters proved more fruitful. Phase-transfer diazenation of **2.14a** and methoxy-substituted **2.16a** afforded the corresponding α-azo compounds in excellent ee, though re-optimization of reaction conditions was required (Scheme 9).

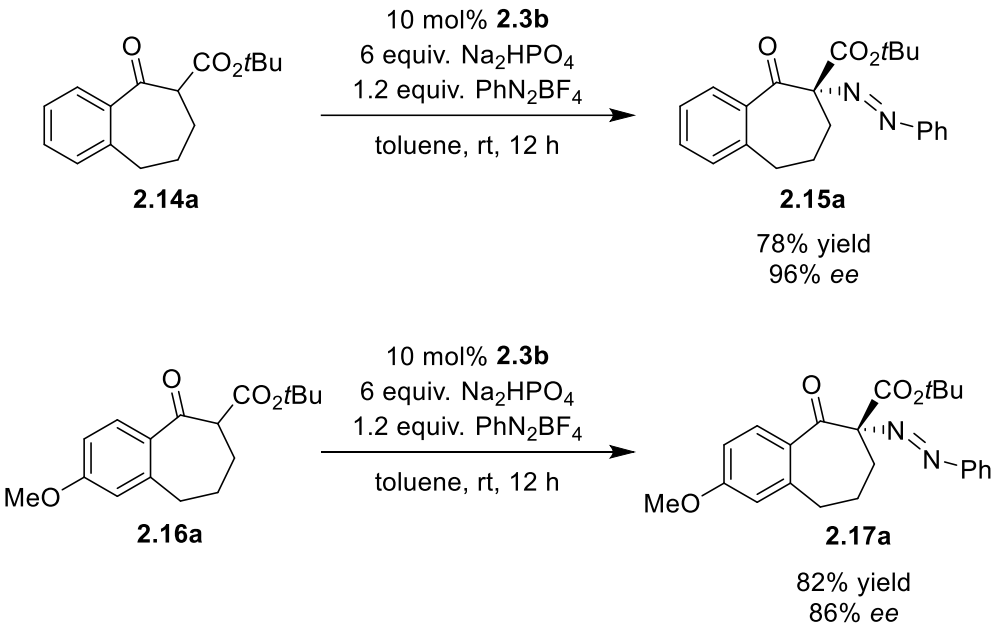

Scheme 9. Diazenation of benzosuberone-derived β-keto esters **2.14a** and **2.16a**.

At this juncture, we had only employed cyclic substrates and were interested in expanding the scope to acyclic starting materials. Unfortunately, when β-keto ester **2.18a** was subjected to phase-transfer amination conditions, no desired product was observed (Scheme 10). Crude ^{1}H NMR analysis indicated return of starting material. The absence of any reactivity may be explained by the decreased nucleophilicity and lower enolic character of **2.18a** relative to its cyclic counterparts.

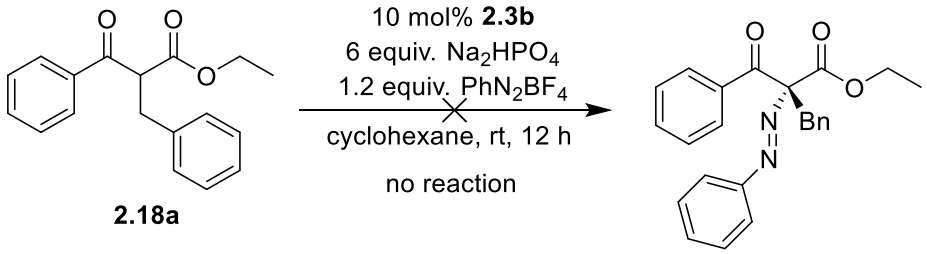

Scheme 10. Failed diazenation of **2.18a**.

Having determined a set of β-keto esters that displayed sufficient reactivity and the desired enantioselectivity, we next looked at the scope of the aryldiazonium salt. We found that diazonium salts with *ortho*-, *meta*-, and *para*-substituents were well tolerated (Figure 5). Specifically, diazonium salts with electron-donating groups (**2.7h**, **2.7m-o**) and electron-withdrawing groups (**2.7i-l**) afforded their corresponding diazene products in high yields and high enantioselectivities.

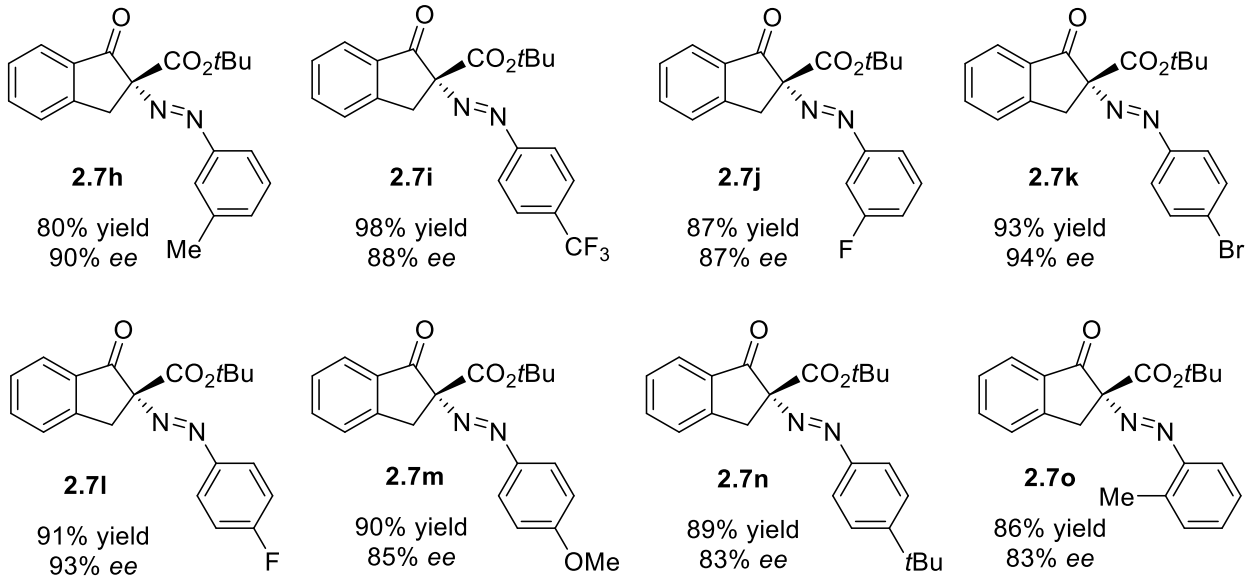

Figure 5. Aryldiazonium scope.

To investigate potential applications of our chemistry, we aimed to expand substrate scope beyond β-keto esters. In an effort to also maintain sufficient nucleophilicity, we synthesized β-keto amides **2.19a** and **2.21a** and subjected them to phase-transfer amination conditions (Table 8). While optimization efforts were not successful with respect to **2.19a** (<25% ee, entries 1-4), moderate levels of enantioinduction were observed using sterically bulkier **2.21a** (entries 4-9). As **2.19a** and **2.21a** were both minimally soluble in hexanes, MTBE and toluene were used as solvents.

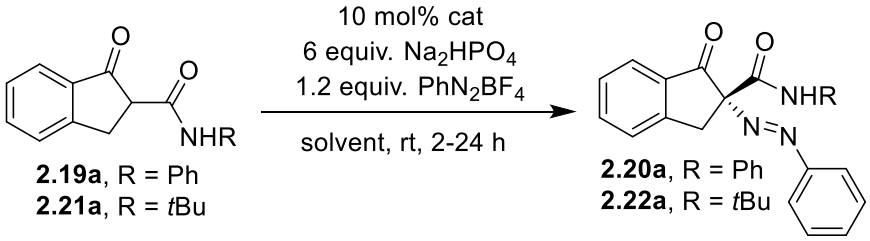

Entry	SM	Cat.	Solvent	Conv. (%)	*ee* (%)
1	**2.19a**	**2.3a**	MTBE	> 95	4
2	**2.19a**	**2.3b**	MTBE	> 95	22
3[a]	**2.19a**	**2.3b**	MTBE	> 95	25
4	**2.19a**	**2.3i**	MTBE	> 95	4
5	**2.21b**	**2.3a**	MTBE	> 95	33
6	**2.21b**	**2.3b**	MTBE	> 95	43
7[a]	**2.21b**	**2.3b**	MTBE	> 95	53
8[a]	**2.21b**	**2.3b**	toluene	> 95	69
9	**2.21b**	**2.3i**	MTBE	> 95	3

[a]6 equiv. Na_3PO_4 used as base

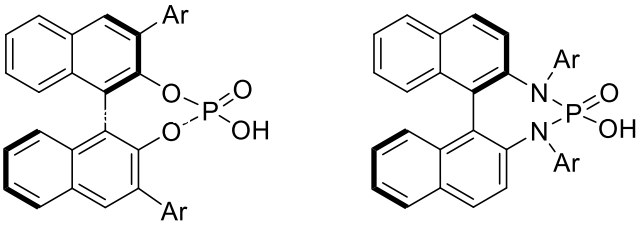

2.3a, Ar = 2,4,6-(*i*Pr)$_3$C$_6$H$_2$
2.3b, Ar = 2,4,6-(Cy)$_3$C$_6$H$_2$
2.3i, Ar = 4-CF$_3$-C$_6$H$_4$

Table 8. Diazenation of β-keto amides **2.19a** and **2.21a**.

With modest ee achieved for **2.19a** (entry 8), we looked at the dependence of enantioinduction on the use of different aryldiazonium salts (Table 9). We were pleased to find that halogen substitution at the 4-position afforded the desired diazene compounds in good enantioselectivity (entries 1-2), a marked improvement over use of phenyldiazonium tetrafluoroborate. The sensitivity of ee to subtle electronic changes was not particularly surprising, as we had observed a similar phenomenon during our initial optimization experiments (Table 3).

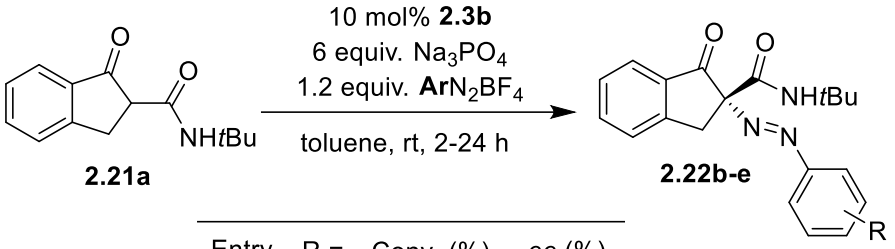

Entry	R =	Conv. (%)	*ee* (%)
1	4-Br	91[a]	90
2	4-F	85[a]	85
3	3-Me	> 95	60
4	4-CF_3	> 95	76

[a]isolated yield

Table 9. Effect of aryldiazonium salt on diazenation of **2.21a**.

As a last examination of scope, we chose to pursue enecarbamates, a class of substrates that our group had previously employed in a chiral anion phase-transfer fluorination reaction.[14] Of these compounds, **2.23a** showed the desired reactivity, affording desired α-azo imine **2.24a** in good yield. Subsequent work focused on improving ee (Table 10), which we found to be sensitive to solvent (entries 1-4) and base (entries 7-11). While moderate ee was observed with BINAM-derived catalyst **2.2j** (entry 6), use of BINOL-derived **2.2b** in Et_2O solvent with Cs_2CO_3 was optimal (entry 11).

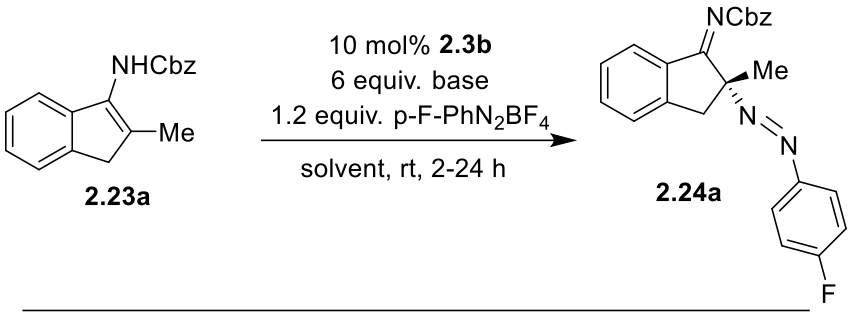

Entry	Cat.	Solvent	Base	Conv. (%)	*ee* (%)
1	**2.3a**	hexanes	Na_2CO_3	< 20	20
2	**2.3a**	MTBE	Na_2CO_3	> 95	72
3	**2.3b**	hexanes	Na_2CO_3	< 20	10
4	**2.3b**	MTBE	Na_2CO_3	> 95	80
5	**2.3i**	MTBE	Na_2CO_3	> 95	3
6	**2.3j**	MTBE	Na_2CO_3	> 95	59
7	**2.3b**	Et_2O	Na_2CO_3	> 95	80
8	**2.3b**	Et_2O	Na_3PO_4	> 95	67
9	**2.3b**	Et_2O	K_2CO_3	> 95	80
10	**2.3b**	Et_2O	Na_2HPO_4	> 95	56
11	**2.3b**	Et_2O	Cs_2CO_3	> 95	81

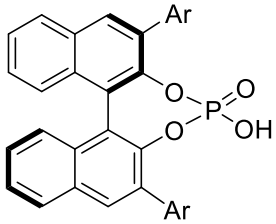

2.3a, Ar = 2,4,6-(*i*Pr)$_3$C$_6$H$_2$
2.3b, Ar = 2,4,6-(Cy)$_3$C$_6$H$_2$

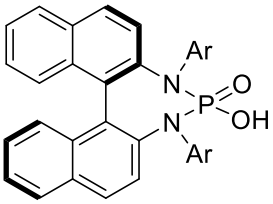

2.3i, Ar = 4-CF$_3$-C$_6$H$_4$
2.3j, Ar = 4-Me-C$_6$H$_4$

Table 10. Diazenation of enecarbamate **2.23a**.

Since the utility of our transformation was dependent on the ability to unmask the free amine, we next aimed to develop deprotection conditions. Attempts to convert **2.7a** directly to an amide *via* Zn^0/AcOH mediated reduction and *in situ* protection failed. Unexpectedly, the reaction afforded β-keto ester **2.6a** (Scheme 11). Similar results were obtained using stoichiometric Fe^0.

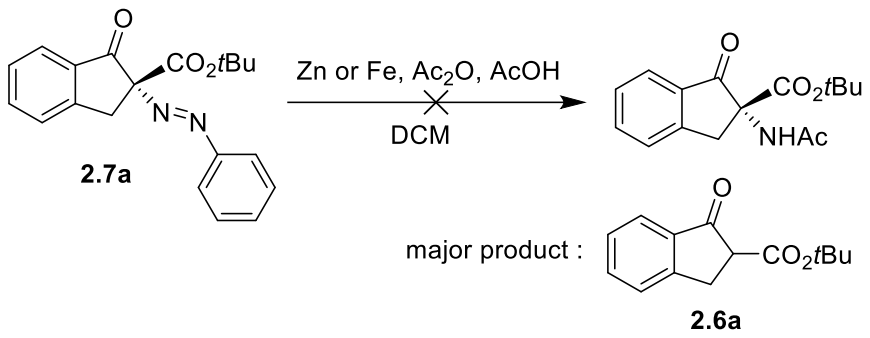

Scheme 11. Failed attempt to reduce **2.7a** with Zn or Fe.

Milder reductants such as $NaBH_4$ did not afford the desired product, and instead resulted in retro-aldol chemistry (Scheme 12). Retro-aldol products were evidenced by the formation of achiral species in the crude ^{1}H NMR.

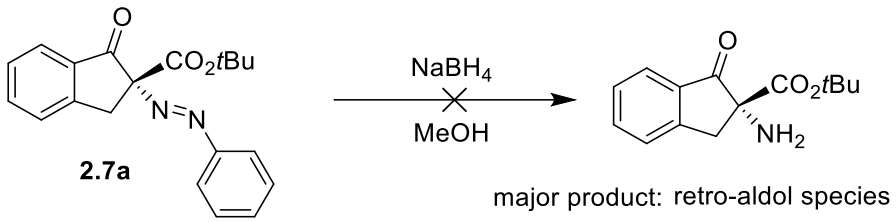

Scheme 12. Attempts to reduce **2.7a** with $NaBH_4$.

High pressure hydrogenations of **2.7a** and **2.14a** did afford *trans*-amino alcohols **2.25a** and **2.26a** respectively, with hydrogenation predominantly occurring on the opposite face of the ester (Scheme 13). High pressures were needed to avoid isolation of the partially reduced hydrazinyl intermediates. Enantioenrichment was retained in both cases.

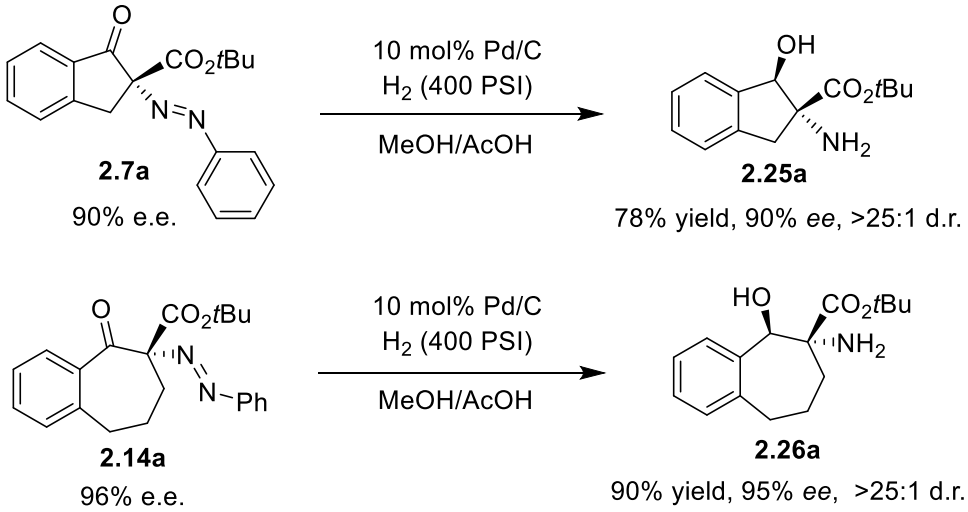

Scheme 13. High pressure hydrogenations of **2.7a** and **2.14a**.

When examining the structure of amino alcohol **2.25a**, we noticed a similarity to conformationally constrained tyrosine analogues (CCTAs) such as Hai, which is currently being investigated for

their properties as δ-opioid agonists (Figure 6). These compounds have been previously prepared in 12 steps *via* classical resolution.[15] We envision that reduction and deprotection of **2.7g** (Figure 4) may provide an efficient entry towards this scaffold.

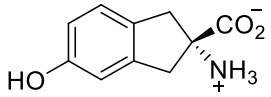

Hai

Figure 6. Structure of CCTA Hai.

Furthermore, ^{15}N-labeling of β-hydroxy amino acid derivatives may be a notable application of our methodology, as similarly prepared analogues could be used for mass spectrometric or NMR studies. Towards this end, isotopically enriched **2.25b** was synthesized in a 3 step sequence starting from $Na^{15}NO_2$ (Scheme 14).

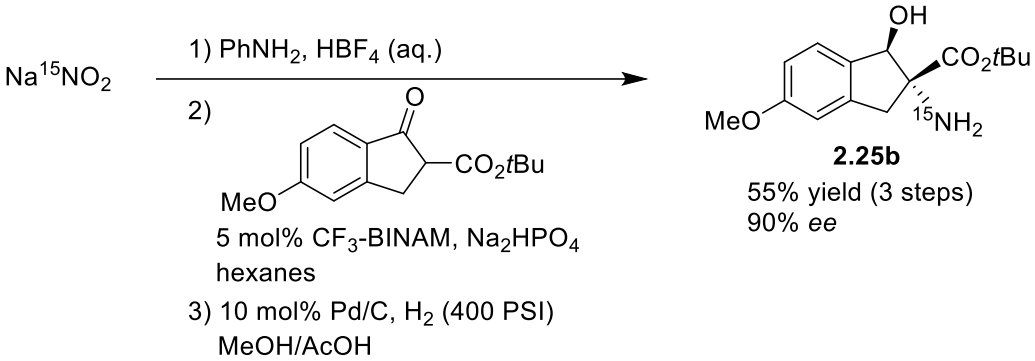

Scheme 14. Synthesis of ^{15}N-labeled **2.25b**.

Lastly, we attempted photolysis of **2.7a** in hopes of generated the corresponding α-arylated product. Unfortunately, a variety of conditions (including multiple sources of UV light) either led to no reaction or decomposition of starting material (Scheme 15).

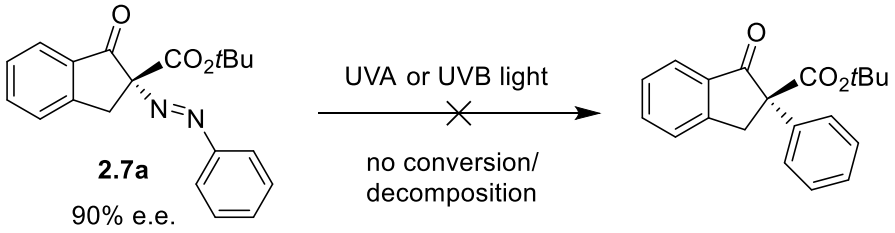

Scheme 15. Attempted photolysis of **2.7a**.

Conclusions

We have developed an asymmetric α-amination of activated ketone derivatives *via c*hiral anion phase-transfer of aryldiazonium salts. Key to obtaining high levels of enantioselectivity was the design and synthesis of a new catalyst scaffold, specifically a library of catalysts derived from BINAM. Reaction conditions were tolerant to a variety of substitution patterns on both the β-keto ester and aryldiazonium salt. Reductions of the resultant diazene compounds yielded

enantioenriched β-hydroxy amino acid derivatives in high diastereoselectivity and with complete retention of enantioenrichment.

Experimental details

General. Unless otherwise noted, reagents were obtained from commercial sources and used without further purification. Dry and degassed THF, diethyl ether, dichloromethane, toluene, triethylamine, and dimethylformamide were obtained by passage through activated alumina under argon. All diazonium tetrafluoroborates were stored at 0˚C and warmed to room temperature before use. Phase-transfer diazenation reactions were run in 1 dram (15 mm x 45 mm) vials fitted with a screw cap and stirred using an 8 mm magnetic stirrer bar. Vigorous stirring was maintained over the course of the reaction to obtain optimal and reproducible results. TLC analysis was performed on Merck silica gel 60 F254 TLC plates and visualized by UV, I_2, or p-anisaldehyde staining. Flash chromatography was carried out with ICN SiliTech 32-63 D 60 Å silica gel. ^{1}H, ^{13}C, ^{31}P and ^{19}F NMR spectra were recorded with Bruker AV-300, AVQ-400, AVB-400, AV-500, DRX-500, and AV-600 spectrometers and were referenced to ^{1}H and ^{13}C residual signals of the deuterated solvents.[16] Solvent abbreviations are reported as follows: MTBE = Methyl *tert*-butyl ether, EtOAc = ethyl acetate, hex = hexanes, DCM = dichloromethane, Et_2O = diethyl ether, MeOH = methanol, *i*PrOH = isopropanol, THF = tetrahydrofuran, DMF = N,N-dimethylformamide, Et_3N = triethylamine. Mass spectral data were obtained from the Micro-Mass/Analytical Facility operated by the College of Chemistry, University of California, Berkeley. Enantiomeric excesses were determined on a Shimadzu VP Series Chiral HPLC using IA, IB, IC and AD columns. Racemic products were obtained by vigorous stirring of all reaction components without any phase-transfer catalyst.

General procedure for synthesis of substrates

All β-keto esters were prepared according to literature procedure.[17] Trans-esterification to afford *tert*-butyl esters was achieved *via* known procedure.[18]

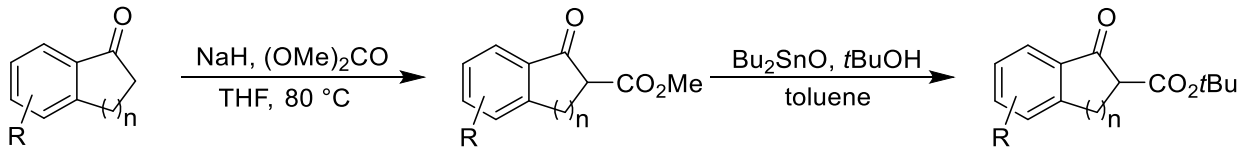

For the following compounds, spectral data was in accordance with literature:

R = H, **n** = 1[19]

R = 5-Cl, **n** = 1[20]

R = 5-OMe, **n** = 1[21]

R = 6-Me, **n** = 1[22]

R = 6-Br, **n** = 1[22]

R = H, **n** = 2[23]

β-keto amide **2.21a** was prepared according to literature procedure[24]:

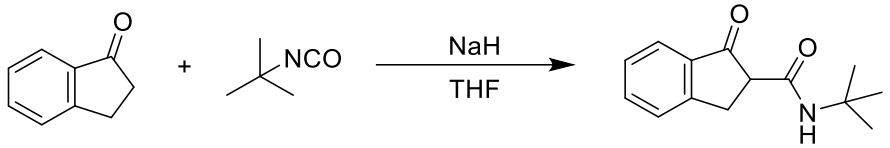

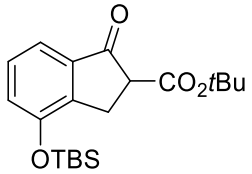

S2.1. ^{1}H NMR (600 MHz, $CDCl_3$) (ketone form) δ 7.37 (d, *J* = 7.5 Hz, 1H), 7.30 – 7.22 (m, 1H), 7.01 (d, *J* = 7.8 Hz, 1H), 3.59 (dd, *J* = 8.1, 3.8 Hz, 1H), 3.34 (d, *J* = 3.8 Hz, 1H), 3.27 – 3.20 (m, 1H), 1.49 (s, 9H), 1.03 (s, 9H), 0.26 (d, *J* = 5.9 Hz, 6H). (enol form) δ 10.61 (s, 1H), 7.30 – 7.22 (m, 2H), 7.01 (d, *J* = 7.8 Hz, 1H), 6.86 – 6.83 (m, 1H), 3.37 (s, 2H), 1.58 (s, 9H), 1.03 (s, 9H), 0.23 (s, 6H). ^{13}C NMR (151 MHz, $CDCl_3$) (keto and enol) δ 200.06, 168.32, 153.25, 151.67, 144.59, 139.11, 137.33, 132.93, 128.96, 128.22, 124.32, 119.72, 117.07, 113.94, 81.93, 54.30, 28.47, 28.00, 27.48, 25.65, 25.59, 18.15, -4.18, -4.27, -4.28. HRMS (ESI) Calcd. for $[M+Na]^+$ $C_{20}H_{30}O_4NaSi$: 385.1806; found: 385.1808.

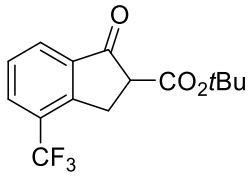

S2.2. ^{1}H NMR (400 MHz, $CDCl_3$) (60% keto ester form) δ 7.95 (d, *J* = 7.7 Hz, 1H), 7.89 (d, *J* = 7.6 Hz, 1H), 7.52 (m, 1H), 3.69 (m, 2H), 3.53 (dd, *J* = 18.6, 9.0 Hz, 1H), 1.50 (s, 9H). (40 % enol form). δ 10.49 (s, 1H), 7.79 (d, *J* = 7.6 Hz, 1H), 7.65 (d, *J* = 7.7 Hz, 1H), 7.52 (m, 1H), 3.66 (s, 2H), 1.59 (s, 9H). ^{13}C NMR (151 MHz, $CDCl_3$) (keto and enol) δ 198.52, 167.48, 150.81 (q, $J_{C\text{-}F}$ = 2.1 Hz), 140.09 (q, $J_{C\text{-}F}$ = 2.3 Hz), 138.87, 136.90, 131.73 (q, $J_{C\text{-}F}$ = 4.6 Hz), 128.54, 128.32, 128.12, 127.94, 127.27, 126.83, 126.62, 125.45 (q, $J_{C\text{-}F}$ = 4.5 Hz), 125.00, 124.52, 123.73, 123.19, 122.71, 104.82, 82.45, 81.52, 53.93, 32.11, 29.19, 28.37, 27.92. ^{19}F NMR (376 MHz, $CDCl_3$) (enol) δ -61.23. (ketone) -61.53. HRMS (ESI) Calcd. for $[M+Na]^+$ $C_{15}H_{15}O_3F_3Na$: 323.0866; found: 323.0868.

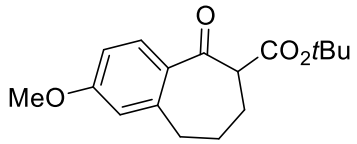

2.16a. ^{1}H NMR (500 MHz, CD_2Cl_2) (1:1 keto : enol) δ 12.89 (s, 1H), 7.80 (d, *J* = 8.6 Hz, 1H), 7.57 (d, *J* = 8.5 Hz, 1H), 6.90 – 6.86 (m, 2H), 6.82 (d, *J* = 2.6 Hz, 1H), 6.77 (d, *J* = 2.5 Hz, 1H), 3.88 (s, 3H), 3.87 (s, 3H), 3.72 – 3.69 (m, 1H), 3.06 – 2.87 (m, 2H), 2.65 (t, *J* = 6.6 Hz, 2H), 2.24 – 1.96 (m, 7H), 1.94 – 1.78 (m, 1H), 1.60 (s, 9H), 1.49 (s, 9H). ^{13}C NMR (126 MHz, CD_2Cl_2) δ 246.68, 233.53 199.04, 173.09, 169.88, 169.75, 162.78, 160.78, 144.35, 143.22, 131.48, 130.90,

128.50, 114.91, 114.29, 111.87, 111.39, 100.83, 81.03, 80.98, 57.32, 55.39, 55.23, 53.87, 33.37, 33.05, 32.18, 28.09, 27.71, 24.83, 24.23, 22.45. HRMS (ESI) Calcd. for $[M+Na]^+$ $C_{17}H_{22}O_4Na$: 313.1410; found: 313.1413.

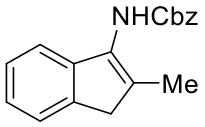

S2.3. ^{1}H NMR (600 MHz,$CDCl_3$) δ 7.51 – 7.30 (m, 6H), 7.24 (d, *J* = 7.4 Hz, 1H), 7.19 (d, *J* = 7.7 Hz, 1H), 7.15 (t, *J* = 7.3 Hz, 1H), 6.20 (s, 1H), 5.22 (s, 2H), 3.33 (s, 2H), 2.06 (s, 3H). ^{13}C NMR (151 MHz, $CDCl_3$) δ 142.49, 140.85, 136.17, 131.05, 128.54, 128.27, 128.24, 128.11, 126.17, 124.90, 124.40, 123.45, 117.68, 67.26, 40.67, 13.81. HRMS (ESI) Calcd. for $[M+Na]^+$ $C_{18}H_{17}O_2NNa$: 302.1152; found: 302.1151.

Catalyst synthesis

Catalysts were synthesized analogously to literature reports[13]:

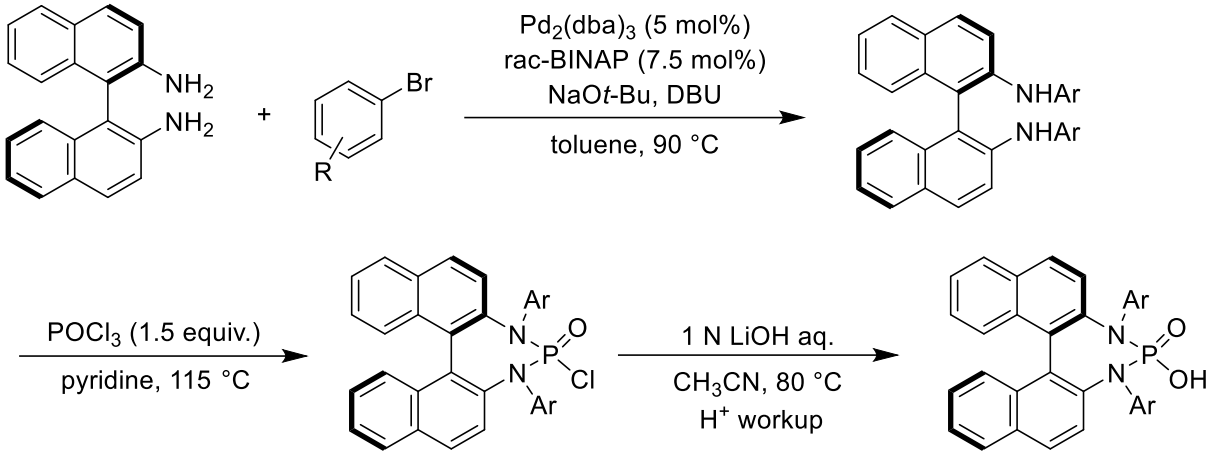

Note: To afford the desired acid as a fine powder, the crude product of the hydrolysis was sonicated in acetonitrile and collected *via* vacuum filtration (column chromatography was not used).

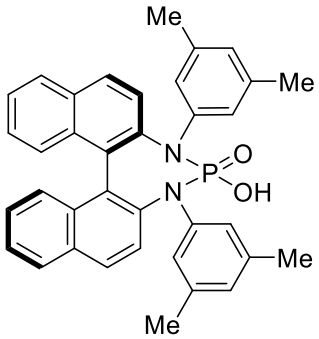

2.3f. ^{1}H NMR (600 MHz, DMSO-d_6) δ 8.01 (dd, *J* = 8.4, 5.7 Hz, 4H), 7.51 (t, *J* = 7.4 Hz, 2H), 7.39 (t, *J* = 7.7 Hz, 2H), 7.32 (d, *J* = 8.5 Hz, 2H), 7.28 (d, *J* = 8.7 Hz, 2H), 6.58 – 6.56 (m, 6H), 2.01 (s, 12H). ^{31}P NMR (243 MHz, DMSO-d_6) δ 8.37. ^{13}C NMR (151 MHz, DMSO-d_6) δ 144.61

(d, $J_{C\text{-}P}$ = 7.5 Hz), 141.03, 137.89, 132.29, 131.90, 130.79, 130.49, 128.83, 127.18, 127.11, 126.87, 126.27, 125.53, 122.25 (d, $J_{C\text{-}P}$ = 3.0 Hz), 21.27. HRMS (ESI) Calcd. for $[M]^-$ $C_{36}H_{30}O_2N_2P$: 553.2050; found: 553.2050.

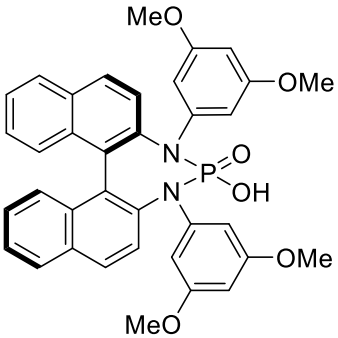

2.3g. ^{1}H NMR (600 MHz, DMSO-d_6) δ 8.04 (dd, J = 16.8, 8.4 Hz, 4H), 7.51 (t, J = 7.4 Hz, 2H), 7.43 – 7.26 (m, 6H), 6.17 – 6.00 (m, 6H), 3.46 (s, 12H). ^{31}P NMR (243 MHz, DMSO-d_6) δ 7.40. ^{13}C NMR (151 MHz, DMSO-d_6) δ 160.56, 146.32 (d, $J_{C\text{-}P}$ = 9.1 Hz), 140.43, 132.23, 132.12, 131.01, 130.67, 128.94, 127.36, 127.23, 126.79, 126.45, 102.72 (d, $J_{C\text{-}P}$ = 7.5 Hz), 95.96, 55.39. HRMS (ESI) Calcd. for $[M]^-$ $C_{36}H_{30}O_6N_2P$: 617.1847; found: 617.1830.

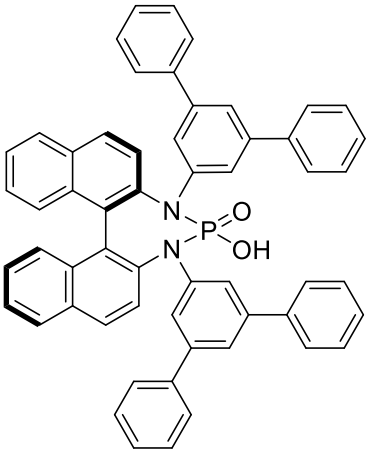

2.3h. ^{1}H NMR (600 MHz, DMSO-d_6) δ 8.11 (d, J = 8.7 Hz, 2H), 8.07 (d, J = 8.1 Hz, 2H), 7.60 (t, J = 7.3 Hz, 2H), 7.55 (d, J = 8.7 Hz, 2H), 7.51 – 7.45 (m, 6H), 7.40 – 7.36 (m, 16H), 7.32 – 7.30 (m, 4H), 7.18 (s, 4H). ^{13}C NMR (151 MHz, DMSO-d_6) δ 145.74 (d, $J_{C\text{-}P}$ = 7.6 Hz), 141.69, 140.41, 139.94, 132.38, 132.33, 131.82, 131.15, 129.30, 129.14, 128.17, 127.65, 127.54, 127.08, 126.87, 126.70, 121.40, 120.75. ^{31}P NMR (243 MHz, DMSO-d_6) δ 7.23. HRMS (ESI) Calcd. for $[M]^-$ $C_{56}H_{38}O_2N_2P$: 801.2676; found: 801.2657.

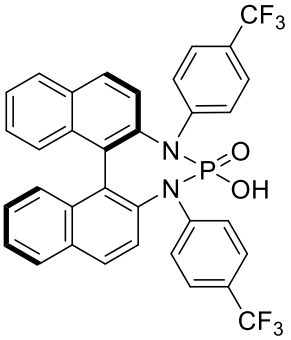

2.3i was prepared according to the general procedure described above, with Cs_2CO_3 (2 equiv.) in place of NaO*t*-Bu and DBU.

2.3i. ^{1}H NMR (400 MHz, DMSO-d_6) δ 8.08 (d, J = 8.7 Hz, 2H), 8.03 (d, J = 8.2 Hz, 2H), 7.53 (m, 2H), 7.48 – 7.41 (m, 4H), 7.39 (m, 2H), 7.34 (m, 4H), 7.13 (d, J = 8.5 Hz, 4H). ^{13}C NMR (151 MHz, DMSO) δ 148.68, 138.73, 134.40, 130.87, 129.32, 128.57, 126.74, 126.19, 126.00, 125.52, 124.59, 124.40, 123.83, 122.82, 118.60 (q, $J_{C\text{-}F}$ = 32.1 Hz), 115.37. ^{31}P NMR (162 MHz, DMSO-d_6) δ 6.58. ^{19}F NMR (376 MHz, DMSO-d_6) δ -59.60. HRMS (ESI) Calcd. for $[M]^-$ $C_{34}H_{20}O_2N_2F_6P$: 633.1172; found: 633.1158.

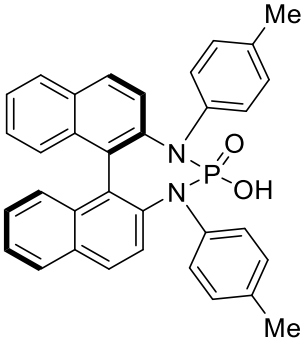

2.3j. ^{1}H NMR (600 MHz, DMSO-d_6) δ 8.01 – 8.79 (m, 4H), 7.50 – 7.47 (m, 2H), 7.37 – 7.34 (m, 2H), 7.29 – 7.25 (m, 4H), 6.94 – 6.92 (m, 4H), 6.84 – 6.82 (m, 4H), 2.12 (d, J = 3.4 Hz, 6H). ^{13}C NMR (151 MHz, DMSO) δ 142.24 (d, $J_{C\text{-}P}$ = 7.3 Hz), 141.13, 133.23, 132.29, 131.83, 130.59, 130.44, 129.49, 128.81, 127.26, 126.96, 126.93, 126.23, 124.39 (d, $J_{C\text{-}P}$ = 3.8 Hz), 20.65. ^{31}P NMR (243 MHz, DMSO) δ 8.56. HRMS (ESI) m/z $[M]^-$ calc'd for $C_{34}H_{26}N_2O_2P$ 525.1737, found 527.1732.

General procedure for phase-transfer diazenation

A one-dram vial was charged with catalyst (10 mol %), appropriate nucleophile (1 equiv.), and base (6 equiv.). Bench-top grade solvent was added (0.025 M) and the mixture was stirred for 10 minutes. The corresponding diazonium tetrafluoroborate (1.2 equiv.) was then added and the mixture was stirred vigorously at room temperature until completion, as monitored by TLC. The crude mixture was diluted with diethyl ether (1 mL) and filtered over cotton to remove precipitates. The crude product was concentrated and purified by flash chromatography on silica gel (pentanes: Et_2O) to afford the desired product.

Conditions **A**: cyclohexane solvent, catalyst **2.3h**

Conditions **B**: MTBE solvent, catalyst **2.3h**

Conditions **C**: toluene solvent, catalyst **2.3b**

Note: All reactions were run using conditions **A** unless otherwise noted.

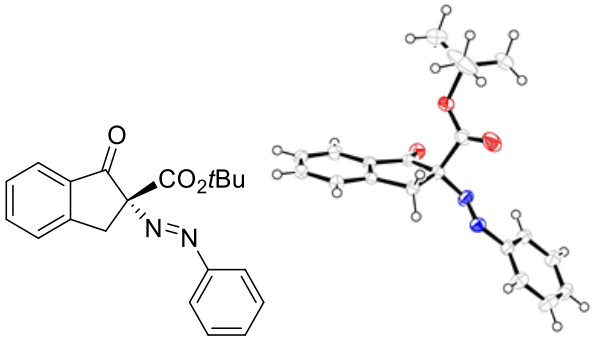

2.7a. Isolated as a yellow oil (16.0 mg, 95%). ^{1}H NMR (300 MHz, CD_2Cl_2) δ 7.78 (d, *J* = 7.7 Hz, 1H), 7.74 – 7.62 (m, 3H), 7.56 (d, *J* = 7.7 Hz, 1H), 7.51 – 7.40 (m, 4H), 3.94 (d, *J* = 17.6 Hz, 1H), 3.77 (d, *J* = 17.6 Hz, 1H), 1.47 (s, 10H). ^{13}C NMR (126 MHz, CD_2Cl_2) δ 196.78, 167.28, 152.29, 151.56, 135.61, 134.68, 131.46, 129.05, 127.98, 126.51, 124.68, 122.51, 87.90, 83.02, 36.01, 27.66. HRMS (ESI) Calcd. for $[M+Na]^+$ $C_{20}H_{20}O_3N_2Na$: 359.1366; found: 359.1366. HPLC (ChiralPak IA column) 98:02 (hexane/iPrOH) 1mL/min; T_{major} (13.9 min), T_{minor} (21.3 min); 90% ee.

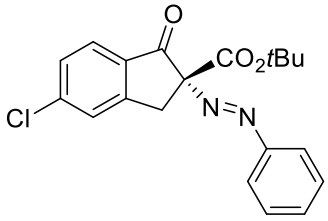

2.7b. Isolated as a yellow oil (8.1 mg, 88%). ^{1}H NMR (500 MHz, CD_2Cl_2) δ 7.74 (t, *J* = 7.3 Hz, 3H), 7.59 (s, 1H), 7.51 (s, 3H), 7.46 (d, *J* = 8.1 Hz, 1H), 3.95 (d, *J* = 17.7 Hz, 1H), 3.78 (d, *J* = 17.8 Hz, 1H), 1.50 (s, 9H). ^{13}C NMR (126 MHz, CD_2Cl_2) δ 195.41, 166.91, 153.75, 151.47, 141.99, 133.15, 131.60, 129.08, 128.79, 126.71, 125.86, 122.56, 87.91, 83.29, 35.58, 27.65. HPLC (ChiralPak IA column) 97:03 (hexane/iPrOH) 1mL/min; T_{major} (11.2 min), T_{minor} (20.2 min); 88% ee. HRMS (ESI) Calcd. for $[M+Na]^+$ $C_{20}H_{19}O_3N_2ClNa$: 393.0976; found: 393.0975.

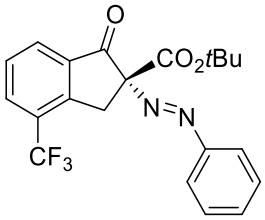

2.7c. Isolated as a yellow oil (9.0 mg, 89%). ^{1}H NMR (600 MHz, CD_2Cl_2) δ 7.99 (d, *J* = 7.6 Hz, 1H), 7.95 (d, *J* = 7.5 Hz, 1H), 7.72 (d, *J* = 7.4 Hz, 2H), 7.61 (t, *J* = 7.6 Hz, 1H), 7.53 – 7.49 (m, 3H), 4.11 (d, *J* = 18.2 Hz, 1H), 3.94 (d, *J* = 18.1 Hz, 1H), 1.48 (s, 9H). ^{13}C NMR (151 MHz,

CD_2Cl_2) δ 195.41, 166.47, 151.39, 149.33, 136.08, 132.11 (q, $J_{C\text{-}F}$ = 3.0 Hz), 131.63, 129.02, 128.52, 128.23, 127.98, 124.61, 122.54, 87.35, 83.47, 34.77, 27.56. ^{19}F NMR (376 MHz, CD_2Cl_2) δ -61.74. HRMS (ESI) Calcd. for $[M+Na]^+$ $C_{21}H_{19}O_3N_2F_3Na$: 427.1240; found: 427.1239. HPLC (ChiralPak IB column) 99:01 (hexane/iPrOH) 1mL/min; T_{major} (12.3 min), T_{minor} (13.0 min); 81% ee.

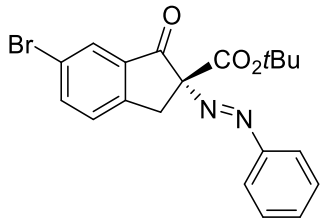

2.7d. Isolated as a yellow oil (9.2 mg, 89%). ^{1}H NMR (600 MHz, CD_2Cl_2) δ 7.91 (d, *J* = 1.9 Hz, 1H), 7.78 (dd, *J* = 8.1, 2.0 Hz, 1H), 7.73 – 7.69 (m, 2H), 7.51 – 7.45 (m, 4H), 3.87 (d, *J* = 17.6 Hz, 1H), 3.73 (d, *J* = 17.7 Hz, 1H), 1.47 (s, 9H). ^{13}C NMR (151 MHz, CD_2Cl_2) δ 195.52, 166.74, 151.46, 150.79, 138.19, 136.46, 131.53, 129.00, 128.06, 127.39, 122.48, 121.87, 88.05, 83.27, 35.59, 27.59. HRMS (ESI) Calcd. for $[M+Na]^+$ $C_{20}H_{19}O_3N_2Na$: 437.0471; found: 437.0471. HPLC (ChiralPak IA column) 98:02 (hexane/iPrOH) 1mL/min; T_{major} (11.3 min), T_{minor} (16.1 min); 81% ee.

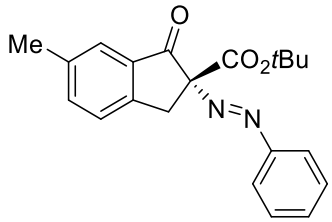

2.7e. Isolated as a yellow oil (15.7 mg, 89%). ^{1}H NMR (300 MHz, CD_2Cl_2) δ 7.74 – 7.65 (m, 2H), 7.57 (s, 1H), 7.54 – 7.39 (m, 5H), 3.87 (d, *J* = 17.4 Hz, 1H), 3.71 (d, *J* = 17.5 Hz, 1H), 2.42 (s, 3H), 1.46 (s, 9H). ^{13}C NMR (151 MHz, CD_2Cl_2) δ 196.74, 167.34, 151.59, 149.57, 138.17, 136.81, 134.82, 131.32, 128.96, 126.06, 124.47, 122.43, 88.22, 82.86, 35.69, 27.61, 20.72. HRMS (ESI) Calcd. for $[M+Na]^+$ $C_{21}H_{22}O_3N_2Na$: 373.1523; found: 373.1522. HPLC (ChiralPak IA column) 98:02 (hexane/iPrOH) 1mL/min; T_{major} (13.6 min), T_{minor} (19.3 min); 77% ee.

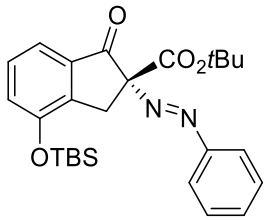

2.7f. Isolated as a yellow oil (10.2 mg, 90%). ^{1}H NMR (600 MHz, CD_2Cl_2) δ 7.73 – 7.69 (m, 2H), 7.51 – 7.46 (m, 3H), 7.40 (dd, *J* = 7.6, 1.1 Hz, 1H), 7.34 (t, *J* = 7.7 Hz, 1H), 7.11 (dd, *J* = 7.9, 1.1 Hz, 1H), 3.81 (d, *J* = 17.7 Hz, 1H), 3.64 (d, *J* = 17.7 Hz, 1H), 1.48 (s, 9H), 1.06 (s, 9H), 0.29 (d, *J* = 1.9 Hz, 6H). ^{13}C NMR (151 MHz, CD_2Cl_2) δ 196.72, 167.26, 153.23, 151.57, 143.10, 136.40, 131.35, 129.33, 128.96, 125.12, 122.45, 117.26, 87.78, 82.91, 33.31, 27.61, 25.35, 18.06, -4.56. HRMS (ESI) Calcd. for $[M+Na]^+$ $C_{26}H_{34}O_4N_2NaSi$: 489.2180; found: 489.2177. HPLC (ChiralPak WHELK column) 99:01 (hexane/iPrOH) 0.5mL/min; T_{major} (14.9 min), T_{minor} (18.9 min); 92% ee.

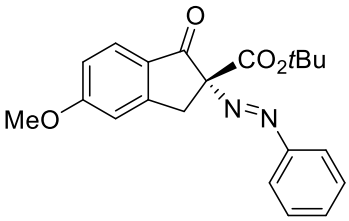

2.7g. Isolated a yellow oil (16.3 mg, 89%) using conditions **B**. ^{1}H NMR (600 MHz, CD_2Cl_2) δ 7.71 (dd, *J* = 6.9, 3.3 Hz, 3H), 7.51 – 7.45 (m, 3H), 7.00 (d, *J* = 2.1 Hz, 1H), 6.97 (dd, *J* = 8.7, 2.1 Hz, 1H), 3.92 (s, 3H), 3.89 (d, *J* = 17.5 Hz, 1H), 3.71 (d, *J* = 17.5 Hz, 1H), 1.48 (s, 9H). ^{13}C NMR (151 MHz, CD_2Cl_2) δ 194.48, 167.45, 166.02, 155.35, 151.60, 131.28, 128.96, 127.68, 126.38, 122.43, 115.98, 109.55, 88.21, 82.78, 55.79, 35.79, 27.62. HRMS (ESI) Calcd. for $[M+Na]^+$ $C_{21}H_{22}O_4N_2Na$: 389.1472; found: 389.1472. HPLC (ChiralPak IA column) 98:02 (hexane/iPrOH) 1mL/min; T_{major} (16.9 min), T_{minor} (35.1); 93% ee.

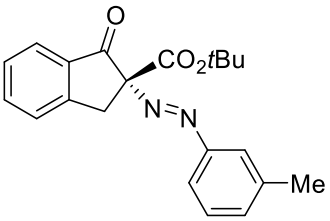

2.7h. Isolated as a yellow oil (13.9 mg, 80%). ^{1}H NMR (600 MHz, CD_2Cl_2) δ 7.78 (d, *J* = 7.7 Hz, 1H), 7.68 (t, *J* = 7.5 Hz, 1H), 7.57 (d, *J* = 7.7 Hz, 1H), 7.51 (d, *J* = 8.6 Hz, 2H), 7.45 (t, *J* = 7.5 Hz, 1H), 7.36 (t, *J* = 7.6 Hz, 1H), 7.31 (d, *J* = 7.5 Hz, 1H), 3.94 (d, *J* = 17.5 Hz, 1H), 3.77 (d, *J* = 17.5 Hz, 1H), 2.41 (s, 3H), 1.47 (s, 9H). ^{13}C NMR (151 MHz, CD_2Cl2) δ 196.76, 167.24, 152.22, 151.61, 139.16, 135.49, 134.67, 132.11, 128.73, 127.89, 126.42, 124.60, 122.48, 120.06, 87.81, 82.92, 35.92, 27.61, 20.90. HRMS (ESI) Calcd. for $[M+Na]^+$ $C_{21}H_{22}O_3N_2Na$: 373.1523; found: 373.1522. HPLC (ChiralPak IA column) 98:02 (hexane/iPrOH) 1mL/min; T_{major} (12.5 min), T_{minor} (14.1 min); 90% ee.

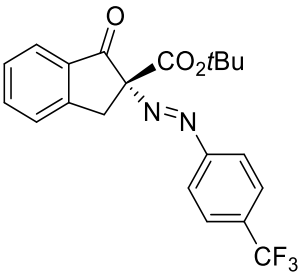

2.7i. Isolated as a yellow oil (19.8 mg, 98%). ^{1}H NMR (600 MHz, CD_2Cl_2) δ 7.83 – 7.79 (m, 3H), 7.76 (d, *J* = 8.3 Hz, 2H), 7.70 (t, *J* = 7.5 Hz, 1H), 7.58 (d, *J* = 7.7 Hz, 1H), 7.46 (t, *J* = 7.5 Hz, 1H), 3.96 (d, *J* = 17.5 Hz, 1H), 3.81 (d, *J* = 17.5 Hz, 1H), 1.47 (s, 9H). ^{13}C NMR (151 MHz, CD_2Cl_2) δ 196.09, 166.85, 153.45, 152.06, 135.67, 134.48, 132.54, 132.33, 128.03, 126.45, 126.23 (q, J_{C-F} = 3.8 Hz), 124.73, 122.77, 88.41, 83.25, 35.95, 27.58. ^{19}F NMR (376 MHz, CD_2Cl2) δ -62.22. HRMS (ESI) Calcd. for $[M+Na]^+$ $C_{21}H_{19}O_3N_2F_3Na$: 472.1240; found: 472.1237. HPLC (ChiralPak IA column) 98:02 (hexane/iPrOH) 1mL/min; T_{major} (14.7 min), T_{minor} (20.4 min); 88% ee.

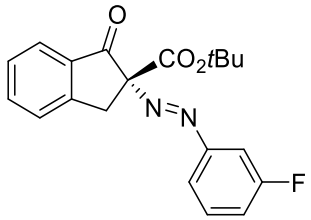

2.7j. Isolated as a yellow oil (15.2 mg, 87%). ^{1}H NMR (600 MHz, CD_2Cl_2) δ 7.79 (d, *J* = 7.7 Hz, 1H), 7.69 (t, *J* = 7.4 Hz, 1H), 7.57 (d, *J* = 7.8 Hz, 2H), 7.50 – 7.45 (m, 2H), 7.41 (d, *J* = 9.6 Hz, 1H), 7.24 – 7.17 (m, 1H), 3.93 (d, *J* = 17.5 Hz, 1H), 3.80 (d, *J* = 17.5 Hz, 1H), 1.47 (s, 9H). ^{13}C NMR (151 MHz, CD_2Cl_2) δ 196.28, 166.97, 163.05 (d, $J_{C\text{-}F}$ = 247.5 Hz), 152.93 (d, $J_{C\text{-}F}$ = 7.0 Hz), 152.09, 135.61, 134.55, 130.30, 127.98, 126.44, 124.68, 119.94 (d, $J_{C\text{-}F}$ = 2.9 Hz), 118.10 (d, $J_{C\text{-}F}$ = 21.9 Hz), 107.98 (d, $J_{C\text{-}F}$ = 23.2 Hz), 88.04, 83.13, 36.00, 27.59. ^{19}F NMR (376 MHz, CD_2Cl_2) δ -111.77 – -111.85 (m). HRMS (ESI) Calcd. for $[M+Na]^+$ $C_{20}H_{19}O_3N_2FNa$: 377.1272; found: 377.1270. HPLC (ChiralPak IA column) 98:02 (hexane/iPrOH) 1mL/min; T_{major} (11.5 min), T_{minor} (13.9 min); 87% ee.

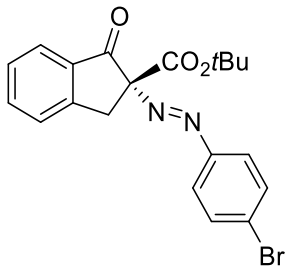

2.7k. Isolated as a yellow oil (19.4 mg, 94%). ^{1}H NMR (600 MHz, CD_2Cl_2) δ 7.82 – 7.73 (m, 3H), 7.68 (td, *J* = 7.4, 1.3 Hz, 1H), 7.57 (d, *J* = 7.7, 1H), 7.50 – 7.38 (m, 1H), 7.21 – 7.13 (m, 2H), 3.93 (d, *J* = 17.5 Hz, 1H), 3.78 (d, *J* = 17.5 Hz, 1H), 1.47 (s, 9H). ^{13}C NMR (151 MHz, CD_2Cl2) δ 196.38, 167.01, 152.13, 150.29, 135.59, 134.56, 132.24, 127.97, 126.43, 125.78, 124.66, 124.05, 88.00, 83.09, 35.97, 27.59. HRMS (ESI) Calcd. for $[M+Na]^+$ $C_{20}H_{19}O_3N_2BrNa$: 437.0471; found: 437.0471. HPLC (ChiralPak IA column) 98:02 (hexane/iPrOH) 1mL/min; T_{major} (14.6 min), T_{minor} (21.6 min); 93% ee.

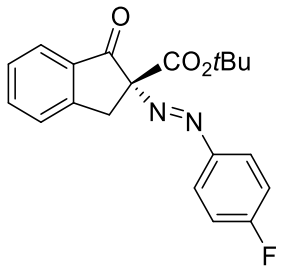

2.7l. Isolated as a yellow oil (16.2 mg, 91%). ^{1}H NMR (600 MHz, CD_2Cl_2) δ 7.78 (d, *J* = 7.7 Hz, 1H), 7.69 (td, *J* = 7.5, 1.3 Hz, 1H), 7.65 – 7.59 (m, 4H), 7.57 (d, *J* = 7.7 Hz, 1H), 7.45 (t, *J* = 7.4 Hz, 1H), 3.93 (d, *J* = 17.5 Hz, 1H), 3.78 (d, *J* = 17.5 Hz, 1H), 1.47 (s, 9H). ^{13}C NMR (151 MHz, CD_2Cl_2) δ 196.58, 167.15, 164.57 (d, $J_{C\text{-}F}$ = 251.7 Hz), 152.16, 148.10 (d, $J_{C\text{-}F}$ = 3.1 Hz), 135.54, 134.63, 127.93, 126.42, 124.70, 124.63 (d, $J_{C\text{-}F}$ = 1.3 Hz), 115.88 (d, $J_{C\text{-}F}$ = 23.1 Hz), 87.74, 83.00, 35.99, 27.59. ^{19}F NMR (376 MHz, CD_2Cl_2) δ -108.63 – -108.70 (m). HRMS (ESI) Calcd. for

[M+Na]$^+$ $C_{20}H_{19}O_3N_2FNa$: 377.1272; found: 377.1272. HPLC (ChiralPak IA column) 98:02 (hexane/iPrOH) 1mL/min; T_{major} (17.5 min), T_{minor} (25.2 min); 94 % ee.

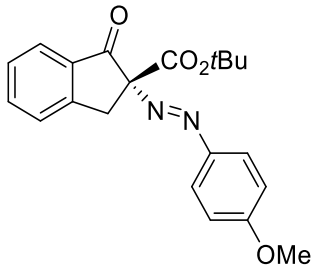

2.7m. Isolated as a yellow oil (16.5 mg, 90%). ^{1}H NMR (500 MHz, CD_2Cl_2) δ 7.80 (d, *J* = 7.6 Hz, 1H), 7.77 – 7.72 (m, 2H), 7.70 (td, *J* = 7.5, 1.2 Hz, 1H), 7.58 (d, *J* = 7.7 Hz, 1H), 7.46 (t, *J* = 7.5 Hz, 1H), 7.02 – 6.95 (m, 2H), 3.94 (d, *J* = 17.5 Hz, 1H), 3.88 (s, 3H), 3.78 (d, *J* = 17.5 Hz, 1H), 1.49 (s, 9H). ^{13}C NMR (126 MHz, CD_2Cl_2) δ 197.21, 167.56, 162.45, 152.39, 145.72, 135.51, 134.78, 127.90, 126.48, 124.61, 124.48, 114.04, 87.31, 82.83, 55.58, 36.13, 27.65. HRMS (ESI) Calcd. for [M+Na]$^+$ $C_{21}H_{22}O_4N_2Na$: 389.1472; found: 389.1472. HPLC (ChiralPak IA column) 98:02 (hexane/iPrOH) 1mL/min; T_{major} (15.7 min), T_{minor} (26.1 min); 85% ee.

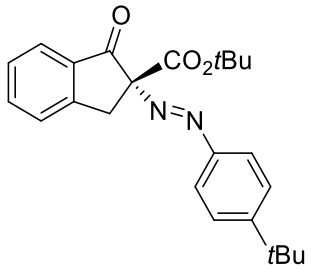

2.7n. Isolated as a yellow oil (17.5 mg, 89%). ^{1}H NMR (500 MHz, CD_2Cl_2) δ 7.80 (d, *J* = 7.7 Hz, 1H), 7.74 – 7.64 (m, 3H), 7.59 (d, *J* = 7.8 Hz, 1H), 7.52 (d, *J* = 8.5 Hz, 2H), 7.47 (t, *J* = 7.5 Hz, 1H), 3.96 (d, *J* = 17.5 Hz, 1H), 3.79 (d, *J* = 17.6 Hz, 1H), 1.49 (s, 9H), 1.37 (s, 9H). ^{13}C NMR (126 MHz, CD_2Cl_2) δ 196.95, 167.40, 155.21, 152.32, 149.43, 135.54, 134.74, 127.93, 126.49, 125.98, 124.64, 122.23, 87.72, 82.90, 36.04, 34.89, 30.92, 27.66. HRMS (ESI) Calcd. for [M+Na]$^+$ $C_{24}H_{28}O_3N_2Na$: 415.1992; found: 415.1991. HPLC (ChiralPak IA column) 98:02 (hexane/iPrOH) 1mL/min; T_{major} (13.7 min), T_{minor} (22.5 min); 83% ee.

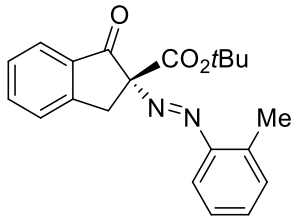

2.7o. Isolated as a yellow oil (7.5 mg, 86%). ^{1}H NMR (500 MHz, CD_2Cl_2) δ 7.80 (d, *J* = 7.6 Hz, 1H), 7.70 (t, *J* = 7.2 Hz, 1H), 7.58 (d, *J* = 7.7 Hz, 1H), 7.46 (t, *J* = 7.0 Hz, 1H), 7.41 – 7.34 (m, 2H), 7.31 (d, *J* = 7.4 Hz, 1H), 7.23 (t, *J* = 7.7 Hz, 1H), 3.92 (d, *J* = 17.6 Hz, 1H), 3.81 (d, *J* = 17.6 Hz, 1H), 2.47 (s, 3H), 1.54 – 1.47 (s, 9H). ^{13}C NMR (126 MHz, CD_2Cl_2) δ 196.94, 167.41, 152.14, 149.79, 137.41, 135.50, 134.63, 131.21, 131.05, 127.93, 126.45, 126.33, 124.59, 115.62, 88.42, 82.93, 36.20, 27.66, 16.85. HRMS (ESI) Calcd. for [M+Na]$^+$ $C_{21}H_{22}O_3N_2Na$: 373.1523; found:

373.1523. HPLC (ChiralPak IA column) 98:02 (hexane/iPrOH) 1mL/min; T_{major} (10.9 min), T_{minor} (12.7 min); 83% ee.

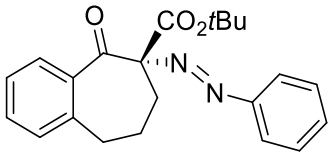

2.15a. Isolated as a yellow oil (88%) using conditions **C**. ^{1}H NMR (300 MHz, CD_2Cl_2) δ 7.74 – 7.62 (m, 2H), 7.57 (dd, *J* = 7.6, 1.5 Hz, 1H), 7.53 – 7.47 (m, 3H), 7.43 (td, *J* = 7.5, 1.6 Hz, 1H), 7.33 (td, *J* = 7.5, 1.3 Hz, 1H), 7.24 – 7.17 (m, 1H), 3.03 (ddd, *J* = 15.8, 8.5, 3.8 Hz, 1H), 2.87 (ddd, *J* = 15.8, 8.3, 3.8 Hz, 1H), 2.51 (t, *J* = 6.5 Hz, 2H), 2.19 – 1.91 (m, 2H), 1.30 (s, 9H). ^{13}C NMR (126 MHz, CD_2Cl_2) δ 200.61, 167.05, 151.55, 139.76, 139.21, 131.52, 131.35, 129.56, 129.46, 129.06, 126.35, 122.35, 90.03, 82.53, 33.42, 32.36, 27.38, 23.36. HRMS (ESI) Calcd. for $[M+Na]^+$ $C_{22}H_{24}O_3N_2Na$: 387.1679; found: 387.1677. HPLC (ChiralPak IA column) 97:03 (hexane/iPrOH) 1mL/min; T_{major} (8.6 min), T_{minor} (9.7 min); 97% ee.

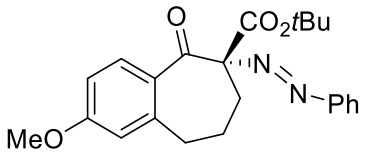

2.17a. Isolated as a yellow oil (8.1 mg, 82%) using conditions **C**. ^{1}H NMR (600 MHz, CD_2Cl_2) δ 7.73 – 7.66 (m, 2H), 7.62 (d, *J* = 8.6 Hz, 1H), 7.51 – 7.49 (m, 3H), 6.86 (dd, *J* = 8.6, 2.6 Hz, 1H), 6.71 (d, *J* = 2.4 Hz, 1H), 3.86 (s, 3H), 2.99 (ddd, *J* = 15.8, 9.1, 3.8 Hz, 1H), 2.82 (ddd, *J* = 15.7, 8.2, 3.8 Hz, 1H), 2.59 – 2.45 (m, 2H), 2.15 – 2.05 (m, 1H), 2.05 – 1.93 (m, 1H), 1.34 (s, 9H). ^{13}C NMR (151 MHz, CD_2Cl_2) δ 198.62, 167.25, 162.37, 151.55, 142.52, 132.04, 131.71, 131.18, 128.98, 122.28, 114.38, 111.86, 89.81, 82.31, 55.32, 33.46, 31.60, 27.41, 23.06. HRMS (ESI) Calcd. for $[M+Na]^+$ $C_{23}H_{26}O_4N_2Na$: 417.1785; found: 417.1788. HPLC (ChiralPak IA column) 96:04 (hexane/iPrOH) 1mL/min; T_{major} (23.3 min), T_{minor} (24.5 min); 86% ee.

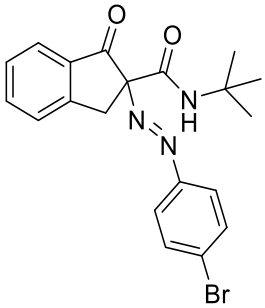

2.22b. Isolated as a yellow oil (8.8 mg, 91%) using conditions **C**. ^{1}H NMR (600 MHz, CD_2Cl_2) δ 7.74 – 7.66 (m, 2H), 7.66 – 7.62 (m, 2H), 7.61 – 7.56 (m, 3H), 7.45 – 7.38 (m, 1H), 7.31 (s, 1H), 4.01 (d, *J* = 17.5 Hz, 1H), 3.78 (d, *J* = 17.4 Hz, 1H), 1.43 (s, 9H). ^{13}C NMR (151 MHz, CD_2Cl_2) δ 198.25, 164.84, 153.95, 150.03, 135.89, 133.50, 132.36, 127.73, 126.41, 126.07, 124.74, 124.02, 89.80, 51.61, 33.51, 28.37. HRMS (ESI) Calcd. for $[M+Na]^+$ $C_{20}H_{20}O_2N_3Na$: 436.0631; found: 436.0637. HPLC (ChiralPak IC column) 90:10 (hexane/iPrOH) 1mL/min; T_{minor} (9.6 min), T_{major} (11.1 min); 90% ee.

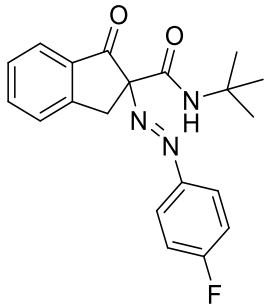

2.22c. Isolated as a yellow oil (6.9 mg, 85%) using conditions **C**. ^{1}H NMR (600 MHz, CD_2Cl_2) δ 7.76 – 7.67 (m, 4H), 7.59 (d, *J* = 7.8 Hz, 1H), 7.44 – 7.38 (m, 1H), 7.33 (s, 1H), 7.21 – 7.15 (m, 2H), 4.01 (d, *J* = 17.4 Hz, 1H), 3.77 (d, *J* = 17.5 Hz, 1H), 1.43 (s, 9H). ^{13}C NMR (151 MHz, CD_2Cl2) δ 198.47, 165.07, 164.68 (d, $J_{C\text{-}F}$ = 252.2 Hz), 153.99, 147.83 (d, $J_{C\text{-}F}$ = 3.0 Hz), 135.83, 133.59, 127.70, 126.40, 124.70, 116.03 (d, $J_{C\text{-}F}$ = 23.0 Hz), 89.40, 51.58, 33.61, 28.37. *one resonance missing. ^{19}F NMR (376 MHz, CD_2Cl_2) δ -108.08 – -108.15 (m). HRMS (ESI) Calcd. for $[M+Na]^+$ $C_{20}H_{20}O_2N_3Na$: 376.1432; found: 376.1435. HPLC (ChiralPak IC column) 90:10 (hexane/iPrOH) 1mL/min; T_{minor} (9.5 min), T_{major} (11.5 min); 85% ee.

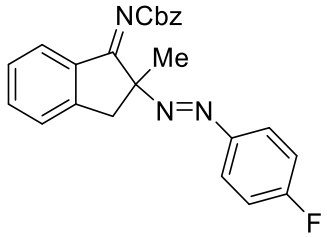

2.24a. Isolated as a yellow oil (11.8 mg, 59%) using conditions **C**. ^{1}H NMR (400 MHz, CD_2Cl_2) δ 7.80 – 7.62 (m, 2H), 7.57 – 7.53 (t, *J* = 7.7 Hz, 2H), 7.44 (d, *J* = 7.8 Hz, 1H), 7.43 – 7.22 (m, 6H), 7.12 (t, *J* = 8.5 Hz, 2H), 5.24 (d, *J* = 11.9 Hz, 1H), 5.14 (d, *J* = 12.6 Hz, 1H), 3.72 (d, *J* = 17.1 Hz, 1H), 3.11 (d, *J* = 17.1 Hz, 1H), 1.72 (s, 3H). ^{13}C NMR (151 MHz, CD_2Cl_2) δ 175.06, 164.26 (d, $J_{C\text{-}F}$ = 252.2 Hz), 161.89, 148.70, 148.24 (d, $J_{C\text{-}F}$ = 3.0 Hz), 135.46, 133.87, 128.58, 128.43, 128.32, 127.58, 126.19, 124.76, 124.53 (d, $J_{C\text{-}F}$ = 9.1 Hz), 115.79 (d, $J_{C\text{-}F}$ = 24.2 Hz), 68.09, 40.73, 29.64, 8.34. (one resonance missing). ^{19}F NMR (376 MHz, CD_2Cl_2) δ -109.63. HRMS (ESI) Calcd. for $[M+H]^+$ $C_{24}H_{21}O_2N_3F$: 402.1612; found: 402.1613. HPLC (ChiralPak IC column) 95:05 (hexane/iPrOH) 1mL/min; T_{major} (15.2 min), T_{minor} (14.0 min); 80% ee.

General procedure for hydrogenation of diazene compounds

A one dram vial was charged with diazene (1 equiv), Pd/C (10 wt %, 10 mol %), and a magnetic stir bar. MeOH and AcOH (10:1, 0.05M) were then added and the vial was placed in a Parr bomb. The bomb was purged with H_2 and pressurized to 800 psi. After 24 h, Na_2CO_3 (20 equiv.) and celite were added and the mixture was stirred for 30 min. The mixture was filtered and concentrated. The crude product was purified by column chromatography on Et_3N treated silica gel (100 % EtOAc) to afford the corresponding amino alcohol.

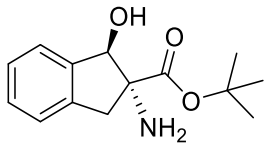

2.25a. Isolated as a white solid (78%). ^{1}H NMR (600 MHz, $CDCl_3$) δ 7.40 (d, *J* = 6.3 Hz, 1H), 7.28 – 7.24 (m, 2H), 7.21 (d, *J* = 6.6 Hz, 1H), 4.91 (s, 1H), 3.60 (d, *J* = 16.1 Hz, 1H), 2.83 (d, *J* = 16.1 Hz, 1H), 2.40 (s, 3H), 1.44 (s, 9H). ^{13}C NMR (151 MHz, $CDCl_3$) δ 174.02, 142.24, 140.63, 128.75, 127.20, 124.83, 124.83, 84.29, 82.05, 69.57, 42.07, 27.93. HRMS (ESI) Calcd. for $[M+H]^+$ $C_{14}H_{20}O_3N$: 250.1438; found: 250.1437. HPLC (ChiralPak AD-H column) 98:02 (hexane/iPrOH) 1mL/min; T_{major} (39.6 min), T_{minor} (43.1 min); 90% ee. The relative stereochemistry agrees with reported NMR spectra of the same compound.[23]

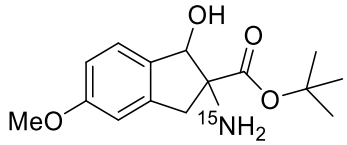

2.25b was prepared in a 3-step sequence starting with ^{15}N-labeled $NaNO_2$.
2.25b. ^{1}H NMR (500 MHz, CD_2Cl_2) δ 7.31 (d, *J* = 8.1 Hz, 1H), 6.80 – 6.82 (m, 2H), 4.77 (d, *J* = 2.4 Hz, 1H), 3.82 (s, 3H), 3.64 (dd, *J* = 16.2, 3.3 Hz, 1H), 2.73 (dd, *J* = 16.4, 2.9 Hz, 1H), 2.41 (br s, 3H), 1.50 (s, 9H). ^{13}C NMR (126 MHz, CD_2Cl_2) δ 174.05, 160.50, 143.38, 134.66, 125.98, 112.91, 110.05, 83.58 (d, $J_{C\text{-}N}$ = 4.4 Hz), 81.60, 69.80 (d, $J_{C\text{-}N}$ = 3.9 Hz), 55.35, 41.72, 27.74. HRMS (ESI) Calcd. for $[M+Na]^+$ $C_{15}H_{21}O_4{}^{15}NNa$: 303.1333; found: 303.1334. HPLC (ChiralPak AD-H column) 98:02 (hexane/iPrOH) 1mL/min; T_{major} (41.9 min), T_{minor} (46.7 min); 90% ee.

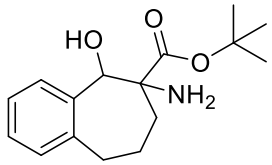

2.26a. Isolated as a white solid (90%). ^{1}H NMR (300 MHz, CD_2Cl_2) δ 7.37 – 7.34 (m, 1H), 7.21 – 7.13 (m, 2H), 7.13 – 7.04 (m, 1H), 4.71 (s, 1H), 3.11 – 3.03 (m, 1H), 2.74 – 2.33 (m, 5H), 1.84 – 1.69 (m, 3H), 1.31 (s, 9H). ^{13}C NMR (H-Cl salt, 151 MHz, MeOD) δ 167.42, 139.03, 138.27, 128.38, 127.61, 125.90, 83.44, 65.44, 64.18, 34.26, 32.97, 26.38, 22.33, 13.98. HRMS (ESI) Calcd. for $[M+H]^+$ $C_{16}H_{24}O_3N$: 278.1751; found: 278.1750.

Notes and references:

(1) Nugent, T. C. *Chiral Amine Synthesis: Methods, Developments and Applications*; John Wiley & Sons, 2011.
(2) Reetz, M. T. *Angew. Chem. Int. Ed. Engl.* **1991**, *30* (12), 1531.
(3) Nájera, C.; Sansano, J. M. *Chem. Rev.* **2007**, *107* (11), 4584.
(4) Nair, V.; Biju, A. T.; Mathew, S. C.; Babu, B. P. *Chem. – Asian J.* **2008**, *3* (5), 810.
(5) Huisgen, R.; Jakob, F. *Justus Liebigs Ann. Chem.* **1954**, *590* (1), 37.
(6) Evans, D. A.; Nelson, S. G. *J. Am. Chem. Soc.* **1997**, *119* (27), 6452.
(7) Bøgevig, A.; Juhl, K.; Kumaragurubaran, N.; Zhuang, W.; Jørgensen, K. A. *Angew. Chem.* **2002**, *114* (10), 1868.

(8) List, B. *J. Am. Chem. Soc.* **2002**, *124* (20), 5656.
(9) Kumaragurubaran, N.; Juhl, K.; Zhuang, W.; Bøgevig, A.; Jørgensen, K. A. *J. Am. Chem. Soc.* **2002**, *124* (22), 6254.
(10) Nelson, H. M.; Reisberg, S. H.; Shunatona, H. P.; Patel, J. S.; Toste, F. D. *Angew. Chem. Int. Ed.* **2014**, *53* (22), 5600.
(11) Rauniyar, V.; Lackner, A. D.; Hamilton, G. L.; Toste, F. D. *Science* **2011**, *334* (6063), 1681.
(12) Wang, Y.-M.; Wu, J.; Hoong, C.; Rauniyar, V.; Toste, F. D. *J. Am. Chem. Soc.* **2012**, *134* (31), 12928.
(13) Hatano, M.; Ikeno, T.; Matsumura, T.; Torii, S.; Ishihara, K. *Adv. Synth. Catal.* **2008**, *350* (11-12), 1776.
(14) Phipps, R. J.; Hiramatsu, K.; Toste, F. D. *J. Am. Chem. Soc.* **2012**, *134* (20), 8376.
(15) Murigi, F. N.; Nichol, G. S.; Mash, E. A. *J. Org. Chem.* **2010**, *75* (4), 1293.
(16) Gottlieb, H. E.; Kotlyar, V.; Nudelman, A. *J. Org. Chem.* **1997**, *62* (21), 7512.
(17) Emelen, K. V.; De Wit, T.; Hoornaert, G. J.; Compernolle, F. *Tetrahedron* **2002**, *58* (21), 4225.
(18) Capuzzi, M.; Perdicchia, D.; Jørgensen, K. A. *Chem. – Eur. J.* **2008**, *14* (1), 128.
(19) Nakajima, M.; Yamamoto, S.; Yamaguchi, Y.; Nakamura, S.; Hashimoto, S. *Tetrahedron* **2003**, *59* (37), 7307.
(20) Wu, F.; Li, H.; Hong, R.; Deng, L. *Angew. Chem. Int. Ed.* **2006**, *45* (6), 947.
(21) Kobayashi, S.; Gustafsson, T.; Shimizu, Y.; Kiyohara, H.; Matsubara, R. *Org. Lett.* **2006**, *8* (21), 4923.
(22) Cao, W.; Liu, X.; Peng, R.; He, P.; Lin, L.; Feng, X. *Chem. Commun.* **2013**, *49* (33), 3470.
(23) Poulsen, T. B.; Bernardi, L.; Alemán, J.; Overgaard, J.; Jørgensen, K. A. *J. Am. Chem. Soc.* **2007**, *129* (2), 441.
(24) Moss, T. A.; Alba, A.; Hepworth, D.; Dixon, D. J. *Chem. Commun.* **2008**, No. 21, 2474.

NMR Spectra

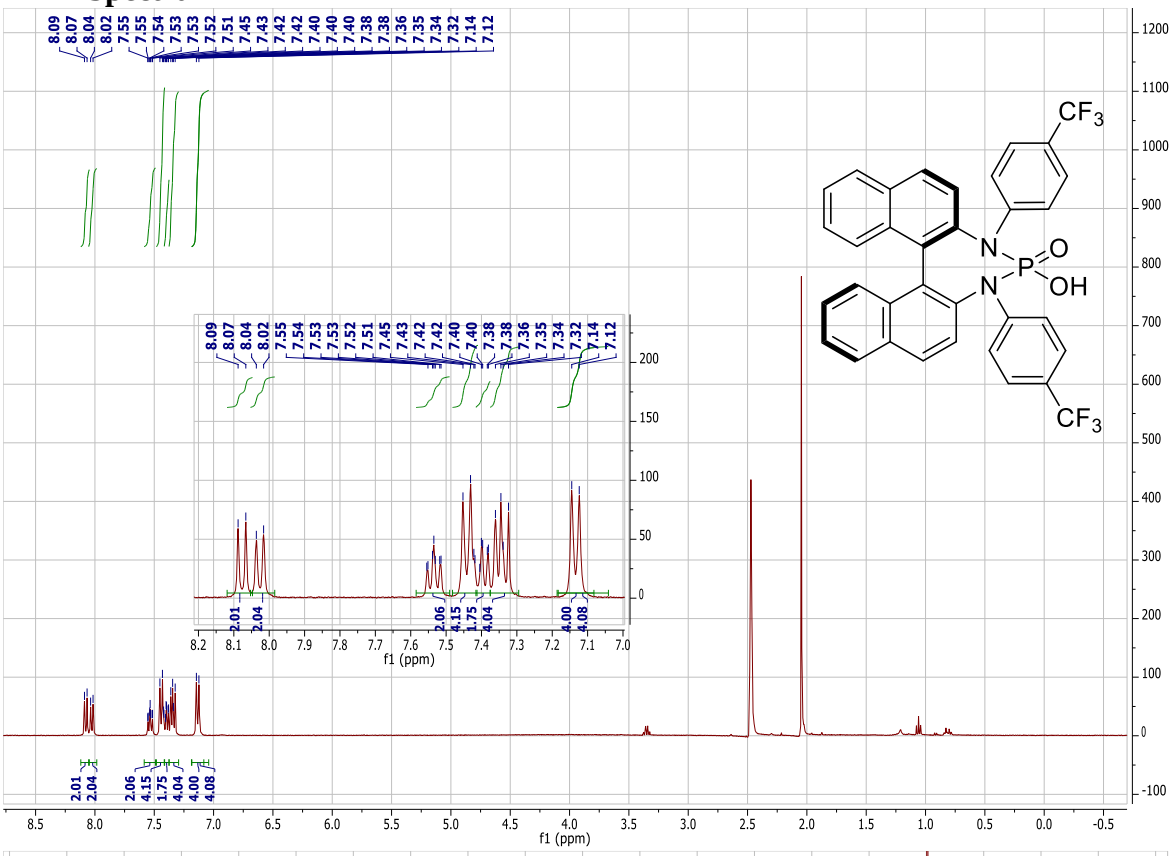
8.09 8.07 8.04 8.02 7.55 7.55 7.54 7.53 7.53 7.53 7.52 7.51 7.45 7.43 7.42 7.42 7.40 7.40 7.40 7.38 7.38 7.36 7.35 7.34 7.32 7.14 7.12
2.01 2.04 2.06 4.15 1.75 4.04 4.00 4.08
f1 (ppm)
CF3
N
P
O
OH
N
CF3

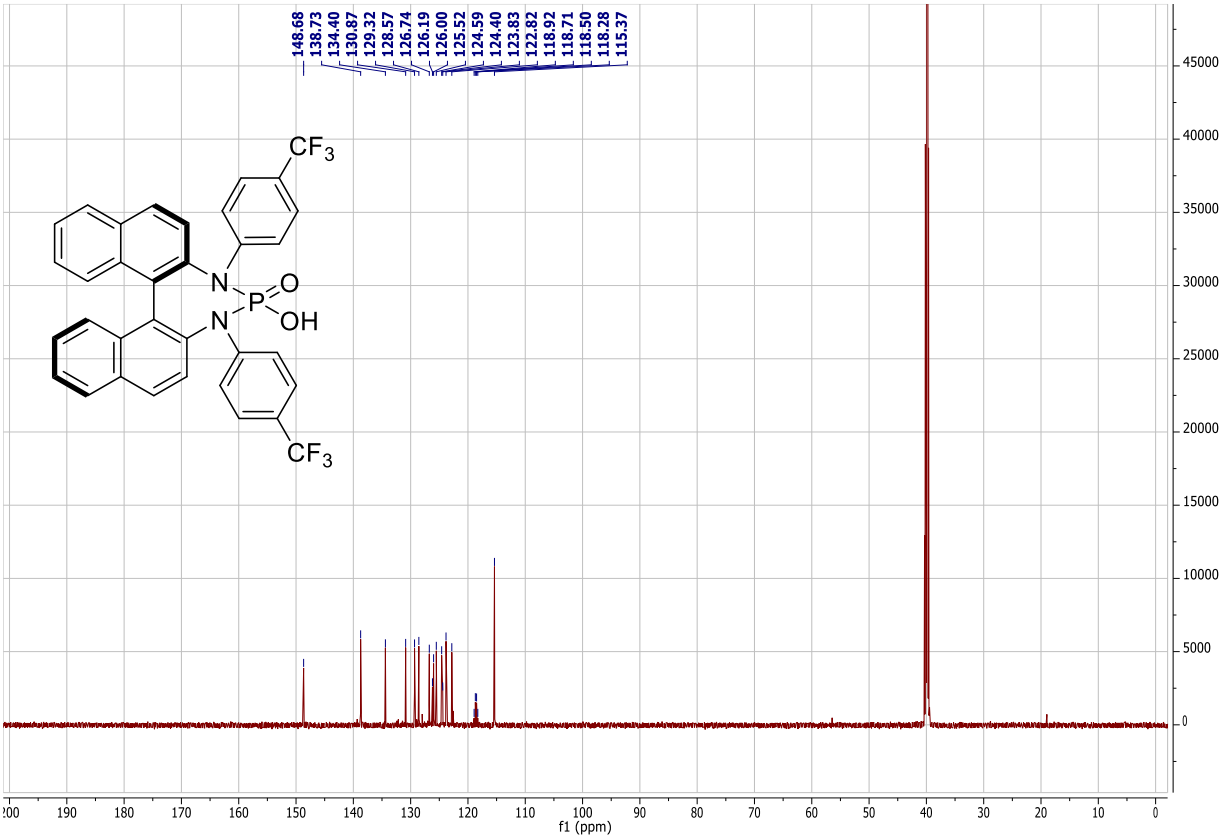
148.68 138.73 134.40 130.87 129.32 128.57 126.74 126.19 126.00 125.52 124.59 124.40 123.83 122.82 118.92 118.71 118.50 118.28 115.37
f1 (ppm)
CF3
N
P
O
OH
N
CF3

^{19}F NMR

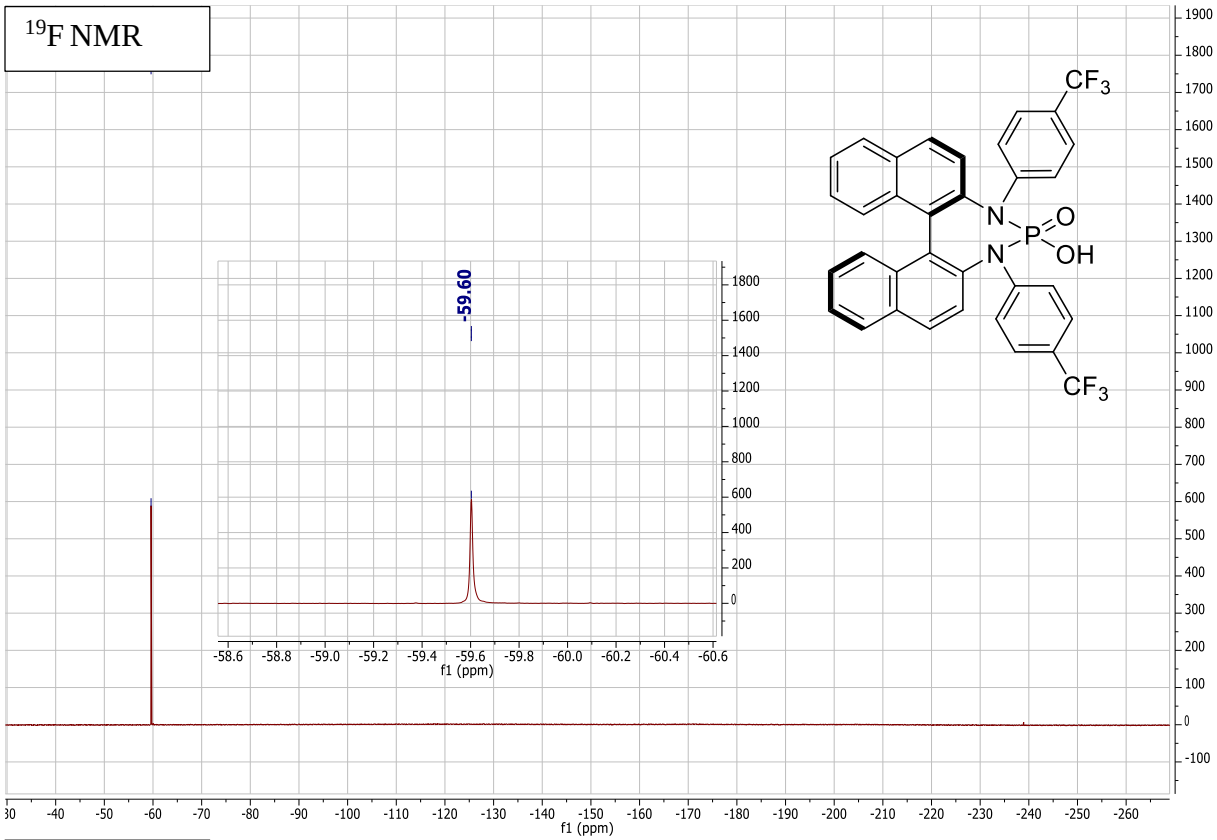

^{31}P NMR

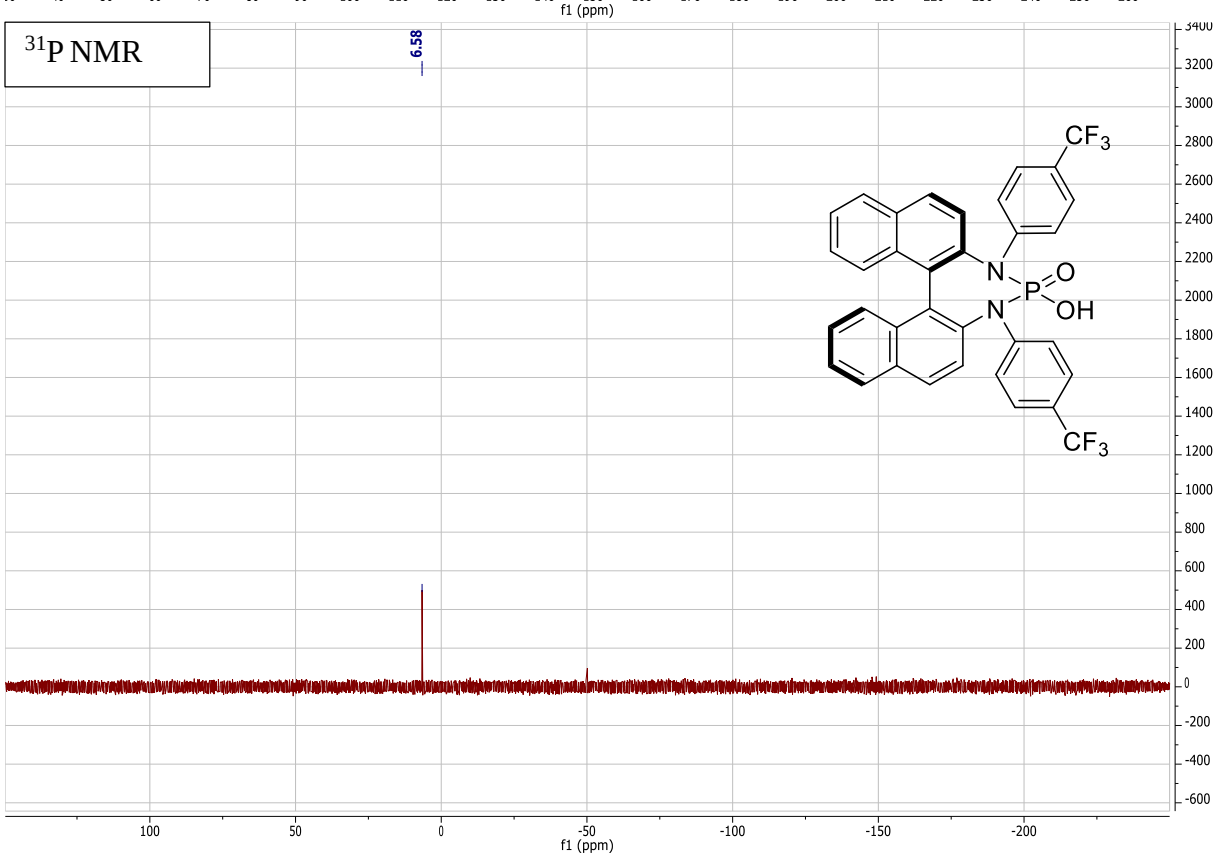

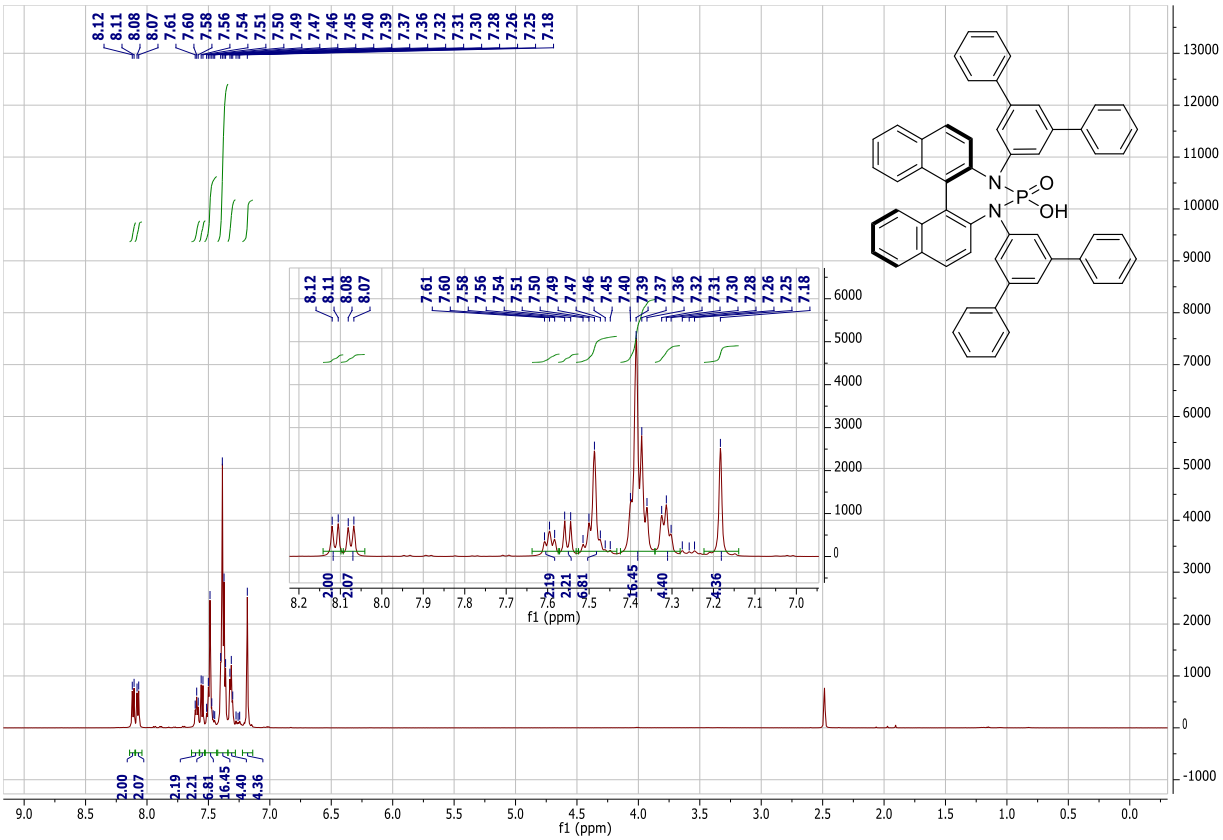
8.12 8.11 8.08 8.07 7.61 7.60 7.58 7.56 7.54 7.51 7.50 7.49 7.47 7.46 7.45 7.40 7.39 7.37 7.36 7.32 7.31 7.30 7.28 7.26 7.25 7.18
2.00 2.07 2.19 2.21 6.81 16.45 4.40 4.36
f1 (ppm)
N
P
O
OH
N

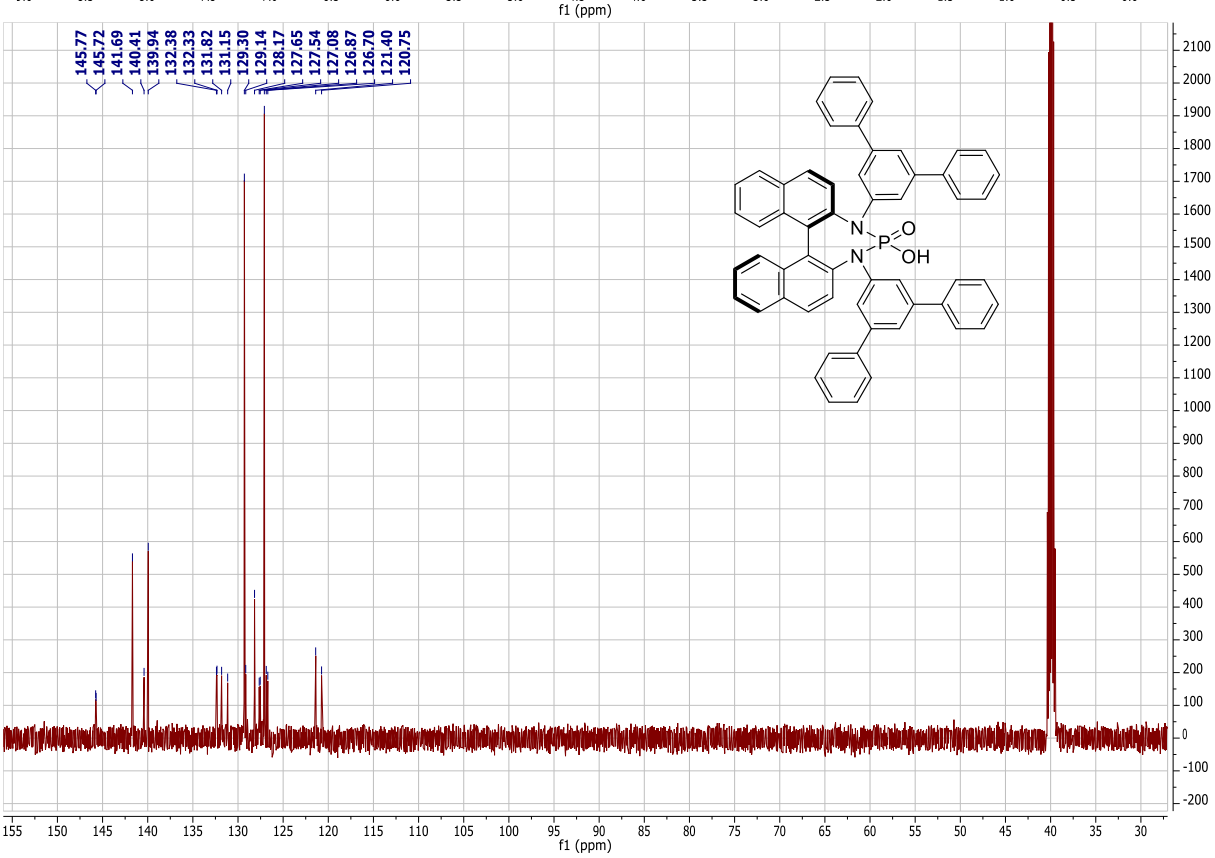
145.77 145.72 141.69 140.41 139.94 132.38 132.33 131.82 131.15 129.30 129.14 128.17 127.65 127.54 127.08 126.87 126.70 121.40 120.75
f1 (ppm)
N
P
O
OH
N

^{31}P NMR

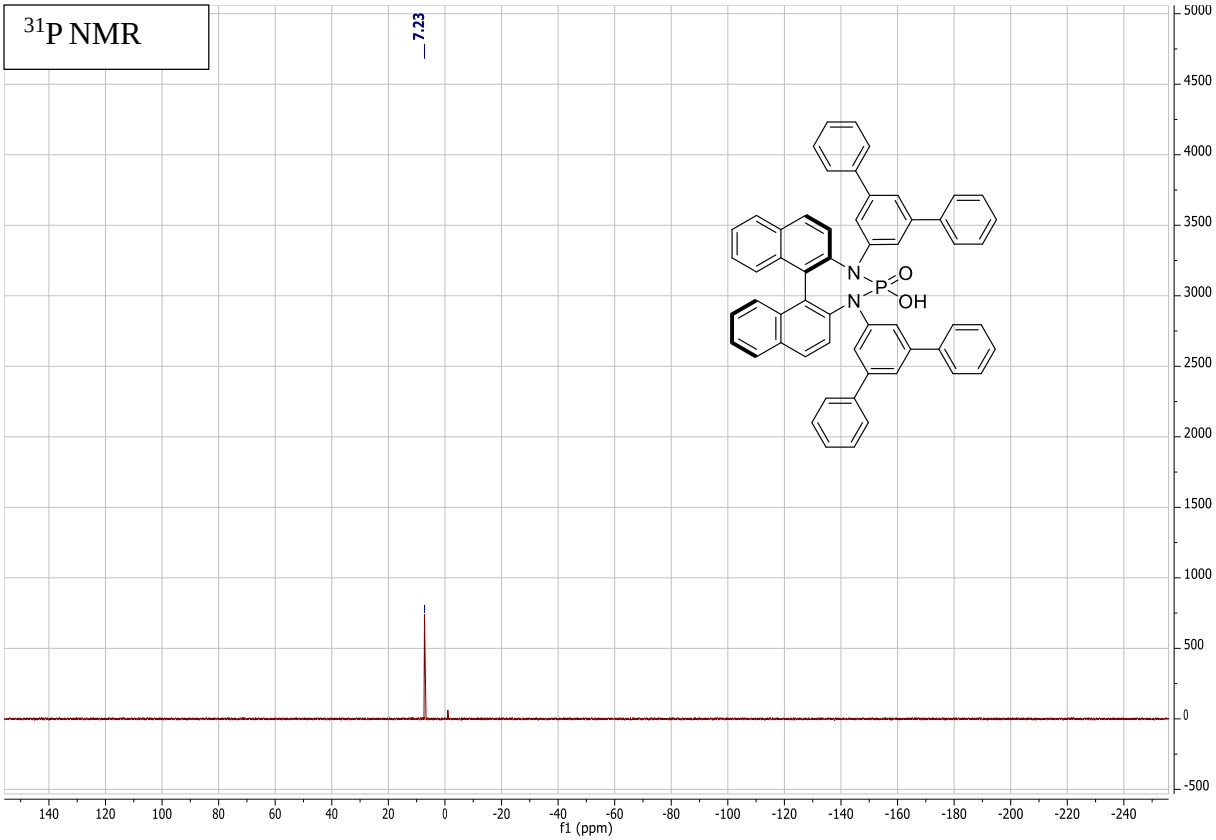
7.23
N
P
O
OH
N
f1 (ppm)

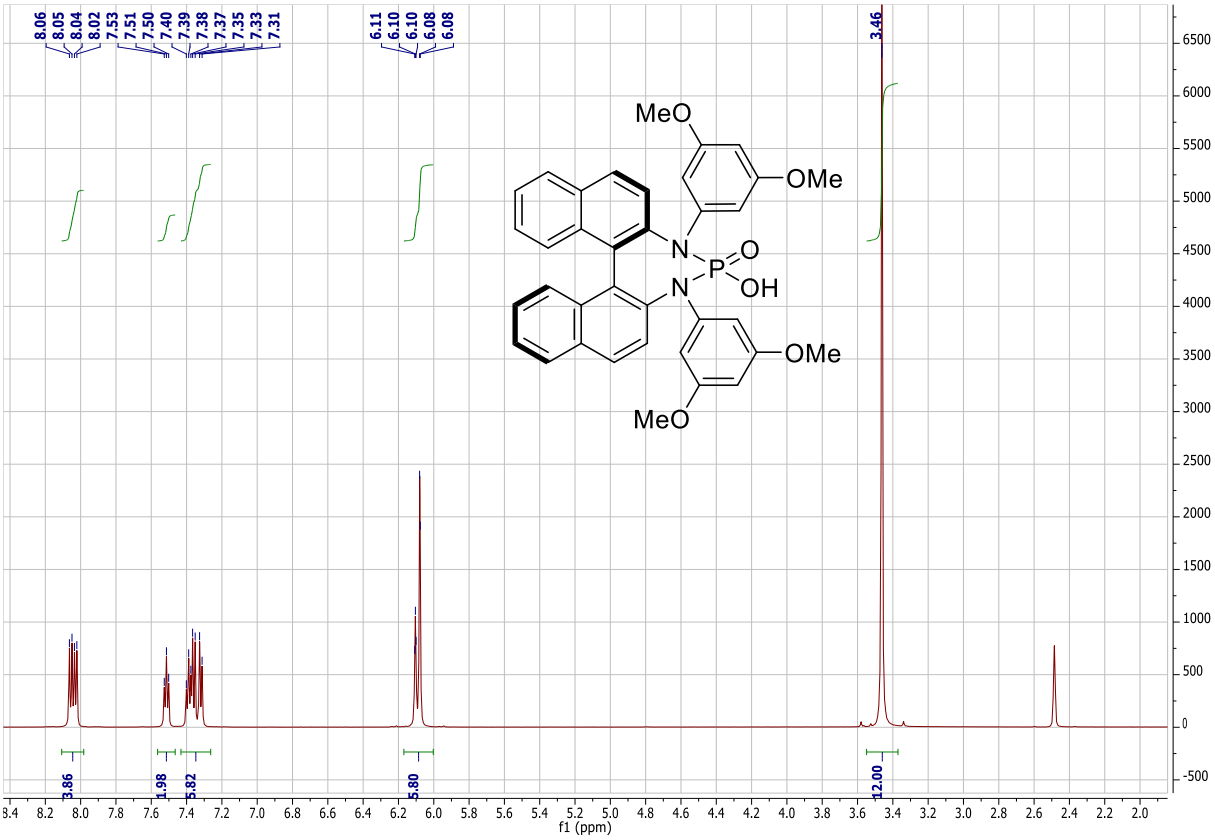
8.06
8.05
8.04
8.02
7.53
7.51
7.50
7.40
7.39
7.38
7.37
7.35
7.33
7.31
6.11
6.10
6.10
6.08
6.08
3.46
MeO
OMe
N
P
O
OH
N
OMe
MeO
3.86
1.98
5.82
5.80
12.00
f1 (ppm)

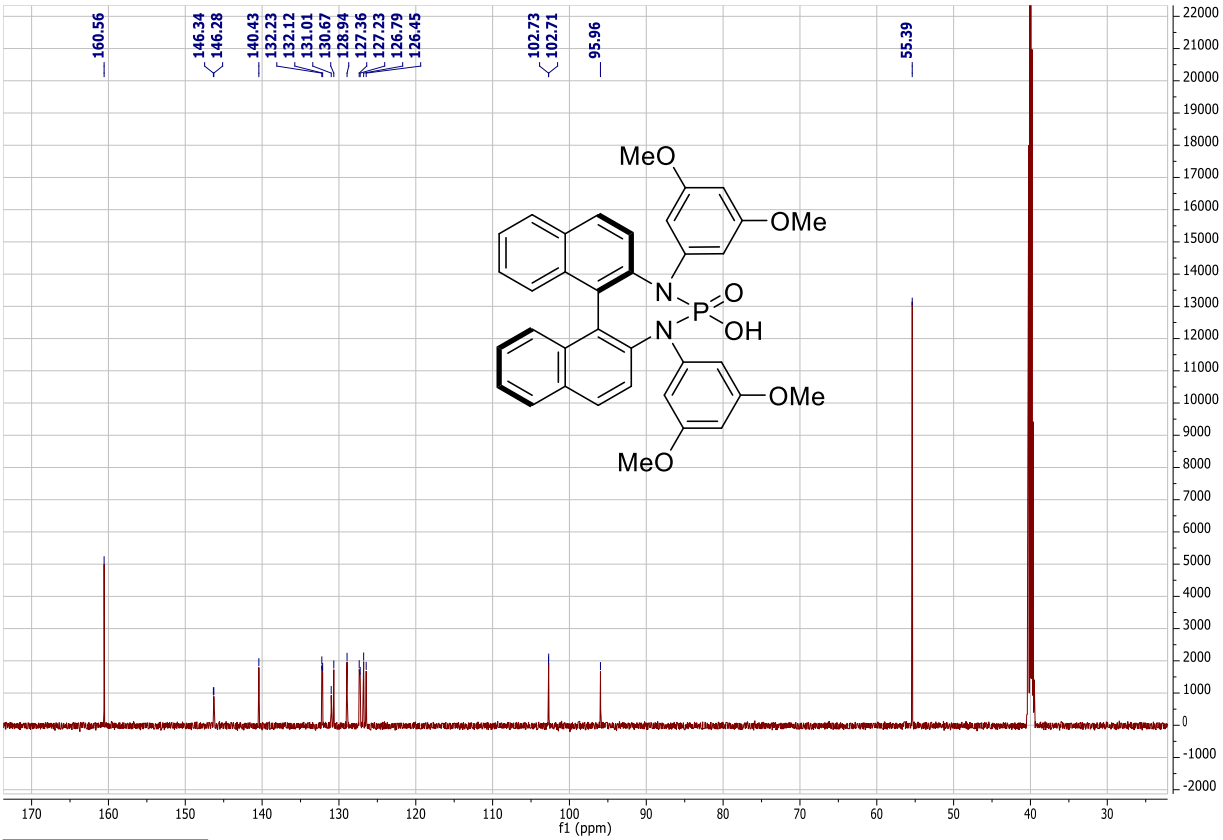
160.56
146.34
146.28
140.43
132.23
132.12
131.01
130.67
128.94
127.36
127.23
126.79
126.45
102.73
102.71
95.96
55.39
MeO
OMe
N
P
O
OH
N
OMe
MeO
f1 (ppm)

^{31}P NMR

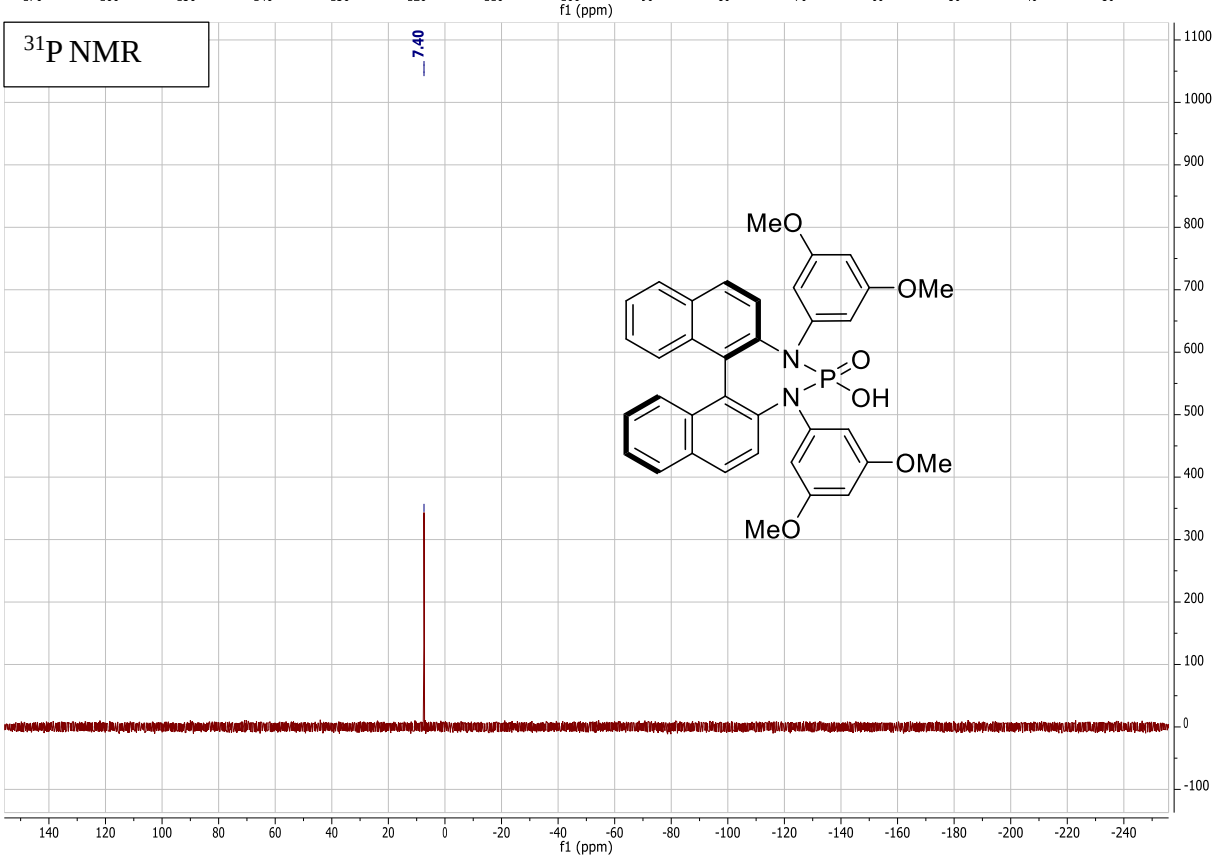
7.40
MeO
OMe
N
P
O
OH
N
OMe
MeO
f1 (ppm)

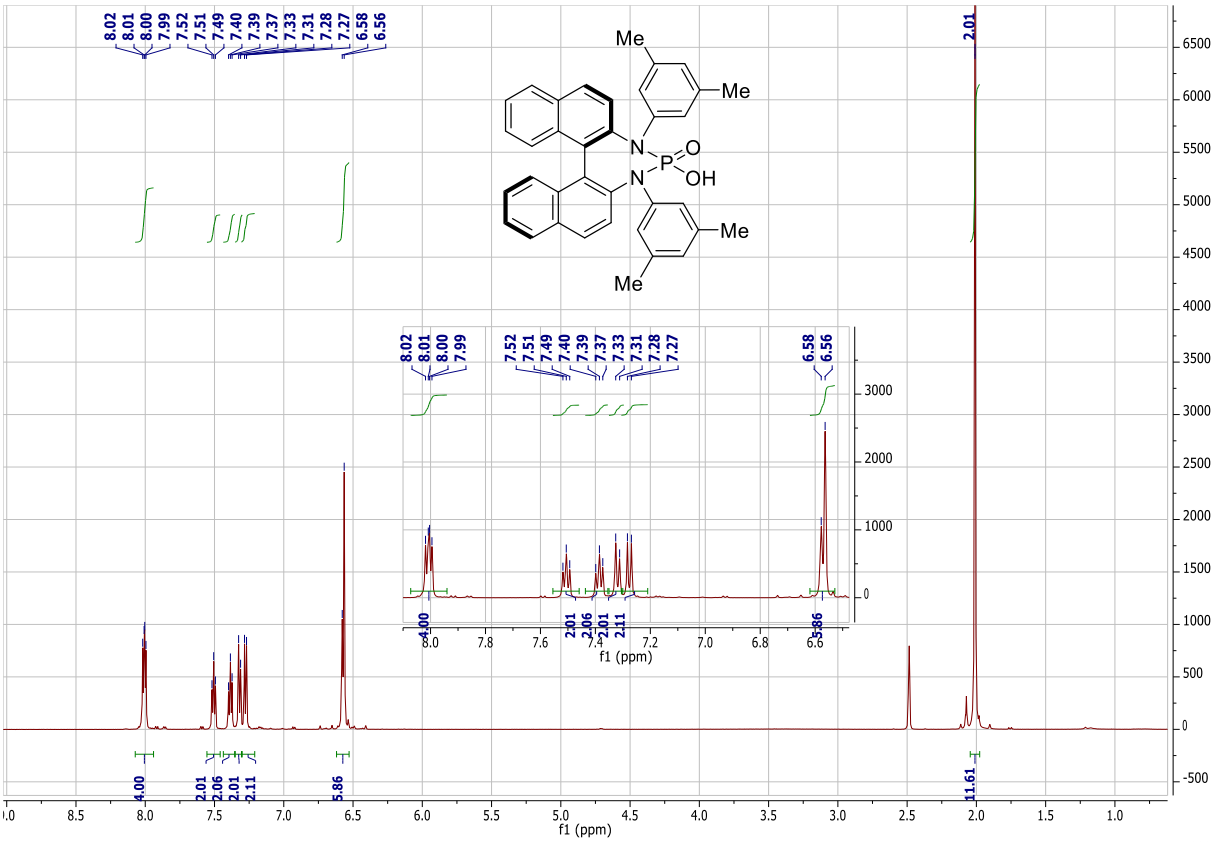
8.02
8.01
8.00
7.99
7.52
7.51
7.49
7.40
7.39
7.37
7.33
7.31
7.28
7.27
6.58
6.56
2.01
Me
Me
N
P
O
OH
N
Me
Me
4.00
2.01
2.06
2.01
2.11
5.86
11.61
f1 (ppm)

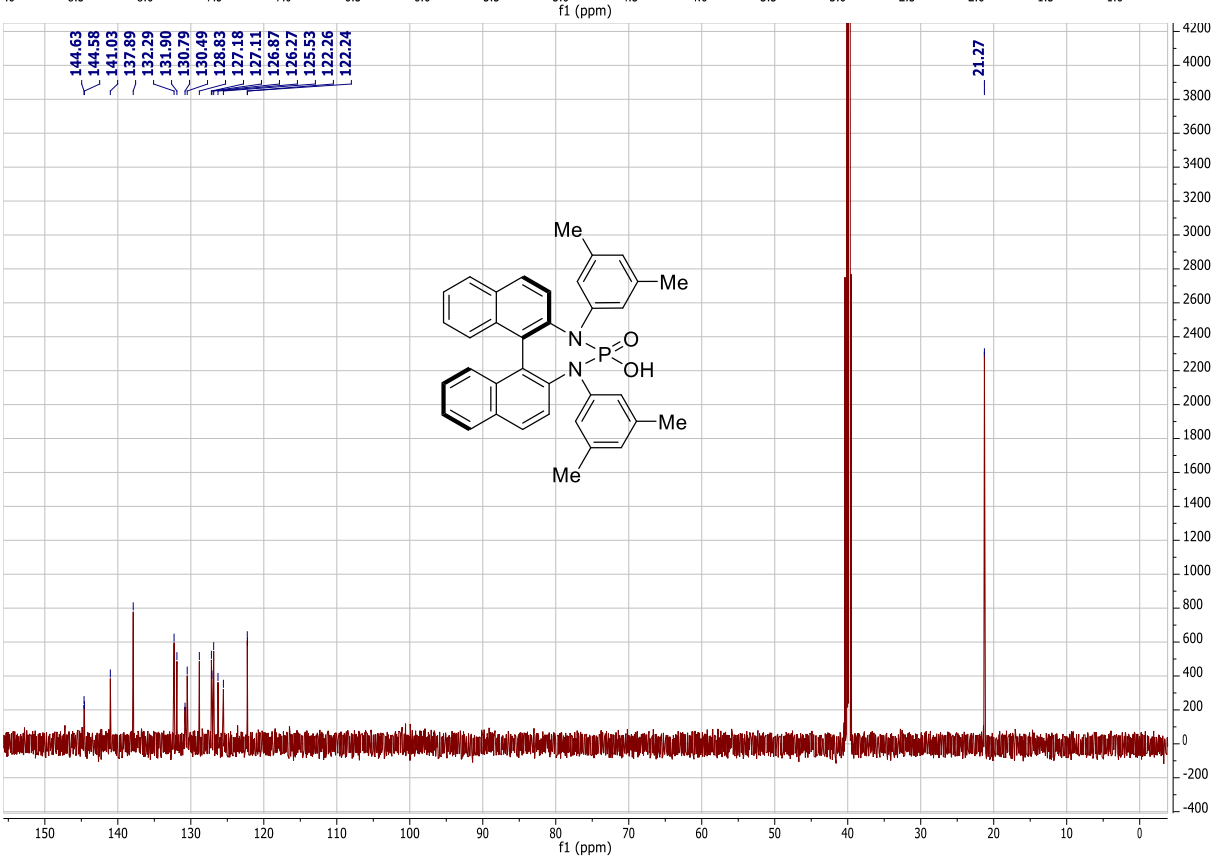
144.63
144.58
141.03
137.89
132.29
131.90
130.79
130.49
128.83
127.18
127.11
126.87
126.27
125.53
122.26
122.24
21.27
Me
Me
N
P
O
OH
N
Me
Me
f1 (ppm)

^{31}P NMR

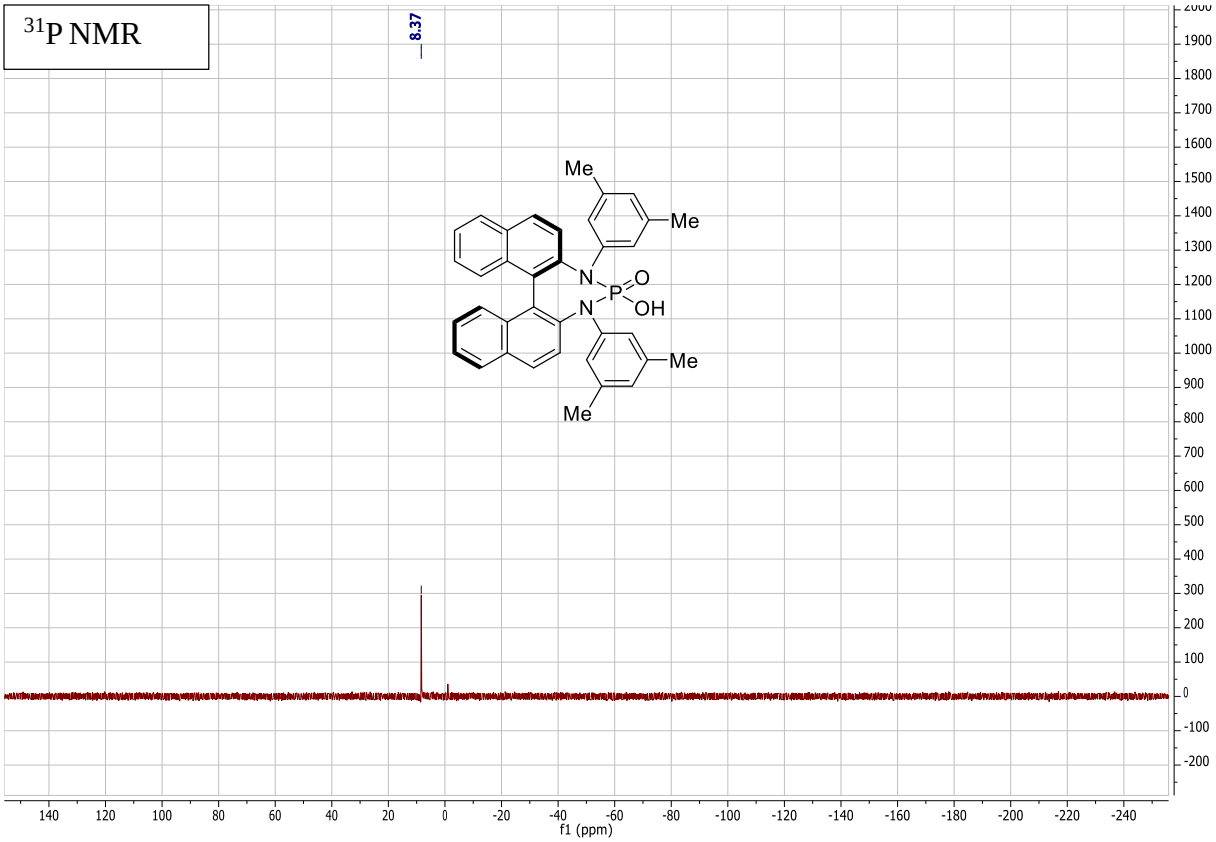
8.37
Me
Me
N
P
O
OH
N
Me
Me
f1 (ppm)

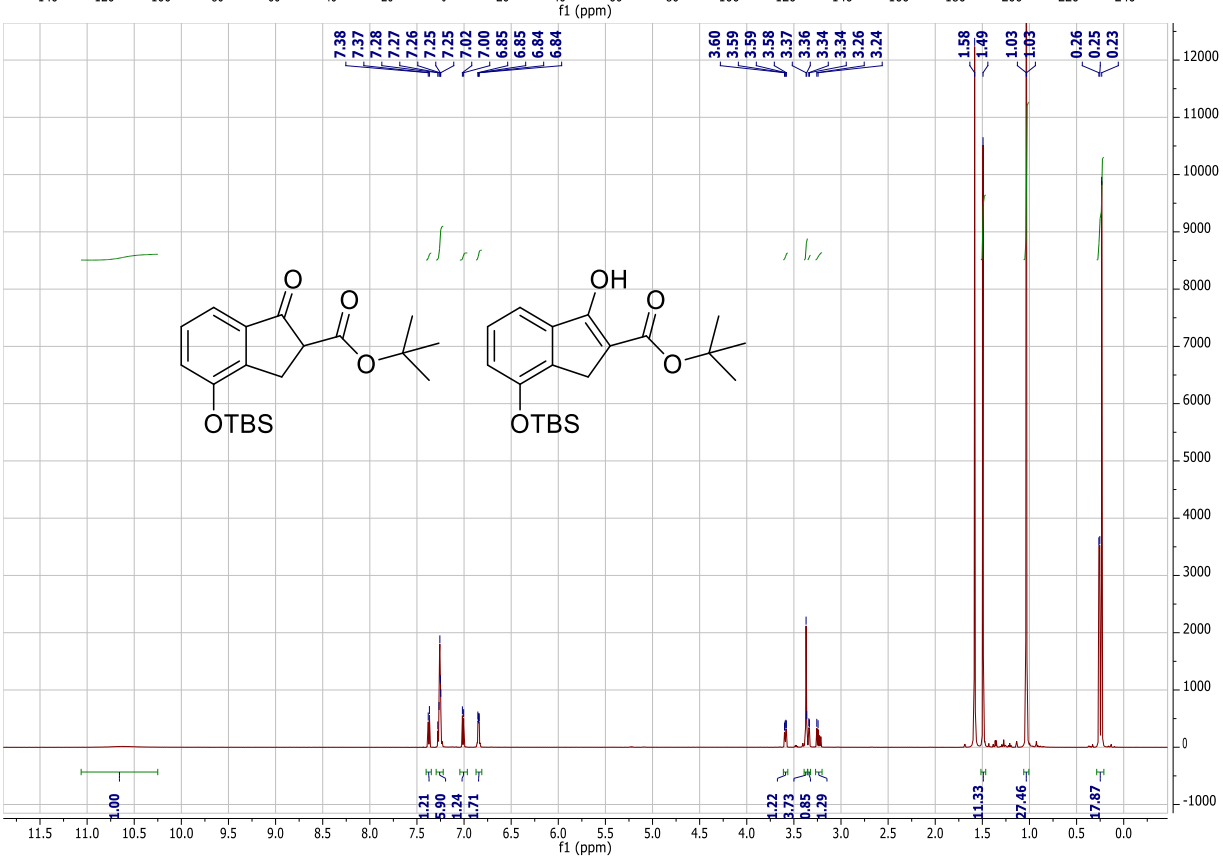
7.38
7.37
7.28
7.27
7.26
7.25
7.25
7.02
7.00
6.85
6.85
6.84
6.84
3.60
3.59
3.59
3.58
3.37
3.36
3.34
3.34
3.26
3.24
1.58
1.49
1.03
1.03
0.26
0.25
0.23
O
O
O
OTBS
OH
O
O
OTBS
1.00
1.21
5.90
1.24
1.71
1.22
3.73
0.85
1.29
11.33
27.46
17.87
f1 (ppm)

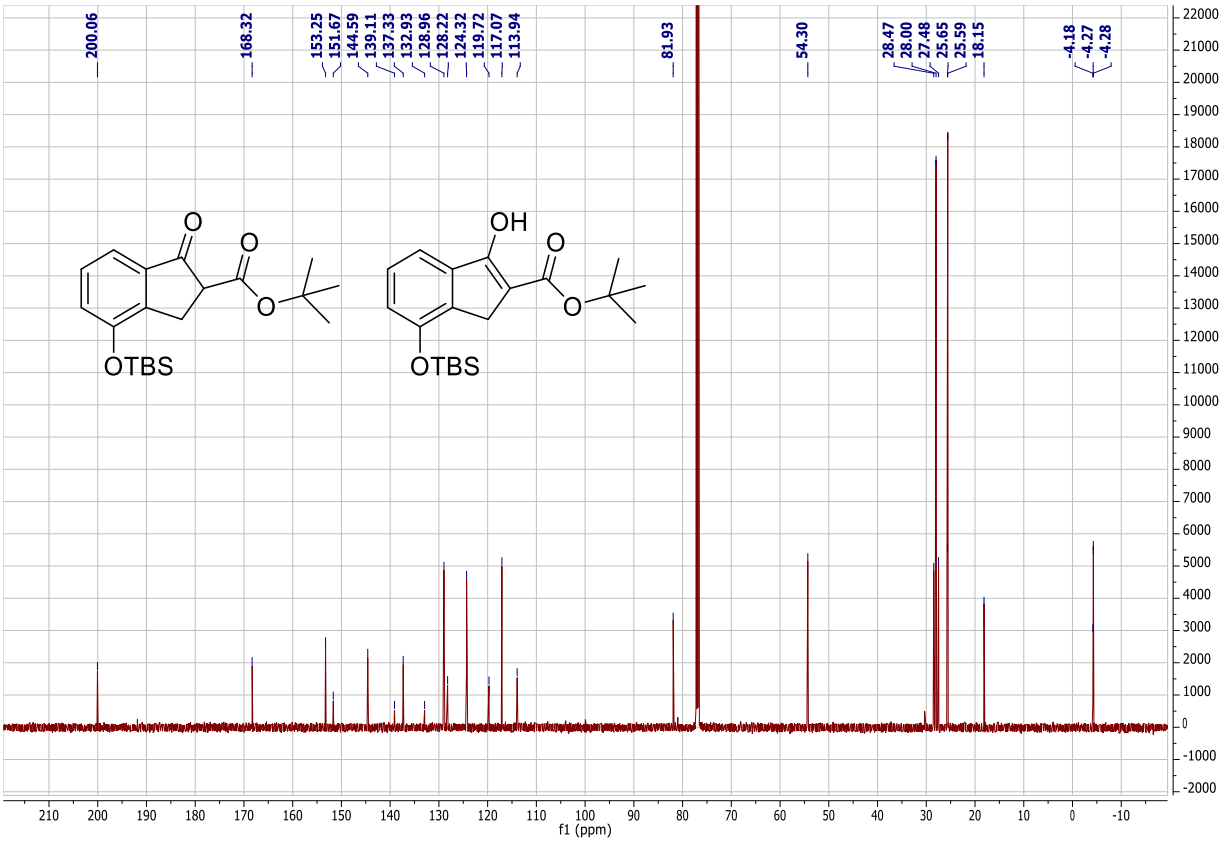
200.06
168.32
153.25
151.67
144.59
139.11
137.33
132.93
128.96
128.22
124.32
119.72
117.07
113.94
81.93
54.30
28.47
28.00
27.48
25.65
25.59
18.15
-4.18
-4.27
-4.28
OTBS
OH
OTBS
f1 (ppm)

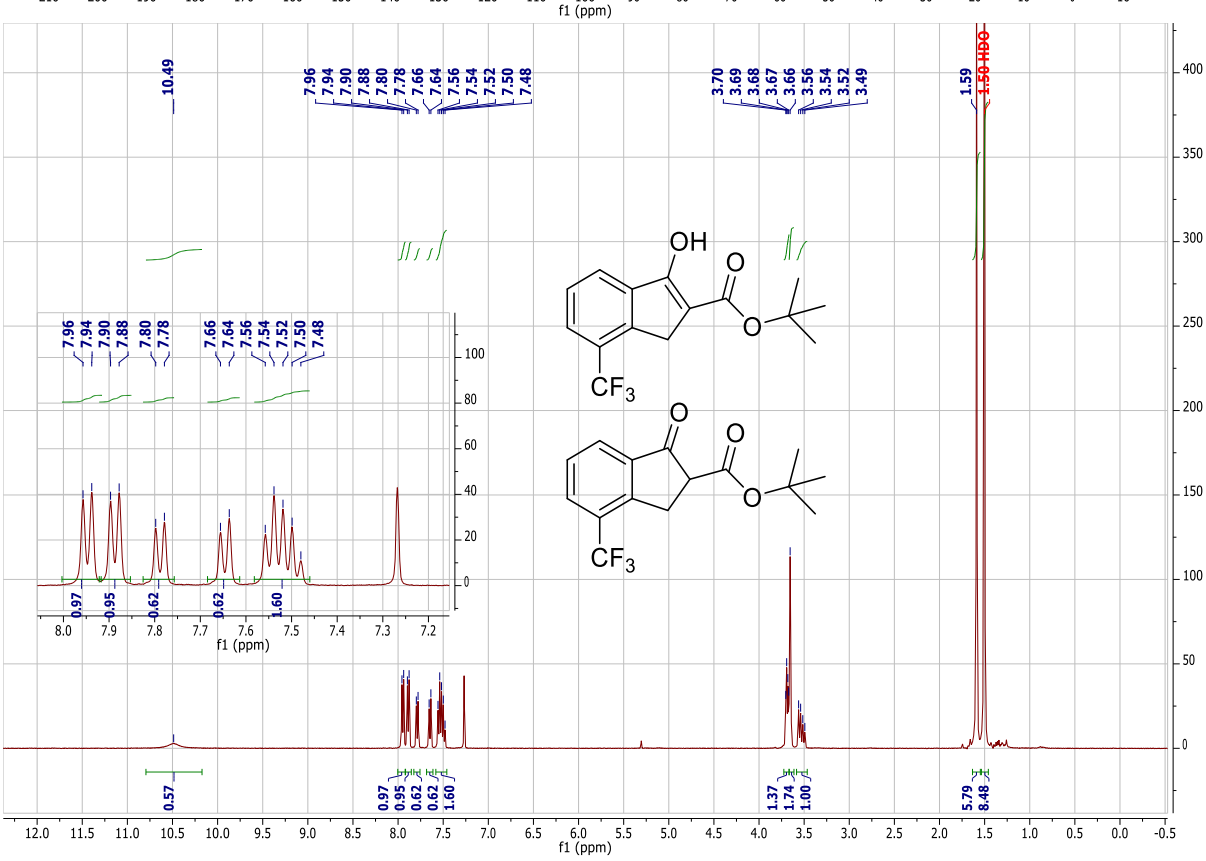
10.49
7.96
7.94
7.90
7.88
7.80
7.78
7.66
7.64
7.56
7.54
7.52
7.50
7.48
3.70
3.69
3.68
3.67
3.66
3.56
3.54
3.52
3.49
1.59
1.50 HDO
OH
CF3
CF3
0.57
0.97
0.95
0.62
0.62
1.60
1.37
1.74
1.00
5.79
8.48
f1 (ppm)

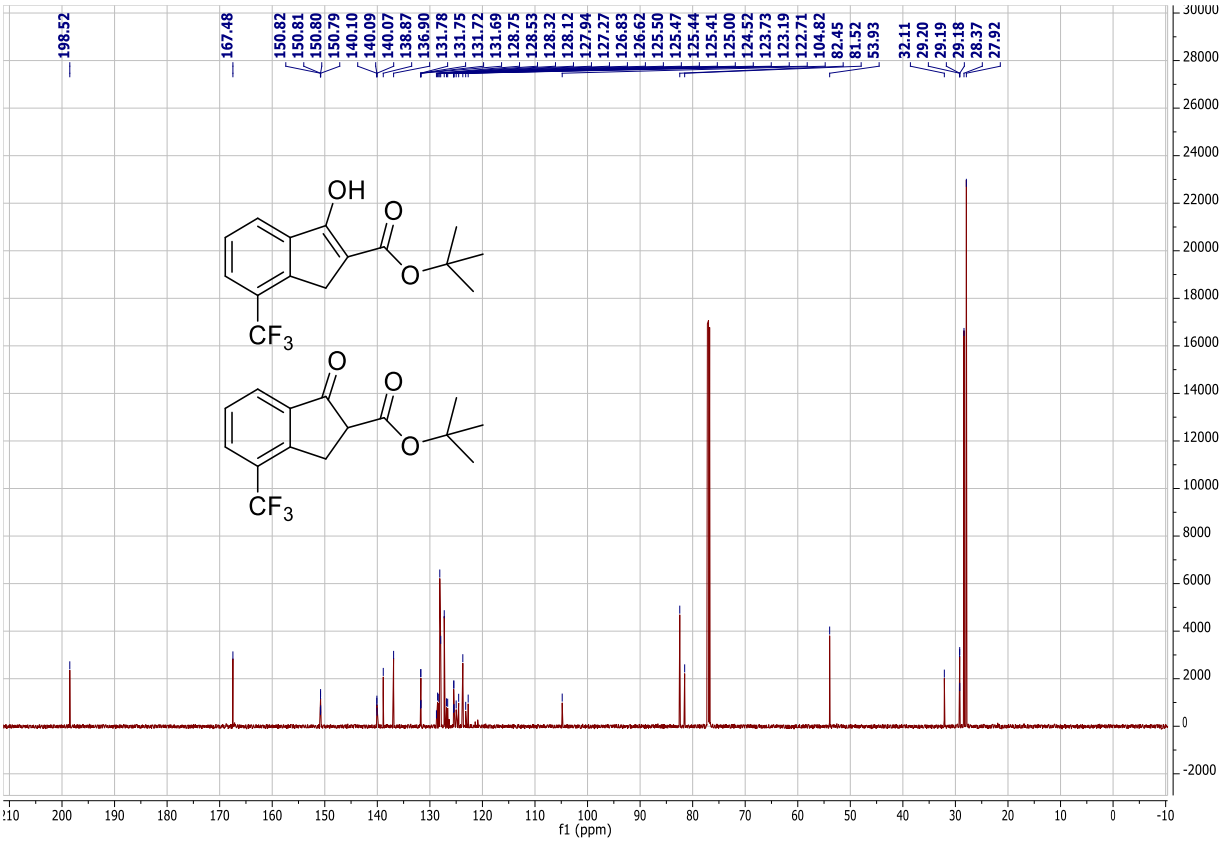
198.52
167.48
150.82
150.81
150.80
150.79
140.10
140.09
140.07
138.87
136.90
131.78
131.75
131.72
131.69
128.75
128.53
128.32
128.12
127.94
127.27
126.83
126.62
125.50
125.47
125.44
125.41
125.00
124.52
123.73
123.19
122.71
104.82
82.45
81.52
53.93
32.11
29.20
29.19
29.18
28.37
27.92
OH
O
O
CF3
O
O
O
CF3
f1 (ppm)

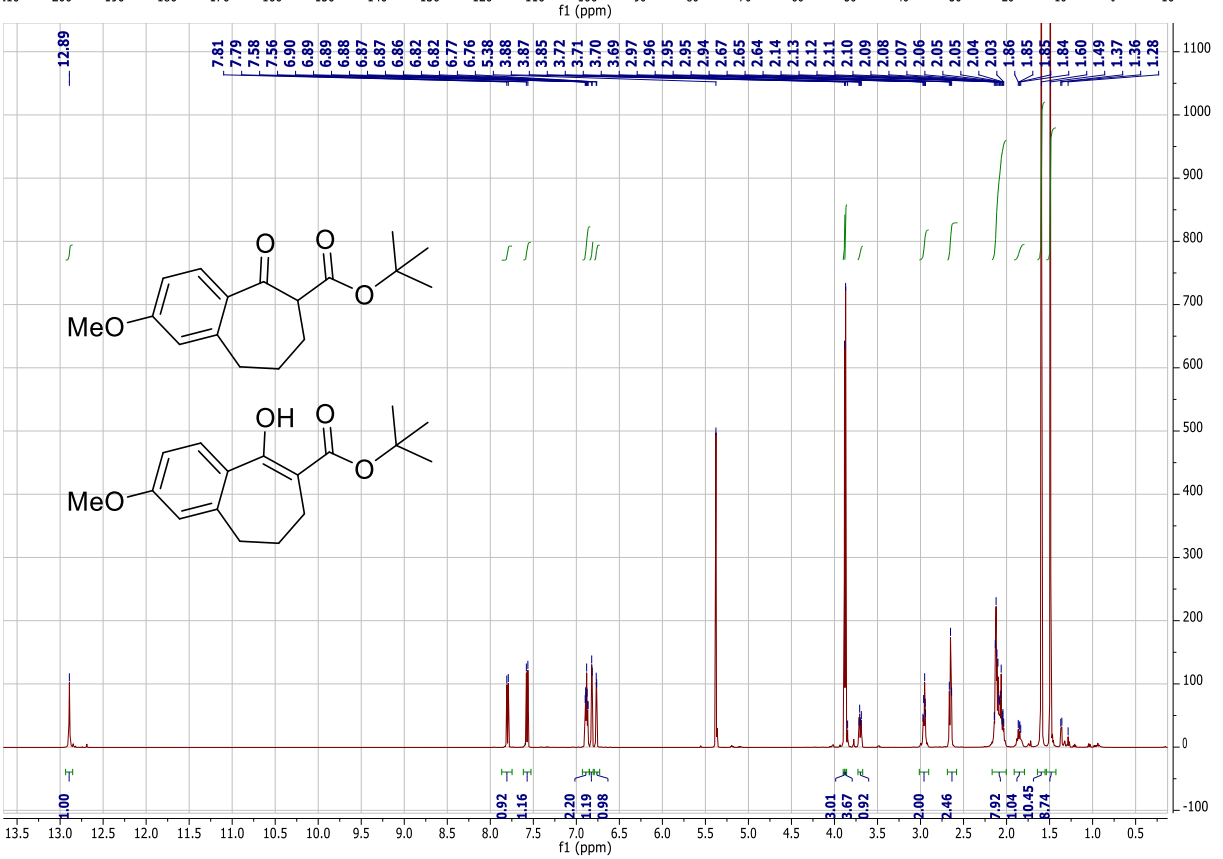
12.89
7.81
7.79
7.58
7.56
6.90
6.89
6.89
6.88
6.87
6.87
6.86
6.82
6.82
6.77
6.76
5.38
3.88
3.87
3.85
3.72
3.71
3.70
3.69
2.97
2.96
2.95
2.95
2.94
2.67
2.65
2.64
2.14
2.13
2.12
2.11
2.10
2.09
2.08
2.07
2.06
2.05
2.05
2.04
2.03
1.86
1.85
1.85
1.84
1.60
1.49
1.37
1.36
1.28
O
O
O
MeO
OH
O
O
MeO
1.00
0.92
1.16
2.20
1.19
0.98
3.01
3.67
0.92
2.00
2.46
7.92
1.04
10.45
3.74
f1 (ppm)

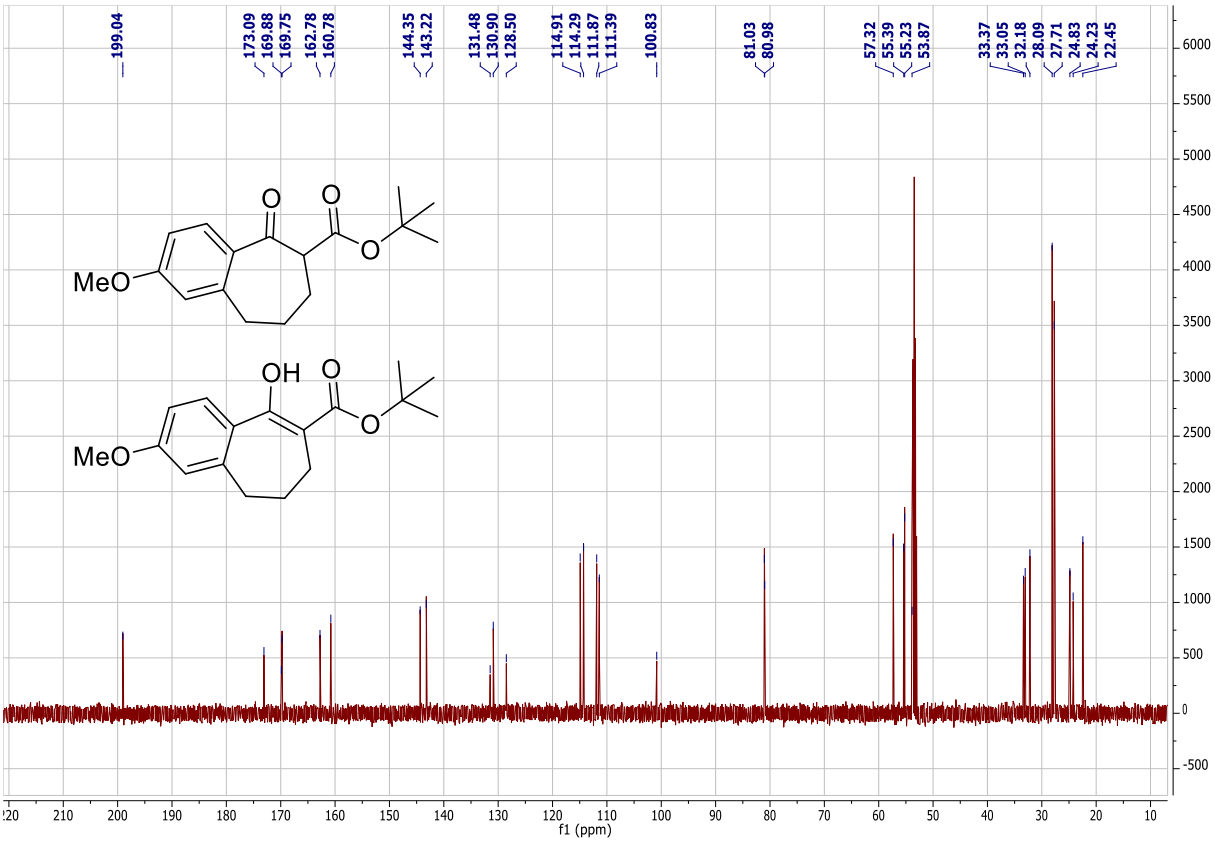
199.04
173.09
169.88
169.75
162.78
160.78
144.35
143.22
131.48
130.90
128.50
114.91
114.29
111.87
111.39
100.83
81.03
80.98
57.32
55.39
55.23
53.87
33.37
33.05
32.18
28.09
27.71
24.83
24.23
22.45
MeO
OH
f1 (ppm)

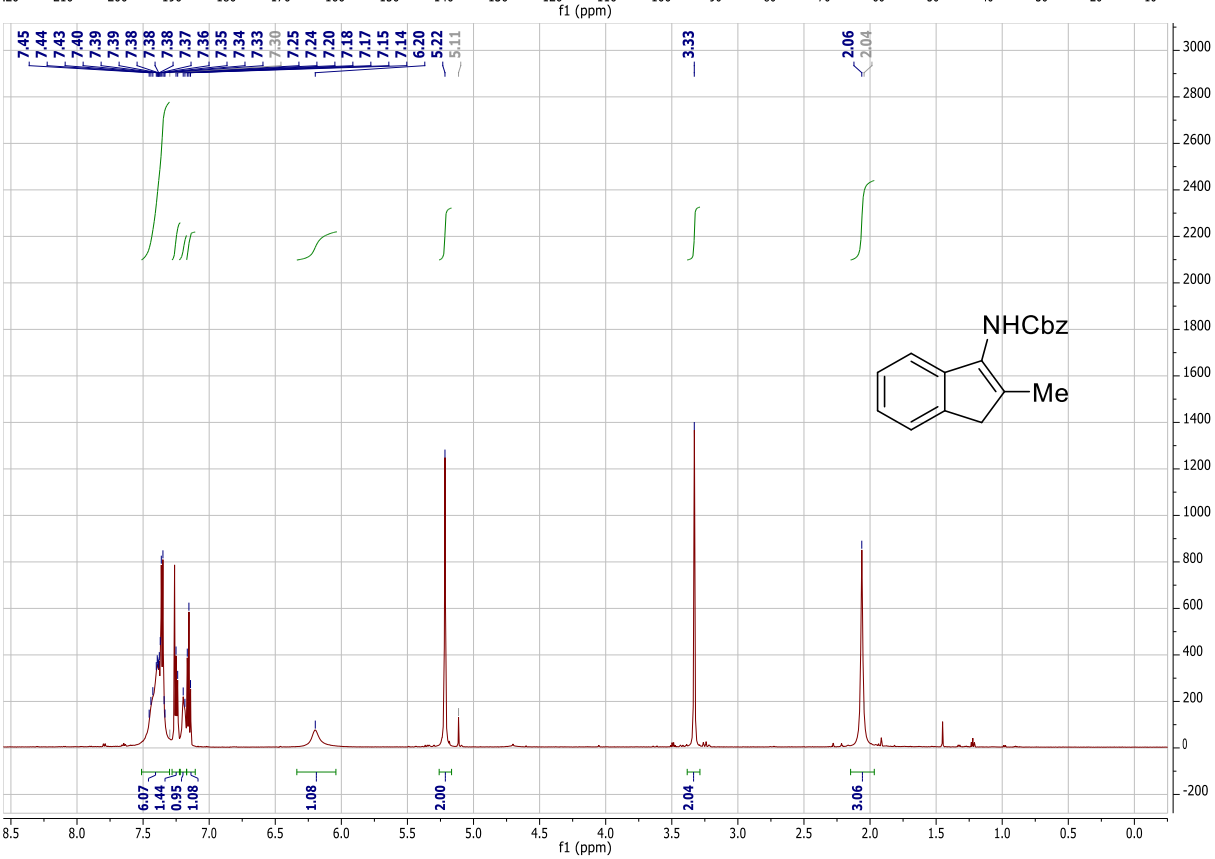
7.45
7.44
7.43
7.40
7.39
7.39
7.38
7.38
7.38
7.37
7.36
7.35
7.34
7.33
7.30
7.25
7.24
7.20
7.18
7.17
7.15
7.14
6.20
5.22
5.11
3.33
2.06
2.04
NHCbz
Me
6.07
1.44
0.95
1.08
1.08
2.00
2.04
3.06
f1 (ppm)

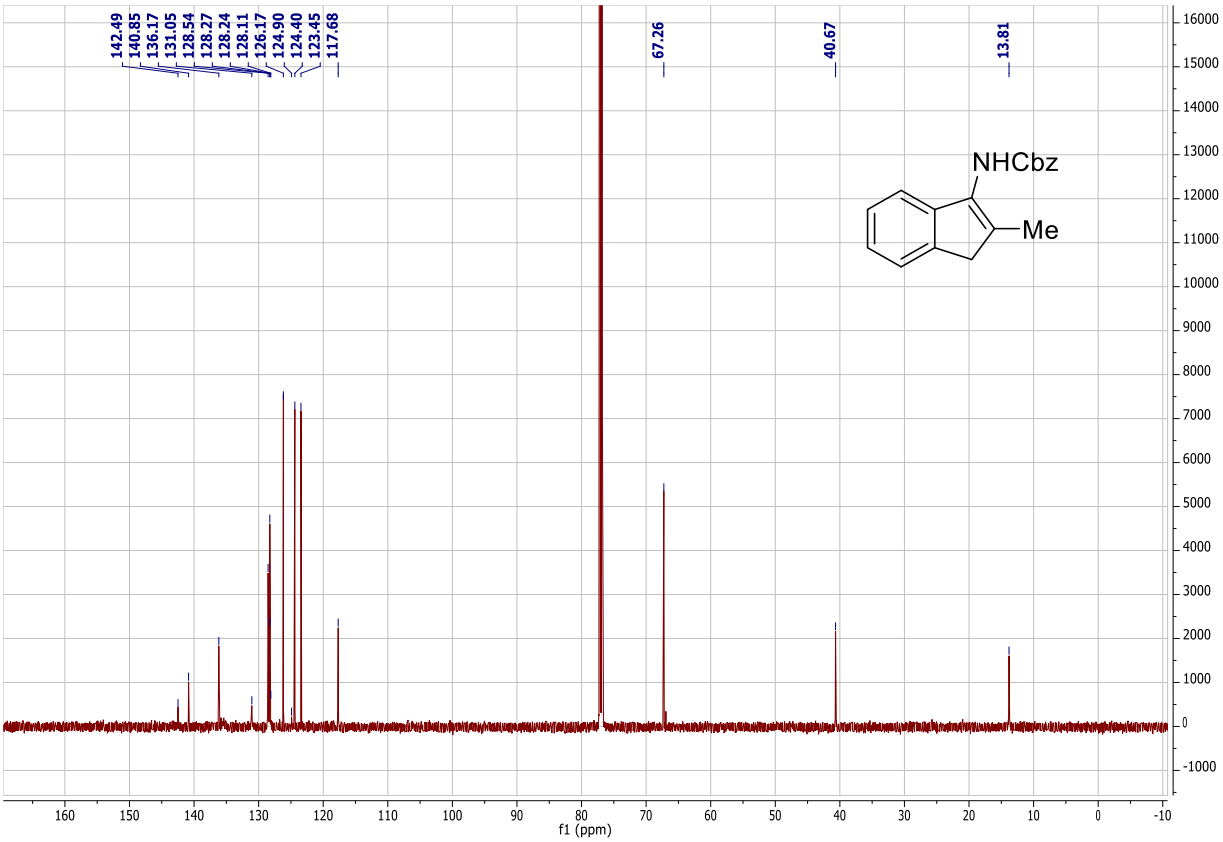
142.49
140.85
136.17
131.05
128.54
128.27
128.24
128.11
126.17
124.90
124.40
123.45
117.68
67.26
40.67
13.81
NHCbz
Me
f1 (ppm)

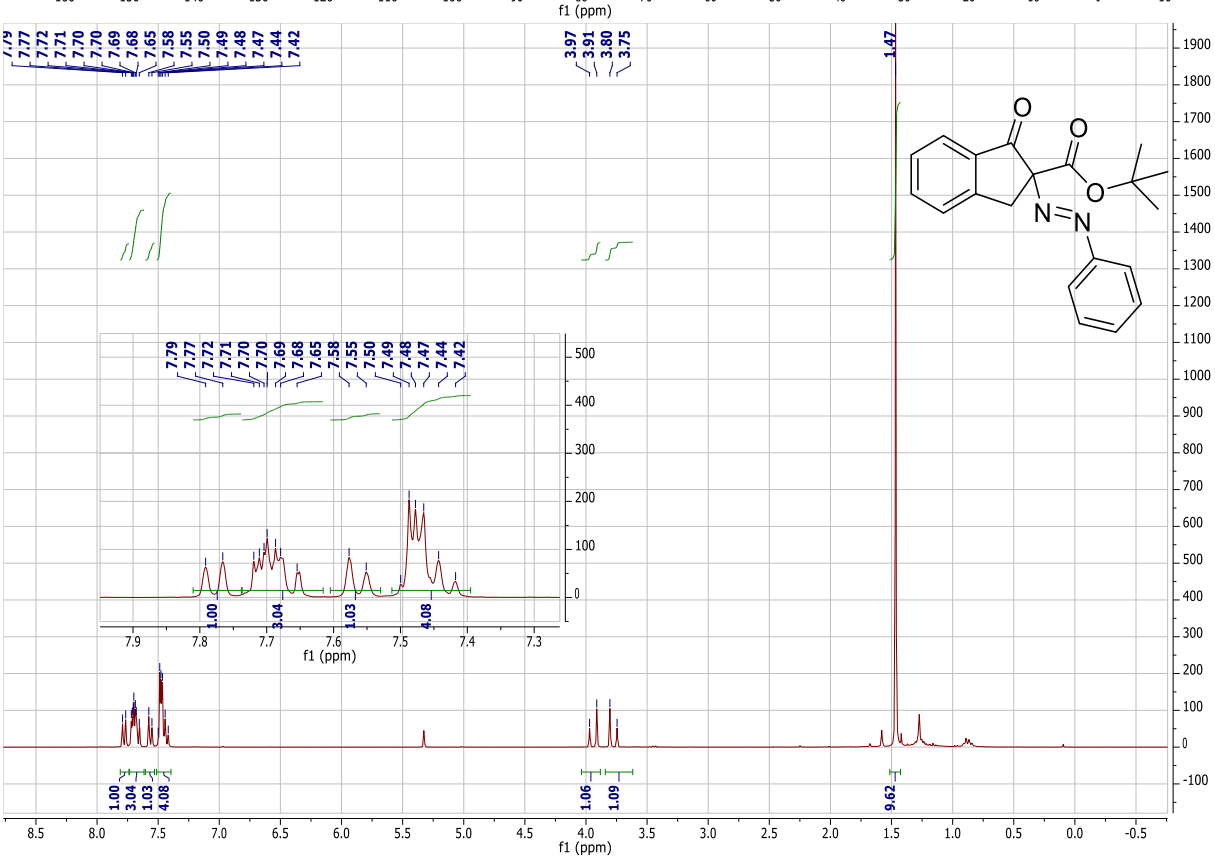
7.79
7.77
7.72
7.71
7.70
7.70
7.69
7.68
7.65
7.58
7.55
7.50
7.49
7.48
7.47
7.44
7.42
3.97
3.91
3.80
3.75
1.47
O
O
O
N
N
1.00
3.04
1.03
4.08
1.06
1.09
9.62
f1 (ppm)

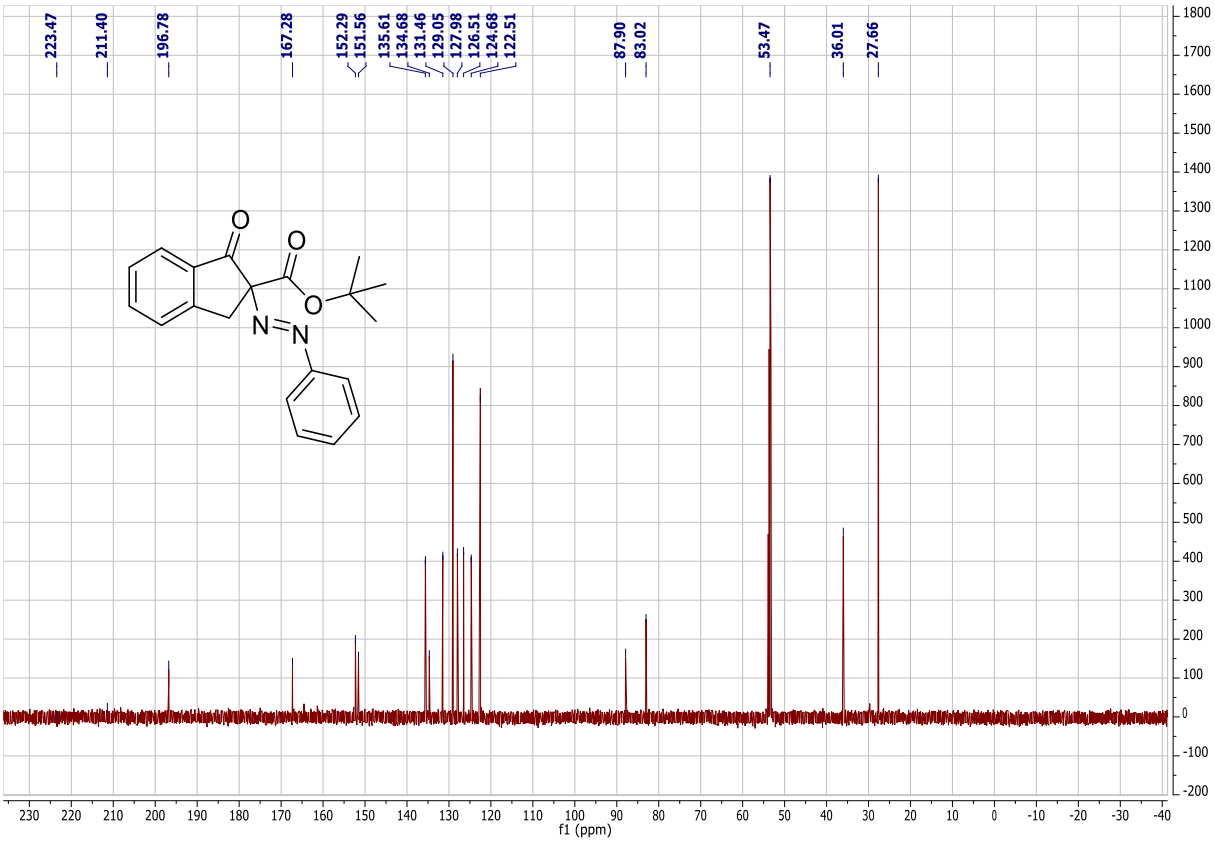
223.47
211.40
196.78
167.28
152.29
151.56
135.61
134.68
131.46
129.05
127.98
126.51
124.68
122.51
87.90
83.02
53.47
36.01
27.66
f1 (ppm)

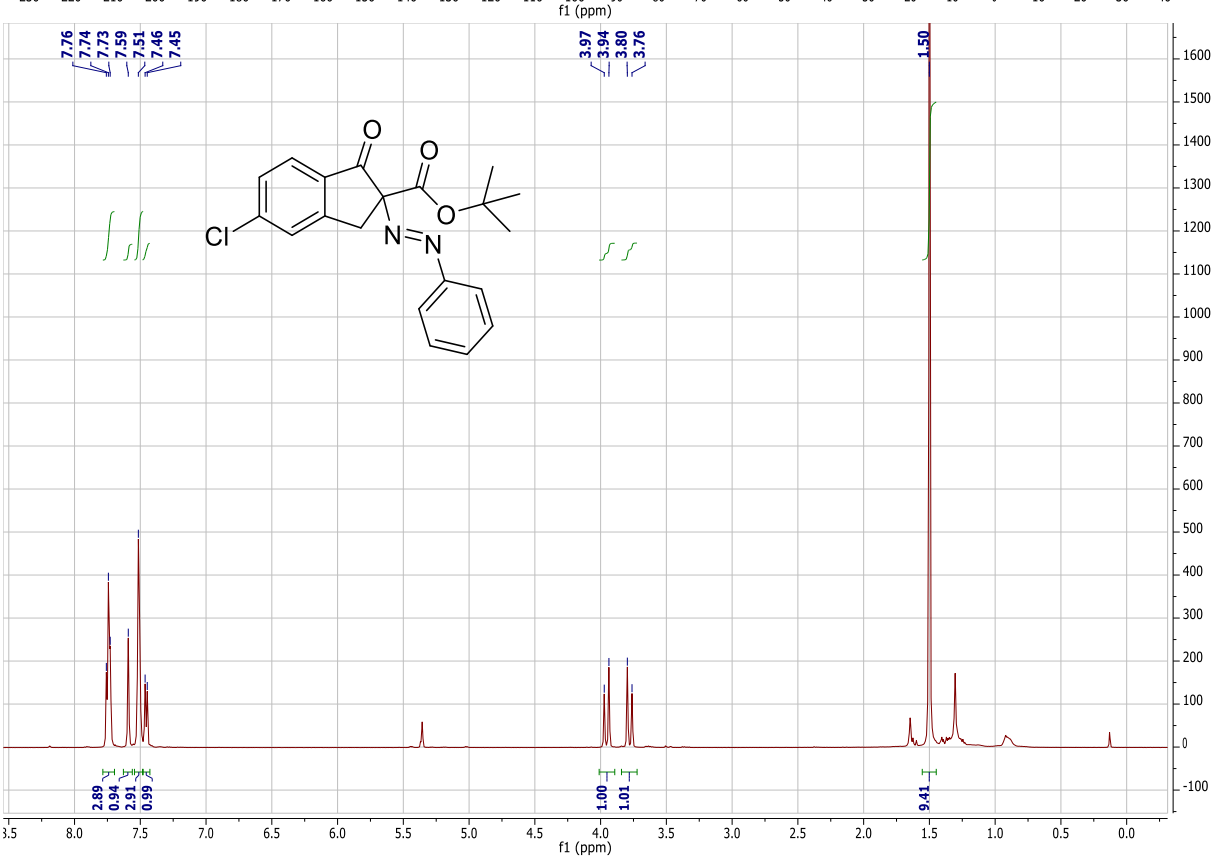
7.76
7.74
7.73
7.59
7.51
7.46
7.45
3.97
3.94
3.80
3.76
1.50
2.89
0.94
2.91
0.99
1.00
1.01
9.41
f1 (ppm)

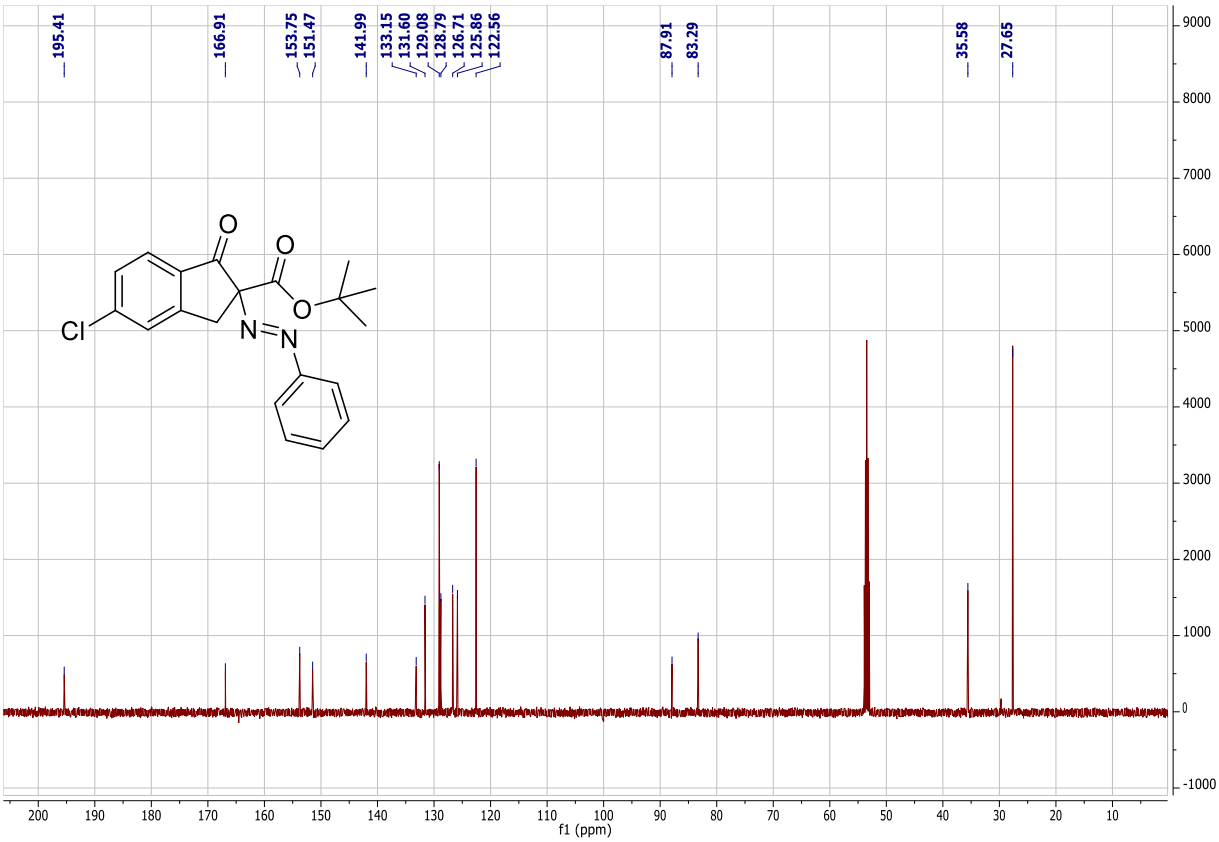
195.41
166.91
153.75
151.47
141.99
133.15
131.60
129.08
128.79
126.71
125.86
122.56
87.91
83.29
35.58
27.65
Cl
O
O
O
N
N
f1 (ppm)

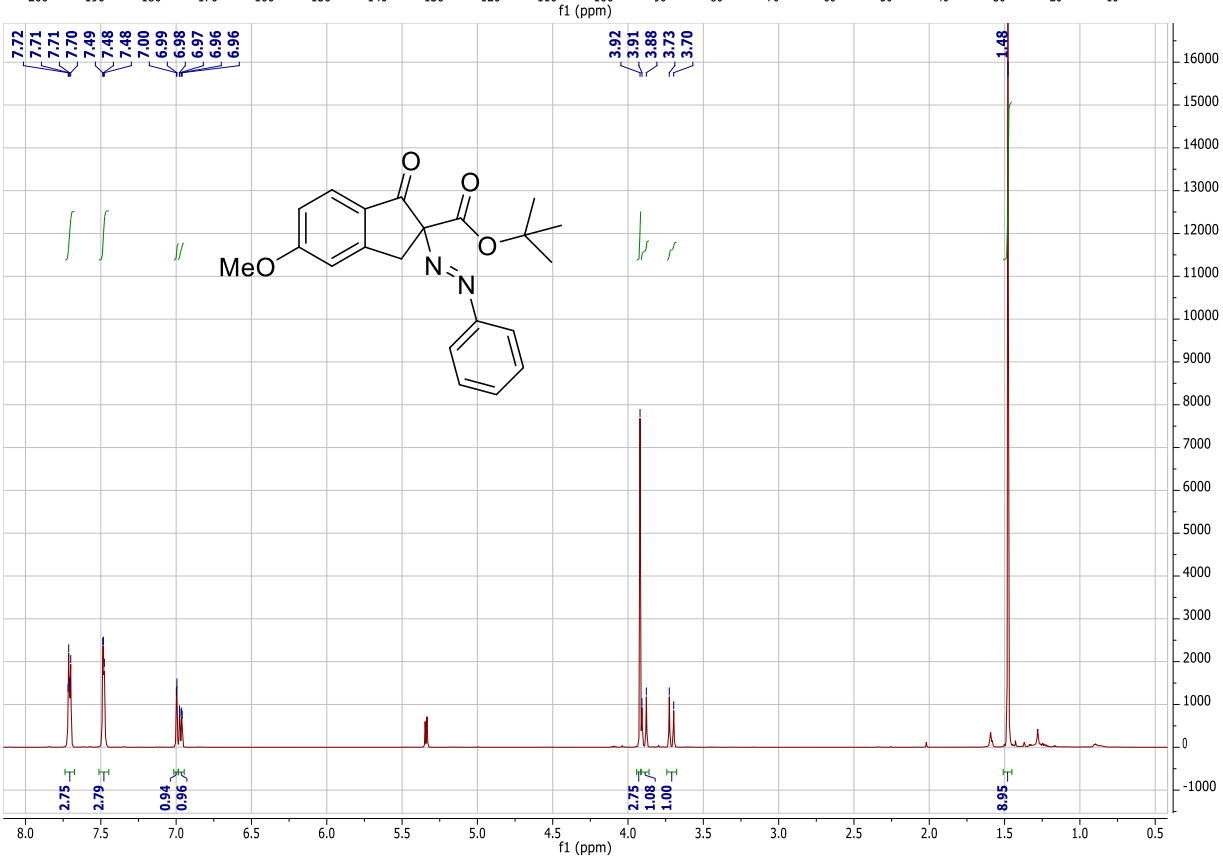
7.72
7.71
7.71
7.70
7.49
7.48
7.48
7.00
6.99
6.98
6.97
6.96
6.96
3.92
3.91
3.88
3.73
3.70
1.48
MeO
O
O
O
N
N
2.75
2.79
0.94
0.96
2.75
1.08
1.00
8.95
f1 (ppm)

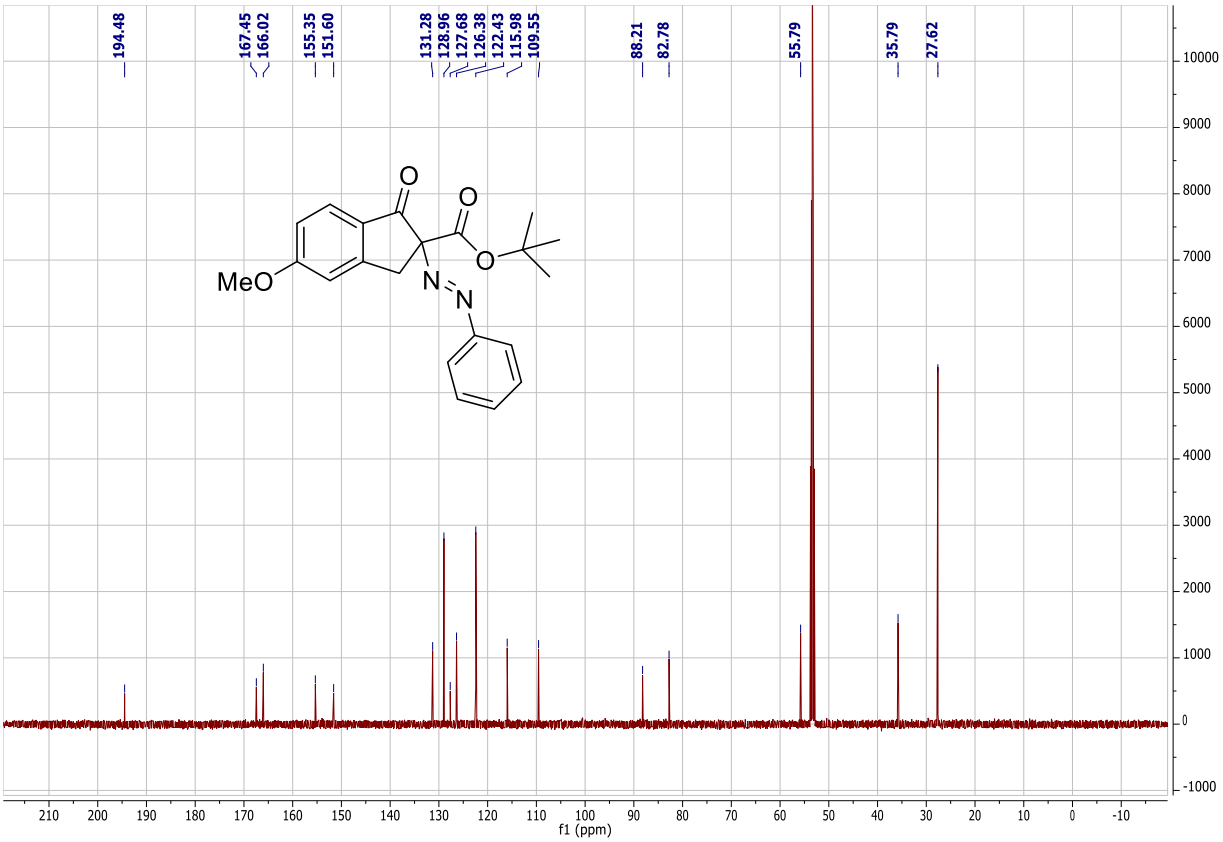
194.48
167.45
166.02
155.35
151.60
131.28
128.96
127.68
126.38
122.43
115.98
109.55
88.21
82.78
55.79
35.79
27.62
MeO
f1 (ppm)

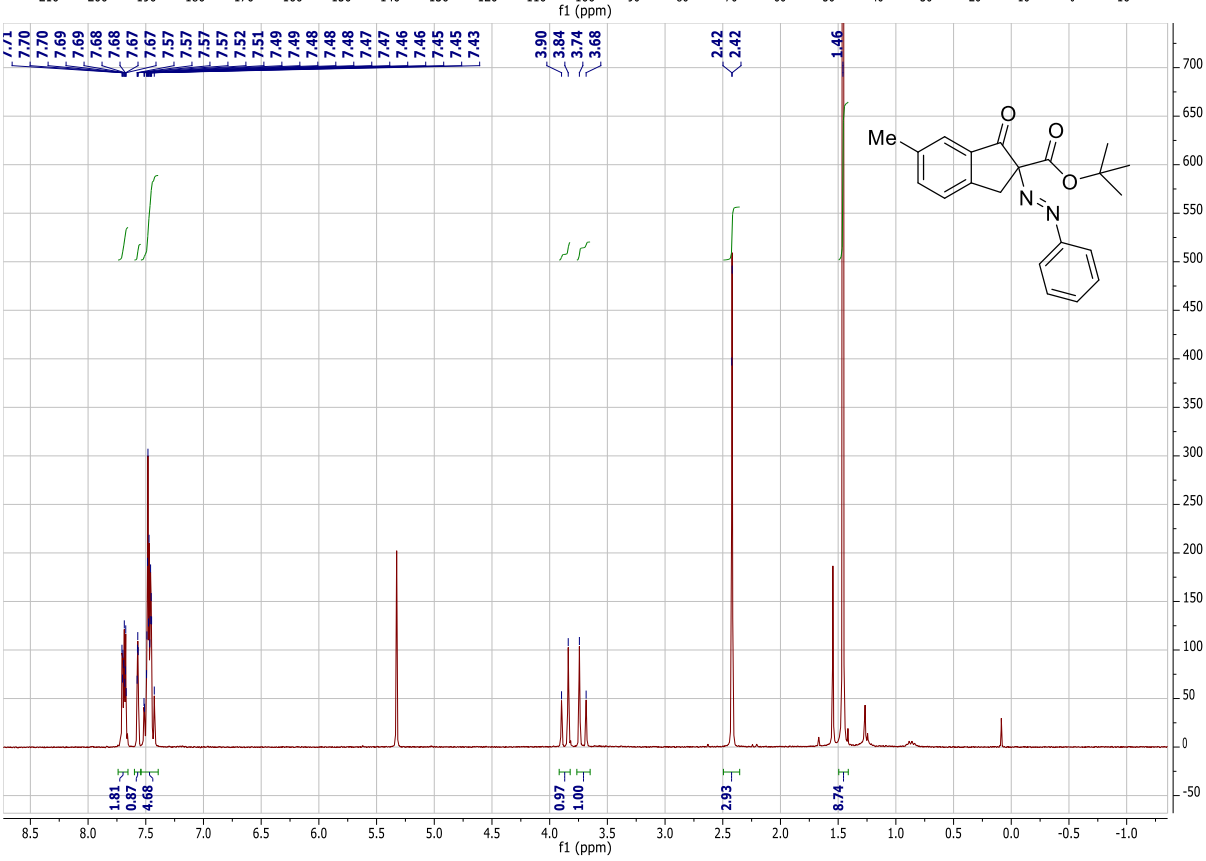
7.70
7.69
7.68
7.67
7.57
7.52
7.51
7.49
7.48
7.47
7.46
7.45
7.43
3.90
3.84
3.74
3.68
2.42
1.46
Me
1.81
0.87
4.68
0.97
1.00
2.93
8.74
f1 (ppm)

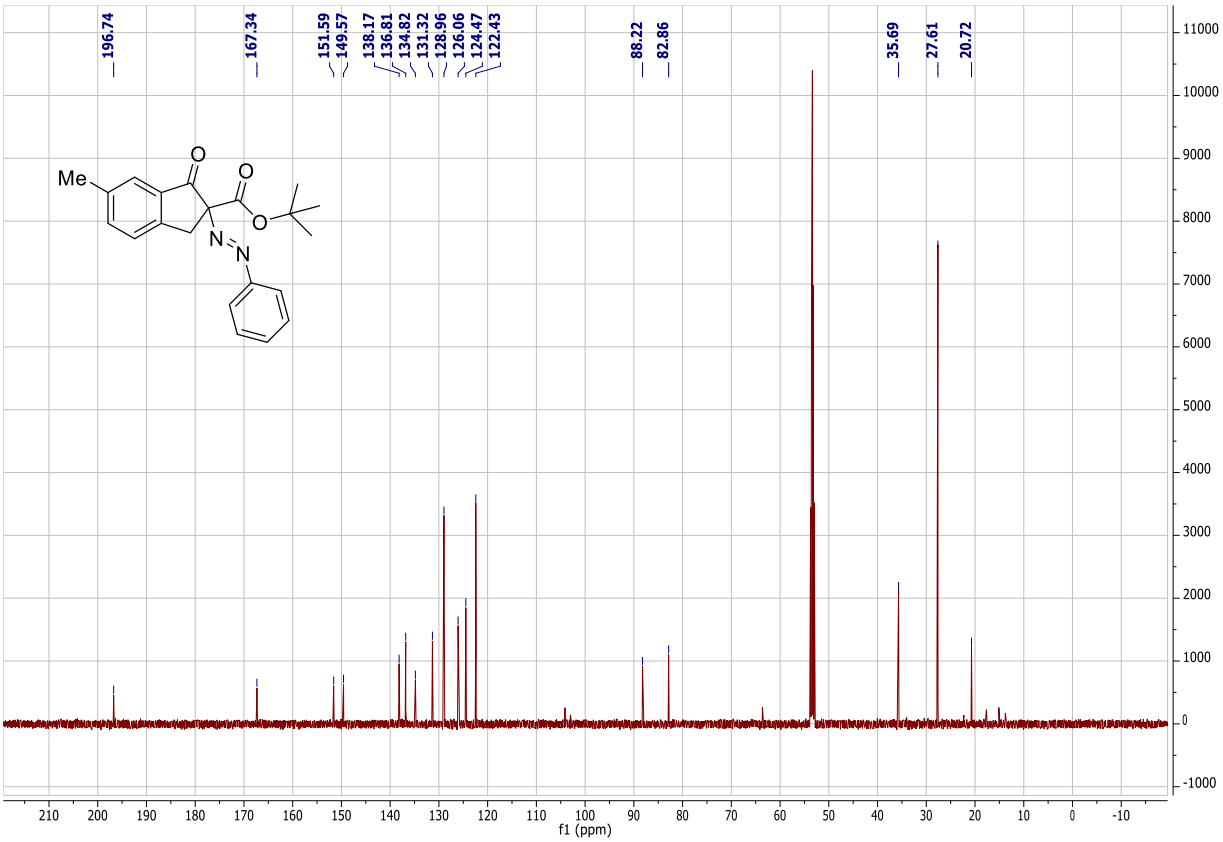
196.74
167.34
151.59
149.57
138.17
136.81
134.82
131.32
128.96
126.06
124.47
122.43
88.22
82.86
35.69
27.61
20.72
Me
O
O
O
N
N
f1 (ppm)

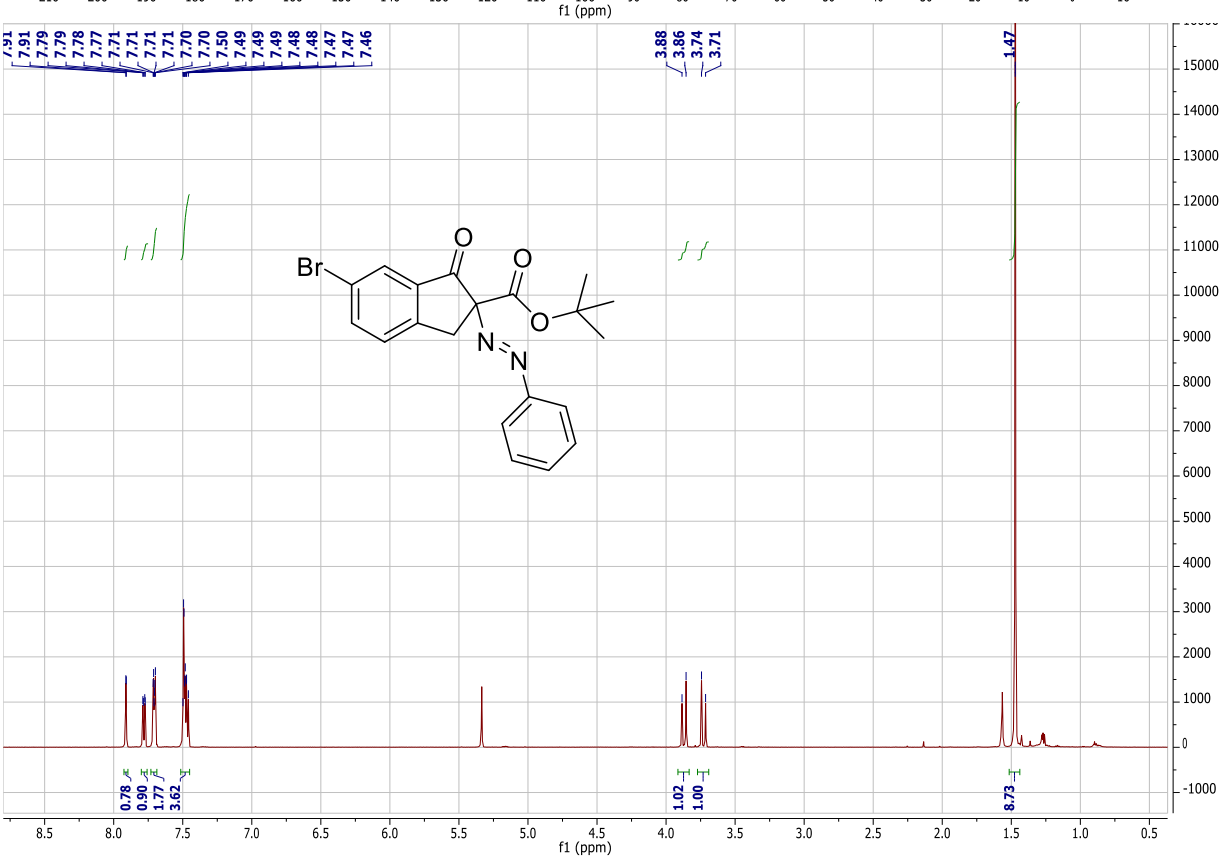
7.91
7.91
7.79
7.79
7.78
7.77
7.71
7.71
7.71
7.71
7.70
7.70
7.50
7.49
7.49
7.49
7.48
7.48
7.47
7.47
7.46
3.88
3.86
3.74
3.71
1.47
Br
O
O
O
N
N
0.78
0.90
1.77
3.62
1.02
1.00
8.73
f1 (ppm)

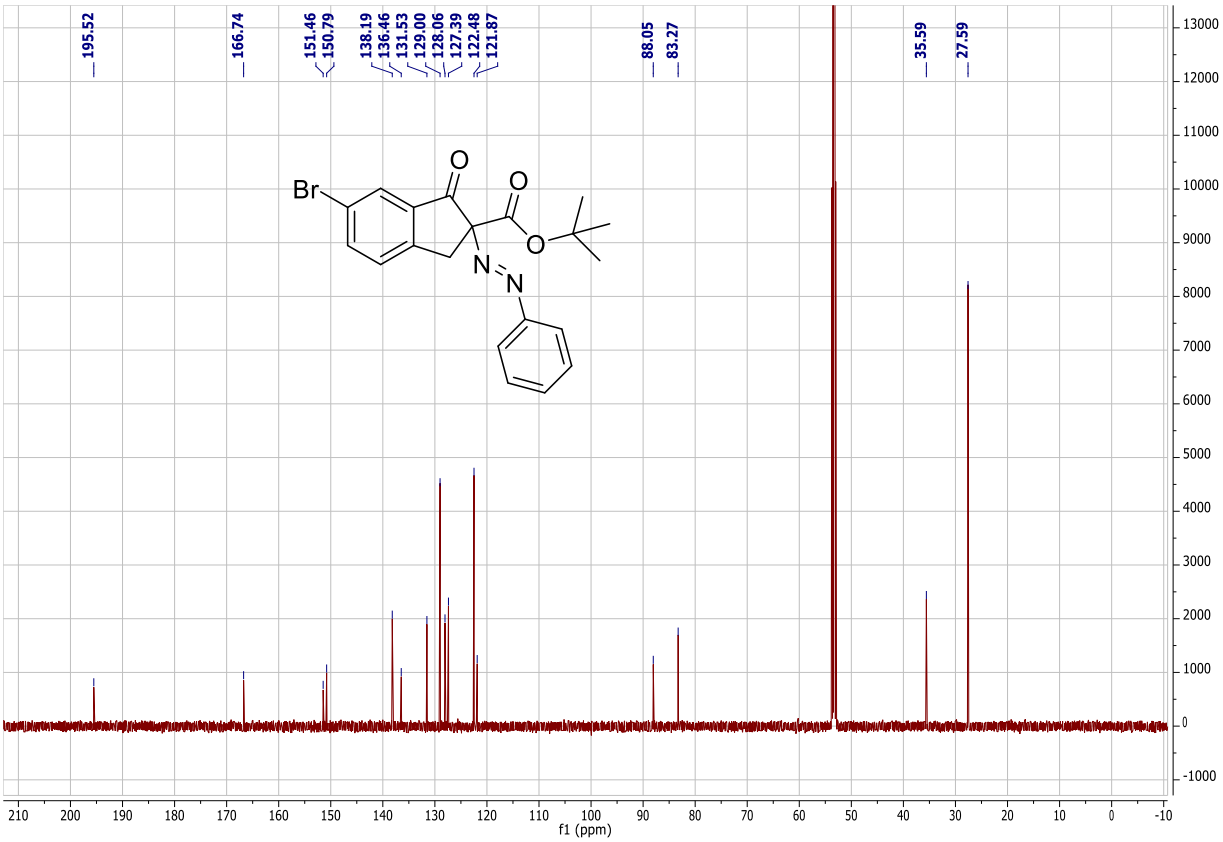
195.52
166.74
151.46
150.79
138.19
136.46
131.53
129.00
128.06
127.39
122.48
121.87
88.05
83.27
35.59
27.59
Br
O
O
O
N
N
f1 (ppm)

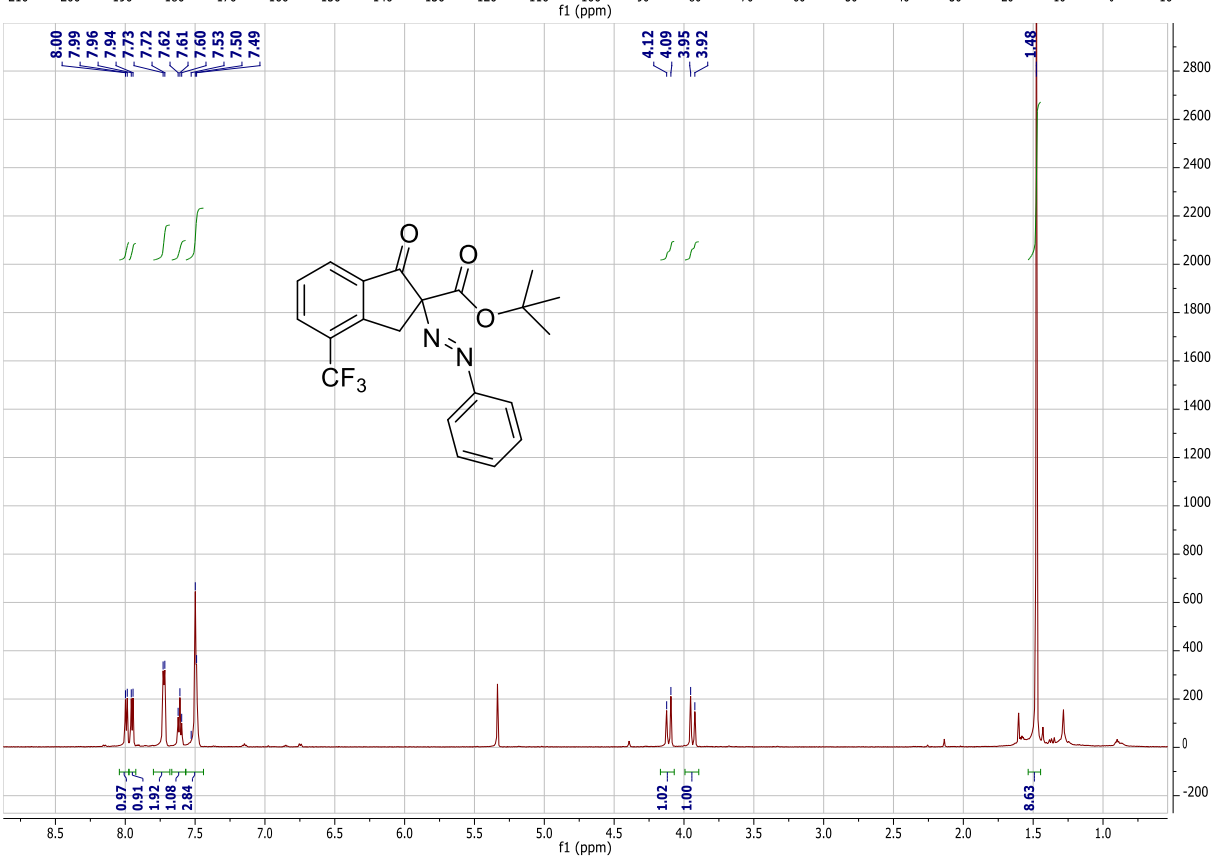
8.00
7.99
7.96
7.94
7.73
7.72
7.62
7.61
7.60
7.53
7.50
7.49
4.12
4.09
3.95
3.92
1.48
O
O
O
N
N
CF3
0.97
0.91
1.92
1.08
2.84
1.02
1.00
8.63
f1 (ppm)

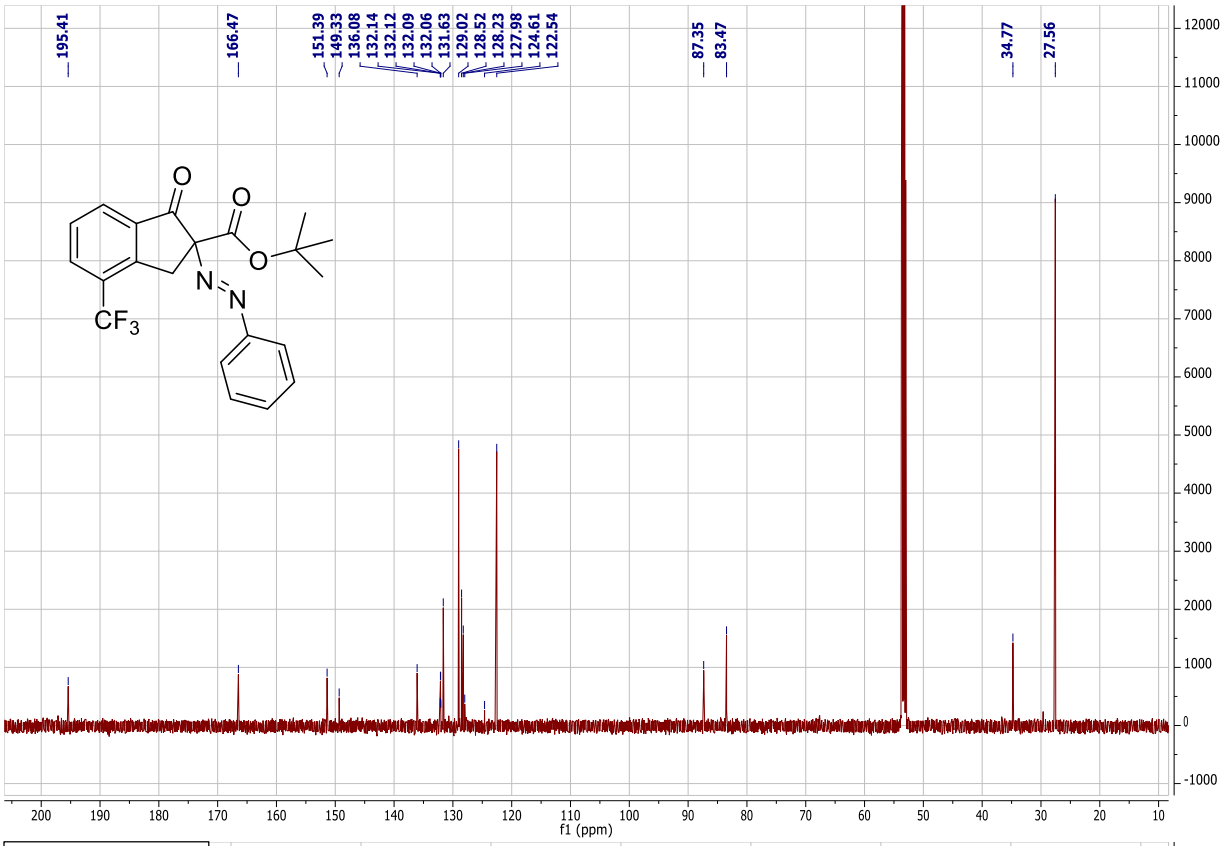
195.41
166.47
151.39
149.33
136.08
132.14
132.12
132.09
132.06
131.63
129.02
128.52
128.23
127.98
124.61
122.54
87.35
83.47
34.77
27.56
f1 (ppm)

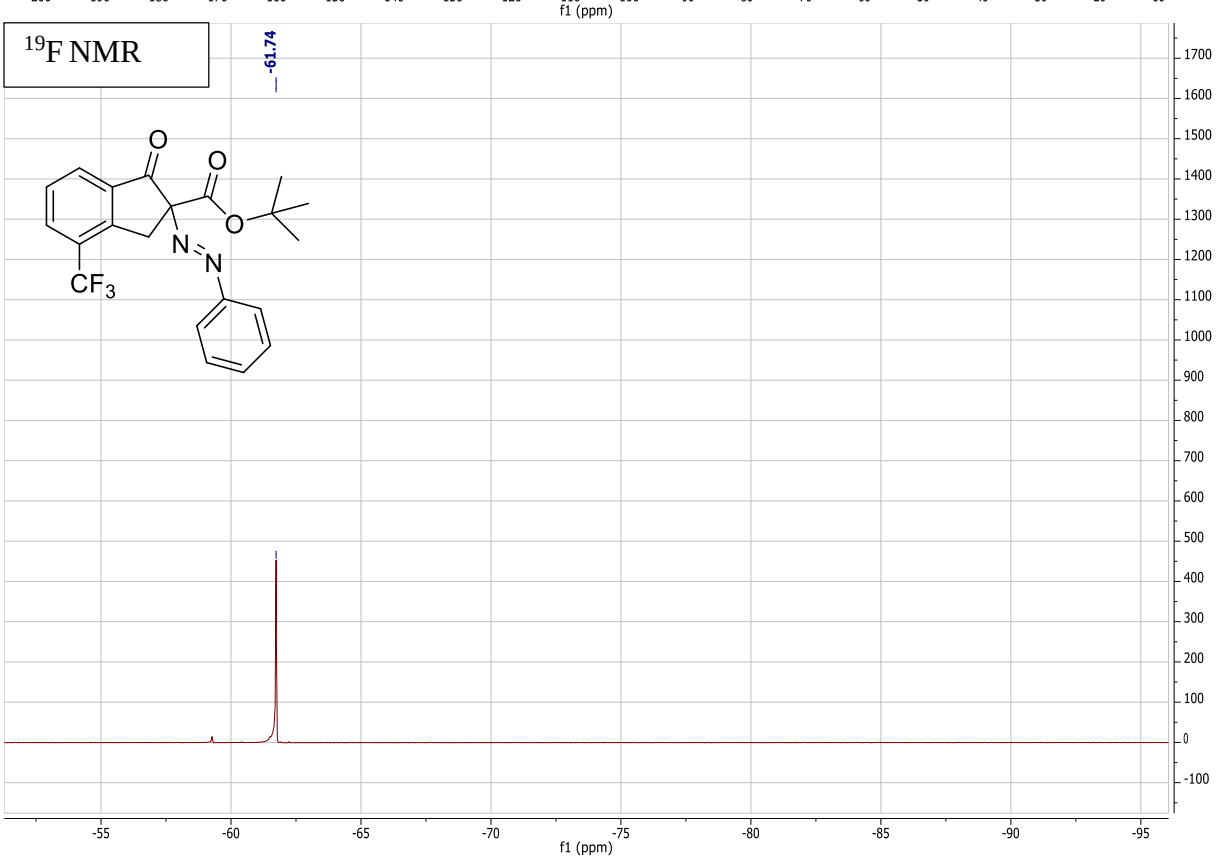
^{19}F NMR
-61.74
f1 (ppm)

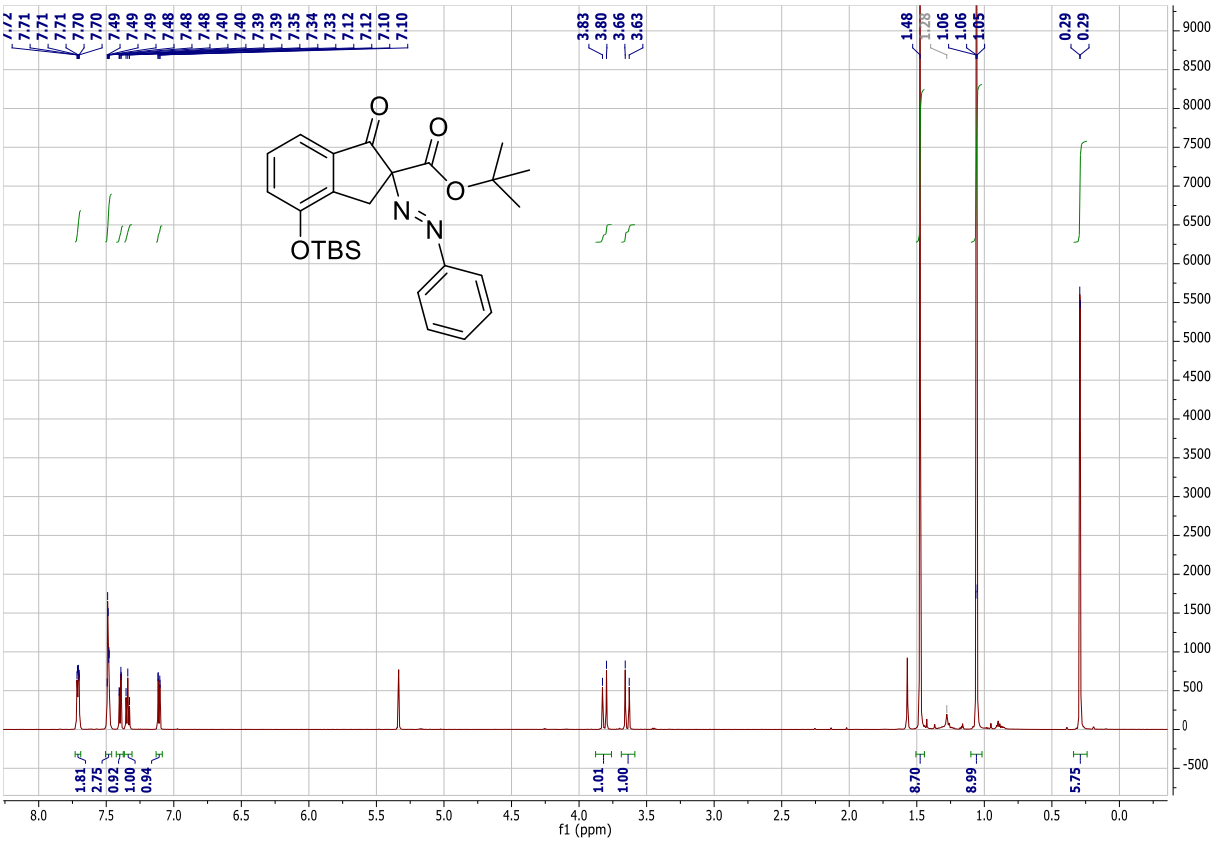
7.71
7.71
7.71
7.70
7.70
7.49
7.49
7.49
7.48
7.48
7.48
7.40
7.40
7.39
7.39
7.35
7.34
7.33
7.12
7.12
7.10
7.10
3.83
3.80
3.66
3.63
1.48
1.06
1.06
1.05
0.29
0.29
1.81
2.75
0.92
1.00
0.94
1.01
1.00
8.70
8.99
5.75
f1 (ppm)
OTBS

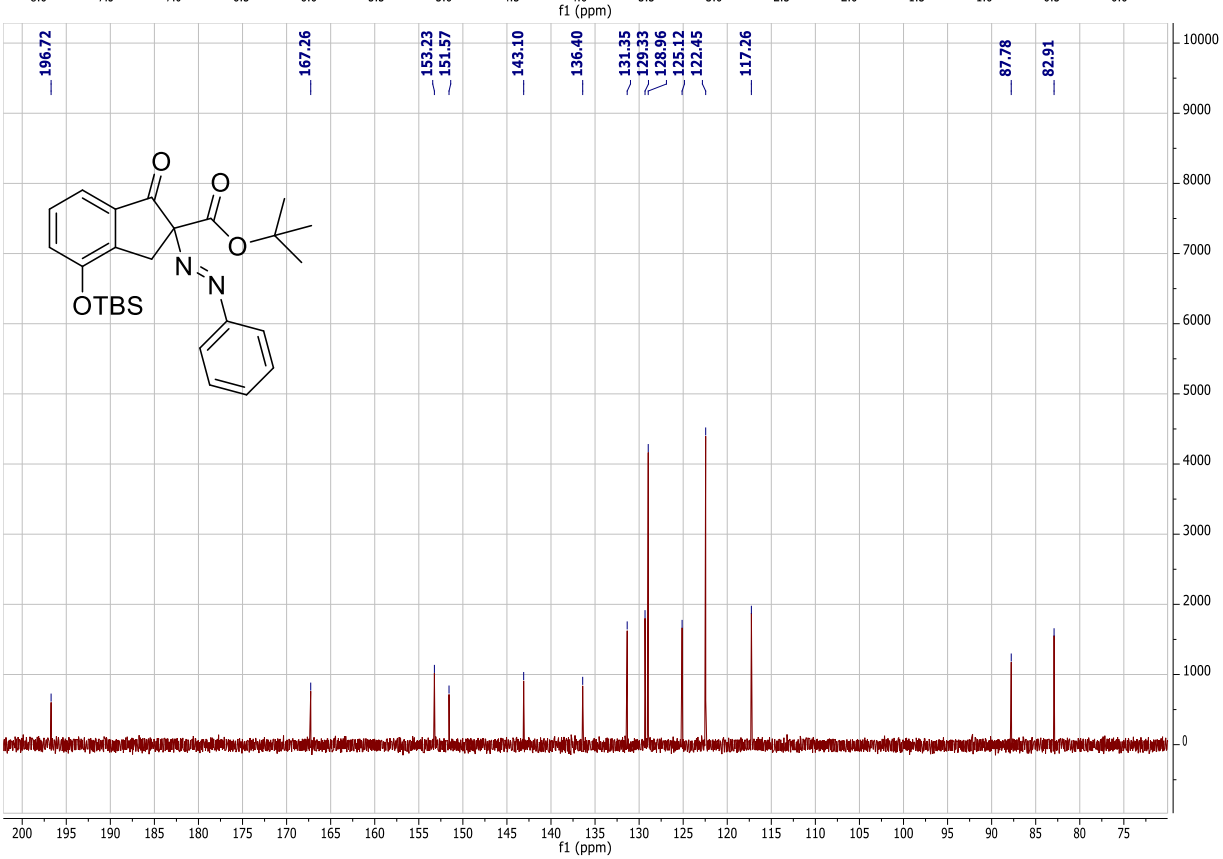
196.72
167.26
153.23
151.57
143.10
136.40
131.35
129.33
128.96
125.12
122.45
117.26
87.78
82.91
f1 (ppm)
OTBS

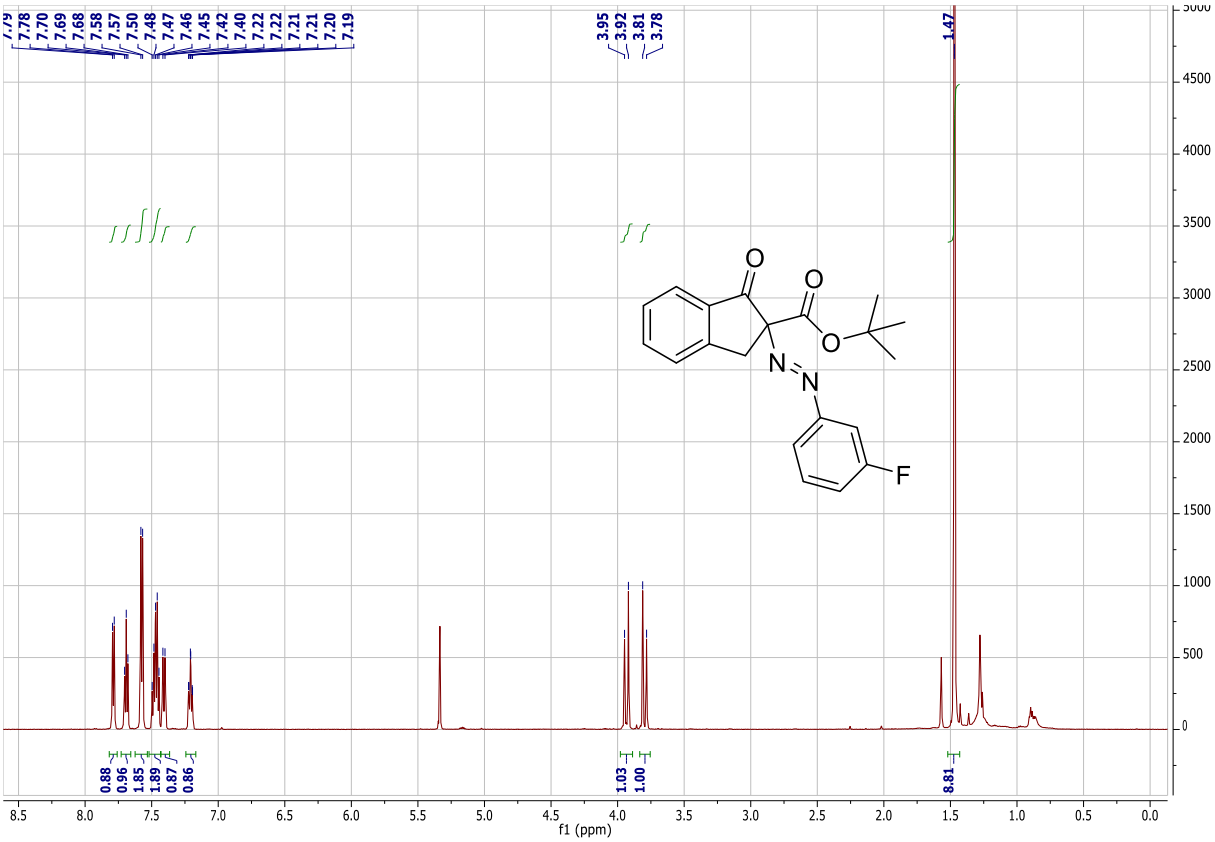
7.79
7.78
7.70
7.69
7.68
7.58
7.57
7.50
7.48
7.47
7.46
7.45
7.42
7.40
7.22
7.22
7.21
7.21
7.20
7.19
3.95
3.92
3.81
3.78
1.47
0.88
0.96
1.85
1.89
0.87
0.86
1.03
1.00
8.81
f1 (ppm)

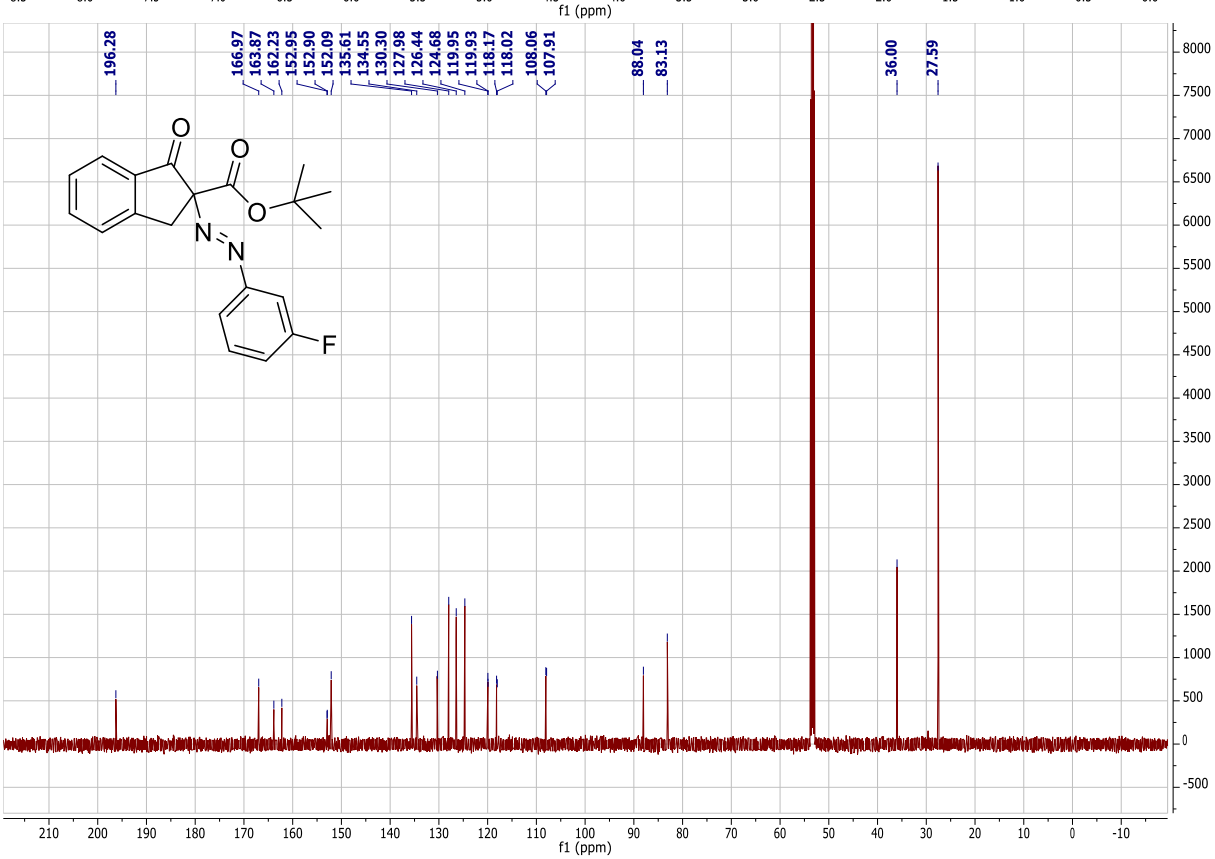
196.28
166.97
163.87
162.23
152.95
152.90
152.09
135.61
134.55
130.30
127.98
126.44
124.68
119.95
119.93
118.17
118.02
108.06
107.91
88.04
83.13
36.00
27.59
f1 (ppm)

^{19}F NMR

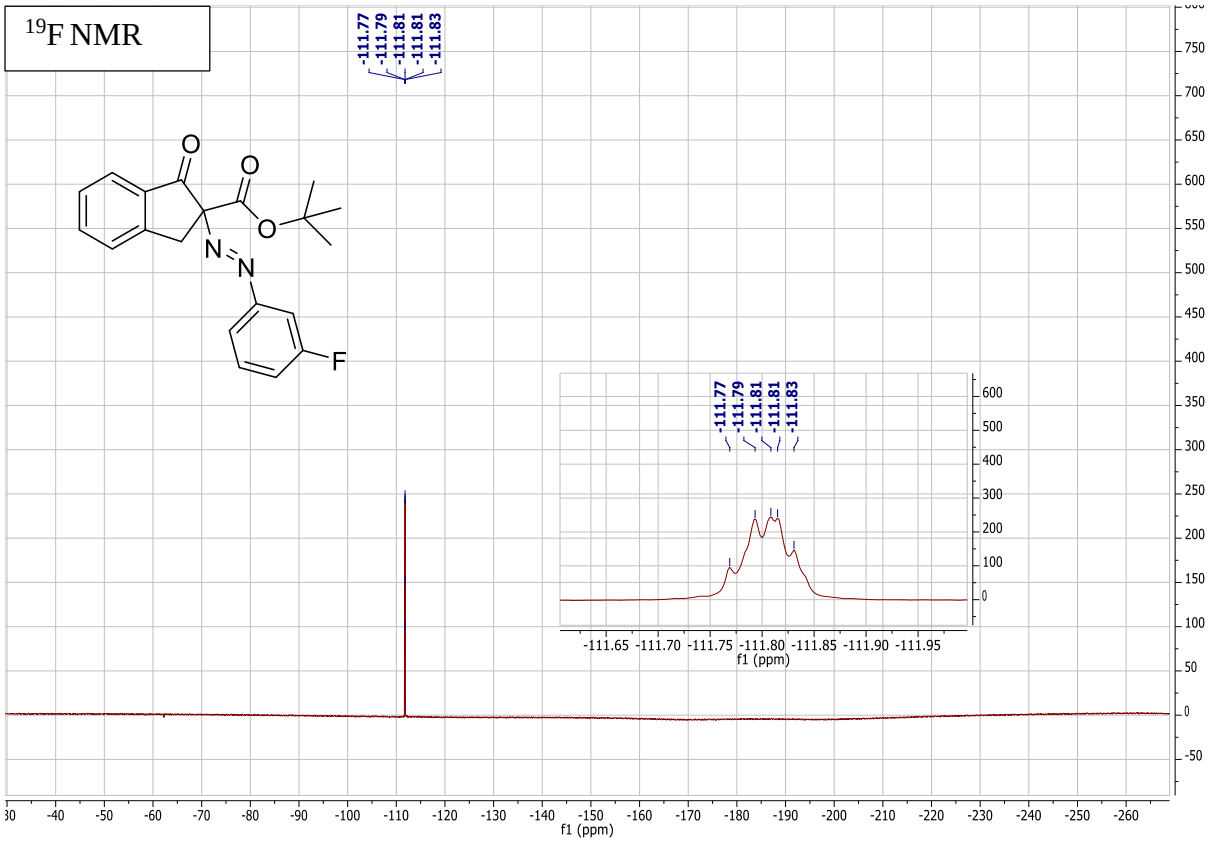
-111.77
-111.79
-111.81
-111.81
-111.83
O
O
O
N
N
F
f1 (ppm)

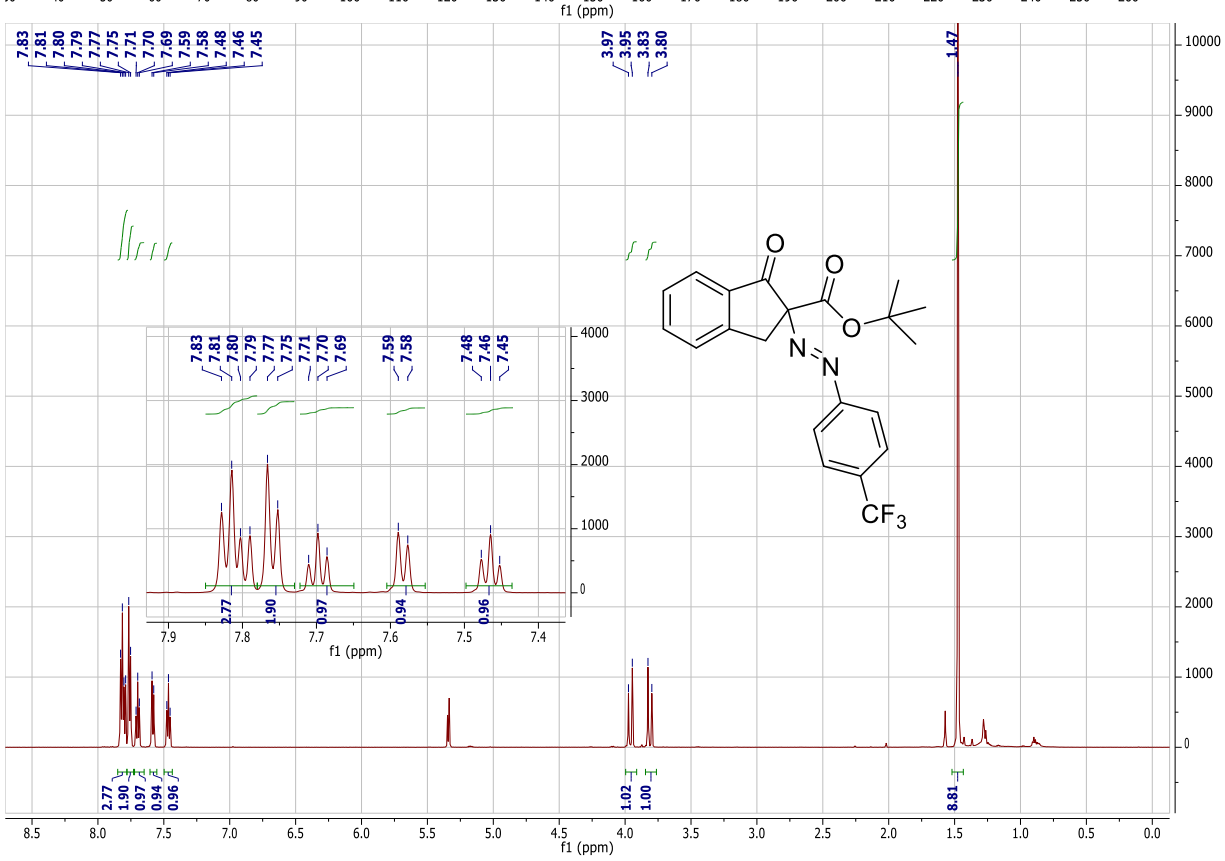
7.83
7.81
7.80
7.79
7.77
7.75
7.71
7.70
7.69
7.59
7.58
7.48
7.46
7.45
3.97
3.95
3.83
3.80
1.47
O
O
O
N
N
CF3
2.77
1.90
0.97
0.94
0.96
1.02
1.00
8.81
f1 (ppm)

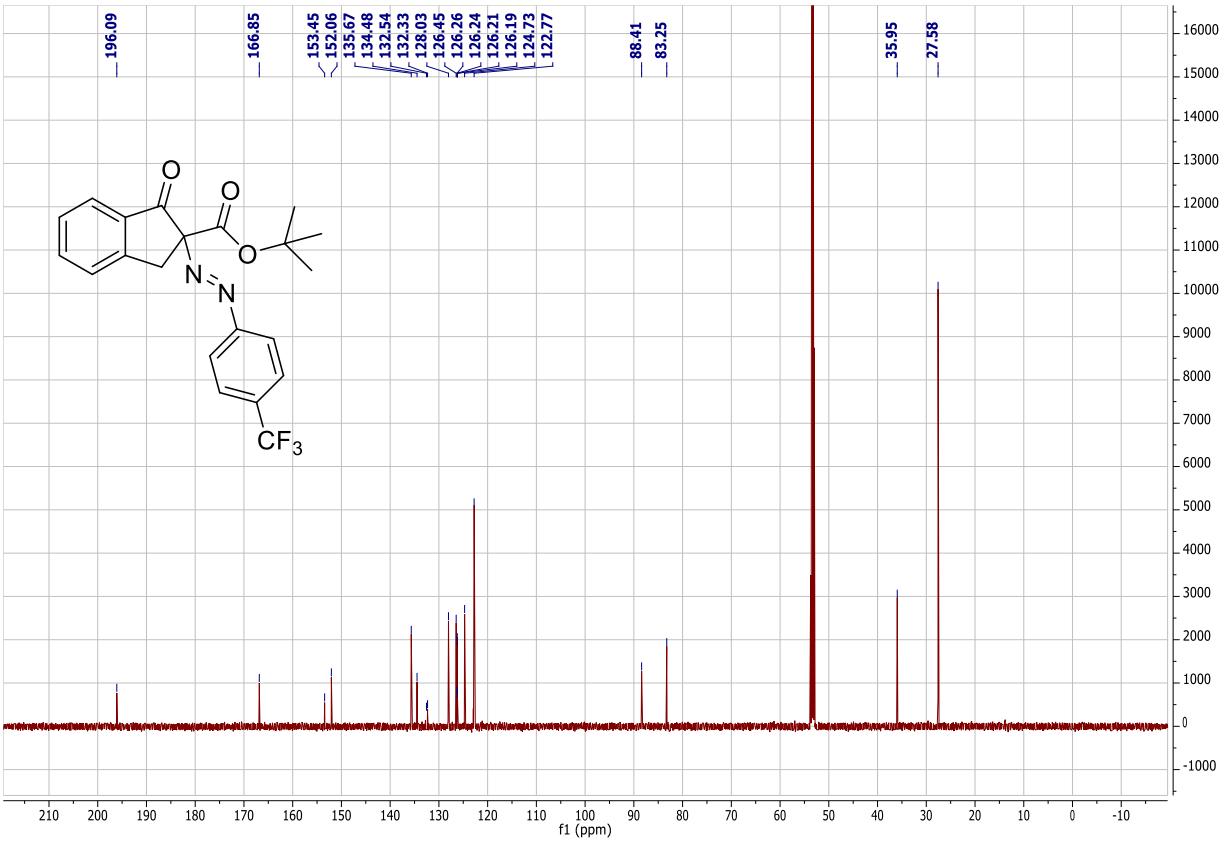
196.09
166.85
153.45
152.06
135.67
134.48
132.54
132.33
128.03
126.45
126.26
126.24
126.21
126.19
124.73
122.77
88.41
83.25
35.95
27.58
f1 (ppm)

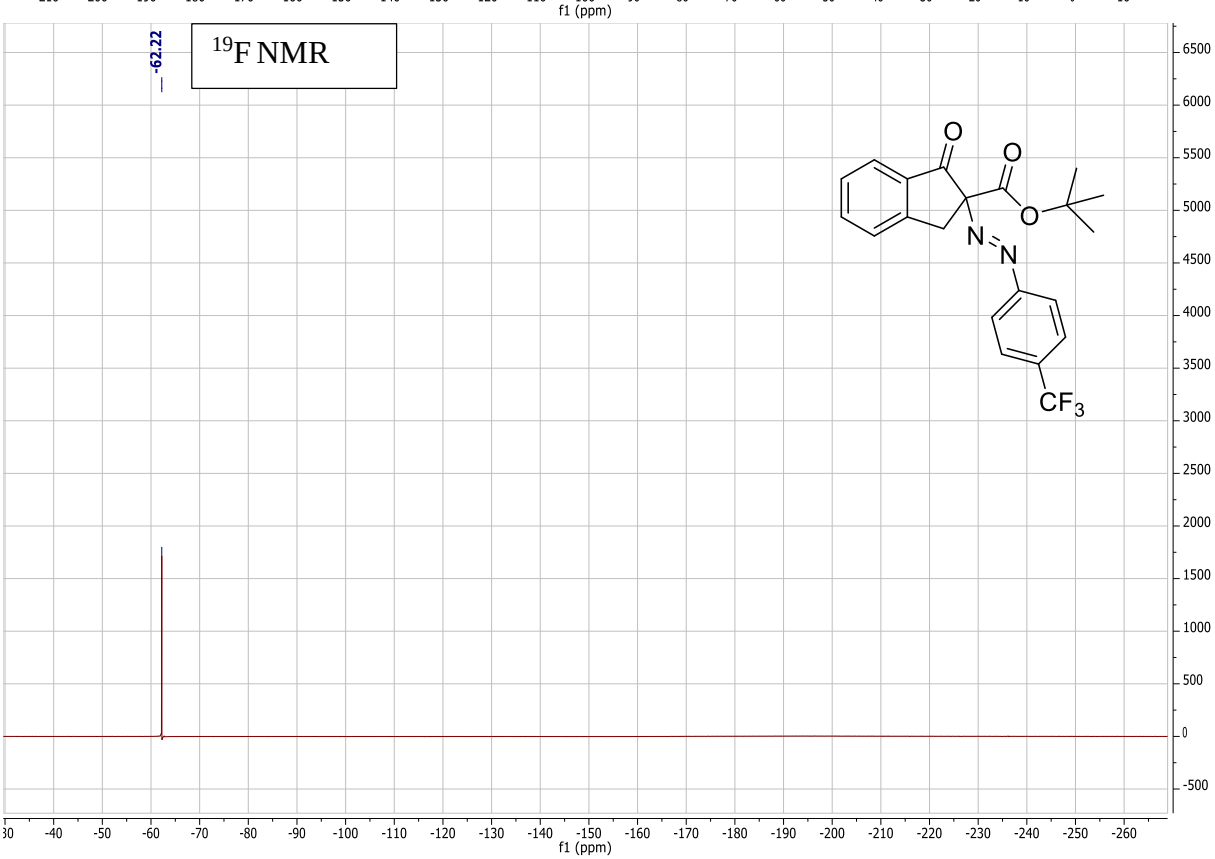
-62.22
^{19}F NMR
f1 (ppm)

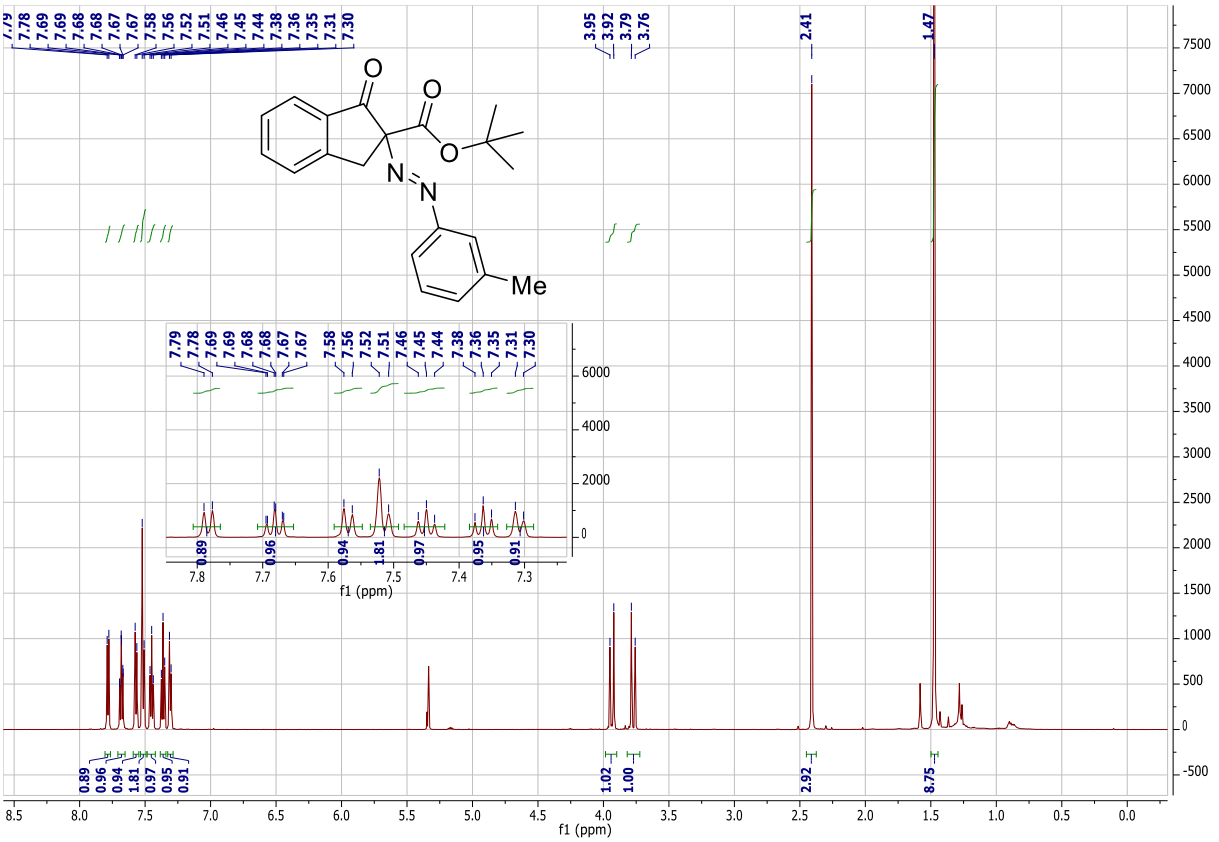
7.79 7.78 7.69 7.69 7.68 7.68 7.67 7.67 7.58 7.56 7.52 7.51 7.46 7.45 7.44 7.38 7.36 7.35 7.31 7.30
3.95 3.92 3.79 3.76
2.41
1.47
O
O
O
N
N
Me
0.89 0.96 0.94 1.81 0.97 0.95 0.91
1.02 1.00
2.92
8.75
f1 (ppm)

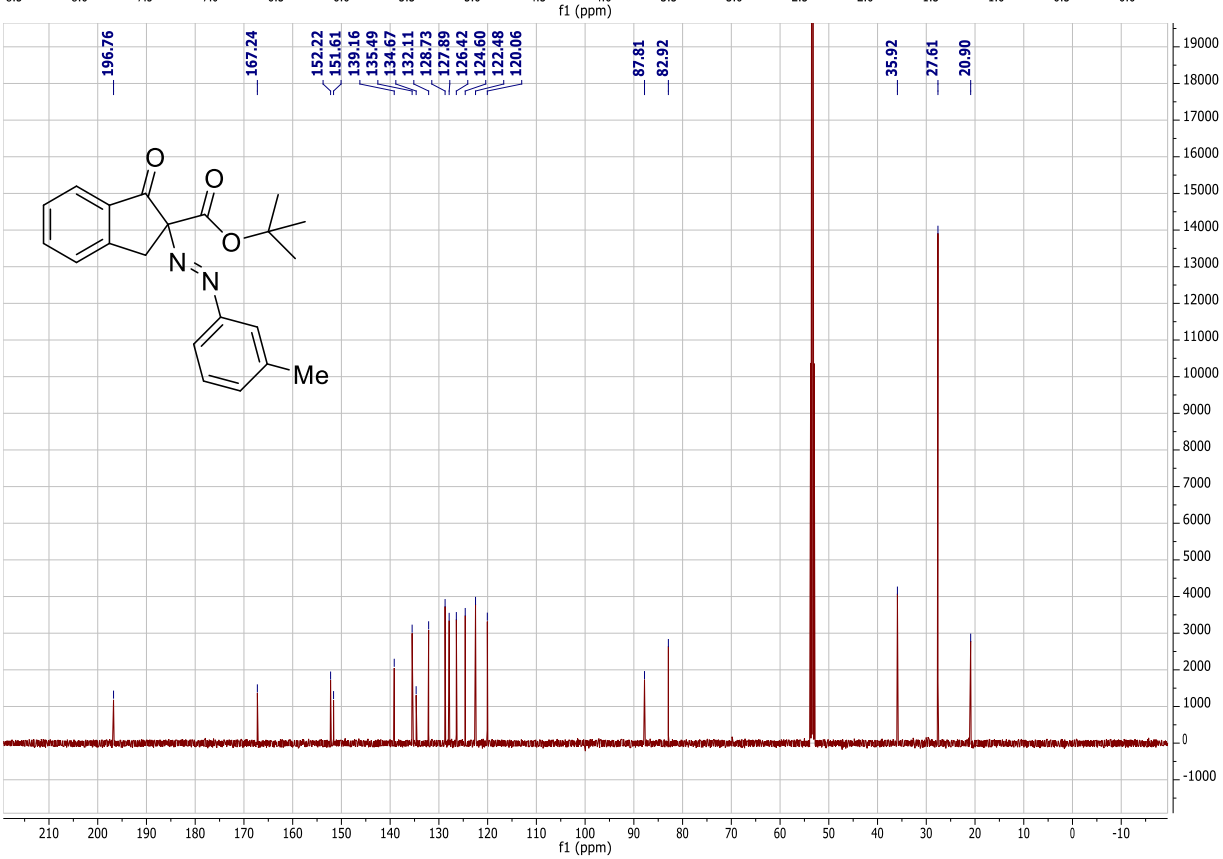
196.76
167.24
152.22 151.61 139.16 135.49 134.67 132.11 128.73 127.89 126.42 124.60 122.48 120.06
87.81 82.92
35.92 27.61 20.90
O
O
O
N
N
Me
f1 (ppm)

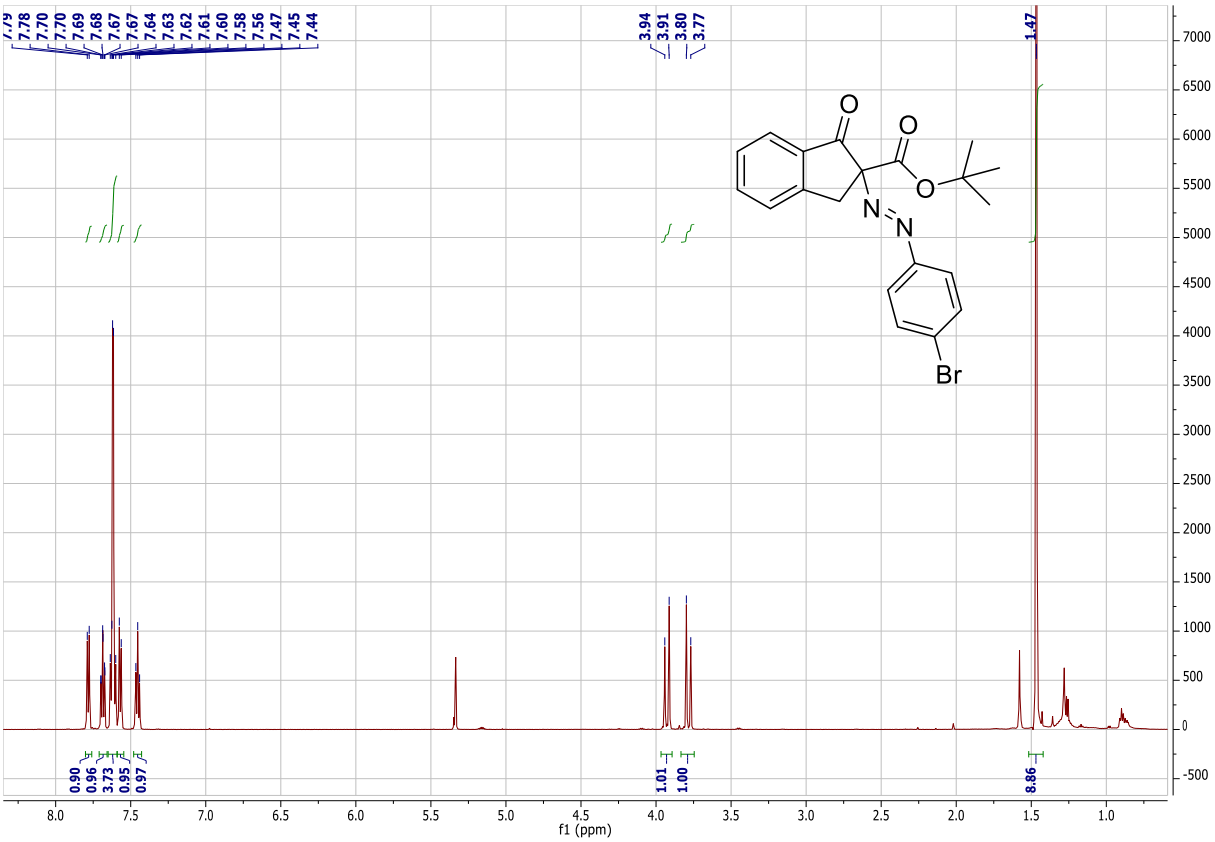
7.79
7.78
7.70
7.70
7.69
7.68
7.67
7.67
7.64
7.63
7.62
7.61
7.60
7.58
7.56
7.47
7.45
7.44
3.94
3.91
3.80
3.77
1.47
0.90
0.96
3.73
0.95
0.97
1.01
1.00
8.86
f1 (ppm)

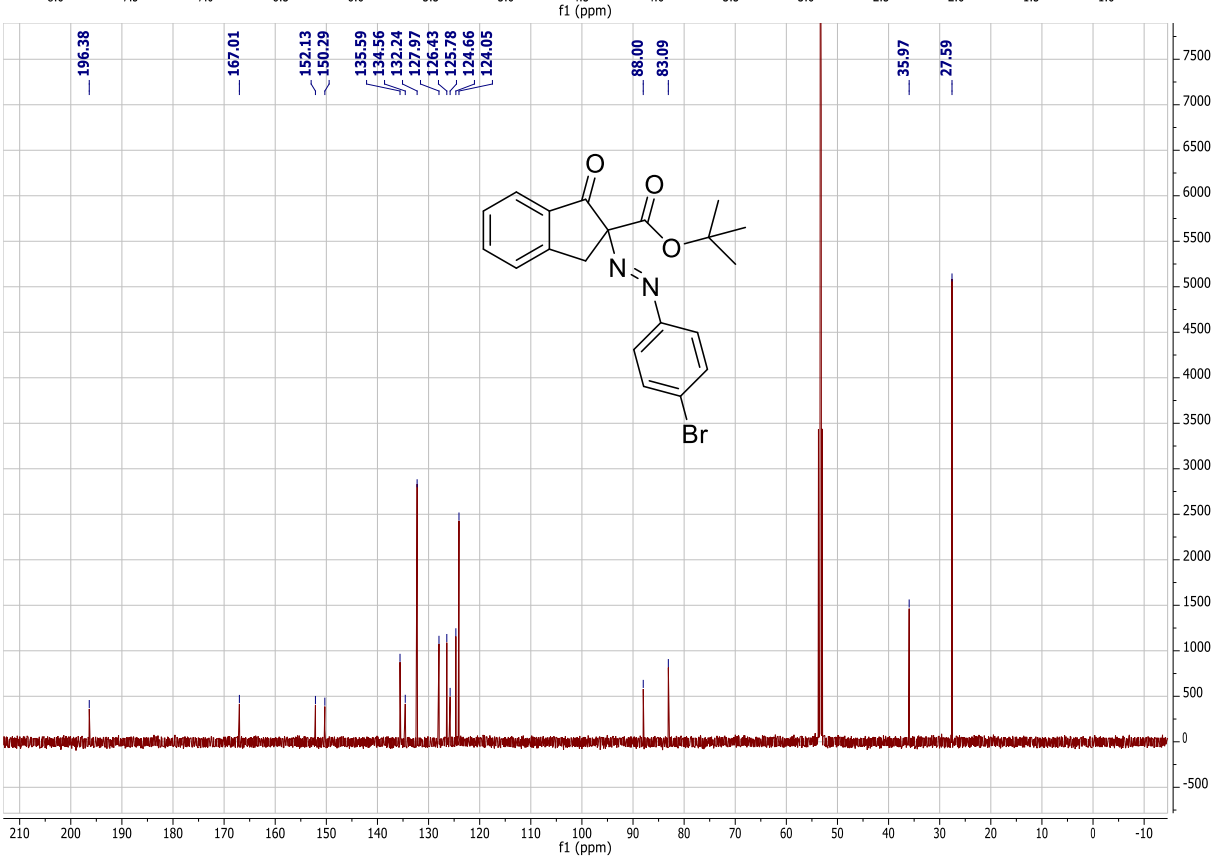
196.38
167.01
152.13
150.29
135.59
134.56
132.24
127.97
126.43
125.78
124.66
124.05
88.00
83.09
35.97
27.59
f1 (ppm)

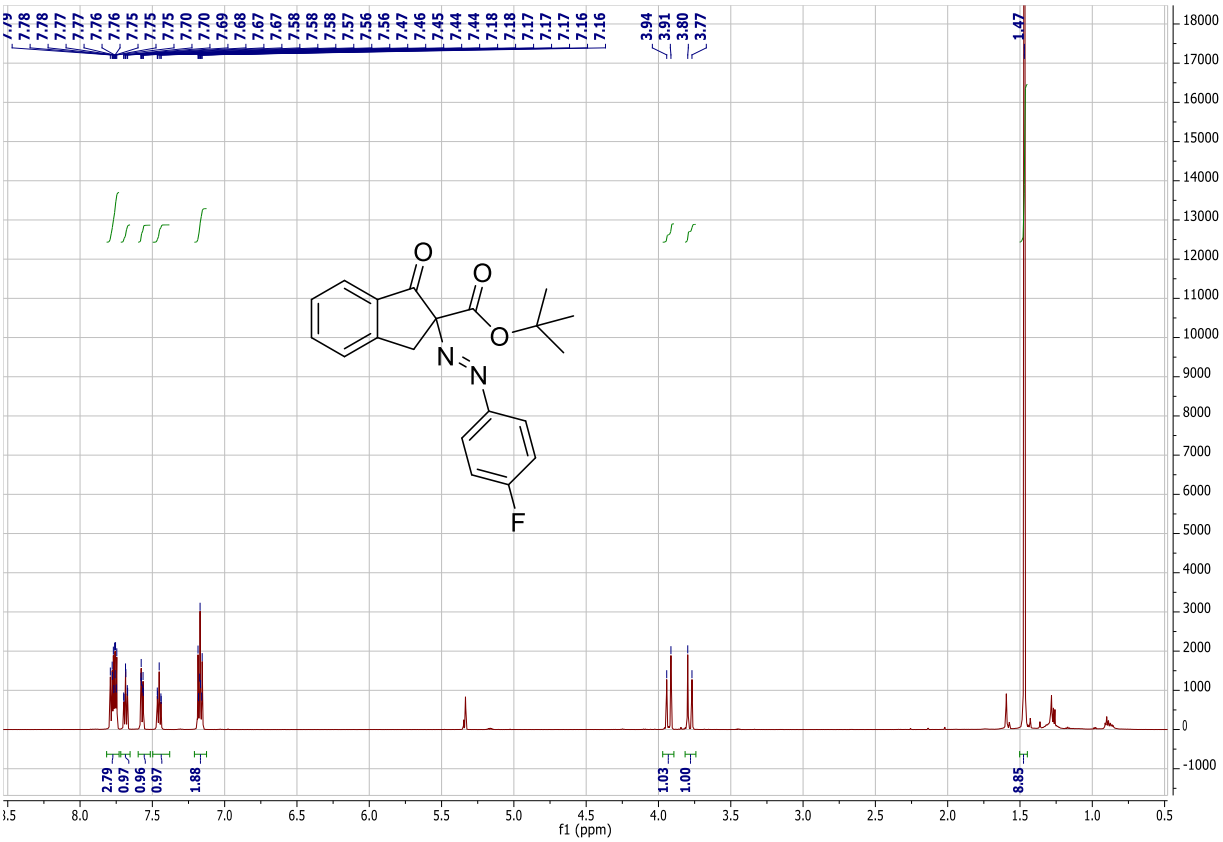
7.79 7.78 7.78 7.77 7.77 7.76 7.76 7.75 7.75 7.75 7.70 7.70 7.69 7.68 7.67 7.67 7.58 7.58 7.58 7.57 7.56 7.56 7.47 7.46 7.45 7.44 7.44 7.18 7.18 7.17 7.17 7.17 7.16 7.16
3.94 3.91 3.80 3.77
1.47
2.79 0.97 0.96 0.97 1.88
1.03 1.00
8.85
f1 (ppm)

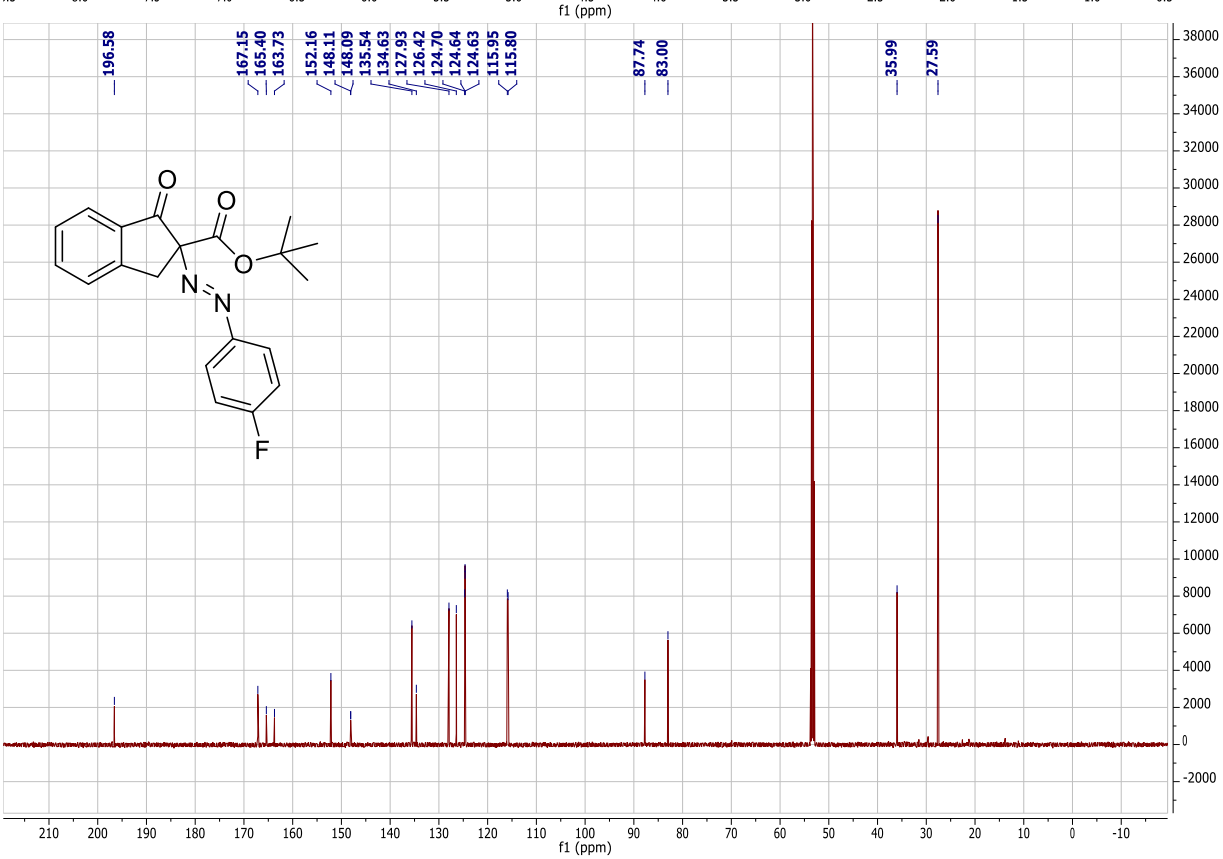
196.58
167.15 165.40 163.73
152.16 148.11 148.09 135.54 134.63 127.93 126.42 124.70 124.64 124.63 115.95 115.80
87.74 83.00
35.99 27.59
f1 (ppm)

^{19}F NMR

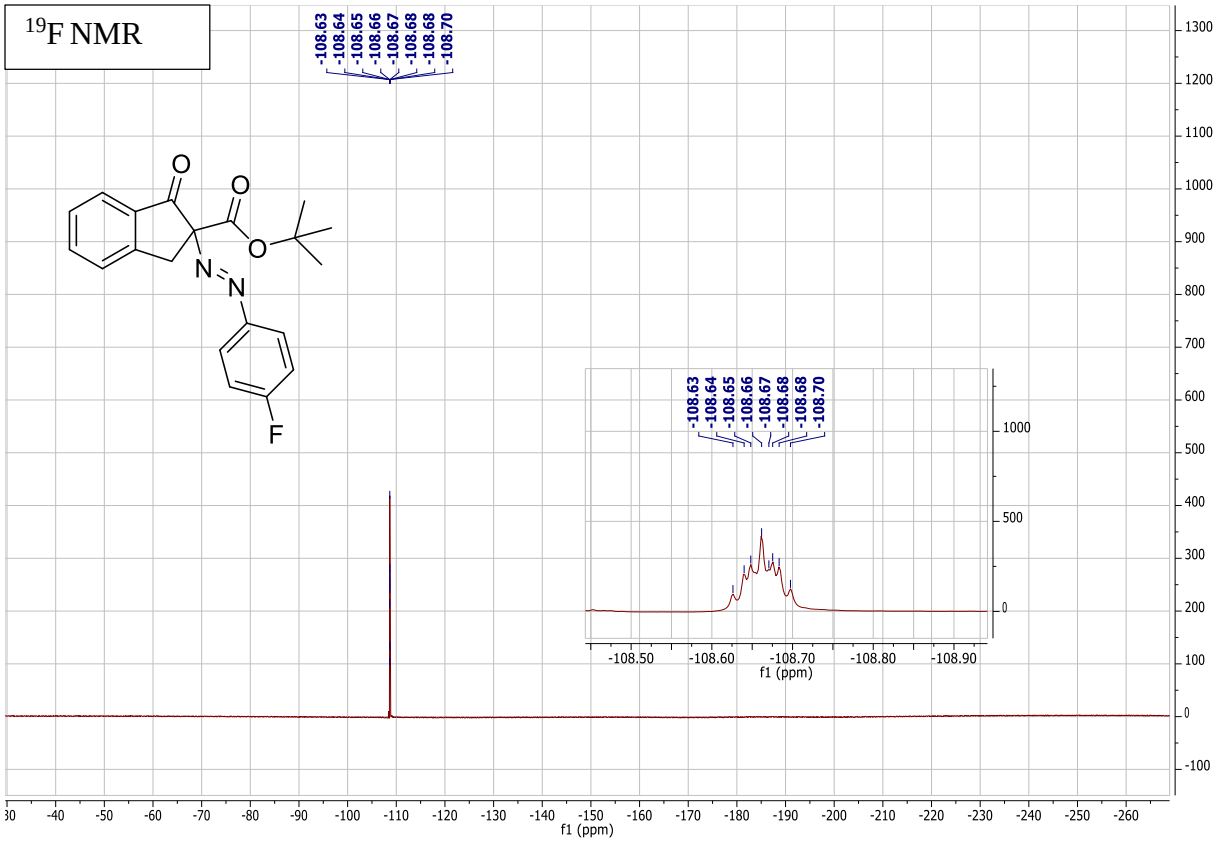
-108.63
-108.64
-108.65
-108.66
-108.67
-108.68
-108.68
-108.70
f1 (ppm)

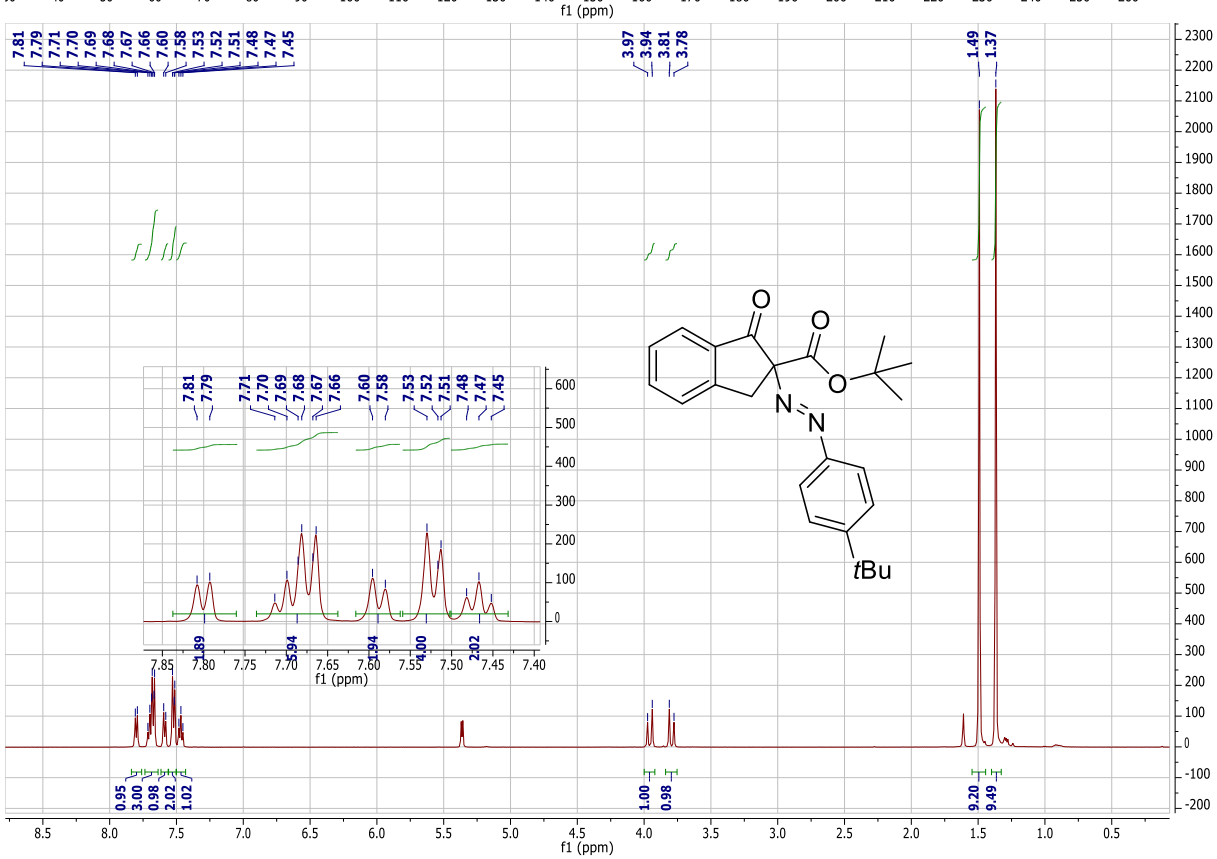
7.81
7.79
7.71
7.70
7.69
7.68
7.67
7.66
7.60
7.58
7.53
7.52
7.51
7.48
7.47
7.45
3.97
3.94
3.81
3.78
1.49
1.37
tBu
0.95
3.00
0.98
2.02
1.02
1.00
0.98
9.20
9.49
f1 (ppm)

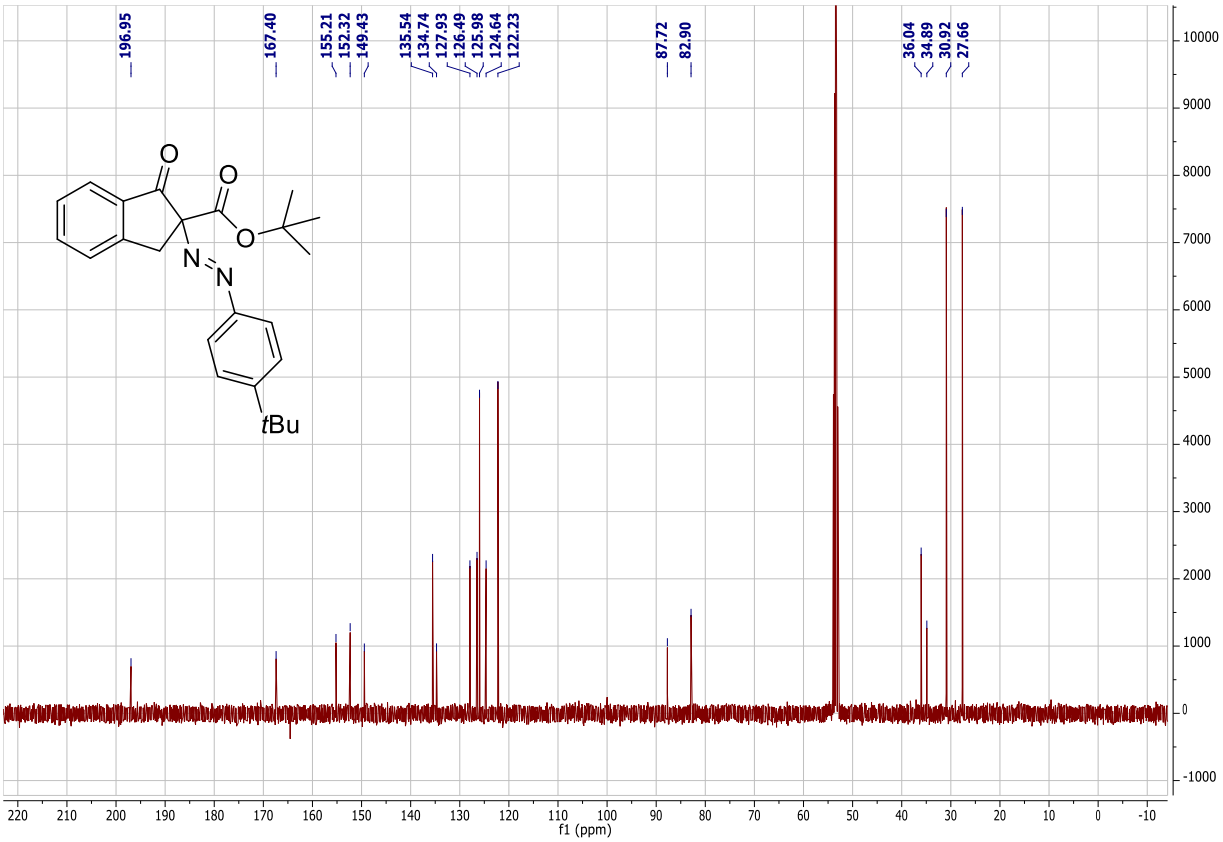
196.95
167.40
155.21
152.32
149.43
135.54
134.74
127.93
126.49
125.98
124.64
122.23
87.72
82.90
36.04
34.89
30.92
27.66
tBu
f1 (ppm)

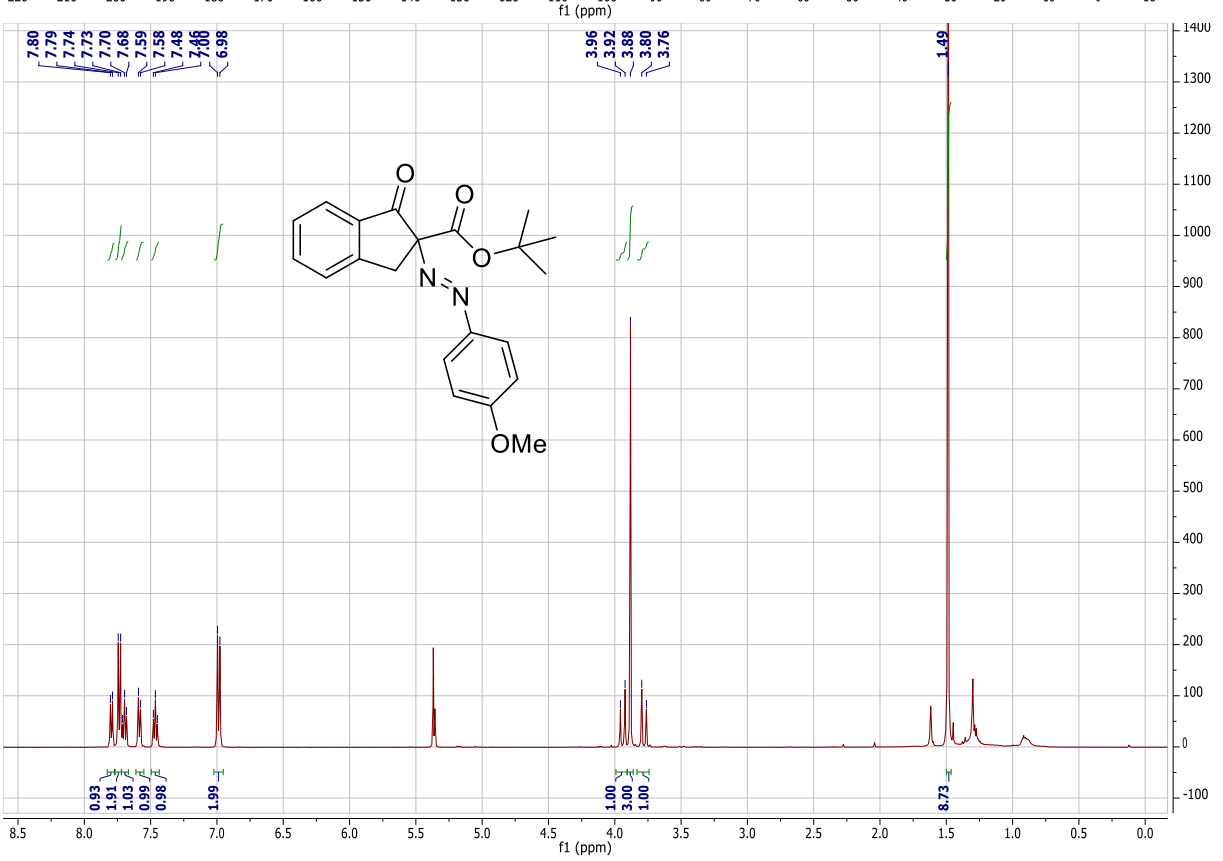
7.80
7.79
7.74
7.73
7.70
7.68
7.59
7.58
7.48
6.98
3.96
3.92
3.88
3.80
3.76
1.49
OMe
0.93
1.91
1.03
0.99
0.98
1.99
1.00
3.00
1.00
8.73
f1 (ppm)

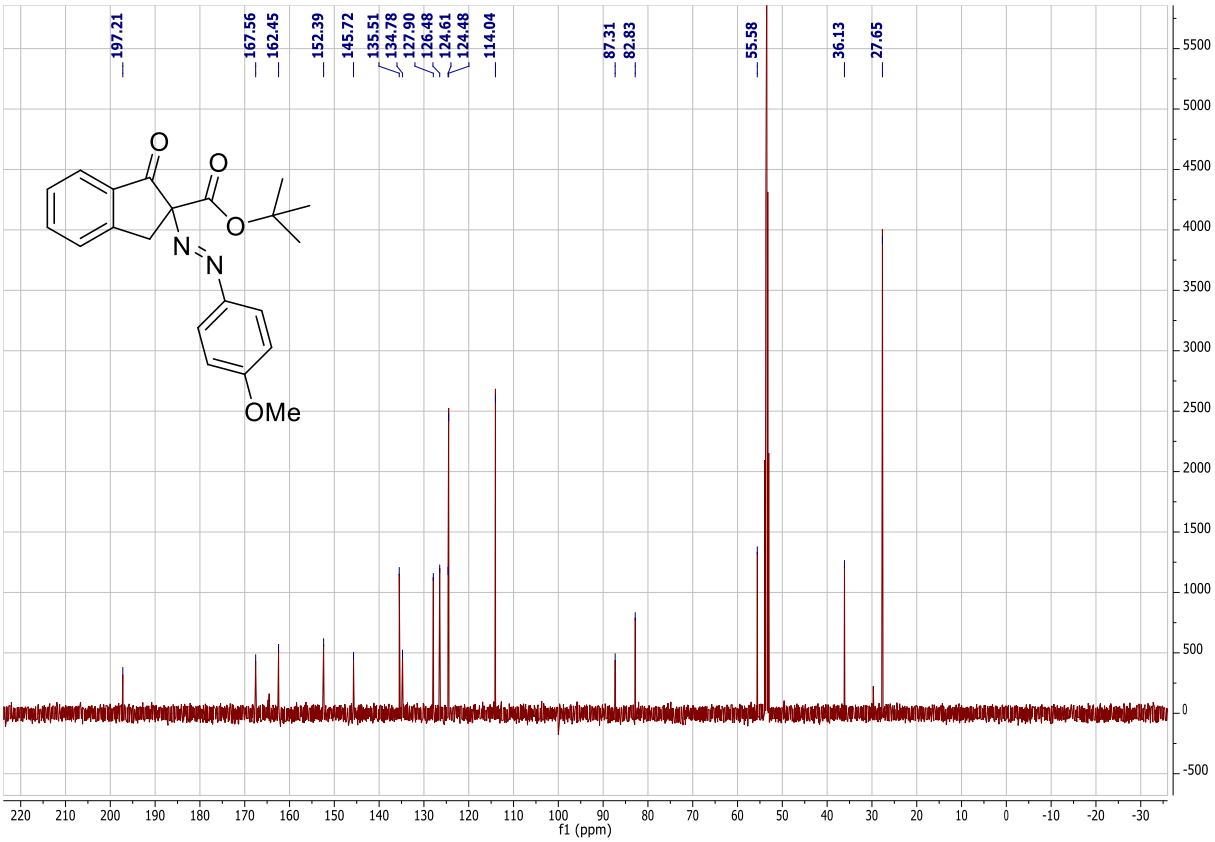
197.21
167.56
162.45
152.39
145.72
135.51
134.78
127.90
126.48
124.61
124.48
114.04
87.31
82.83
55.58
36.13
27.65
OMe
f1 (ppm)

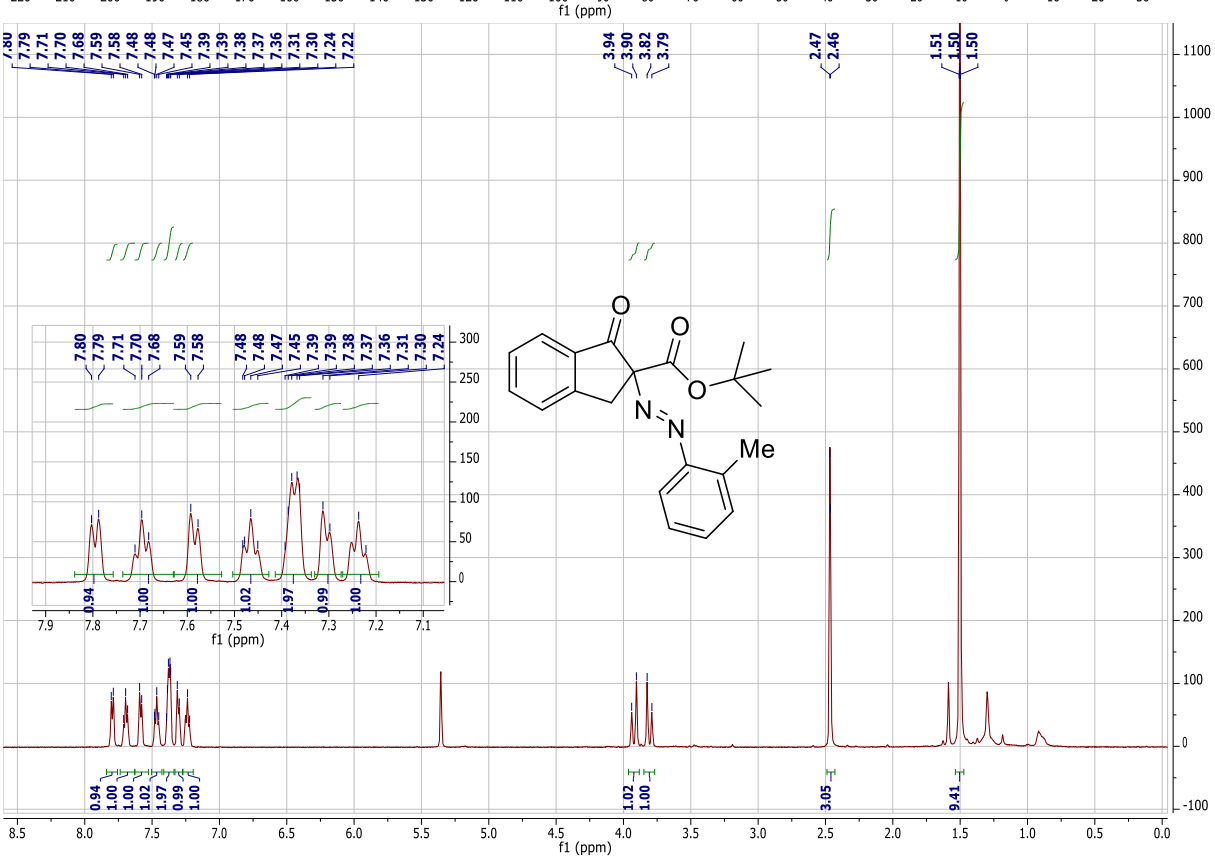
Me
f1 (ppm)

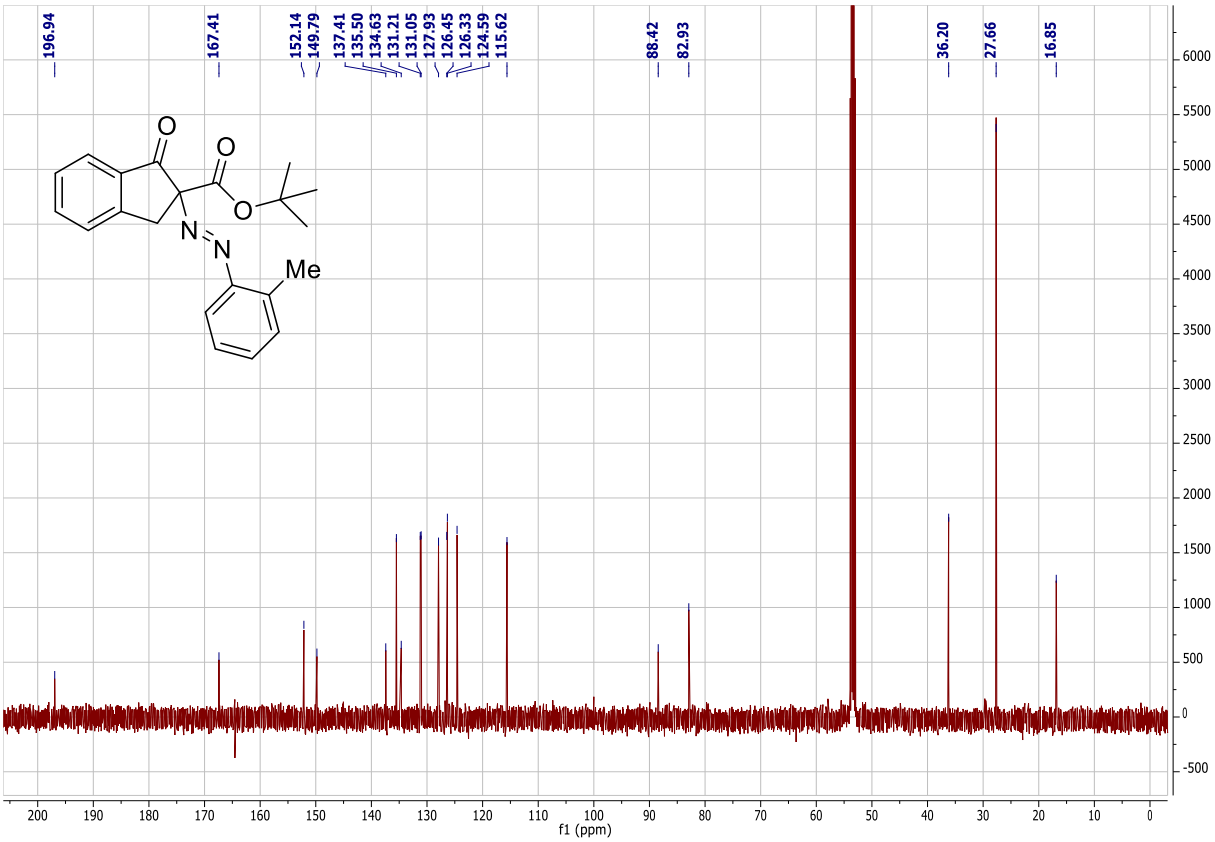
196.94
167.41
152.14
149.79
137.41
135.50
134.63
131.21
131.05
127.93
126.45
126.33
124.59
115.62
88.42
82.93
36.20
27.66
16.85
O
O
O
N
N
Me
f1 (ppm)

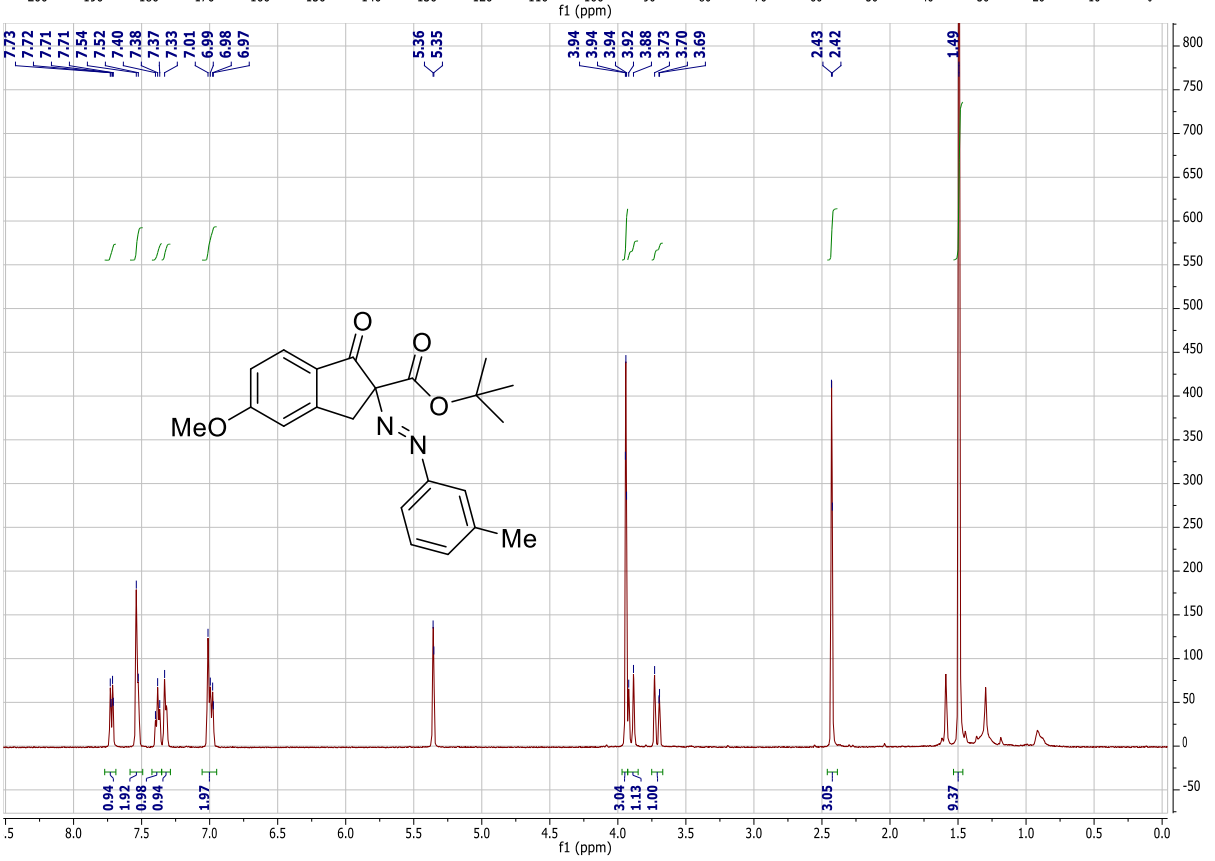
7.73
7.72
7.71
7.71
7.54
7.52
7.40
7.38
7.37
7.33
7.01
6.99
6.98
6.97
5.36
5.35
3.94
3.94
3.94
3.92
3.88
3.73
3.70
3.69
2.43
2.42
1.49
0.94
1.92
0.98
0.94
1.97
3.04
1.13
1.00
3.05
9.37
O
O
O
MeO
N
N
Me
f1 (ppm)

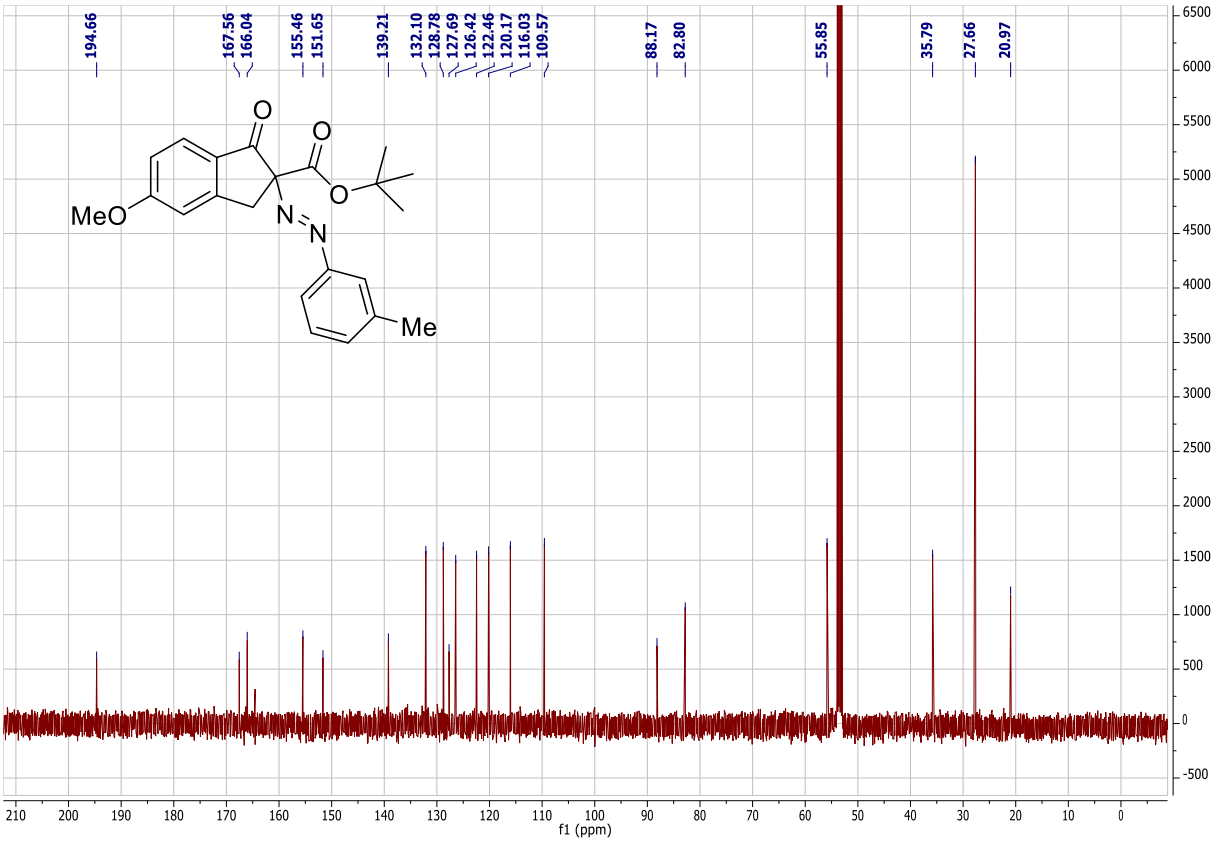
194.66
167.56
166.04
155.46
151.65
139.21
132.10
128.78
127.69
126.42
122.46
120.17
116.03
109.57
88.17
82.80
55.85
35.79
27.66
20.97
MeO
Me
f1 (ppm)

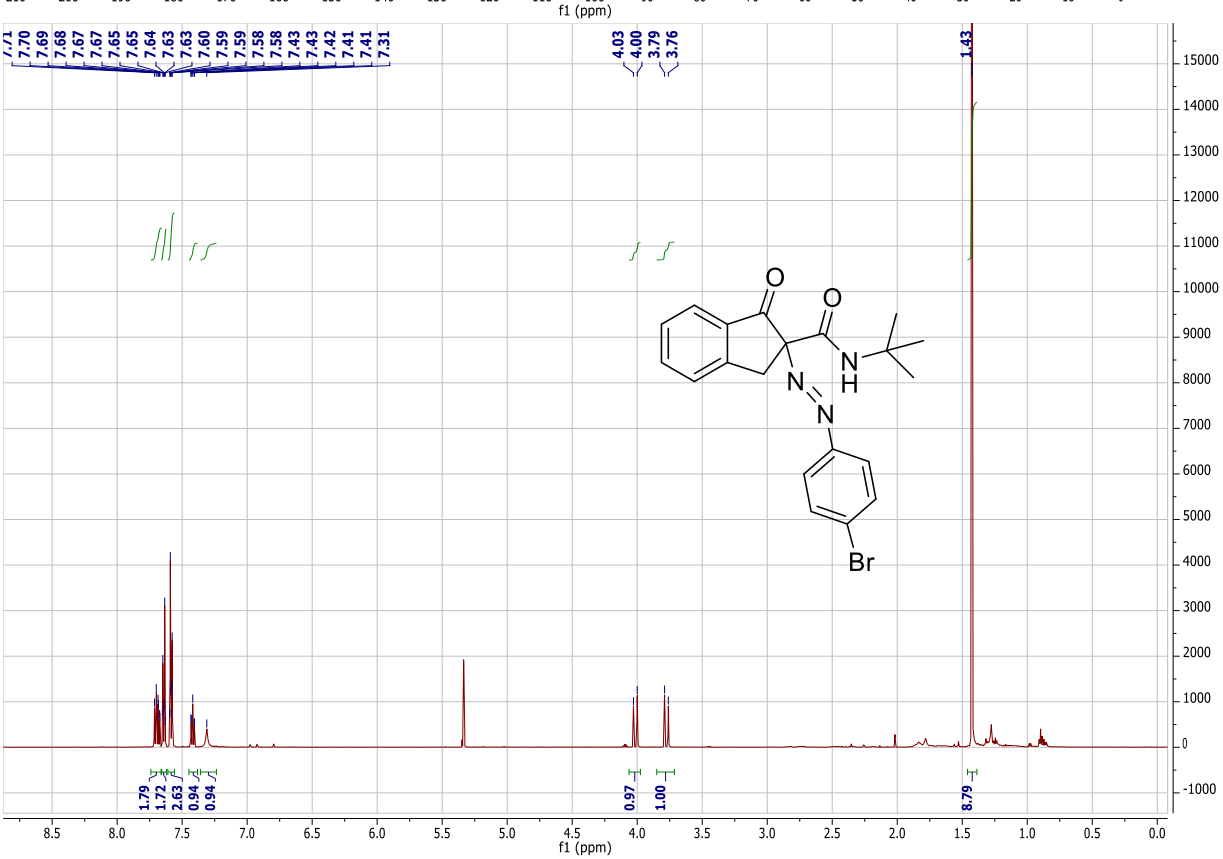
7.71
7.70
7.69
7.68
7.67
7.67
7.65
7.65
7.64
7.63
7.63
7.60
7.59
7.59
7.58
7.58
7.43
7.43
7.42
7.41
7.41
7.31
4.03
4.00
3.79
3.76
1.43
Br
1.79
1.72
2.63
0.94
0.94
0.97
1.00
8.79
f1 (ppm)

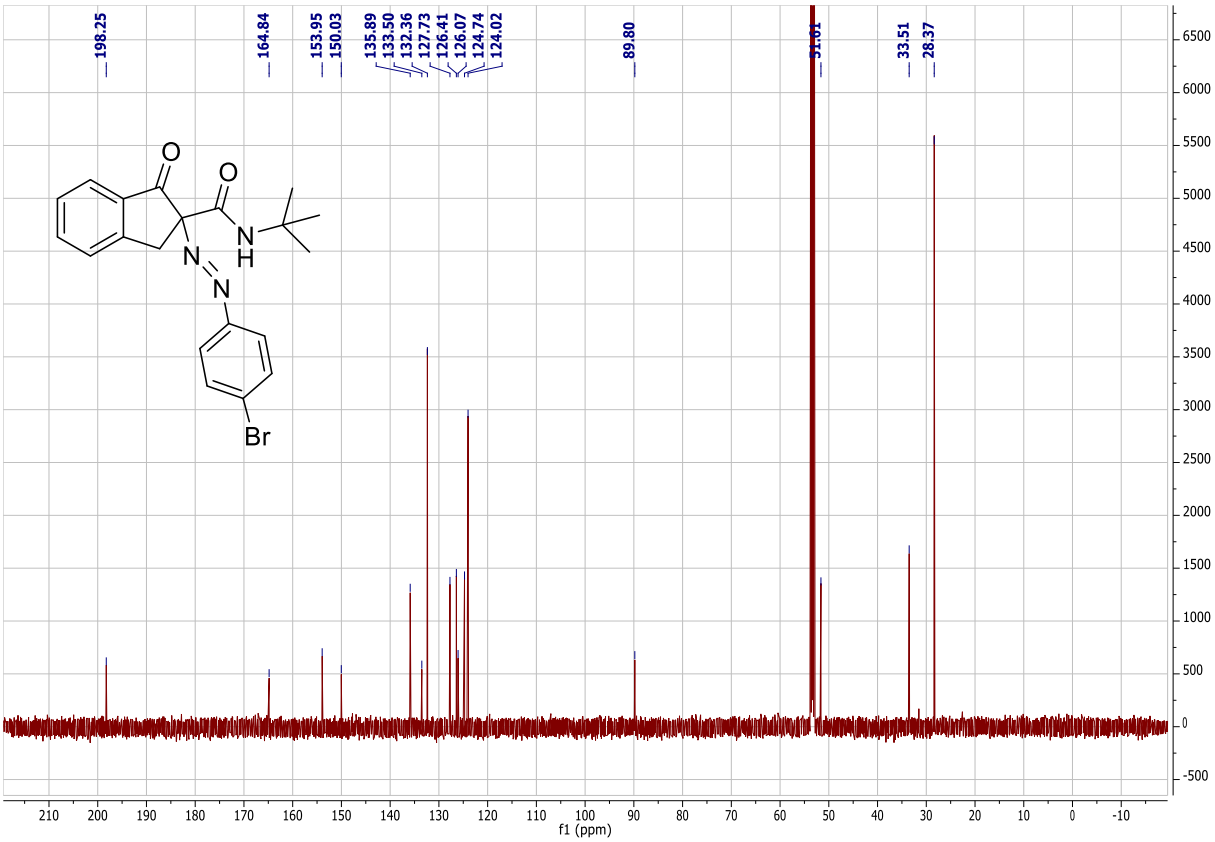
198.25
164.84
153.95
150.03
135.89
133.50
132.36
127.73
126.41
126.07
124.74
124.02
89.80
51.01
33.51
28.37
O
O
N
H
N
N
Br
f1 (ppm)

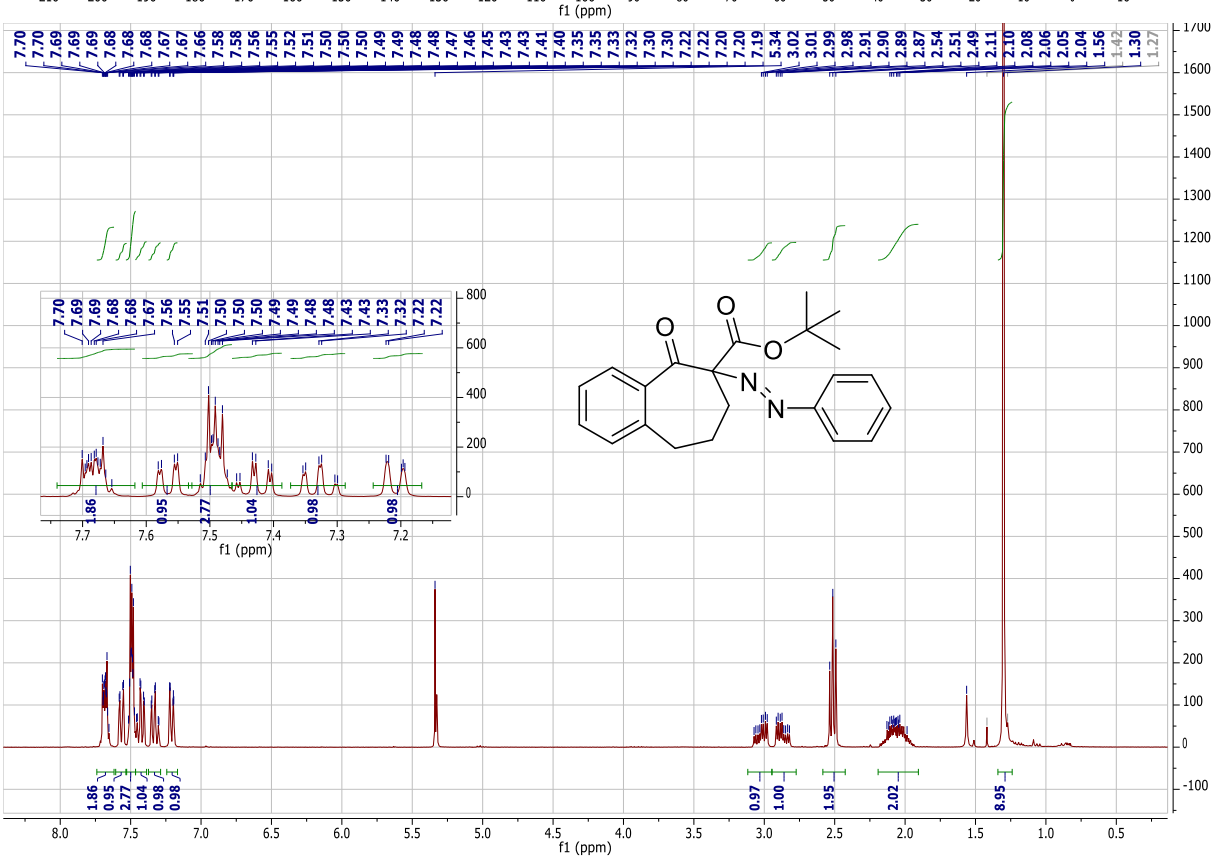
O
O
O
O
N
N
1.86
0.95
2.77
1.04
0.98
0.98
0.97
1.00
1.95
2.02
8.95
f1 (ppm)

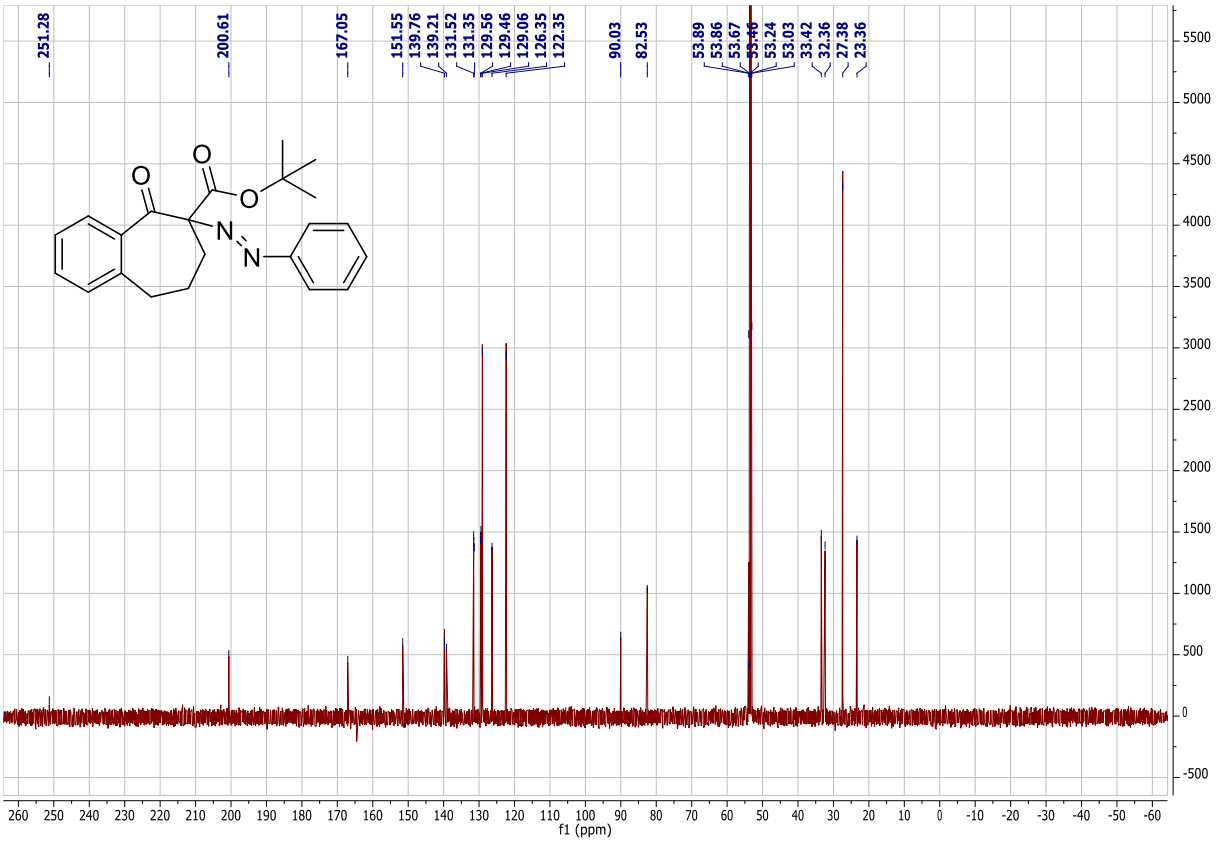
251.28
200.61
167.05
151.55
139.76
139.21
131.52
131.35
129.56
129.46
129.06
126.35
122.35
90.03
82.53
53.89
53.86
53.67
53.40
53.24
53.03
33.42
32.36
27.38
23.36
f1 (ppm)

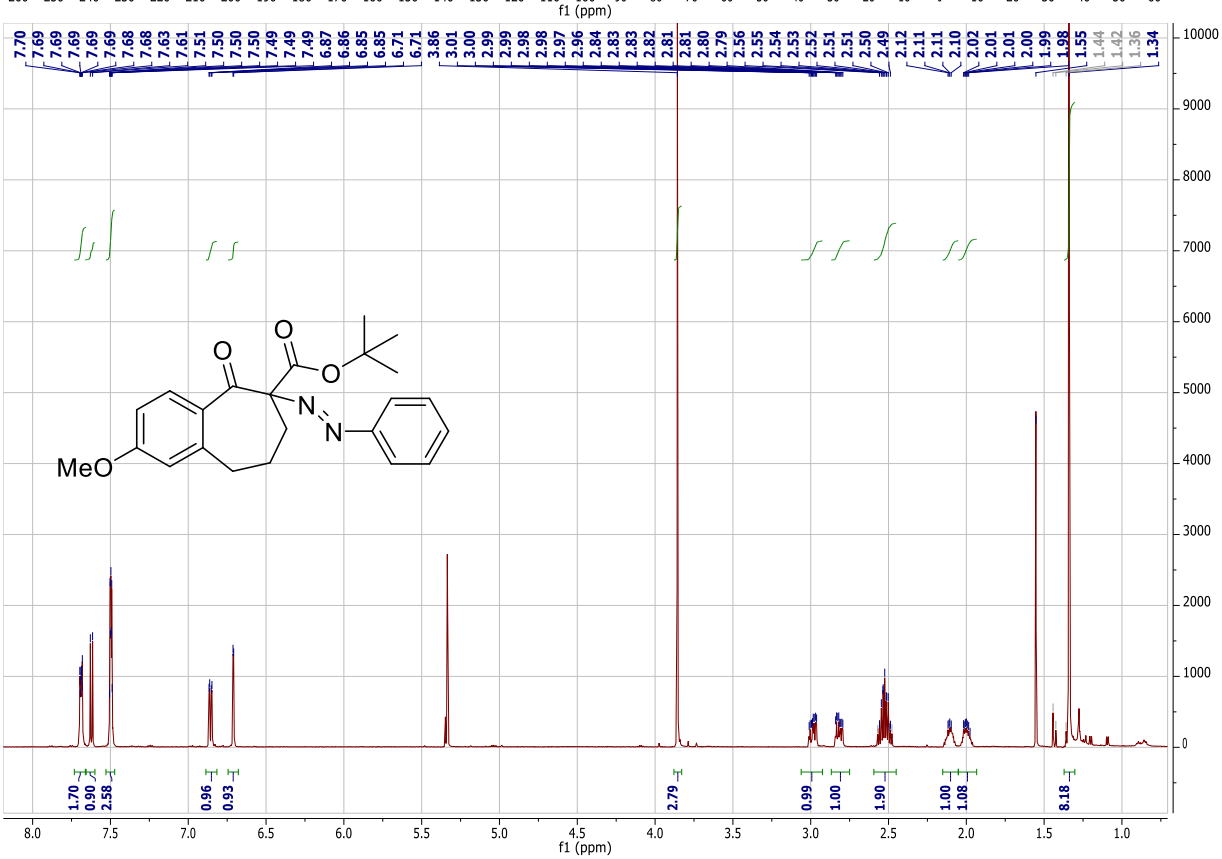
MeO
1.70
0.90
2.58
0.96
0.93
2.79
0.99
1.00
1.90
1.00
1.08
8.18
f1 (ppm)

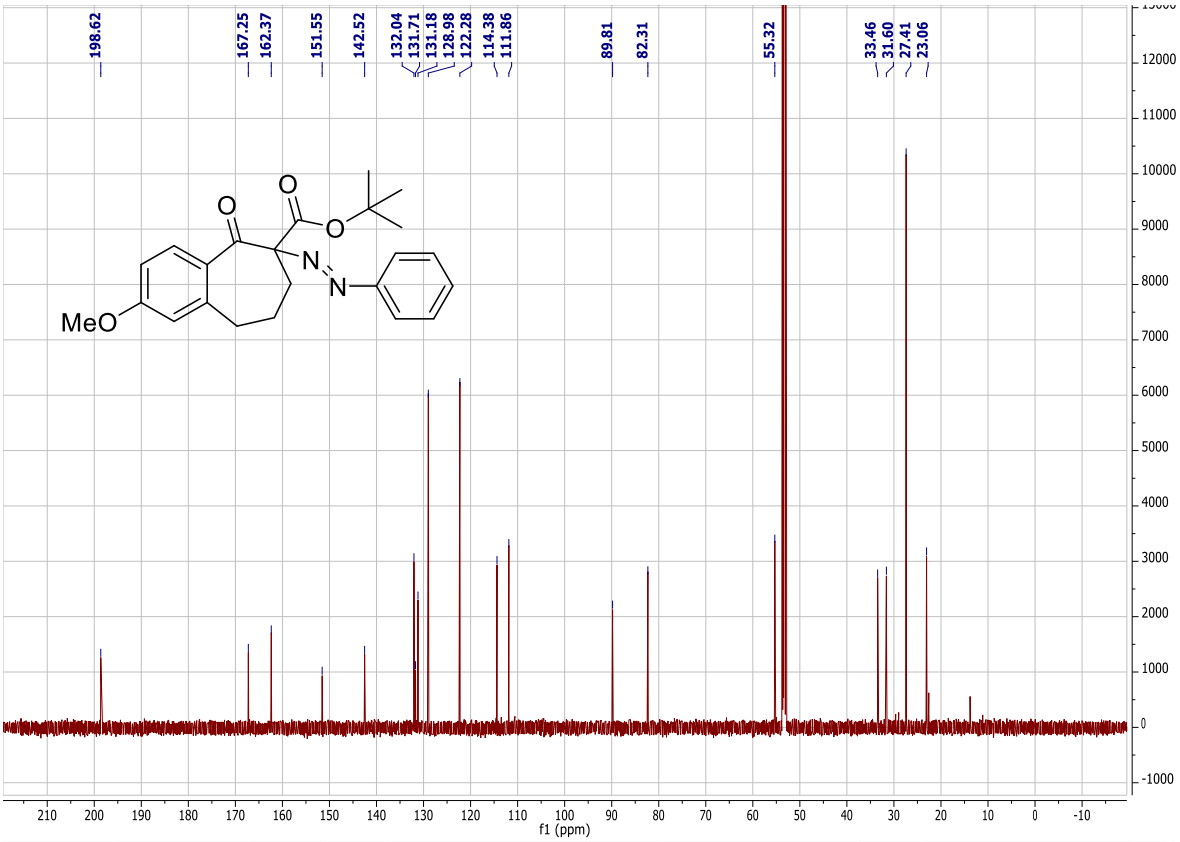
198.62
167.25
162.37
151.55
142.52
132.04
131.71
131.18
128.98
122.28
114.38
111.86
89.81
82.31
55.32
33.46
31.60
27.41
23.06
MeO
f1 (ppm)

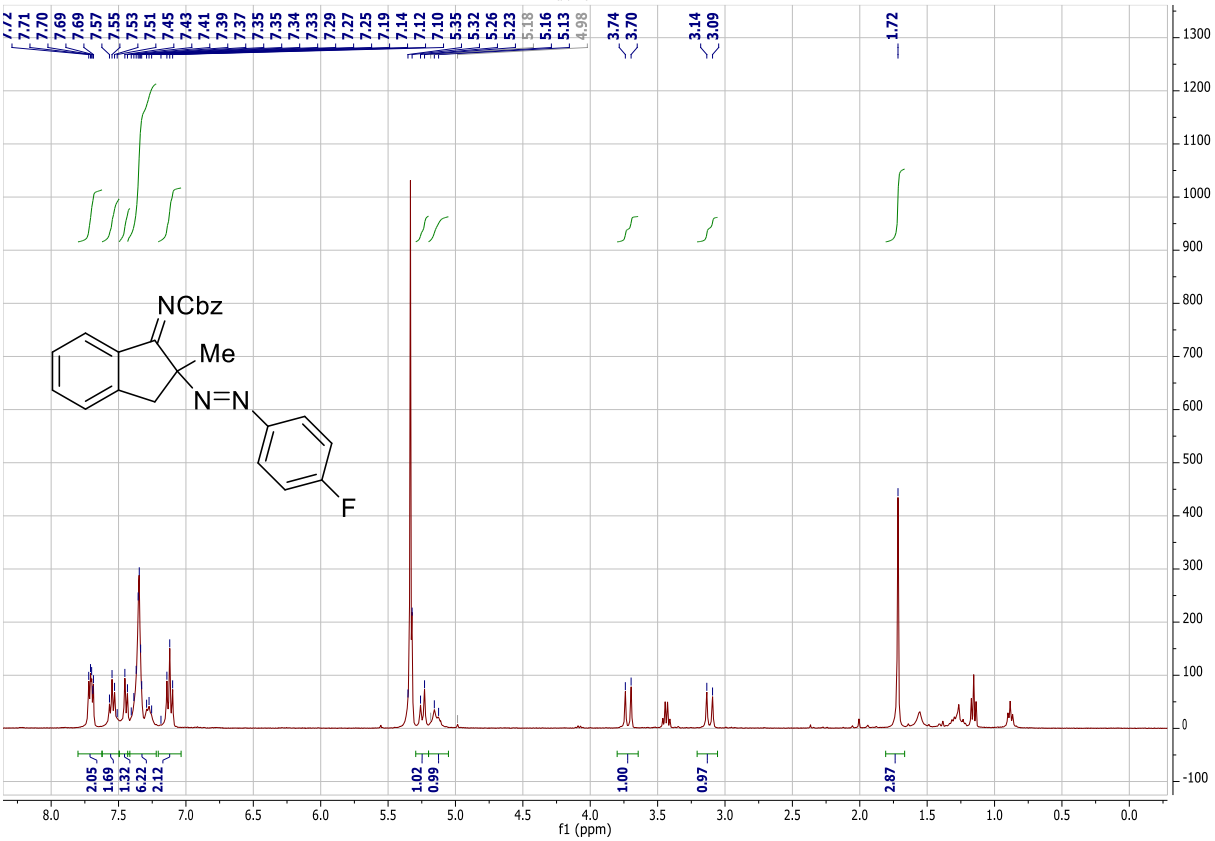
7.71
7.70
7.69
7.69
7.57
7.55
7.53
7.51
7.45
7.43
7.41
7.39
7.37
7.35
7.35
7.34
7.33
7.29
7.27
7.25
7.19
7.14
7.12
7.10
5.35
5.32
5.26
5.23
5.16
5.13
3.74
3.70
3.14
3.09
1.72
NCbz
Me
N=N
F
2.05
1.69
1.32
6.22
2.12
1.02
0.99
1.00
0.97
2.87
f1 (ppm)

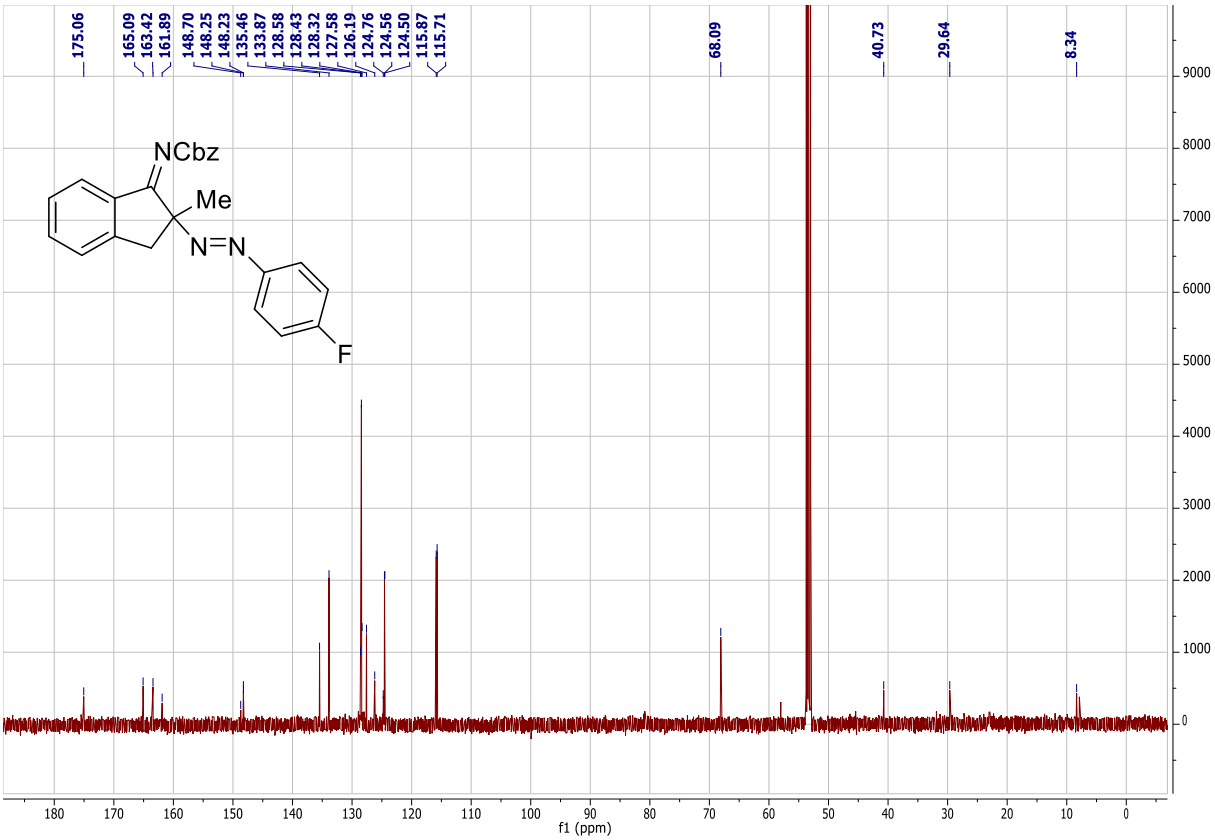
175.06
165.09
163.42
161.89
148.70
148.25
148.23
135.46
133.87
128.58
128.43
128.32
127.58
126.19
124.76
124.56
124.50
115.87
115.71
68.09
40.73
29.64
8.34
NCbz
Me
N=N
F
f1 (ppm)

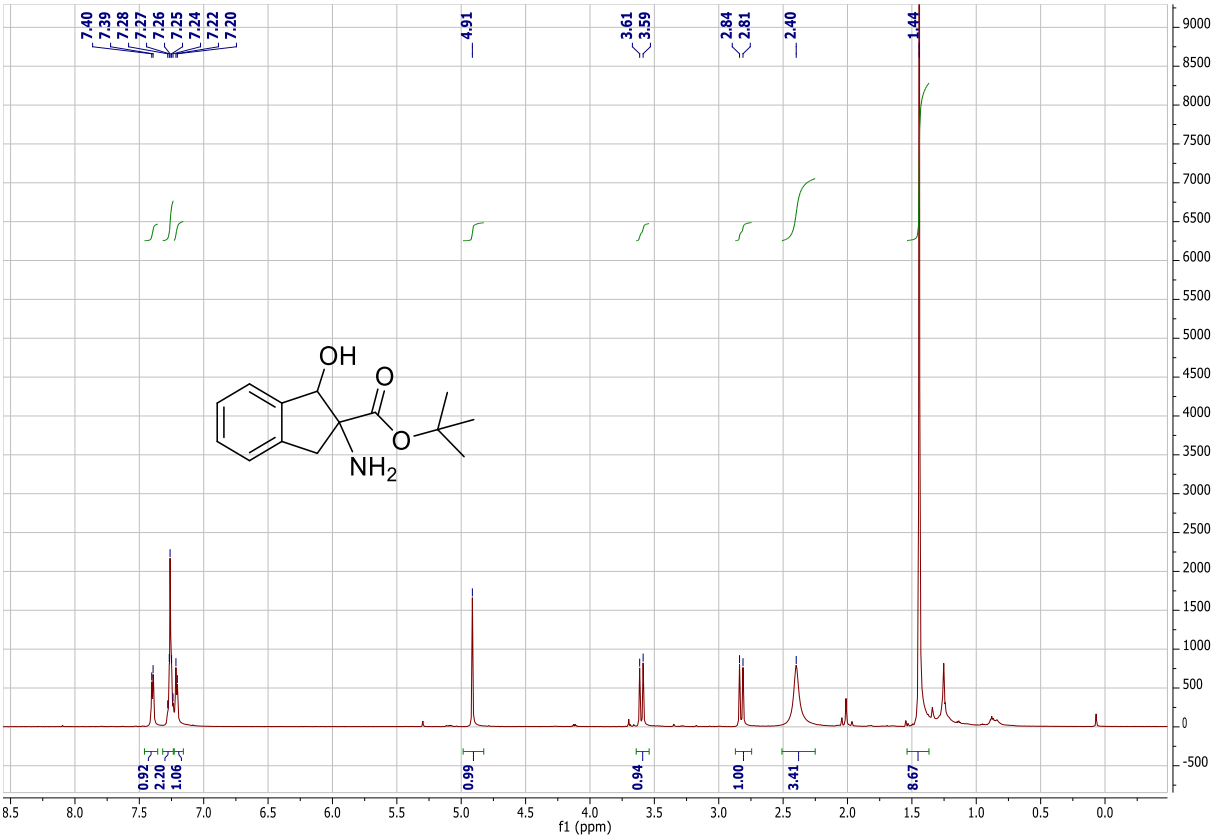
7.40
7.39
7.28
7.27
7.26
7.25
7.24
7.22
7.20
4.91
3.61
3.59
2.84
2.81
2.40
1.44
OH
O
O
NH2
0.92
2.20
1.06
0.99
0.94
1.00
3.41
8.67
f1 (ppm)

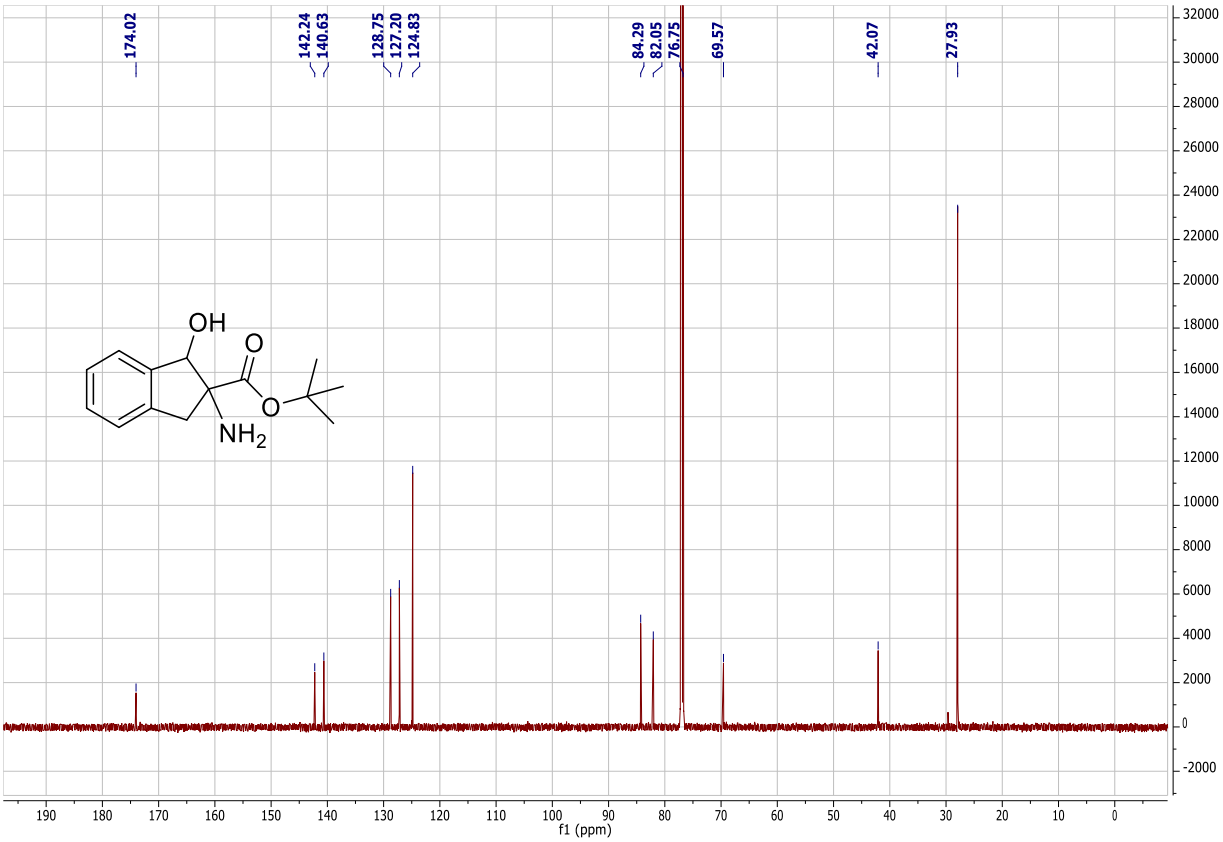
174.02
142.24
140.63
128.75
127.20
124.83
84.29
82.05
76.75
69.57
42.07
27.93
OH
O
O
NH2
f1 (ppm)

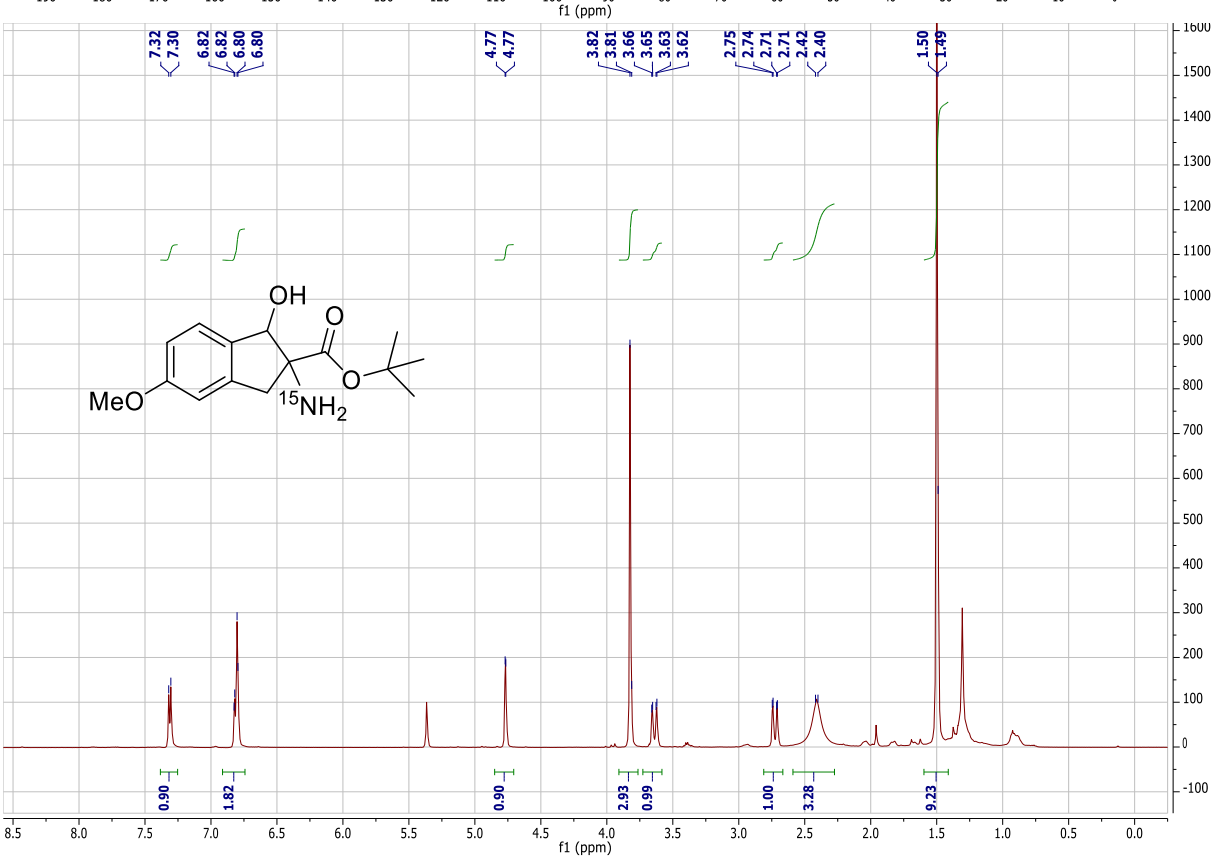
7.32
7.30
6.82
6.82
6.80
6.80
4.77
4.77
3.82
3.81
3.66
3.65
3.63
3.62
2.75
2.74
2.71
2.71
2.42
2.40
1.50
1.49
OH
O
O
MeO
15NH2
0.90
1.82
0.90
2.93
0.99
1.00
3.28
9.23
f1 (ppm)

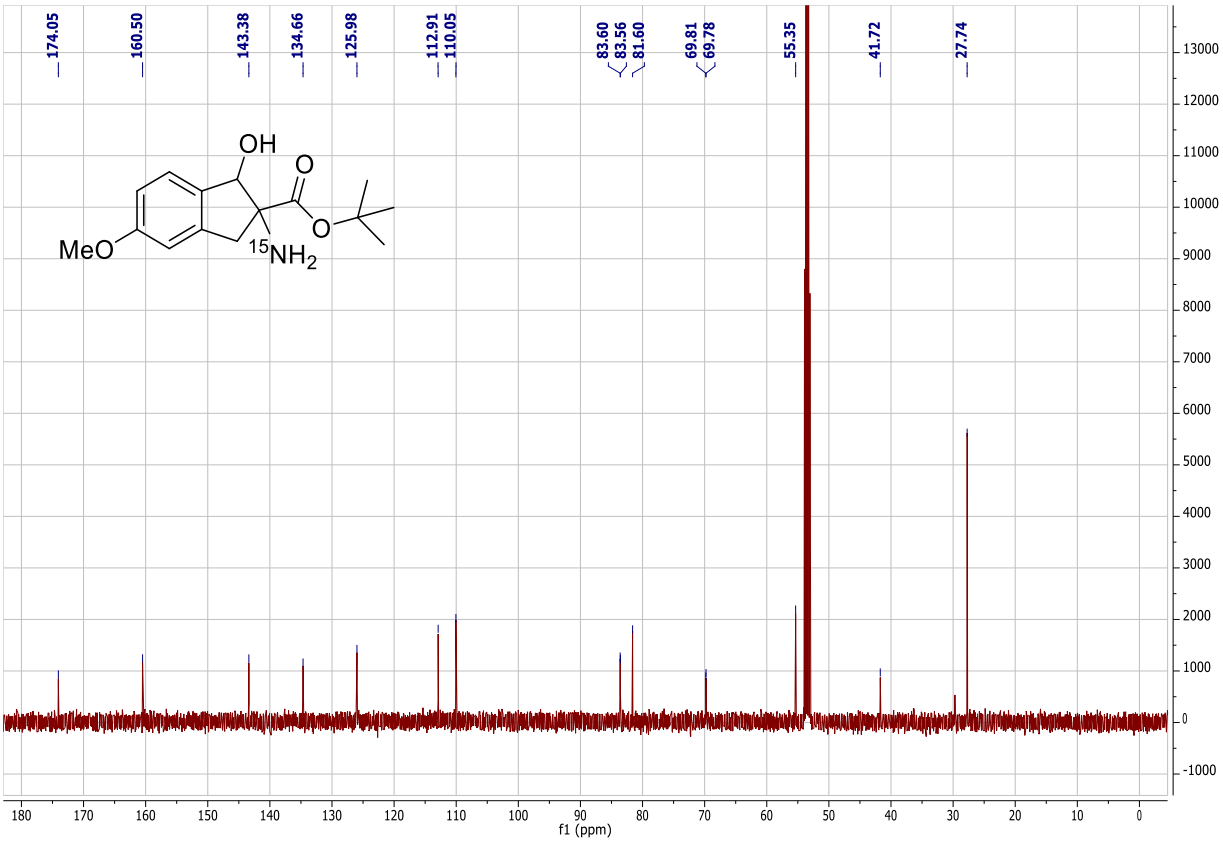
174.05
160.50
143.38
134.66
125.98
112.91
110.05
83.60
83.56
81.60
69.81
69.78
55.35
41.72
27.74
OH
O
O
MeO
15NH2
f1 (ppm)

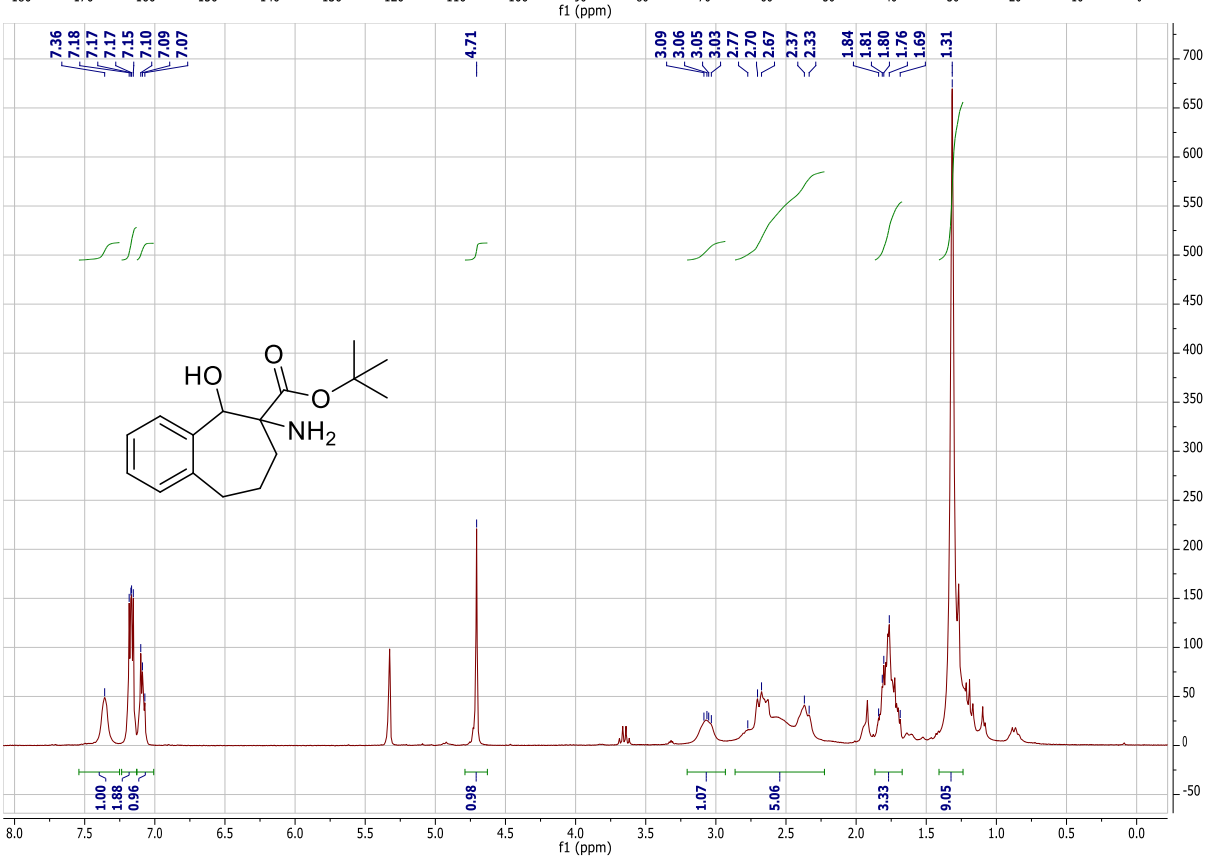
7.36
7.18
7.17
7.17
7.15
7.10
7.09
7.07
4.71
3.09
3.06
3.05
3.03
2.77
2.70
2.67
2.37
2.33
1.84
1.81
1.80
1.76
1.69
1.31
HO
O
O
NH2
1.00
1.88
0.96
0.98
1.07
5.06
3.33
9.05
f1 (ppm)

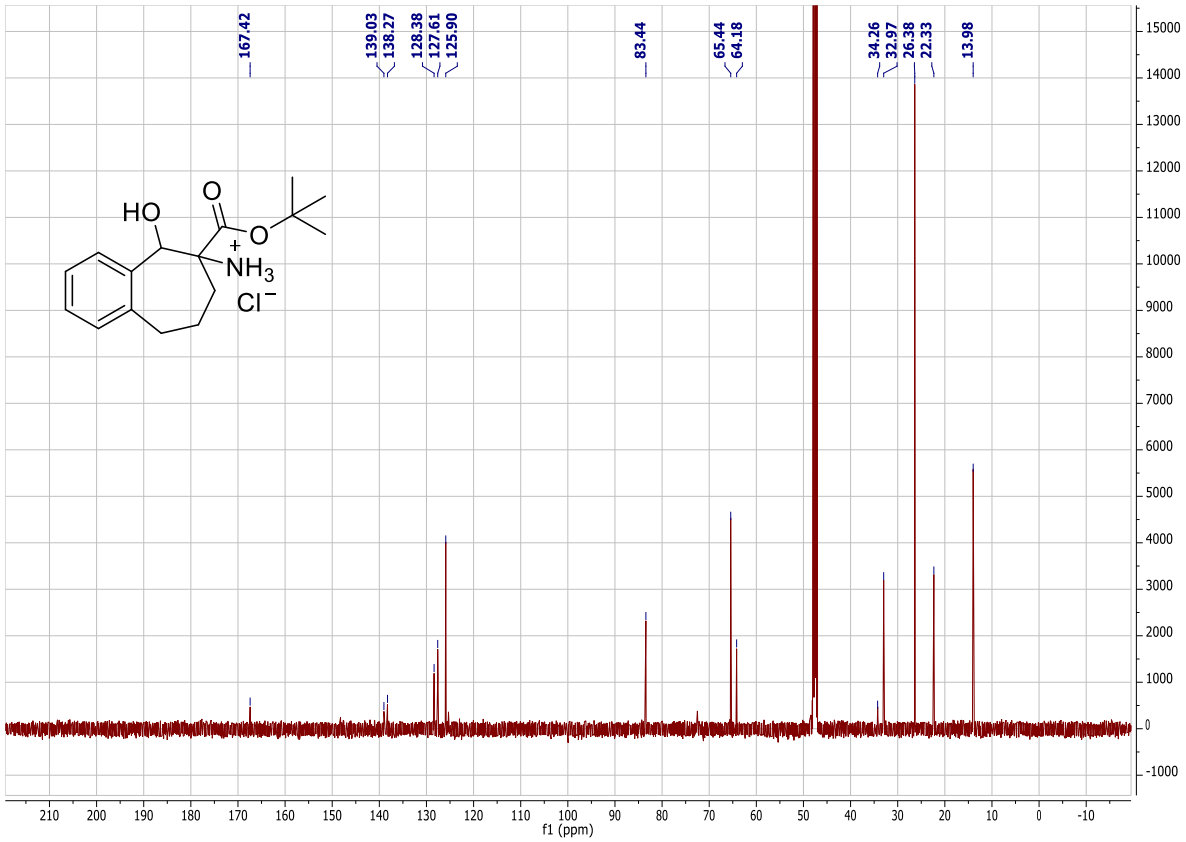
167.42
139.03
138.27
128.38
127.61
125.90
83.44
65.44
64.18
34.26
32.97
26.38
22.33
13.98
HO
O
O
NH3
Cl−
f1 (ppm)

HPLC Traces

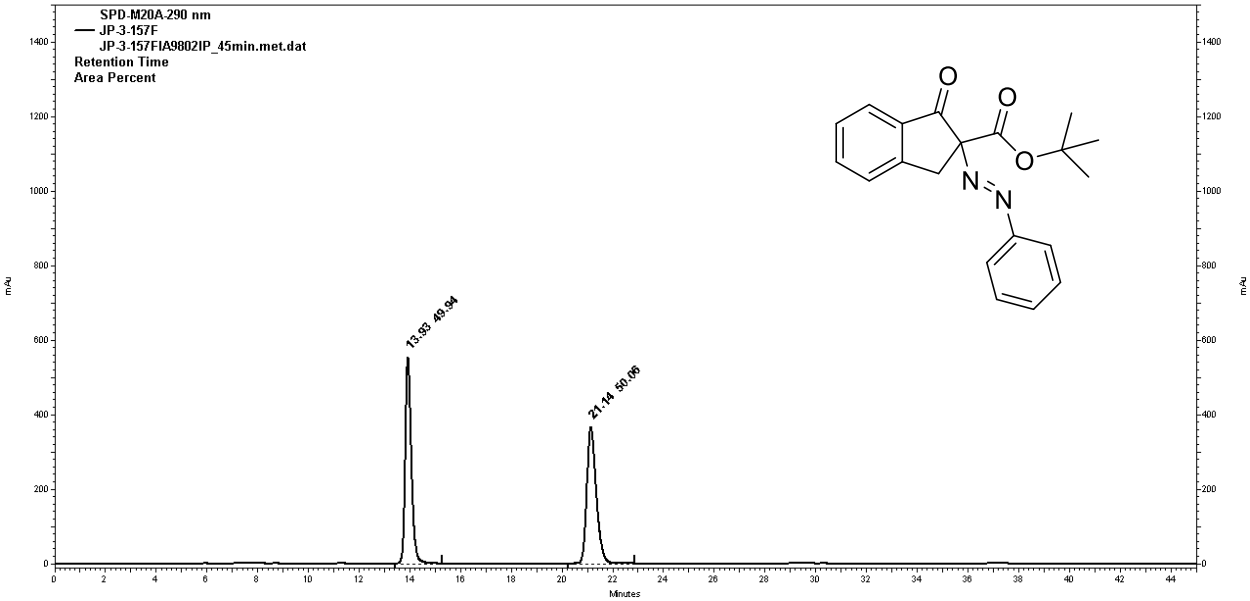
SPD-M20A-290 nm
JP-3-157F
JP-3-157FIA9802IP_45min.met.dat
Retention Time
Area Percent
13.33 49.94
21.14 50.06
m/Au
Minutes

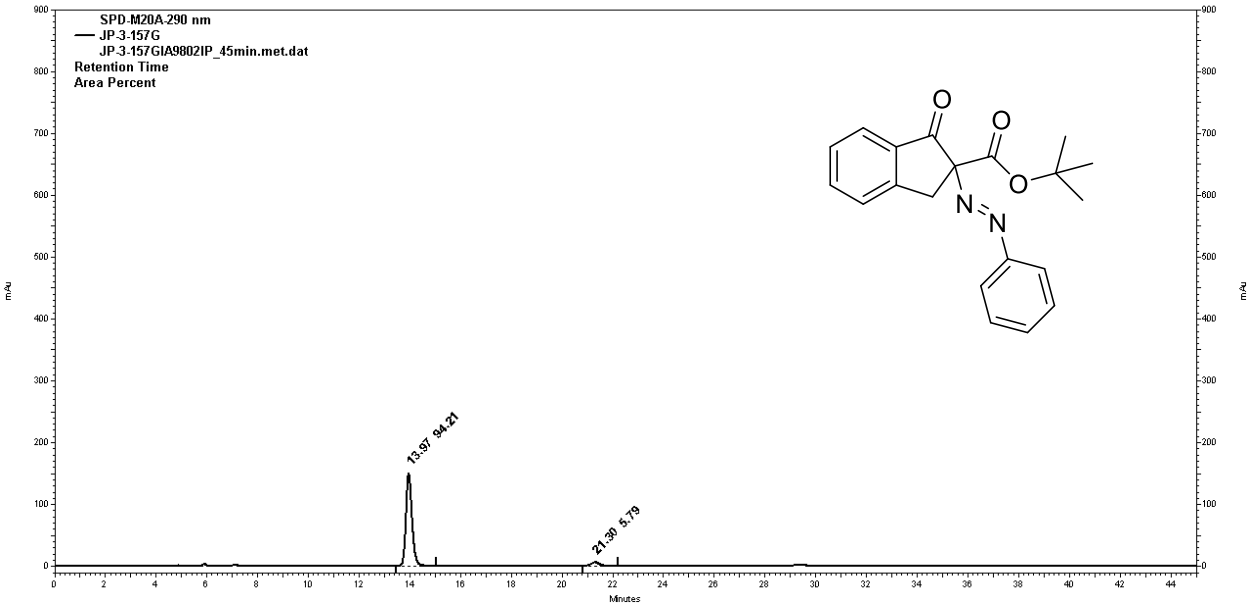
SPD-M20A-290 nm
JP-3-157G
JP-3-157GIA9802IP_45min.met.dat
Retention Time
Area Percent
13.97 94.21
21.30 5.79
m/Au
Minutes

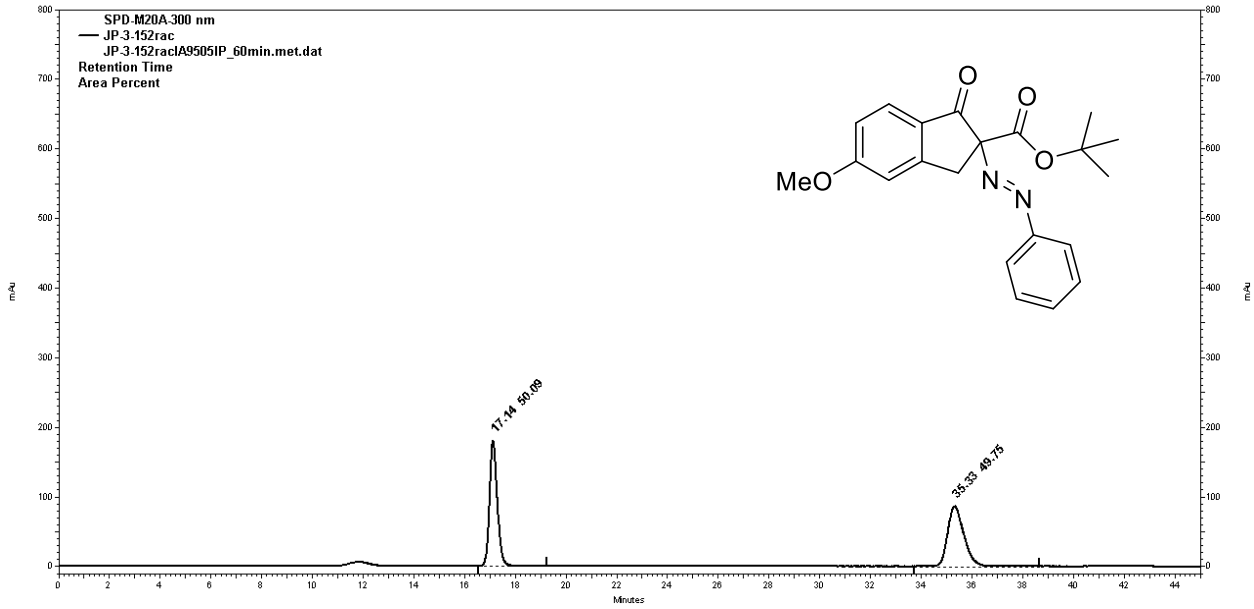
SPD-M20A-300 nm
JP-3-152rac
JP-3-152racIA9505IP_60min.met.dat
Retention Time
Area Percent
17.44 50.09
35.33 49.75
m/Au
Minutes
MeO
O
O
O
N
N

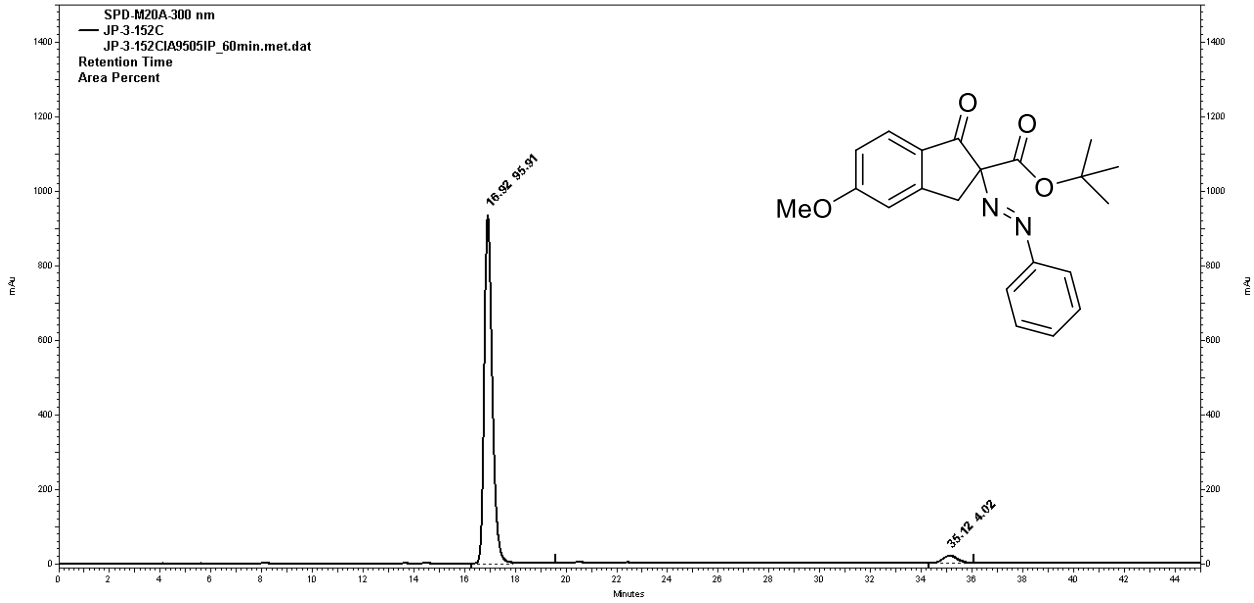
SPD-M20A-300 nm
JP-3-152C
JP-3-152CIA9505IP_60min.met.dat
Retention Time
Area Percent
16.92 95.91
35.12 4.02
m/Au
Minutes
MeO
O
O
O
N
N

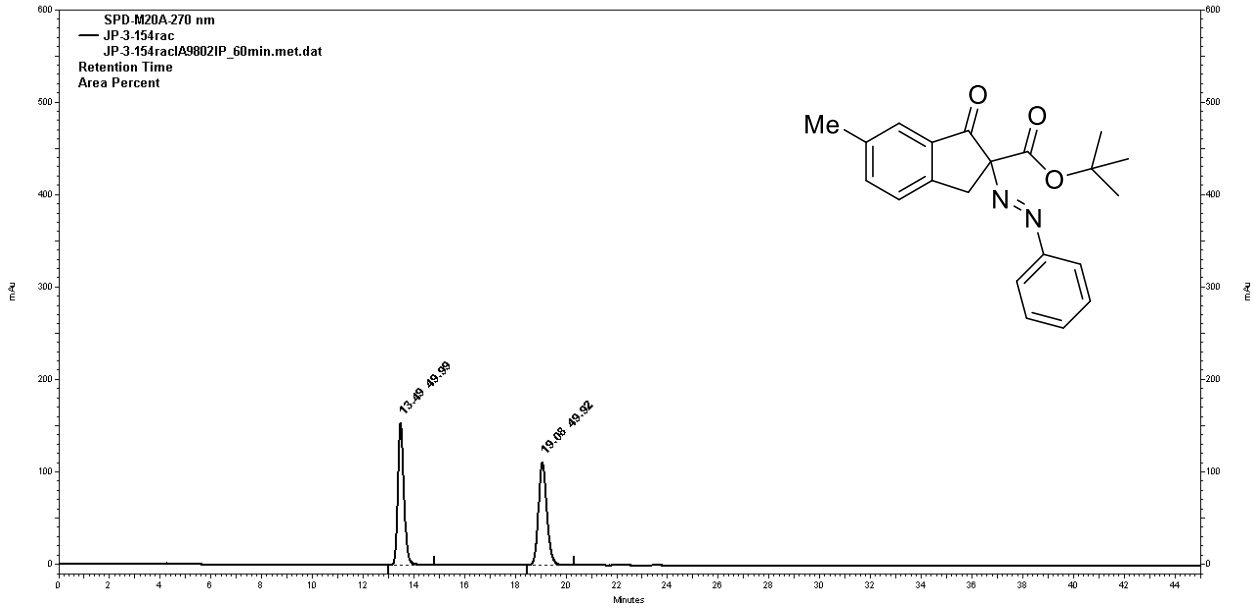
SPD-M20A-270 nm
JP-3-154rac
JP-3-154racIA9802IP_60min.met.dat
Retention Time
Area Percent
13.49 49.59
19.08 49.92
m/Au
Minutes
Me
O
O
O
N
N

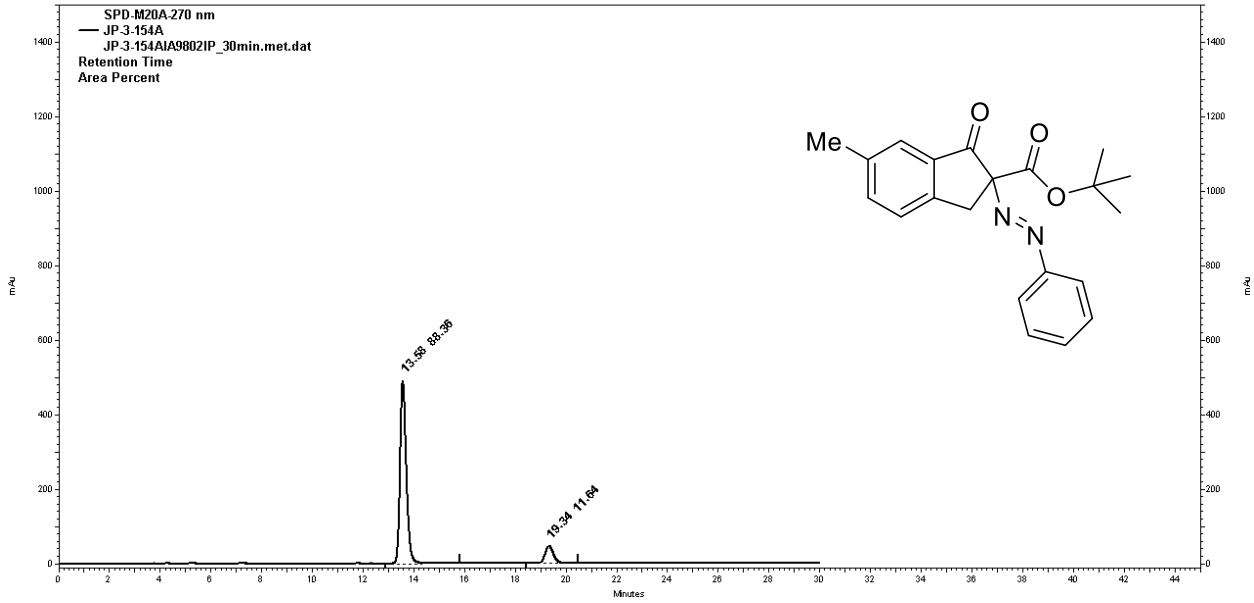
SPD-M20A-270 nm
JP-3-154A
JP-3-154AIA9802IP_30min.met.dat
Retention Time
Area Percent
13.58 88.36
19.34 11.64
m/Au
Minutes
Me
O
O
O
N
N

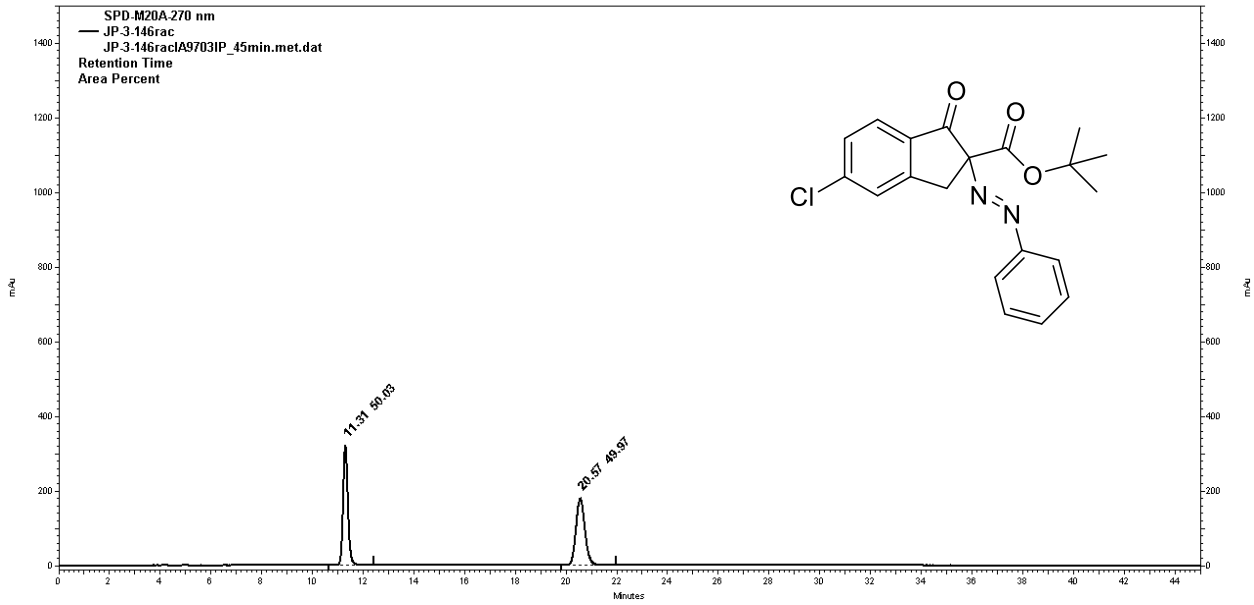
SPD-M20A-270 nm
JP-3-146rac
JP-3-146racIA9703IP_45min.met.dat
Retention Time
Area Percent
11.31 50.03
20.57 49.97
m/Au
Minutes
Cl
N
N
O
O
O

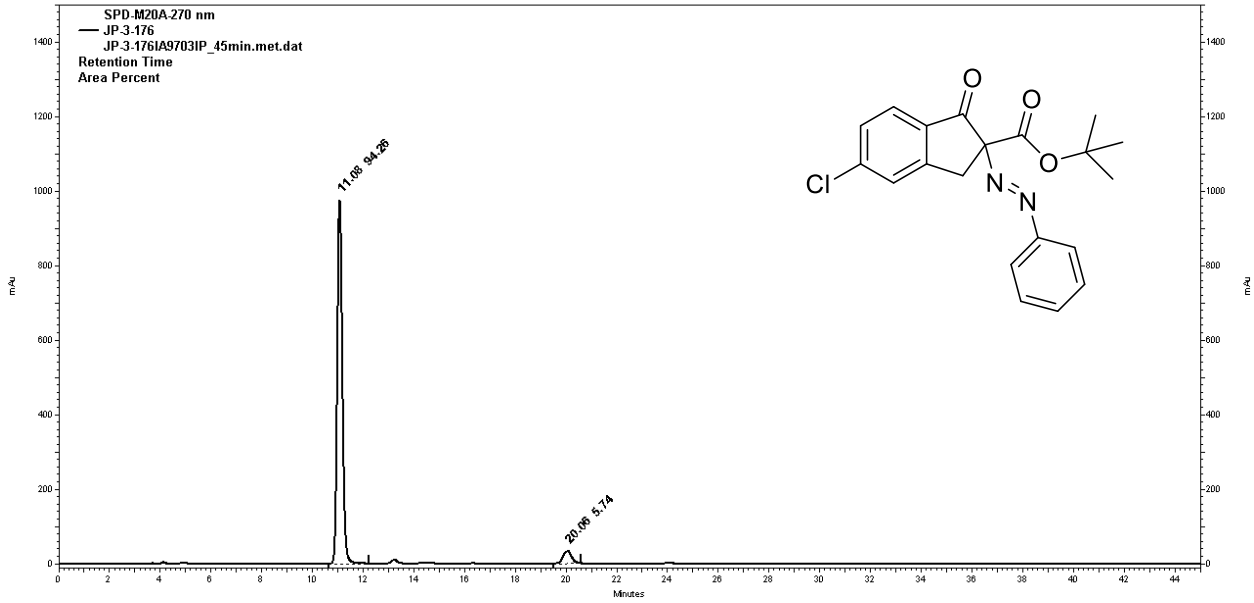
SPD-M20A-270 nm
JP-3-176
JP-3-176IA9703IP_45min.met.dat
Retention Time
Area Percent
11.08 94.26
20.06 5.74
m/Au
Minutes
Cl
N
N
O
O
O

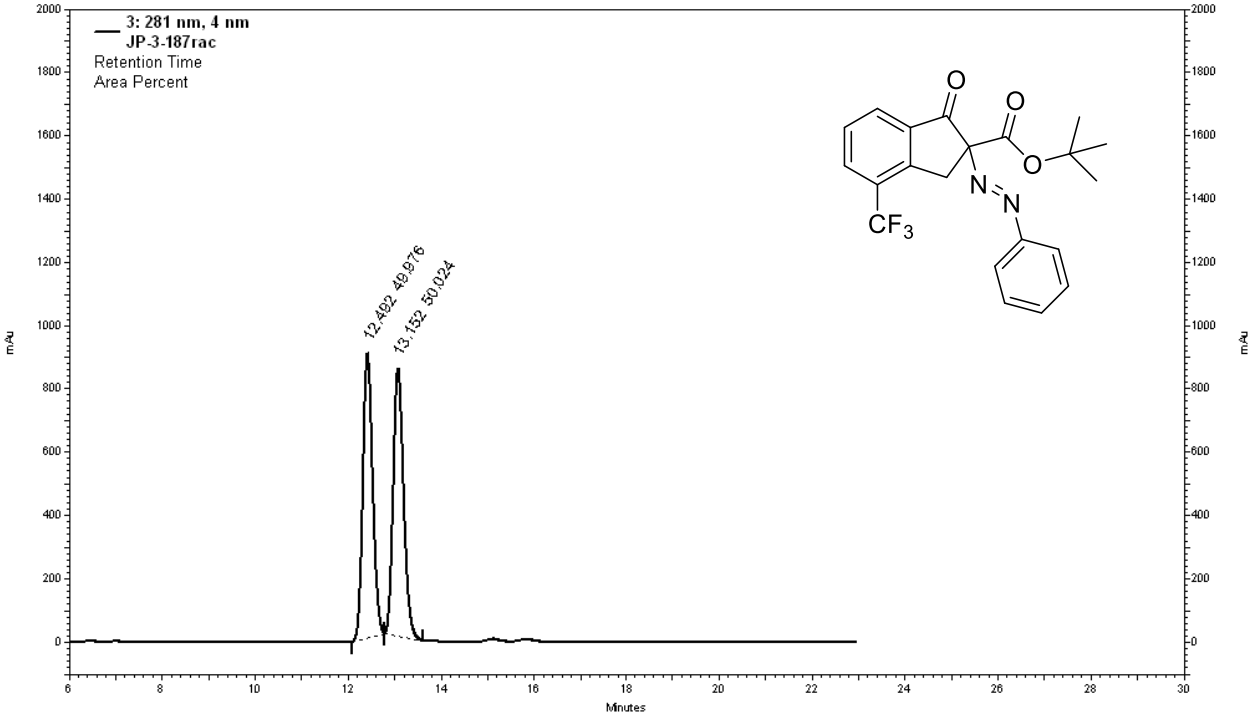
3: 281 nm, 4 nm
JP-3-187rac
Retention Time
Area Percent
12.492 49.976
13.152 50.024
mAu
Minutes
O
O
O
N
N
CF3

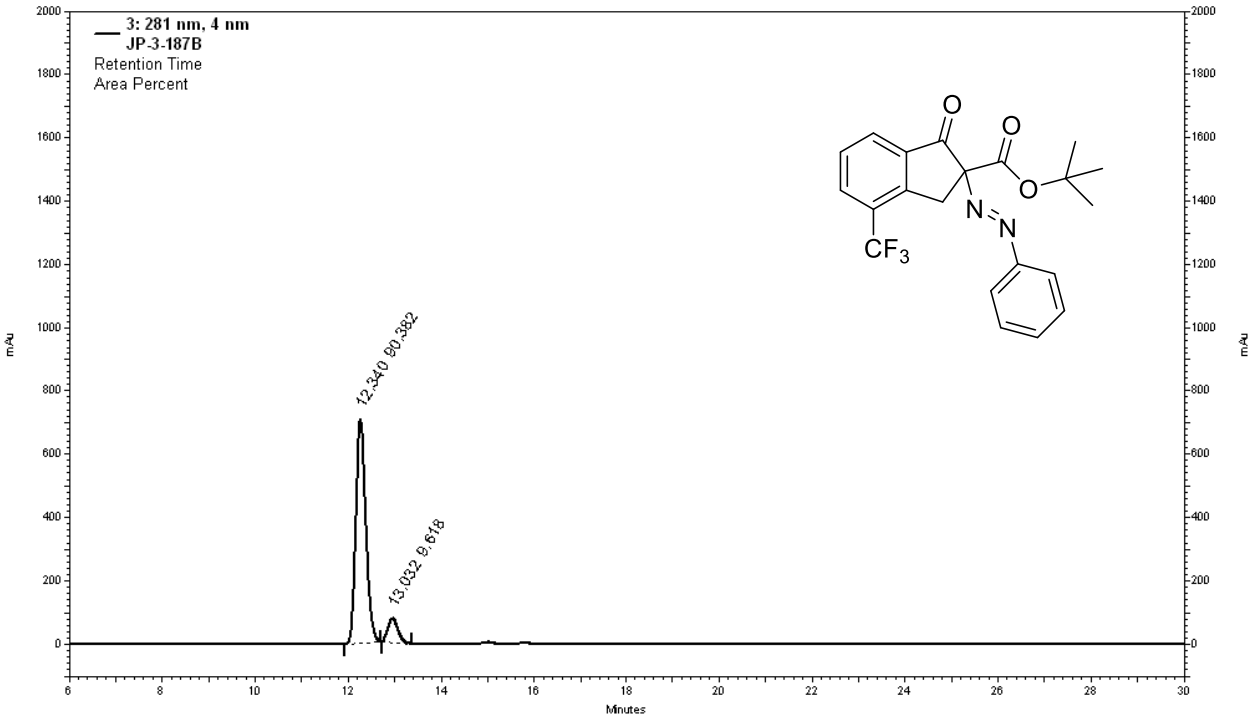
3: 281 nm, 4 nm
JP-3-187B
Retention Time
Area Percent
12.340 90.382
13.032 9.618
mAu
Minutes
O
O
O
N
N
CF3

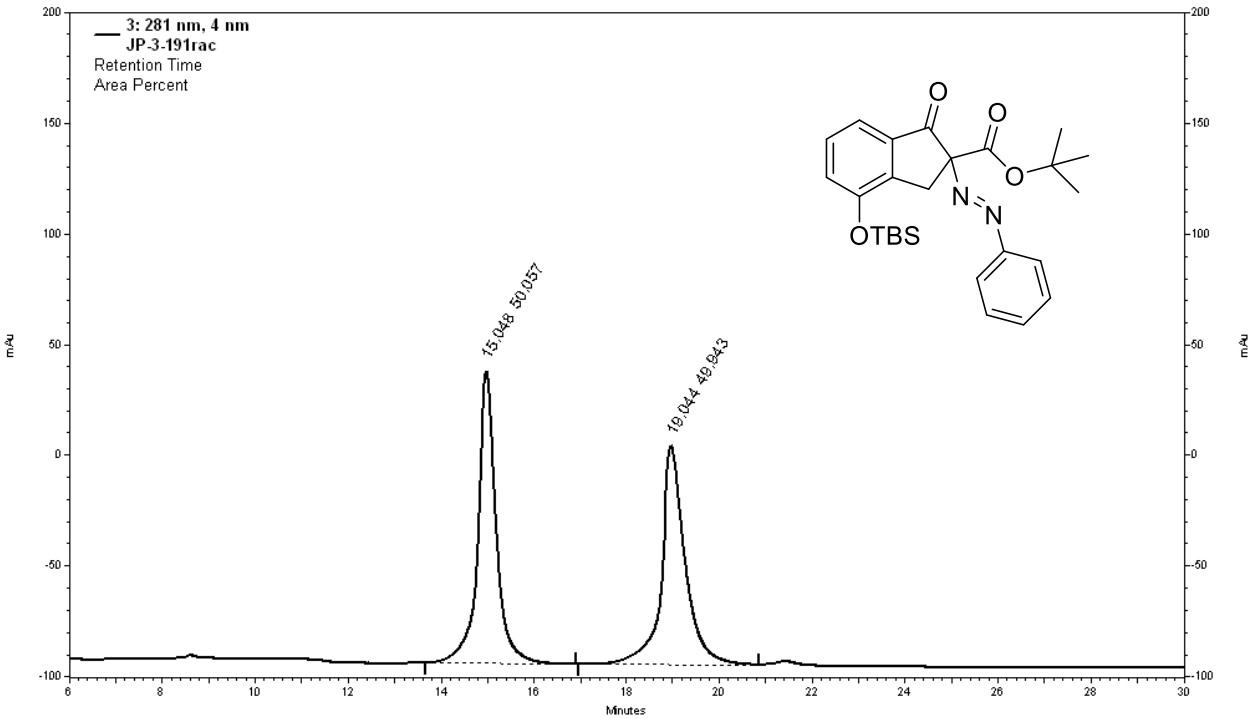
3: 281 nm, 4 nm
JP-3-191rac
Retention Time
Area Percent
15.048 50.057
19.044 49.943
OTBS
mAu
Minutes

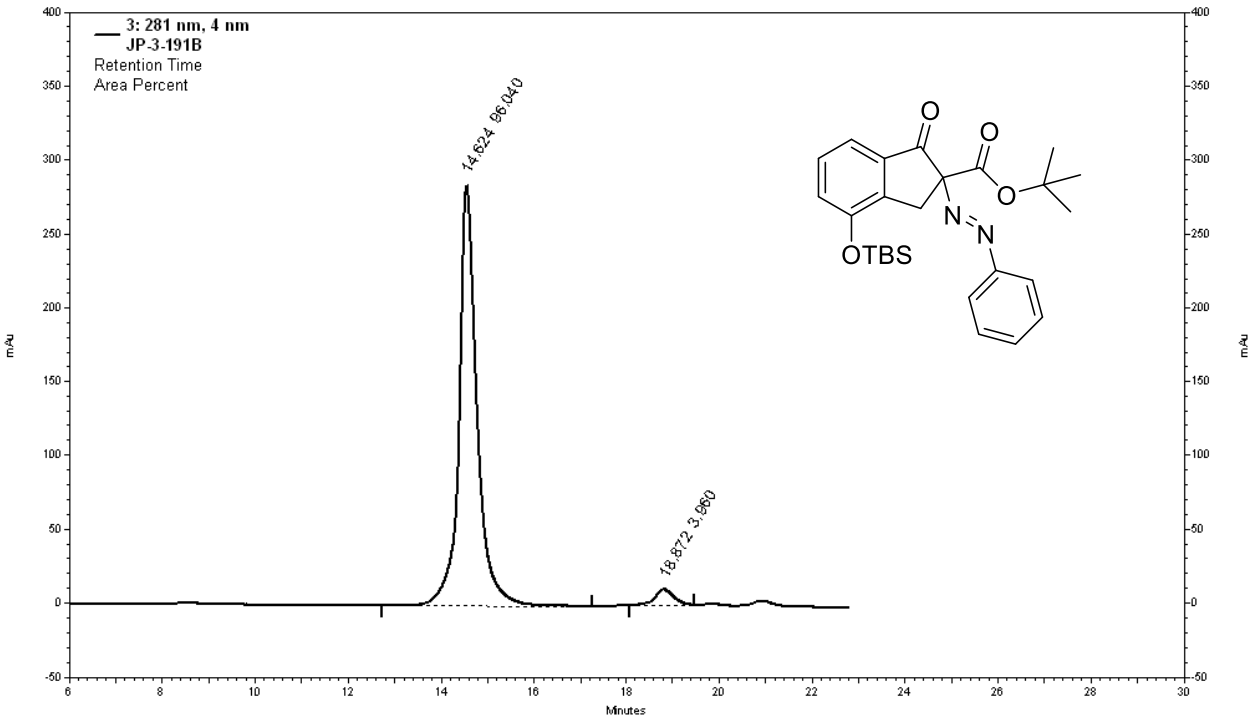
3: 281 nm, 4 nm
JP-3-191B
Retention Time
Area Percent
14.624 96.040
18.872 3.960
OTBS
mAu
Minutes

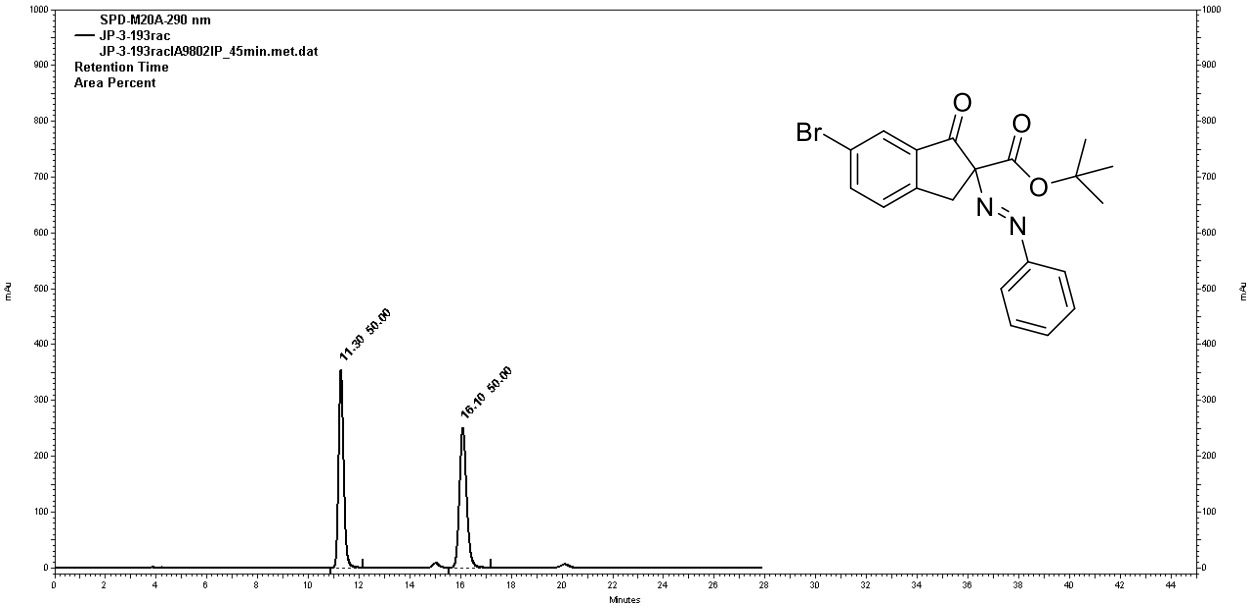
SPD-M20A-290 nm
JP-3-193rac
JP-3-193racIA9802IP_45min.met.dat
Retention Time
Area Percent
11.30 50.00
16.10 50.00
m/Au
Minutes
Br
O
O
O
N
N

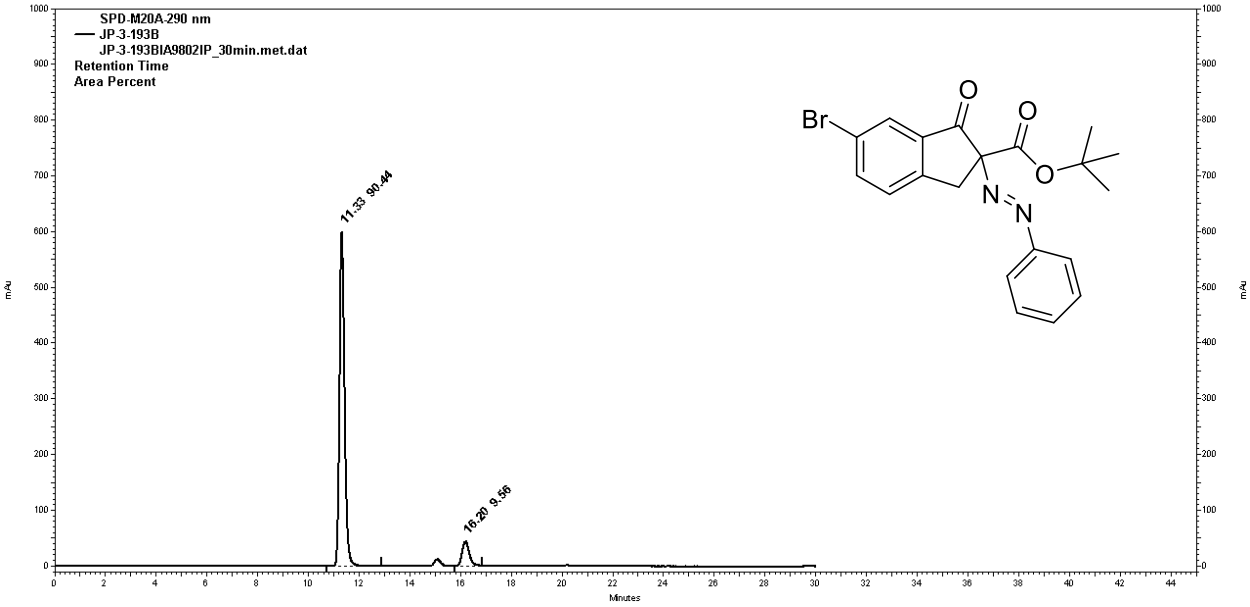
SPD-M20A-290 nm
JP-3-193B
JP-3-193BIA9802IP_30min.met.dat
Retention Time
Area Percent
11.33 90.44
16.20 9.56
m/Au
Minutes
Br
O
O
O
N
N

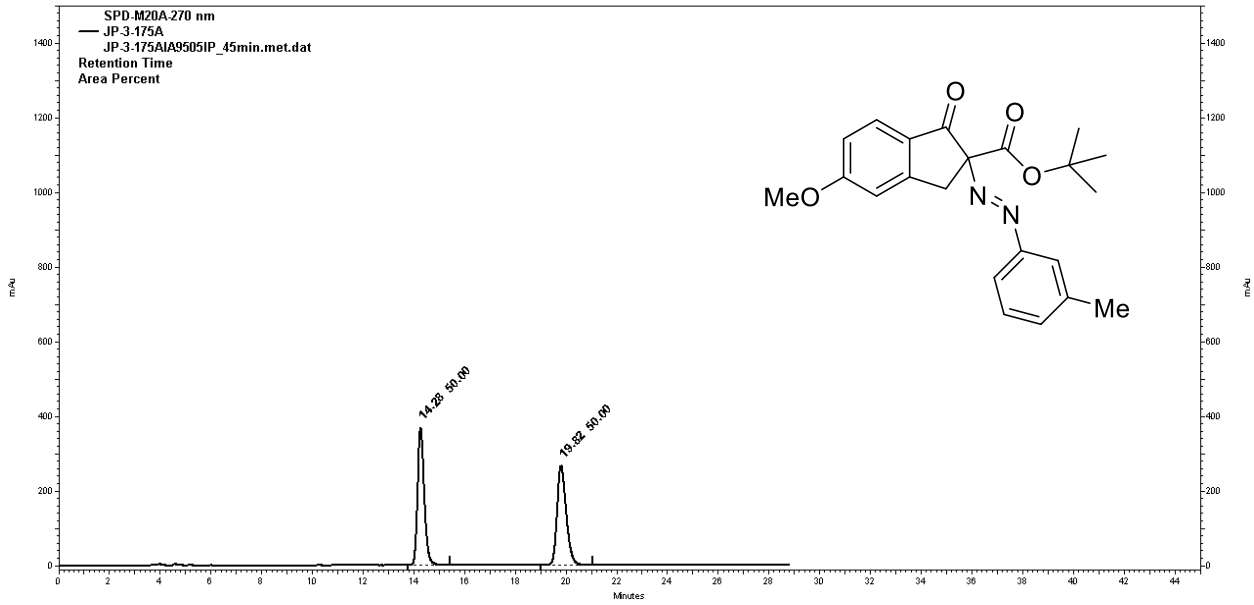
SPD-M20A-270 nm
JP-3-175A
JP-3-175AIA9505IP_45min.met.dat
Retention Time
Area Percent
14.23 50.00
19.82 50.00
m/Au
Minutes
MeO
Me

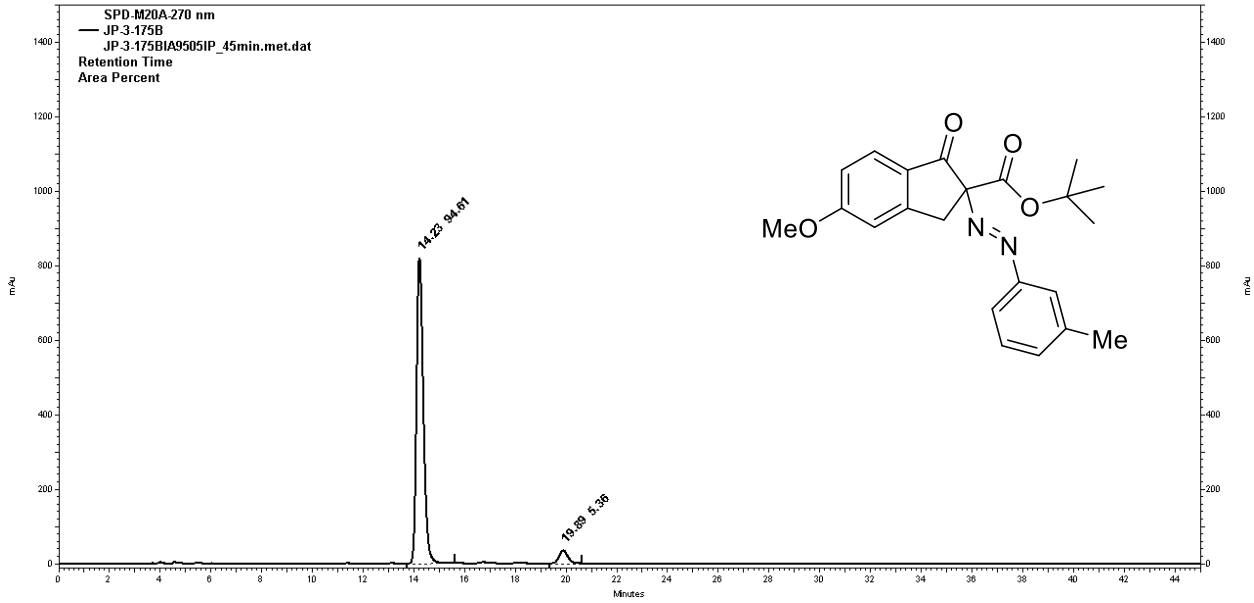
SPD-M20A-270 nm
JP-3-175B
JP-3-175BIA9505IP_45min.met.dat
Retention Time
Area Percent
14.23 94.61
19.89 5.36
m/Au
Minutes
MeO
Me

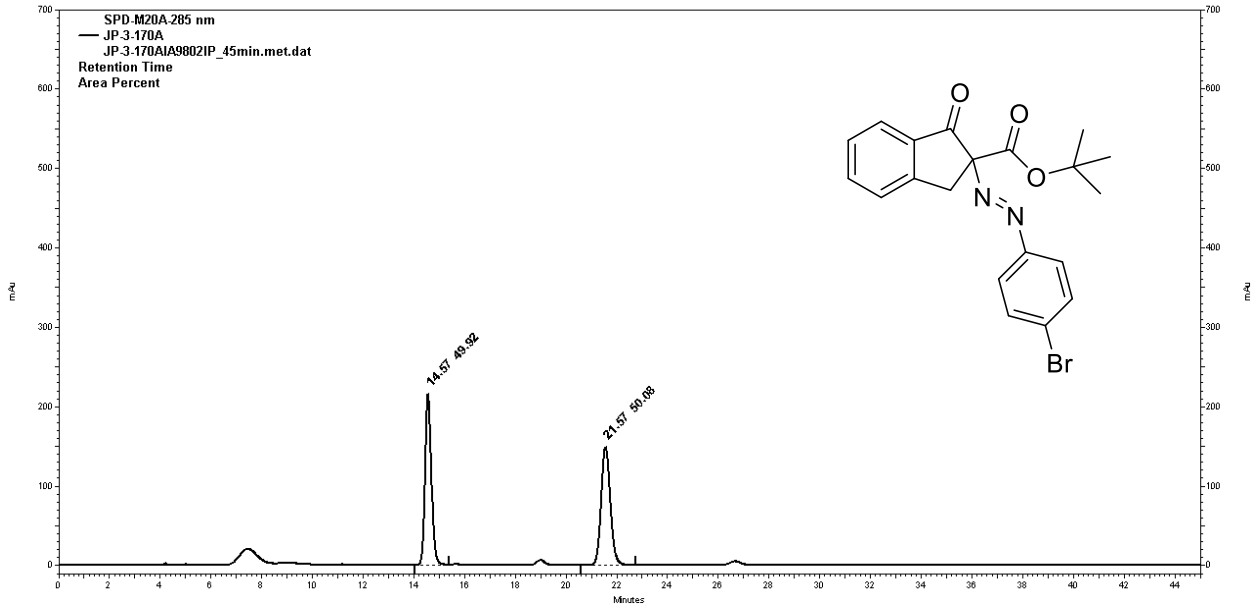
SPD-M20A-285 nm
JP-3-170A
JP-3-170AIA9802IP_45min.met.dat
Retention Time
Area Percent
14.57 49.92
21.57 50.08
m/Au
Minutes
O
O
O
N
N
Br

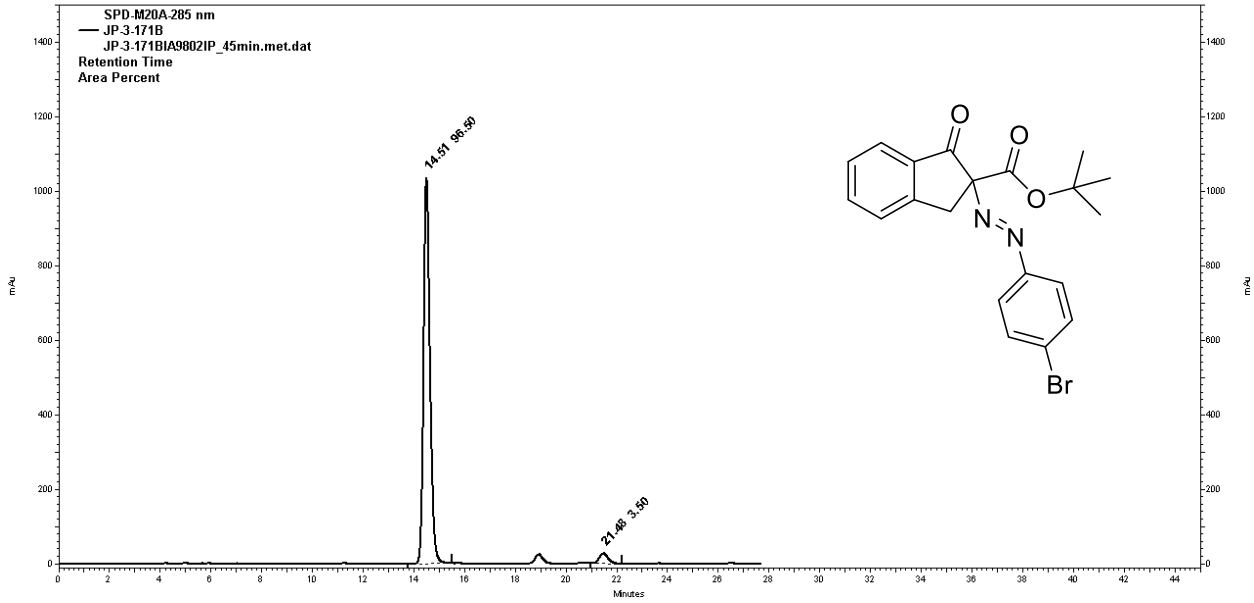
SPD-M20A-285 nm
JP-3-171B
JP-3-171BIA9802IP_45min.met.dat
Retention Time
Area Percent
14.51 96.50
21.48 3.50
m/Au
Minutes
O
O
O
N
N
Br

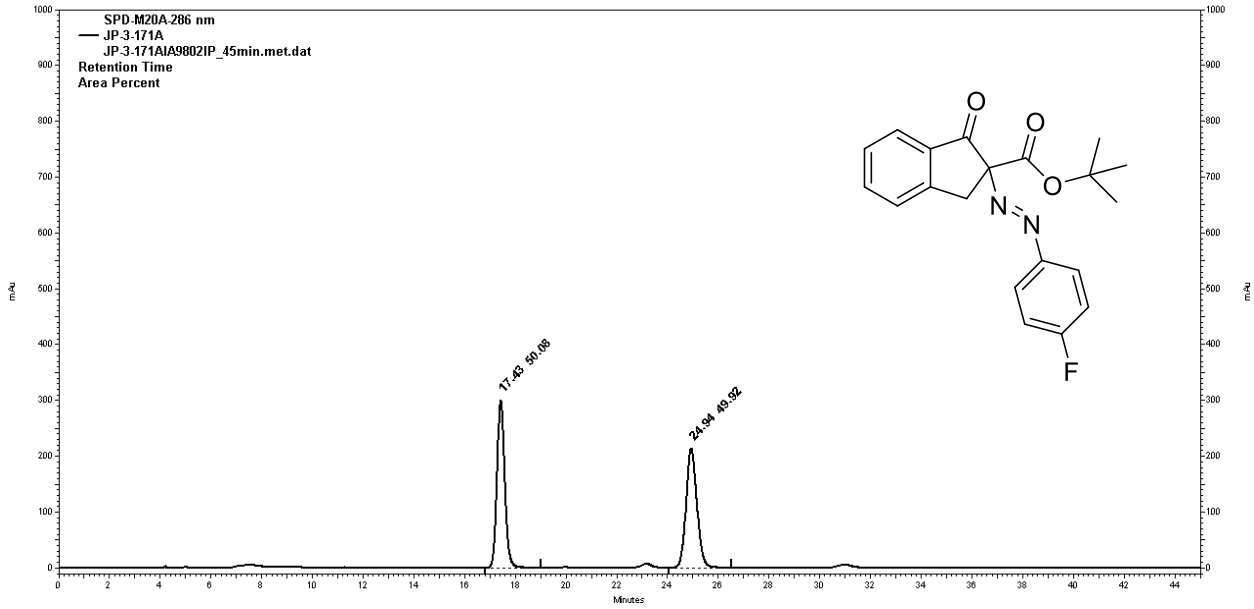
SPD-M20A-286 nm
JP-3-171A
JP-3-171AIA9802IP_45min.met.dat
Retention Time
Area Percent
17.43 50.08
24.94 49.92
m-Au
Minutes
O
O
O
N
N
F

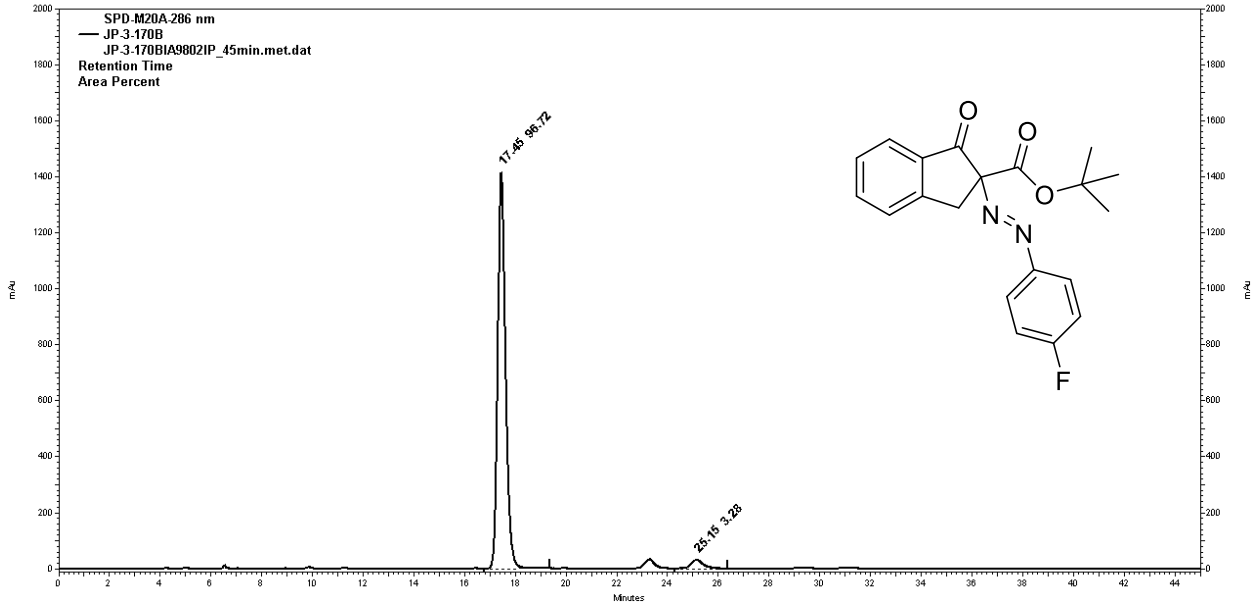
SPD-M20A-286 nm
JP-3-170B
JP-3-170BIA9802IP_45min.met.dat
Retention Time
Area Percent
17.45 96.72
25.15 3.28
m-Au
Minutes
O
O
O
N
N
F

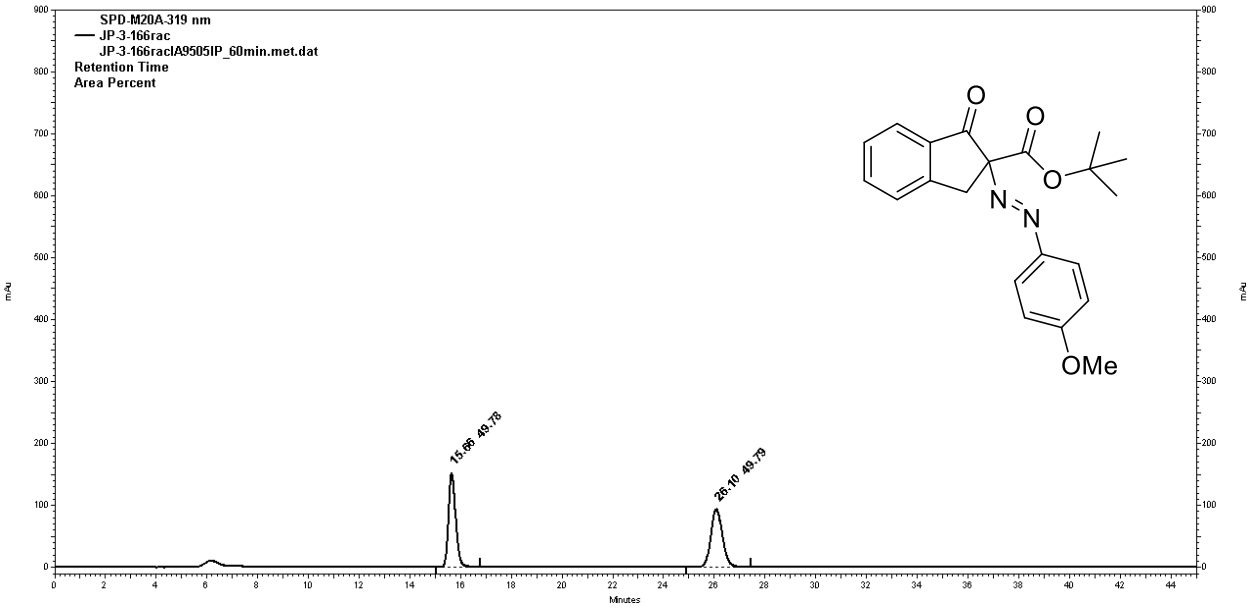
SPD-M20A-319 nm
JP-3-166rac
JP-3-166racIA9505IP_60min.met.dat
Retention Time
Area Percent
15.66 49.78
26.10 49.79
m-Au
Minutes
OMe

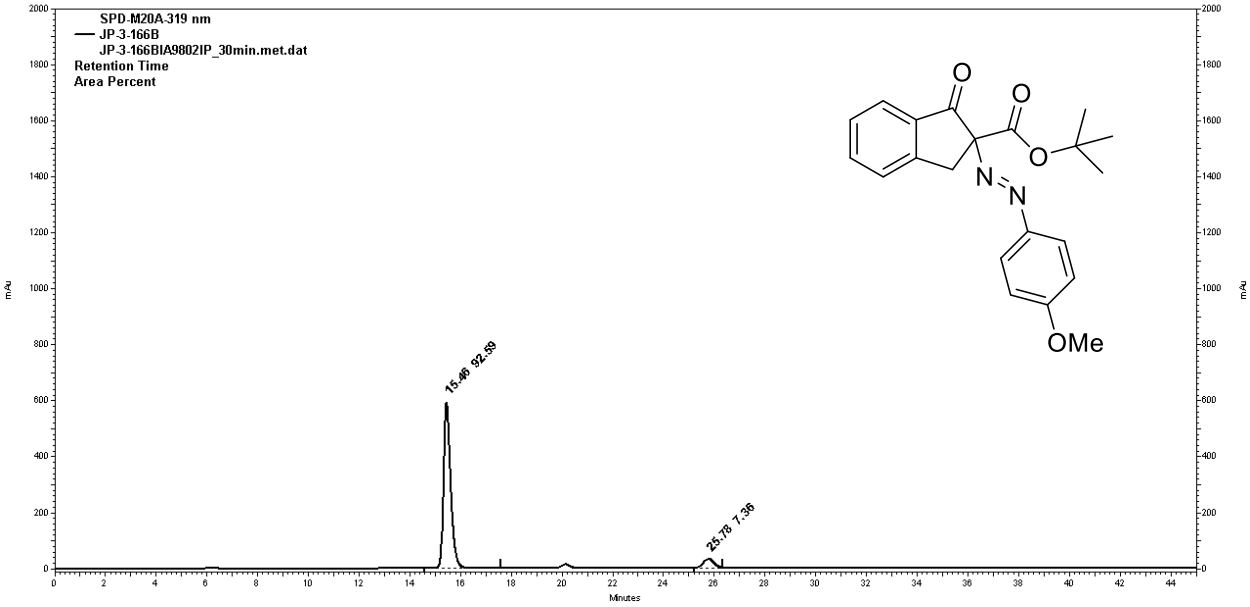
SPD-M20A-319 nm
JP-3-166B
JP-3-166BIA9802IP_30min.met.dat
Retention Time
Area Percent
15.46 92.59
25.78 7.36
m-Au
Minutes
OMe

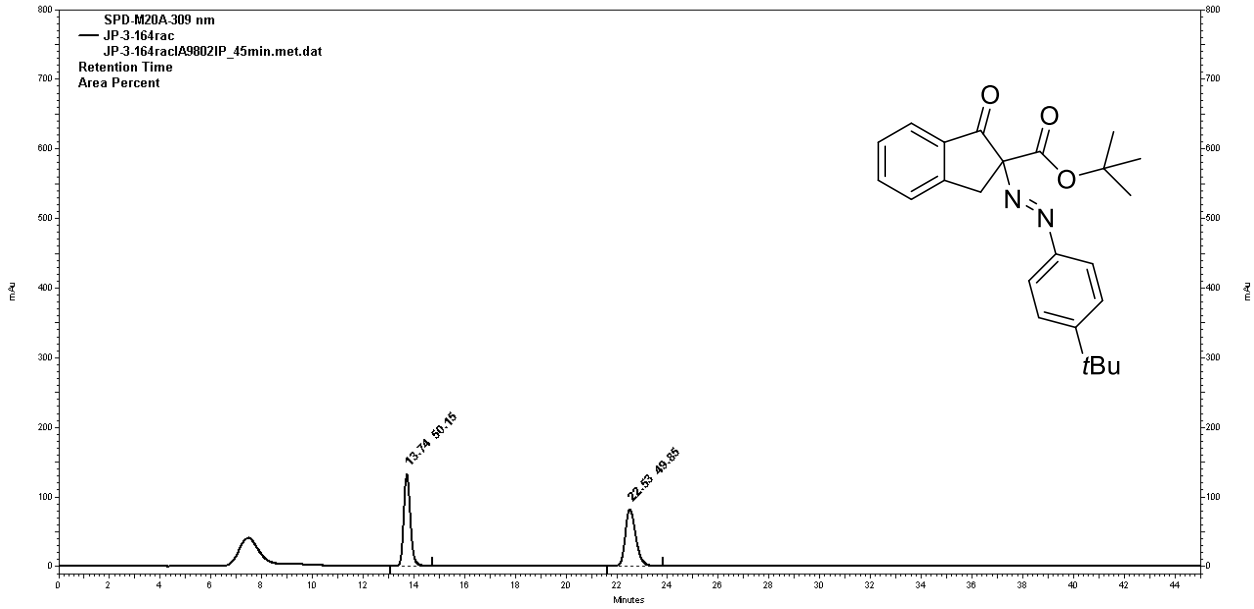
SPD-M20A-309 nm
JP-3-164rac
JP-3-164racIA9802IP_45min.met.dat
Retention Time
Area Percent
13.74 50.15
22.53 49.85
m/Au
Minutes
O
O
O
N
N
tBu

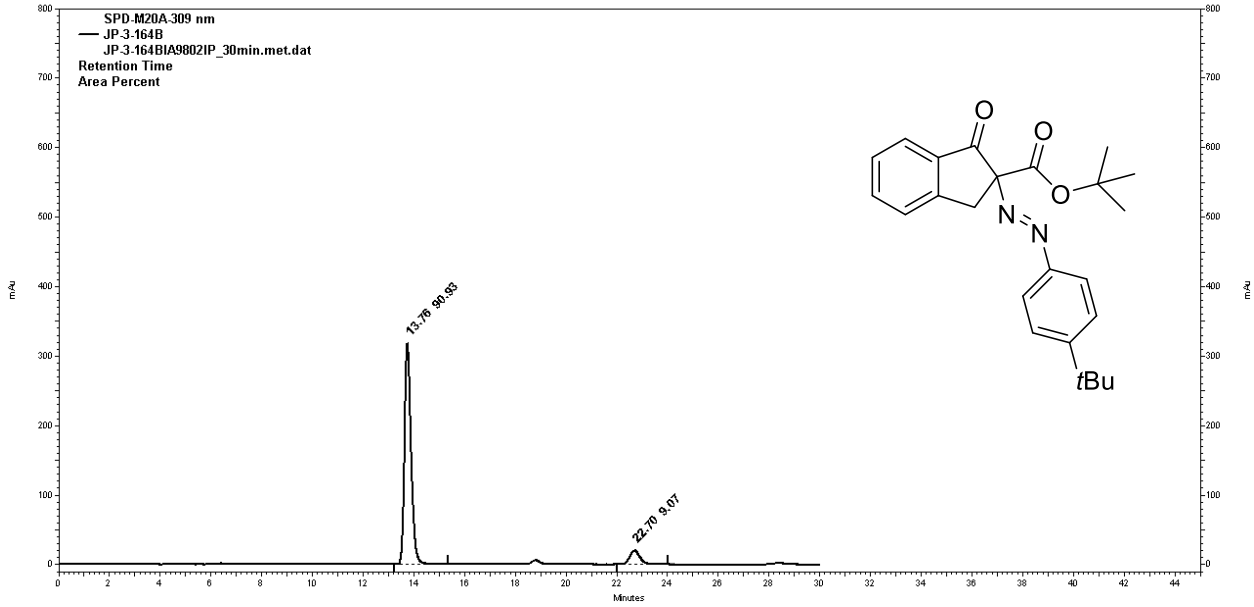
SPD-M20A-309 nm
JP-3-164B
JP-3-164BIA9802IP_30min.met.dat
Retention Time
Area Percent
13.76 90.93
22.70 9.07
m/Au
Minutes
O
O
O
N
N
tBu

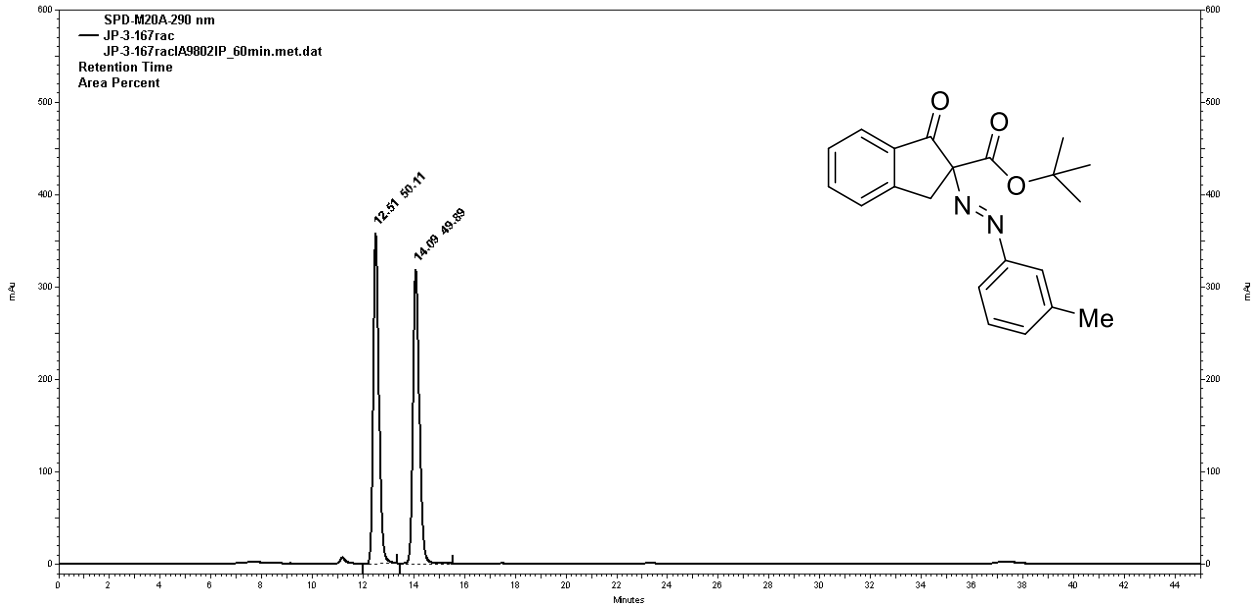
SPD-M20A-290 nm
JP-3-167rac
JP-3-167racIA9802IP_60min.met.dat
Retention Time
Area Percent
12.51 50.11
14.09 49.89
m/Au
Minutes
O
O
O
N
N
Me

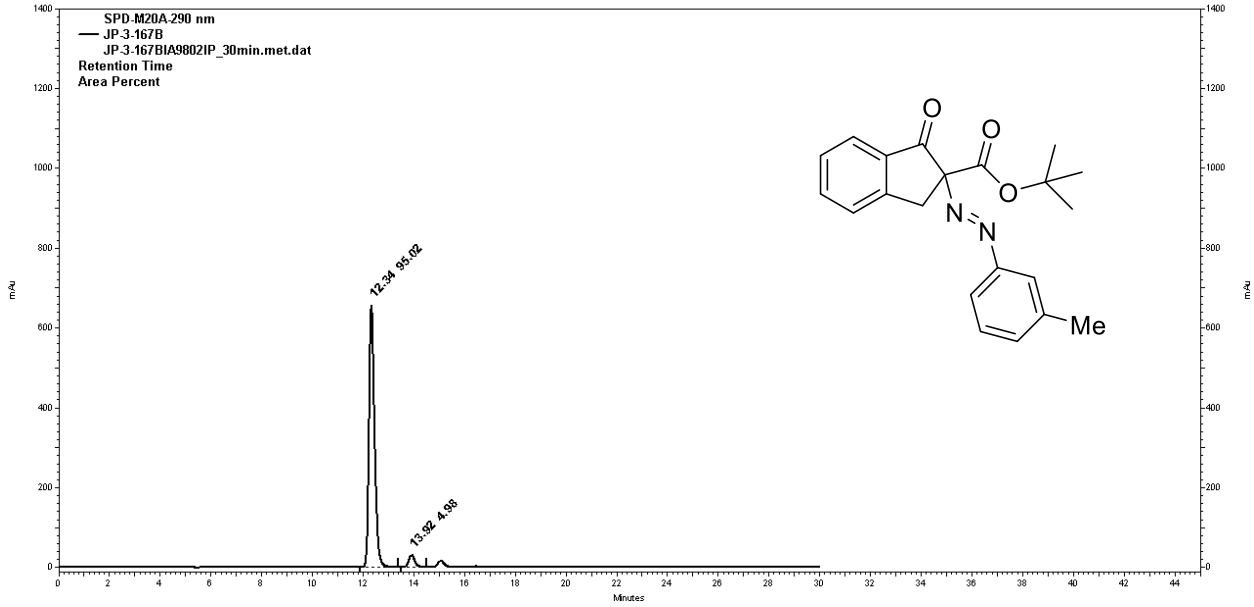
SPD-M20A-290 nm
JP-3-167B
JP-3-167BIA9802IP_30min.met.dat
Retention Time
Area Percent
12.34 95.02
13.92 4.98
m/Au
Minutes
O
O
O
N
N
Me

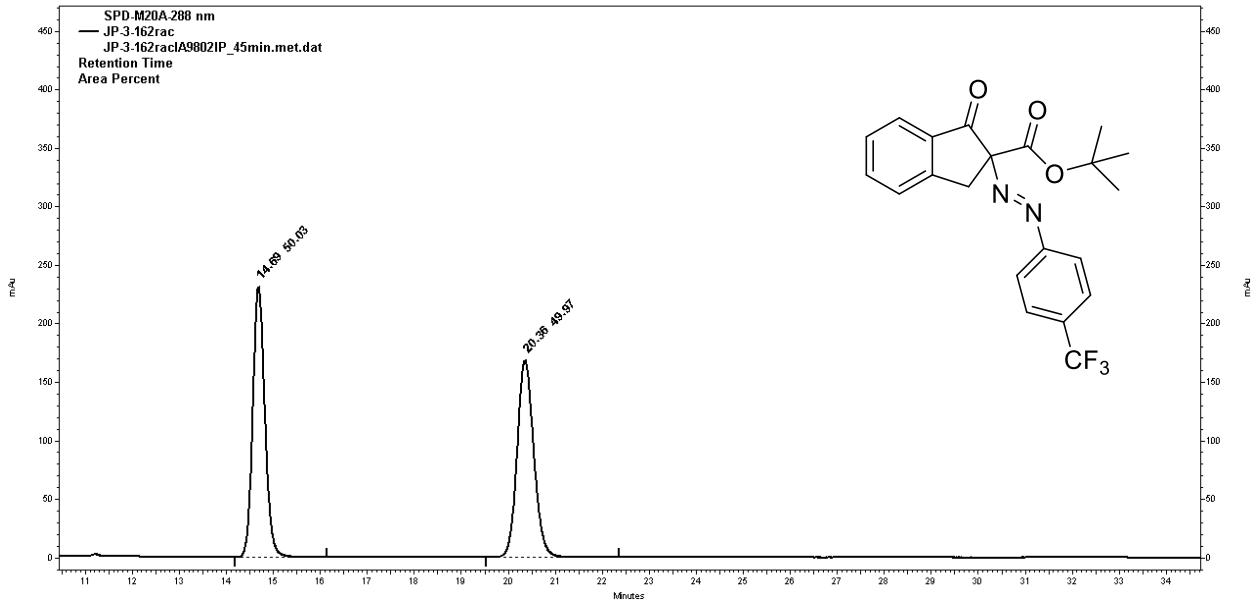
SPD-M20A-288 nm
JP-3-162rac
JP-3-162racIA9802IP_45min.met.dat
Retention Time
Area Percent
14.69 50.03
20.36 49.97
m/Au
Minutes
O
O
O
N
N
CF3

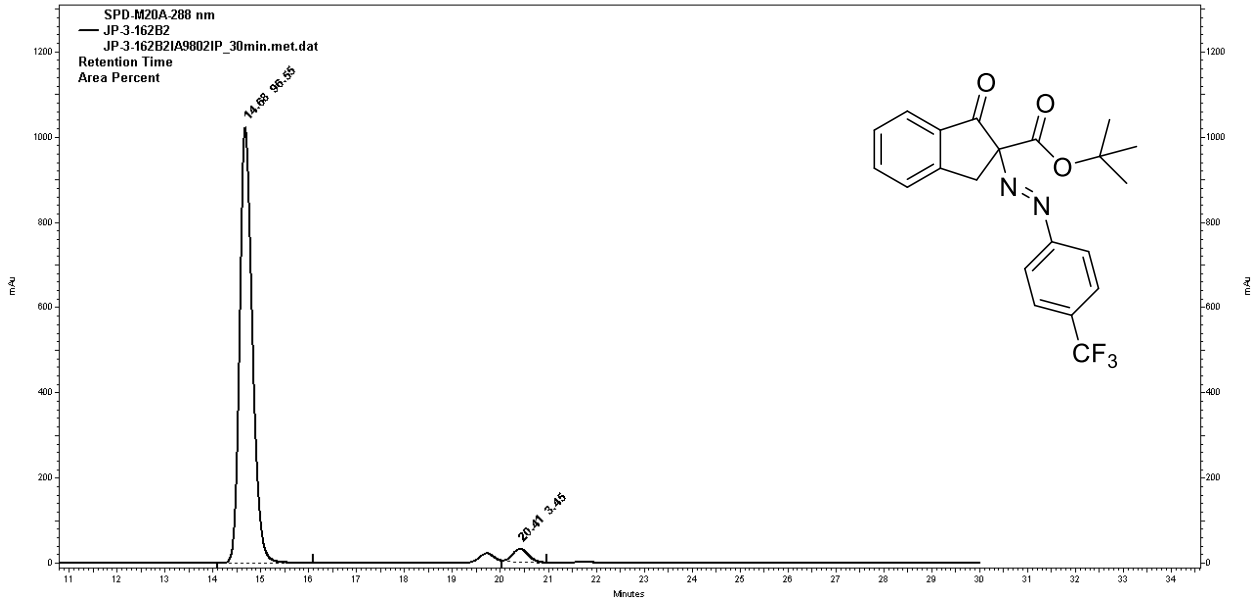
SPD-M20A-288 nm
JP-3-162B2
JP-3-162B2IA9802IP_30min.met.dat
Retention Time
Area Percent
14.69 96.55
20.41 3.45
m/Au
Minutes
O
O
O
N
N
CF3

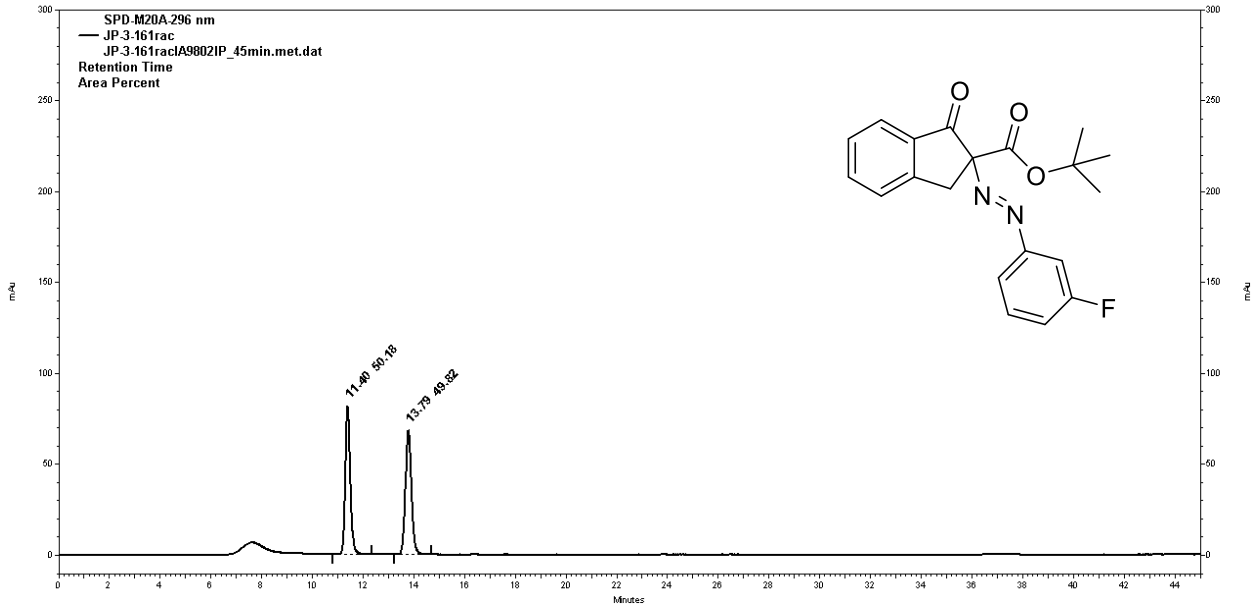
SPD-M20A-296 nm
JP-3-161rac
JP-3-161racIA9802IP_45min.met.dat
Retention Time
Area Percent
11.40 50.18
13.79 49.82
m/Au
Minutes
O
O
O
N
N
F

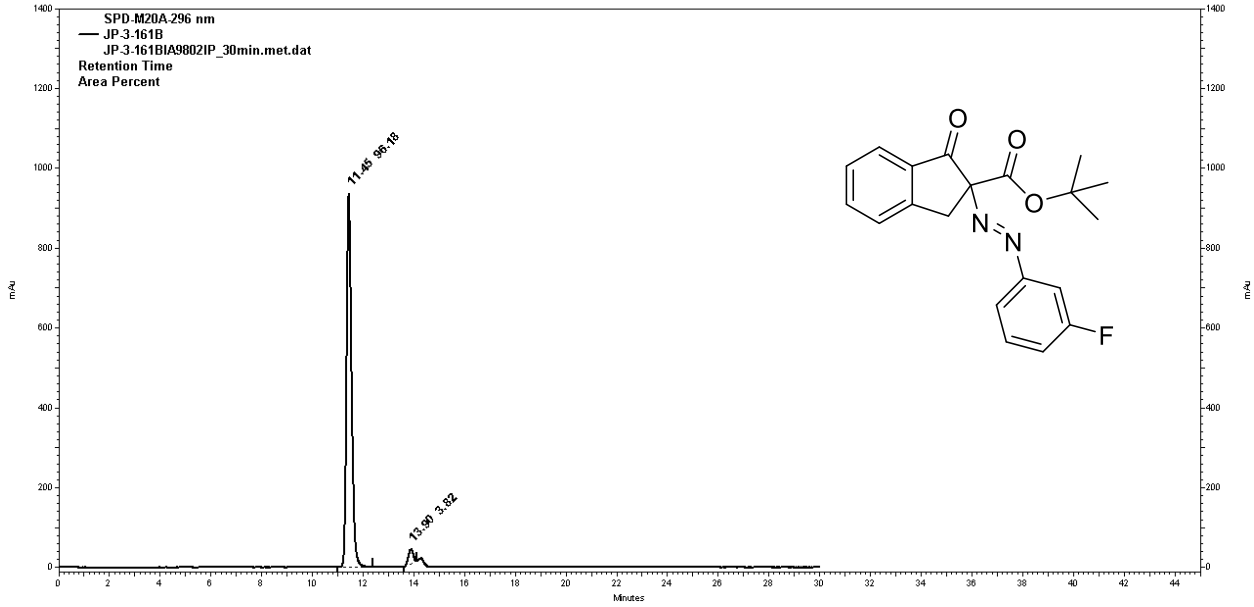
SPD-M20A-296 nm
JP-3-161B
JP-3-161BIA9802IP_30min.met.dat
Retention Time
Area Percent
11.45 96.18
13.90 3.82
m/Au
Minutes
O
O
O
N
N
F

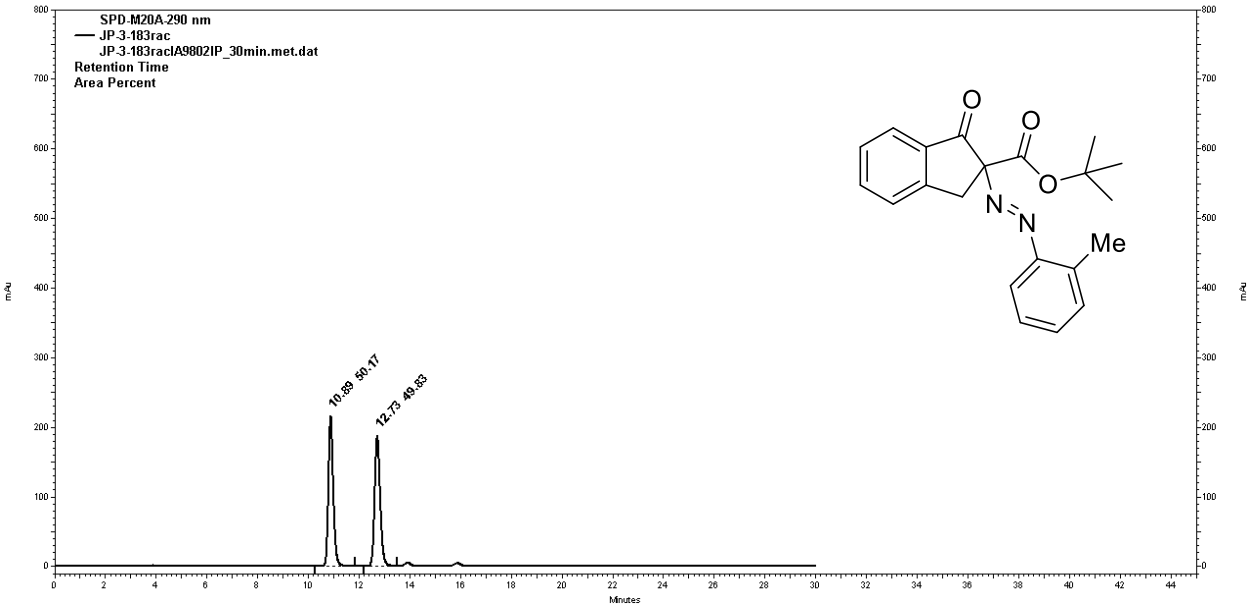
SPD-M20A-290 nm
JP-3-183rac
JP-3-183racIA9802IP_30min.met.dat
Retention Time
Area Percent
10.89 50.17
12.73 49.83
m/Au
Minutes
O
O
O
N
N
Me

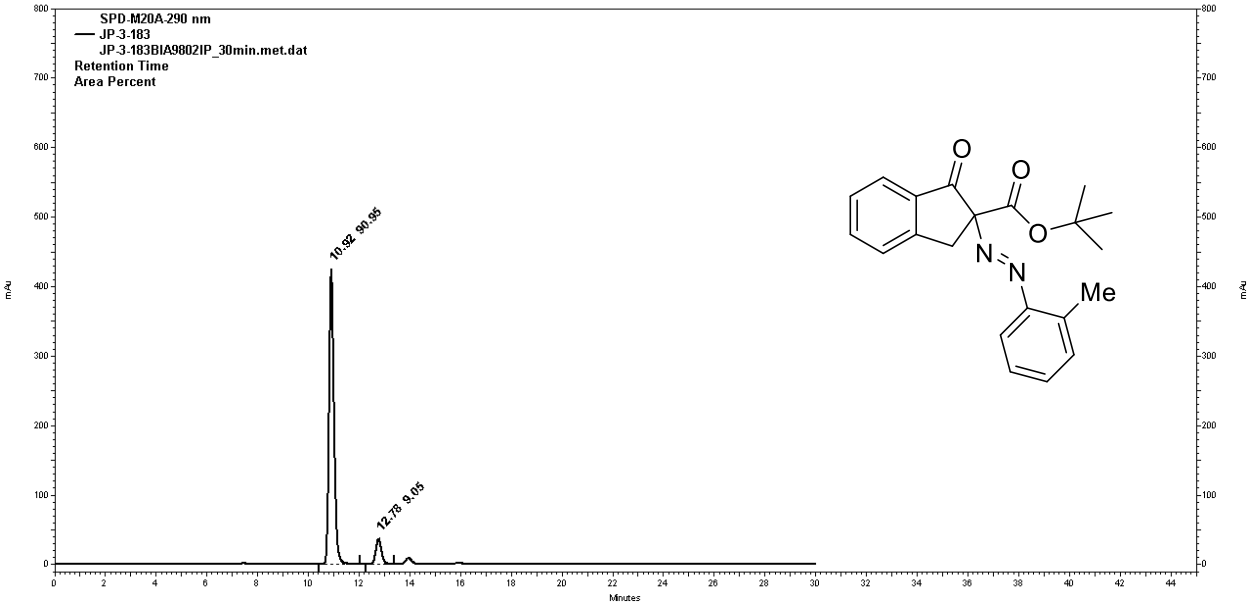
SPD-M20A-290 nm
JP-3-183
JP-3-183BIA9802IP_30min.met.dat
Retention Time
Area Percent
10.92 90.95
12.78 9.05
m/Au
Minutes
O
O
O
N
N
Me

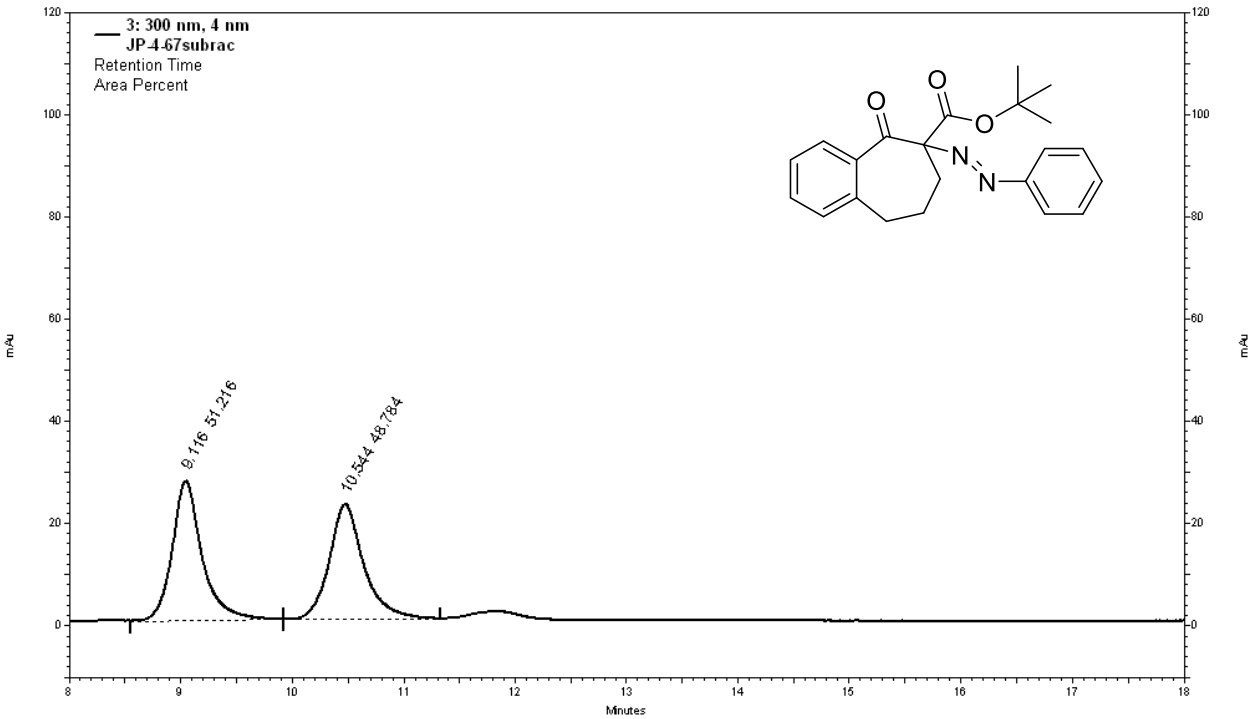
3: 300 nm, 4 nm
JP-4-67subrac
Retention Time
Area Percent
9.116 51.216
10.544 48.784
mAu
Minutes

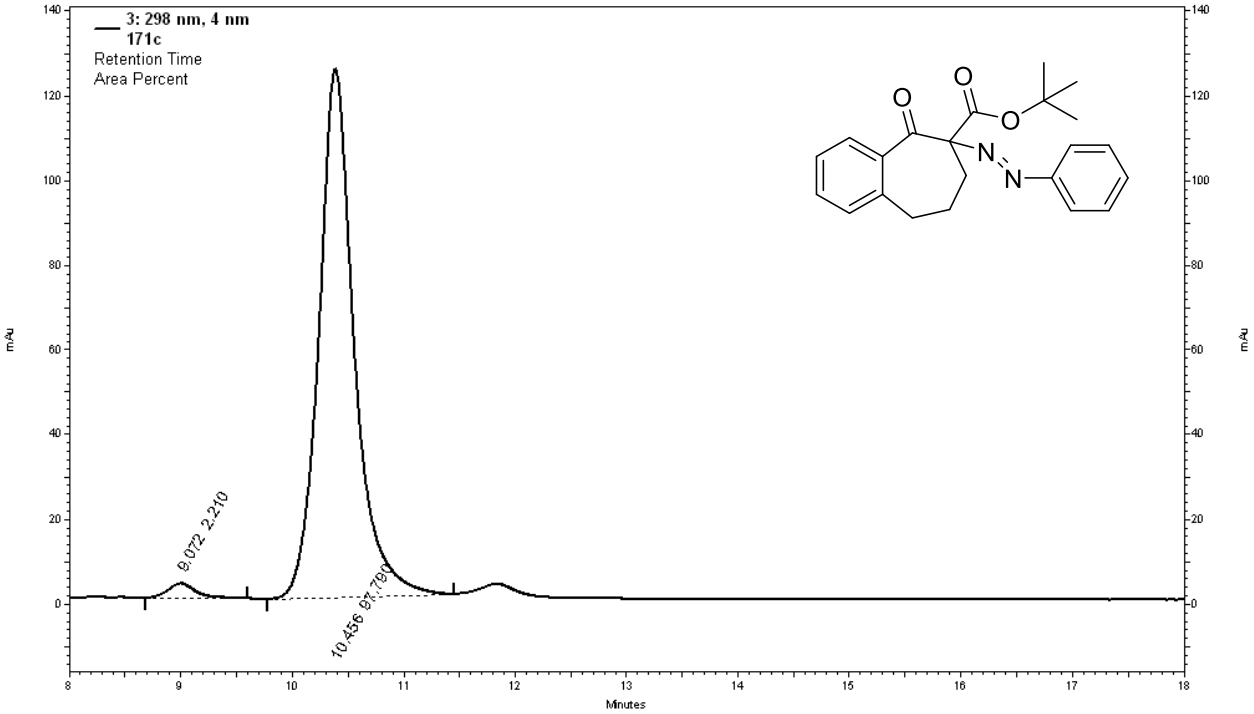
3: 298 nm, 4 nm
171c
Retention Time
Area Percent
9.072 2.210
10.456 97.790
mAu
Minutes

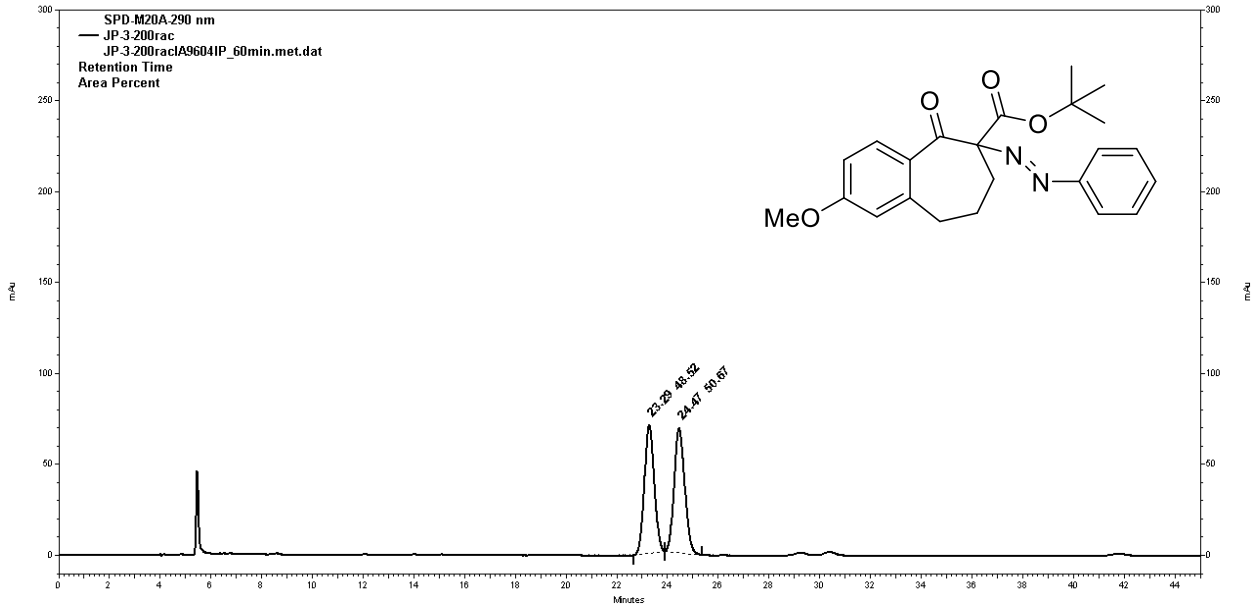
SPD-M20A-290 nm
JP-3-200rac
JP-3-200racIA9604IP_60min.met.dat
Retention Time
Area Percent
23.29 49.52
24.47 50.67
m/Au
Minutes
MeO
O
O
O
N
N

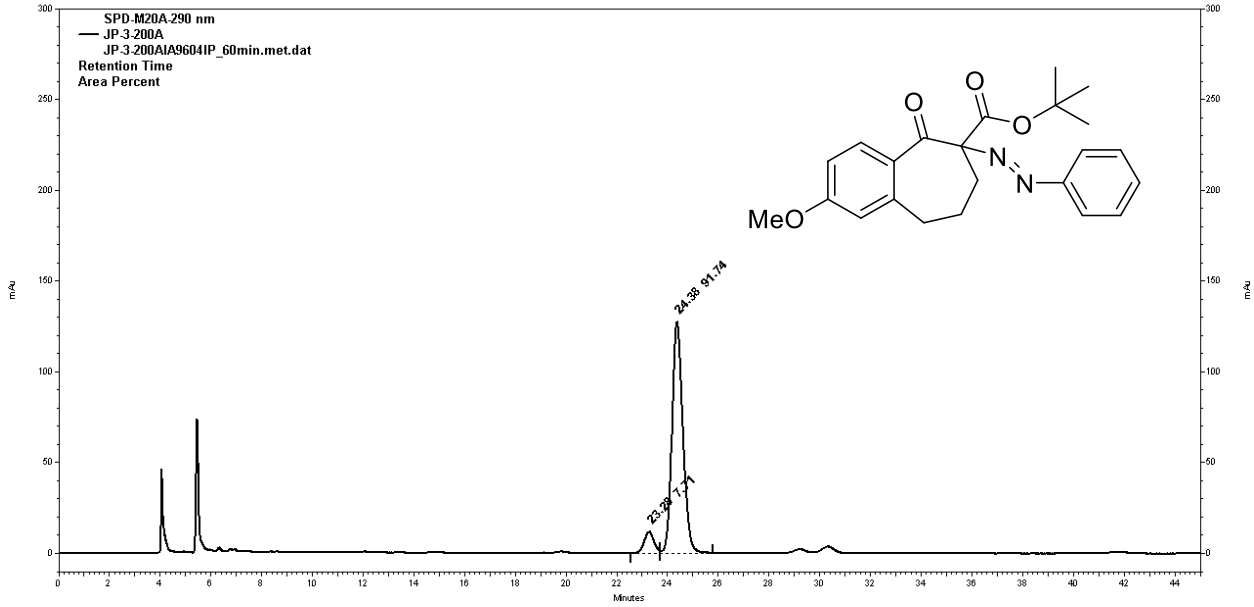
SPD-M20A-290 nm
JP-3-200A
JP-3-200AIA9604IP_60min.met.dat
Retention Time
Area Percent
24.38 91.74
23.29 7.71
m/Au
Minutes
MeO
O
O
O
N
N

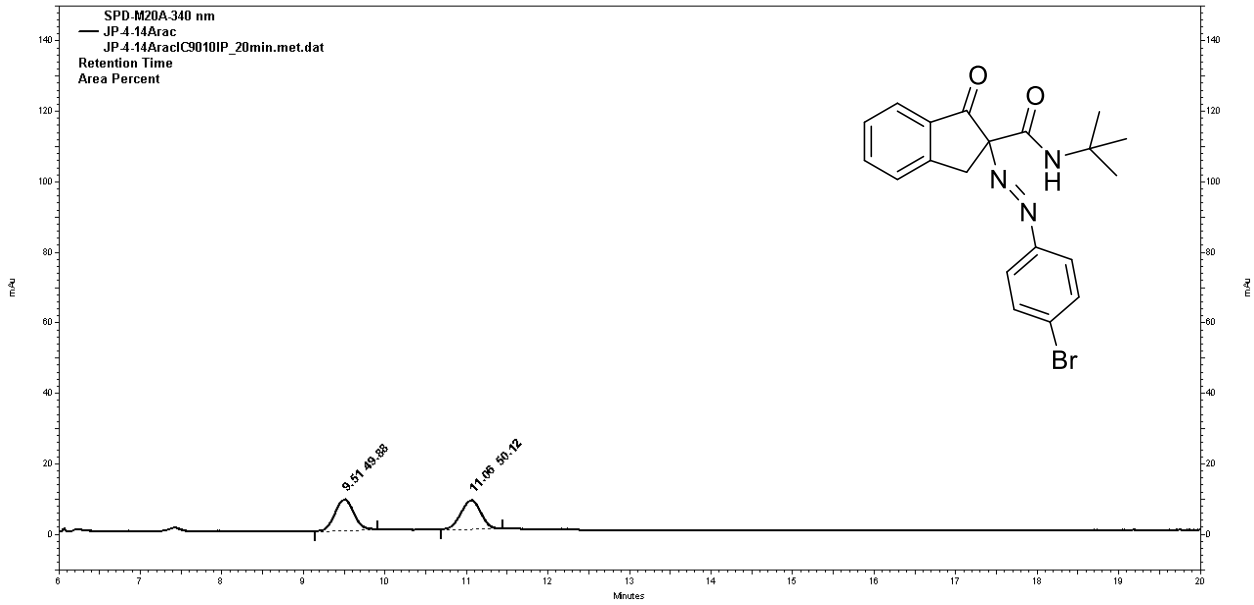
SPD-M20A-340 nm
JP-4-14Arac
JP-4-14AracIC9010IP_20min.met.dat
Retention Time
Area Percent
9.51 49.88
11.06 50.12
m/Au
Minutes
O
O
N
H
N
N
Br

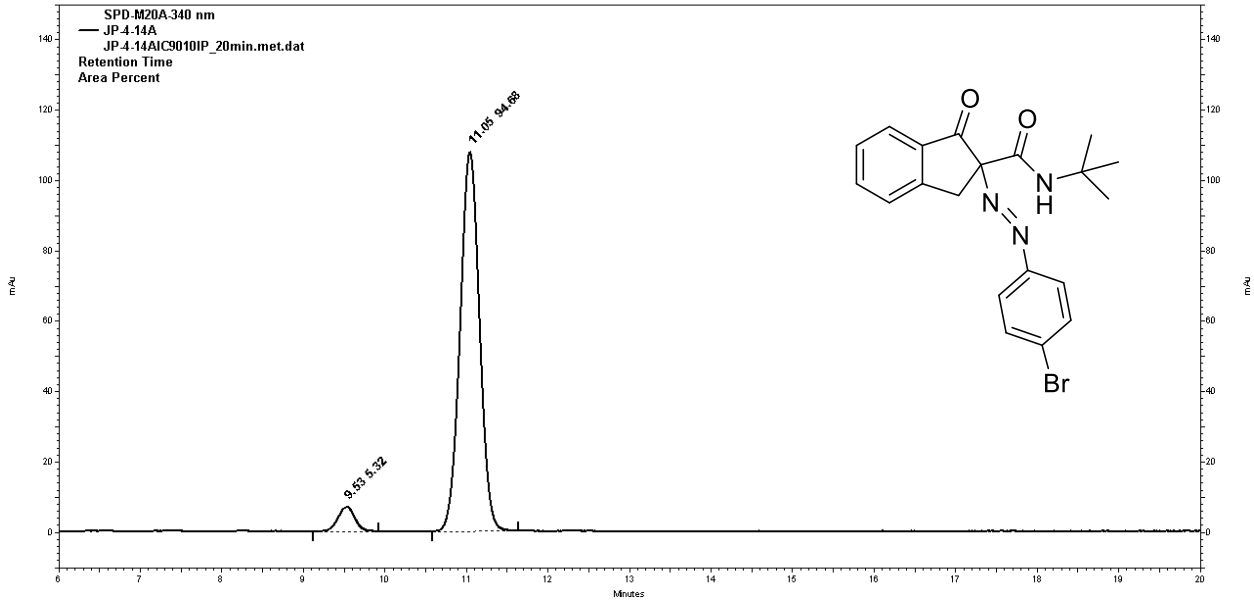
SPD-M20A-340 nm
JP-4-14A
JP-4-14AIC9010IP_20min.met.dat
Retention Time
Area Percent
9.53 5.32
11.05 94.68
m/Au
Minutes
O
O
N
H
N
N
Br

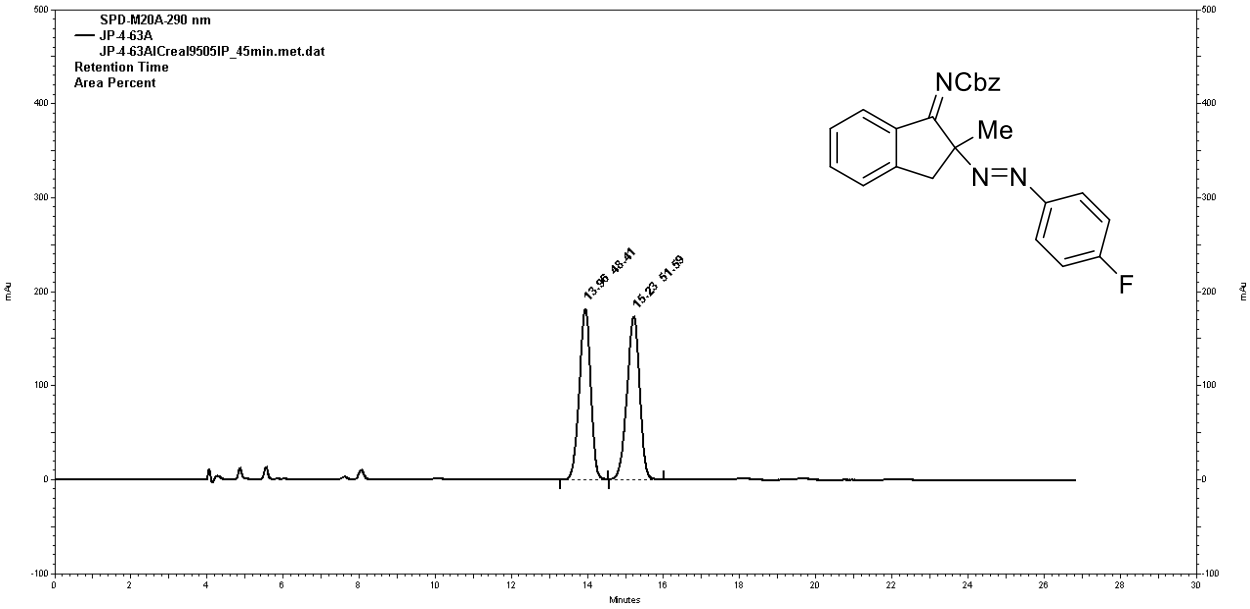
SPD-M20A-290 nm
JP-4-63A
JP-4-63AICreal9505IP_45min.met.dat
Retention Time
Area Percent
13.96 48.41
15.23 51.59
NCbz
Me
N=N
F
m/Au
Minutes

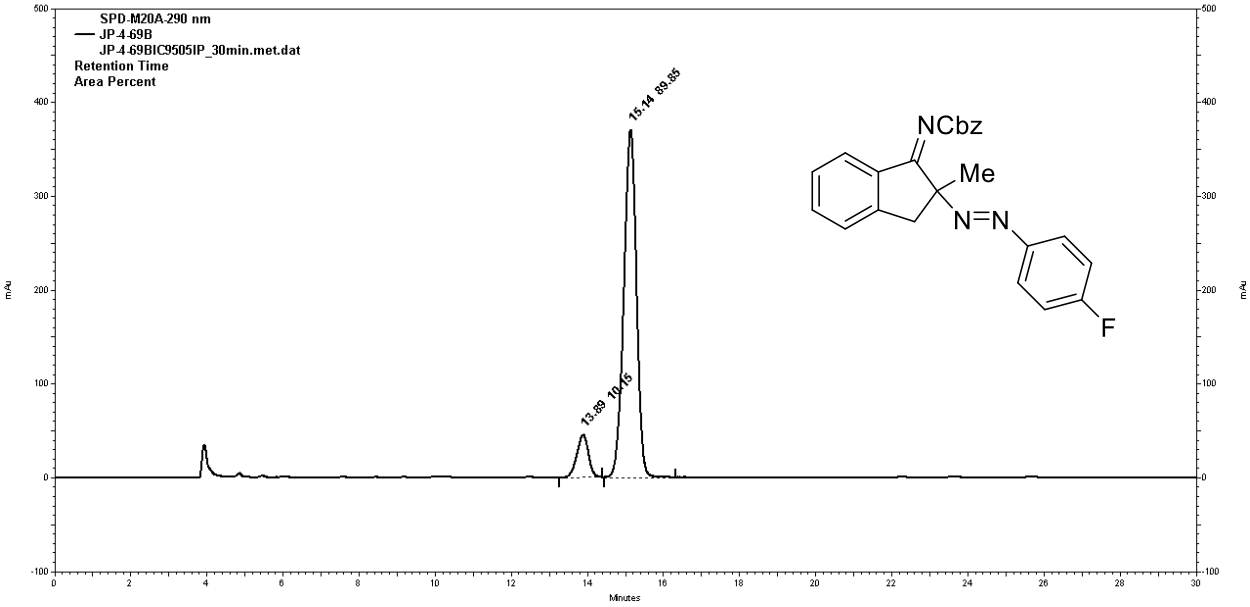
SPD-M20A-290 nm
JP-4-69B
JP-4-69BIC9505IP_30min.met.dat
Retention Time
Area Percent
13.89 10.15
15.14 89.85
NCbz
Me
N=N
F
m/Au
Minutes

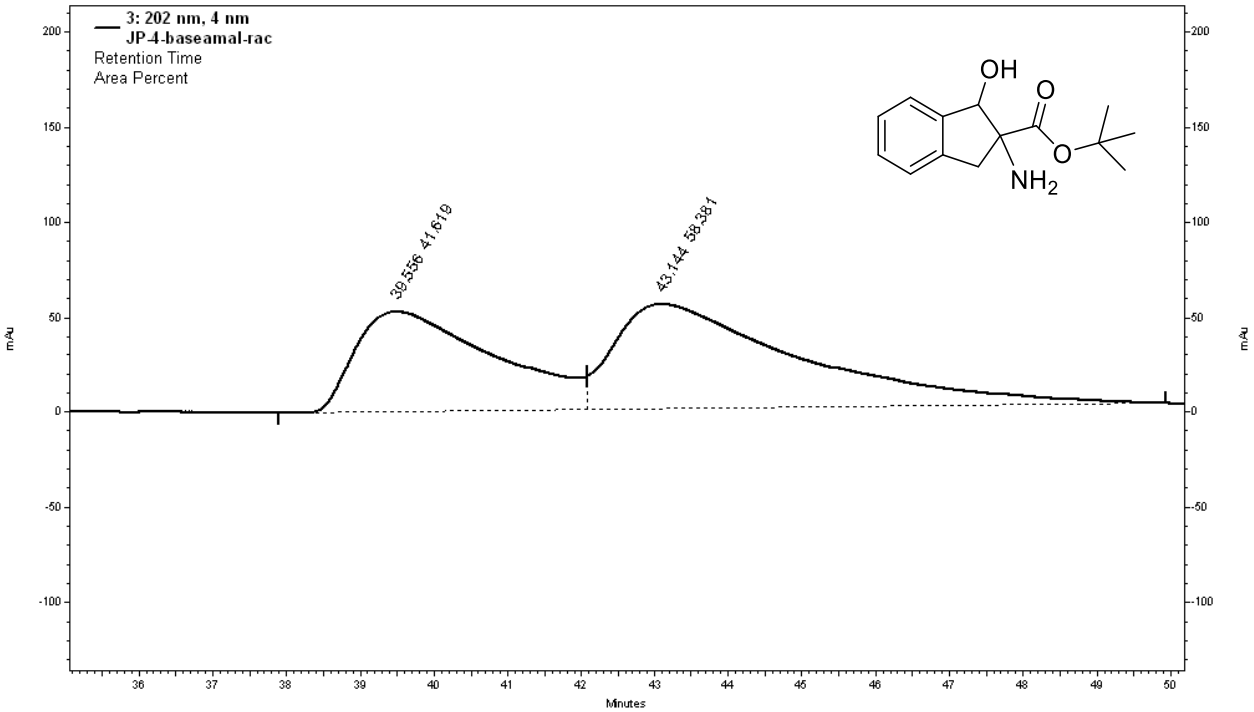
3: 202 nm, 4 nm
JP-4-baseamal-rac
Retention Time
Area Percent
39.556 41.619
43.144 58.381
OH
O
O
NH2
mAu
Minutes

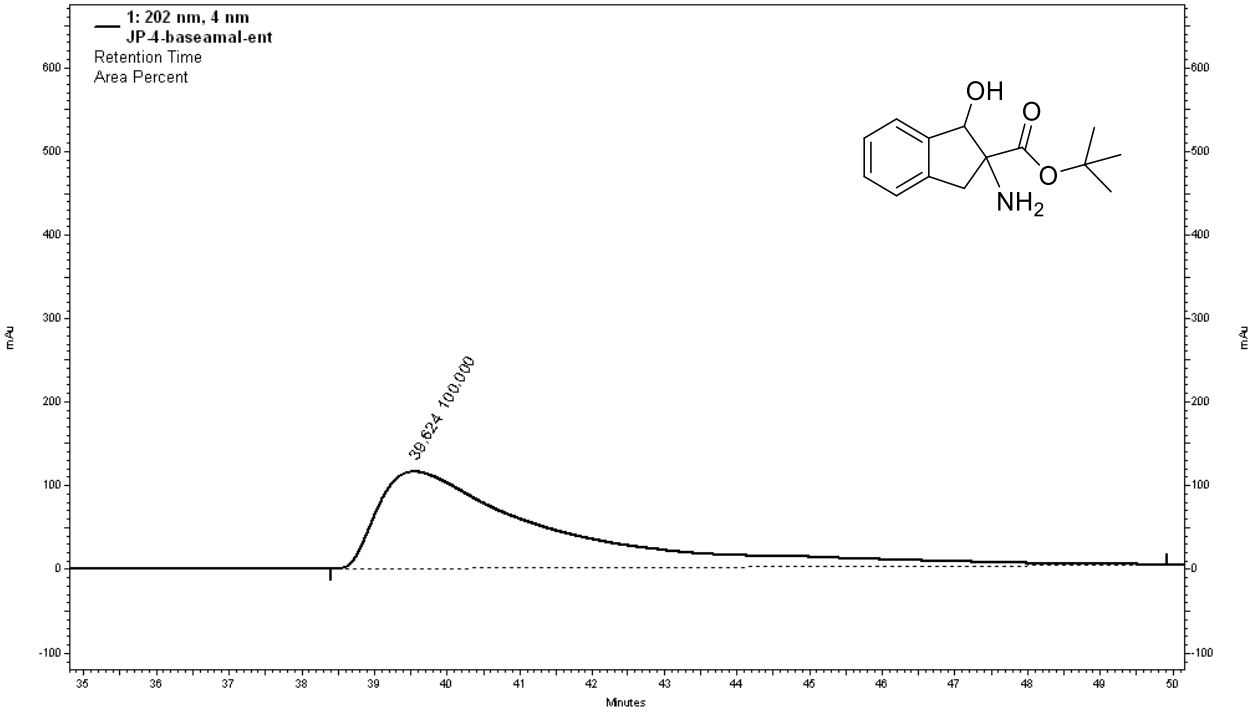
1: 202 nm, 4 nm
JP-4-baseamal-ent
Retention Time
Area Percent
39.624 100.000
OH
O
O
NH2
mAu
Minutes

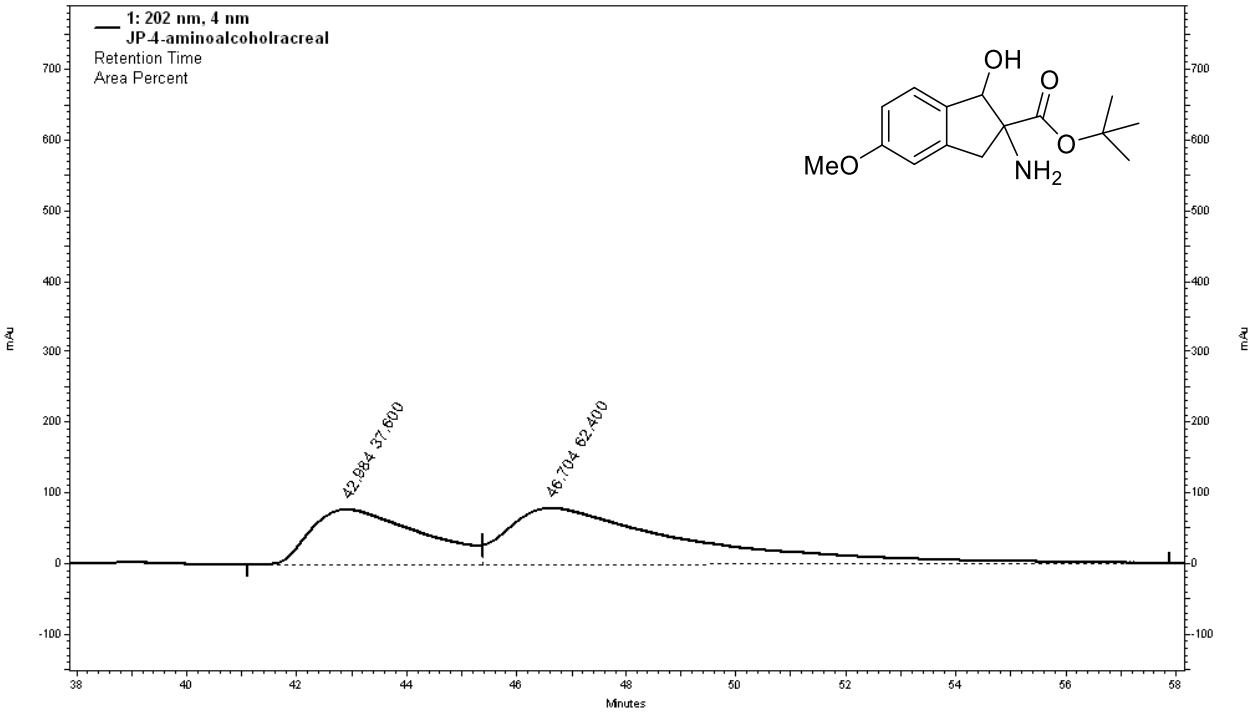
1: 202 nm, 4 nm
JP-4-aminoalcoholracreal
Retention Time
Area Percent
42.984 37.600
46.704 62.400
mAu
Minutes
OH
O
O
MeO
NH2

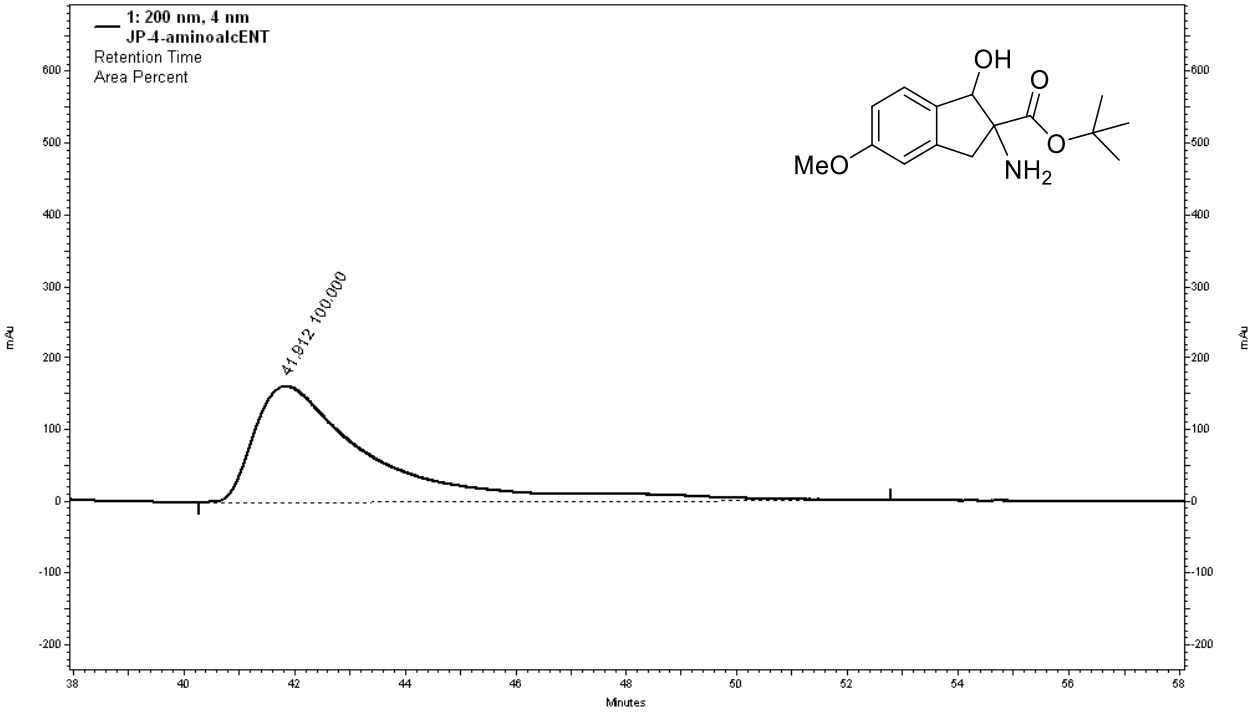
1: 200 nm, 4 nm
JP-4-aminoalcENT
Retention Time
Area Percent
41.912 100.000
mAu
Minutes
OH
O
O
MeO
NH2

Chapter 3. Enantioselective Heck-Matsuda Arylations *via* Phase-Transfer of Aryl Diazonium Cations

Aryldiazonium salts are extensively employed in cross coupling reactions, yet enantioselective variants of these transformations are rare. This challenge is primarily associated with the incompatibility of diazonium salts and most chiral phosphine ligands, which tend to react directly. To overcome this problem, we utilize a chiral anion phase-transfer strategy in combination with Pd^0 catalysis to achieve an enantioselective Heck-Matsuda reaction. Key to obtaining high yields and enantioselectivities is the design and application of new phase-transfer phosphates, which we believe serve as counterions to cationic Pd^{II} intermediates. In addition to controlling enantioselectivity, chiral anions are used to modulate chemical reactivity, indicating a potentially larger role of chiral anions in transition metal-mediated processes.

Portions of this chapter are based on work done in collaboration with Carolina Avila, Hosea Nelson, Hunter Shunatona, Yernaidu Reddi, and Raghavan Sunoj. H.N. and C.A. made significant intellectual contributions and performed optimization experiments. C.A. also assisted with determination of substrate scope. H.S. contributed to catalyst synthesis. Y.R. and R.S. performed computational experiments.

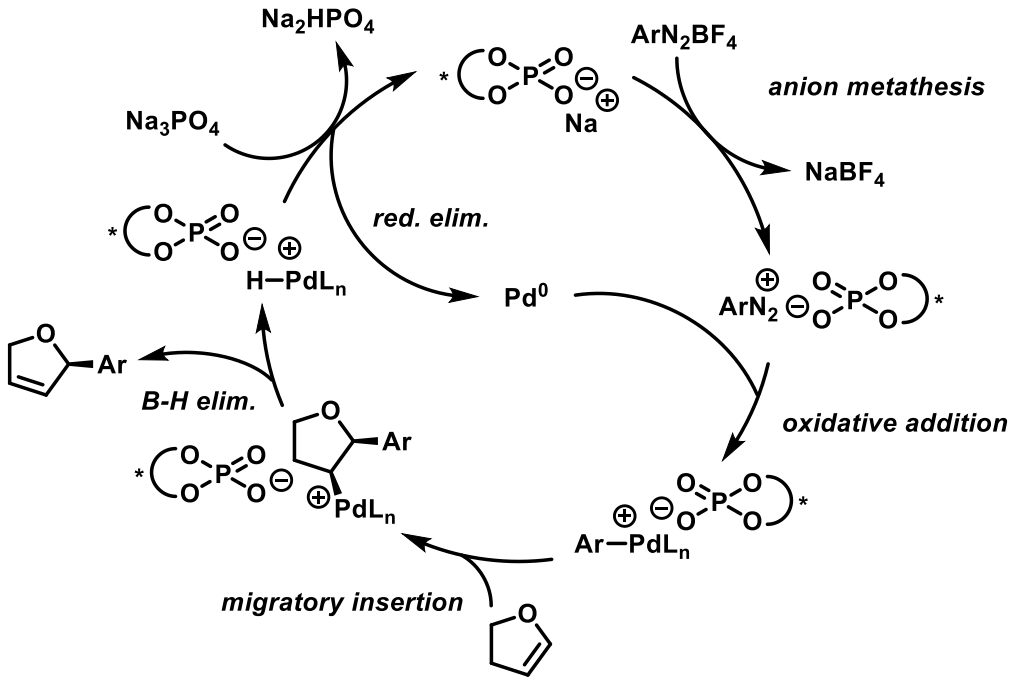

Introduction

Chapters 1 and 2 detail asymmetric amination reactions enabled by chiral anion phase-transfer of aryldiazonium salts. While high enantioselectivity can be obtained, these transformations require substrates with "built-in" reactivity, such as β-keto esters and tryptamine derivatives, primarily because aryldiazonium salts are weak π-electrophiles. Achieving broad substrate scope presented a difficult, yet intriguing challenge, as the ability to start with unactivated starting materials would be a significant advance in our methodology.

Given literature precedent and recent work in our group, we were interested in the possibility of combining phase-transfer catalysis with transition metal catalysis to develop an enantioselective cross coupling reaction using aryldiazonium salts, a reaction that would allow us to functionalize simple olefins. Furthermore, substitution of the diazonium salt would be incorporated into the product, providing stark contrast to much of our previously reported phase-transfer chemistry that has been limited to the addition of single atoms such as fluorine and bromine.

Additionally, enantioselective cross coupling reactions using diazonium salts (Heck-Matsuda reactions) are extremely rare in literature, proving us an opportunity to directly address a synthetic problem. This challenge is largely due to the incompatibility of commonly used chiral phosphine ligands and diazonium salts. Generally, reactions between these species result in dediazoniation and the formation of the corresponding phosphine oxide (Scheme 1).[1,2] We proposed that the use of chiral phosphate anions to achieve enantioinduction could provide a solution, especially given the compatibility of chiral phosphates and diazonium cations that we had already demonstrated (Chapters 1 and 2).

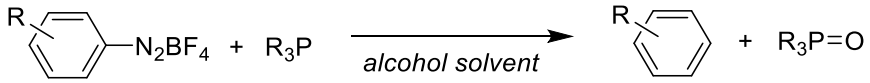

Scheme 1. Decomposition of aryldiazonium salts *via* reduction by phosphines (ref. 1).

While the scarcity of viable chiral ligands has limited the development of enantioselective Heck-Matsuda reactions, a few examples have been reported by the Correia[3,4] and Sigman[5] groups who have utilized chiral bisoxazoline and pyridine oxazoline ligands respectively. Correia and co-workers have developed arylative desymmetrizations of cyclic and acyclic olefins (Scheme 2a), while the Sigman Group has developed enantio- and regioselective arylations of acyclic alkenyl alcohols *via* a redox-relay process (Scheme 2b).

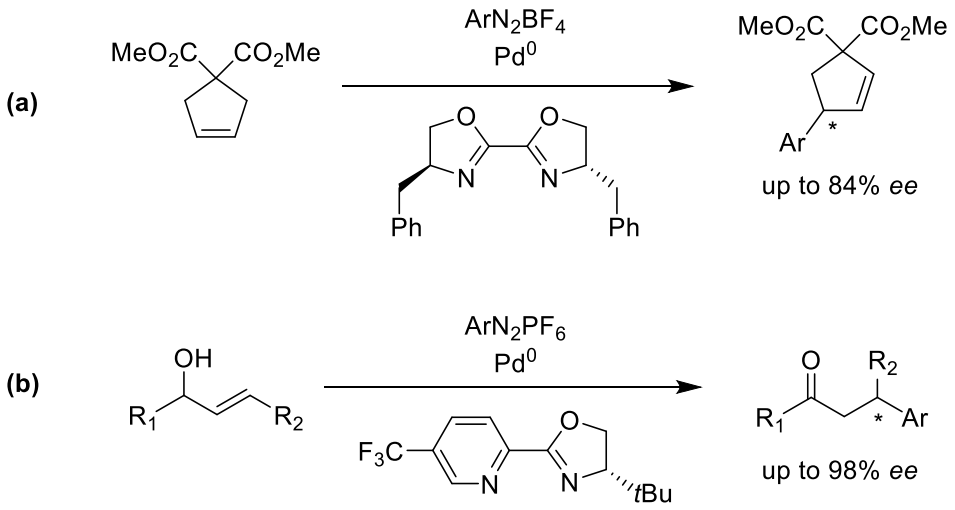

Scheme 2. Previously developed enantioselective Heck-Matsuda arylations (ref. 3, 5).

As a complementary approach, we sought to achieve enantioinduction *via* ion-pairing. We hypothesized that the chiral anion used to solubilize the aryldiazonium salt could function as a counterion to a cationic Pd^{II} intermediate formed after oxidative addition (Scheme 3).

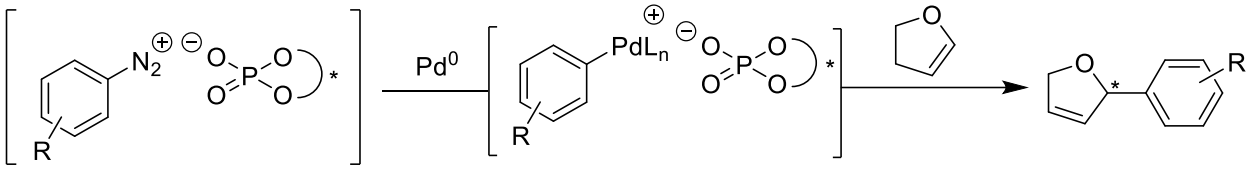

Scheme 3. Chiral ion-pairing with cationic Pd^{II}.

Similar oxidative additions to generate chiral ion-paired cationic Pd^{II} intermediates have been proposed. In 2007, List and coworkers reported an asymmetric allylation of aldehydes catalyzed by Pd^0 and TRIP (Scheme 4).[6] Notably, the authors proposed an oxidative addition of Pd^0 to an enaminium ion pair. The resultant cationic Pd^{II}-allyl intermediate is paired to a chiral phosphate counterion that subsequently directs an enantioselective allylation.

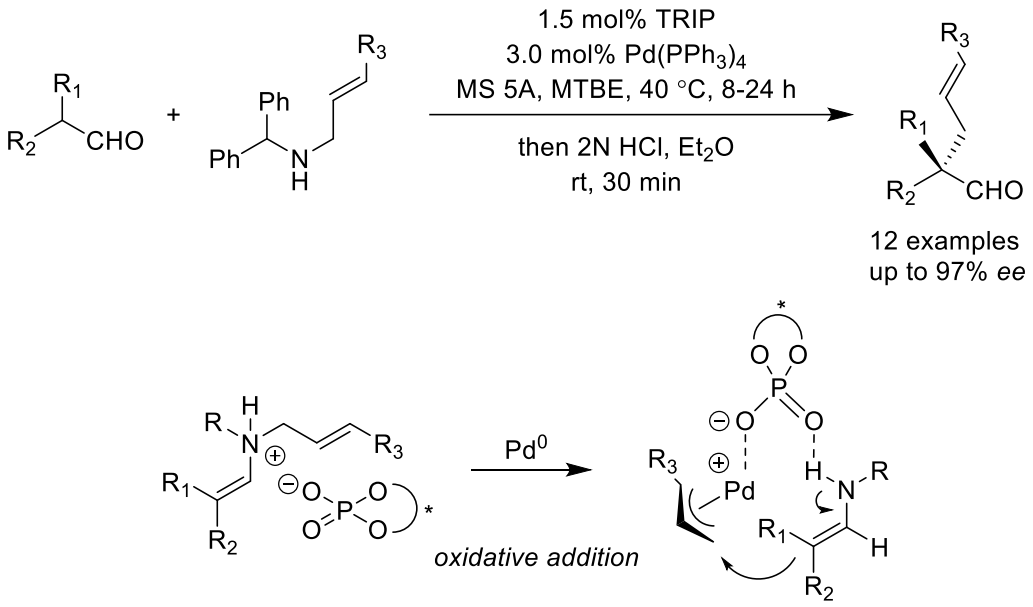

Scheme 4. Oxidative addition of Pd^0 to a chiral ion pair (ref 5).

Recently, our group reported an enantioselective 1,1-arylborylation of alkenes using aryldiazonium salts and a similar catalytic system of Pd^0 and chiral phosphate (Scheme 5).[7] In the proposed mechanism, Pd^0 undergoes oxidative addition to a chiral ion-paired aryldiazonium salt. The intermediate cationic Pd^{II} species then undergoes an enantiodetermining migratory insertion, with asymmetry induced by the chiral counteranion.

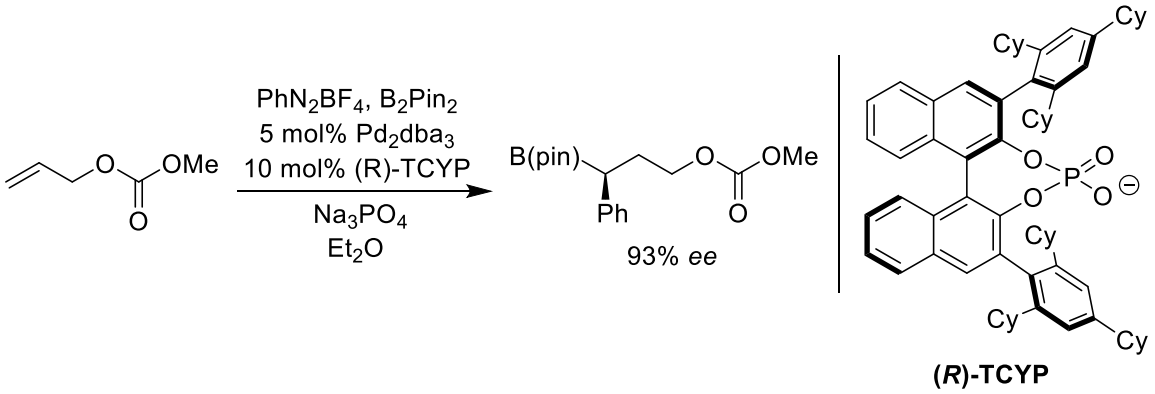

Scheme 5. Enantioselective 1,1-arylborylation of alkenes using Pd and chiral anion phase-transfer catalysis (ref. 6).

In light of literature precedent, we proposed the following mechanism for an enantioselective Heck-Matsuda reaction *via* palladium and chiral anion phase-transfer catalysis (Figure 1).

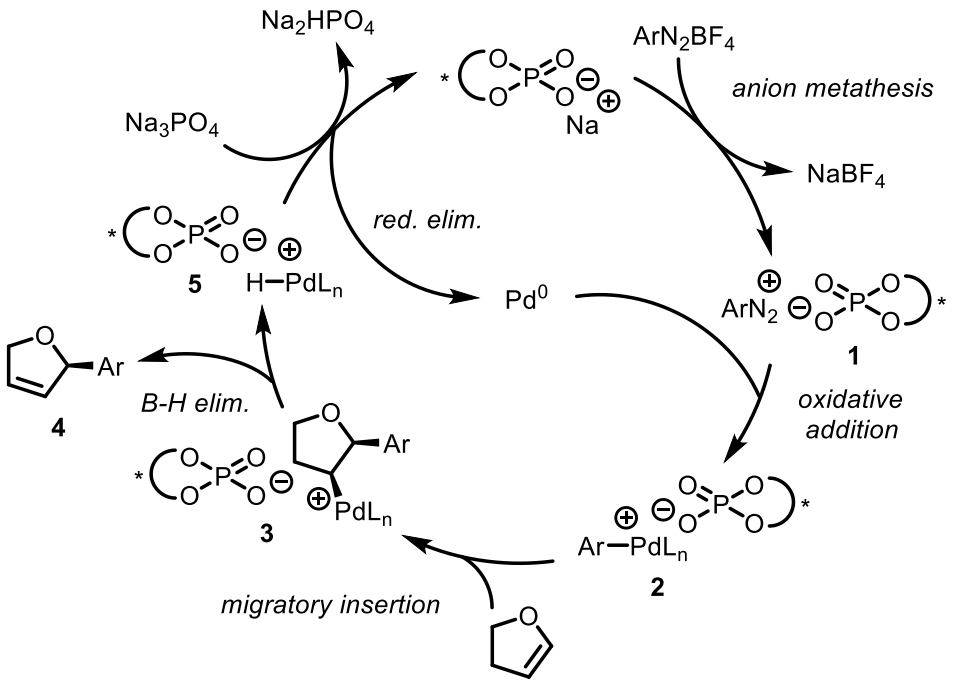

Figure 1. Proposed mechanism for Heck-Matsuda arylation.

The insoluble aryl diazonium salt is first brought into solution *via* chiral anion metathesis, forming ion pair **1**. Oxidative addition of Pd^0 forms cationic Pd^{II} intermediate **2**. The chiral counterion associated to **2** subsequently directs an enantiodetermining migratory insertion of a cyclic olefin to generate intermediate **3**. Intermediate **3** then undergoes a stereospecific β-hydride elimination to generate desired product **4** and Pd-hydride **5**. **5** then undergoes formal reductive elimination *via* deprotonation, either by the counterion or inorganic base, to regenerate Pd^0 and the chiral phosphate phase-transfer catalyst.

Results and Discussion

To test this hypothesis, we examined 2,3-dihydrofuran (**3.1a**) as a model substrate. Treatment of **3.1a** with 5 mol% Pd_2dba_3, 10 mol% (*R*)-TRIP (**3.3a**), 0.5 equivalents of p-$MePhN_2BF_4$, and 3 equivalents of Na_3PO_4 in hexanes led to the formation of desired product **3.2a** in moderate yield and 30% ee (Scheme 6).

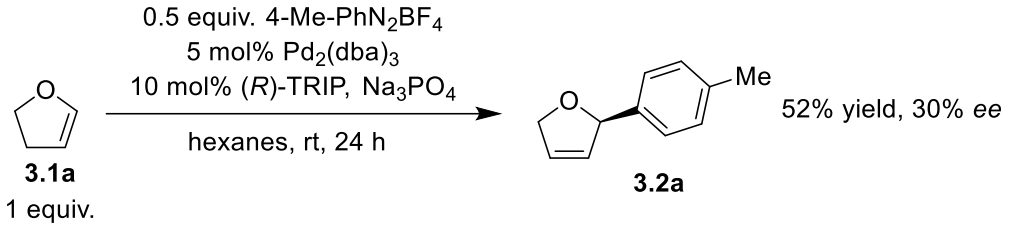

Scheme 6. Phase-transfer Heck-Matsuda arylation of **3.1a** – initial hit.

While enantioselectivity was modest, this promising result showed that some levels of enantioinduction could be achieved using a fairly unbiased substrate. To improve ee, we next examined different phase-transfer catalysts (Table 1).

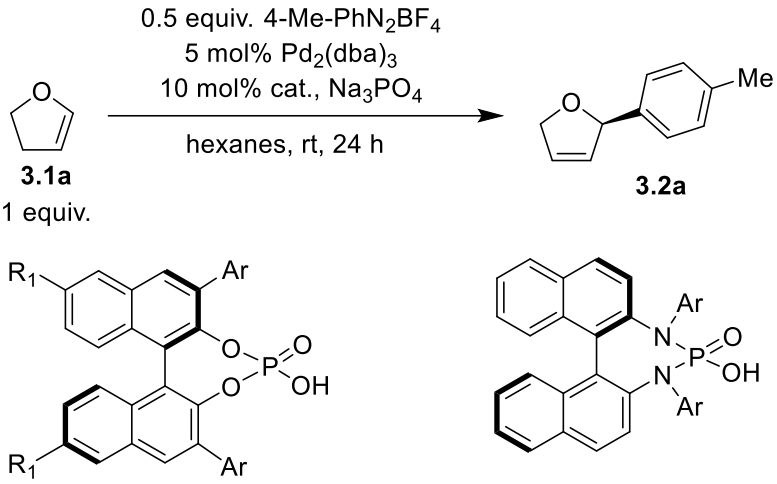

Entry	Cat.	*ee* (%)
1	**3.3a**	30
2	**3.3b**	30
3	**3.3c**	-5
4	**3.3d**	5
5	**3.3e**	0
6	**3.3f**	33
7	**3.3g**	0
8	**3.3h**	-15
9	**3.3i**	20

3.3a, R_1 = H, Ar = 2,4,6-(*i*Pr)$_3$C$_6$H$_2$
3.3b, R_1 = C$_8$H$_{17}$, Ar = 2,4,6-(*i*Pr)$_3$C$_6$H$_2$
3.3c, R_1 = H, Ar = 2,4,6-(Cy)$_3$C$_6$H$_2$
3.3d, R_1 = C$_8$H$_{17}$, Ar = 2,4,6-(Cy)$_3$C$_6$H$_2$
3.3e, Ar = Ph
3.3f, Ar = 3,5-Me-C$_6$H$_3$
3.3g, Ar = 3,5-*t*Bu-C$_6$H$_3$
3.3h, Ar = 3,5-OMe-C$_6$H$_3$
3.3i, Ar = 2-Napthyl

Table 1. Catalyst optimization.

Screening a subset of BINOL- and BINAM-derived chiral phosphoric acids did not result in any significant improvement in enantioselectivity (entries 1-9). Long alkyl chains on the backbone of the catalyst (entries 2, 4), which could increase solubilizing potential, did not make a major impact. As catalysts **3.3a**, **3.3b**, and **3.3f** provided similar ee values, all three phosphoric acids were taken forward and evaluated with various inorganic bases (Table 2).

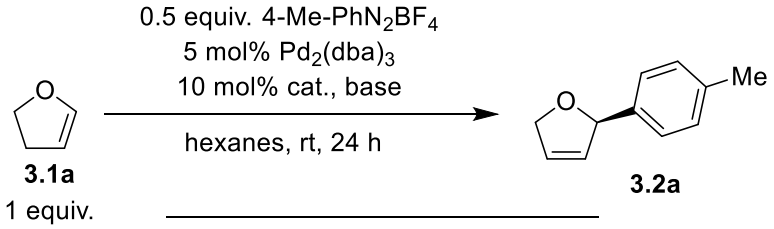

Entry	Cat.	Base	*ee* (%)
1	**3.3a**	Na_3PO_4	30
2	**3.3a**	Na_2HPO_4	30
3	**3.3b**	Na_3PO_4	30
4	**3.3b**	Na_2HPO_4	33
5	**3.3f**	Na_3PO_4	33
6	**3.3f**	K_3PO_4	36
7	**3.3f**	$NaHCO_3$	48
8	**3.3f**	Na_2HPO_4	49
9	**3.3f**	NaOAc	20
10	**3.3f**	Li_2CO_3	38

Table 2. Base optimization.

Enantioselectivities were improved up to 49% with judicious choice of base. Specifically, a combination of catalyst **3.3f** and Na_2HPO_4 gave the best results (entry 8). Notably, the identity of the inorganic base only had an impact when **3.3f** was used as a phase-transfer catalyst (entries 5-10). When BINOL-derived phosphoric acids were employed, base identity had little impact on ee (entries 1-4).

Next, concentration of **3.1a**, phase-transfer catalyst loading, and palladium loading were investigated (Table 3). Increasing the loading of **3.3f** did not increase ee (entry 3), indicating a minimal background reaction. At a 0.30 M concentration of **3.1a** we observed our highest levels of enantioselectivity (entry 5), with higher concentrations eventually leading to a decrease (entry 6).

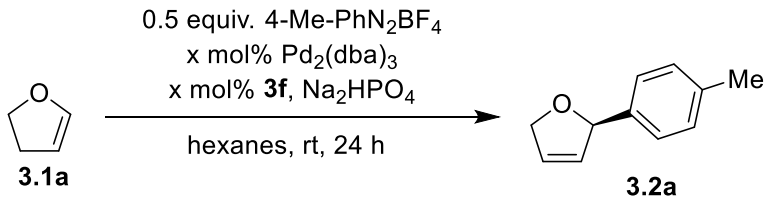

entry	furan [M]	mol% Pd_2dba_3	mol% **3f**	*ee* (%)
1	0.15	5	5	41
2	0.15	10	10	45
3	0.15	5	20	47
4	0.15	5	10	32[a]
5	0.30	5	10	56
6	0.50	5	10	52

[a] with mol sieves

Table 3. Further optimization using catalyst **3.3f**.

While optimization experiments had been somewhat fruitful, we had exhausted variations of most of our reaction parameters. Furthermore, we were concerned that further reaction optimization would be increasingly substrate specific and would not necessarily translate across a wide array of cyclic olefins and aryldiazonium salts. To get a sense for scope, we examined different diazonium salts under our optimized reaction conditions (Table 4).

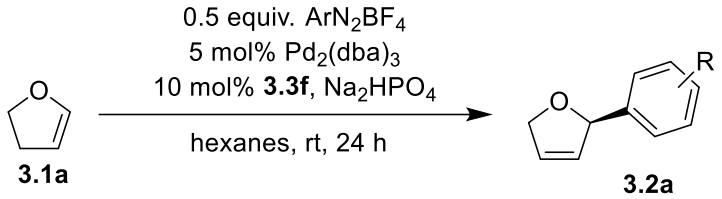

entry	R =	*ee* (%)
1	H	47
2	2-Me	22
3	3-Me	51
4	4-OMe	24
5[a]	4-CF_3	-
6[a]	4-CO_2Me	-

[a]no product observed

Table 4. Aryldiazonium scope.

Only modest levels of enantioselectivity were observed for most aryldiazonium salts (entries 1-4). Electron-withdrawing substituents were not well tolerated, leading to minimal product formation (entries 5-6). Given these limitations (poor scope and low ee) we chose to pursue other substrate classes.

We next examined cyclopentene derivative **3.3a** which had been previously employed by the Correia group.[3] An initial screen of phase-transfer catalysts revealed use of H8-TCYP (**3.3j**) to be optimal. Further solvent and temperature optimization experiments were then conducted (Table 5). Generally, yields were good (up to 80%) while enantioselectivities remained modest (<60% ee, entries 1-5). Notably, we found a significant increase in enantioselectivity by using MTBE solvent, decreasing the reaction temperature to 0 ˚C, and using K_2CO_3 as base (entry 6).

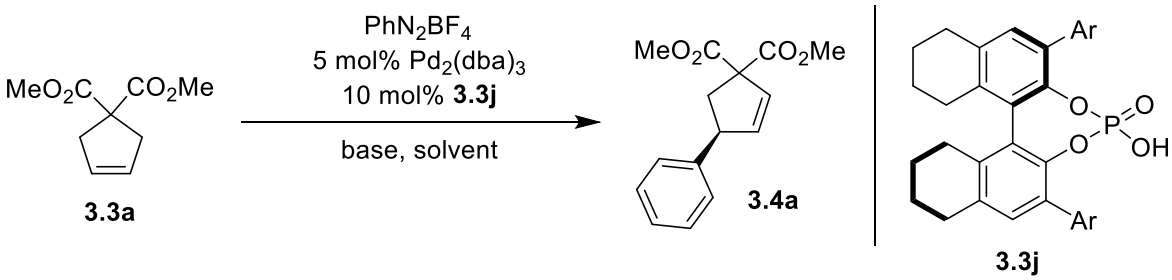

Entry	Solvent	Base	Temp	*ee* (%)	yield (%)
1	toluene	Na_2CO_3	r.t.	49	76
2	benzene	Na_2CO_3	r.t.	57	80
3	*m*-xylene	Na_2CO_3	r.t.	50	76
4	*n*Bu_2O	Na_2CO_3	r.t.	48	45
5	MTBE	Na_2CO_3	r.t.	59	68
6	MTBE	K_2CO_3	0 °C	70	75

Table 6. Arylation of **3.3a** - initial optimizations.

To further improve ee, we examined mixed solvent systems and additional bases (Table 7). Ultimately, we obtained our best results by using benzene/MTBE co-solvents (3:2) and K_2CO_3 at 10 ˚C (entry 5).

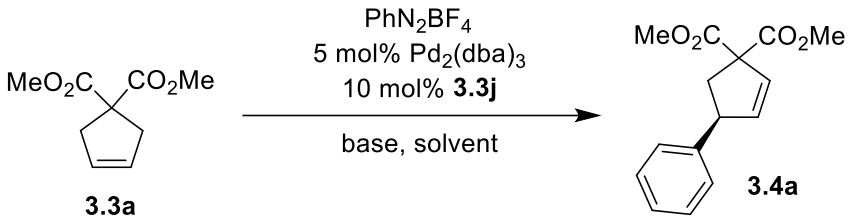

Entry	Solvent	Base	Temp	*ee* (%)	yield (%)
1	benzene/MTBE 1:1	Na_2CO_3	r.t.	66	72
2	benzene/MTBE 3:2	Na_2CO_3	r.t.	68	86
3	benzene/MTBE 3:2	$NaHCO_3$	r.t.	58	52
4	benzene/MTBE 3:2	K_2CO_3	r.t.	70	97
5	benzene/MTBE 3:2	K_2CO_3	10 °C	85	80
6	benzene/MTBE 3:2	Na_3PO_4	r.t.	64	63

Table 7. Solvent and base optimization.

Using these optimized conditions, we re-evaluated our library of phase-transfer catalysts to ensure that we did not miss an optimal result through pure linear screening (Table 8). Control experiments omitting phase-transfer catalyst (entry 6) and inorganic base (entry 7) resulted in both low yield and low ee, supporting the proposed phase-transfer hypothesis.

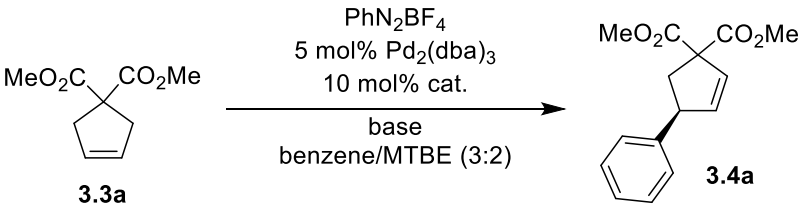

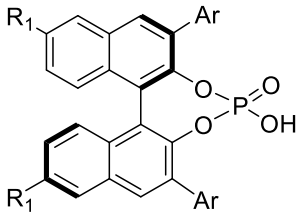

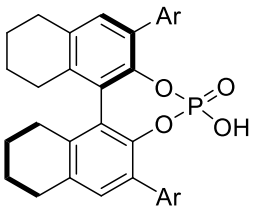

3.3a, R_1 = H, Ar = 2,4,6-(*i*Pr)$_3$C$_6$H$_2$
3.3b, R_1 = C_8H_{17}, Ar = 2,4,6-(*i*Pr)$_3$C$_6$H$_2$
3.3c, R_1 = H, Ar = 2,4,6-(Cy)$_3$C$_6$H$_2$
3.3d, R_1 = C_8H_{17}, Ar = 2,4,6-(Cy)$_3$C$_6$H$_2$
3.3j, Ar = 2,4,6-(Cy)$_3$C$_6$H$_2$
3.3k, Ar = 2,4,6-(*i*Pr)$_3$C$_6$H$_2$

Entry	Cat.	*ee* (%)	yield (%)
1	**3.3a**	63	61
2	**3.3b**	43	88
3	**3.3c**	40	94
4	**3.3d**	36	82
5	**3.3k**	45	85
6	-	-	9
7[a]	**3.3j**	40	7

[a]no base added

Table 8. Phase-transfer catalyst screen.

Having reached the upper limit of enantioselectivity that could be achieved through reagent optimization, we explored aryldiazonium scope (Table 9). In addition to phenyldiazonium tetrafluoroborate (entry 1), aryldiazonium salts with electron withdrawing groups (entries 2-3) and electron donating groups (entries 4-8) were well tolerated, affording the corresponding arylated products in good yield and acceptable enantioselectivity. A disubstituted aryldiazonium salt was also amenable (entry 9). Generally, *meta*- and *para*-substitution was tolerated, with *ortho*-substitution leading to poor conversion and low ee.

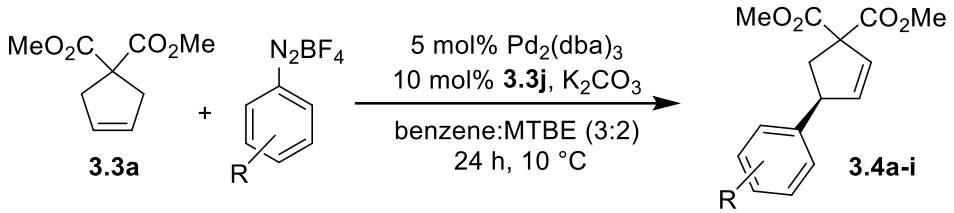

entry	R =	yield (%)	*ee* (%)
1	H (**3.4a**)	82	85
2	3-CF_3 (**3.4b**)	70	84
3	4-F (**3.4c**)	81	85
4	3-OMe (**3.4d**)	81	79
5	4-OMe (**3.4e**)	73	82
6	3,5-Me (**3.4f**)	79	82
7	4-*t*Bu (**3.4g**)	82	-87
8	4-Ph (**3.4h**)	66	85
9	4-OMe,3-Cl (**3.4i**)	80	80

Table 9. Aryldiazonium scope.

Reactions using 2,3-dihydrofuran (**3.1a**) and cyclopentene di-ester **3.3a** substrates were fairly clean, with crude NMR spectra predominantly showing the desired product in addition to smaller peaks corresponding to phase-transfer catalyst and free dba ligand. When employing spirocyclic cyclopentene substrates, we were surprised to see additional NMR peaks in the alkene region that did not correspond to arylated product. We were later able to assign these peaks to olefin isomers (Scheme 7). For example, subjection of **3.5a**, **3.7a**, and **3.9a** to phase-transfer arylation conditions afforded significant amounts of olefin isomers **3.5b**, **3.7b**, and **3.9b** in addition to desired products.

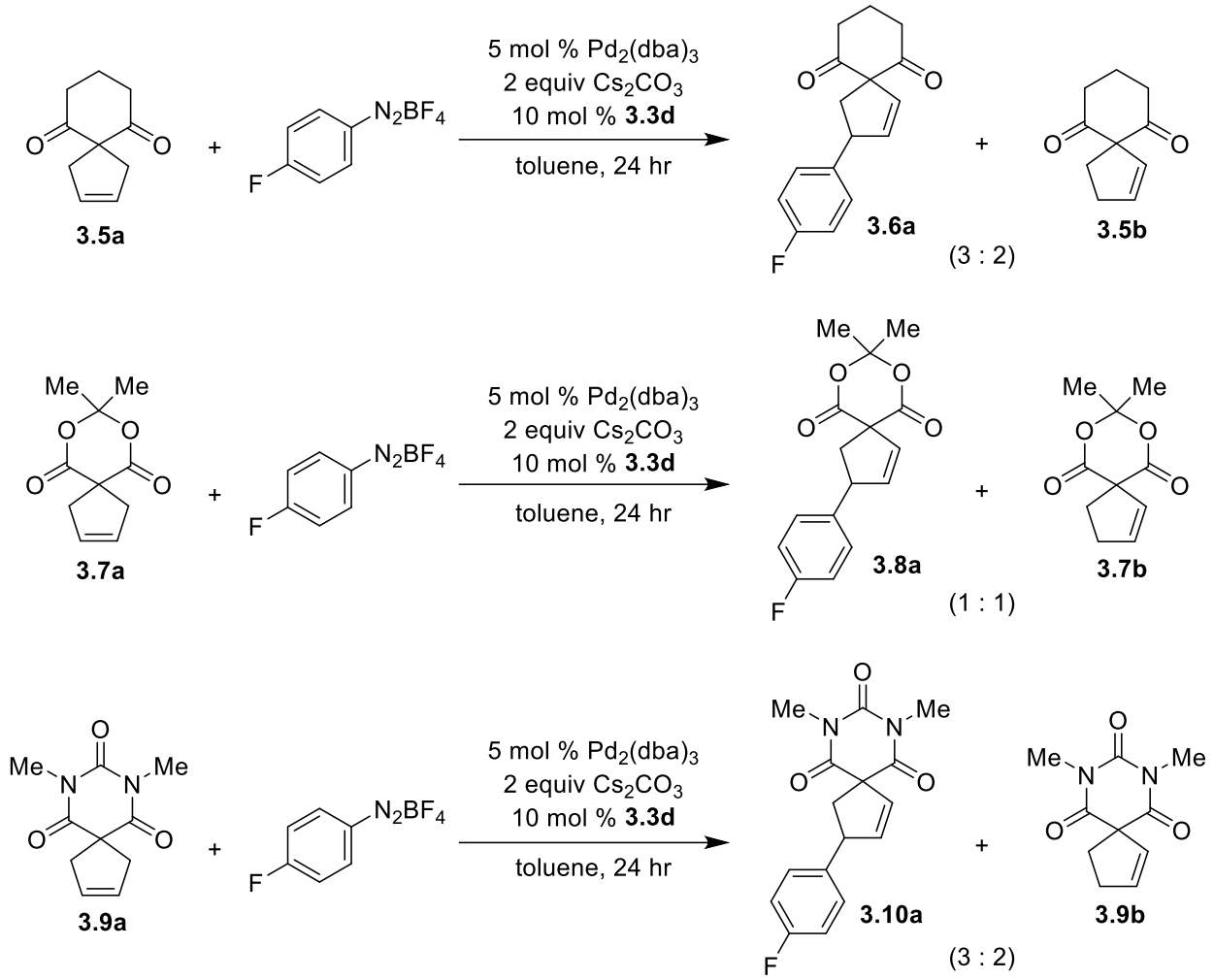

Scheme 7. Olefin isomerization of spirocyclic substrates.

To understand the mechanism of olefin isomerization, we performed a few control experiments (Scheme 8). Treatment of **3.9a** with Pd_2dba_3 did not result in isomerization, nor did treatment with chiral phosphoric acid (TRIP). A combination of both Pd_2dba_3 and TRIP, which could potentially form a palladium hydride species, did not result in substrate isomerization either. Finally, adding base to the mixture produced the same result. These controls indicated that the aryldiazonium salt was necessary for isomerization, presumably through formation of a palladium hydride species (**5**, Figure 1).

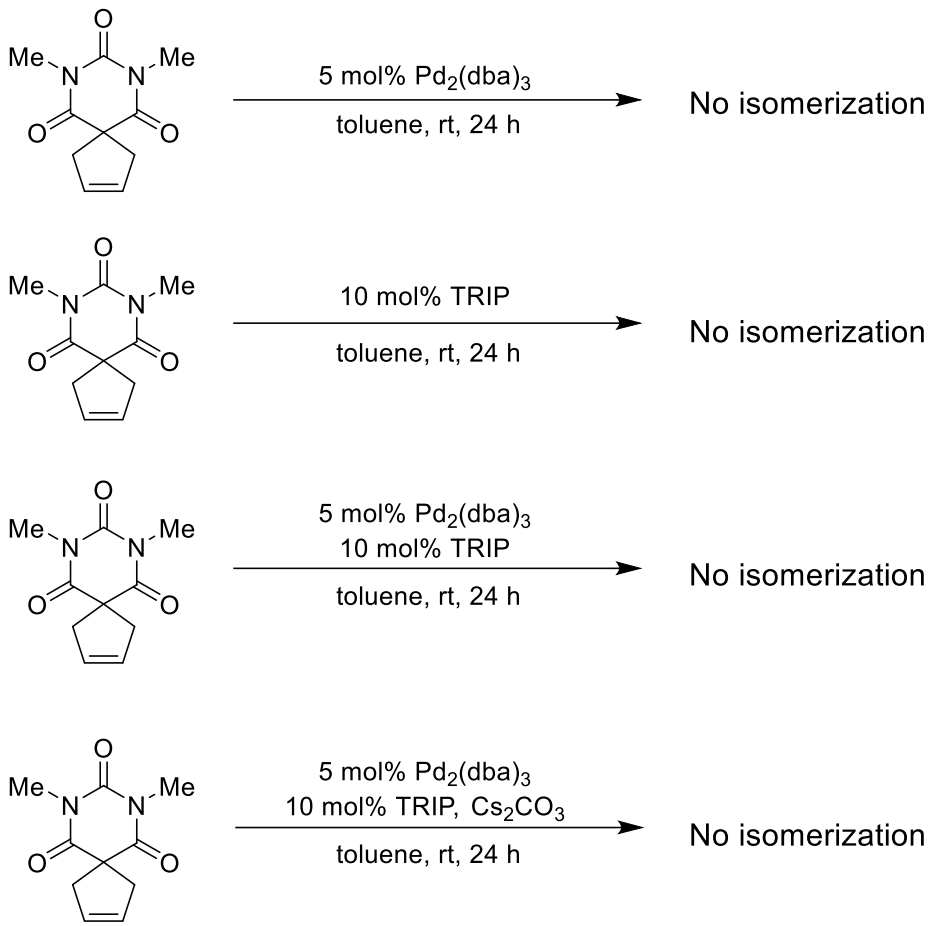

Scheme 8. Control experiments for the isomerization of **3.9a**

We thus hypothesized that olefin isomerization requires a palladium hydride species that can only be accessed after arylation and β-hydride elimination. Substrate coordination to this palladium hydride and subsequent insertion and β-hydride elimination (Scheme 9) affords the olefin isomer. For spirocyclic substrates, the isomerization pathway and the desired reductive elimination pathway are likely to be kinetically competitive, resulting in a mixture of products.

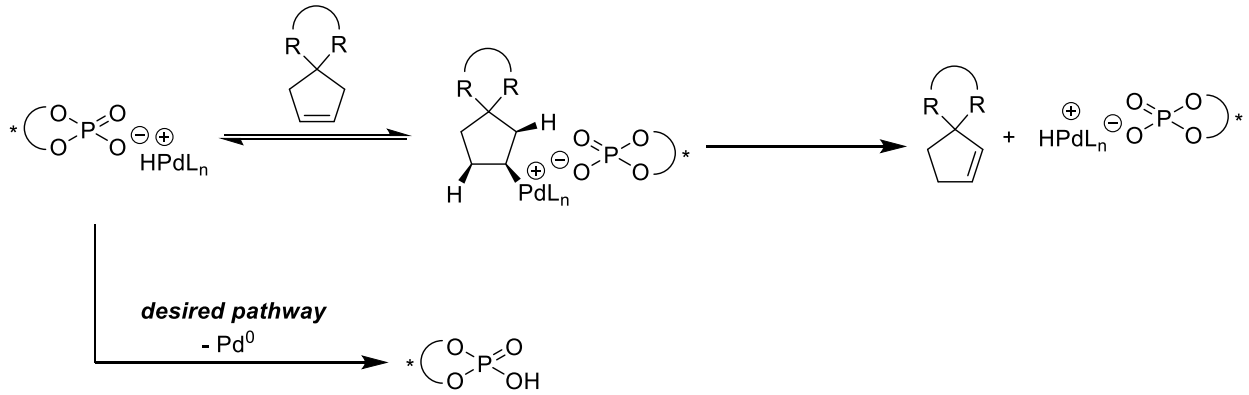

Scheme 9. Proposed mechanism of isomerization.

Furthermore, we hypothesized that limiting the lifetime of a palladium hydride species by accelerating reductive elimination could lead to higher product selectivity. To favor the productive reductive elimination pathway, which we believed was occurring *via* deprotonation, we proposed utilizing more basic chiral counterions, specifically BINAM-derived phosphates developed previously (Scheme 10, $k_1 > k_2$).

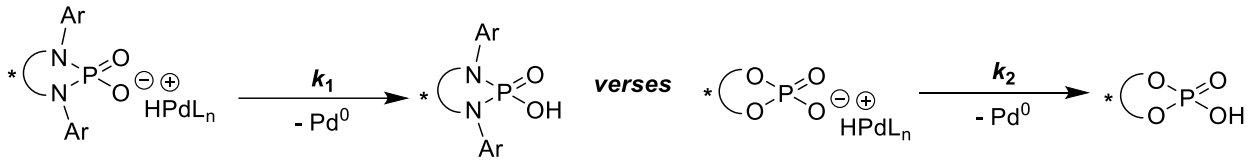

Scheme 10. Relative rates of reductive elimination with different counterions.

To test this proposal, we subjected substrate **3.9a** to two sets of reaction conditions, one with BINOL-derived phosphate **3.3d** and the other with BINAM-derived phosphate **3.3l** (Table 10).

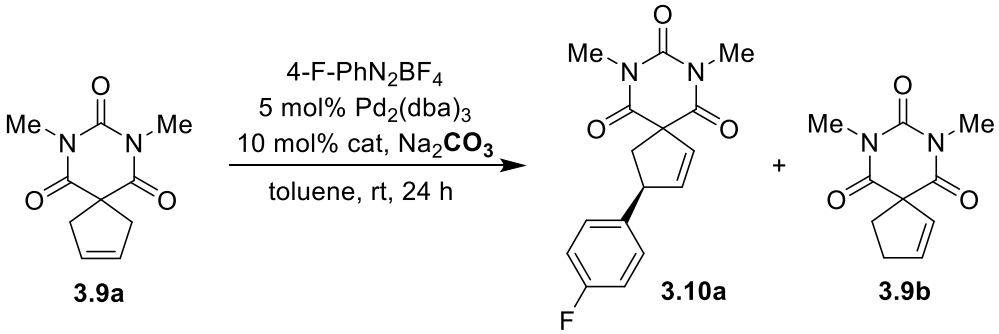

Entry	Cat.	**3.10a**:**3.9b**	conv. (%)	*ee* (%)
1	**3.3d**	3:2	50	40
2	**3.3l**	> 20:1	78	55

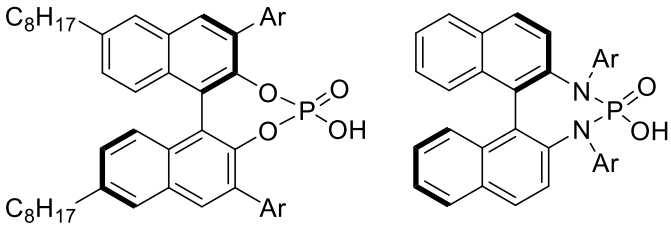

3.3d, Ar = (2,4,6)-$(Cy)_3C_6H_2$ **3.3l**, Ar = 4-Me-C_6H_4

Table 10. Increased product selectivity with **3.3l**.

While use of BINOL phosphate **3.3d** resulted in a 3:2 mixture of desired product **3.10a** and olefin isomer **3.9b** (entry 1), use of BINAM phosphate **3.3l** led to exclusive arylation and no isomerization as observed by crude ^{1}H NMR (entry 2). Notably, the desired product was formed in excellent conversion and moderate enantioselectivity.

With a new optimal catalyst scaffold for the arylation of spirocycle **3.9a**, we next aimed to increase ee. A screen of our library of BINAM-derived phosphates indicated that higher enantioselectivities were correlated with increasing steric bulk at the 4-position of the *N*-aryl group, as well as with

use of weaker inorganic bases (Table 11). Using catalyst **3.3p**, which has a *t*-butyl group at the 4-position, we were able to increase ee up to 74% (entry 8). In all cases, no isomerization of **3.9a** was observed.

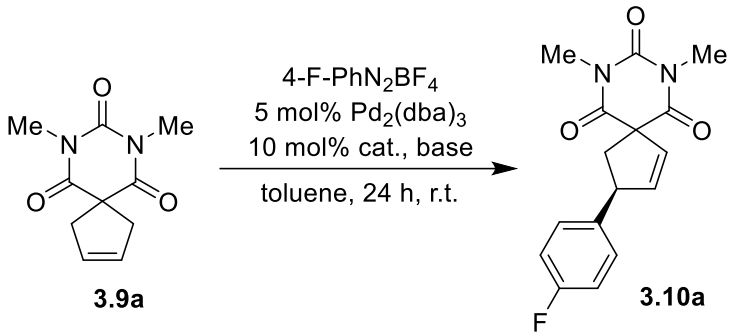

Entry	Cat.	Base	conv. (%)	*ee* (%)
1	**3.3f**	Na_2HPO_4	67	0
2	**3.3h**	Na_2HPO_4	87	0
3	**3.3l**	Na_2CO_3	78	55
4	**3.3l**	Na_2HPO_4	95	57
5	**3.3m**	Na_2CO_3	64	35
6	**3.3n**	Na_2HPO_4	75	-36
7	**3.3o**	Na_2HPO_4	90	67
8	**3.3p**	Na_2HPO_4	96	74

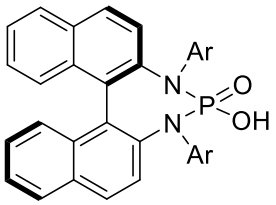

3.3f, Ar = 3,5-Me-C_6H_3
3.3h, Ar = 3,5-OMe-C_6H_3
3.3l, Ar = 4-Me-C_6H_4
3.3m, Ar = 3,5-Ph-C_6H_3
3.3n, Ar = 4-CF_3-C_6H_4
3.3o, Ar = 4-F-C_6H_4
3.3p, Ar = 4-*t*Bu-C_6H_4

Table 11. Screen of BINAM-derived phosphoric acids.

Given the trend in Table 11, we synthesized catalysts with sterically larger groups, specifically mesityl-substituted **3.3q** and adamantyl-substituted **3.3r** (Table 12). Use of the latter in MTBE solvent gave the highest enantioselectivity (entry 3).

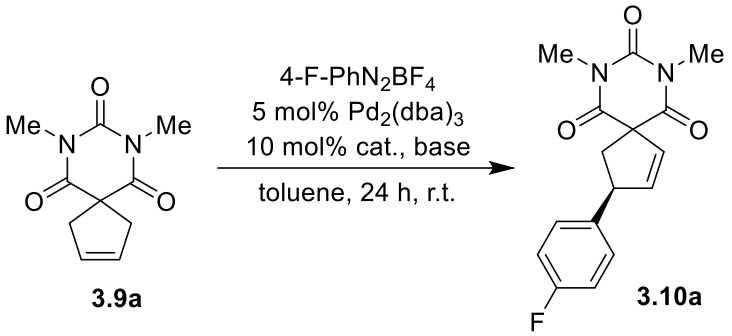

Entry	Cat.	solvent	Base	conv. (%)	*ee* (%)
1	**3.3q**	tol/MTBE 1:1	Na_2HPO_4	50	82
2	**3.3r**	tol/MTBE 1:1	Na_2HPO_4	95	82
3	**3.3r**	MTBE	Na_2HPO_4	95	87

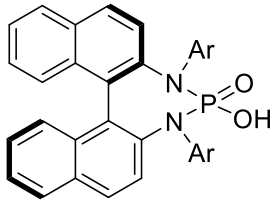

3.3q, Ar = 4-Mes-C_6H_4
3.3r, Ar = 4-Ad-C_6H_4

Table 12. Rational design of catalysts **3.3q** and **3.3r**.

Moving forward with catalyst **3.3r**, we investigated a series of aryldiazonium salts (Table 13). We found that mildly electron donating (entries 1-3) and electron withdrawing (entries 4-6) substituents were tolerated at the *meta*- and *para*-positions of the aryl group, with enantioselectivities as high as 92% (entry 2).

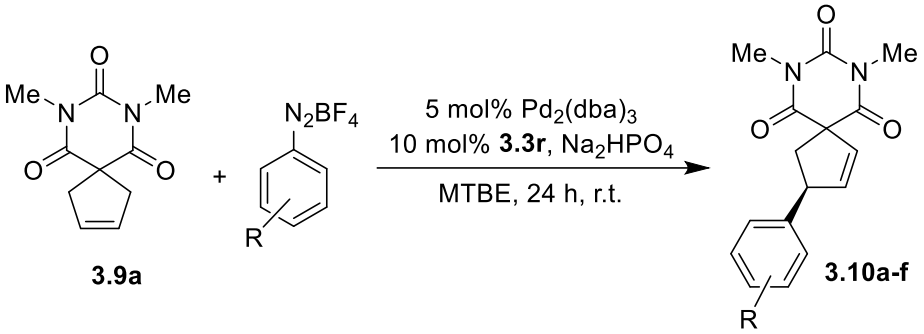

entry	R =	yield (%)	ee (%)
1	Ph (**3.10a**)	70	86
2	4-*t*Bu (**3.10b**)	92	92
3	4-Me (**3.10c**)	67	90
4	4-F (**3.10d**)	79	85
5	3-F (**3.10e**)	92	84
6	3-CF_3 (**3.10f**)	94	90

Table 13. Aryldiazonium scope.

To gain further mechanistic insight, we collaborated with the Sunoj Group, who carried out density functional theory computations (B3LYP-D3) on the reductive elimination and isomerization steps with both BINOL- and BINAM-derived phosphate counterions (Figure 2a). The Gibbs free energy of activation for the reductive elimination step was calculated to be 2.2 kcal/mol lower with a BINAM-phosphate than with a BINOL-phosphate, affirming our initial hypothesis. Presumably, the presence of less inductively withdrawing and more π-donating *N*-aryl substituents results in a more basic phosphate and consequently, a more favorable reductive elimination.

When examining the isomerization of spirocyclic olefin **3.9a**, cationic (dba)Pd-hydride (intermediate **5**, Figure 1) and the chiral phosphate were both found to be involved in the transition state. The optimized geometry indicates that the olefinic carbon accepts the hydride from the palladium while the phosphate oxygen simultaneously abstracts a methylene proton (Figure 2b).

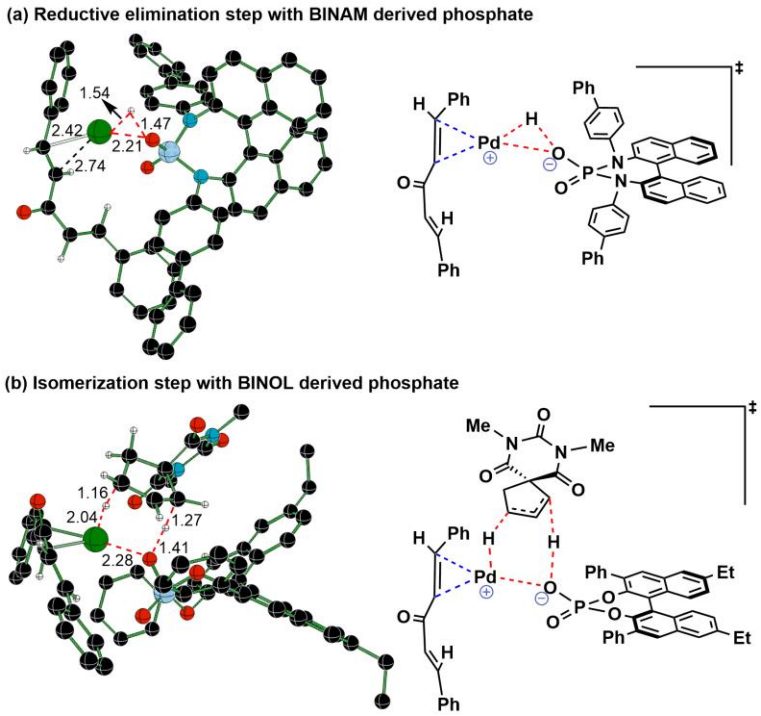

Figure 2. Optimized transition state geometries for (a) reductive elimination and (b) isomerization of **3.9a** in the presence of chiral phosphates at the $SMD_{(Toluene)}$/B3LYP-D3/6-31G**, LANL2DZ(Pd) level of theory. The distances are in Å. Only selected hydrogen atoms are shown for improved clarity. C=black, O=red, H=gray, N=cyan, P=blue and Pd=green.

To further probe the divergent reactivity observed when using different phosphates, the Sunoj Group calculated Gibbs free energies of activation for the isomerization of **3.9a**. When comparing BINOL- and BINAM-phosphates, they found these barriers to be higher by 2.5 and 5.5 kcal/mol compared to reductive elimination respectively. This is in agreement with our experimental observations, as we see a competitive isomerization process with the use BINOL-phosphates and no isomerization with the use of BINAM-phosphates.

Given our results for disubstituted and spirocyclic cyclopentene derivatives, we became interested in pursuing monosubstituted cyclopentene substrates, with the immediate goal of achieving both high diastereo- and enantioselectivity. We believed that high diastereoselectivity could be achieved in either of two scenarios (Scheme 11). If R is a directing group, the cationic palladium aryl intermediate would reside on the same face on the olefin, affording the *cis* product. Alternatively, if R is sterically large, the palladium would reside on the opposite face of the olefin, resulting in the *trans* product.

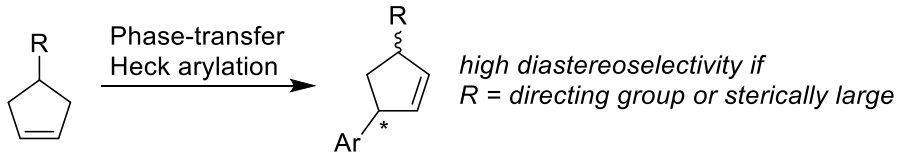

Scheme 11. Diastereoselective Phase-transfer Heck arylation of monosubstituted cyclopentene substrates.

We thus prepared a series of cyclopentene derivatives with different functional groups. Unfortunately, we failed to see both the desired reactivity and high diastereoselectivity in a majority of cases (Figure 3).

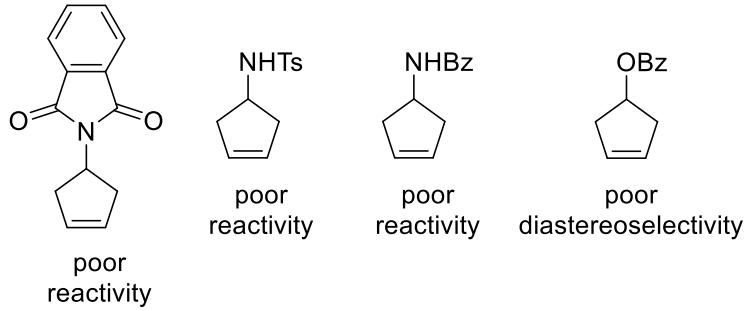

Figure 3. Monosubstituted olefins – failed substrates.

It was not until we examined N-tosyl carbamate **3.11a** that we observed full conversion to a single diastereomer (**3.12a**, Table 14). After slight modification of previously employed reaction conditions, namely use of Cs_2CO_3 as inorganic base and Pd_2(4-OMe-dba)$_3$ as the palladium source, we were able to obtain the desired product in high enantioselectivity. As we only observed the *trans*-diastereomer (confirmed by X-ray crystallographic analysis), the large tertiary amine likely blocks one face of the olefin, resulting in arylation on the opposite face. A small array of aryldiazonium salts were examined, with both electron rich and electron poor diazonium salts affording the desired product in good yield and high optical purity (entries 1-4).

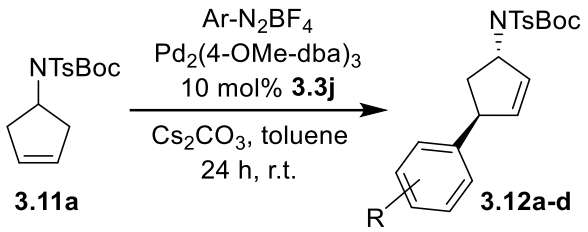

R =	yield[b]	ee[c]
4-F (**3.12a**)	86	90
3,5-Me (**3.12b**)	62	86
4-Ph (**3.12c**)	53	84
3-OMe (**3.12d**)	70	83

Table 14. Diastereo- and enantioselective arylation of **3.11a**.

As an application of this method, hydantoin derivative **3.13a**, an amino acid precursor, was synthesized and subjected to phase-transfer arylation conditions (Table 15). After catalyst, solvent, and base optimization, we were able to isolate the desired product **3.14a** as a single diastereomer in high yield and good enantioselectivity (entry 5). Furthermore, **3.14a** could be isolated in excellent optical purity after a single recrystallization (97% ee). The absolute structure of **3.14a** was determined by X-ray crystallography.

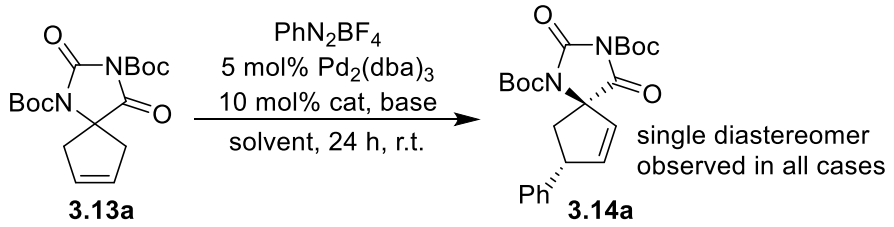

Entry	Cat.	solvent	Base	conv. (%)	*ee* (%)
1	**3.3s**	toluene	K_2CO_3	80	40
2	**3.3p**	toluene	K_2CO_3	30	67
3	**3.3p**	MTBE	K_2CO_3	18	51
4	**3.3p**	benzene	K_2CO_3	21	54
5	**3.3p**	toluene	Na_2HPO_4	89	81
6	**3.3p**	toluene	Na_3PO_4	76	80
7	**3.3p**	*m*-xylene	Na_2HPO_4	63	79
8	**3.3p**	*m*-xylene	Na_3PO_4	66	76
9	**3.3t**	toluene	Na_2HPO_4	66	66
10	**3.3t**	toluene	Na_3PO_4	75	66
11	**3.3r**	toluene	Na_2HPO_4	80	17

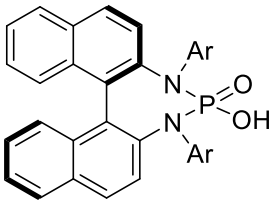

3.3p, Ar = 4-*t*Bu-C_6H_4
3.3r, Ar = 4-Ad-C_6H_4
3.3s, Ar = 4-Ph-C_6H_4
3.3t, Ar = 4-Cy-C_6H_4

Table 15. Enantioselective arylation of **3.13a**.

Deprotection of **3.14a** was accomplished using KOH in refluxing THF and afforded arylated amino acid derivative **3.15a** in 66% yield (Scheme 12). Conformationally constrained amino acids similar in structure to **3.15a** are known $S1P_1$ receptor agonists,[8] and have been previously prepared from optically active starting materials in 3 or more steps.[9] Thus, our methodology may provide an efficient entryway into this bioactive scaffold.

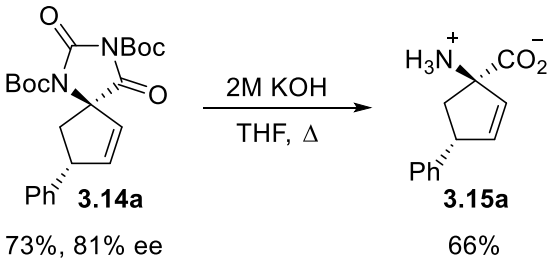

Scheme 12. Deprotection of **3.14a** to yield amino acid derivative **3.15a**.

Conclusions

We have developed an asymmetric Heck-Matsuda arylation of cyclopentene derivatives by combining chiral anion phase-transfer catalysis with traditional palladium cross-coupling catalysis. Undesired olefin isomerization of spirocyclic substrates was circumvented by the synthesis and application of BINAM-derived phosphates, a rare instance in which chiral anions can be used to optimize both enantioselectivity and chemical reactivity. Mechanistic insights into

an undesired isomerization pathway were gained through DFT computations in collaboration with the Sunoj Group and provided additional rationale for experimental observations. Lastly, an asymmetric synthesis of arylated amino acid **3.15a** was developed.

Experimental details

General. Unless otherwise noted, all chemical reagents were purchased from commercial suppliers and used without further purification. Phase-transfer reactions were performed in 1-dram (0.5" x 1.75") vials equipped with a screw cap and were vigorously stirred using a magnetic Teflon stir bar (1/2" x 5/16"). Fast and efficient stirring was maintained over the course of the reaction in order to obtain optimal and reproducibile results. Thin-layer chromatography (TLC) analysis of reaction mixtures was performed using Merck silica gel 60 F254 TLC plates, and visualized under UV or by staining with ceric ammonium molybdate, $KMnO_4$, *p*-anisaldehyde, or vanillin. Column chromatography was performed on Merck Silica Gel 60 Å, 230 X 400 mesh. Nuclear magnetic resonance (NMR) spectra were recorded using Bruker AV-600, AV-500, DRX-500, AVQ-400, AVB-400 and AV-300 spectrometers. ^{1}H and ^{13}C chemical shifts are reported in ppm and referenced to residual solvent peak ($CHCl_3$, δH = 7.27 ppm and δC = 77.00 ppm; DMSO, δH = 2.50 and δC = 39.5 ppm; MeOH δH =3.31 ppm and δC = 49 ppm).[6] ^{19}F spectra are referenced to $CFCl_3$ (0.00 ppm, external). Multiplicities are reported using the following abbreviations: s = singlet, d = doublet, t = triplet, q = quartet, app t = apparent triplet, m = multiplet, br = broad resonance. Mass spectral data were obtained in the QB3/Chemistry Mass Spectrometry Facility, University of California, Berkeley. Enantiomeric excesses were measured on a Shimadzu VP Series Chiral HPLC.

The syntheses of chiral phosphoric acids TRIP (**3.3a**),[10] C8-TRIP (**3.3b**),[11] TCYP (**3.3c**),[12] C8-TCYP (**3.3d**)[13] and H8-TRIP (**3.3k**)[14] have been previously reported. Olefins **3.3a** and **3.9a** were prepared according to a published procedures.[15] Aryldiazonium salts were prepared according to published procedures.[16] Racemic traces were obtained by substituting $Pd(OAc)_2$ in place of Pd_2dba_3 and using methanol as solvent. A racemic trace of **3.14a** was obtained using (±)-TRIP (**3.a**) as the phase-transfer catalyst.

*Synthesis of (R)-H8-TCYP (**3.3j**)*

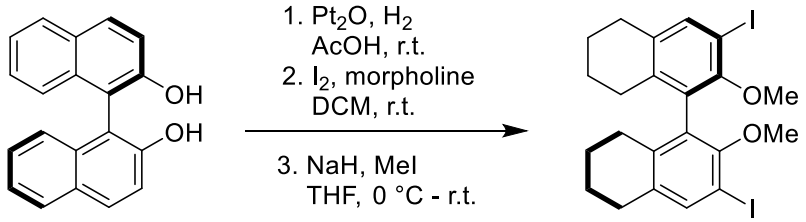

(*R*)-BINOL **S3.1**

S3.1 was prepared from (*R*)-BINOL according to published procedures[17,18,19] (65%, 3 steps). ^{1}H NMR (400 MHz, $CDCl_3$) δ 7.57 (s, 2H), 3.51 (s, 6H), 2.76 (t, *J* = 6.3 Hz, 4H), 2.28 (dt, *J* = 17.3, 6.2 Hz, 2H), 2.09 (dt, *J* = 17.2, 6.3 Hz, 2H), 1.78 – 1.69 (m, 4H), 1.64 (dd, *J* = 11.7, 6.0 Hz, 5H). Spectral data are in accordance with literature.[17,18,19]

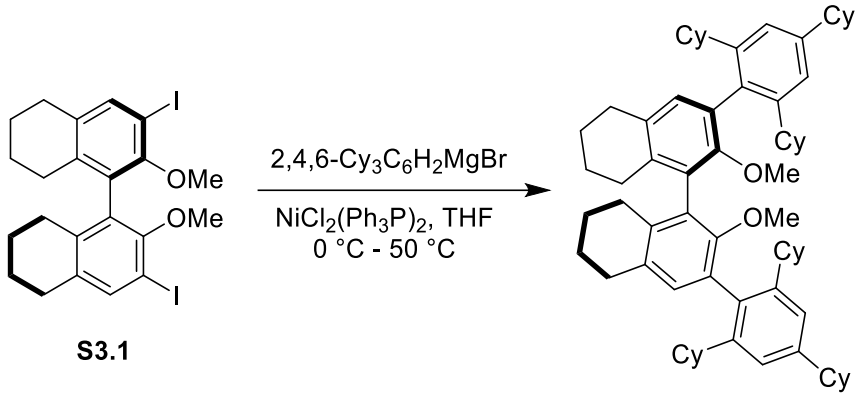

S3.1 **S3.2**

S3.2. (2,4,6-Tricyclohexylphenyl)magnesium bromide were prepared according to published procedures.[12] To a stirred suspension of **S3.1** (1.60 g, 2.78 mmol) and $NiCl_2(Ph_3P)_2$ (0.182 g, 0.28 mmol) in anhydrous and degassed THF (15 mL), was added the Grignard solution (18.6 mmol, 0.37 M) over 5 min at 0 °C. The resultant brown suspension was stirred for 24 h at 50 °C under N_2 atmosphere. During this time, the formation of large amount of precipitate was observed. The reaction was quenched by dropwise addition of cold satd. NH_4Cl (30 mL) at 0 °C. After stirring for 15 min the layers were separated, and the aqueous phase extracted with EtOAc (3 x 50 mL). The combined organic phases were dried over $MgSO_4$, filtered and concentrated under reduced pressure. The crude product was purified by column chromatography (hex/DCM/MeOH 92:07:01 to 90:09:01) to afford **S3.2** as a white foam (1.5 g, 56%). ^{1}H NMR (600 MHz, $CDCl_3$) δ 7.00 – 6.93 (m, 4H), 6.73 (s, 2H), 3.09 (s, 6H), 2.73 (d, *J* = 6.4 Hz, 4H), 2.59 – 2.46 (m, 4H), 2.43 – 2.32 (m, 4H), 2.21 (dd, *J* = 14.8, 9.0 Hz, 2H), 1.94 (d, *J* = 12.2 Hz, 4H), 1.88 – 1.72 (m, 21H), 1.69 – 1.62 (m, 8H), 1.51 – 1.36 (m, 14H), 1.32 – 1.13 (m, 14H), 1.06 (ddt, *J* = 16.4, 12.7, 3.3 Hz, 4H), 0.97 – 0.90 (m, 2H). ^{13}C NMR (101 MHz, $CDCl_3$) δ 152.15, 146.32, 145.86, 145.44, 135.36, 134.48, 133.79, 133.60, 131.29, 131.16, 130.40, 129.73, 128.66, 128.48, 128.41, 121.67, 121.56, 58.87, 44.67, 41.47, 41.43, 35.76, 35.24, 34.57, 33.53, 33.40, 29.43, 27.24, 27.08, 26.93, 26.43, 26.32, 26.26, 23.31, 23.23. HRMS (ESI) m/z $[M+Na]^+$ calc'd for $C_{70}H_{94}O_2Na$ 989.7146, found 989.7119.

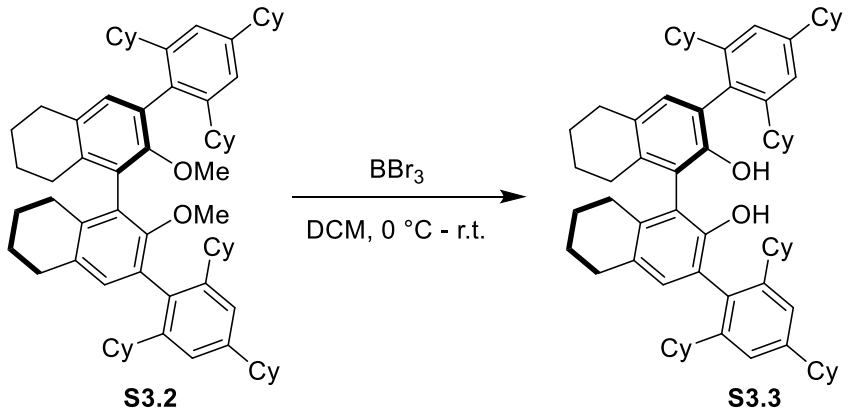

S3.2 **S3.3**

To a solution of **S3.2** (0.885 g; 0.91 mmol) in anhydrous DCM (20 mL) under N_2 atmosphere, was added BBr_3 (3.7 mL, 1M solution in DCM) at 0 °C. The orange solution was stirred at r.t. for 3 h after which an NMR aliquot indicated full conversion. The reaction was quenched by addition of cold satd. $NaHCO_3$ (20 mL) at 0 °C and was stirred for 30 min at r.t. The layers were separated,

and the aqueous phase extracted with DCM (3 x 50 mL). The combined organic phases were dried over $MgSO_4$, filtered and concentrated under reduced pressure. The crude product was purified by column chromatography (hex/DCM/MeOH 90:09:01) to afford **S3.3** as a white foam (0.700 g, 81%). ^{1}H NMR (400 MHz, $CDCl_3$) δ 7.09 (d, *J* = 1.7 Hz, 2H), 7.06 (d, *J* = 1.7 Hz, 2H), 6.84 (s, 2H), 4.47 (s, 2H), 2.79 (s, 4H), 2.56 (tt, *J* = 11.8, 3.4 Hz, 2H), 2.47 – 2.41 (m, 2H), 2.42 – 2.35 (m, 2H), 2.29 (ddt, *J* = 15.1, 12.0, 3.5 Hz, 2H), 2.00 (d, *J* = 11.4 Hz, 4H), 1.93 – 1.88 (m, 4H), 1.84 – 1.68 (m, 24H), 1.57 (dt, *J* = 8.2, 4.1 Hz, 4H), 1.52 – 1.43 (m, 8H), 1.46 – 1.29 (m, 14H), 1.28 – 1.06 (m, 10H), 0.93 (dt, *J* = 9.2, 3.1 Hz, 2H). ^{13}C NMR (151 MHz, $CDCl_3$) δ 148.50, 147.16, 146.67, 146.28, 135.45, 132.00, 131.23, 129.14, 124.19, 122.00, 121.95, 119.99, 44.80, 41.77, 41.45, 34.75, 34.53, 34.47, 34.46, 34.30, 33.94, 29.70, 29.21, 27.07, 27.03, 26.99, 26.94, 26.81, 26.30, 26.16, 23.26, 23.24. HRMS (ESI) m/z $[M+Na]^+$ calc'd for $C_{68}H_{90}O_2Na$ 961.6809, found 961.6833.

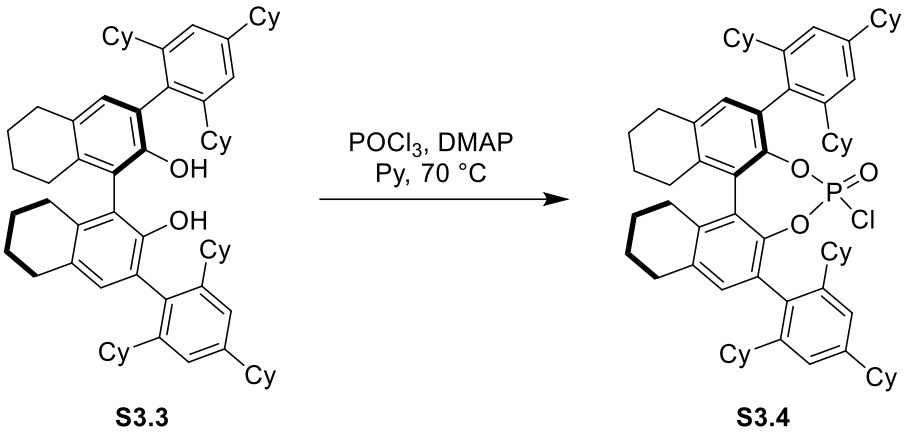

S3.4. To a stirred solution of **S3.3** (0.700 g, 0.74 mmol) and DMAP (0.023 g, 0.19 mmol) in anhydrous pyridine was added fleshly distilled phosphoryl chloride (0.17 mL, 1.83 mmol) dropwise over 3 min. The yellow solution was then stirred for 24 h at 70 °C. The reaction was allowed to cool to r.t. and DCM (50 mL) was added. The reaction mixture was washed with water (3 x 50 mL), dried over $MgSO_4$, filtered and concentrated under reduced pressure. The residual pyridine was removed by co-evaporation with *n*-heptane. The crude white solid was purified by column chromatography (hex/DCM 90:10 to DCM) to afford **S3.4** as white solid (0.555 g, 73%). ^{1}H NMR (400 MHz, $CDCl_3$) δ 7.04 (d, *J* = 5.9 Hz, 2H), 7.00 (d, *J* = 3.1 Hz, 2H), 6.95 (d, *J* = 2.8 Hz, 2H), 2.98 – 2.65 (m, 6H), 2.56 – 2.10 (m, 8H), 2.09 – 1.54 (m, 40H), 1.50 – 1.37 (m, 12H), 1.35 – 1.16 (m, 10H), 1.12 – 1.00 (m, 4H), 0.93 (tdd, *J* = 16.5, 11.1, 6.8 Hz, 2H). ^{13}C NMR (101 MHz, $CDCl_3$) δ 147.23, 147.07, 146.59, 145.99, 145.24, 145.19, 144.15, 144.04, 143.75, 143.64, 136.83, 136.71, 135.01, 134.64, 133.14, 132.89, 131.18, 130.64, 129.97, 128.93, 126.09, 126.04, 122.50, 122.31, 121.31, 44.71, 44.60, 42.44, 42.07, 41.98, 37.81, 36.89, 35.20, 34.77, 34.52, 34.44, 34.36, 34.28, 33.78, 33.56, 32.83, 29.09, 28.97, 27.76, 27.72, 27.54, 27.40, 27.18, 27.03, 26.93, 26.80, 26.68, 26.43, 26.29, 22.75, 22.64, 22.57. ^{31}P NMR (162 MHz, $CDCl_3$) δ 5.55. HRMS (ESI) m/z $[M+Na]^+$ calc'd for $C_{68}H_{88}O_3ClNaP$ 1041.6052, found 1041.6077.

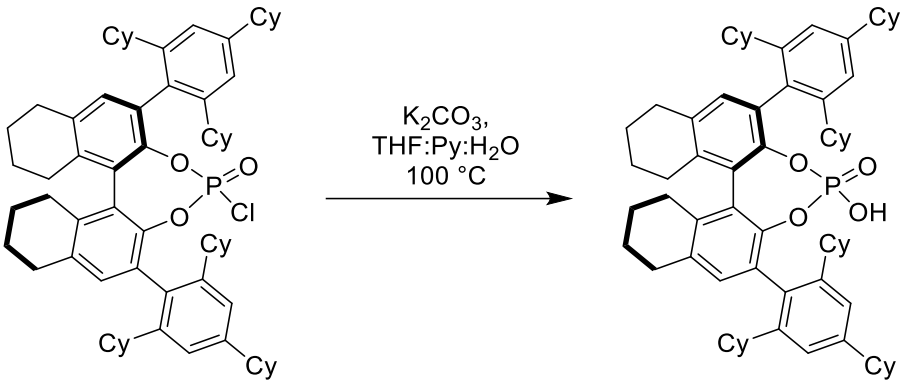

S3.4 (*R*)-H8-TCYP (**3.3j**)

3.3j. To a stirred solution of **S3.4** (0.555 g, 0.54 mmol) in THF:pyridine:H_2O (2:1:1, 48 mL) was added K_2CO_3 (0.301 g, 2.18 mmol). The reaction mixture was stirred for 48 h at 90 °C, after which a ^{31}P NMR aliquot indicated total consumption of the starting material (^{31}P NMR shows a singlet at δ 3.21 ppm). HCl (12M, 10 mL) was added dropwise and the reaction was allowed to cool to r.t. The layers were separated, and the aqueous phase extracted with DCM (3 x 50 mL). The combined organic phases were washed once with HCl (12M, 100 mL), dried over $MgSO_4$, filtered and concentrated under reduced pressure. The crude solid was triturated 3 times with MeCN and filtered *in vacuo* to afford **3.3j** as a white solid (0.350 g, 64%). ^{1}H NMR (500 MHz, $CDCl_3$) δ 6.89 – 6.81 (m, 6H), 2.77 (dtd, *J* = 34.7, 17.7, 17.2, 10.1 Hz, 6H), 2.43 (d, *J* = 10.4 Hz, 2H), 2.32 (d, *J* = 15.8 Hz, 2H), 2.15 (t, *J* = 12.2 Hz, 4H), 1.92 – 1.71 (m, 20H), 1.62 (t, *J* = 15.7 Hz, 12H), 1.44 (dt, *J* = 32.4, 8.2 Hz, 12H), 1.32 – 1.09 (m, 16H), 0.93 (tt, *J* = 26.2, 15.0 Hz, 8H). ^{13}C NMR (151 MHz, $CDCl_3$) δ 146.38, 145.75, 144.78, 144.72, 136.05, 133.19, 132.13, 129.42, 126.63, 122.15, 121.33, 44.67, 41.82, 41.63, 37.04, 34.90, 34.60, 34.18, 33.42, 32.71, 29.00, 27.86, 27.39, 27.19, 27.15, 27.13, 26.83, 26.68, 26.43, 26.38, 26.24, 22.94, 22.82. ^{31}P NMR (162 MHz, $CDCl_3$) δ -1.10. Spectral data are in accordance with literature.[13]

<u>*Synthesis of BINAM-derived phosphoric acids*</u>

BINAM-derived phosphoric acids were synthesized analogously to literature reports.[20]

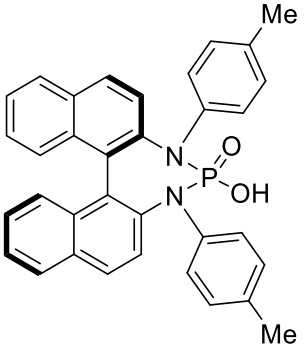

^{1}H NMR (600 MHz, DMSO-d_6) δ 8.01 – 8.79 (m, 4H), 7.50 – 7.47 (m, 2H), 7.37 – 7.34 (m, 2H), 7.29 – 7.25 (m, 4H), 6.94 – 6.92 (m, 4H), 6.84 – 6.82 (m, 4H), 2.12 (d, *J* = 3.4 Hz, 6H). ^{13}C NMR (151 MHz, DMSO-d_6) δ 142.24 (d, $J_{C\text{-}P}$ = 7.3 Hz), 141.13, 133.23, 132.29, 131.83, 130.59, 130.44, 129.49, 128.81, 127.26, 126.96, 126.93, 126.23, 124.39 (d, $J_{C\text{-}P}$ = 3.8 Hz), 20.65. ^{31}P NMR (243

MHz, DMSO-d_6) δ 8.56. HRMS (ESI) m/z [M]$^-$ calc'd for $C_{34}H_{26}N_2O_2P$ 525.1737, found 527.1732.

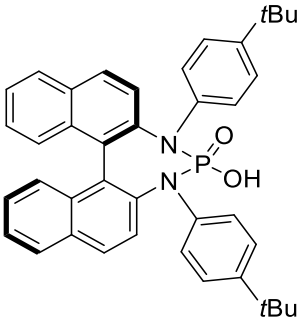

^{1}H NMR (600 MHz, DMSO-d_6) δ 8.03 (dd, J = 8.5, 5.7 Hz, 4H), 7.53 (t, J = 7.5 Hz, 2H), 7.41 (t, J = 7.7 Hz, 2H), 7.31 (dd, J = 15.7, 8.7 Hz, 4H), 7.14 (d, J = 8.4 Hz, 4H), 6.86 (d, J = 8.4 Hz, 4H), 1.15 (s, 18H). ^{13}C NMR (126 MHz, DMSO-d_6) δ 145.91, 141.81 (d, $J_{C\text{-}P}$ = 7.6 Hz), 140.61, 131.88, 131.52, 130.41, 130.16, 128.46, 126.94, 126.80, 126.54, 125.91, 125.63, 125.39, 123.45 (d, $J_{C\text{-}P}$ = 3.8 Hz), 118.71, 33.96, 31.11. ^{31}P NMR (162 MHz, DMSO-d_6) δ 7.99. HRMS (ESI) m/z [M]$^-$ calc'd for $C_{40}H_{38}N_2O_2P$ 609.2676, found 609.2673.

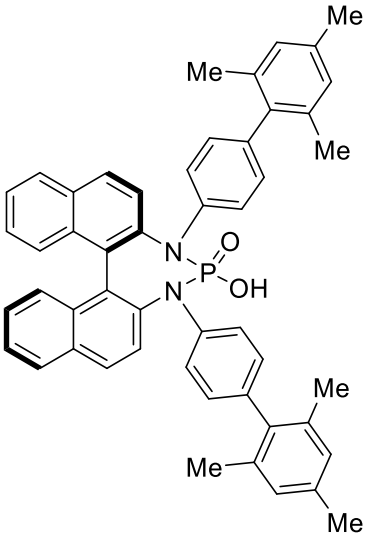

^{1}H NMR (600 MHz, DMSO-d_6) δ 8.08 (dd, J = 8.8, 3.8 Hz, 2H), 8.01 (dd, J = 8.6, 3.8 Hz, 2H), 7.50 (dd, J = 8.9, 5.1 Hz, 2H), 7.42 – 7.24 (m, 6H), 7.08 – 6.98 (m, 4H), 6.92 – 6.85 (m, 4H), 6.82 (d, J = 3.8 Hz, 4H), 2.18 (d, J = 3.8 Hz, 6H), 1.81 (d, J = 3.9 Hz, 12H). ^{13}C NMR (151 MHz, DMSO-d_6) δ 143.25 (d, $J_{C\text{-}P}$ = 7.1 Hz), 141.02, 138.26, 136.16, 136.00, 135.56, 132.32, 131.93, 130.78, 130.72, 129.76, 128.83, 128.26, 127.35, 126.97, 126.93, 126.35, 123.98 (d, $J_{C\text{-}P}$ = 4.1 Hz), 20.89, 1.56. ^{13}C NMR (151 MHz, DMSO-d_6) δ ^{31}P NMR (243 MHz, DMSO-d_6) δ 8.58. HRMS (ESI) m/z [M]$^-$ calc'd for $C_{50}H_{42}N_2O_2P$ 733.2989, found 733.2979.

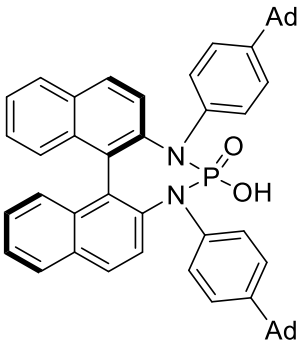

^{1}H NMR (400 MHz, DMSO-d_6) δ 8.03 (dd, J = 8.6, 3.7 Hz, 4H), 7.53 (t, J = 7.4 Hz, 2H), 7.40 (t, J = 7.7 Hz, 2H), 7.31 (dd, J = 13.2, 8.6 Hz, 4H), 7.12 (d, J = 8.3 Hz, 4H), 6.88 (d, J = 8.3 Hz, 4H), 1.99 – 1.96 (m, 6H), 1.82 – 1.55 (m, 24H). ^{13}C NMR (126 MHz, DMSO-d_6) δ 146.66, 142.25, 142.20, 141.01, 132.30, 131.94, 130.79, 130.59, 128.89, 127.37, 127.20, 126.99, 126.34, 125.38, 123.95, 42.95, 36.55, 35.73, 28.69. ^{31}P NMR (162 MHz, DMSO-d_6) δ 8.09. HRMS (ESI) m/z $[M]^-$ calc'd for $C_{52}H_{50}N_2O_2P$ 765.3615, found 765.3597.

*General procedure for Heck-Matsuda arylation of **3.1a**.*

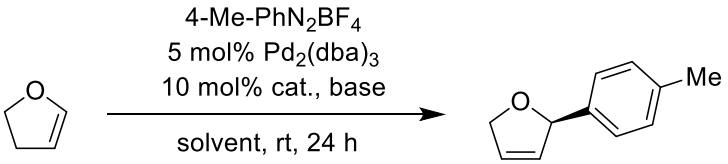

A one-dram vial was charged with **3.1a** (1 equiv.), catalyst (0.10 equiv.), and base (2 equiv.). Solvent was added, and the suspension was stirred vigorously for 10 minutes at room temperature. Aryldiazonium tetrafluoroborate (1.4 equiv.) and Pd_2dba_3 (0.05 equiv.) were then added, and the mixture was stirred vigorously for 24 hours at r.t. The crude reaction mixture was then diluted with diethyl ether (1 mL) and filtered to remove solid precipitates. The mixture was concentrated *in vacuo* and purified by preparatory TLC. NMR spectra of arylated products match those reported in literature.[20]

*General procedure for Heck-Matsuda arylation of **3.3a**.*

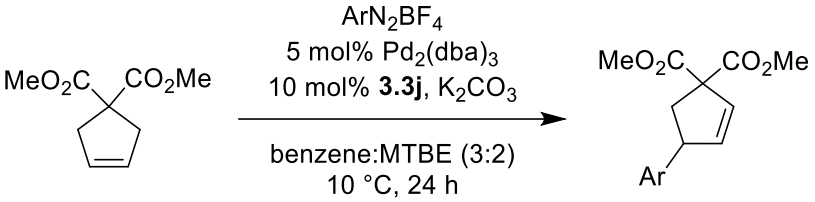

A one-dram vial was charged with **3.3a** (1 equiv., 0.054 mmol), **3.3j** (0.10 equiv.), and K_2CO_3 (2 equiv.). Benzene:MTBE (3:2; 0.03M, 1.6 mL) was added, and the suspension was stirred vigorously for 10 minutes at room temperature. Aryldiazonium tetrafluoroborate (1.4 equiv.) and Pd_2dba_3 (0.05 equiv.) were then added, and the mixture was stirred vigorously for 24 hours at 10 °C. The crude reaction mixture was then diluted with diethyl ether (1 mL) and filtered to remove solid precipitates. The mixture was concentrated *in vacuo* and purified by flash column

chromatography using a 1.0 x 20 cm column (hex:EtOAc 98:02 to 95:05) to afford the desired product.

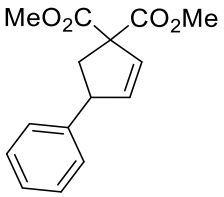

3.4a. Isolated as a colorless oil (82% yield). ^{1}H NMR (600 MHz, $CDCl_3$) δ 7.32 (t, *J* = 7.6 Hz, 2H), 7.23 (t, *J* = 7.4 Hz, 1H), 7.21 – 7.17 (m, 2H), 6.03 (s, 2H), 4.13 (t, *J* = 7.9 Hz, 1H), 3.77 (d, *J* = 6.9 Hz, 6H), 3.15 (dd, *J* = 13.8, 8.3 Hz, 1H), 2.20 (dd, *J* = 13.8, 7.5 Hz, 1H). ^{13}C NMR (151 MHz, CDCl3) δ 170.41, 169.98, 142.58, 137.85, 128.48, 127.39, 126.12, 125.46, 65.47, 51.65, 51.52, 49.40, 40.44. HRMS (EI) m/z $[M]^+$ calc'd for $C_{15}H_{16}O_4$ 260.1049, found 260.1053. HPLC (CHIRALPAK AD-H column) 99:01 (hexane/*i*PrOH) 0.5 mL/min; T_{major} (17.7 min), T_{minor} (20.2 min); 85% ee.

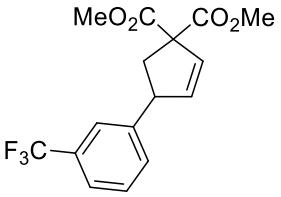

3.4b. Isolated as a yellow oil (70% yield).[3] ^{1}H NMR (600 MHz, $CDCl_3$) δ 7.48 (d, *J* = 7.8 Hz, 1H), 7.46 – 7.39 (m, 2H), 7.37 (d, *J* = 7.8 Hz, 1H), 6.08 (dd, *J* = 5.6, 2.6 Hz, 1H), 6.00 (dd, *J* = 5.6, 2.0 Hz, 1H), 4.23 – 4.12 (m, 1H), 3.76 (d, *J* = 6.7 Hz, 6H), 3.16 (dd, *J* = 13.8, 8.4 Hz, 1H), 2.18 (dd, *J* = 13.8, 7.2 Hz, 1H). ^{13}C NMR (151 MHz, $CDCl_3$) δ 171.31, 170.90, 144.69, 137.95, 130.78, 130.74, 130.73, 130.67, 129.04, 124.04 (q, $J_{C\text{-}F}$ = 3.6 Hz), 123.55 (q, $J_{C\text{-}F}$ = 3.8 Hz), 66.67, 52.95, 52.83, 50.37, 41.45. ^{19}F NMR (376 MHz, $CDCl_3$) δ -61.80. HPLC (CHIRALPAK AD-H column) 99:01 (hexane/*i*PrOH) 0.5 mL/min; T_{major} (15.6 min), T_{minor} (16.5 min); 84% ee.

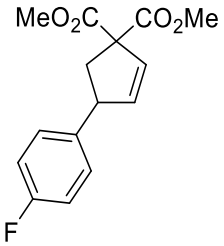

3.4c. Isolated as a yellow oil (81% yield). ^{1}H NMR (600 MHz, $CDCl_3$) δ 7.13 (dd, *J* = 8.5, 5.3 Hz, 2H), 6.98 (t, *J* = 8.5 Hz, 2H), 6.02 (dd, *J* = 5.6, 2.5 Hz, 1H), 5.97 (dd, *J* = 5.6, 1.9 Hz, 1H), 4.14 – 4.04 (m, 1H), 3.76 (d, *J* = 4.7 Hz, 6H), 3.12 (dd, *J* = 13.8, 8.3 Hz, 1H), 2.14 (dd, *J* = 13.8, 7.3 Hz, 1H). ^{13}C NMR (151 MHz, $CDCl_3$) δ 171.54, 171.09, 162.50, 160.88, 139.49, 138.82, 129.87, 128.79, 115.42, 115.28, 66.62, 52.88, 52.77, 49.87, 41.70. ^{19}F NMR (376 MHz, $CDCl_3$) δ -115.58 – -115.66 (m). HRMS (EI) m/z $[M]^+$ calc'd for $C_{15}H_{15}O_4F$ 279.0988, found 279.0989. HPLC (CHIRALPAK AD-H column) 99:01 (hexane/*i*PrOH) 0.5 mL/min; T_{major} (19.9 min), T_{minor} (22.5 min); 85% ee.

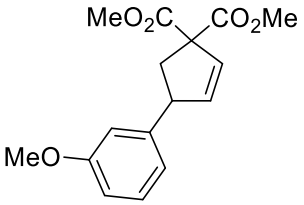

3.4d. Isolated as a yellow oil (81% yield). ^{1}H NMR (600 MHz, $CDCl_3$) δ 7.22 (t, *J* = 7.9 Hz, 1H), 6.80 – 6.74 (m, 2H), 6.73 (t, *J* = 2.1 Hz, 1H), 6.01 (s, 2H), 4.09 (t, *J* = 7.8 Hz, 1H), 3.79 (s, 3H), 3.76 (d, *J* = 6.7 Hz, 6H), 3.12 (dd, *J* = 13.8, 8.3 Hz, 1H), 2.19 (dd, *J* = 13.8, 7.4 Hz, 1H). ^{13}C NMR (151 MHz, $CDCl_3$) δ 171.58, 171.18, 159.85, 145.45, 138.91, 129.75, 129.57, 119.67, 113.00, 112.06, 66.65, 55.18, 52.86, 52.73, 50.62, 41.50. HRMS (EI) m/z $[M]^+$ calc'd for $C_{16}H_{18}O_5$ 291.1188, found 291.1191. HPLC (CHIRALPAK AD-H column) 99:01 (hexane/*i*PrOH) 0.5 mL/min; T_{major} (27.3 min), T_{minor} (32.2 min); 79% ee.

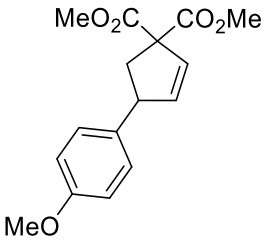

3.4e. Isolated as a colorless oil (73% yield).[3] ^{1}H NMR (600 MHz, $CDCl_3$) δ 7.11 (d, *J* = 8.6 Hz, 2H), 6.90 – 6.78 (m, 2H), 6.00 (s, 2H), 4.08 (t, *J* = 7.8 Hz, 1H), 3.80 (s, 3H), 3.77 (d, *J* = 3.9 Hz, 6H), 3.11 (dd, *J* = 13.8, 8.2 Hz, 1H), 2.16 (dd, *J* = 13.7, 7.4 Hz, 1H). ^{13}C NMR (151 MHz, $CDCl_3$) δ 171.70, 171.25, 158.39, 139.40, 135.91, 129.34, 128.29, 113.99, 66.62, 55.27, 52.83, 52.72, 49.84, 41.79. HPLC (CHIRALPAK AD-H column) 99:01 (hexane/*i*PrOH) 0.5 mL/min; T_{major} (31.4 min), T_{minor} (33.5 min); 82% ee.

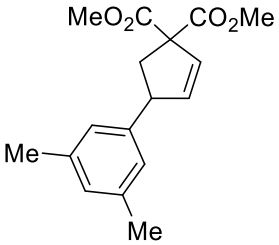

3.4f. Isolated as a yellow oil (79% yield). ^{1}H NMR (600 MHz, $CDCl_3$) δ 6.88 (s, 1H), 6.81 (s, 2H), 6.02 (s, 2H), 4.05 (t, *J* = 7.9 Hz, 1H), 3.77 (d, *J* = 1.4 Hz, 6H), 3.12 (dd, *J* = 13.7, 8.2 Hz, 1H), 2.30 (s, 6H), 2.16 (dd, *J* = 13.7, 7.8 Hz, 1H). ^{13}C NMR (151 MHz, $CDCl_3$) δ 171.69, 171.21, 143.68, 139.35, 138.13, 129.43, 128.30, 125.12, 66.63, 52.83, 52.68, 50.43, 41.74, 21.24. HRMS (EI) m/z $[M]^+$ calc'd for $C_{17}H_{20}O_4$ 288.1362, found 288.1364. HPLC (CHIRALPAK AD-H column) 99:01 (hexane/*i*PrOH) 0.5 mL/min; T_{major} (13.1 min), T_{minor} (15.3 min); 82% ee.

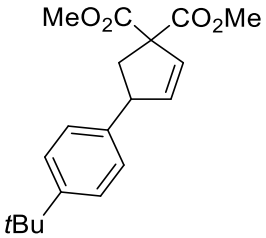

3.4g. Isolated as a yellow solid (82% yield). ^{1}H NMR (400 MHz, $CDCl_3$) δ 7.39 – 7.30 (m, 2H), 7.18 – 7.08 (m, 2H), 6.06 – 5.97 (m, 2H), 4.11 (t, *J* = 7.9 Hz, 1H), 3.80 – 3.73 (m, 6H), 3.13 (dd, *J* = 13.8, 8.2 Hz, 1H), 2.19 (dd, *J* = 13.8, 7.6 Hz, 1H), 1.32 (s, 9H). ^{13}C NMR (151 MHz, $CDCl_3$) δ 171.69, 171.26, 149.54, 140.74, 139.33, 129.41, 126.98, 125.48, 66.66, 52.85, 52.71, 50.12, 41.63, 34.41, 31.35. HRMS (EI) m/z $[M]^+$ calc'd for $C_{19}H_{24}O_4$ 316.1675, found 316.1679. HPLC (CHIRALPAK OD-H column) 99:01 (hexane/*i*PrOH) 0.5 mL/min; T_{minor} (18.3 min), T_{major} (20.4 min); -87% ee.

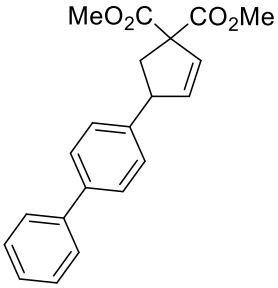

3.4h. Isolated as a yellow solid (66% yield).[3] ^{1}H NMR (600 MHz, $CDCl_3$) δ 7.60 – 7.56 (m, 2H), 7.56 – 7.51 (m, 2H), 7.43 (t, *J* = 7.5 Hz, 2H), 7.34 (t, *J* = 7.5 Hz, 1H), 7.29 – 7.22 (m, 2H), 6.05 (s, 2H), 4.17 (t, *J* = 7.8 Hz, 1H), 3.78 (dd, *J* = 5.3, 1.3 Hz, 6H), 3.17 (dd, *J* = 13.8, 8.2 Hz, 1H), 2.24 (dd, *J* = 13.7, 7.4 Hz, 1H). ^{13}C NMR (151 MHz, $CDCl_3$) δ 171.62, 171.19, 142.88, 140.88, 139.71, 139.00, 129.81, 128.73, 127.76, 127.36, 127.16, 127.02, 66.71, 52.88, 52.76, 50.28, 41.62. HPLC (CHIRALPAK AD-H column) 99:01 (hexane/*i*PrOH) 0.5 mL/min; T_{major} (34.8 min), T_{minor} (38.2 min); 85% ee.

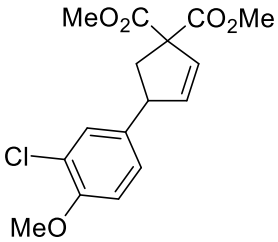

3.4i. Isolated as a colorless oil (80% yield).[3] ^{1}H NMR (600 MHz, $CDCl_3$) δ 7.18 (t, *J* = 2.0 Hz, 1H), 7.04 (dt, *J* = 8.5, 2.1 Hz, 1H), 6.86 (dd, *J* = 8.5, 1.8 Hz, 1H), 6.02 (dt, *J* = 5.6, 2.2 Hz, 1H), 5.96 (dt, *J* = 5.5, 1.9 Hz, 1H), 4.09 – 4.00 (m, 1H), 3.88 (d, *J* = 1.8 Hz, 3H), 3.77 (d, *J* = 1.8 Hz, 6H), 3.10 (ddd, *J* = 13.8, 8.3, 1.9 Hz, 1H), 2.14 (ddd, *J* = 13.7, 7.3, 1.9 Hz, 1H).^{13}C NMR (151 MHz, $CDCl_3$) δ 171.49, 171.07, 153.79, 138.61, 137.02, 130.00, 129.09, 126.52, 122.51, 112.21, 66.59, 56.20, 52.88, 52.78, 49.57, 41.60. HPLC (CHIRALPAK AD-H column) 99:01 (hexane/*i*PrOH) 0.5 mL/min; T_{major} (33.7 min), T_{minor} (35.8 min); 80% ee.

*General procedure for Heck-Matsuda arylation of **3.9a***

A one-dram vial was charged with **3.9a** (1 equiv. 0.025 mmol), **3.3r** (0.10 equiv.), and Na_2HPO_4 (2 equiv.). MTBE (0.05M) was added, and the suspension was stirred for 10 minutes. Aryldiazonium tetrafluoroborate (1.5 equiv.) and Pd_2dba_3 (0.05 equiv.) were then added, and the mixture was stirred vigorously for 24 hours. The crude reaction mixture was then diluted with diethyl ether (1 mL) and filtered to remove solid precipitates. The mixture was concentrated *in vacuo* and purified by flash column chromatography using a pipette column (ether/hex) to afford the desired product.

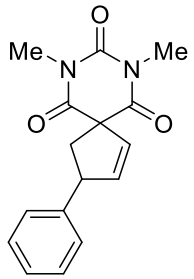

3.10a. Isolated as a white solid (70% yield). ^{1}H NMR (300 MHz, $CDCl_3$) δ 7.41 – 7.19 (m, 5H), 6.14 (dd, *J* = 5.3, 2.0 Hz, 1H), 5.66 (dd, *J* = 5.3, 2.5 Hz, 1H), 4.41 – 4.34 (m, 1H), 3.34 (d, *J* = 4.6 Hz, 5H), 2.97 (dd, *J* = 13.3, 8.5 Hz, 1H), 2.57 (dd, *J* = 13.3, 7.6 Hz, 1H). ^{13}C NMR (151 MHz, $CDCl_3$) δ 170.76, 170.67, 151.35, 143.30, 141.85, 129.15, 128.66, 127.69, 126.90, 64.92, 51.85, 42.41, 29.18, 29.06. HRMS (EI) m/z $[M]^+$ calc'd for $C_{16}H_{16}N_2O_3$ 284.1161, found 284.1165. HPLC (CHIRALPAK AD-H column) 90:10 (hexane/*i*PrOH) 1mL/min; T_{minor} (9.5 min), T_{major} (16.7 min); 86% ee.

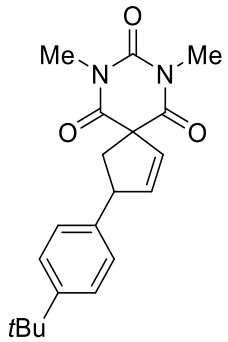

3.10b. Isolated as a white solid (92% yield). ^{1}H NMR (600 MHz, $CDCl_3$) δ 7.36 (d, *J* = 7.7 Hz, 2H), 7.28 – 7.20 (m, 2H), 6.15 – 6.14 (m, 1H), 5.66 – 5.64 (m, 1H), 4.42 – 4.28 (m, 1H), 3.34 (d, *J* = 9.9, 6H), 3.02 – 2.83 (m, 1H), 2.59 – 2.55 (m, 1H), 1.31 (s, 9H). ^{13}C NMR (151 MHz, $CDCl_3$) δ 170.83, 170.72, 151.38, 149.79, 142.07, 140.24, 128.91, 127.34, 125.55, 64.91, 51.37, 42.45, 34.42, 31.32, 29.17, 29.05. HRMS (EI) m/z $[M]^+$ calc'd for $C_{20}H_{24}N_2O_3$ 340.1787, found

340.1791. HPLC (CHIRALPAK AD-H column) 90:10 (hexane/*i*PrOH) 1mL/min; T_{minor} (7.2 min), T_{major} (15.8 min); 92% ee.

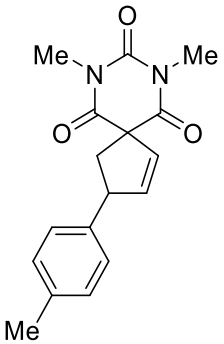

3.10c. Isolated as a white solid (67% yield). ^{1}H NMR (300 MHz, $CDCl_3$) δ 7.19 (d, *J* = 8.1 Hz, 2H), 7.14 (d, *J* = 8.1 Hz, 2H), 6.12 (dd, *J* = 5.3, 2.0 Hz, 1H), 5.64 (dd, *J* = 5.3, 2.6 Hz, 1H), 4.37 – 4.30 (m, 1H), 3.34 (d, *J* = 4.9 Hz, 6H), 2.94 (dd, *J* = 13.2, 8.5 Hz, 1H), 2.54 (dd, *J* = 13.2, 7.7 Hz, 1H), 2.33 (s, 3H). ^{13}C NMR (151 MHz, $CDCl_3$) δ 170.79, 170.71, 151.37, 142.07, 140.27, 136.51, 129.32, 128.92, 127.57, 64.90, 51.45, 42.52, 29.16, 29.04, 20.99. HRMS (EI) m/z $[M]^+$ calc'd for $C_{17}H_{18}N_2O_3$ 298.1317, found 298.1322. HPLC (CHIRALPAK AD-H column) 90:10 (hexane/*i*PrOH) 1mL/min; T_{minor} (9.1 min), T_{major} (13.6 min); 90% ee.

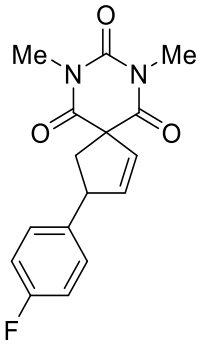

3.10d. Isolated as a white solid (79% yield). ^{1}H NMR (300 MHz, $CDCl_3$) δ 7.46 – 7.18 (m, 2H), 7.10 – 6.79 (m, 2H), 6.09 (dd, *J* = 5.3, 2.0 Hz, 1H), 5.66 (dd, *J* = 5.3, 2.6 Hz, 1H), 4.50 – 4.13 (m, 1H), 3.34 (d, *J* = 5.1 Hz, 6H), 2.97 (dd, *J* = 13.3, 8.6 Hz, 1H), 2.51 (dd, *J* = 13.3, 7.5 Hz, 1H). ^{13}C NMR (151 MHz, $CDCl_3$) δ 170.66, 170.63, 161.84 (d, $J_{C\text{-}F}$ = 245.1 Hz), 151.28, 141.57, 139.04 (d, $J_{C\text{-}F}$ = 3.1 Hz), 129.31, 129.17 (d, $J_{C\text{-}F}$ = 8.0 Hz), 115.43 (d, $J_{C\text{-}F}$ = 21.3 Hz), 64.90, 51.13, 42.31, 29.19, 29.07. ^{19}F NMR (376 MHz, $CDCl_3$) δ -115.20 – -115.27 (m). HRMS (EI) m/z $[M]^+$ calc'd for $C_{16}H_{15}FN_2O_3$ 302.1067, found 302.1072. HPLC (CHIRALPAK AD-H column) 90:10 (hexane/*i*PrOH) 1mL/min; T_{minor} (9.6 min), T_{major} (18.2 min); 85% ee.

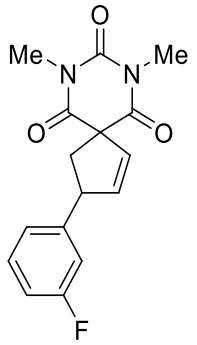

3.10e. Isolated as a white solid (94% yield). ^{1}H NMR (300 MHz, $CDCl_3$) δ 7.34 – 7.26 (m, 1H), 7.10 – 7.06 (m, 1H), 7.05 – 7.00 (m, 1H), 6.97 – 6.90 (m, 1H), 6.11 (dd, *J* = 5.3, 2.0 Hz, 1H), 5.68 (dd, *J* = 5.3, 2.6 Hz, 1H), 4.40 – 4.33 (m, 1H), 3.34 (d, *J* = 5.4 Hz, 6H), 2.97 (dd, *J* = 13.4, 8.6 Hz, 1H), 2.55 (dd, *J* = 13.3, 7.5 Hz, 1H). ^{13}C NMR (151 MHz, $CDCl_3$) δ 170.58, 170.45, 163.02 (d, $J_{C\text{-}F}$ = 246.1 Hz), 151.27, 145.91 (d, $J_{C\text{-}F}$ = 6.8 Hz), 141.07, 130.08 (d, $J_{C\text{-}F}$ = 8.3 Hz), 129.73, 123.29 (d, $J_{C\text{-}F}$ = 2.9 Hz), 114.61 (d, $J_{C\text{-}F}$ = 21.5 Hz), 113.81 (d, $J_{C\text{-}F}$ = 21.1 Hz), 64.90, 51.52, 41.92, 29.21, 29.08. ^{19}F NMR (376 MHz, $CDCl_3$) δ -111.96 – -112.02 (m). (EI) m/z $[M]^+$ calc'd for $C_{16}H_{15}FN_2O_3$ 302.1067, found 302.1072. HPLC (CHIRALPAK AD-H column) 90:10 (hexane/*i*PrOH) 1mL/min; T_{minor} (10.5 min), T_{major} (16.4 min); 84% ee.

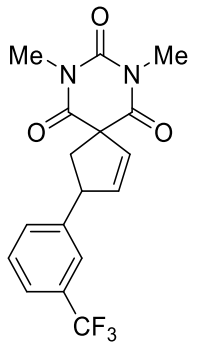

3.10f. Isolated as a clear film (94% yield). ^{1}H NMR (300 MHz, $CDCl_3$) δ 7.62 – 7.36 (m, 4H), 6.12 (dd, *J* = 5.3, 2.0 Hz, 1H), 5.71 (dd, *J* = 5.3, 2.6 Hz, 1H), 4.47 – 4.44 (m, 1H), 3.34 (d, *J* = 5.1 Hz, 6H), 3.09 – 2.90 (m, 1H), 2.56 (dd, *J* = 13.3, 7.5 Hz, 1H). ^{13}C NMR (151 MHz, $CDCl_3$) δ 170.48, 170.37, 151.24, 144.31, 140.77, 131.08, 130.15, 129.18, 124.95, 124.53 (q, $J_{C\text{-}F}$ = 3.7 Hz), 123.82 (q, $J_{C\text{-}F}$ = 3.6 Hz), 123.15, 64.94, 51.61, 41.88, 29.23, 29.11. ^{19}F NMR (376 MHz, $CDCl_3$) δ -61.74. HRMS (EI) m/z $[M]^+$ calc'd for $C_{17}H_{15}F_3N_2O_3$ 352.1035, found 352.1038. HPLC (CHIRALPAK AD-H column) 90:10 (hexane/*i*PrOH) 1mL/min; T_{minor} (8.5 min), T_{major} (8.9 min); 90% ee.

*<u>Synthesis of **3.11a**</u>*

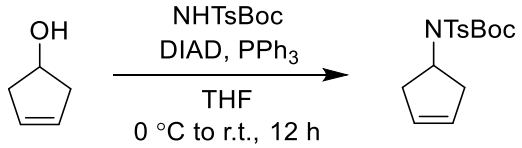

3.11a. To a solution of 3-cyclopentene-1-ol (200 mg, 2.38 mmol), triphenylphosphine (809 mg, 3.09 mmol), and NHTsBoc (838 mg, 3.09 mmol) in THF (15 mL) was added DIAD (608 µL, 3.09

mmol) at 0 ˚C. The reaction was warmed to room temperature and stirred for 12 hours. The crude reaction mixture was concentrated and loaded directly onto a column and purified by flash chromatography (EtOAc/hex) to afford the desired product as a white solid (550 mg, 69%). ^{1}H NMR (600 MHz, $CDCl_3$) δ 7.76 (d, *J* = 8.0 Hz, 2H), 7.30 (d, *J* = 8.0 Hz, 2H), 5.68 (s, 2H), 5.36 – 5.22 (m, 1H), 2.73 – 2.70 (m, 4H), 2.44 (s, 3H), 1.32 (s, 9H). ^{13}C NMR (151 MHz, $CDCl_3$) δ 150.46, 143.85, 137.72, 129.25, 128.74, 127.52, 84.15, 55.66, 37.67, 27.91, 21.56. HRMS (ESI) m/z $[M+Na]^+$ calc'd for $C_{17}H_{23}NO_4SNa$ 360.1240, found 360.1237.

*General procedure for Heck-Matsuda arylation of **3.11a***

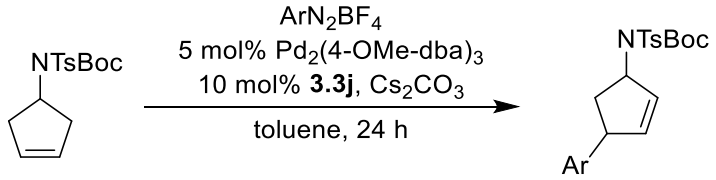

A one-dram vial was charged with **3.11a** (1 equiv.), **3.3j** (0.10 equiv.), and Cs_2CO_3 (2 equiv.). Toluene (0.05M) was added, and the suspension was stirred for 10 minutes. Aryldiazonium tetrafluoroborate (1.5 equiv.) and Pd_2(4-OMe-dba)$_3$ (0.05 equiv.) were then added, and the mixture was stirred vigorously for 24 hours at r.t. The crude reaction mixture was then diluted with diethyl ether (1 mL) and filtered to remove solid precipitates. The mixture was concentrated *in vacuo* and purified by flash column chromatography using a pipette column (Et_2O/hex) to afford the desired product.

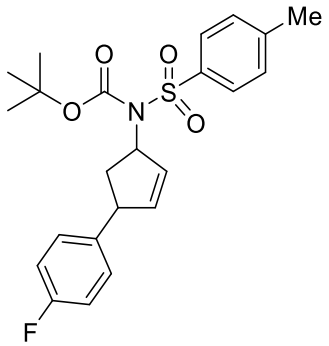

3.12a. Isolated as a clear film (86% yield). ^{1}H NMR (600 MHz, $CDCl_3$) δ 7.78 (d, *J* = 8.3 Hz, 2H), 7.31 (d, *J* = 8.1 Hz, 2H), 7.13 – 7.11 (m, 2H), 6.98 (t, *J* = 8.7 Hz, 2H), 5.97 – 5.91 (m, 1H), 5.89 – 5.79 (m, 2H), 4.24 – 4.22 (m, 1H), 2.63 (ddd, *J* = 14.9, 9.5, 5.2 Hz, 1H), 2.44 (s, 3H), 2.25 (ddd, *J* = 15.3, 7.8, 2.9 Hz, 2H), 1.35 (s, 9H). ^{19}F NMR (376 MHz, $CDCl_3$) δ -116.18. ^{13}C NMR (151 MHz, $CDCl_3$) δ 161.47 (d, $J_{C\text{-}F}$ = 244.4 Hz), 150.44, 143.93, 140.60 (d, $J_{C\text{-}F}$ = 3.2 Hz), 137.81, 136.97, 130.51, 128.52 (d, $J_{C\text{-}F}$ = 7.8 Hz), 129.25, 127.57, 115.28 (d, $J_{C\text{-}F}$ = 21.1 Hz), 84.29, 64.22, 50.21, 38.75, 27.86, 21.55 (one extra resonance). HRMS (ESI) m/z $[M+Na]^+$ calc'd for $C_{23}H_{26}FNO_4SNa$ 454.1459, found 454.1454. HPLC (CHIRALPAK AD-H column) 99:01 (hexane/*i*PrOH) 1mL/min; T_{major} (32.2 min), T_{minor} (26.7 min); 90% ee.

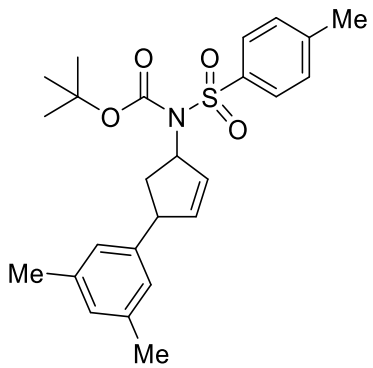

3.12b. ^{1}H NMR (400 MHz, $CDCl_3$) δ 7.80 (d, *J* = 8.1 Hz, 2H), 7.31 (d, *J* = 8.1 Hz, 2H), 6.86 (s, 1H), 6.79 (s, 2H), 5.95 – 5.92 (m, 1H), 5.91 – 5.84 (m, 1H), 5.84 – 5.77 (m, 1H), 4.21 – 4.13 (m, 1H), 2.60 (ddd, *J* = 14.7, 9.5, 6.0 Hz, 1H), 2.45 (s, 3H), 2.31 (m, 7H), 1.36 (s, 9H). ^{13}C NMR (151 MHz, $CDCl_3$) δ 150.50, 144.91, 143.86, 138.10, 137.84, 137.28, 130.14, 129.23, 127.97, 127.60, 124.97, 84.17, 64.49, 50.86, 38.53, 27.87, 21.55, 21.26. HRMS (ESI) m/z $[M+Na]^+$ calc'd for $C_{23}H_{31}NO_4SNa$ 464.1866, found 464.1859. HPLC (CHIRALPAK AD-H column) 99:01 (hexane/*i*PrOH) 1mL/min; T_{major} (15.6 min), T_{minor} (13.4 min); 86% ee.

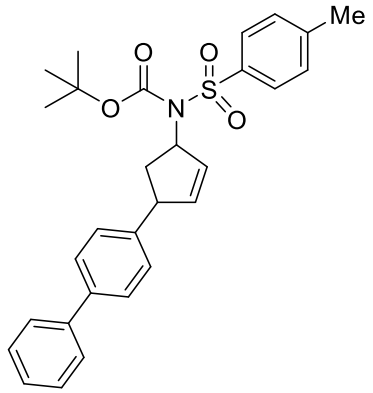

3.12c. Isolated as a clear film (53% yield). ^{1}H NMR (400 MHz, $CDCl_3$) δ 7.88 – 7.81 (m, 2H), 7.66 – 7.61 (m, 2H), 7.61 – 7.55 (m, 2H), 7.53 – 7.43 (m, 2H), 7.42 – 7.33 (m, 3H), 7.32 – 7.26 (m, 2H), 6.06 – 6.03 (m, 1H), 6.01 – 5.92 (m, 1H), 5.91 – 5.89 (m, 1H), 4.42 – 4.22 (m, 1H), 2.71 (ddd, *J* = 13.7, 9.7, 5.4 Hz, 1H), 2.49 (s, 3H), 2.40 (ddd, *J* = 13.7, 9.5, 4.0 Hz, 1H), 1.41 (s, 9H). ^{13}C NMR (151 MHz, $CDCl_3$) δ 150.49, 144.06, 143.90, 140.93, 139.36, 137.83, 137.01, 130.49, 129.25, 128.68, 127.60, 127.59, 127.33, 127.06, 126.99, 84.25, 64.39, 50.63, 38.62, 27.88, 21.56. HRMS (ESI) m/z $[M+Na]^+$ calc'd for $C_{29}H_{31}NO_4SNa$ 512.1866, found 512.1851. HPLC (CHIRALPAK AD-H column) 99:01 (hexane/*i*PrOH) 1mL/min; T_{major} (61.9 min), T_{minor} (42.0 min); 84% ee.

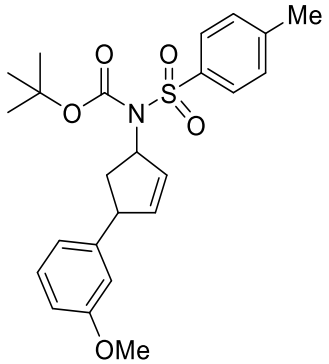

3.12d. Isolated as a clear film (70% yield). ^{1}H NMR (400 MHz, $CDCl_3$) δ 7.86 – 7.76 (m, 2H), 7.41 – 7.32 (m, 2H), 7.27 (t, *J* = 7.9 Hz, 1H), 6.83 – 6.79 (m, 2H), 6.76 (t, *J* = 2.1 Hz, 1H), 6.01 – 5.99 (m, 1H), 5.95 – 5.77 (m, 2H), 4.29 – 4.24 (m, 1H), 3.85 (s, 3H), 2.66 (ddd, *J* = 13.6, 9.6, 5.4 Hz, 1H), 2.48 (s, 3H), 2.35 (ddd, *J* = 13.6, 9.5, 4.0 Hz, 1H), 1.39 (s, 9H). ^{13}C NMR (151 MHz, $CDCl_3$) δ 159.81, 150.47, 146.65, 143.88, 137.82, 136.93, 130.48, 129.55, 129.24, 127.59, 119.54, 112.99, 111.52, 84.22, 64.35, 55.15, 50.99, 38.54, 27.87, 21.55. HRMS (ESI) m/z $[M+Na]^+$ calc'd for $C_{24}H_{29}NO_5SNa$ 466.1659, found 466.1647. HPLC (CHIRALPAK AD-H column) 99:01 (hexane/*i*PrOH) 1mL/min; T_{major} (38.7 min), T_{minor} (36.5 min); 83% ee.

*<u>Synthesis of **3.13a**</u>*

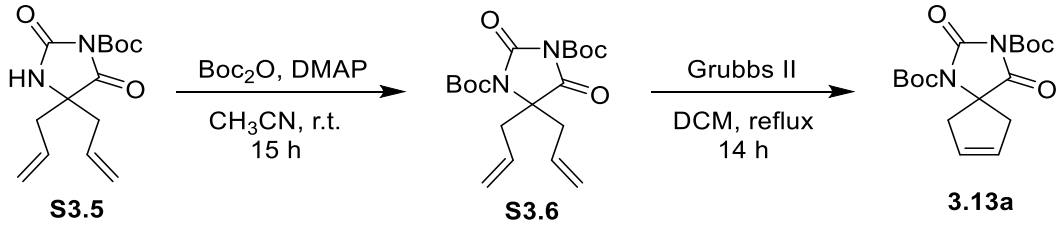

3.13a. To a well stirred solution of Boc_2O (0.935 g, 4.3 mmol) and DMAP (0.024 g, 0.19 mmol) in anhydrous CH_3CN (10 mL) was added a solution of **S3.5**[21,22] (0.55 g, 1.9 mmol) in CH_3CN (10 ml) at r.t. The orange solution was stirred for 15 h. The crude reaction mixture was concentrated and loaded directly onto a column and purified by flash column chromatography (hex:EtOAc 95:5 to 9:1) to afford **S3.6** as a colorless oil (0.50 g, 68%). ^{1}H NMR (400 MHz, $CDCl_3$) δ 5.60 – 5.43 (m, 2H), 5.19 – 5.04 (m, 4H), 2.99 – 2.83 (m, 2H), 2.66 – 2.53 (m, 2H), 1.52 (s, 3H), 1.51 (s, 3H). ^{13}C NMR (101 MHz, $CDCl_3$) δ 169.61, 148.28, 147.60, 144.81, 129.35, 121.34, 86.31, 84.34, 69.10, 58.03, 39.08, 27.80, 27.53, 18.11. HRMS (ESI) m/z $[M+Na]^+$ calc'd for $C_{29}H_{28}O_6N_2Na$ 403.1840, found 403.1841.

To a solution of **S3.6** (0.55 g, 1.4 mmol) in anhydrous DCM (145 mL) was added Grubbs II catalyst (0.061 g, 0.07 mmol) at 40 °C. The solution was stirred and refluxed for 14 h. The solvent was removed and the crude residue was purified by flash chromatography (hex:EtOAc 90:10 to 70:30) to afforded **3.13a** (0.41 g, 80%) as a white solid. ^{1}H NMR (400 MHz, $CDCl_3$) δ 5.73 (s, 2H), 3.03 – 2.87 (m, 4H), 1.59 (s, 9H), 1.53 (s, 9H). ^{13}C NMR (151 MHz, $CDCl_3$) δ 172.06, 147.94, 147.48, 145.11, 127.82, 86.62, 84.89, 67.41, 43.94, 27.99, 27.68. HRMS (ESI) m/z $[M+Na]^+$ calc'd for $C_{17}H_{24}O_6N_2Na$ 375.1527, found 375.1528.

*Procedure for Heck-Matsuda arylation of **3.13**[a]*

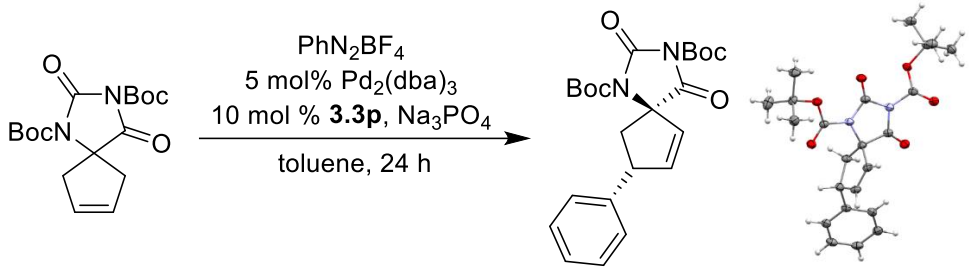

A 20 mL vial was charged with **3.13a** (40.0 mg, 0.11 mmol), **3.3p** (6.9 mg, 0.01 mmol), and Na_3PO_4 (36.0 mg, 0.22 mmol). Toluene (2.3 mL) was added, and the suspension was stirred for 10 minutes. Aryldiazonium tetrafluoroborate (29.0 mg, 0.15 mmol) and Pd_2dba_3 (0.05 equiv.) were then added, and the mixture was stirred vigorously for 24 hours. The crude reaction mixture was then filtered thought a small plug of silica. The mixture was concentrated *in vacuo* and purified by flash column chromatography (*n*-pentane:EtOAc 95:05 to 90:10) to afford the desired product as a white solid (35.5 mg, 73%). ^{1}H NMR (600 MHz, $CDCl_3$) δ 7.38 (d, *J* = 7.5 Hz, 2H), 7.33 (t, *J* = 7.5 Hz, 2H), 7.25 (dd, *J* = 14.4, 7.1 Hz, 1H), 6.24 (dd, *J* = 5.4, 2.1 Hz, 1H), 5.57 (dd, *J* = 5.4, 2.6 Hz, 1H), 4.39 (tt, *J* = 6.1, 2.7 Hz, 1H), 2.83 (dd, *J* = 14.5, 9.0 Hz, 1H), 2.46 (dd, *J* = 14.5, 5.6 Hz, 1H), 1.60 (s, 9H), 1.58 (s, 9H). ^{13}C NMR (151 MHz, $CDCl_3$) δ 170.36, 148.38, 147.42, 145.39, 144.85, 143.14, 128.84, 128.05, 127.04, 126.17, 86.89, 84.91, 52.21, 42.88, 28.18, 27.87. HRMS (ESI) m/z $[M+Na]^+$ calc'd for $C_{21}H_{26}O_5N_5Na$ 451.1826, found 451.1830. HPLC (CHIRALPAK IA column) (hexane/*i*PrOH 98:02) 0.5 mL/min; T_{major} (30.0 min), T_{minor} (27.2 min), 81% ee.

*Synthesis of **3.15a***

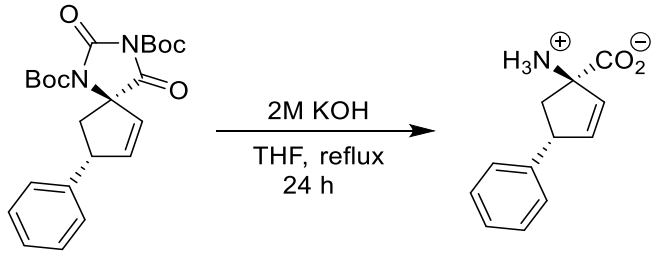

3.15a. A 15 mL round-bottomed flask equipped with a magnetic stirbar was charged with a suspension of the hydantoin **3.14a** (50 mg, 0.16 mmol) in THF (3 mL), and potassium hydroxide (2.0M, 3 mL). The reaction was stirred and refluxed for 24 h. This reaction mixture was cooled at 0 °C, and the pH was adjusted to 7.0 *via* slow addition of 2.0M HCl. The mixture was evaporated to dryness, and the residue was washed 3 times with Et_2O. The solid was solubilized in DCM:MeOH (9:1) and filtered to remove the potassium chloride. The solvent was removed *in vacuo* to afford **3.15a** as a white solid (16 mg, 66%). ^{1}H NMR (600 MHz, CD_3OD) δ 7.42 – 7.15 (m, 5H), 6.42 – 6.27 (m, 1H), 5.94 (dd, *J* = 5.4, 2.6 Hz, 1H), 4.33 (t, *J* = 7.7 Hz, 1H), 2.69 (dd, *J* = 14.8, 8.1 Hz, 1H), 2.51 (dd, *J* = 14.8, 6.9 Hz, 1H). ^{13}C NMR (126 MHz, MeOD) δ 173.13, 146.00, 144.00, 129.82, 129.00, 128.49, 128.12, 71.58, 51.86, 43.89. HRMS (ESI) m/z $[M]^+$ calc'd for $C_{12}H_{14}O_2N$ 204.1019, found 204.1016.

Computational Methods

Computations were performed using Gaussian09 suite of quantum chemical program.[23] The geometries optimization of all stationary points such as transition states, intermediates, substrates and catalysts were carried out in the solvent phase by using the B3LYP-D3 density functional theory[24] using Pople's 6-31G** basis set for all atoms except Pd. The LANL2DZ basis set consisting of an effective core potential (ECP) for 28 core electrons and a double-ζ quality valence basis set for 18 valence electrons was used for palladium.[25] The solvent effects were incorporated using the Cramer−Truhlar continuum solvation model, designated as SMD, that employs quantum mechanical charge density of solutes.[26] Since the reaction was performed in toluene, a continuum solvent dielectric of ε= 2.3741 was employed. All the stationary points were characterized, as minima or a first-order saddle point (transition states) by evaluating the corresponding Hessian indices. The transition states were verified as possessing a unique imaginary frequency in accordance with the anticipated reaction coordinate. The IRC calculations were performed to further authenticate that the transition states on the energy profiles connect to the desired minima on either side of the first order saddle point.[27] These geometries were further optimized by using "opt = calcfc" as implemented in Gaussian09 program. Single point energies were calculated for all stationary points at the $SMD_{(Toluene)}$, B3LYP-D3/6-31G**, SDD(Pd) level of theory. The Gibbs free energies were computed by using the thermal and entropic corrections obtained at the $SMD_{(Toluene)}$/B3LYP-D3/6-31G**, LANL2DZ(Pd) level of theory.

Notes and references

(1) Yasui, S.; Fujii, M.; Kawano, C.; Nishimura, Y.; Ohno, A. *Tetrahedron Lett.* **1991**, *32* (40), 5601.

(2) Yasui, S.; Fujii, M.; Kawano, C.; Nishimura, Y.; Shioji, K.; Ohno, A. *J. Chem. Soc. Perkin Trans. 2* **1994**, No. 2, 177.

(3) Correia, C. R. D.; Oliveira, C. C.; Salles Jr., A. G.; Santos, E. A. F. *Tetrahedron Lett.* **2012**, *53* (26), 3325.

(4) Angnes, R. A.; Oliveira, J. M.; Oliveira, C. C.; Martins, N. C.; Correia, C. R. D. *Chem. – Eur. J.* **2014**, *20* (41), 13117.

(5) Werner, E. W.; Mei, T.-S.; Burckle, A. J.; Sigman, M. S. *Science* **2012**, *338* (6113), 1455.

(6) Mukherjee, S.; List, B. *J. Am. Chem. Soc.* **2007**, *129* (37), 11336.

(7) Nelson, H. M.; Williams, B. D.; Miró, J.; Toste, F. D. *J. Am. Chem. Soc.* **2015**, *137* (9), 3213.

(8) Zhu, R.; Snyder, A. H.; Kharel, Y.; Schaffter, L.; Sun, Q.; Kennedy, P. C.; Lynch, K. R.; Macdonald, T. L. *J. Med. Chem.* **2007**, *50* (25), 6428.

(9) Wallace, G. A.; Gordon, T. D.; Hayes, M. E.; Konopacki, D. B.; Fix-Stenzel, S. R.; Zhang, X.; Grongsaard, P.; Cusack, K. P.; Schaffter, L. M.; Henry, R. F.; Stoffel, R. H. *J. Org. Chem.* **2009**, *74* (13), 4886.

(10) Seayad, J.; Seayad, A. M.; List, B. *J. Am. Chem. Soc.* **2006**, *128* (4), 1086.

(11) Rauniyar, V.; Lackner, A. D.; Hamilton, G. L.; Toste, F. D. *Science* **2011**, *334* (6063), 1681.

(12) Rauniyar, V.; Wang, Z. J.; Burks, H. E.; Toste, F. D. *J. Am. Chem. Soc.* **2011**, *133* (22), 8486.

(13) Yang, X.; Toste, F. D. *J. Am. Chem. Soc.* **2015**, *137* (9), 3205.

(14) Romanov-Michailidis, F.; Romanova-Michaelides, M.; Pupier, M.; Alexakis, A. *Chem. – Eur. J.* **2015**, *21* (14), 5561.
(15) Kammerer, C.; Prestat, G.; Gaillard, T.; Madec, D.; Poli, G. *Org. Lett.* **2008**, *10* (3), 405.
(16) Nelson, H. M.; Reisberg, S. H.; Shunatona, H. P.; Patel, J. S.; Toste, F. D. *Angew. Chem. Int. Ed.* **2014**, *53* (22), 5600.
(17) McDougal, N. T.; Trevellini, W. L.; Rodgen, S. A.; Kliman, L. T.; Schaus, S. E. *Adv. Synth. Catal.* **2004**, *346* (9-10), 1231.
(18) Pousse, G.; Devineau, A.; Dalla, V.; Humphreys, L.; Lasne, M.-C.; Rouden, J.; Blanchet, J. *Tetrahedron* **2009**, *65* (51), 10617.
(19) Schrock, R. R.; Jamieson, J. Y.; Dolman, S. J.; Miller, S. A.; Bonitatebus, Peter J.; Hoveyda, A. H. *Organometallics* **2002**, *21* (2), 409.
(20) Hatano, M.; Ikeno, T.; Matsumura, T.; Torii, S.; Ishihara, K. *Adv. Synth. Catal.* **2008**, *350* (11-12), 1776.
(21) Ulgheri, F.; Giunta, D.; Spanu, P. *Tetrahedron* **2008**, *64* (51), 11768.
(22) Dhara, K.; Midya, G. C.; Dash, J. *J. Org. Chem.* **2012**, *77* (18), 8071.
(23) Gaussian 09, Revision E.01, Frisch, M. J.; Trucks, G. W.; Schlegel, H. B.; Scuseria, G. E.; Robb, M. A.; Cheeseman, J. R.; Scalmani, G.; Barone, V.; Mennucci, B.; Petersson, G. A.; Nakatsuji, H.; Caricato, M.; Li, X.; Hratchian, H. P.; Izmaylov, A. F.; Bloino, J.; Zheng, G.; Sonnenberg, J. L.; Hada, M.; Ehara, M.; Toyota, K.; Fukuda, R.; Hasegawa, J.; Ishida, M.; Nakajima, T.; Honda, Y.; Kitao, O.; Nakai, H.; Vreven, T.; Montgomery, J. A., Jr.; Peralta, J. E.; Ogliaro, F.; Bearpark, M.; Heyd, J. J.; Brothers, E.; Kudin, K. N.; Staroverov, V. N.; Kobayashi, R.; Normand, J.; Raghavachari, K.; Rendell, A.; Burant, J. C.; Iyengar, S. S.; Tomasi, J.; Cossi, M.; Rega, N.; Millam, J. M.; Klene, M.; Knox, J. E.; Cross, J. B.; Bakken, V.; Adamo, C.; Jaramillo, J.; Gomperts, R.; Stratmann, R. E.; Yazyev, O.; Austin, A. J.; Cammi, R.; Pomelli, C.; Ochterski, J. W.; Martin, R. L.; Morokuma, K.; Zakrzewski, V. G.; Voth, G. A.; Salvador, P.; Dannenberg, J. J.; Dapprich, S.; Daniels, A. D.; Farkas, Ö.; Foresman, J. B.; Ortiz, J. V.; Cioslowski, J.; Fox, D. J. Gaussian, Inc., Wallingford CT, 2009.
(24) Grimme, S.; Antony, J.; Ehrlich, S.; Krieg, H. *J. Chem. Phys.* **2010**, *132* (15), 154104.
(25) Hay, P. J.; Wadt, W. R. *J. Chem. Phys.* **1985**, *82* (1), 299.
(26) Marenich, A. V.; Cramer, C. J.; Truhlar, D. G. *J. Phys. Chem. B* **2009**, *113* (18), 6378.
(27) Gonzalez, C.; Schlegel, H. B. *J. Phys. Chem.* **1990**, *94* (14), 5523.

NMR spectra

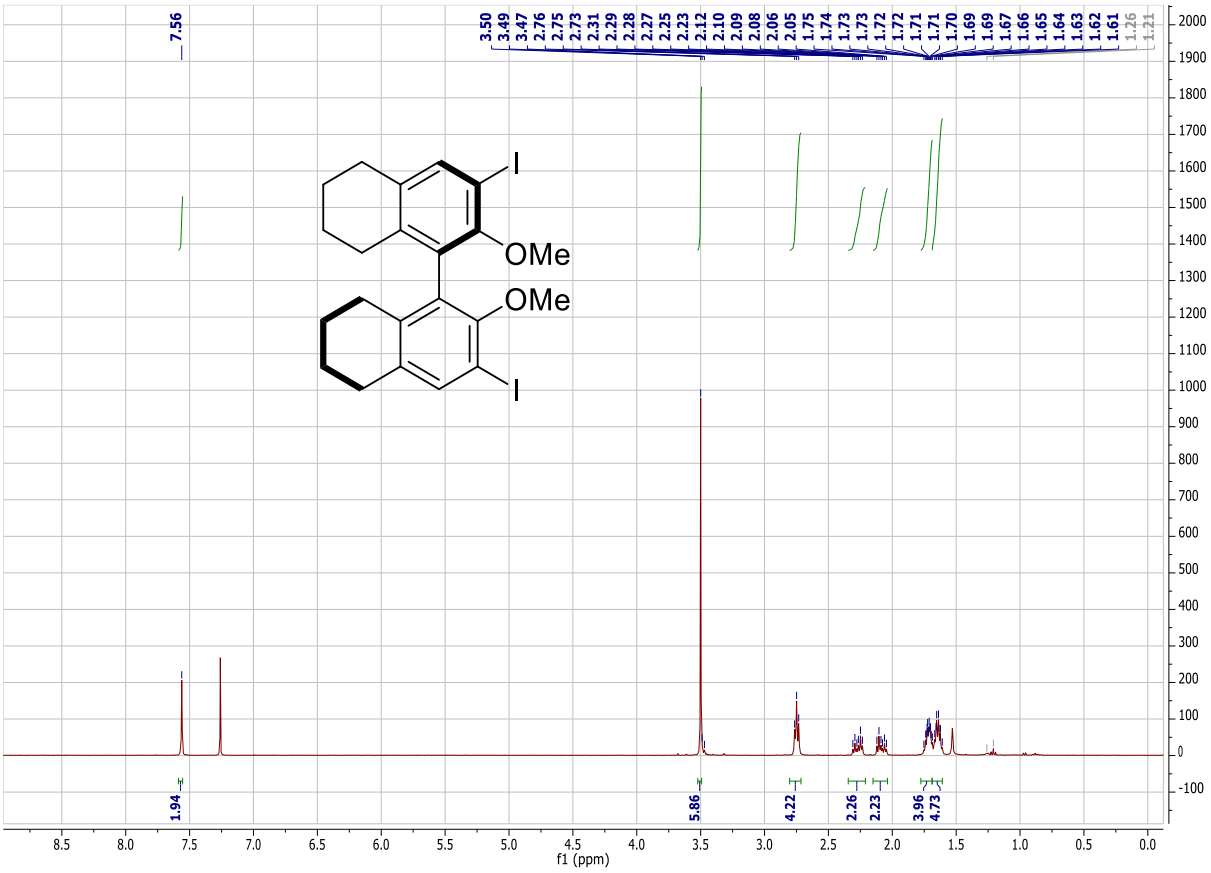
7.56
3.50
3.49
3.47
2.76
2.75
2.73
2.31
2.29
2.28
2.27
2.25
2.23
2.12
2.10
2.09
2.08
2.06
2.05
1.75
1.74
1.73
1.73
1.72
1.72
1.71
1.71
1.70
1.69
1.69
1.67
1.66
1.65
1.64
1.63
1.62
1.61
1.26
1.21
I
OMe
OMe
I
1.94
5.86
4.22
2.26
2.23
3.96
4.73
f1 (ppm)

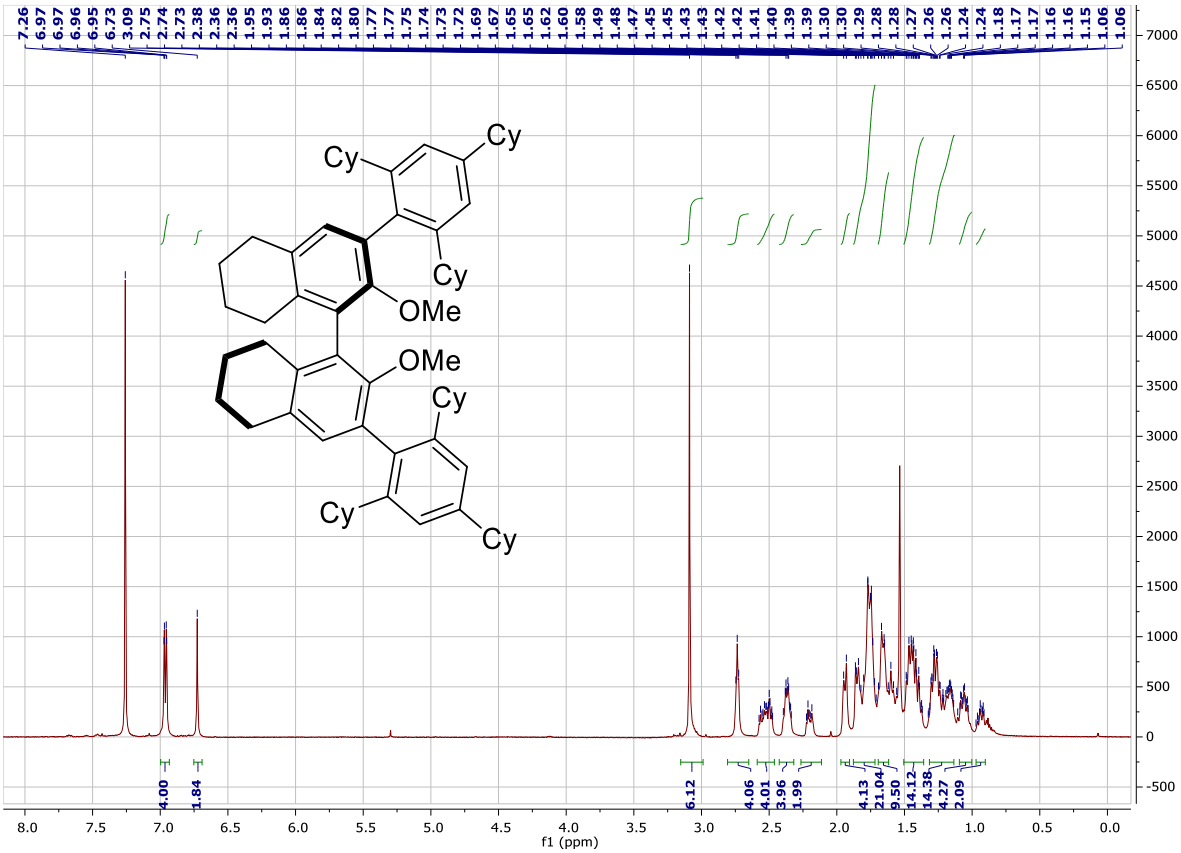
Cy
Cy
Cy
OMe
OMe
Cy
Cy
Cy
f1 (ppm)

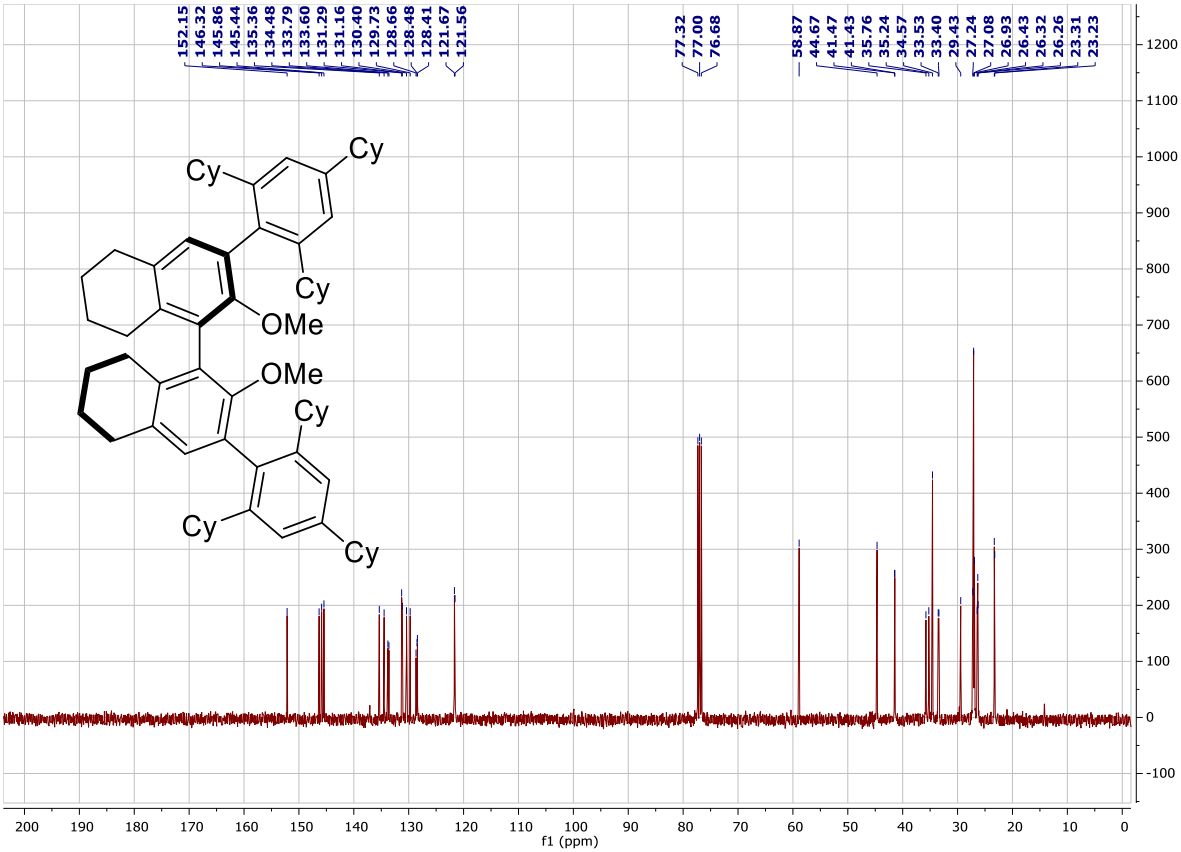
Cy
Cy
Cy
OMe
OMe
Cy
Cy
Cy
f1 (ppm)

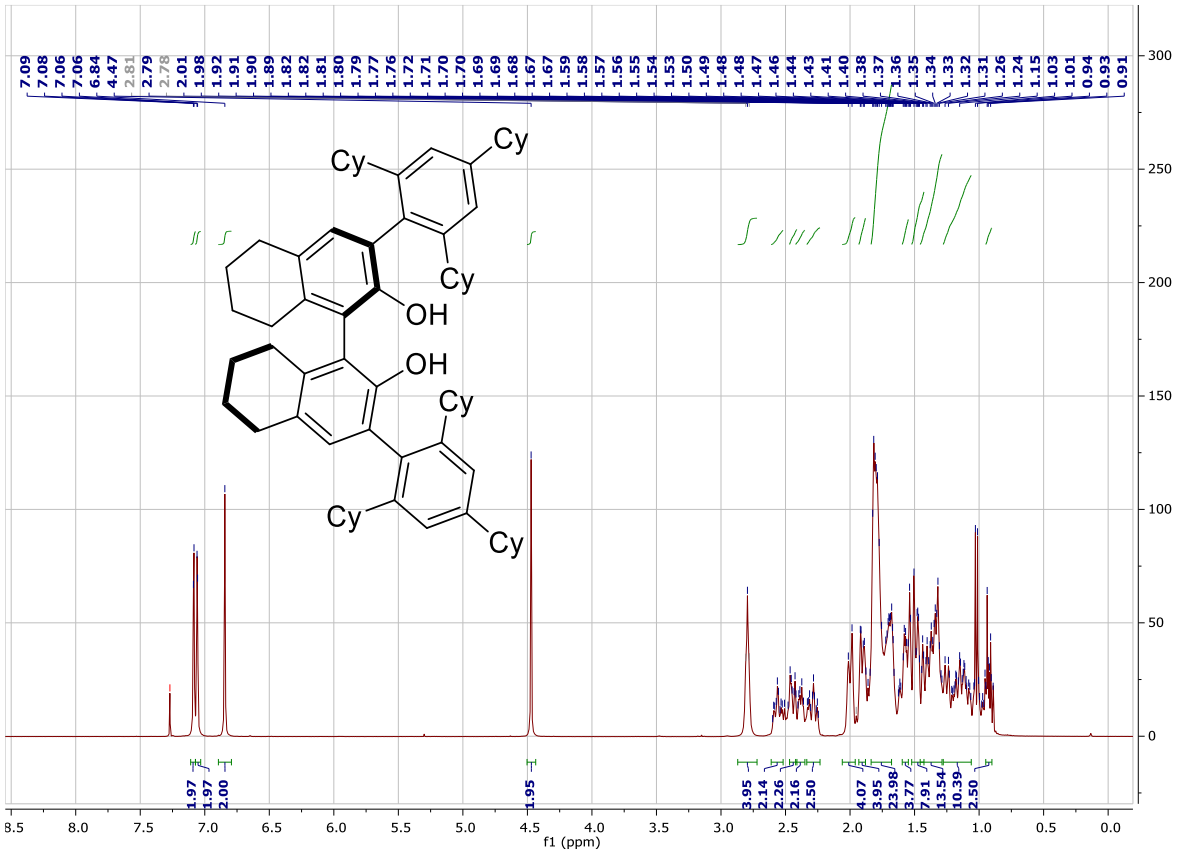
7.09 7.08 7.06 7.06 6.84 4.47 2.81 2.79 2.78 2.01 1.98 1.92 1.91 1.90 1.89 1.82 1.82 1.81 1.80 1.79 1.77 1.76 1.72 1.71 1.70 1.70 1.69 1.69 1.68 1.67 1.67 1.59 1.58 1.57 1.56 1.55 1.54 1.53 1.50 1.49 1.48 1.48 1.47 1.46 1.44 1.43 1.41 1.40 1.38 1.37 1.36 1.35 1.34 1.33 1.32 1.31 1.26 1.24 1.15 1.03 1.01 0.94 0.93 0.91
Cy
OH
1.97 1.97 2.00 1.95 3.95 2.14 2.26 2.16 2.50 4.07 3.95 23.98 3.77 7.91 13.54 10.39 2.50
f1 (ppm)

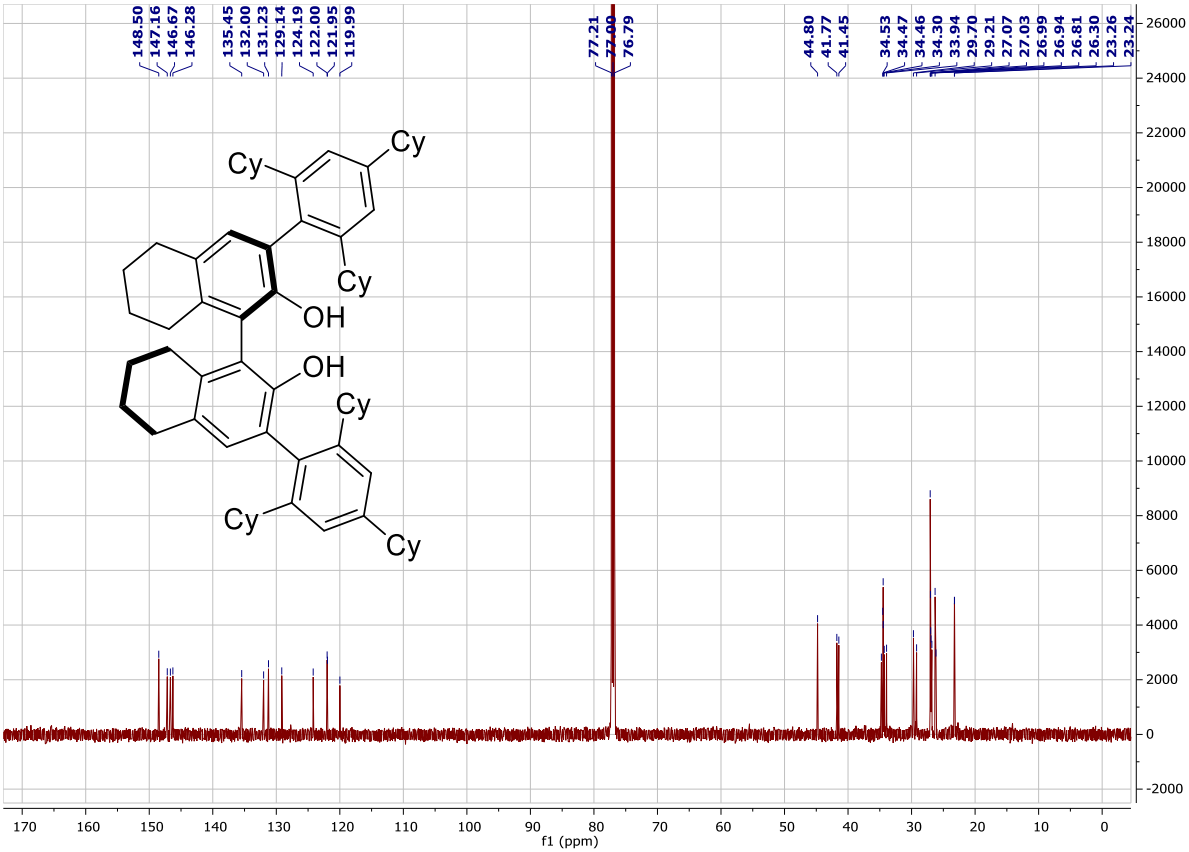
148.50 147.16 146.67 146.28 135.45 132.00 131.23 129.14 124.19 122.00 121.95 119.99 77.21 77.00 76.79 44.80 41.77 41.45 34.53 34.47 34.46 34.30 33.94 29.70 29.21 27.07 27.03 26.99 26.94 26.81 26.30 23.26 23.24
Cy
OH
f1 (ppm)

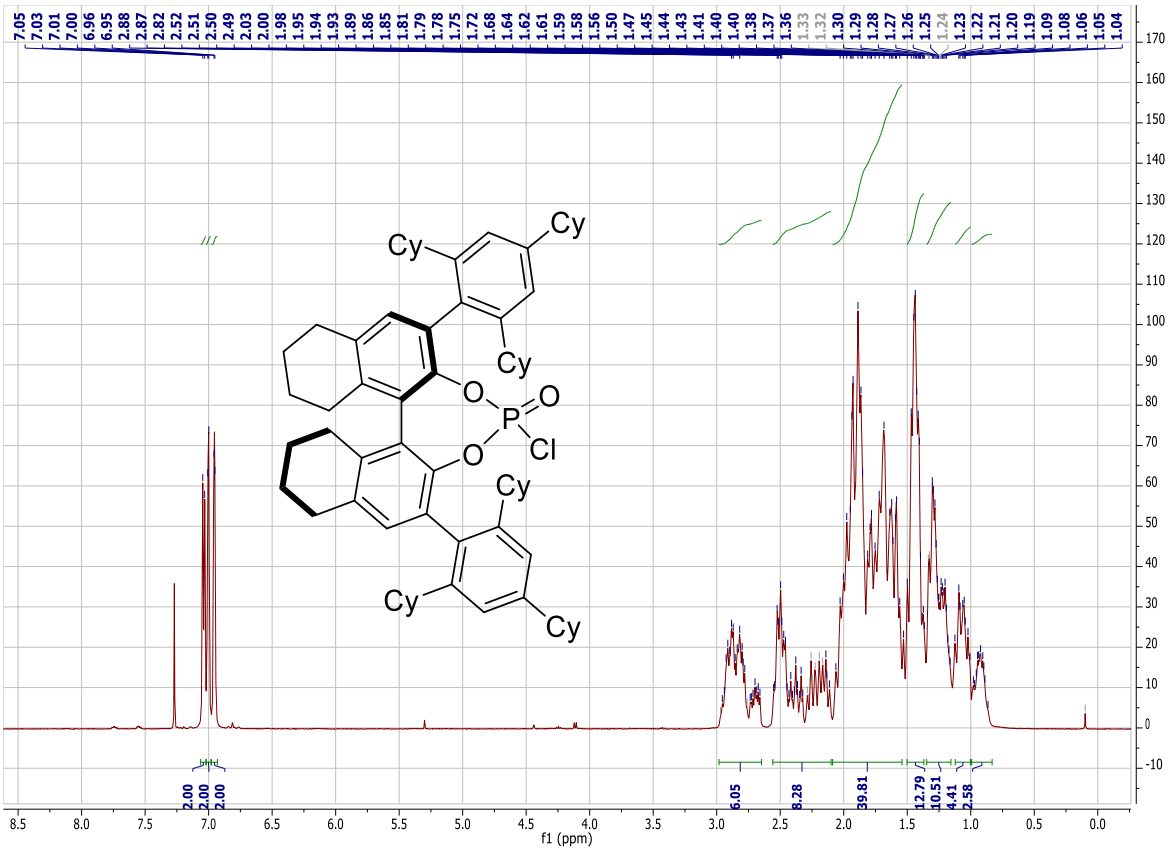
7.05 7.03 7.01 7.00 6.96 6.95 2.88 2.87 2.82 2.52 2.51 2.50 2.49 2.03 2.00 1.98 1.95 1.94 1.93 1.89 1.86 1.85 1.81 1.79 1.78 1.75 1.72 1.68 1.64 1.62 1.61 1.59 1.58 1.56 1.50 1.47 1.45 1.44 1.43 1.41 1.40 1.40 1.38 1.37 1.36 1.33 1.32 1.30 1.29 1.28 1.27 1.26 1.25 1.24 1.23 1.22 1.21 1.20 1.19 1.09 1.08 1.06 1.05 1.04
Cy
Cy
Cy
O
P
O
O
Cl
Cy
Cy
Cy
2.00
2.00
2.00
6.05
8.28
39.81
12.79
10.51
4.41
2.58
f1 (ppm)

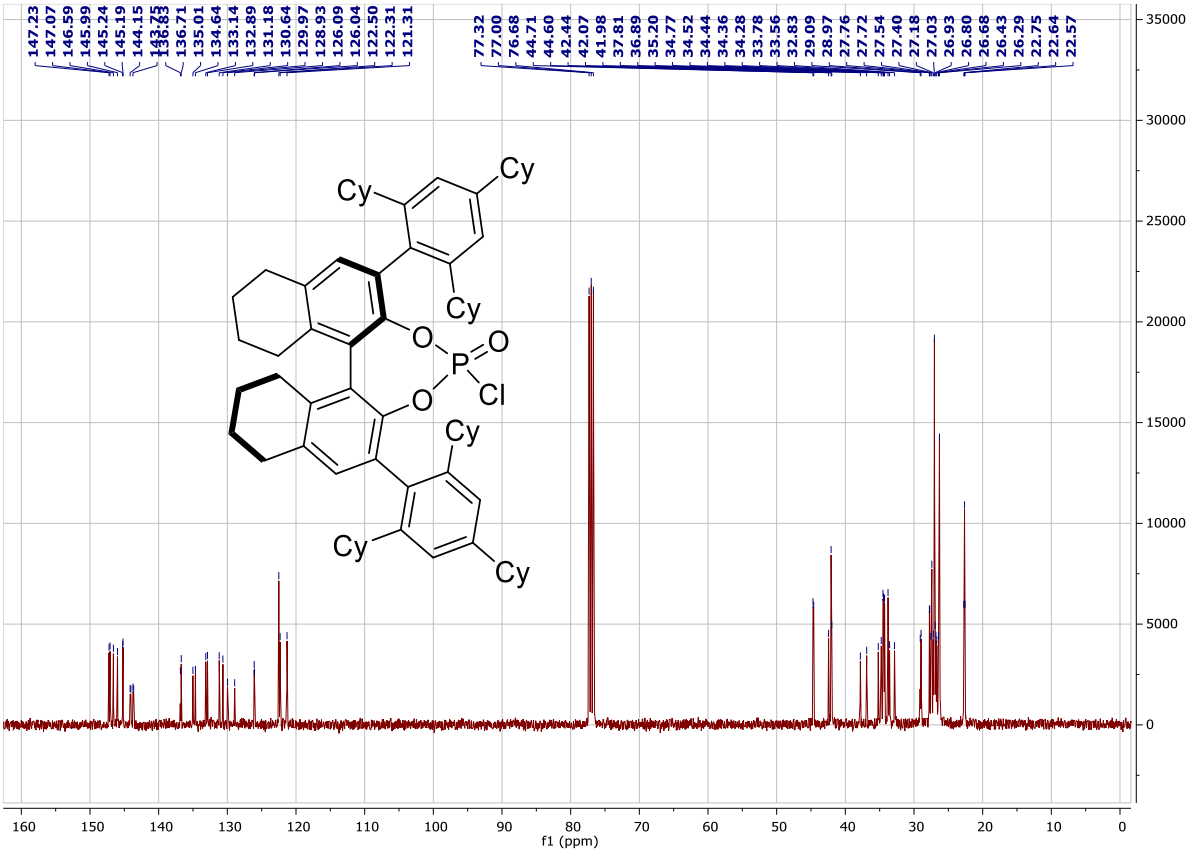
147.23 147.07 146.59 145.99 145.24 145.19 144.15 136.71 135.01 134.64 133.14 132.89 131.18 130.64 129.97 128.93 126.09 126.04 122.50 122.31 121.31
77.32 77.00 76.68 44.71 44.60 42.44 42.07 41.98 37.81 36.89 35.20 34.77 34.52 34.44 34.36 34.28 33.78 33.56 32.83 29.09 28.97 27.76 27.72 27.54 27.40 27.18 27.03 26.93 26.80 26.68 26.43 26.29 22.75 22.64 22.57
Cy
Cy
Cy
O
P
O
O
Cl
Cy
Cy
Cy
f1 (ppm)

^{31}P NMR

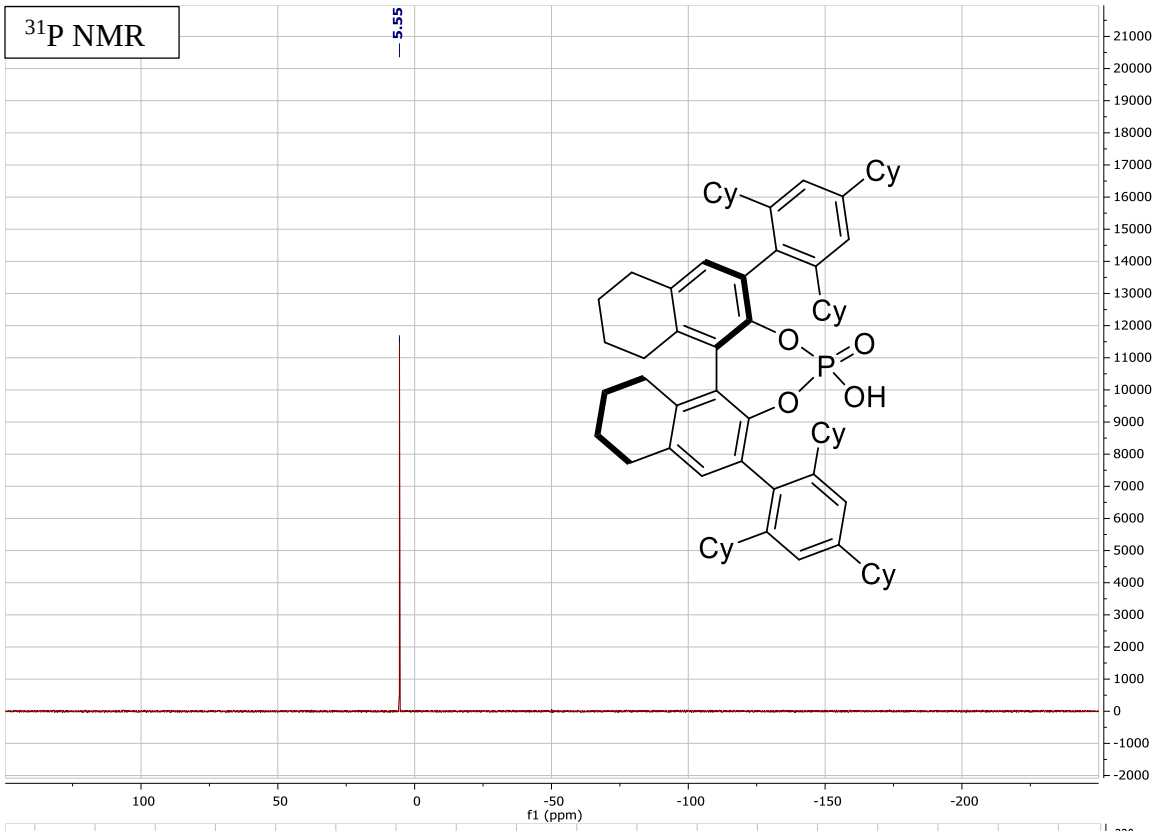
5.55
Cy
Cy
Cy
O
P
O
O
OH
Cy
Cy
Cy
f1 (ppm)

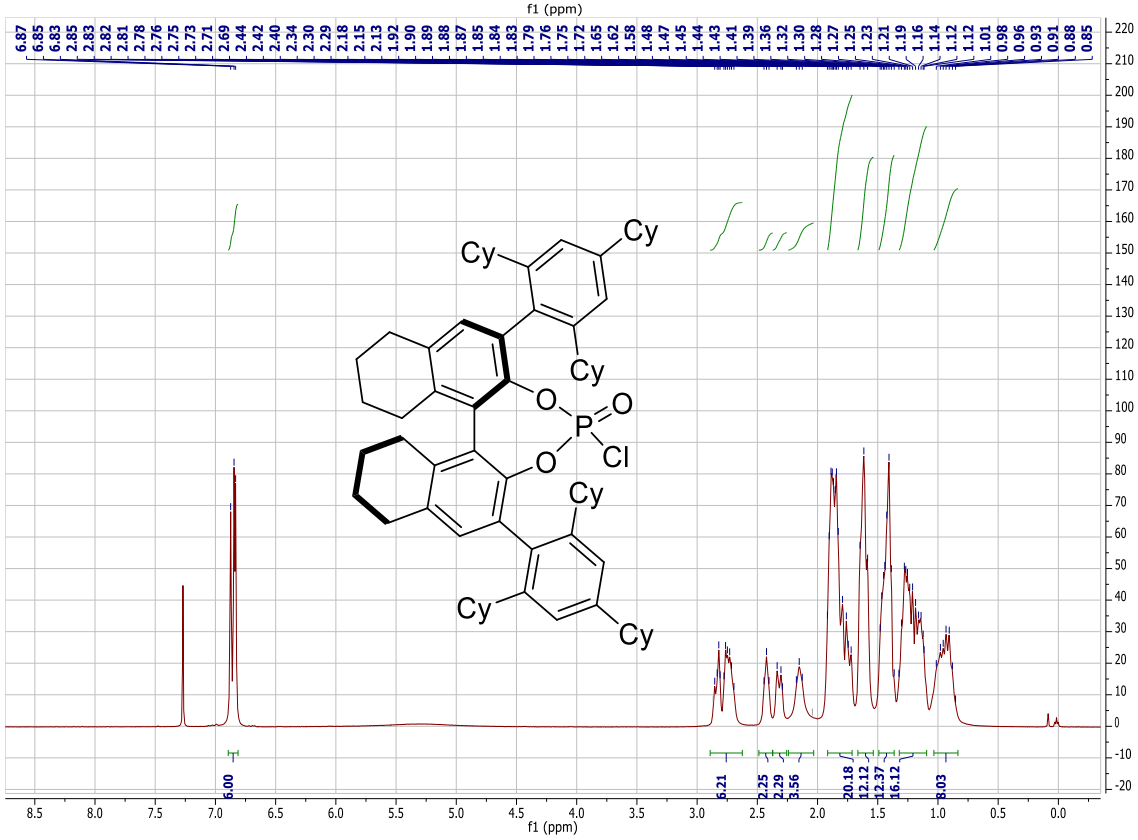
Cy
Cy
Cy
O
P
O
O
Cl
Cy
Cy
Cy
6.00
6.21
2.25
2.29
3.56
20.18
12.12
12.37
16.12
8.03
f1 (ppm)

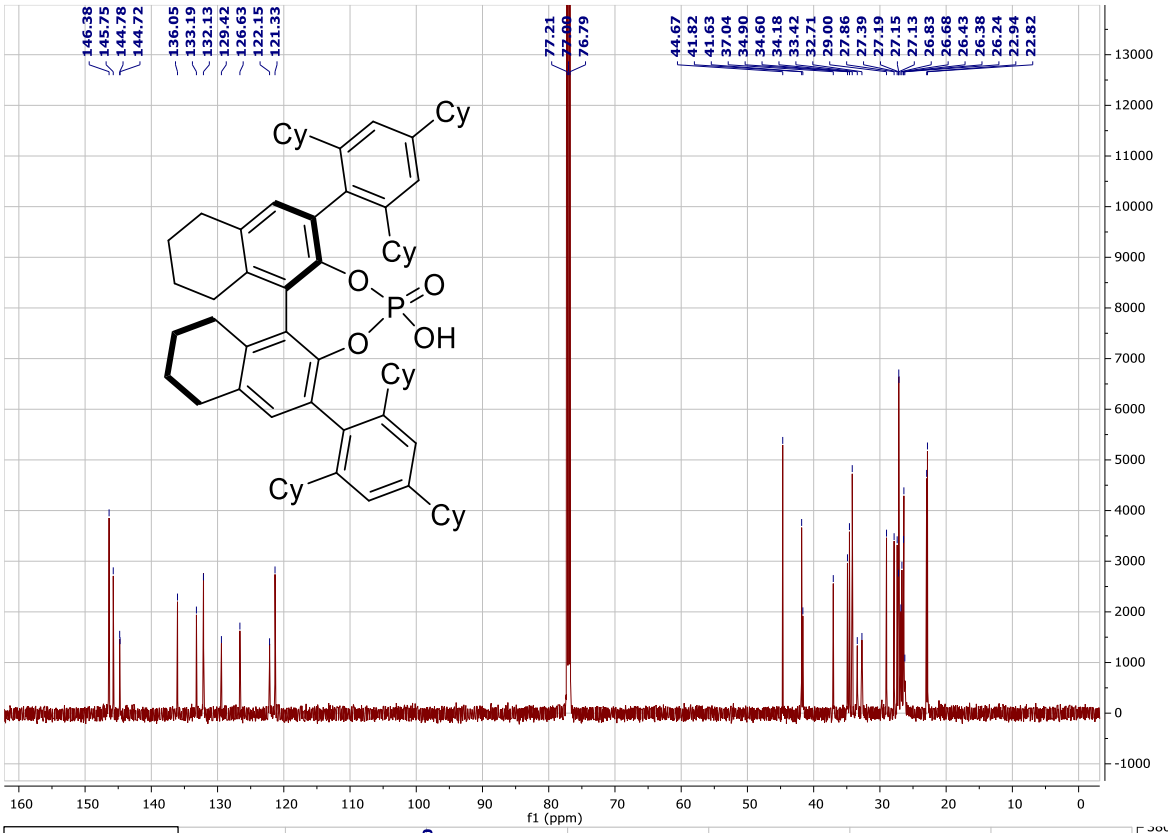
146.38
145.75
144.78
144.72
136.05
133.19
132.13
129.42
126.63
122.15
121.33
77.21
77.00
76.79
44.67
41.82
41.63
37.04
34.90
34.60
34.18
33.42
32.71
29.00
27.86
27.39
27.19
27.15
27.13
26.83
26.68
26.43
26.38
26.24
22.94
22.82
Cy
Cy
Cy
O
P
O
OH
O
Cy
Cy
Cy
f1 (ppm)

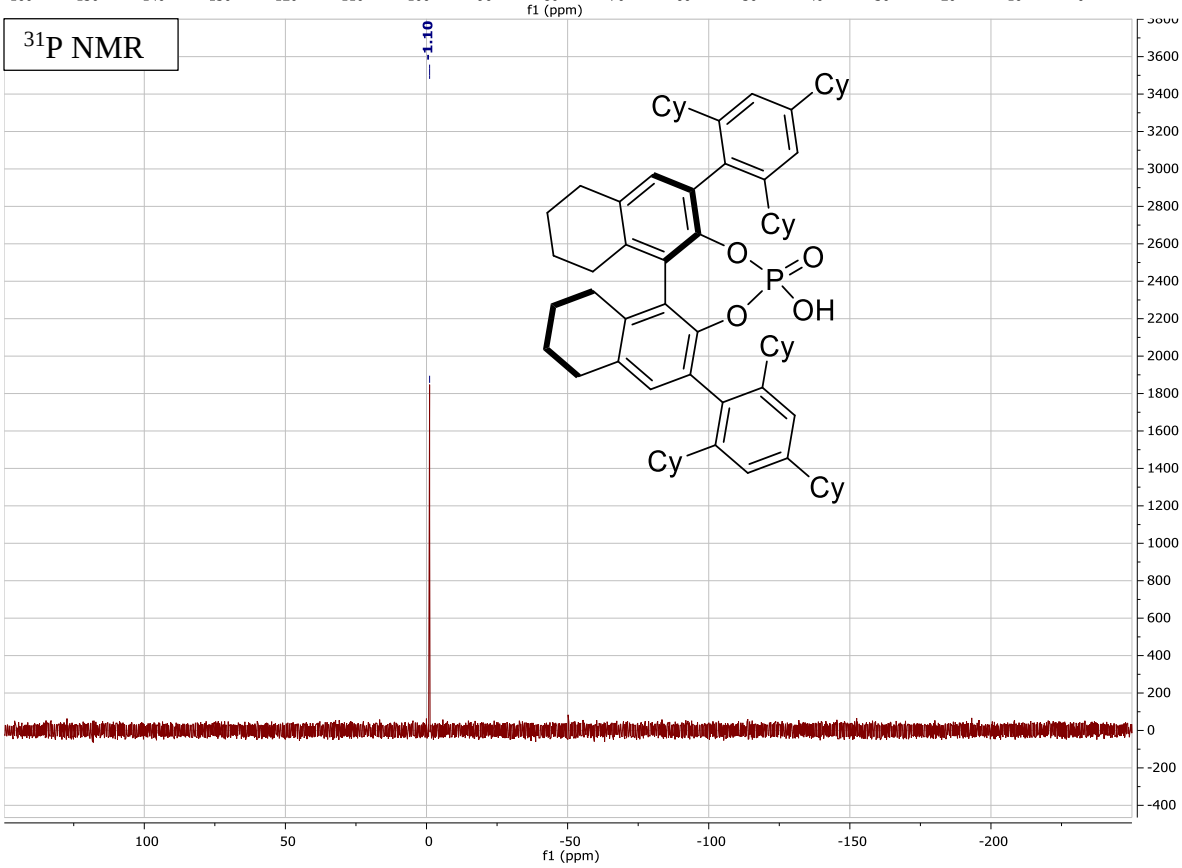
^{31}P NMR
-1.10
Cy
Cy
Cy
O
P
O
OH
O
Cy
Cy
Cy
f1 (ppm)

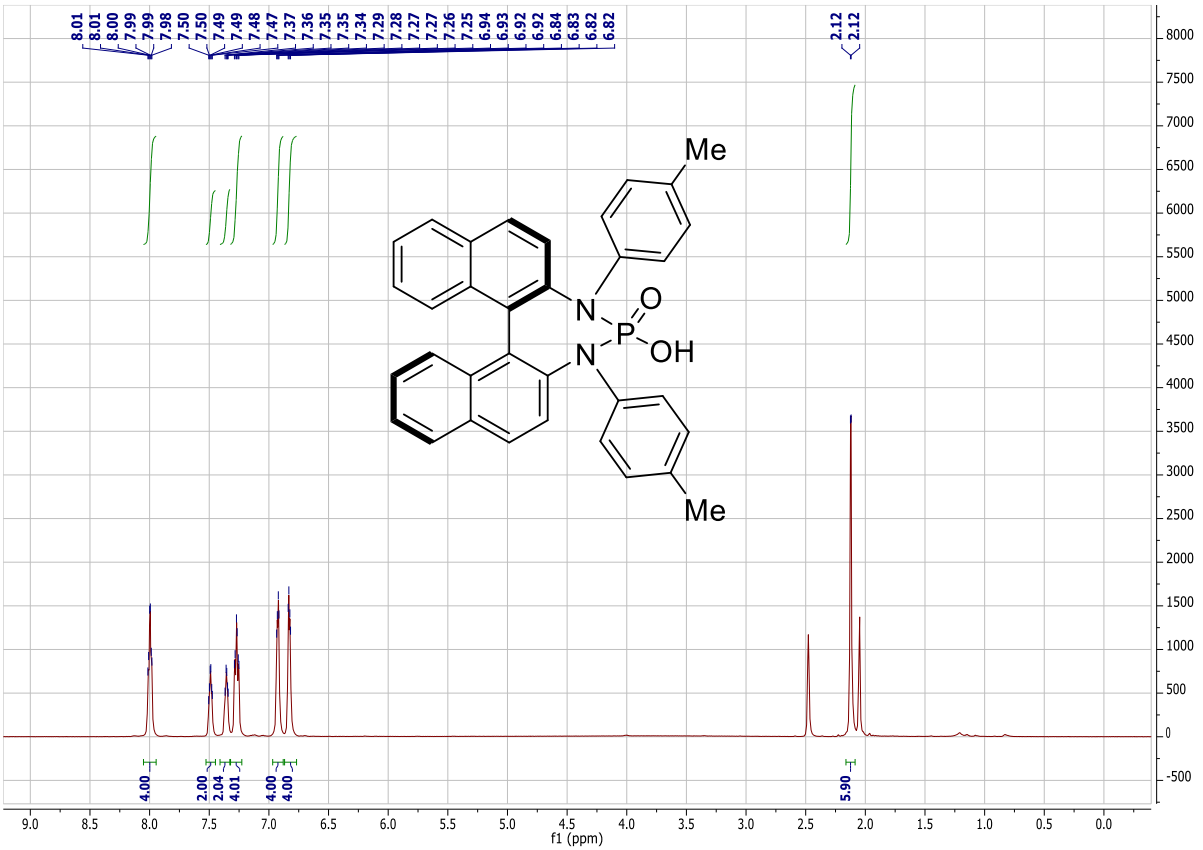
8.01
8.01
8.00
7.99
7.99
7.98
7.50
7.50
7.49
7.49
7.48
7.47
7.37
7.36
7.35
7.35
7.34
7.29
7.28
7.27
7.27
7.26
7.25
6.94
6.93
6.92
6.92
6.84
6.83
6.82
6.82
2.12
2.12
Me
N
P
O
OH
N
Me
4.00
2.00
2.04
4.01
4.00
4.00
5.90
f1 (ppm)

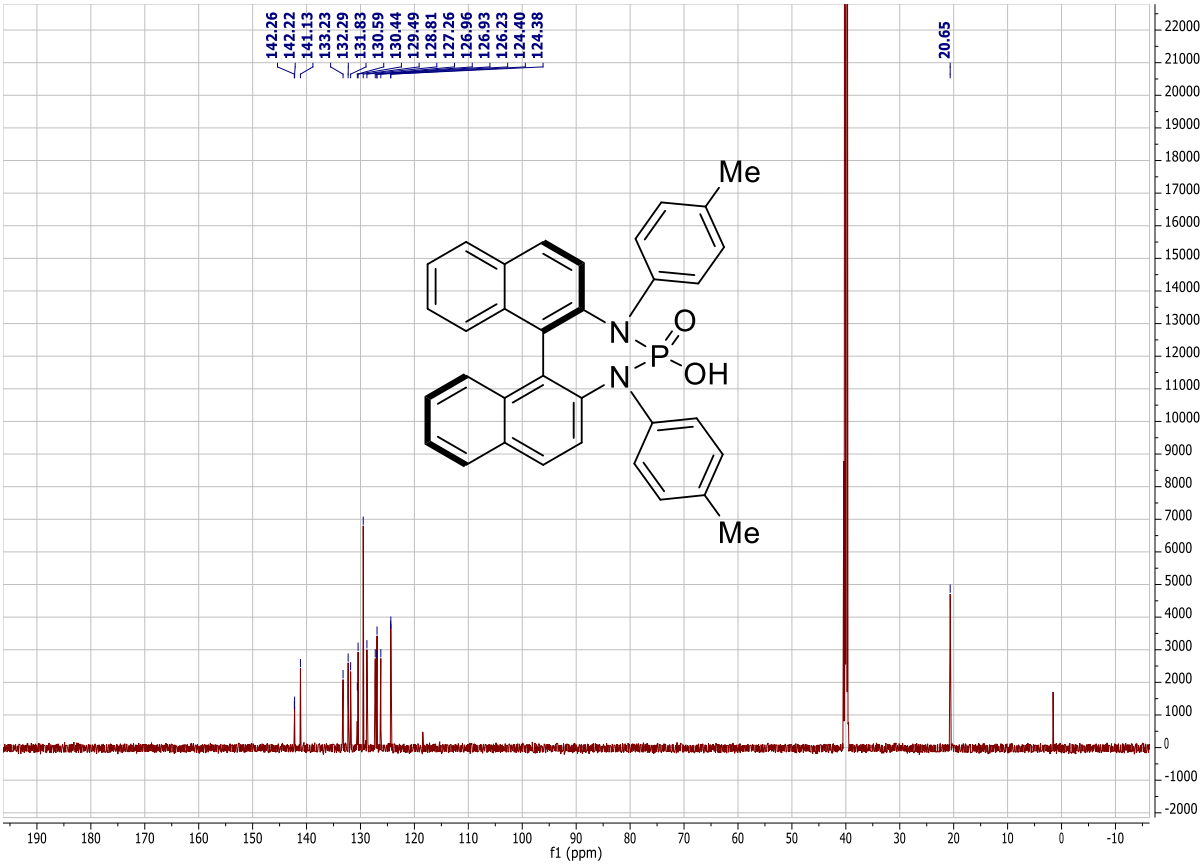
142.26
142.22
141.13
133.23
132.29
131.83
130.59
130.44
129.49
128.81
127.26
126.96
126.93
126.23
124.40
124.38
20.65
Me
N
P
O
OH
N
Me
f1 (ppm)

^{31}P NMR

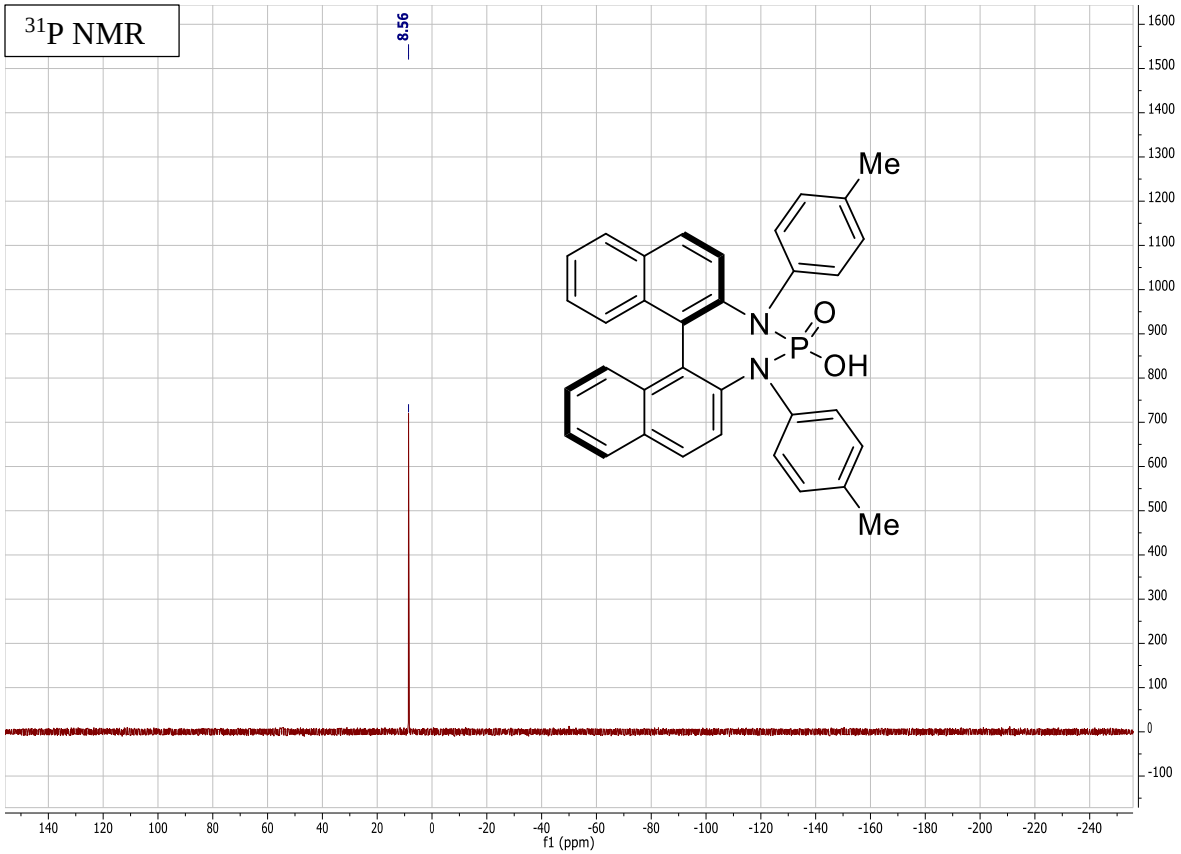
8.56
Me
N
O
P
OH
N
Me
f1 (ppm)

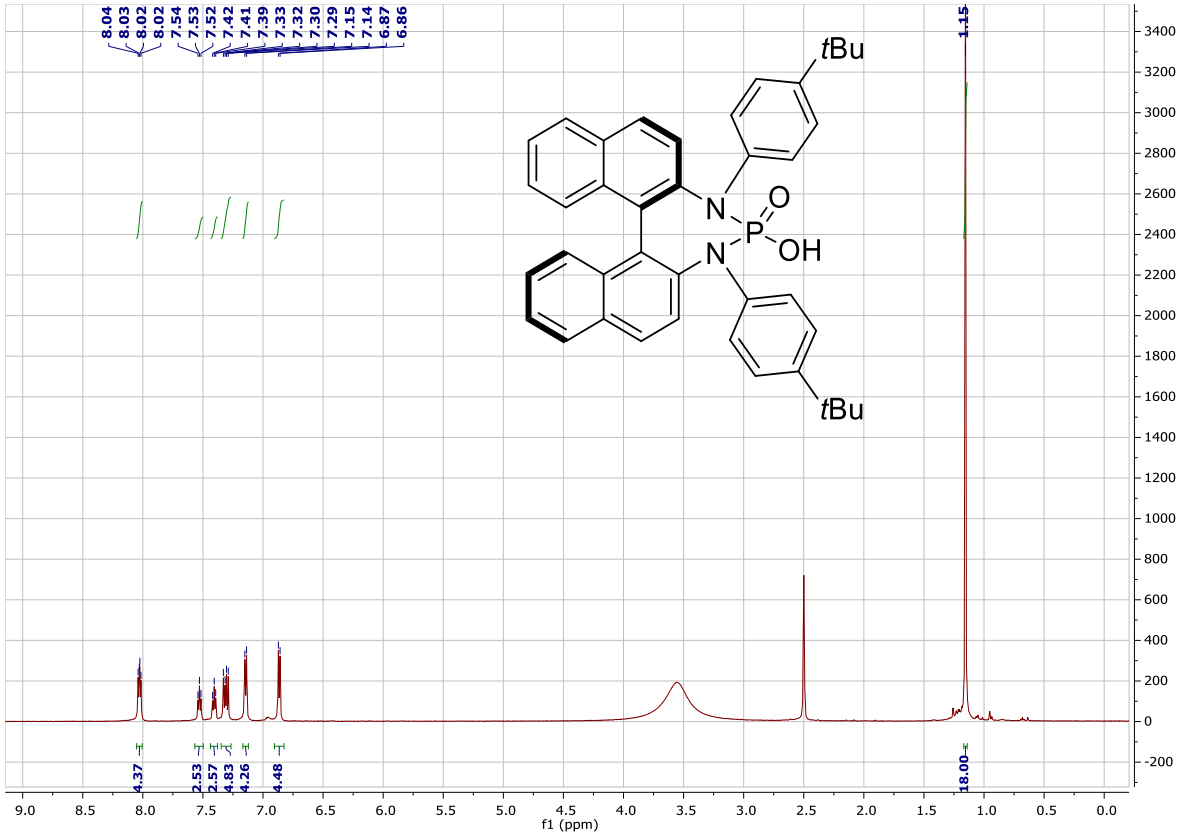
8.04
8.03
8.02
8.02
7.54
7.53
7.52
7.42
7.41
7.39
7.33
7.32
7.30
7.29
7.15
7.14
6.87
6.86
1.15
tBu
N
O
P
OH
N
tBu
4.37
2.53
2.57
4.83
4.26
4.48
18.00
f1 (ppm)

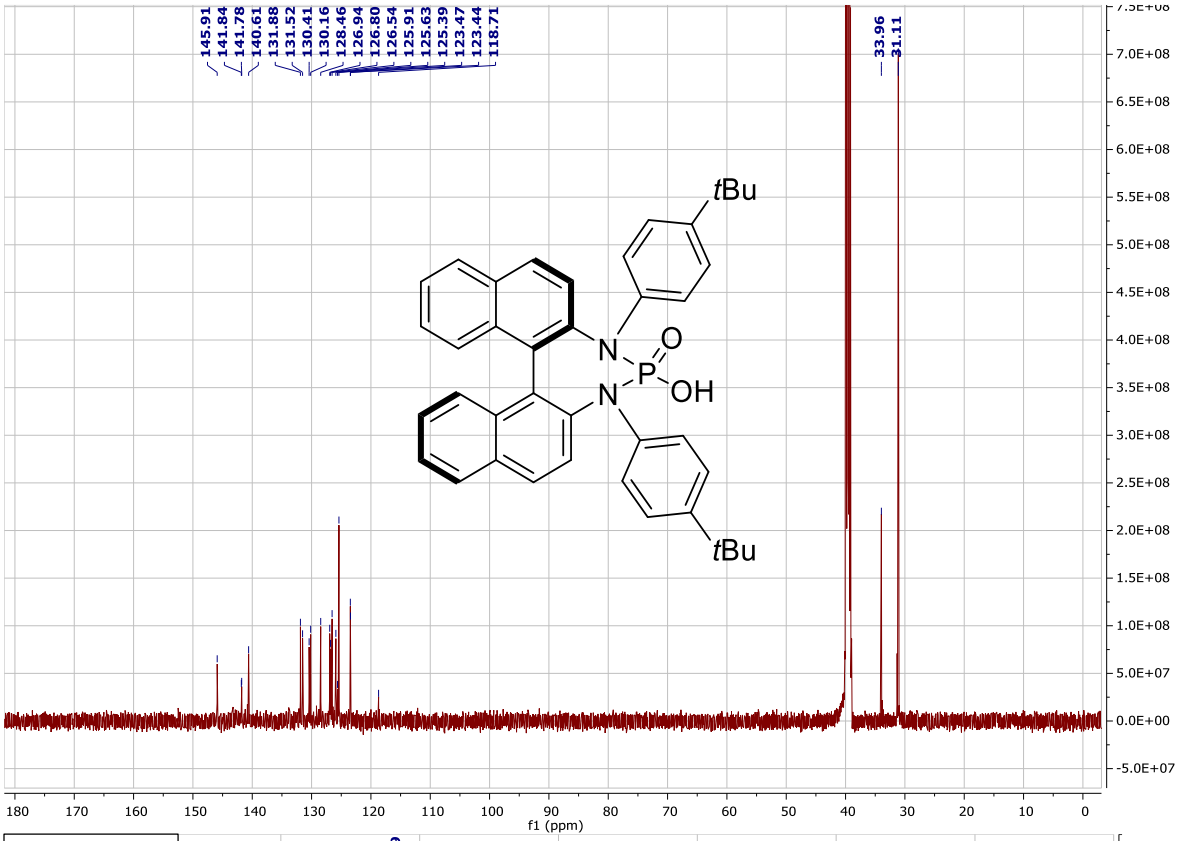
145.91
141.84
141.78
140.61
131.88
131.52
130.41
130.16
128.46
126.94
126.80
126.54
125.91
125.63
125.39
123.47
123.44
118.71
33.96
31.11
tBu
N
O
P
OH
N
tBu
f1 (ppm)

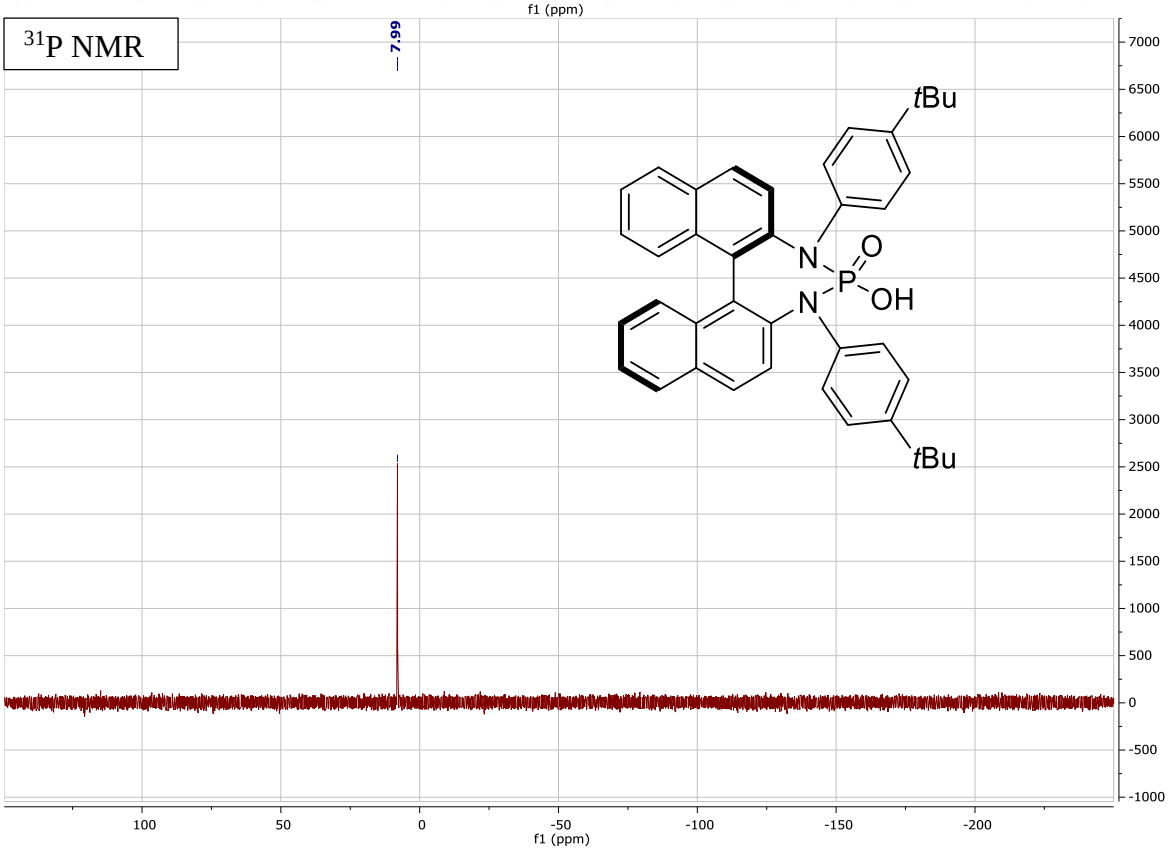
31P NMR
7.99
tBu
N
O
P
OH
N
tBu
f1 (ppm)

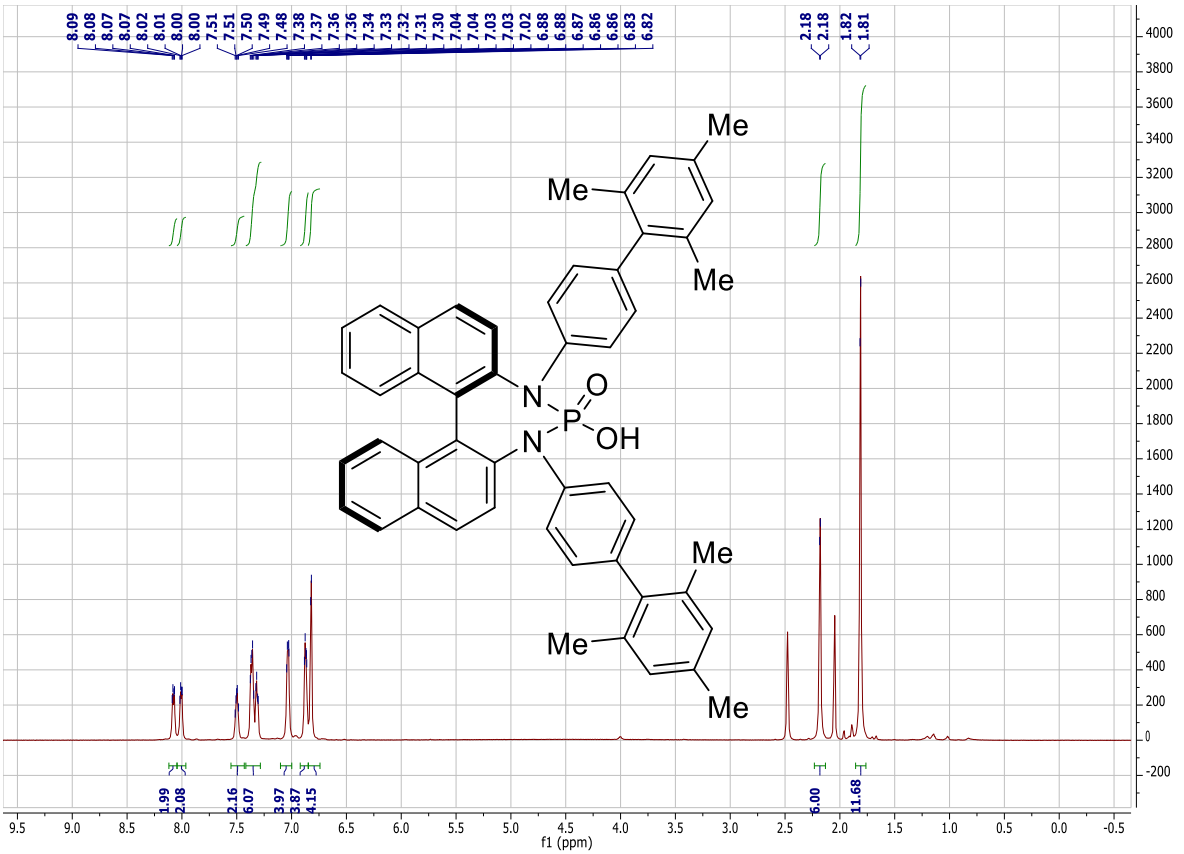
8.09
8.08
8.07
8.07
8.02
8.01
8.00
8.00
7.51
7.51
7.50
7.49
7.48
7.38
7.37
7.36
7.36
7.34
7.33
7.32
7.31
7.30
7.04
7.04
7.03
7.03
7.02
6.88
6.88
6.87
6.86
6.86
6.83
6.82
2.18
2.18
1.82
1.81
Me
Me
Me
N
O
P
OH
N
Me
Me
Me
1.99
2.08
2.16
6.07
3.97
3.87
4.15
6.00
11.68
f1 (ppm)

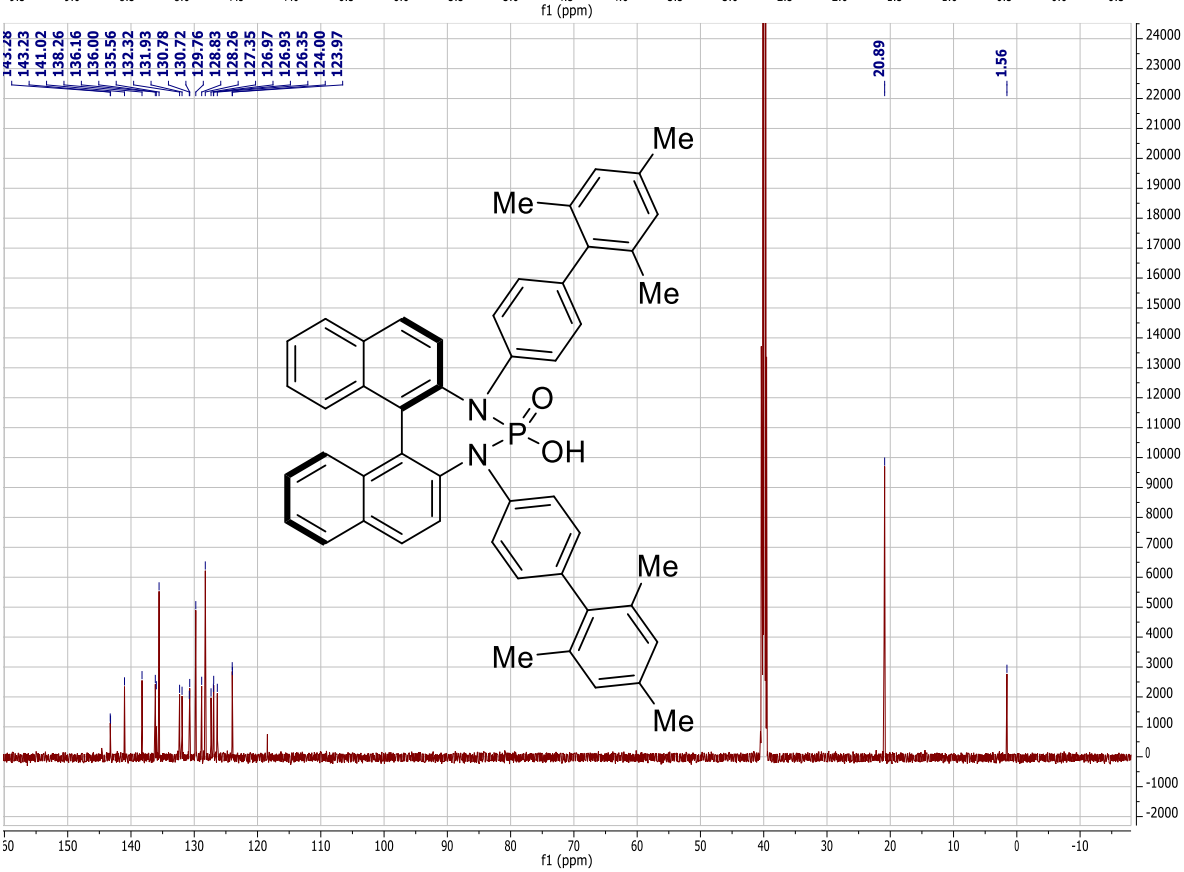
145.28
143.23
141.02
138.26
136.16
136.00
135.56
132.32
131.93
130.78
130.72
129.76
128.83
128.26
127.35
126.97
126.93
126.35
124.00
123.97
20.89
1.56
Me
Me
Me
N
O
P
OH
N
Me
Me
Me
f1 (ppm)

^{31}P NMR

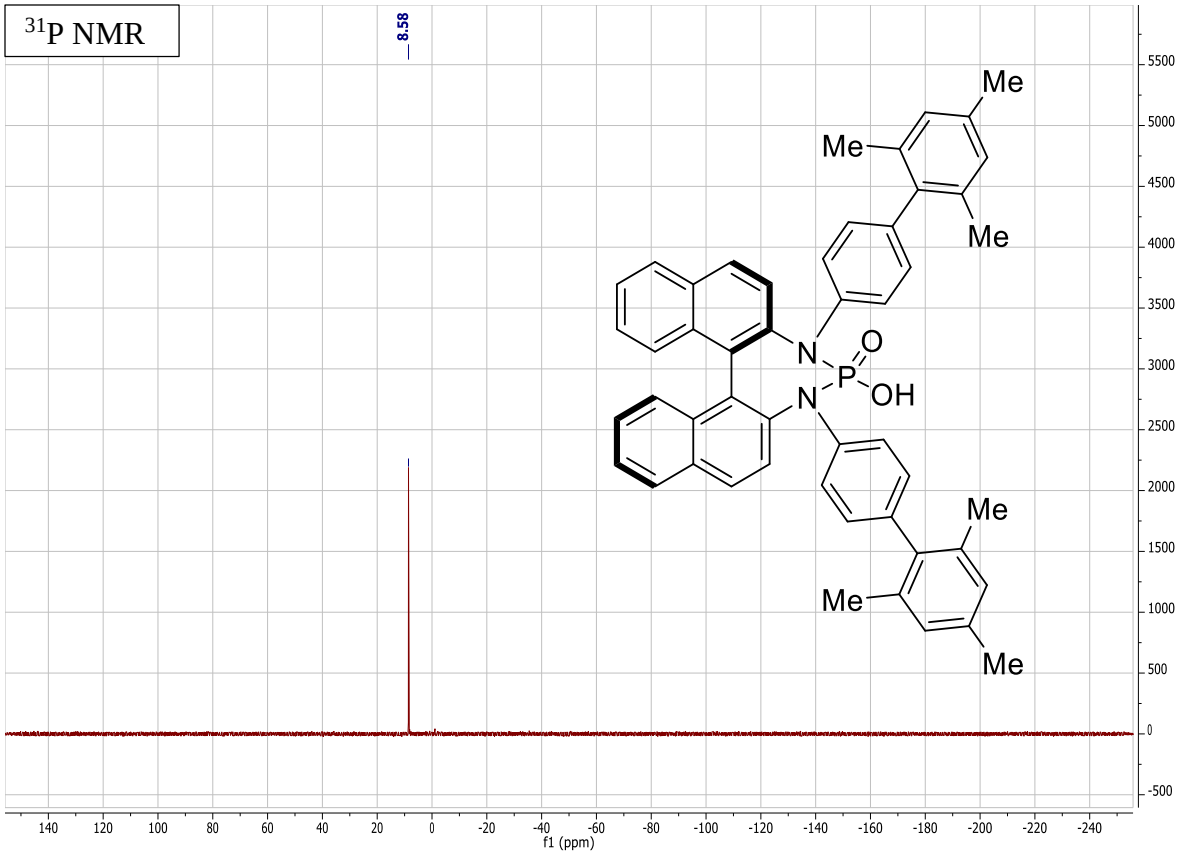
8.58
Me
Me
Me
N
P
O
OH
N
Me
Me
Me
f1 (ppm)

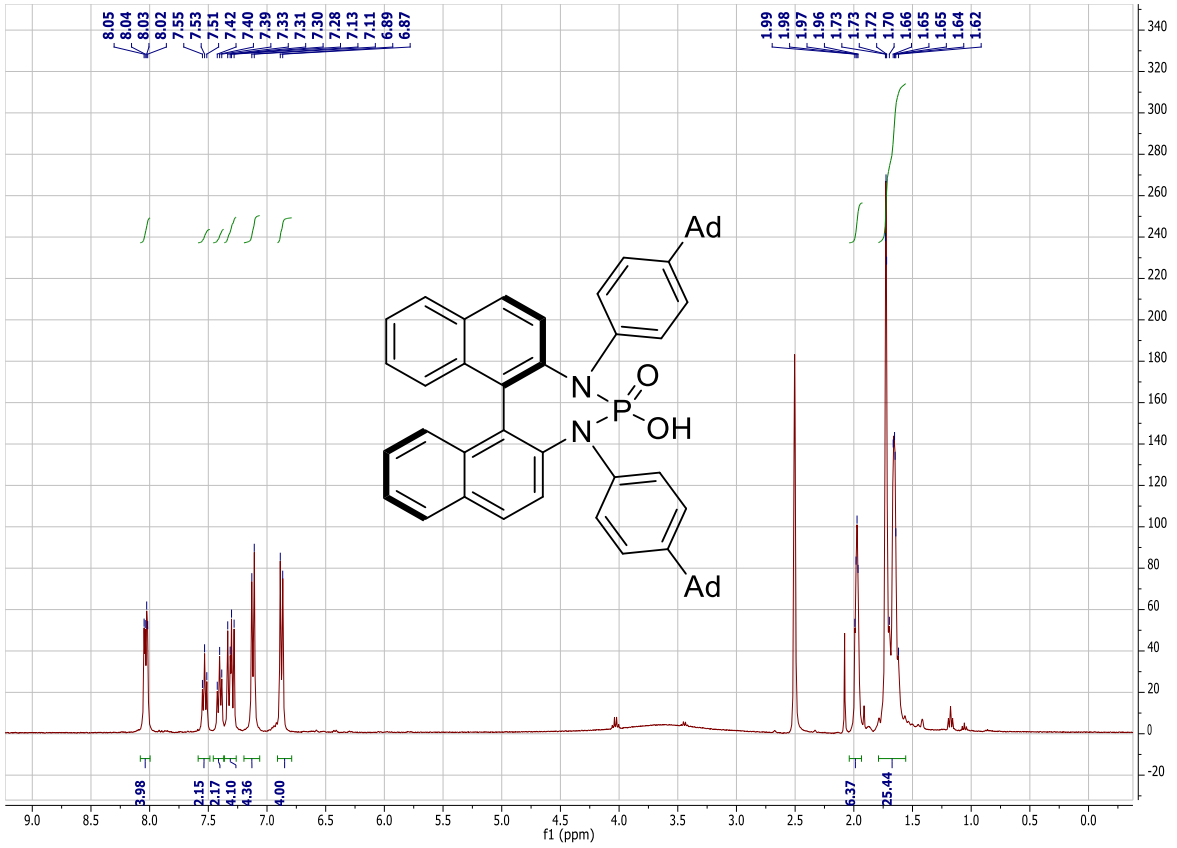
8.05
8.04
8.03
8.02
7.55
7.53
7.51
7.42
7.40
7.39
7.33
7.31
7.30
7.28
7.13
7.11
6.89
6.87
1.99
1.98
1.97
1.96
1.73
1.72
1.70
1.66
1.65
1.64
1.62
Ad
N
P
O
OH
N
Ad
3.98
2.15
2.17
4.10
4.36
4.00
6.37
25.44
f1 (ppm)

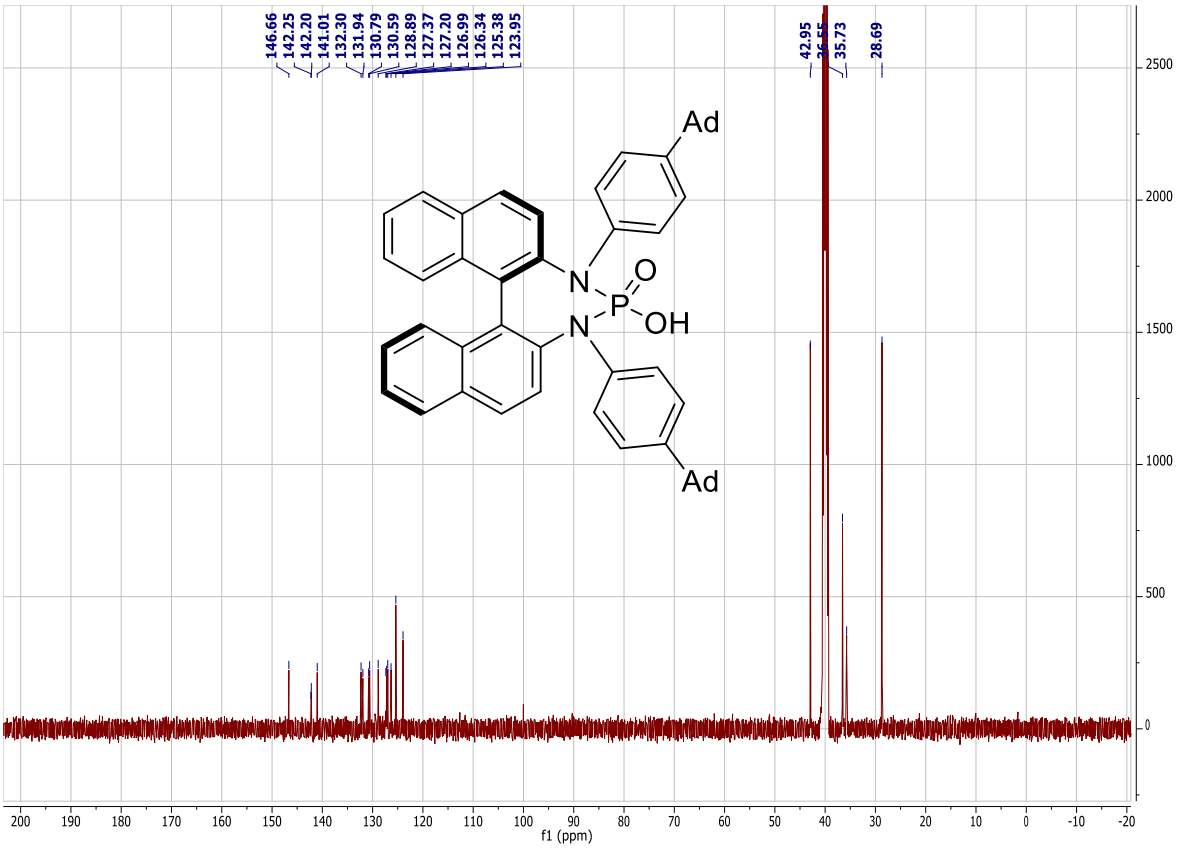
146.66
142.25
142.20
141.01
132.30
131.94
130.79
130.59
128.89
127.37
127.20
126.99
126.34
125.38
123.95
42.95
35.73
28.69
Ad
N
P
O
OH
N
Ad
f1 (ppm)

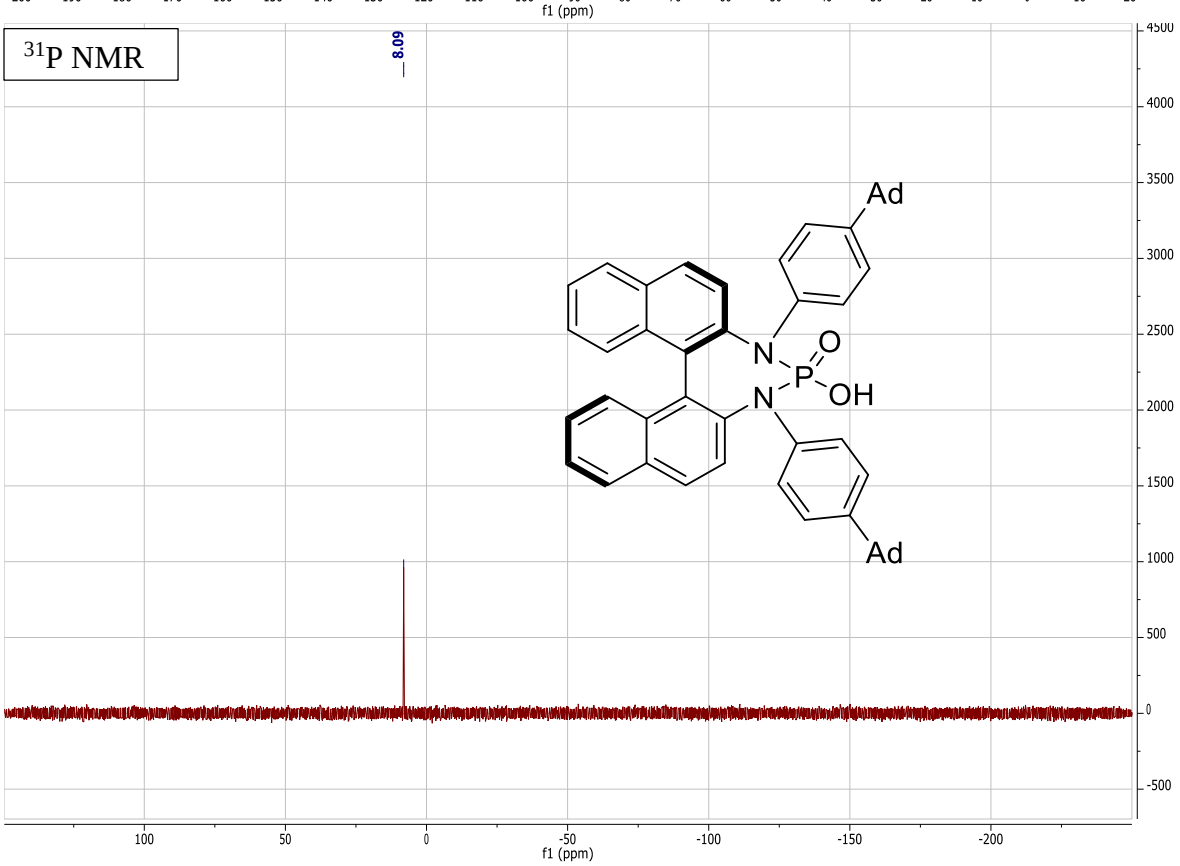
^{31}P NMR
8.09
Ad
N
P
O
OH
N
Ad
f1 (ppm)

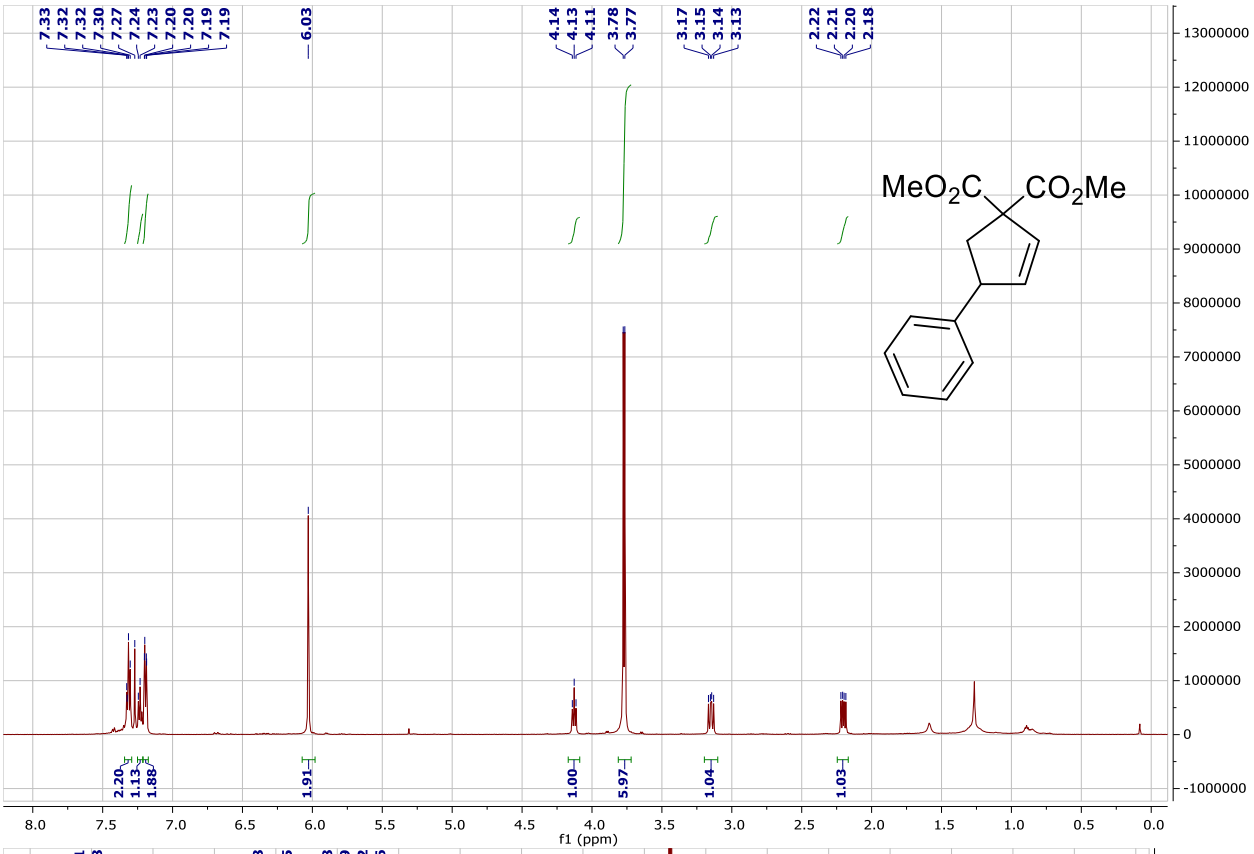
7.33
7.32
7.32
7.30
7.27
7.24
7.23
7.20
7.20
7.19
7.19
6.03
4.14
4.13
4.11
3.78
3.77
3.17
3.15
3.14
3.13
2.22
2.21
2.20
2.18
2.20
1.13
1.88
1.91
1.00
5.97
1.04
1.03
MeO2C
CO2Me
f1 (ppm)

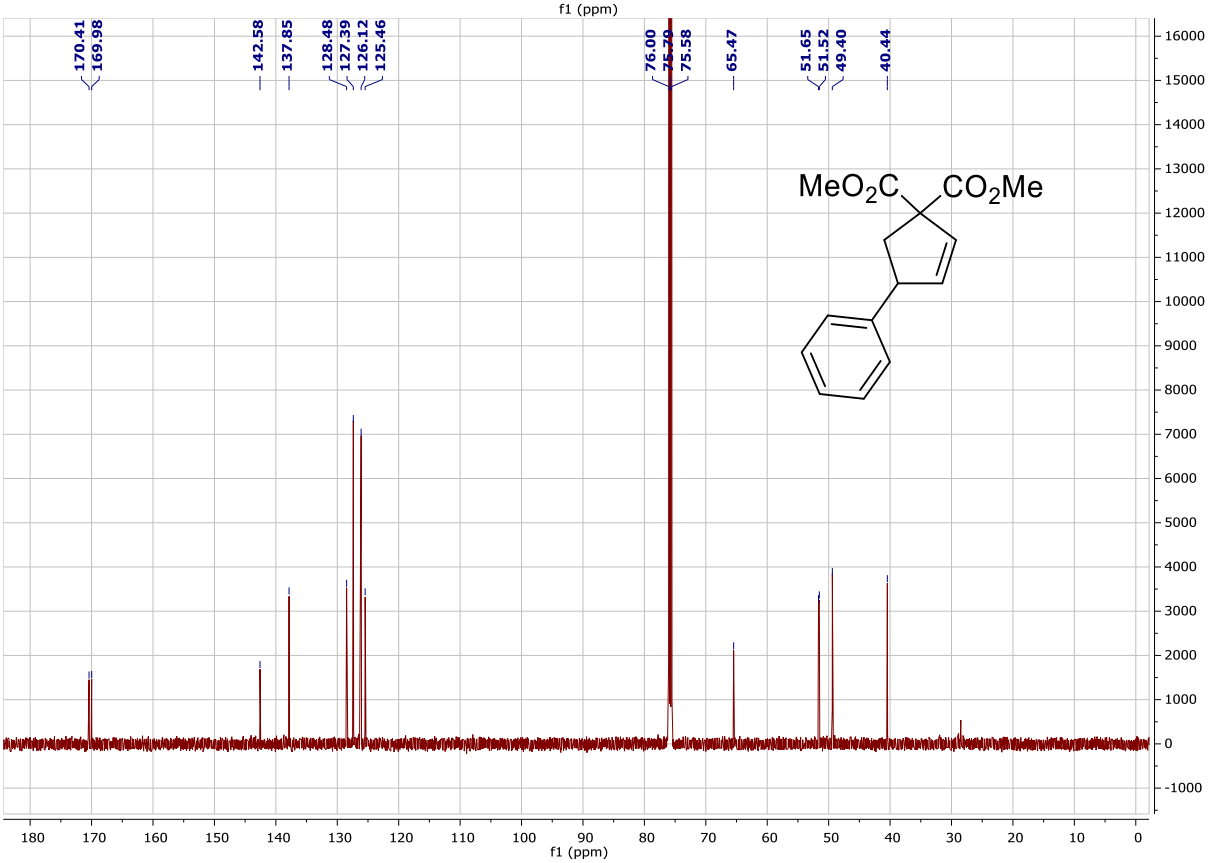
170.41
169.98
142.58
137.85
128.48
127.39
126.12
125.46
76.00
75.70
75.58
65.47
51.65
51.52
49.40
40.44
MeO2C
CO2Me
f1 (ppm)

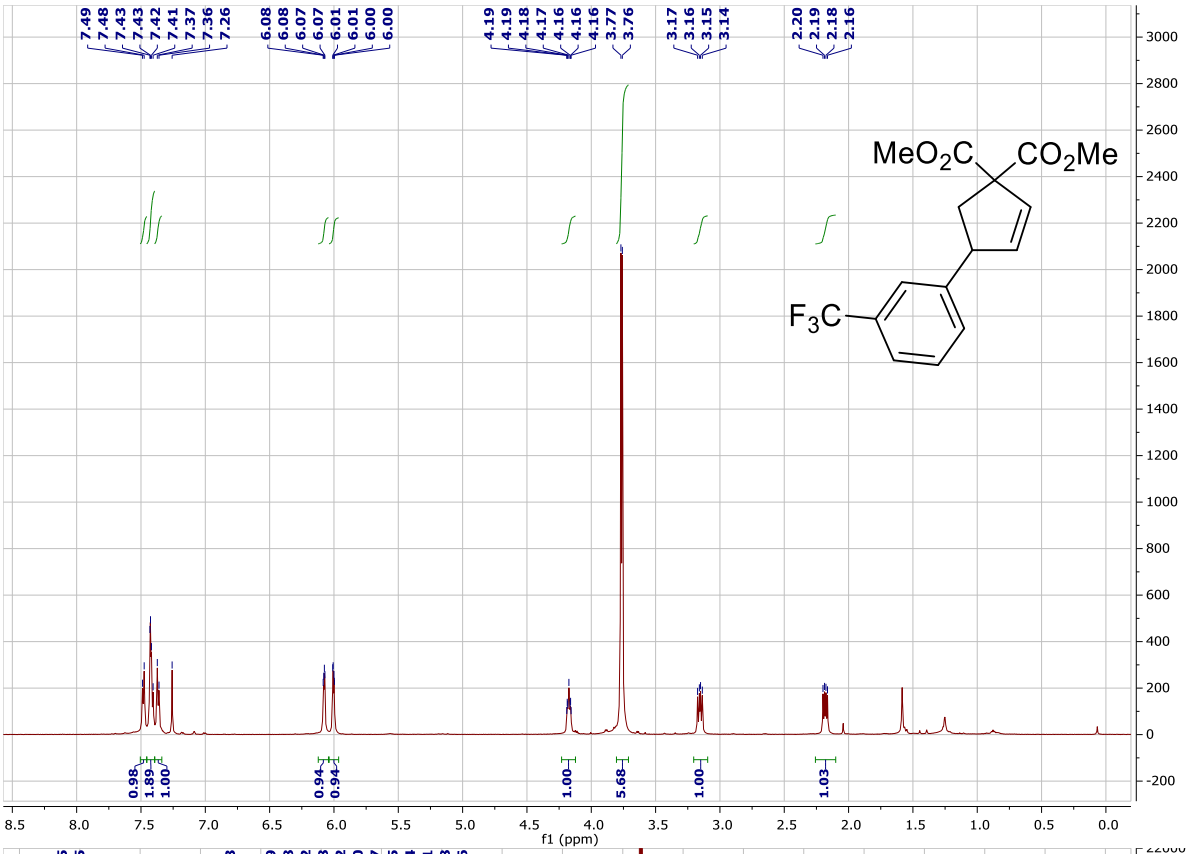
7.49 7.48 7.43 7.43 7.42 7.41 7.37 7.36 7.26
6.08 6.08 6.07 6.07 6.01 6.01 6.00 6.00
4.19 4.19 4.18 4.17 4.16 4.16 4.16
3.77 3.76
3.17 3.16 3.15 3.14
2.20 2.19 2.18 2.16
0.98 1.89 1.00 0.94 0.94 1.00 5.68 1.00 1.03
MeO2C CO2Me
F3C
f1 (ppm)

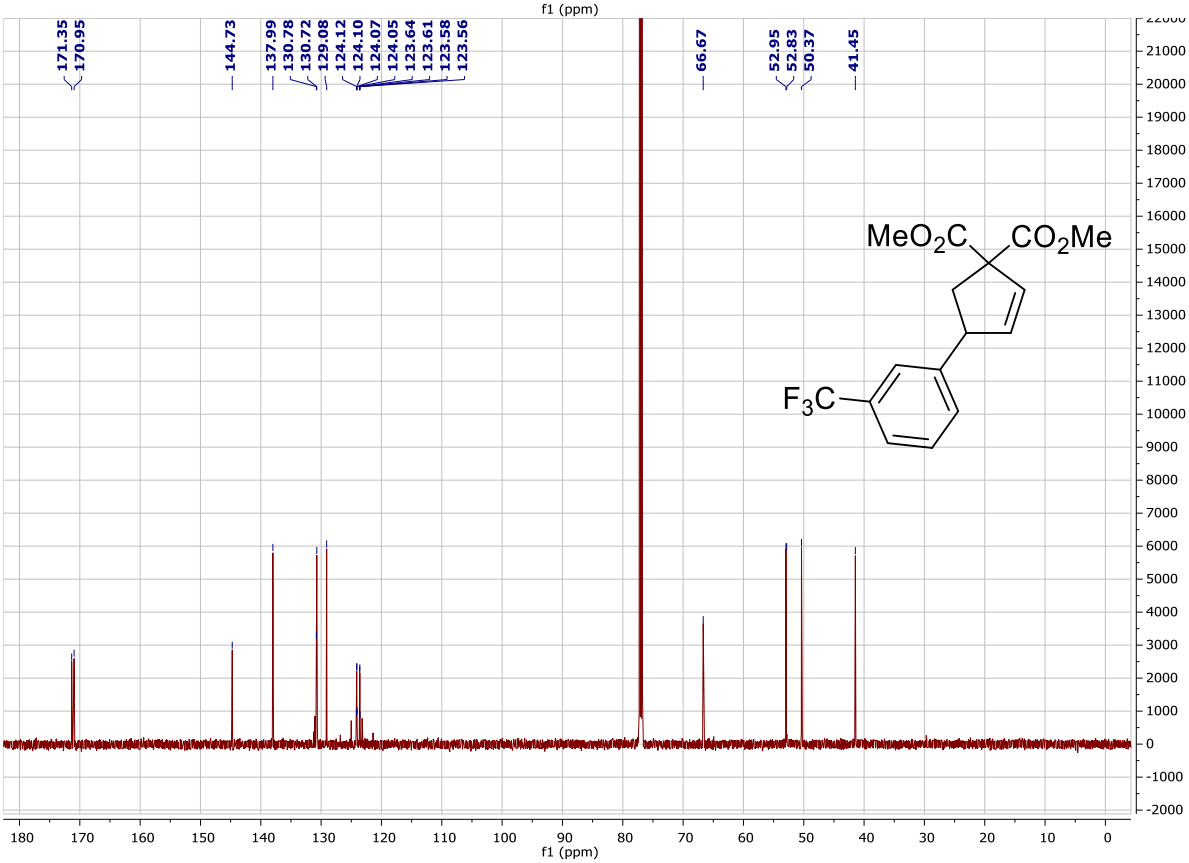
171.35 170.95
144.73
137.99 130.78 130.72 129.08 124.12 124.10 124.07 124.05 123.64 123.61 123.58 123.56
66.67
52.95 52.83 50.37
41.45
MeO2C CO2Me
F3C
f1 (ppm)

^{19}F NMR

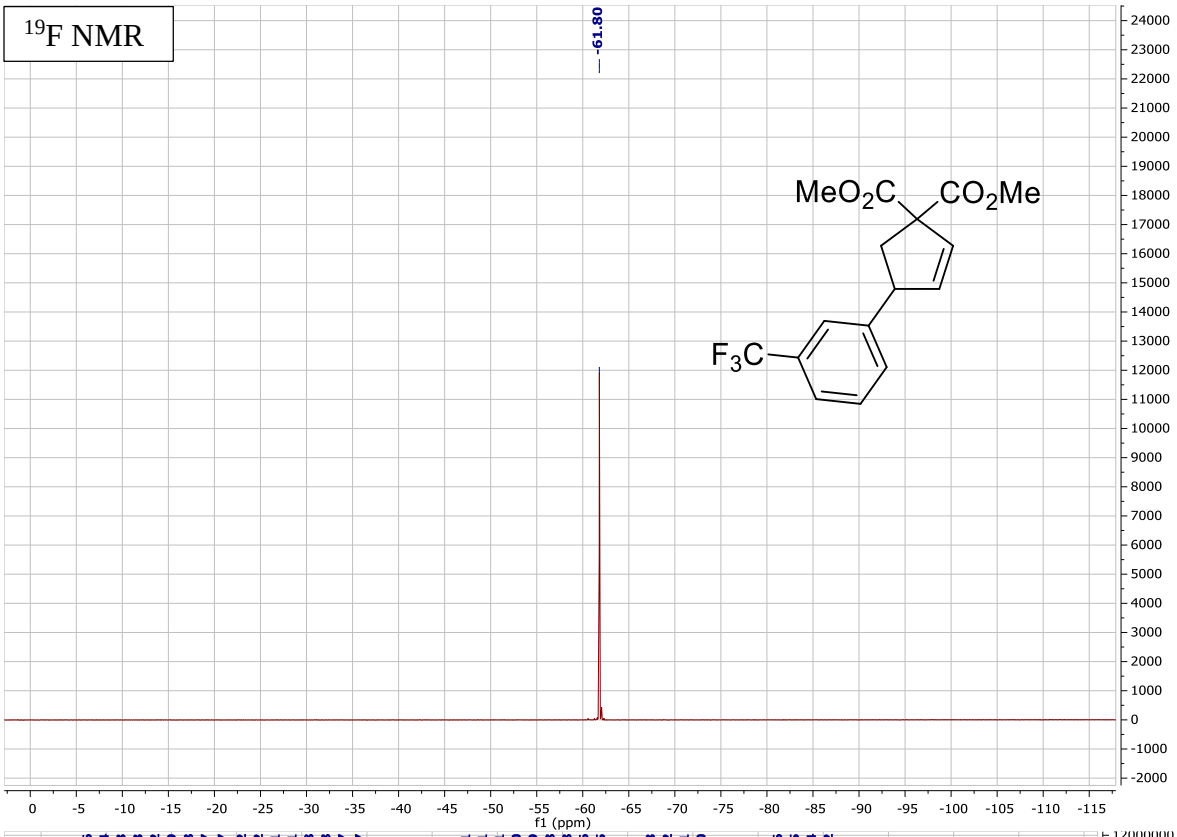
-61.80
MeO2C
CO2Me
F3C
f1 (ppm)

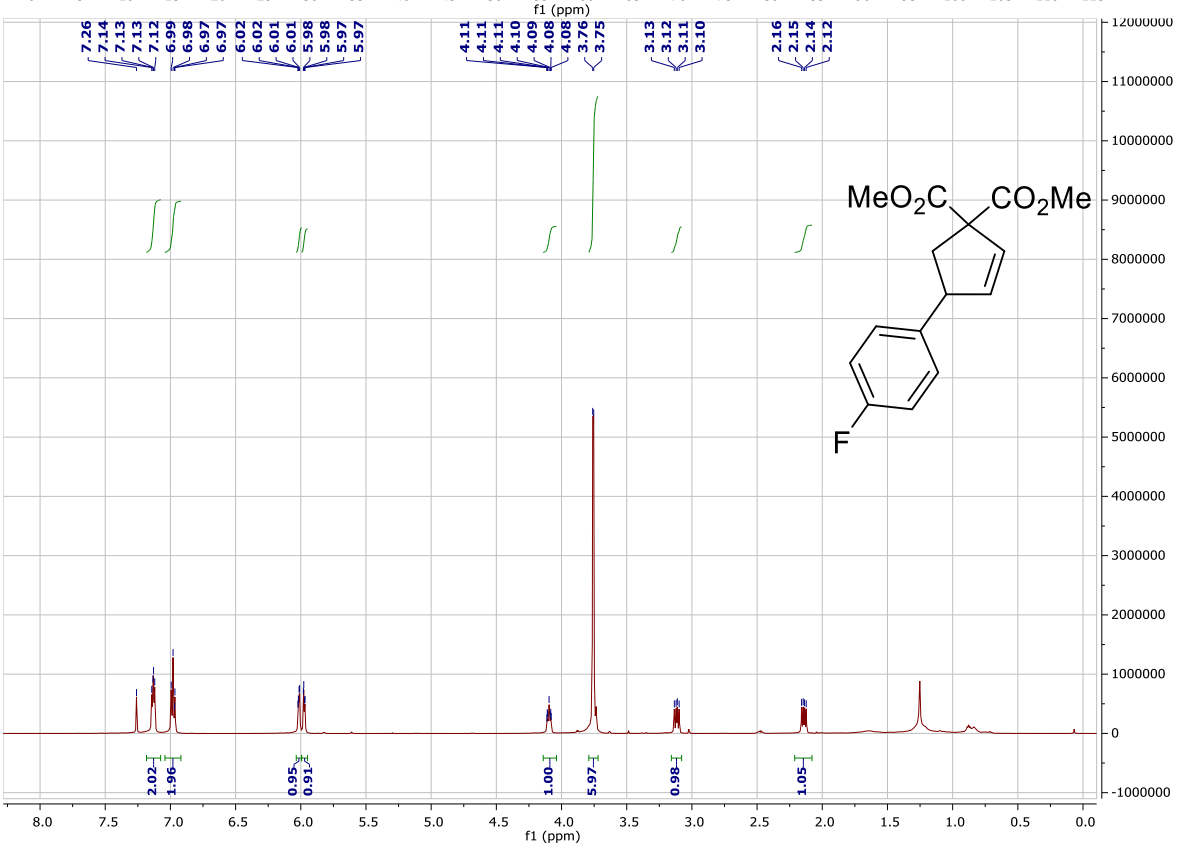
7.26
7.14
7.13
7.13
7.12
6.99
6.98
6.97
6.97
6.02
6.02
6.01
6.01
5.98
5.98
5.97
5.97
4.11
4.11
4.11
4.10
4.09
4.08
4.08
3.76
3.75
3.13
3.12
3.11
3.10
2.16
2.15
2.14
2.12
2.02
1.96
0.95
0.91
1.00
5.97
0.98
1.05
MeO2C
CO2Me
F
f1 (ppm)

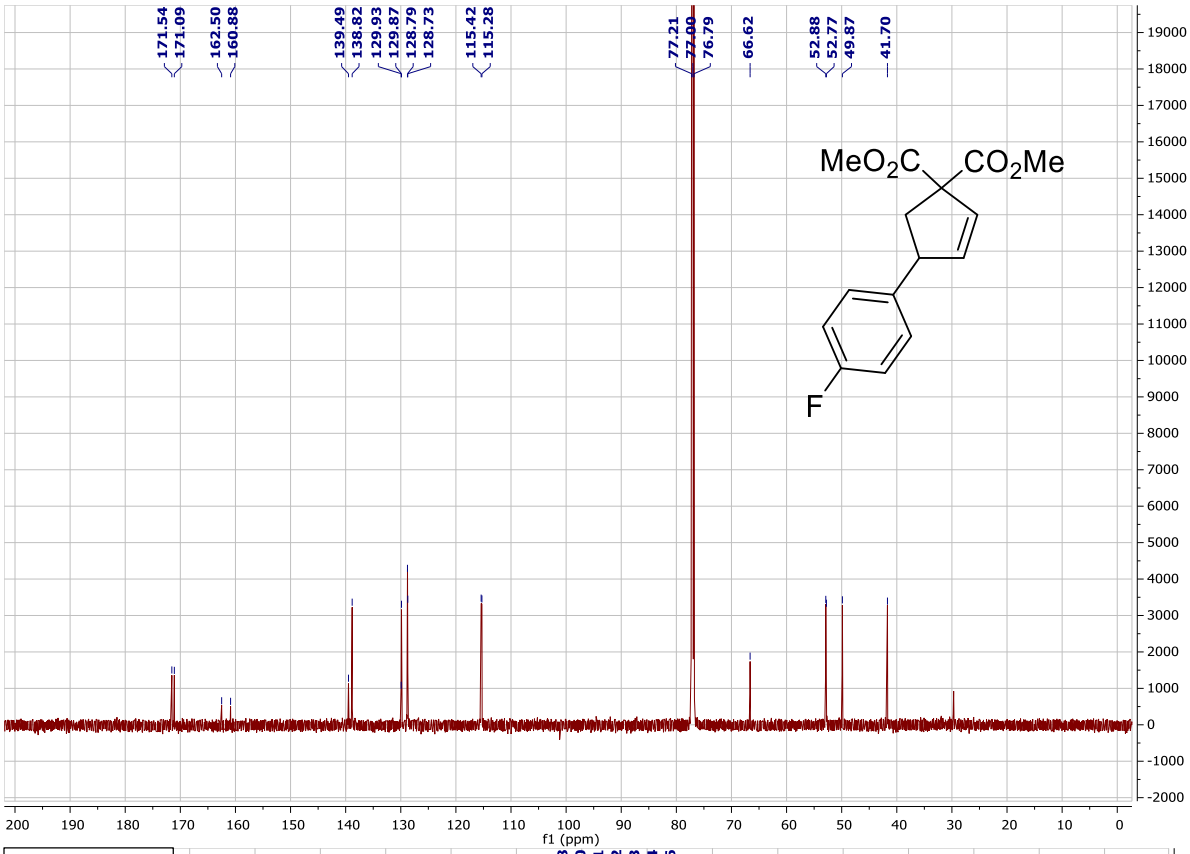
171.54
171.09
162.50
160.88
139.49
138.82
129.93
129.87
128.79
128.73
115.42
115.28
77.21
77.00
76.79
66.62
52.88
52.77
49.87
41.70
MeO2C
CO2Me
F
f1 (ppm)

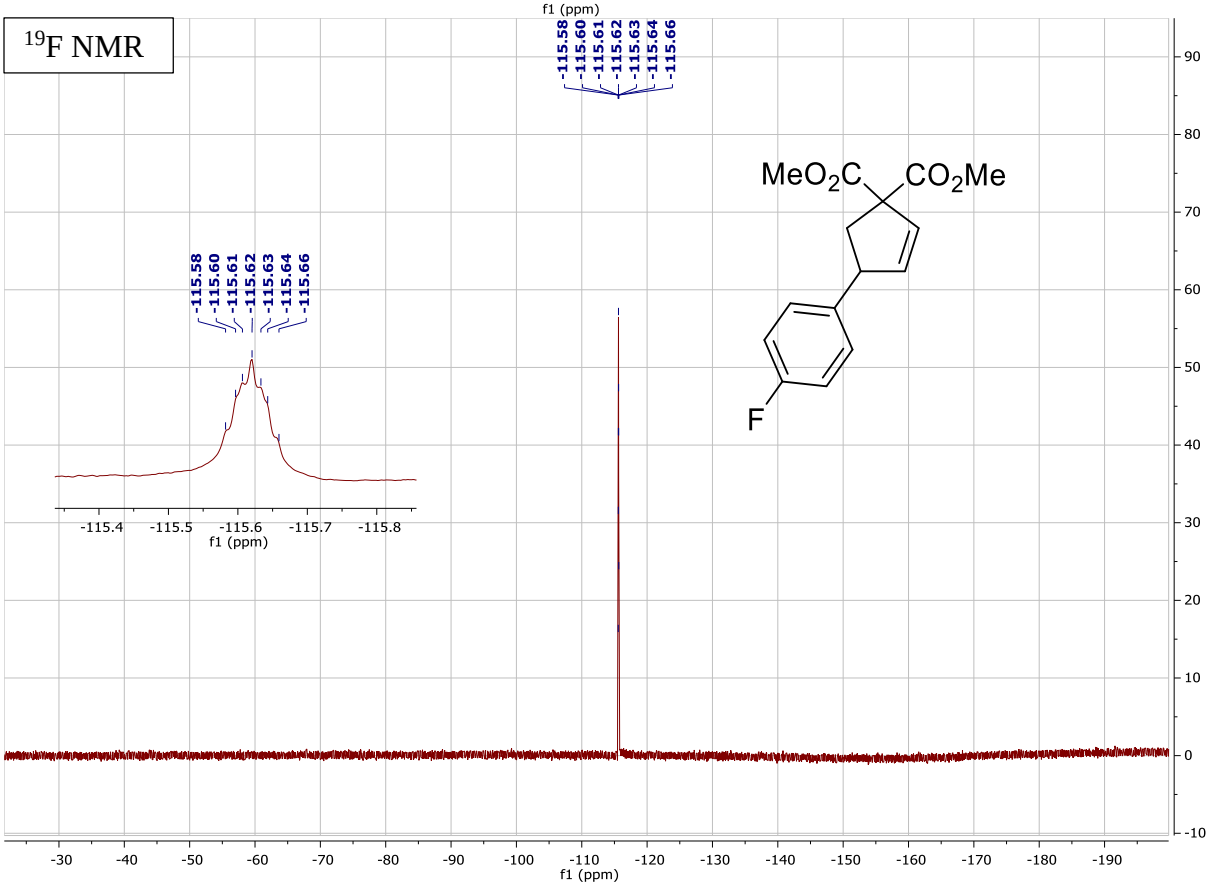
19F NMR
-115.58
-115.60
-115.61
-115.62
-115.63
-115.64
-115.66
MeO2C
CO2Me
F
f1 (ppm)

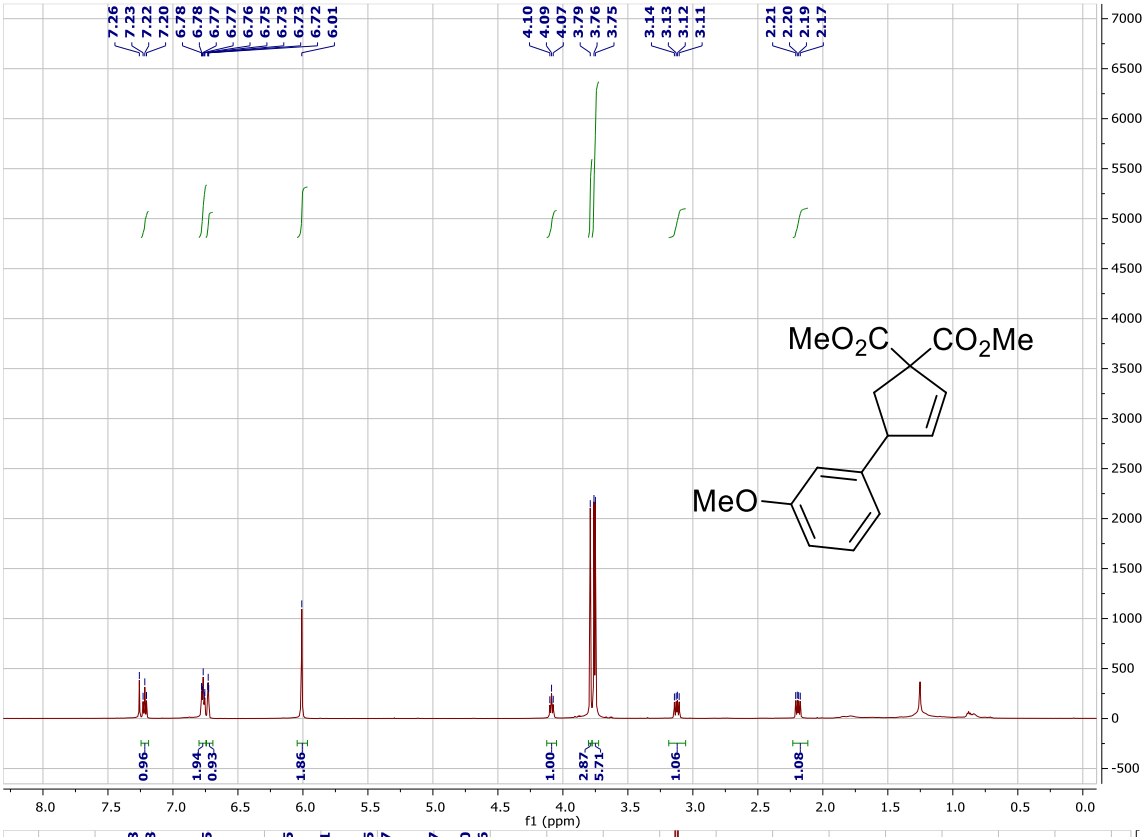
7.26
7.23
7.22
7.20
6.78
6.78
6.77
6.77
6.76
6.75
6.73
6.72
6.01
4.10
4.09
4.07
3.79
3.76
3.75
3.14
3.13
3.12
3.11
2.21
2.20
2.19
2.17
MeO2C
CO2Me
MeO
0.96
1.94
0.93
1.86
1.00
2.87
5.71
1.06
1.08
f1 (ppm)

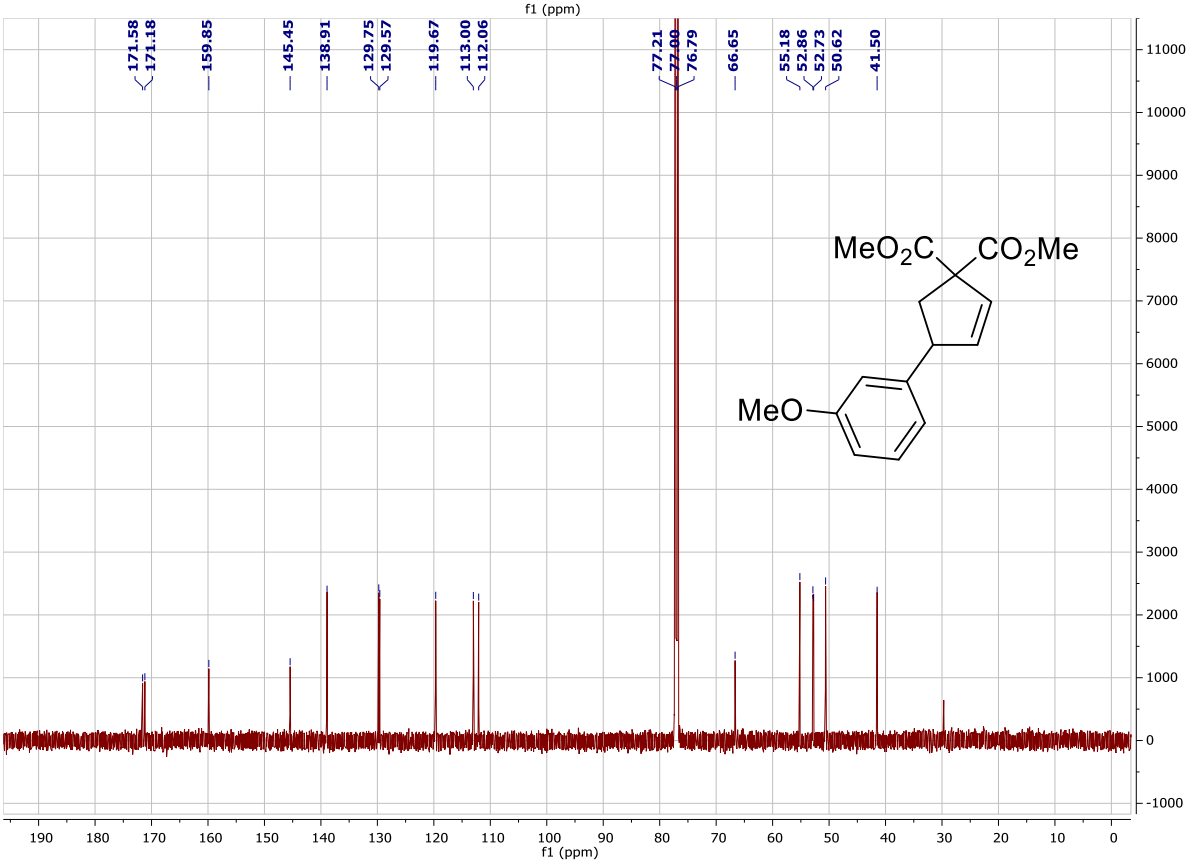
171.58
171.18
159.85
145.45
138.91
129.75
129.57
119.67
113.00
112.06
77.21
77.00
76.79
66.65
55.18
52.86
52.73
50.62
41.50
MeO2C
CO2Me
MeO
f1 (ppm)

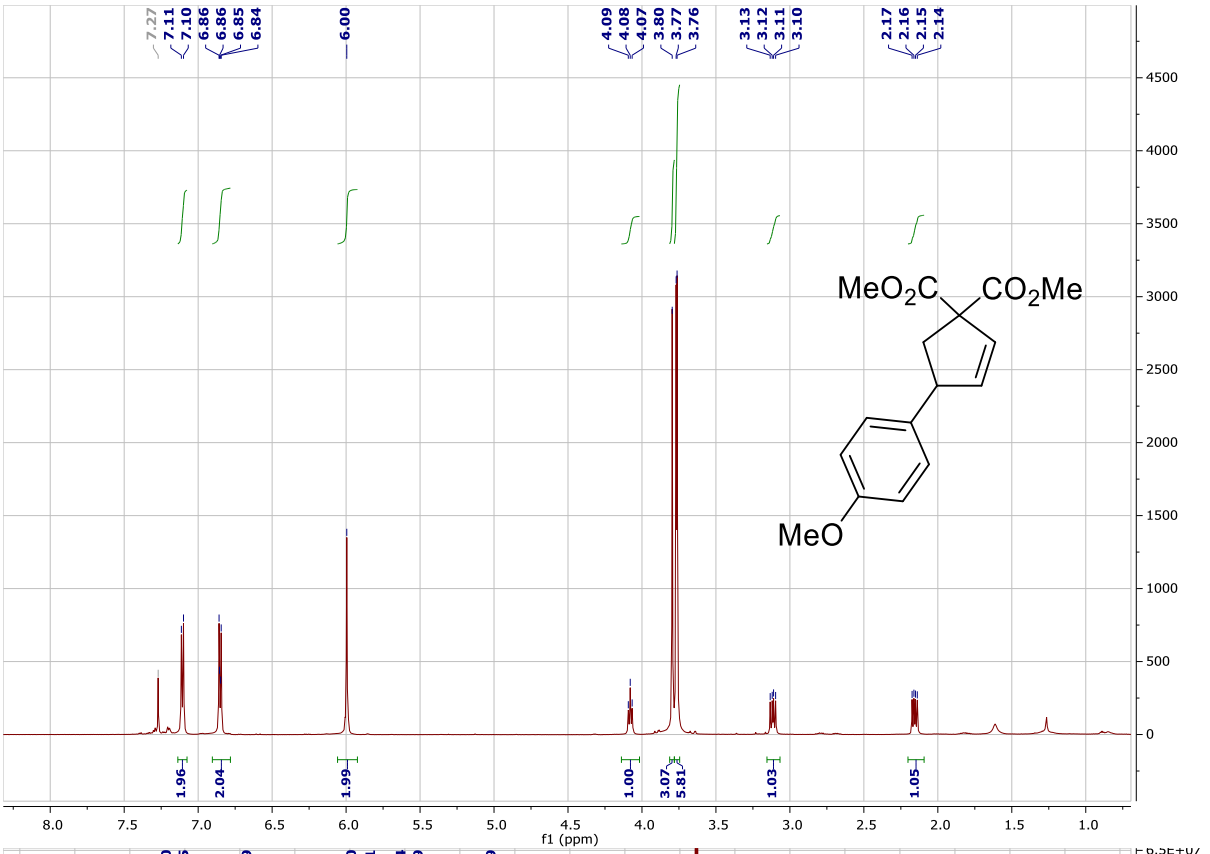
7.27
7.11
7.10
6.86
6.86
6.85
6.84
6.00
4.09
4.08
4.07
3.80
3.77
3.76
3.13
3.12
3.11
3.10
2.17
2.16
2.15
2.14
MeO2C
CO2Me
MeO
1.96
2.04
1.99
1.00
3.07
5.81
1.03
1.05
f1 (ppm)

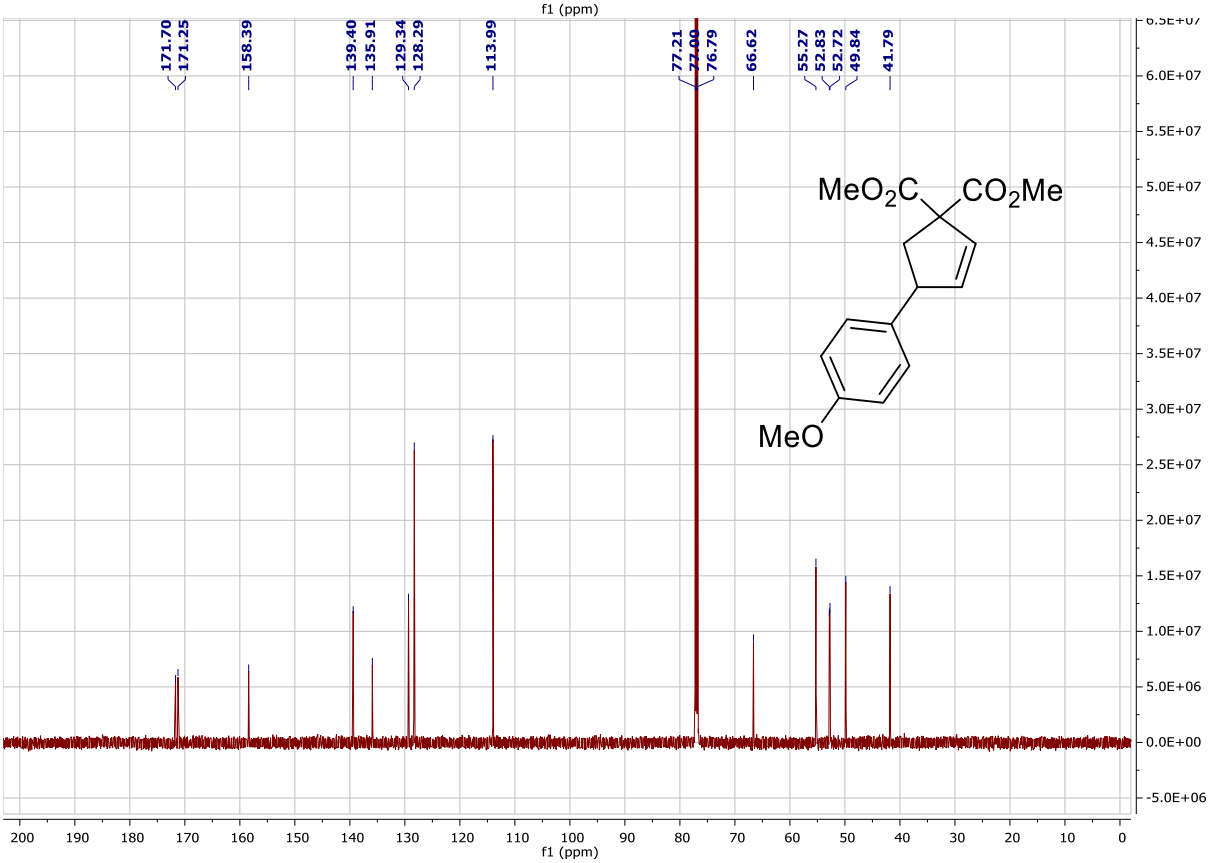
171.70
171.25
158.39
139.40
135.91
129.34
128.29
113.99
77.21
77.00
76.79
66.62
55.27
52.83
52.72
49.84
41.79
MeO2C
CO2Me
MeO
f1 (ppm)

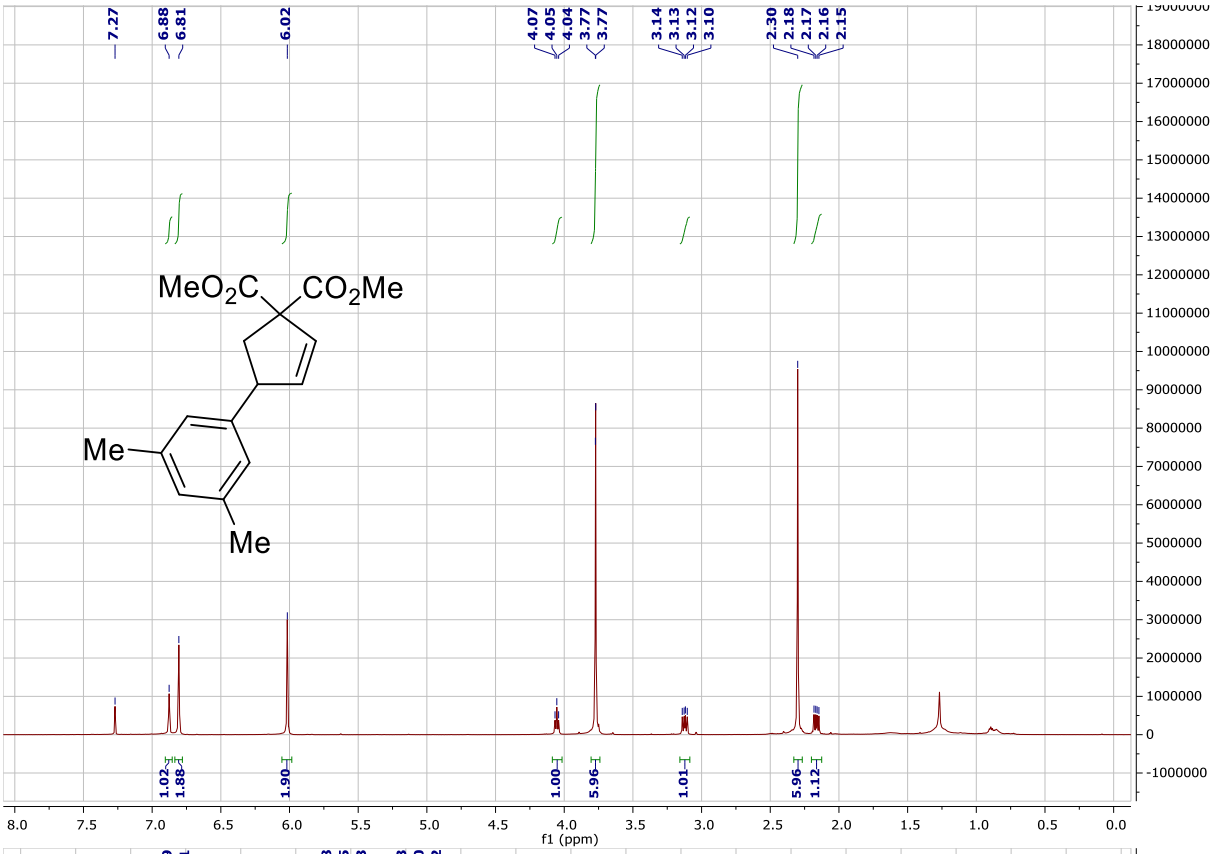
7.27
6.88
6.81
6.02
4.07
4.05
4.04
3.77
3.77
3.14
3.13
3.12
3.10
2.30
2.18
2.17
2.16
2.15
MeO2C
CO2Me
Me
Me
1.02
1.88
1.90
1.00
5.96
1.01
5.96
1.12
f1 (ppm)

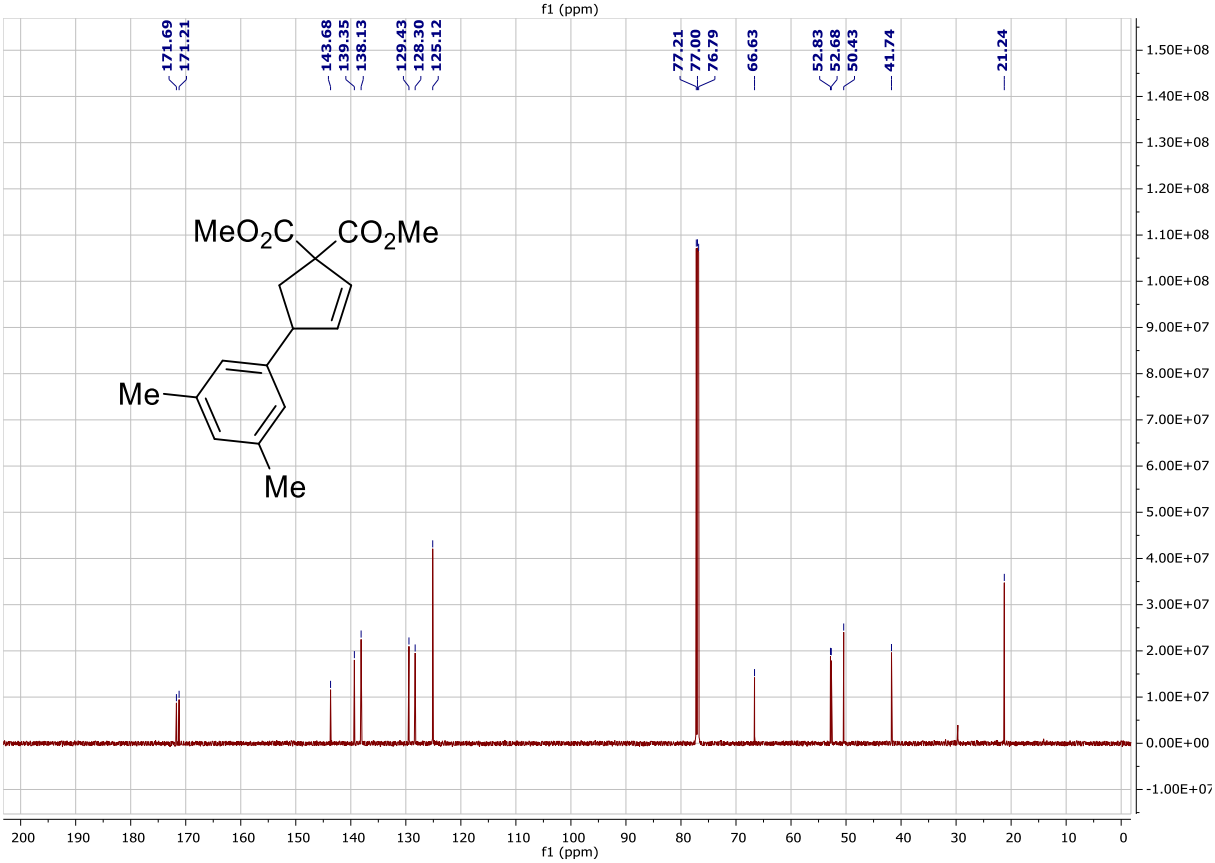
171.69
171.21
143.68
139.35
138.13
129.43
128.30
125.12
77.21
77.00
76.79
66.63
52.83
52.68
50.43
41.74
21.24
MeO2C
CO2Me
Me
Me
f1 (ppm)

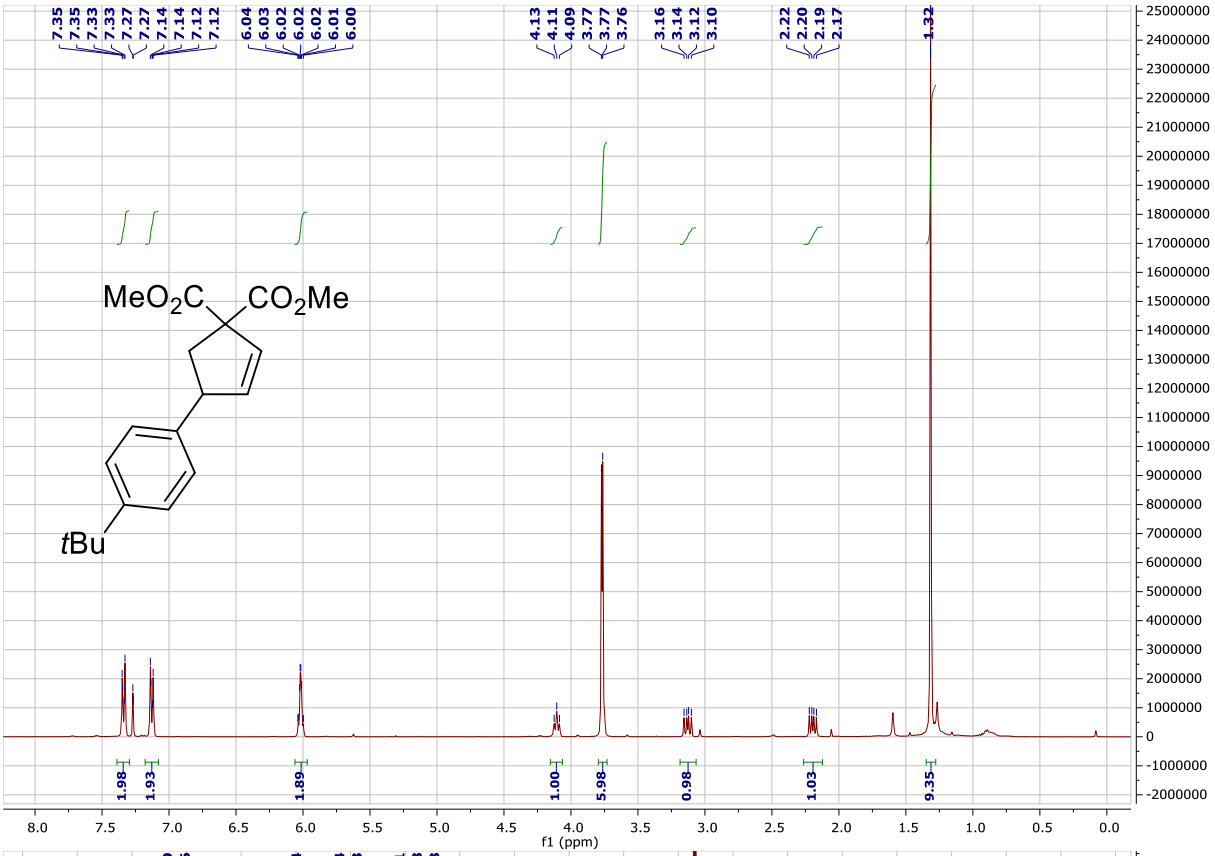
7.35
7.35
7.33
7.33
7.27
7.27
7.14
7.14
7.12
7.12
6.04
6.03
6.02
6.02
6.02
6.01
6.00
4.13
4.11
4.09
3.77
3.77
3.76
3.16
3.14
3.12
3.10
2.22
2.20
2.19
2.17
1.32
MeO2C
CO2Me
tBu
1.98
1.93
1.89
1.00
5.98
0.98
1.03
9.35
f1 (ppm)

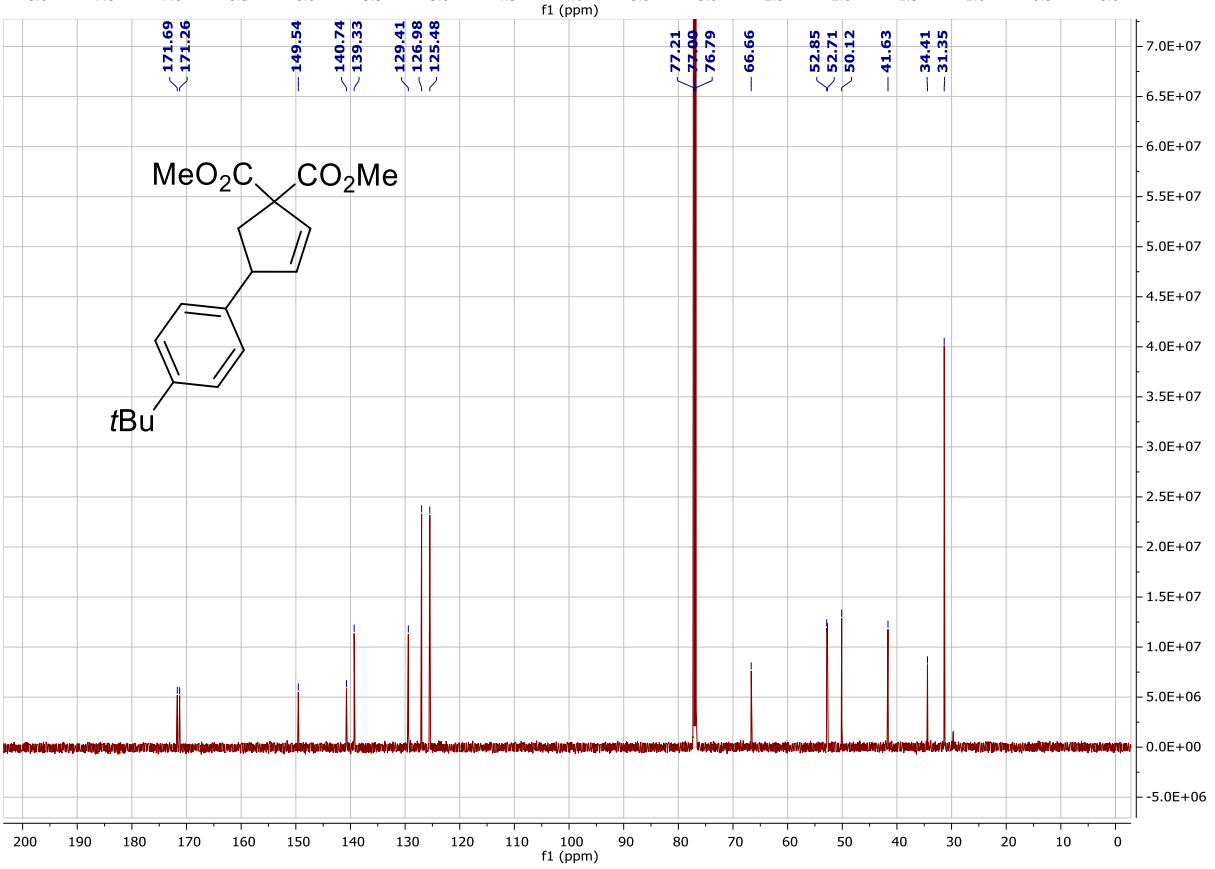
171.69
171.26
149.54
140.74
139.33
129.41
126.98
125.48
77.21
77.00
76.79
66.66
52.85
52.71
50.12
41.63
34.41
31.35
MeO2C
CO2Me
tBu
f1 (ppm)

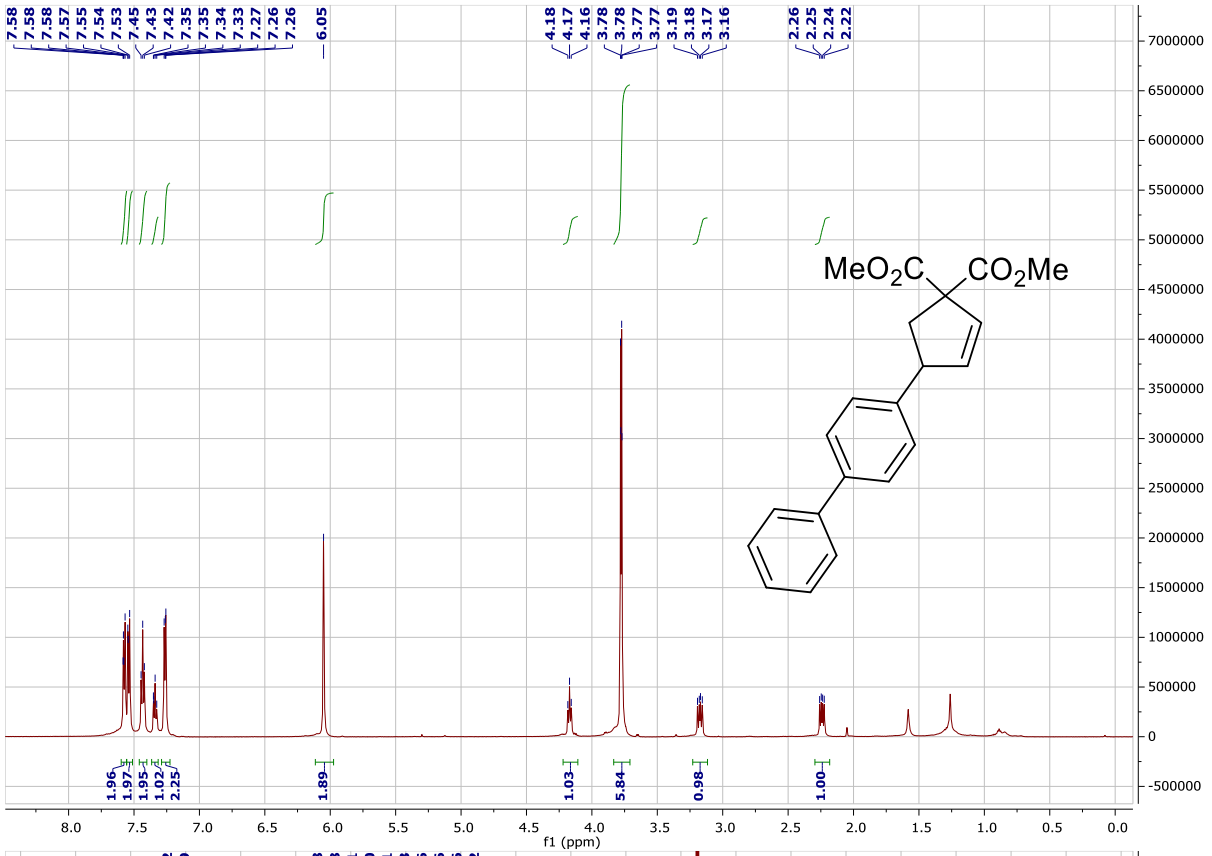
7.58
7.58
7.58
7.57
7.55
7.54
7.53
7.45
7.43
7.42
7.35
7.35
7.34
7.33
7.27
7.26
7.26
6.05
4.18
4.17
4.16
3.78
3.78
3.77
3.77
3.19
3.18
3.17
3.16
2.26
2.25
2.24
2.22
1.96
1.97
1.95
1.02
2.25
1.89
1.03
5.84
0.98
1.00
MeO2C
CO2Me
f1 (ppm)

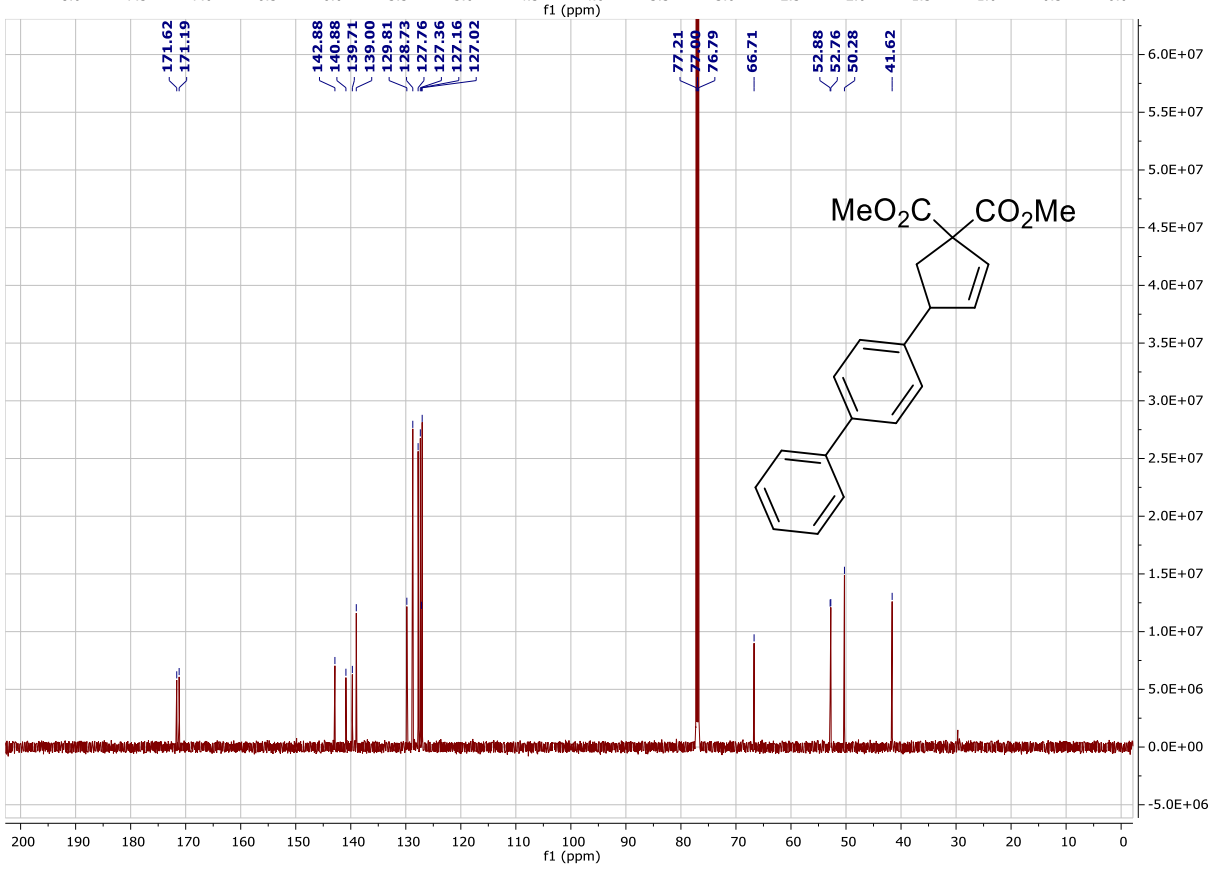
171.62
171.19
142.88
140.88
139.71
139.00
129.81
128.73
127.76
127.36
127.16
127.02
77.21
77.00
76.79
66.71
52.88
52.76
50.28
41.62
MeO2C
CO2Me
f1 (ppm)

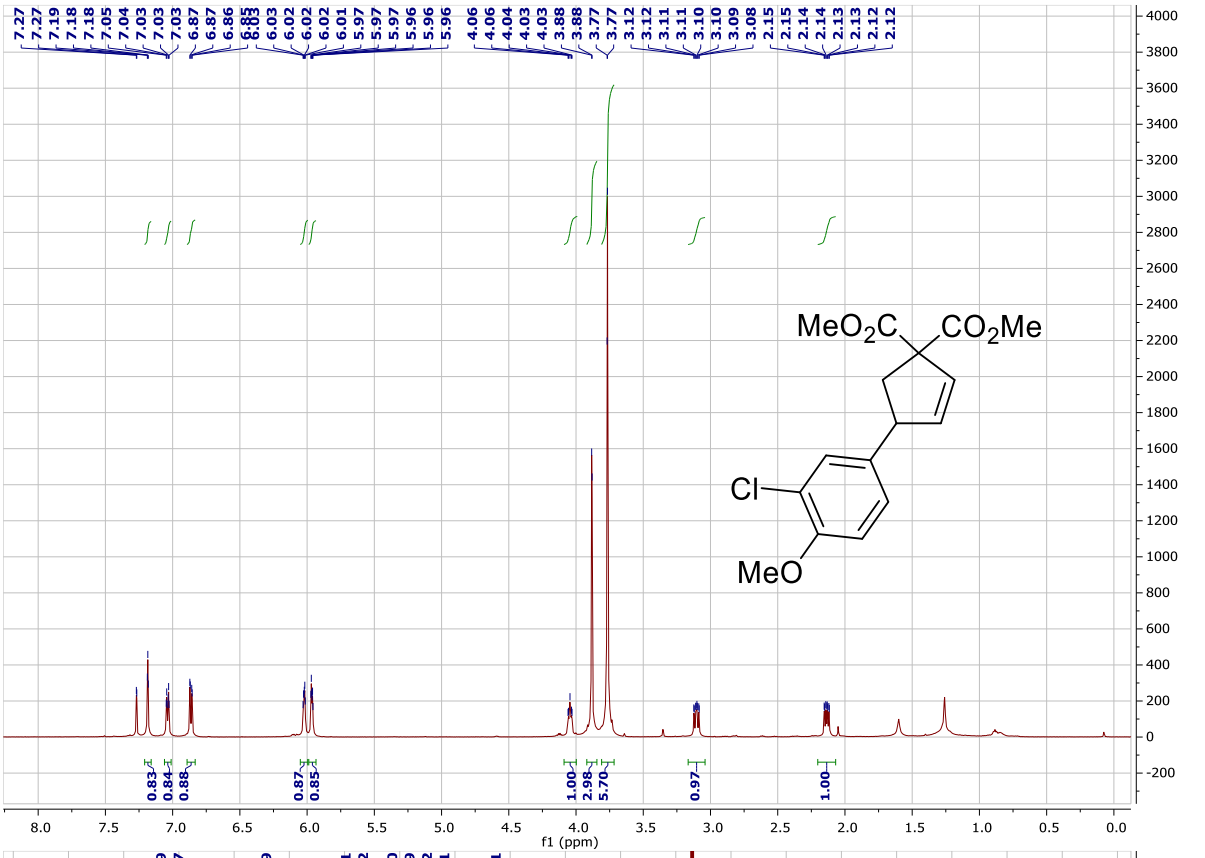
MeO2C
CO2Me
Cl
MeO
f1 (ppm)

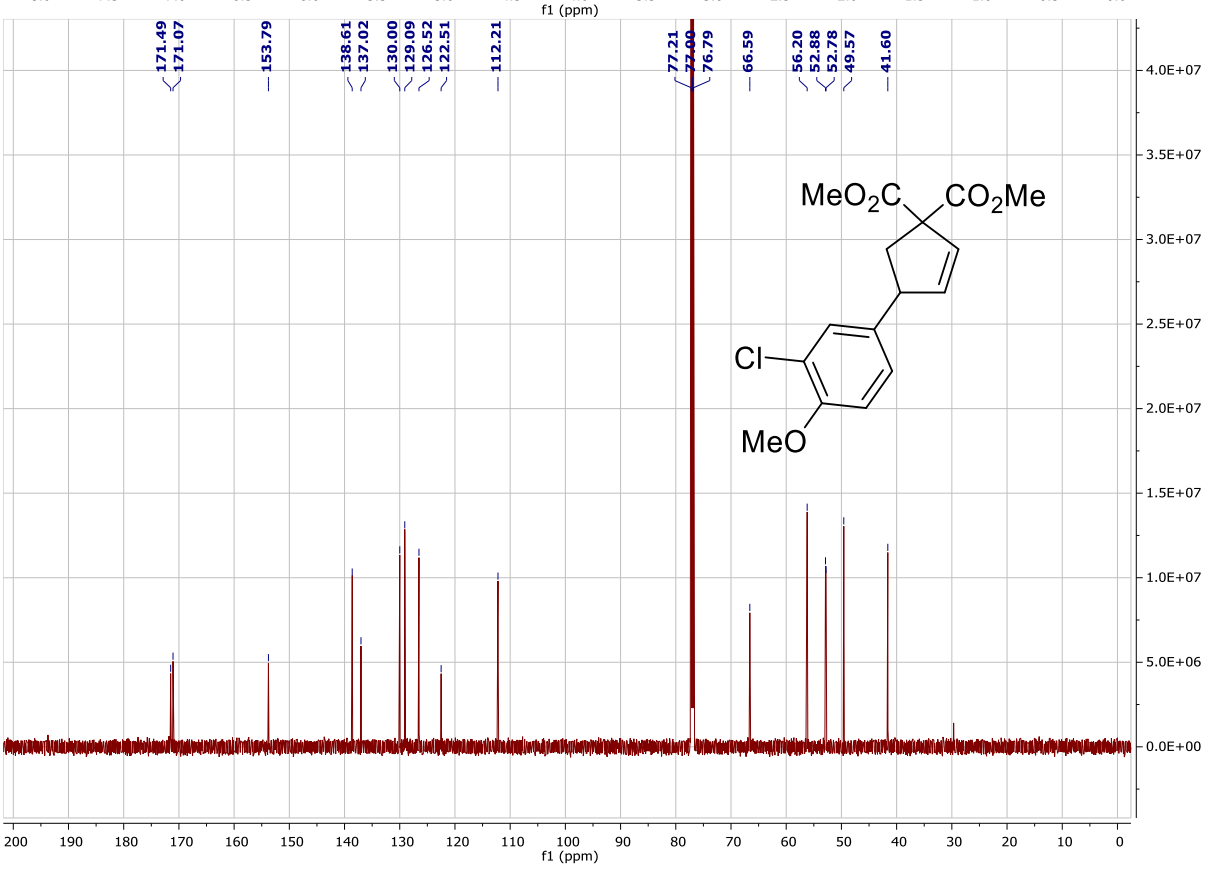
MeO2C
CO2Me
Cl
MeO
f1 (ppm)

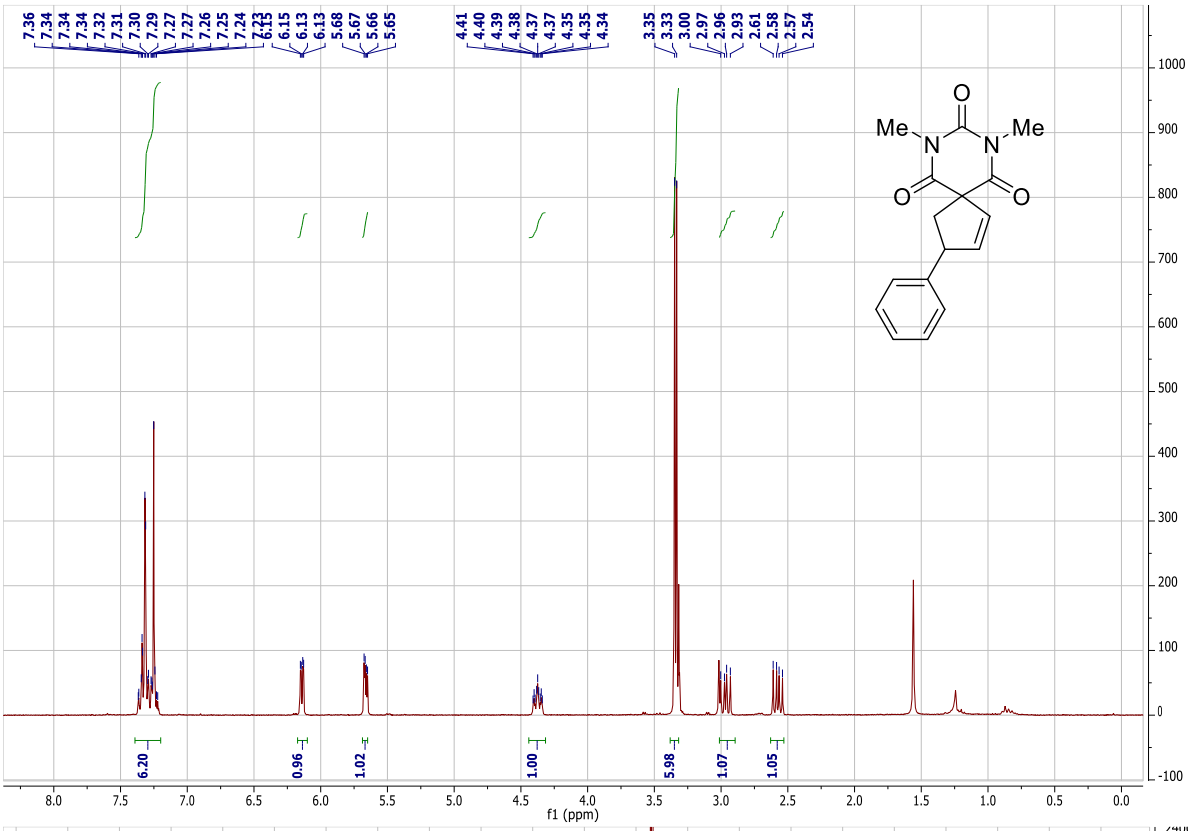
7.36 7.34 7.34 7.34 7.32 7.31 7.30 7.29 7.27 7.27 7.26 7.25 7.24 7.23 6.15 6.15 6.13 6.13 5.68 5.67 5.66 5.65
4.41 4.40 4.39 4.38 4.37 4.37 4.35 4.35 4.34
3.35 3.33 3.00 2.97 2.96 2.93 2.61 2.58 2.57 2.54
6.20 0.96 1.02 1.00 5.98 1.07 1.05
f1 (ppm)

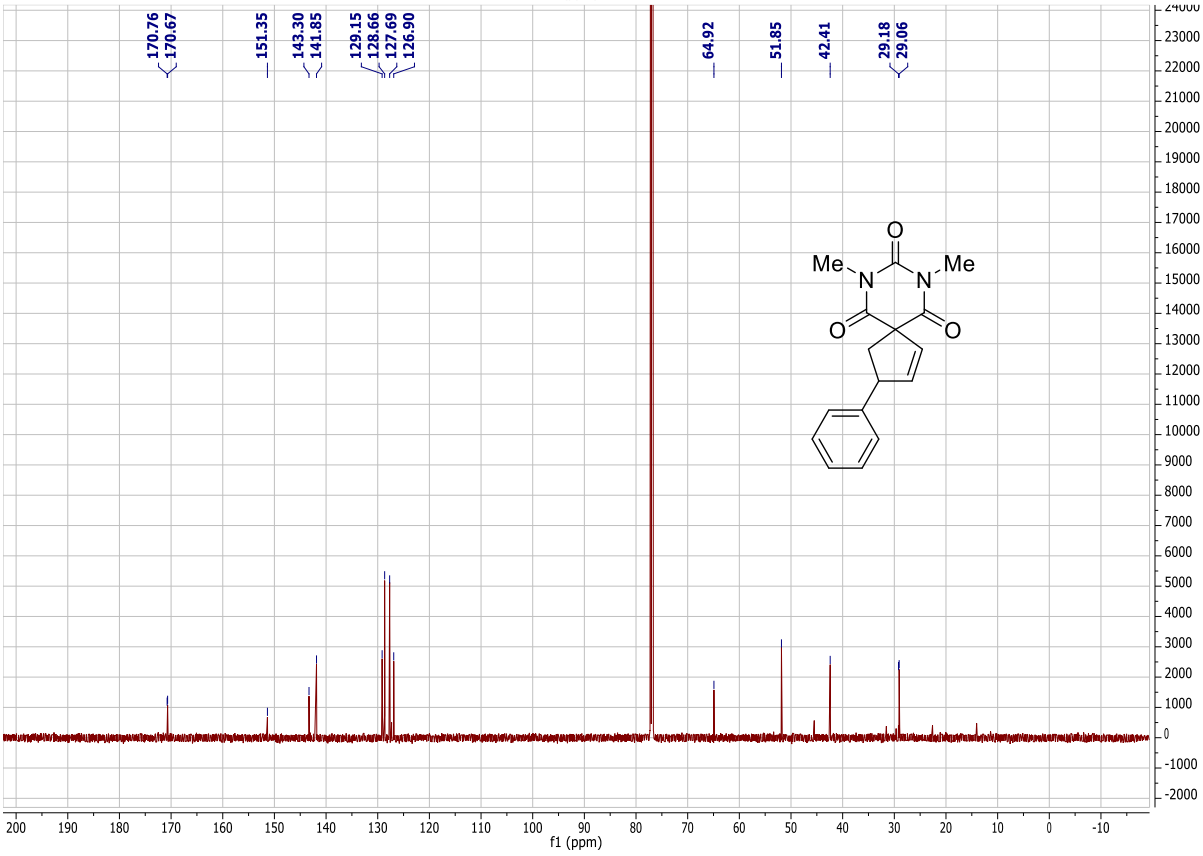
170.76 170.67 151.35 143.30 141.85 129.15 128.66 127.69 126.90 64.92 51.85 42.41 29.18 29.06
f1 (ppm)

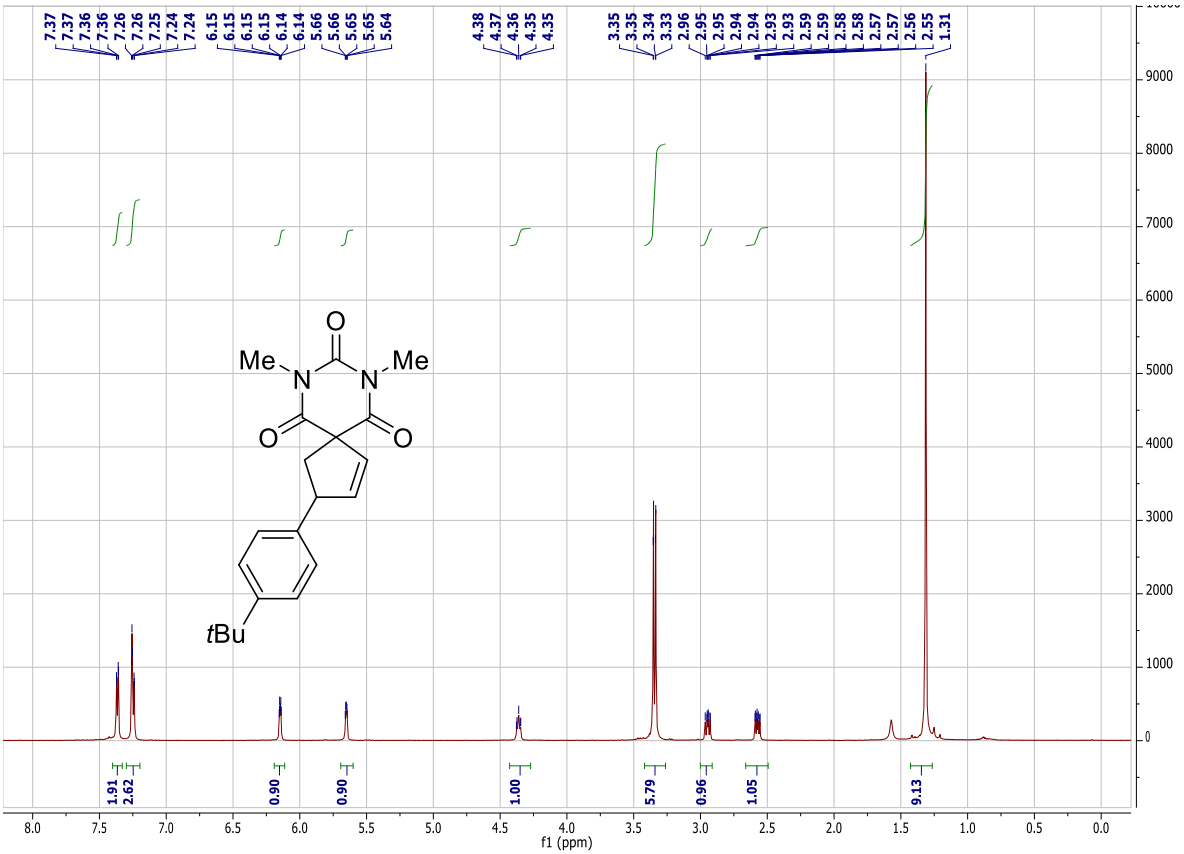
7.37 7.37 7.36 7.36 7.26 7.26 7.25 7.24 7.24
6.15 6.15 6.15 6.15 6.14 6.14
5.66 5.66 5.65 5.65 5.64
4.38 4.37 4.36 4.35 4.35
3.35 3.35 3.34 3.33
2.96 2.95 2.95 2.94 2.94 2.93 2.93 2.59 2.59 2.58 2.58 2.57 2.57 2.56 2.55 1.31
1.91 2.62 0.90 0.90 1.00 5.79 0.96 1.05 9.13
Me N N Me
O O O
tBu
f1 (ppm)

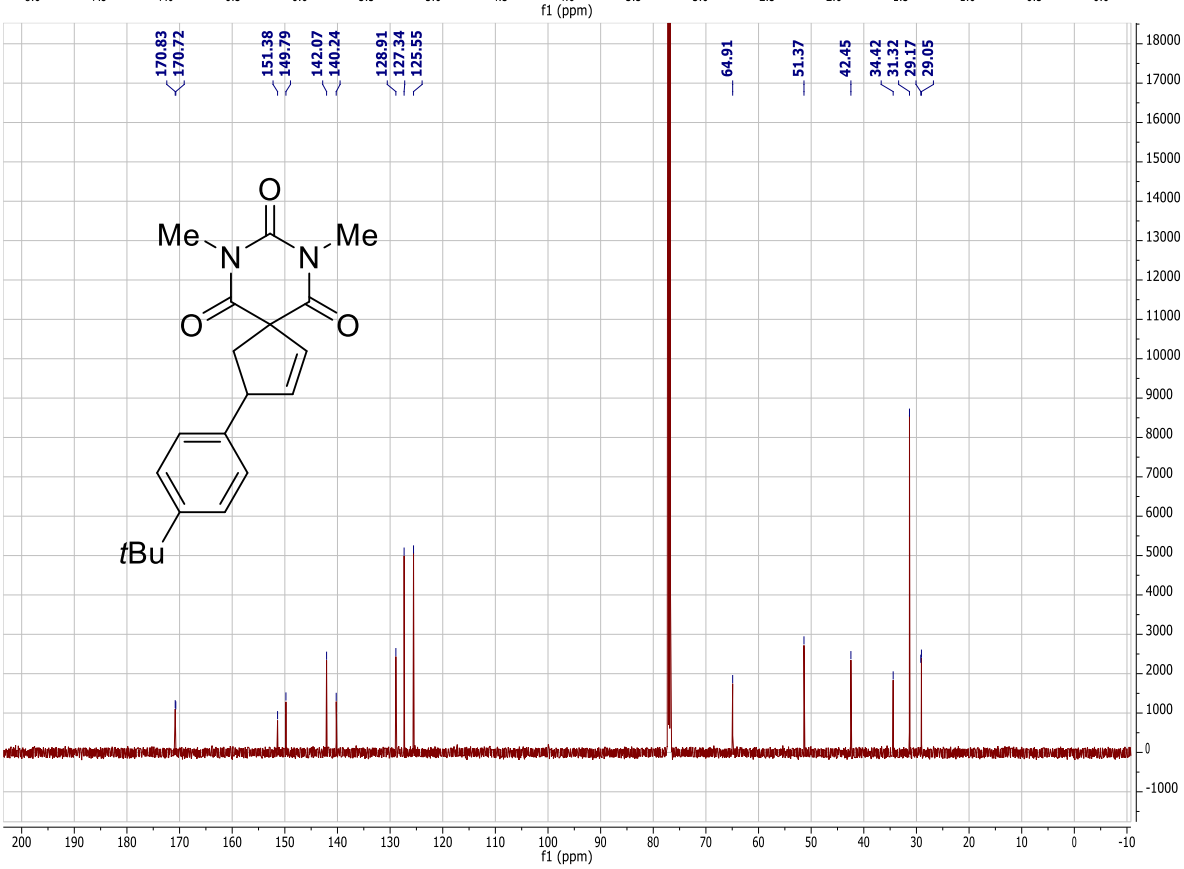
170.83 170.72
151.38 149.79
142.07 140.24
128.91 127.34 125.55
64.91
51.37
42.45
34.42 31.32 29.17 29.05
Me N N Me
O O O
tBu
f1 (ppm)

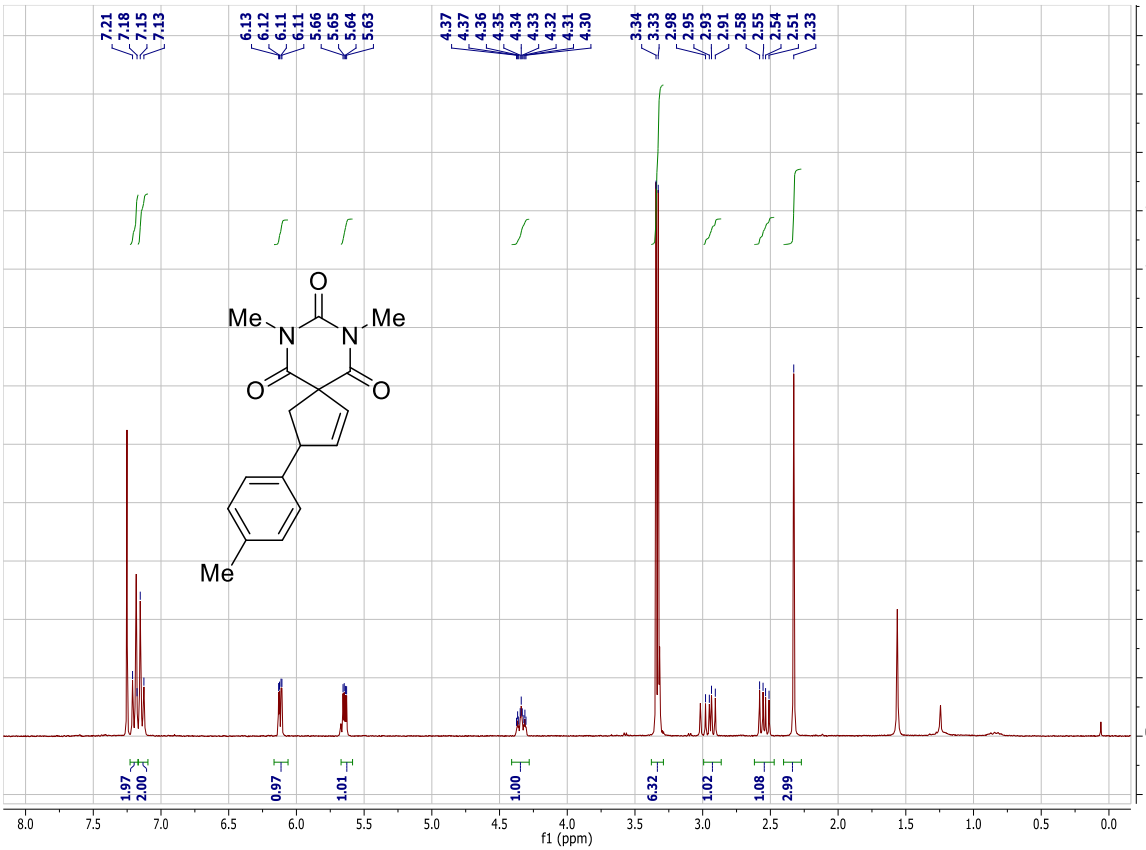
7.21
7.18
7.15
7.13
6.13
6.12
6.11
6.11
5.66
5.65
5.64
5.63
4.37
4.37
4.36
4.35
4.34
4.33
4.32
4.31
4.30
3.34
3.33
2.98
2.95
2.93
2.91
2.58
2.55
2.54
2.51
2.33
1.97
2.00
0.97
1.01
1.00
6.32
1.02
1.08
2.99
Me
N
O
Me
N
O
O
Me
f1 (ppm)

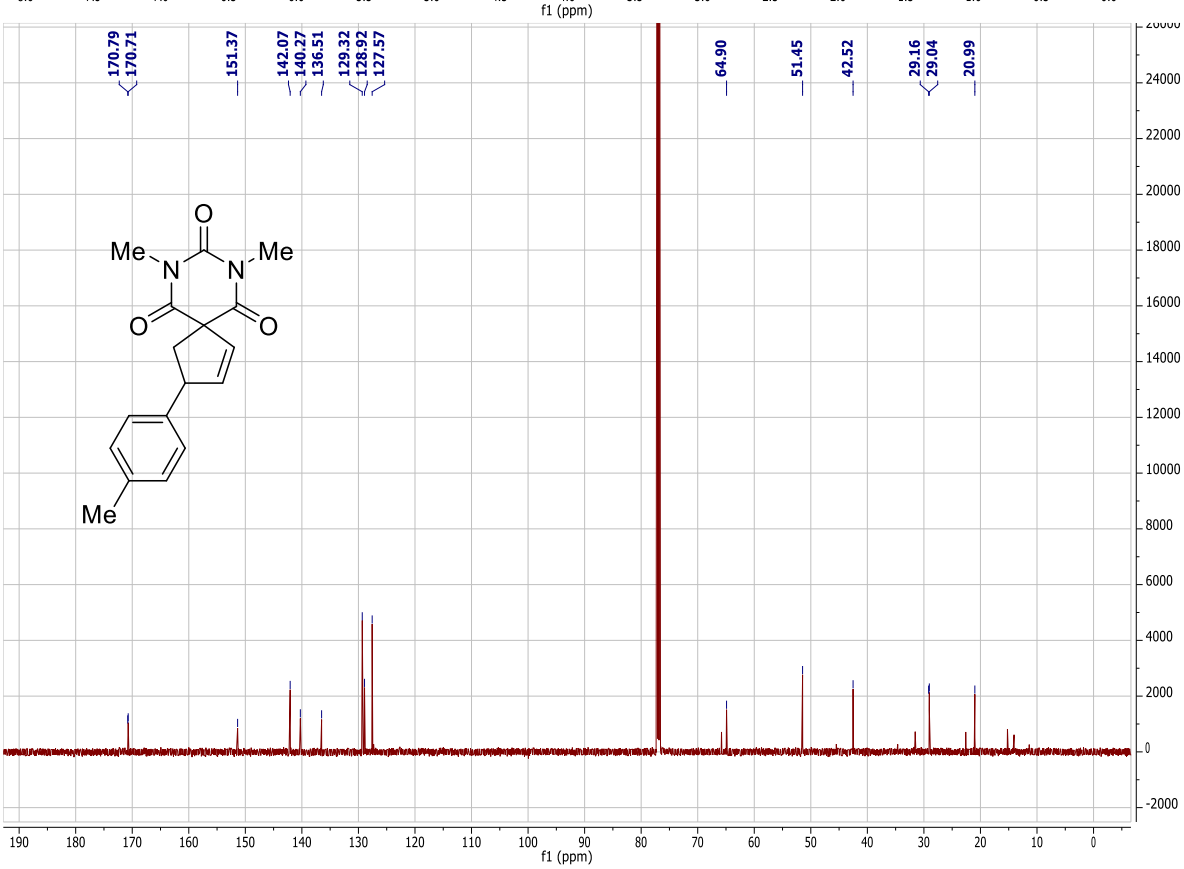
170.79
170.71
151.37
142.07
140.27
136.51
129.32
128.92
127.57
64.90
51.45
42.52
29.16
29.04
20.99
Me
N
O
Me
N
O
O
Me
f1 (ppm)

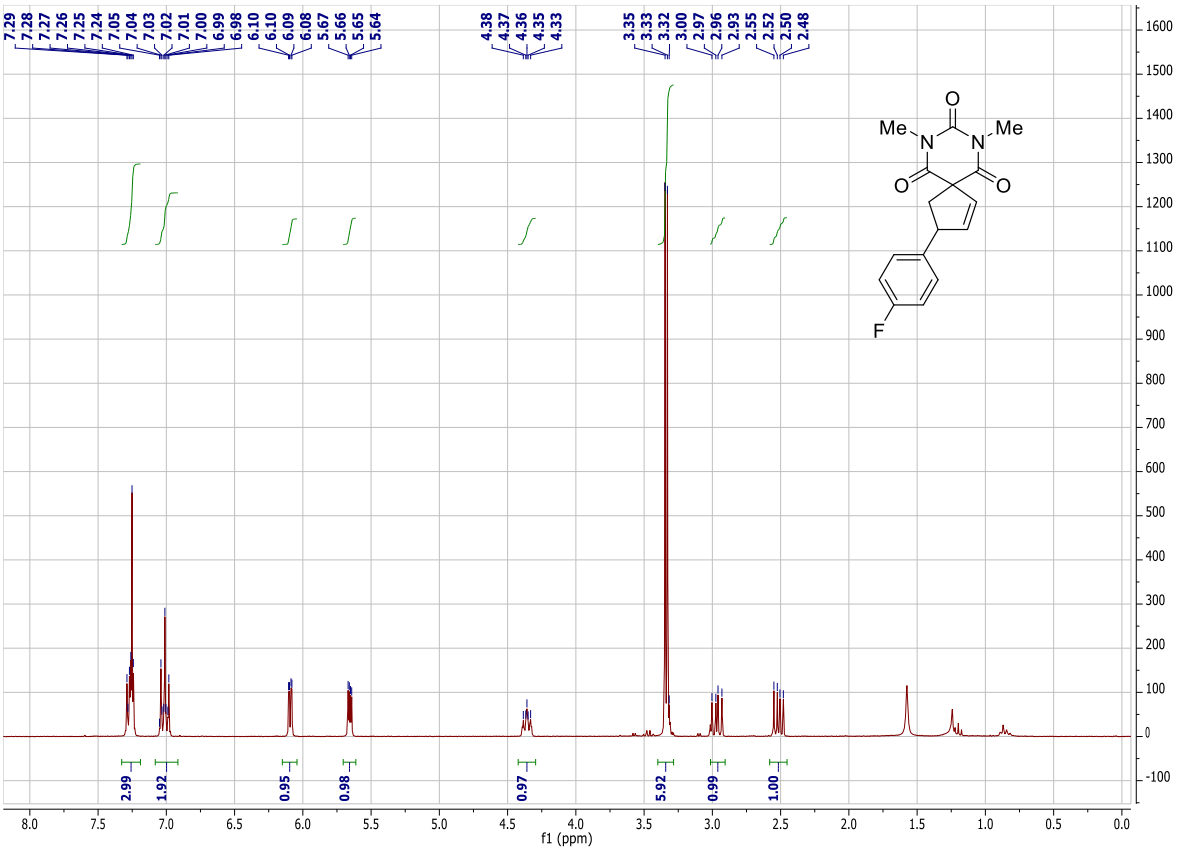
7.29 7.28 7.27 7.26 7.25 7.24 7.05 7.04 7.03 7.02 7.01 7.00 6.99 6.98 6.10 6.09 6.08 5.67 5.66 5.65 5.64
4.38 4.37 4.36 4.35 4.33
3.35 3.33 3.32 3.00 2.97 2.96 2.93 2.55 2.52 2.50 2.48
2.99 1.92 0.95 0.98 0.97 5.92 0.99 1.00
f1 (ppm)

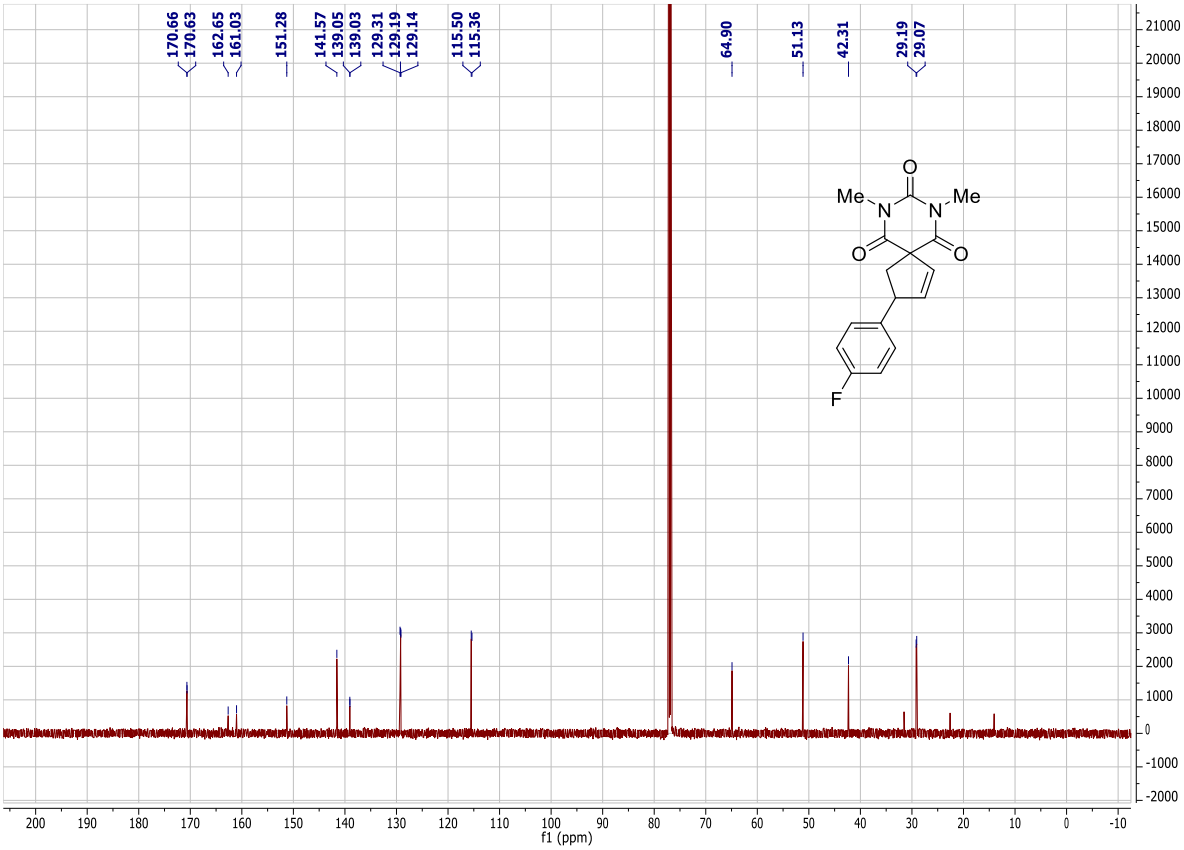
170.66 170.63 162.65 161.03 151.28 141.57 139.05 139.03 129.31 129.19 129.14 115.50 115.36 64.90 51.13 42.31 29.19 29.07
f1 (ppm)

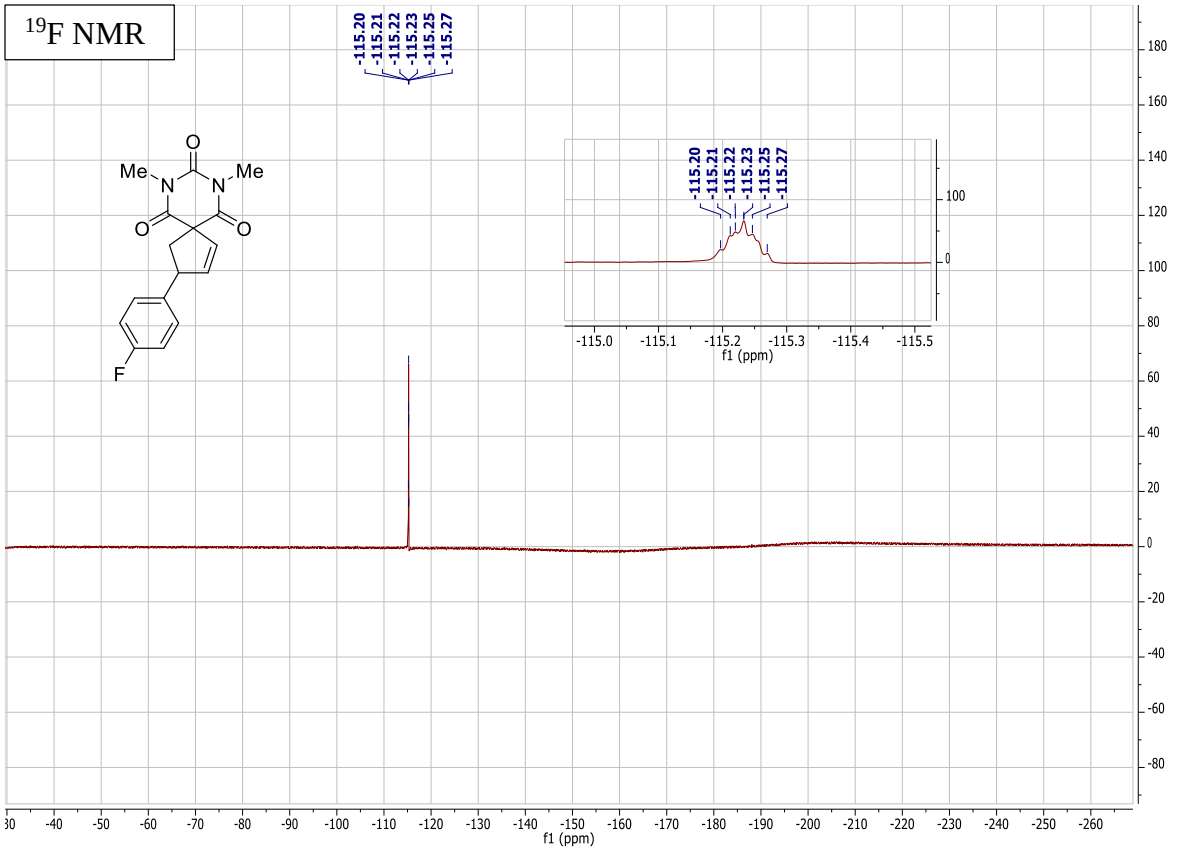
19F NMR
-115.20
-115.21
-115.22
-115.23
-115.25
-115.27
Me
N
N
Me
O
O
O
O
F
f1 (ppm)

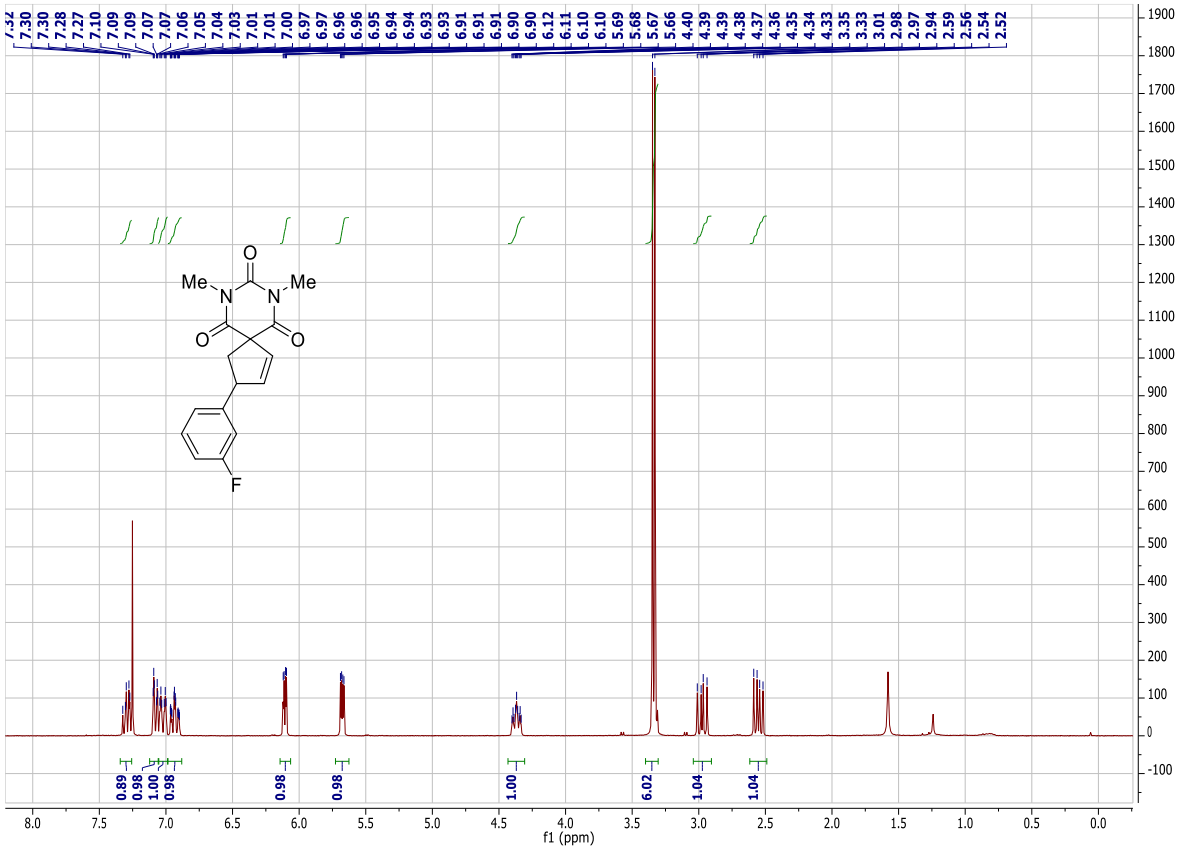
7.30
7.28
7.27
7.10
7.09
7.09
7.07
7.07
7.06
7.05
7.04
7.03
7.01
7.01
7.00
6.97
6.97
6.96
6.96
6.95
6.94
6.94
6.93
6.93
6.91
6.91
6.91
6.90
6.90
6.12
6.11
6.10
6.10
5.69
5.68
5.67
5.66
4.40
4.39
4.39
4.38
4.37
4.36
4.35
4.34
4.33
3.35
3.33
3.01
2.98
2.97
2.94
2.59
2.56
2.54
2.52
Me
N
N
Me
O
O
O
O
F
0.89
0.98
1.00
0.98
0.98
0.98
1.00
6.02
1.04
1.04
f1 (ppm)

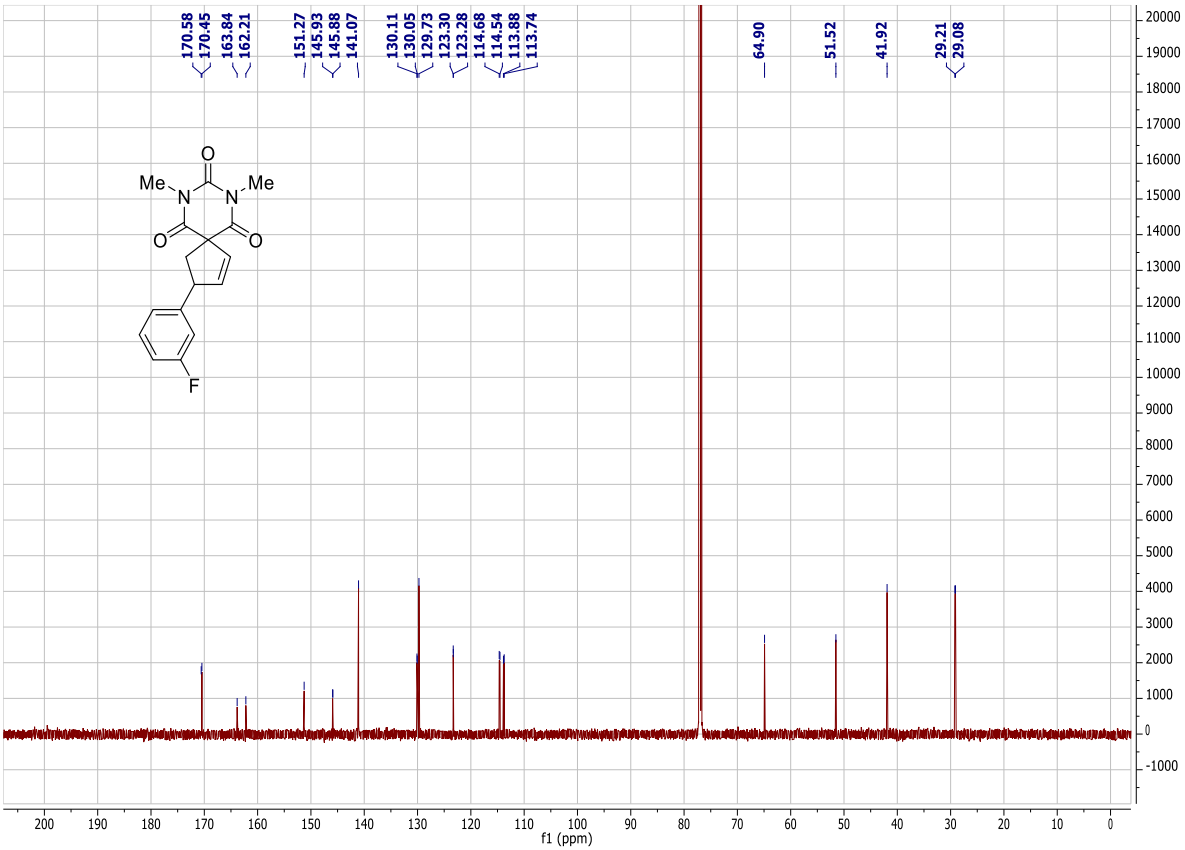
170.58
170.45
163.84
162.21
151.27
145.93
145.88
141.07
130.11
130.05
129.73
123.30
123.28
114.68
114.54
113.88
113.74
64.90
51.52
41.92
29.21
29.08
Me
N
O
N
Me
O
O
F
f1 (ppm)

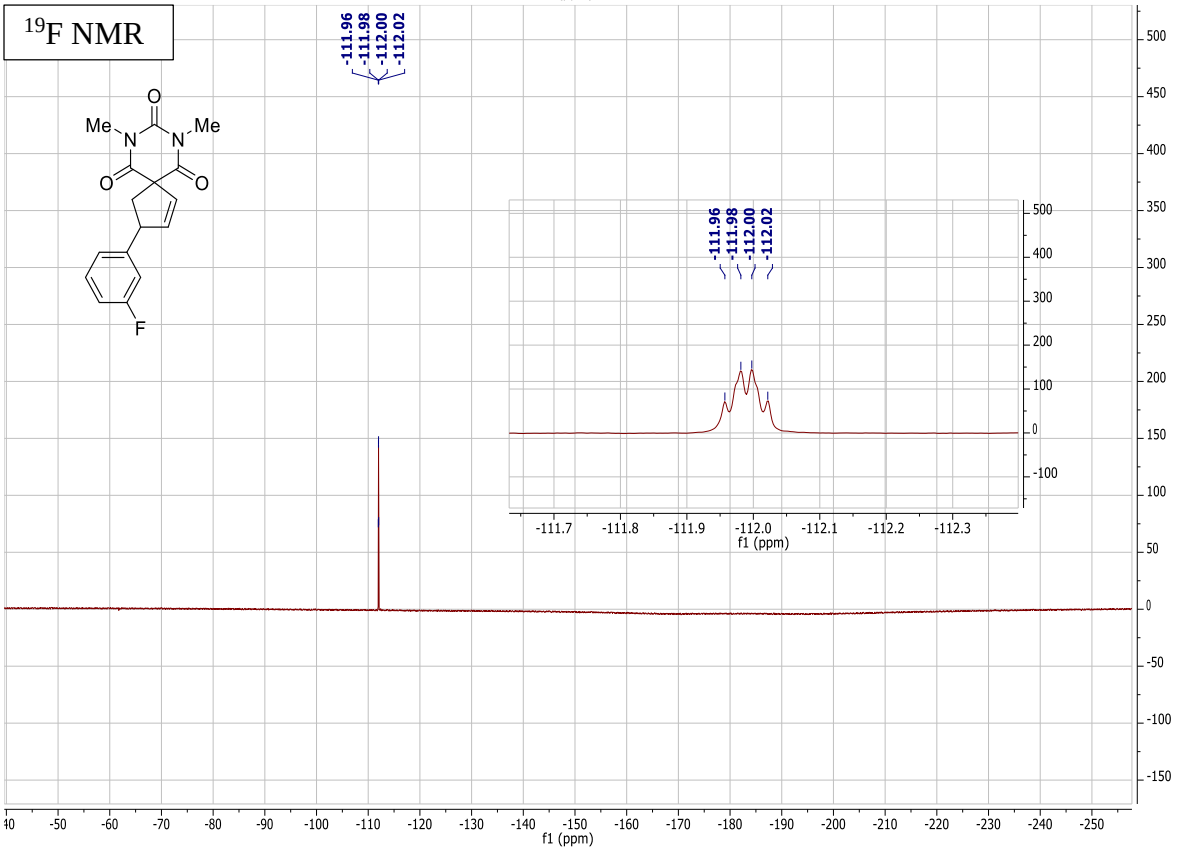
^{19}F NMR
-111.96
-111.98
-112.00
-112.02
Me
N
O
N
Me
O
O
F
f1 (ppm)

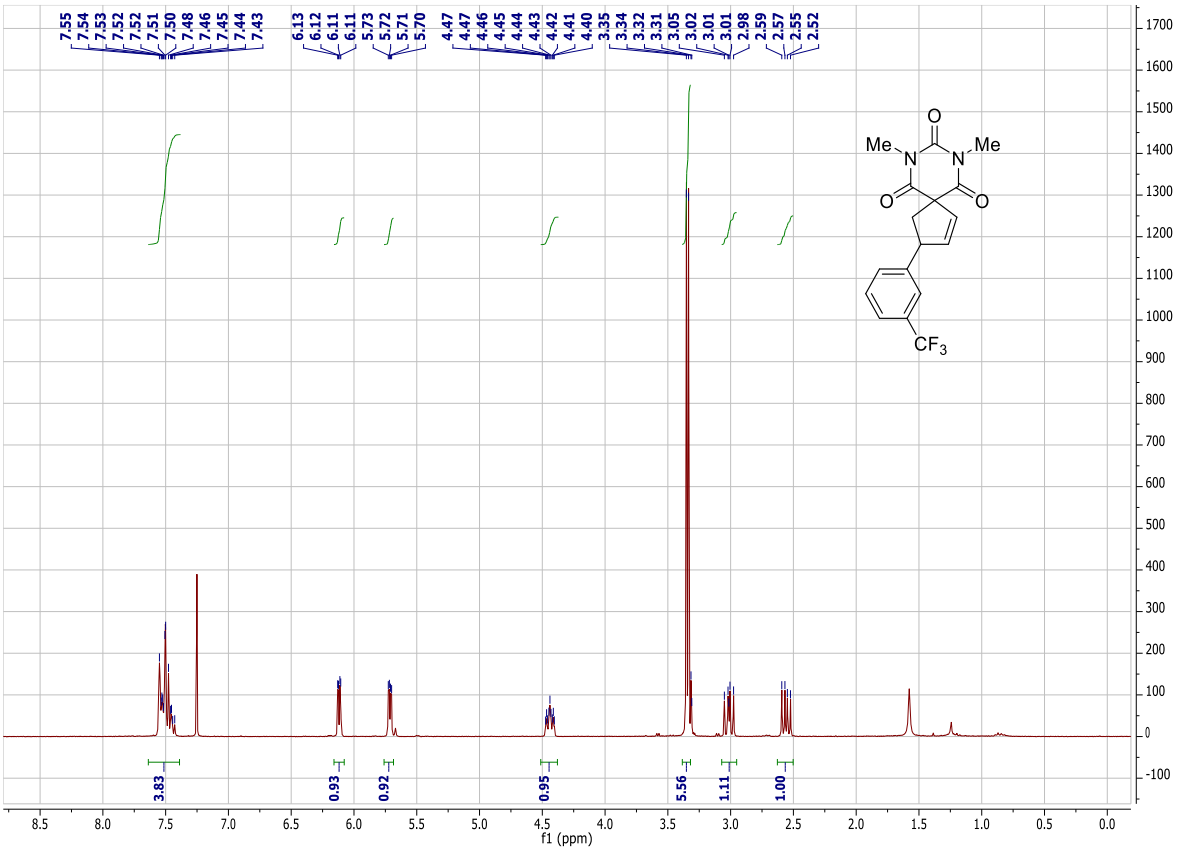
7.55 7.54 7.53 7.52 7.52 7.51 7.50 7.48 7.46 7.45 7.44 7.43
6.13 6.12 6.11 6.11
5.73 5.72 5.71 5.70
4.47 4.47 4.46 4.45 4.44 4.43 4.42 4.41 4.40
3.35 3.34 3.32 3.31 3.05 3.02 3.01 3.01 2.98
2.59 2.57 2.55 2.52
3.83
0.93
0.92
0.95
5.56
1.11
1.00
f1 (ppm)
Me
N
O
N
Me
O
O
CF3

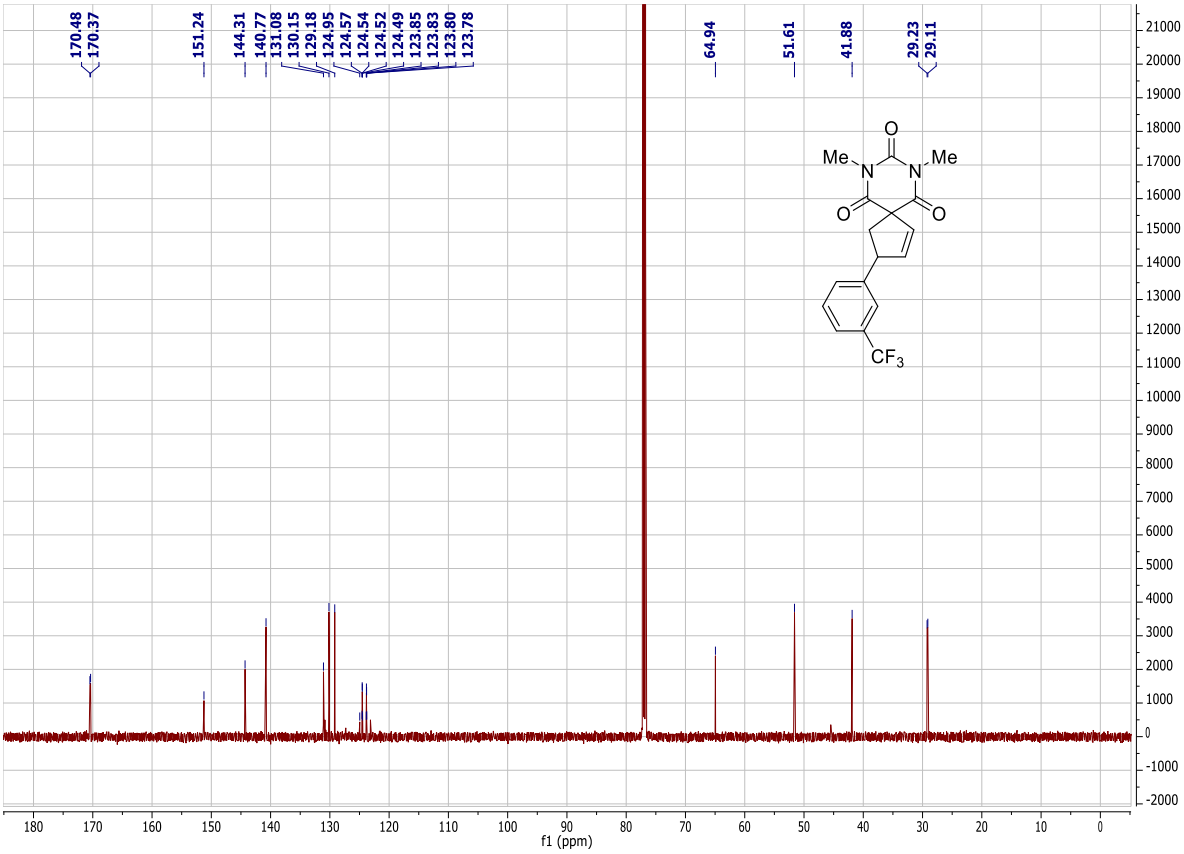
170.48 170.37
151.24
144.31 140.77 131.08 130.15 129.18 124.95 124.57 124.54 124.52 124.49 123.85 123.83 123.80 123.78
64.94
51.61
41.88
29.23 29.11
f1 (ppm)
Me
N
O
N
Me
O
O
CF3

^{19}F NMR

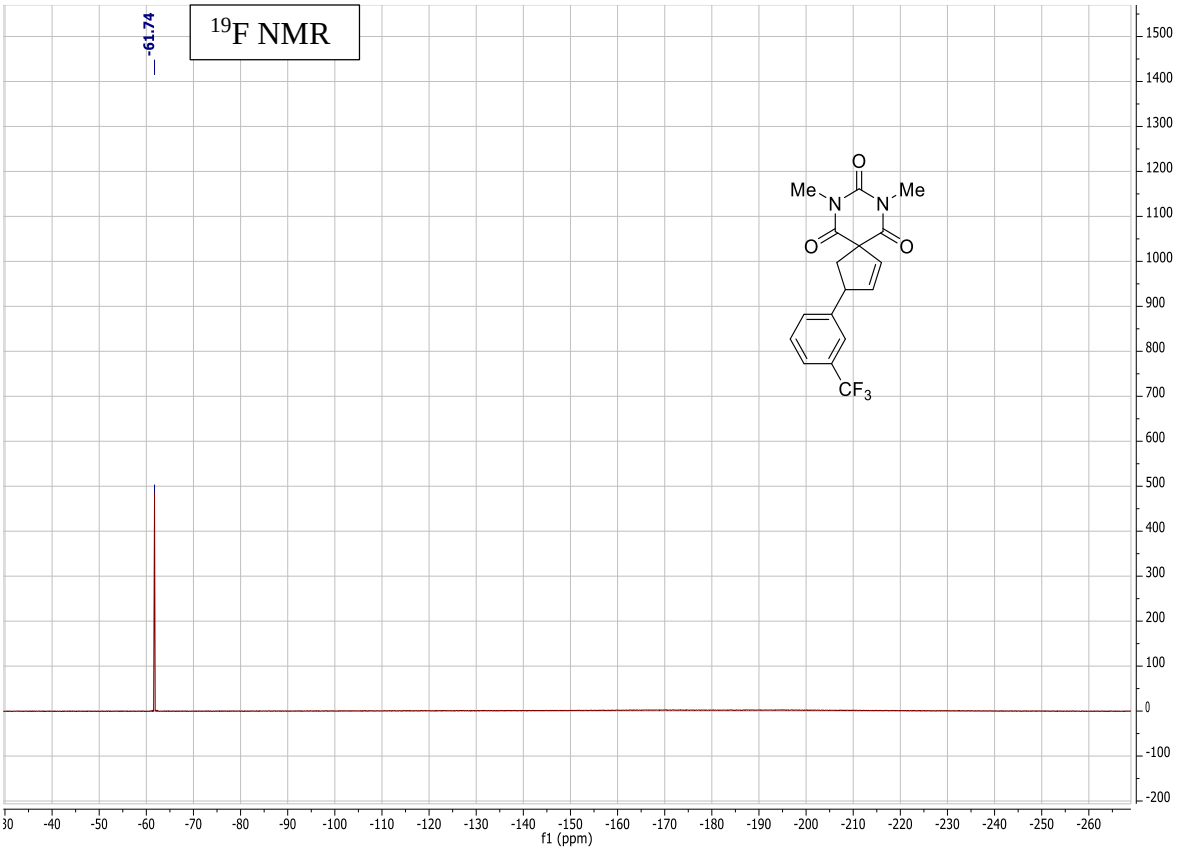
-61.74
Me
N
O
N
Me
O
O
O
CF3
f1 (ppm)

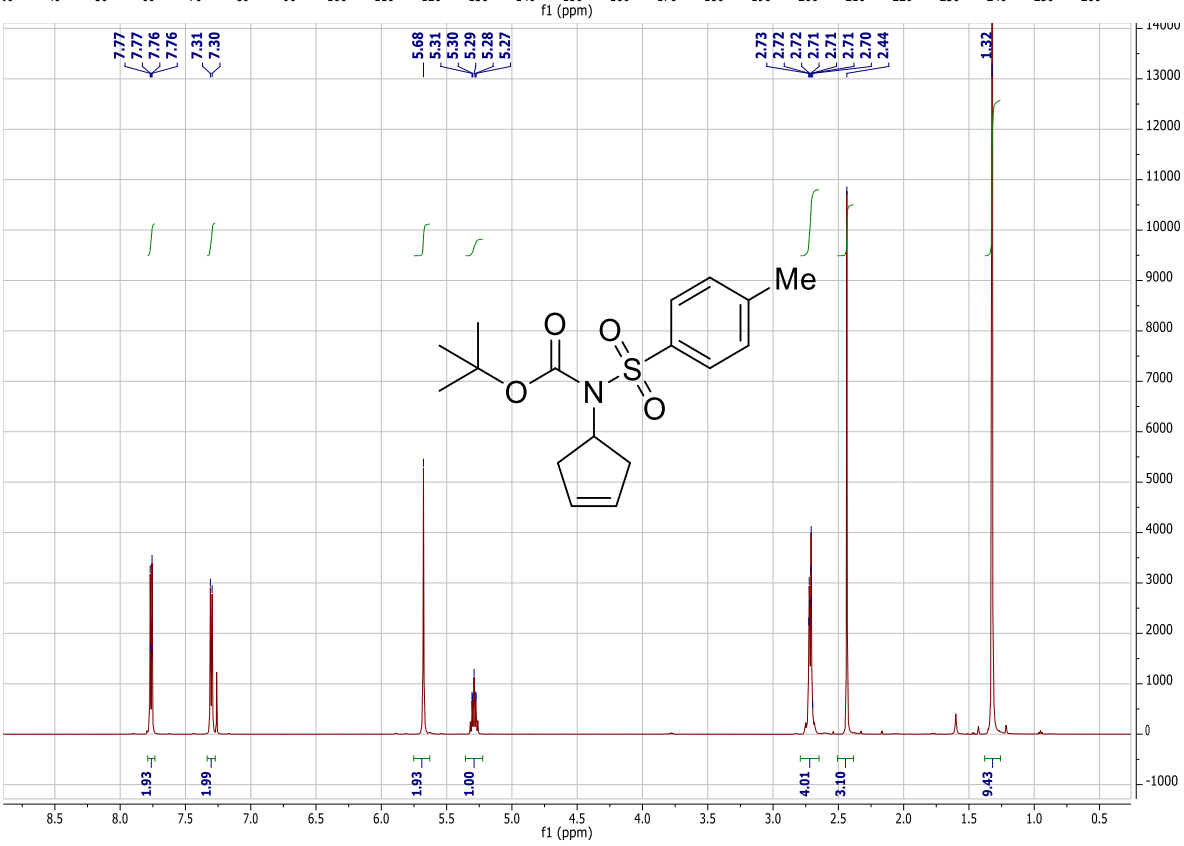
7.77
7.77
7.76
7.76
7.31
7.30
5.68
5.31
5.30
5.29
5.28
5.27
2.73
2.72
2.72
2.71
2.71
2.71
2.70
2.44
1.32
Me
O
O
S
O
O
N
O
1.93
1.99
1.93
1.00
4.01
3.10
9.43
f1 (ppm)

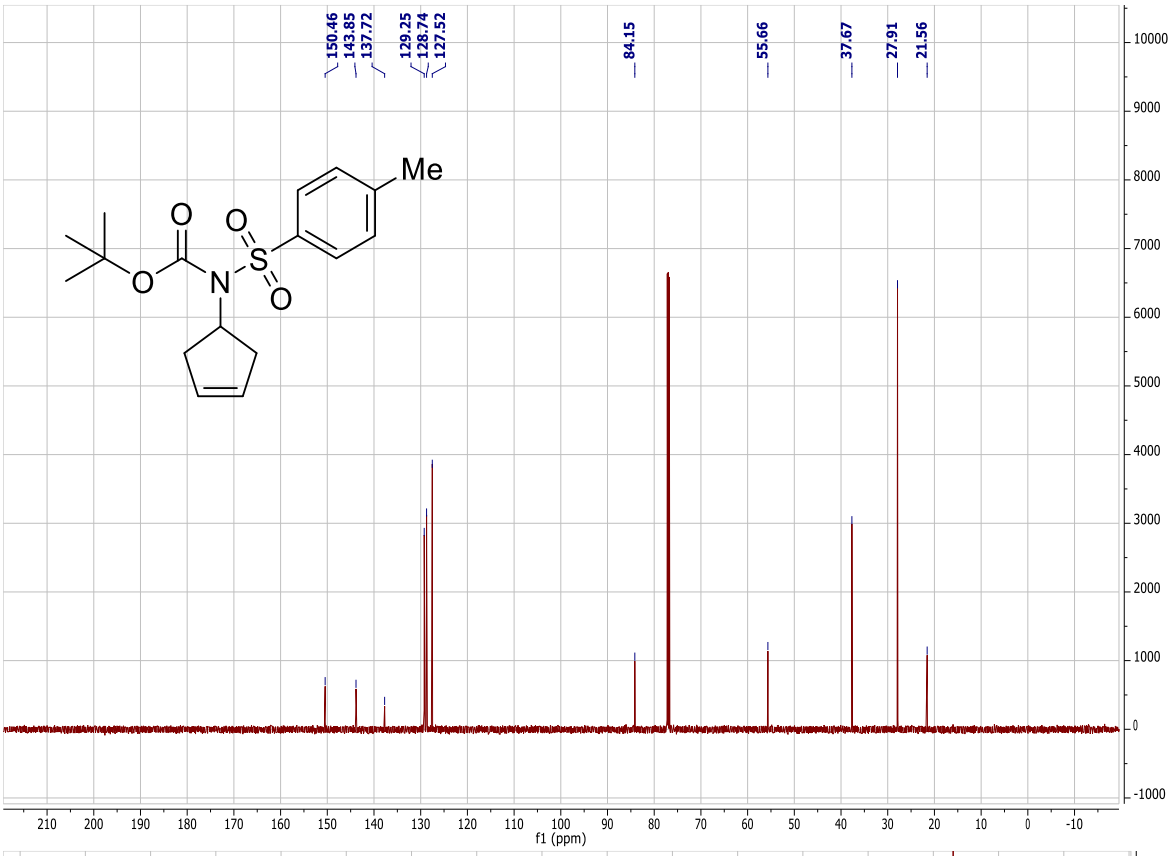
150.46
143.85
137.72
129.25
128.74
127.52
84.15
55.66
37.67
27.91
21.56
Me
O
O
S
O
N
O
O
f1 (ppm)

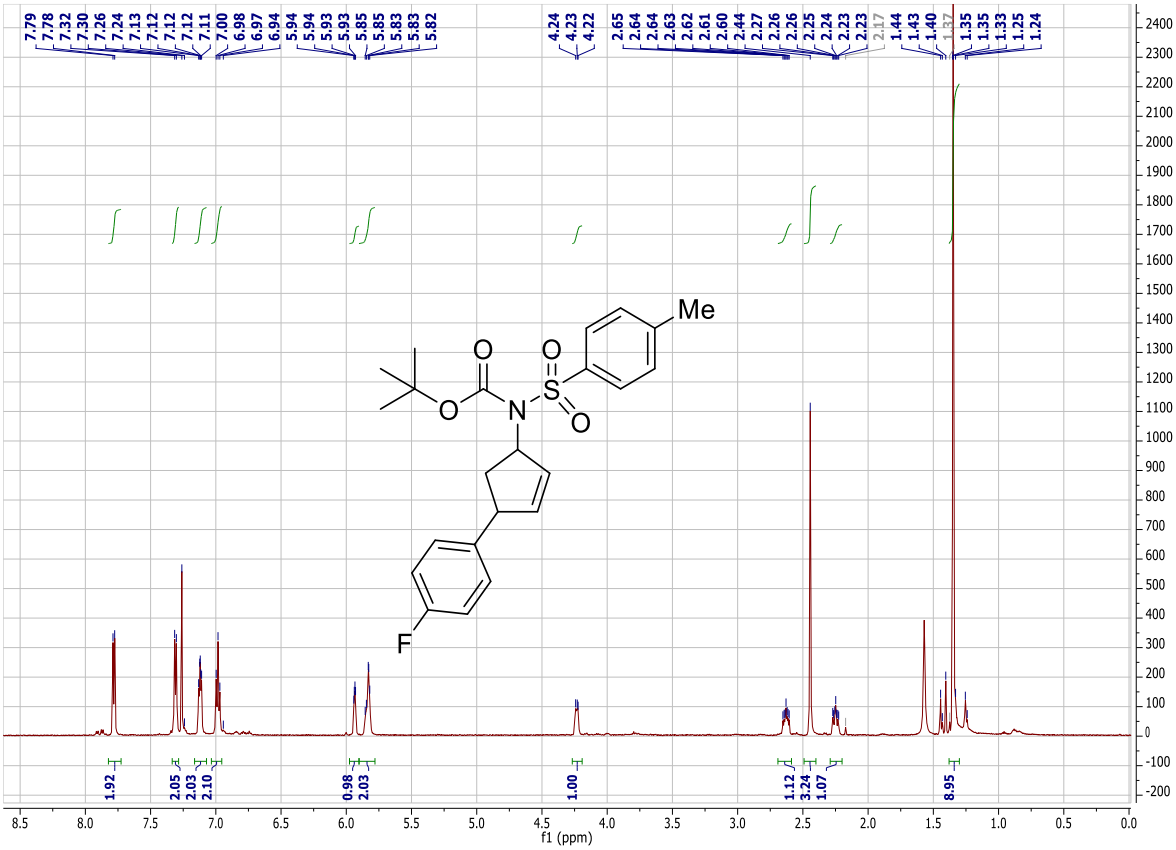
7.79
7.78
7.32
7.30
7.26
7.24
7.13
7.12
7.12
7.12
7.11
7.00
6.98
6.97
6.94
5.94
5.94
5.93
5.93
5.85
5.85
5.83
5.83
5.82
4.24
4.23
4.22
2.65
2.64
2.64
2.63
2.62
2.61
2.60
2.44
2.27
2.26
2.26
2.25
2.24
2.23
2.23
2.17
1.44
1.43
1.40
1.37
1.35
1.35
1.33
1.25
1.24
Me
O
O
S
O
N
O
O
F
1.92
2.05
2.03
2.10
0.98
2.03
1.00
1.12
3.24
1.07
8.95
f1 (ppm)

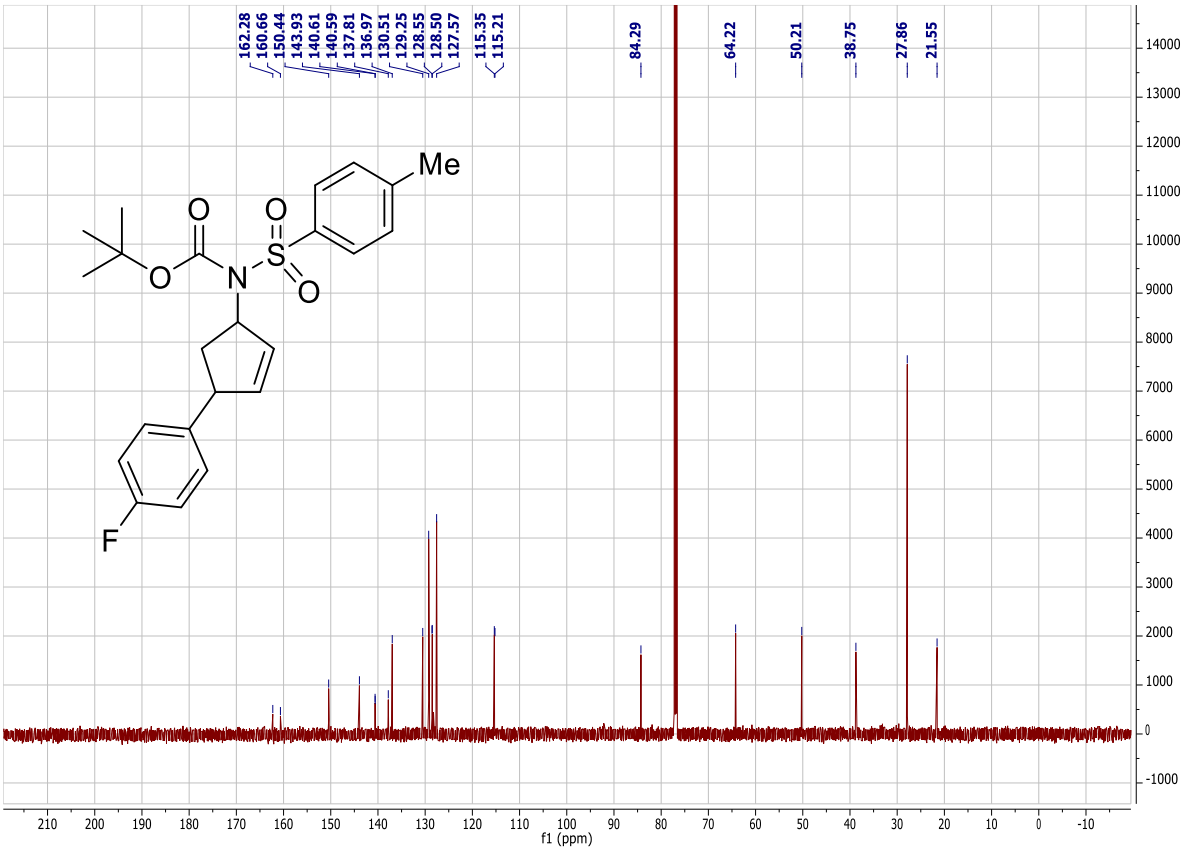
162.28
160.66
150.44
143.93
140.61
140.59
137.81
136.97
130.51
129.25
128.55
128.50
127.57
115.35
115.21
84.29
64.22
50.21
38.75
27.86
21.55
Me
O
O
S
O
N
O
O
F
f1 (ppm)

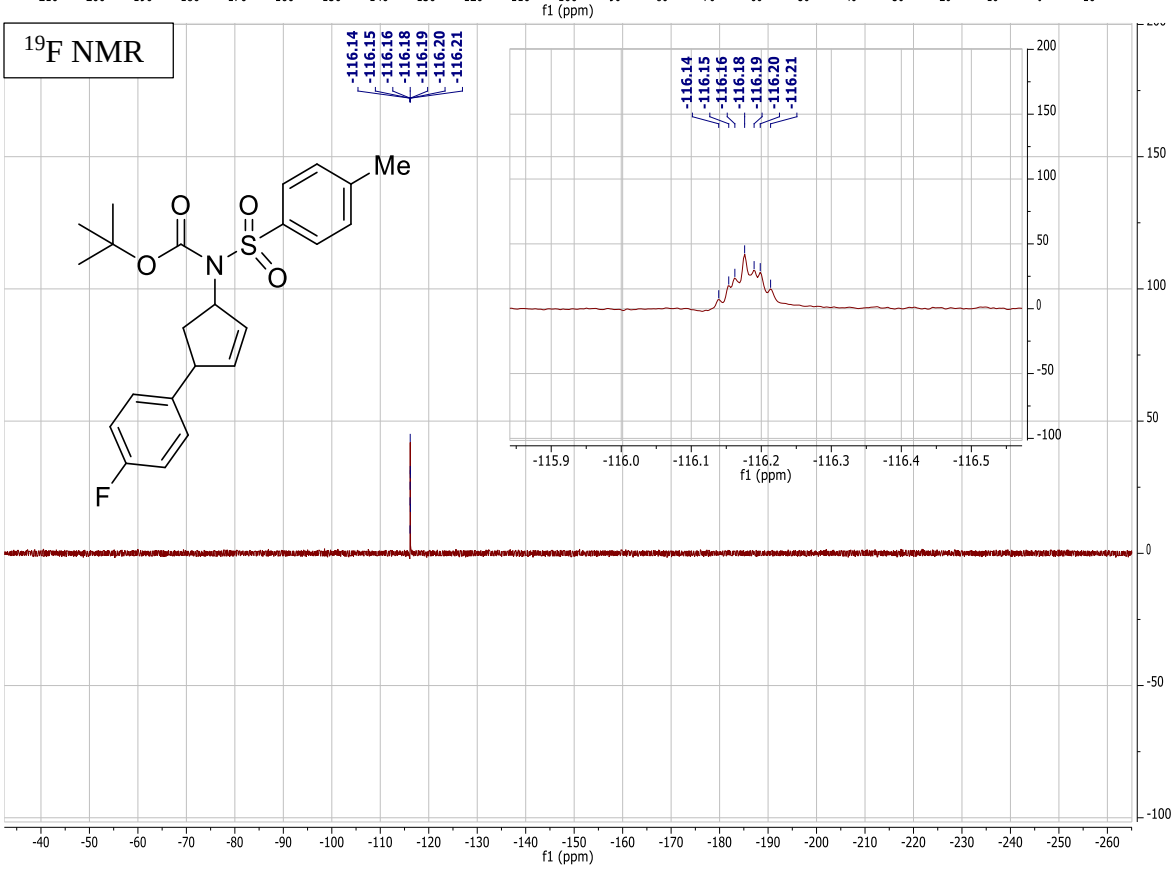
^{19}F NMR
-116.14
-116.15
-116.16
-116.18
-116.19
-116.20
-116.21
Me
O
O
S
O
N
O
O
F
f1 (ppm)

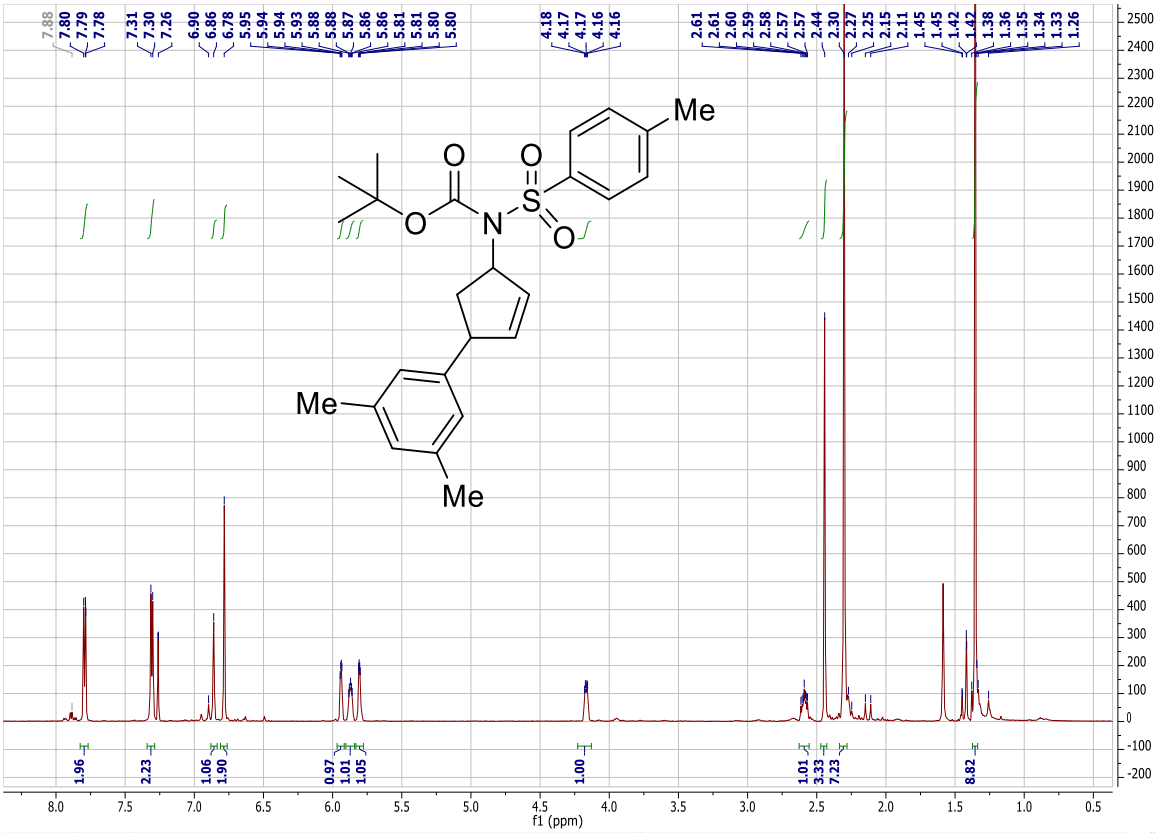
7.88
7.80
7.79
7.78
7.31
7.30
7.26
6.90
6.86
6.78
5.95
5.94
5.94
5.93
5.88
5.88
5.87
5.86
5.86
5.81
5.81
5.80
5.80
4.18
4.17
4.17
4.16
4.16
2.61
2.61
2.60
2.59
2.58
2.57
2.57
2.44
2.30
2.27
2.25
2.15
2.11
1.45
1.45
1.42
1.42
1.38
1.36
1.35
1.34
1.33
1.26
Me
O
O
O
N
S
O
Me
Me
1.96
2.23
1.06
1.90
0.97
1.01
1.05
1.00
1.01
3.33
7.23
8.82
f1 (ppm)

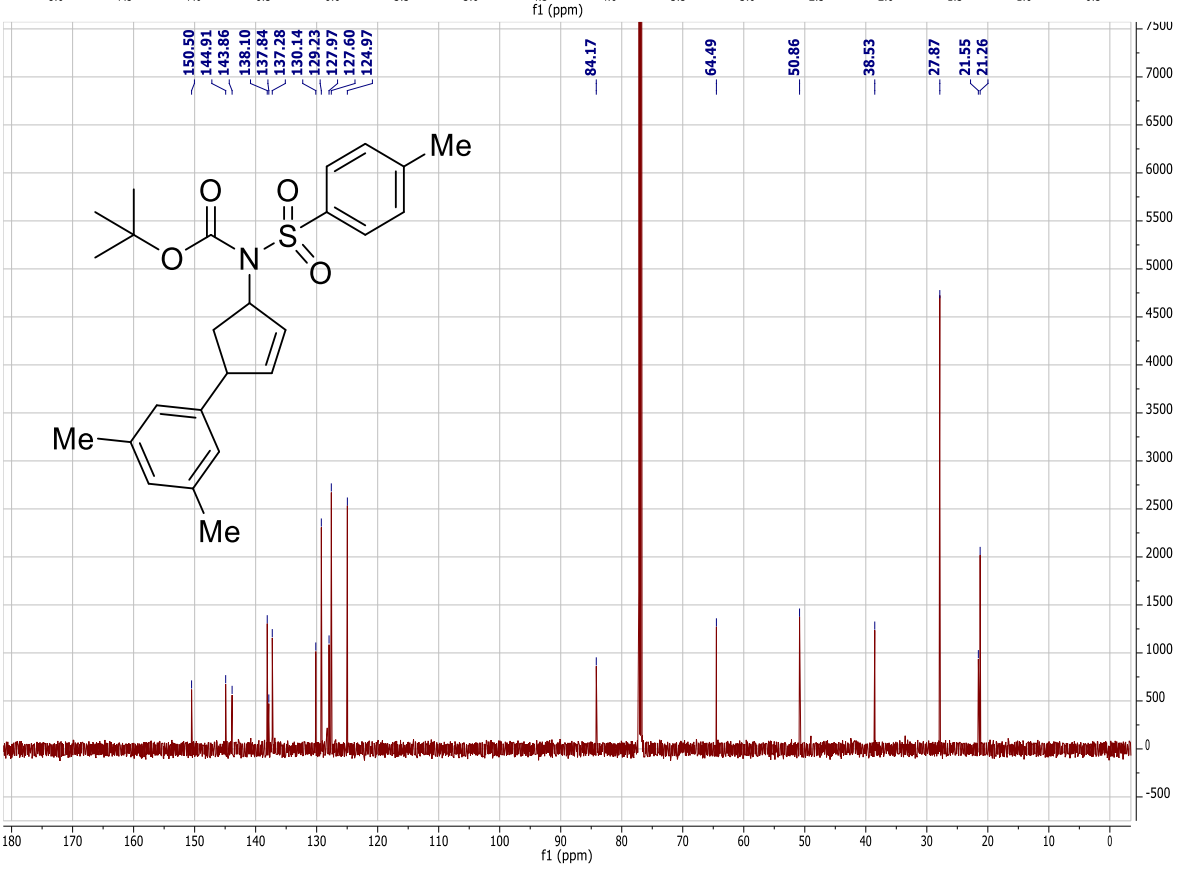
150.50
144.91
143.86
138.10
137.84
137.28
130.14
129.23
127.97
127.60
124.97
84.17
64.49
50.86
38.53
27.87
21.55
21.26
Me
O
O
O
N
S
O
Me
Me
f1 (ppm)

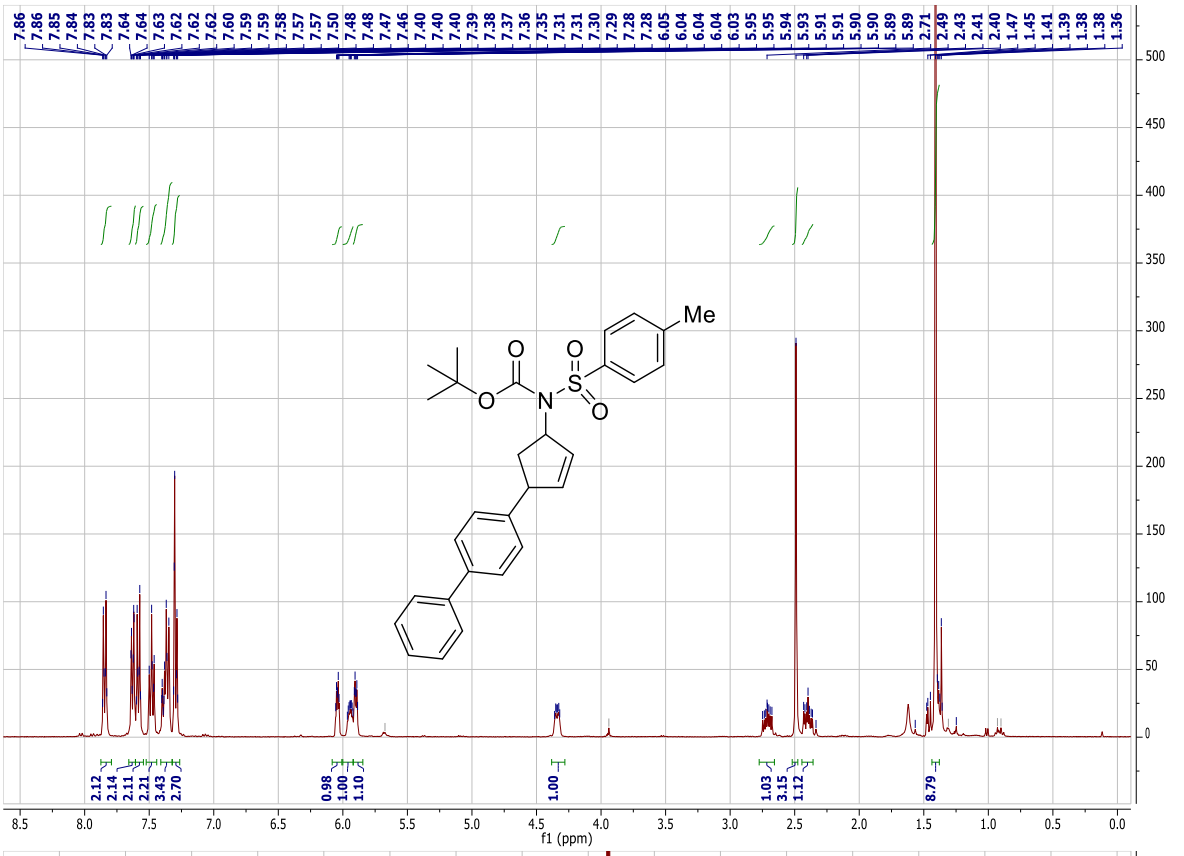
7.86 7.86 7.85 7.84 7.83 7.83 7.64 7.64 7.63 7.62 7.62 7.62 7.60 7.59 7.59 7.58 7.57 7.57 7.50 7.48 7.48 7.47 7.46 7.40 7.40 7.40 7.39 7.38 7.37 7.36 7.35 7.31 7.31 7.30 7.29 7.28 7.28 6.05 6.04 6.04 6.03 5.95 5.95 5.94 5.93 5.91 5.91 5.90 5.90 5.89 5.89 2.71 2.49 2.43 2.41 2.40 1.47 1.45 1.41 1.39 1.38 1.38 1.36
Me
O
O
S
O
N
O
O
2.12 2.14 2.11 2.21 3.43 2.70 0.98 1.00 1.10 1.00 1.03 3.15 1.12 8.79
f1 (ppm)

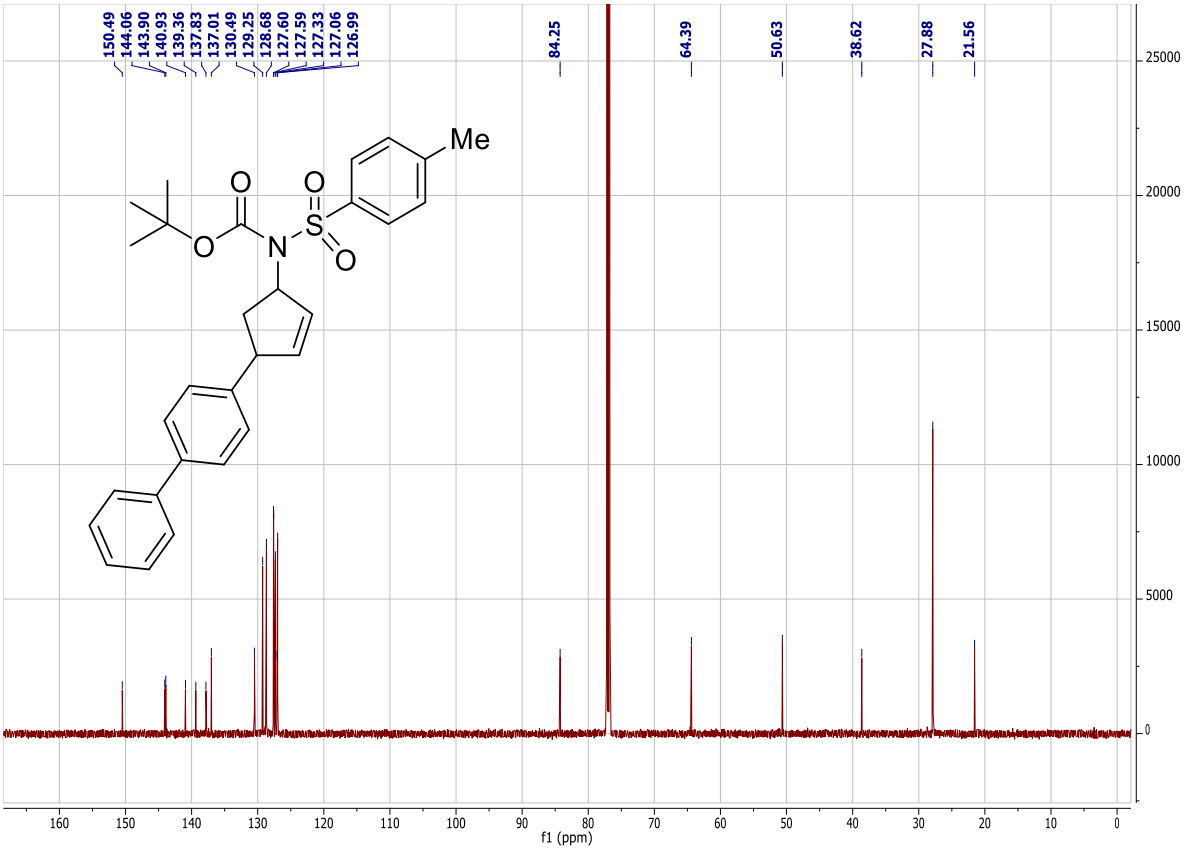
150.49 144.06 143.90 140.93 139.36 137.83 137.01 130.49 129.25 128.68 127.60 127.59 127.33 127.06 126.99
84.25
64.39
50.63
38.62
27.88
21.56
Me
O
O
S
O
N
O
O
f1 (ppm)

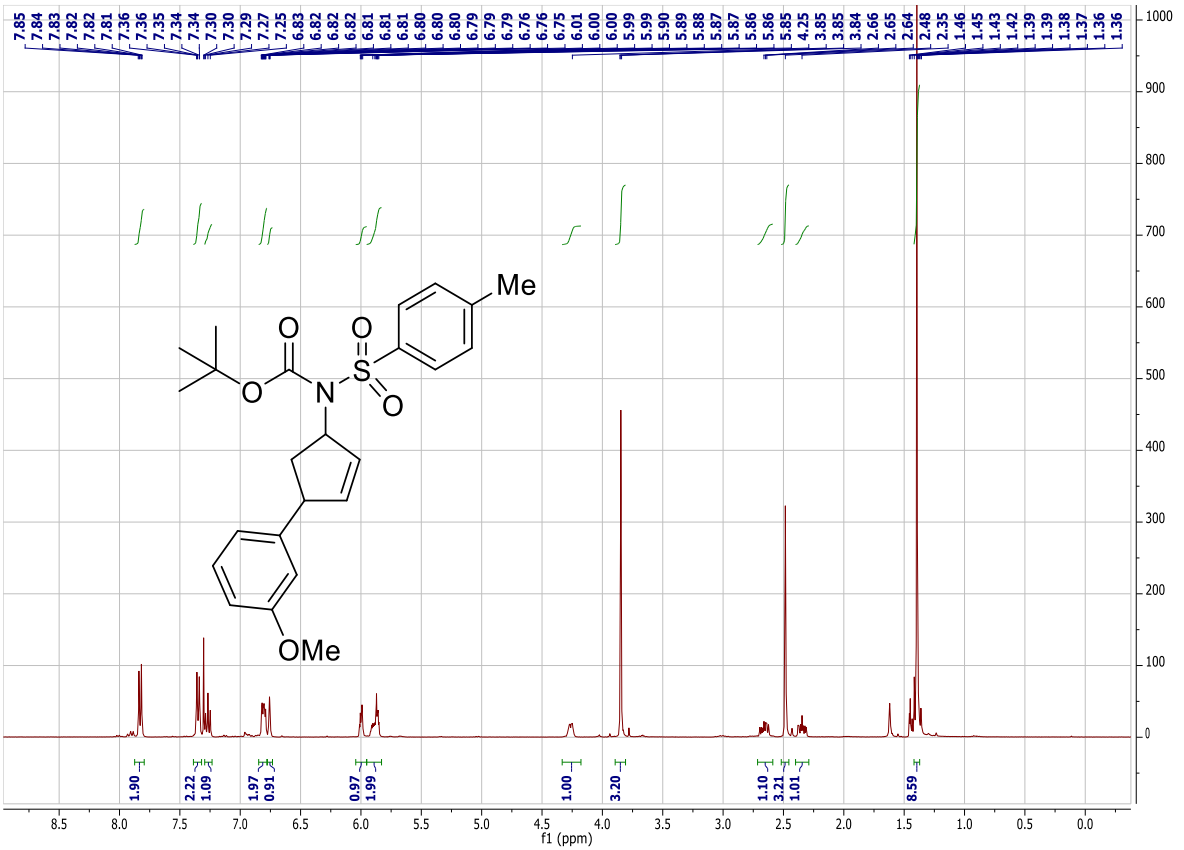
7.85 7.84 7.83 7.82 7.82 7.81 7.36 7.36 7.35 7.34 7.34 7.30 7.30 7.29 7.27 7.25 6.83 6.82 6.82 6.82 6.81 6.81 6.81 6.80 6.80 6.80 6.79 6.79 6.79 6.76 6.76 6.75 6.01 6.00 6.00 5.99 5.99 5.90 5.89 5.88 5.87 5.87 5.86 5.86 5.85 4.25 3.85 3.85 3.84 2.66 2.65 2.64 2.48 2.35 1.46 1.45 1.43 1.42 1.39 1.39 1.38 1.37 1.36 1.36
Me
O
O
O
N
S
O
O
OMe
1.90
2.22
1.09
1.97
0.91
0.97
1.99
1.00
3.20
1.10
3.21
1.01
8.59
f1 (ppm)

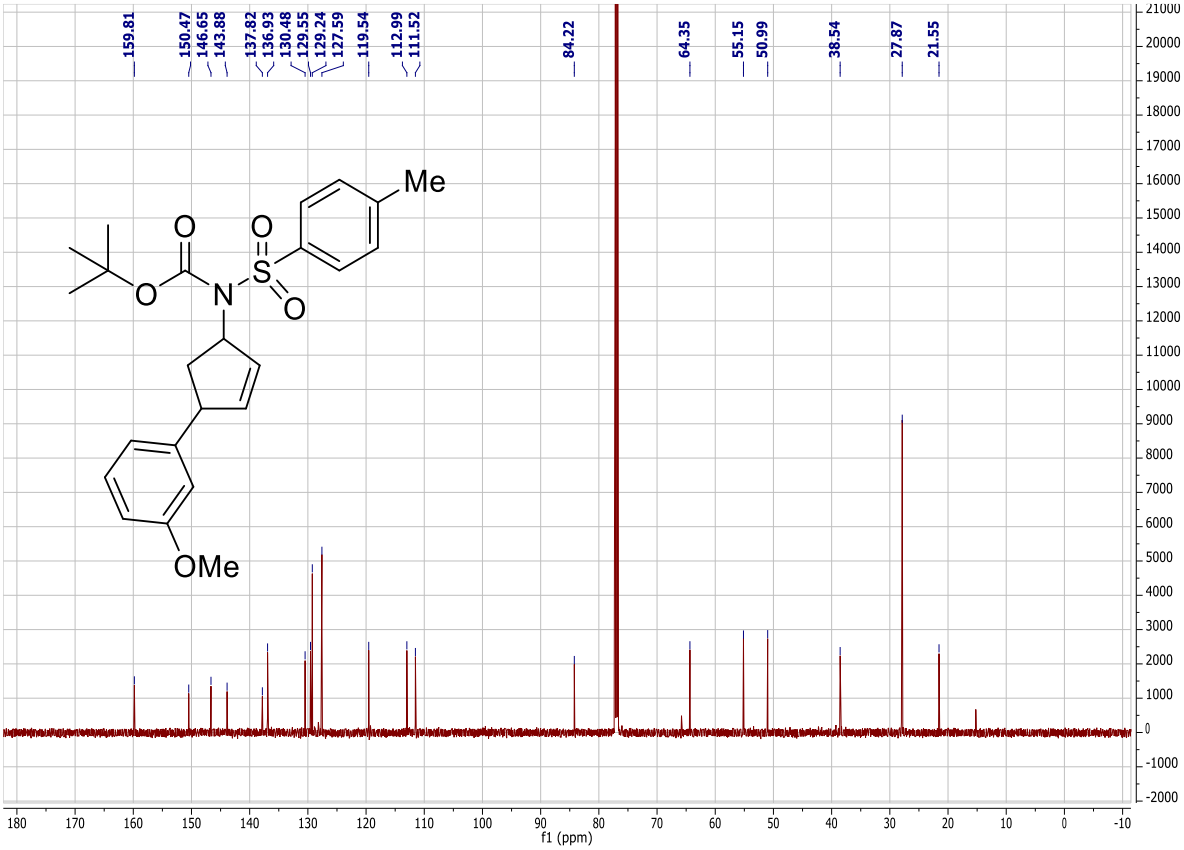
159.81
150.47
146.65
143.88
137.82
136.93
130.48
129.55
129.24
127.59
119.54
112.99
111.52
84.22
64.35
55.15
50.99
38.54
27.87
21.55
Me
O
O
O
N
S
O
O
OMe
f1 (ppm)

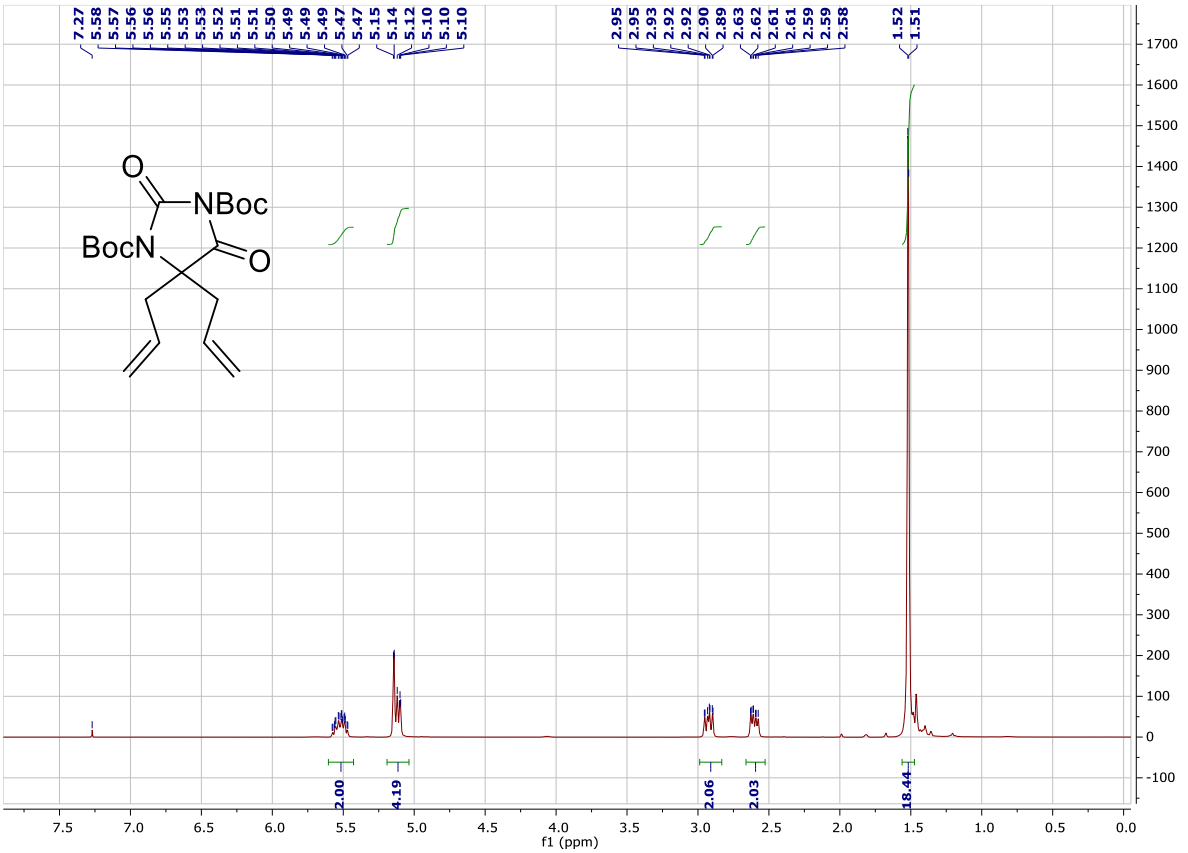
7.27
5.58
5.57
5.56
5.56
5.55
5.53
5.53
5.52
5.51
5.51
5.50
5.49
5.49
5.49
5.47
5.47
5.15
5.14
5.12
5.10
5.10
5.10
2.95
2.95
2.93
2.92
2.92
2.90
2.89
2.63
2.62
2.61
2.61
2.59
2.59
2.58
1.52
1.51
O
NBoc
BocN
O
2.00
4.19
2.06
2.03
18.44
f1 (ppm)

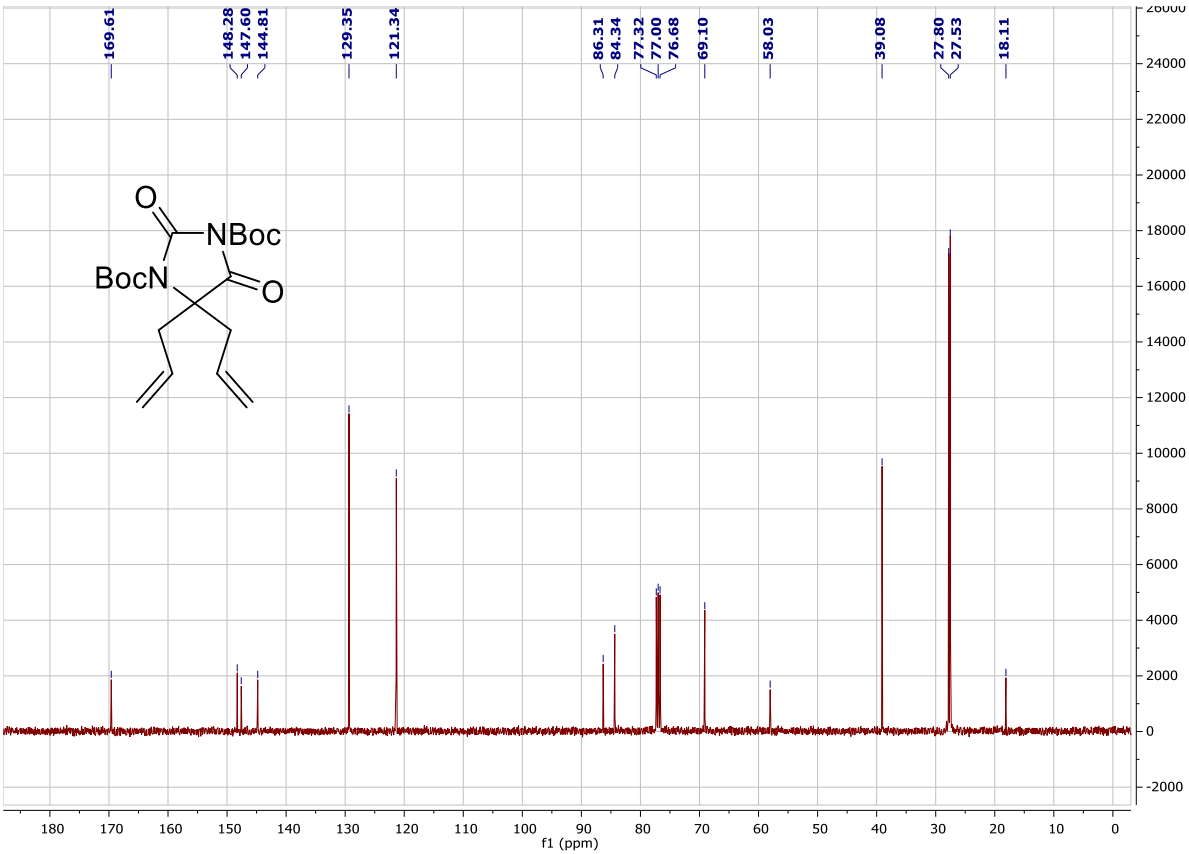
169.61
148.28
147.60
144.81
129.35
121.34
86.31
84.34
77.32
77.00
76.68
69.10
58.03
39.08
27.80
27.53
18.11
O
NBoc
BocN
O
f1 (ppm)

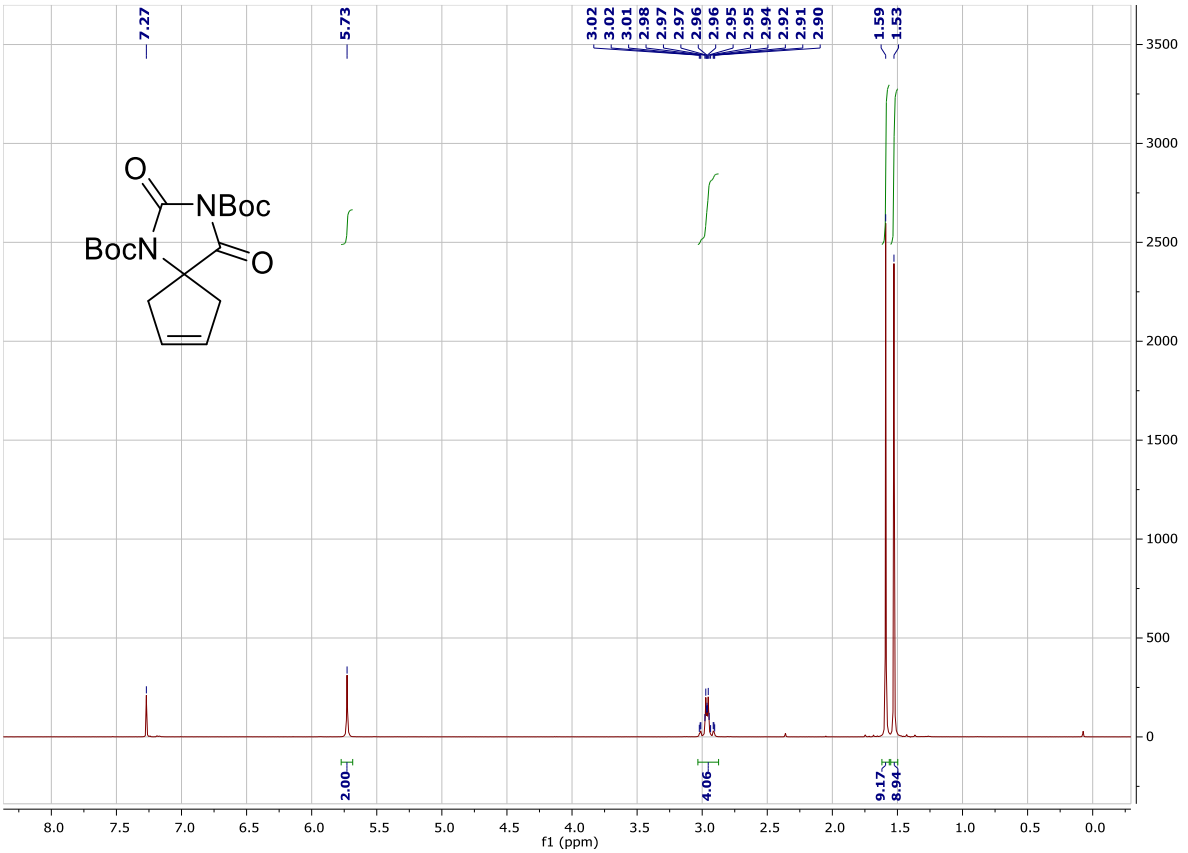
7.27
5.73
3.02
3.02
3.01
2.98
2.97
2.97
2.96
2.96
2.95
2.95
2.94
2.92
2.91
2.90
1.59
1.53
2.00
4.06
9.17
8.94
f1 (ppm)

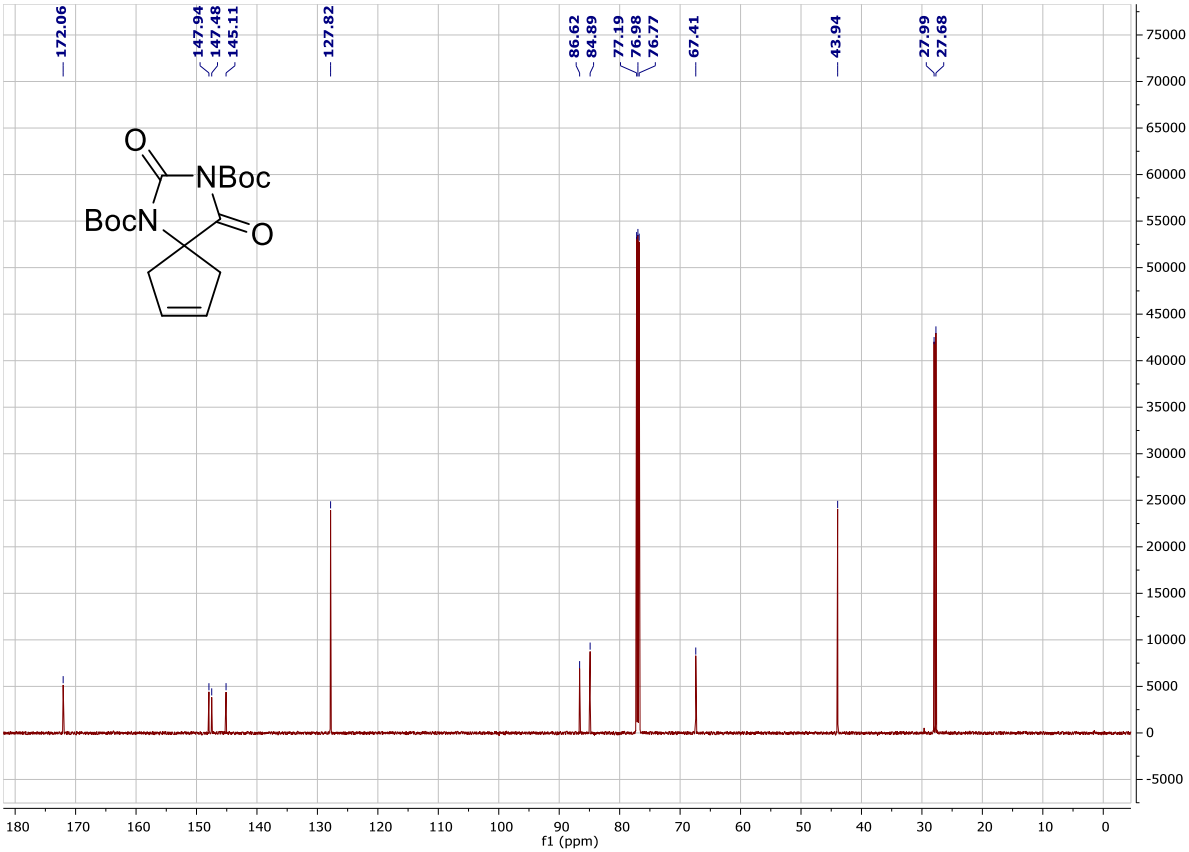
172.06
147.94
147.48
145.11
127.82
86.62
84.89
77.19
76.98
76.77
67.41
43.94
27.99
27.68
f1 (ppm)

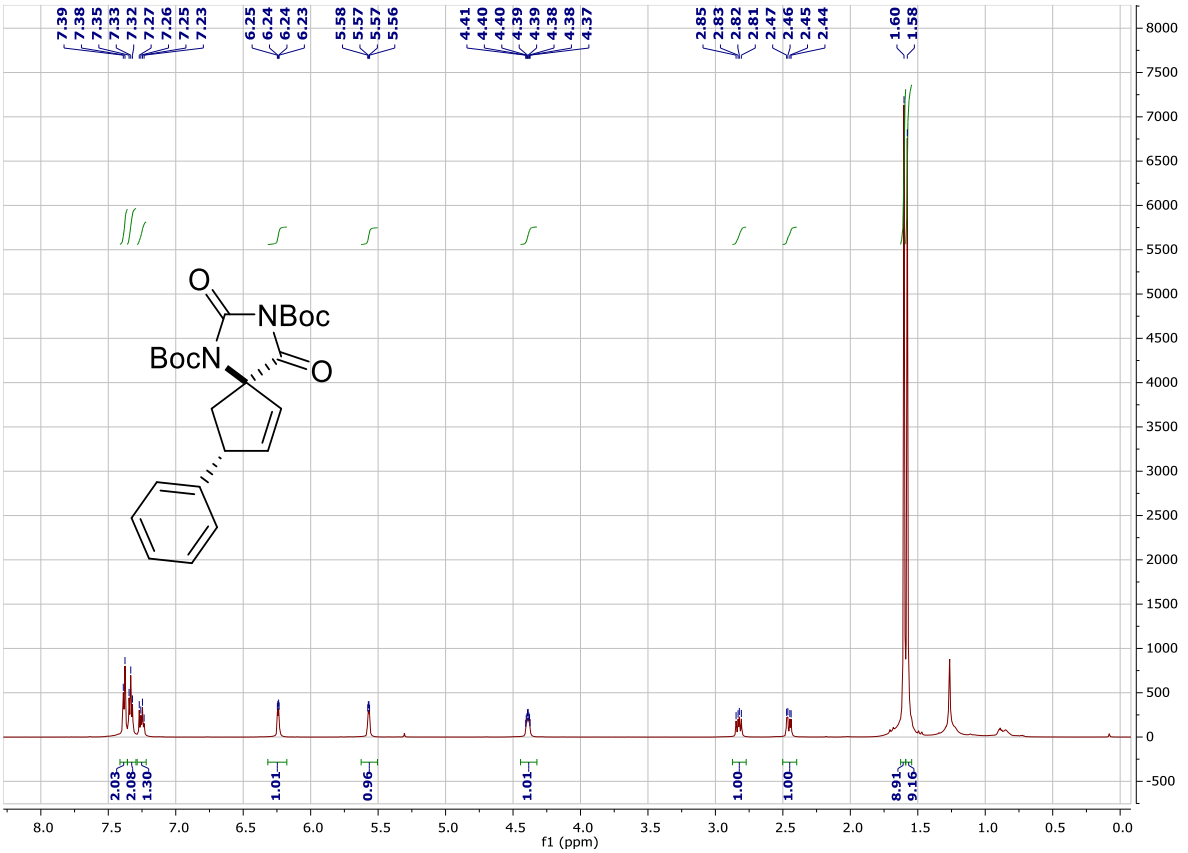
7.39 7.38 7.35 7.33 7.32 7.27 7.26 7.25 7.23
6.25 6.24 6.24 6.23
5.58 5.57 5.57 5.56
4.41 4.40 4.40 4.39 4.39 4.38 4.38 4.37
2.85 2.83 2.82 2.81
2.47 2.46 2.45 2.44
1.60 1.58
O
NBoc
BocN
O
2.03 2.08 1.30
1.01
0.96
1.01
1.00
1.00
8.91 9.16
f1 (ppm)

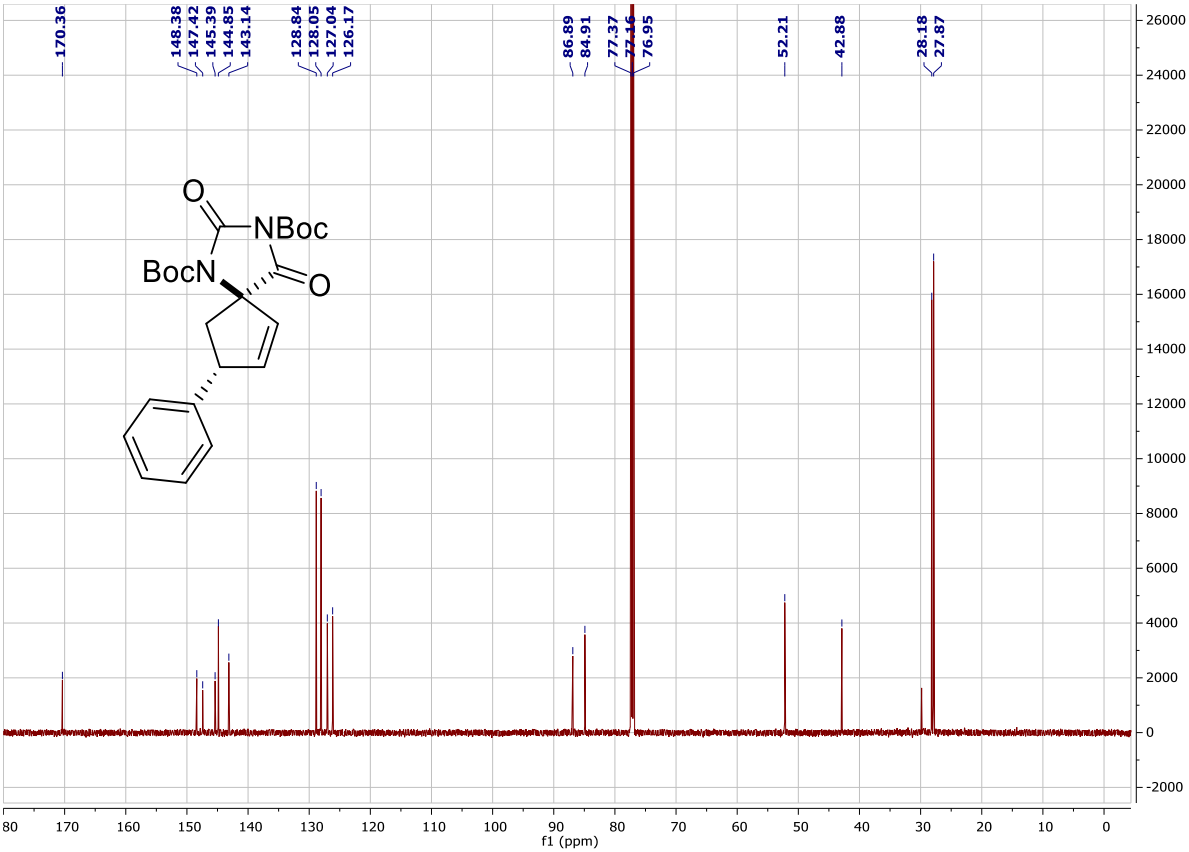
170.36
148.38 147.42 145.39 144.85 143.14
128.84 128.05 127.04 126.17
86.89 84.91
77.37 77.16 76.95
52.21
42.88
28.18 27.87
O
NBoc
BocN
O
f1 (ppm)

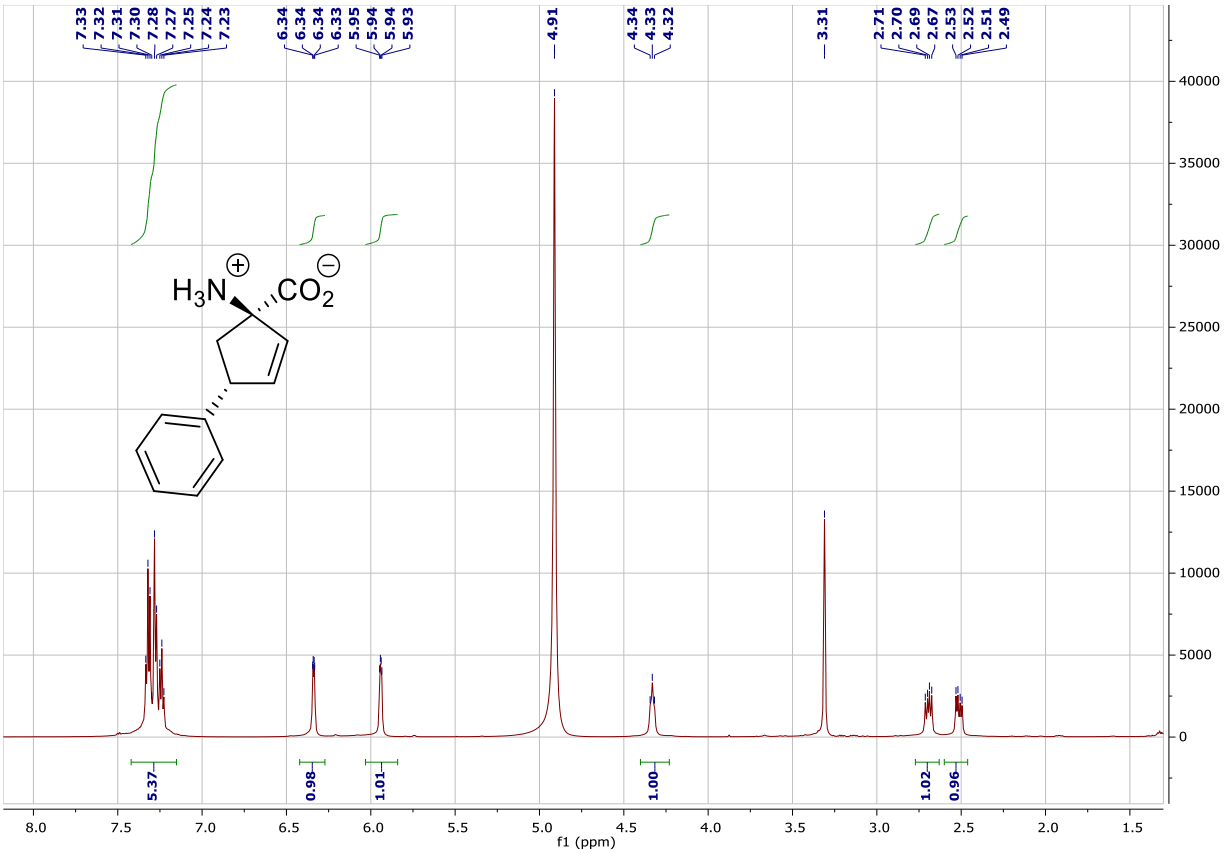
7.33
7.32
7.31
7.30
7.28
7.27
7.25
7.24
7.23
6.34
6.34
6.34
6.33
5.95
5.94
5.94
5.93
4.91
4.34
4.33
4.32
3.31
2.71
2.70
2.69
2.67
2.53
2.52
2.51
2.49
5.37
0.98
1.01
1.00
1.02
0.96
f1 (ppm)

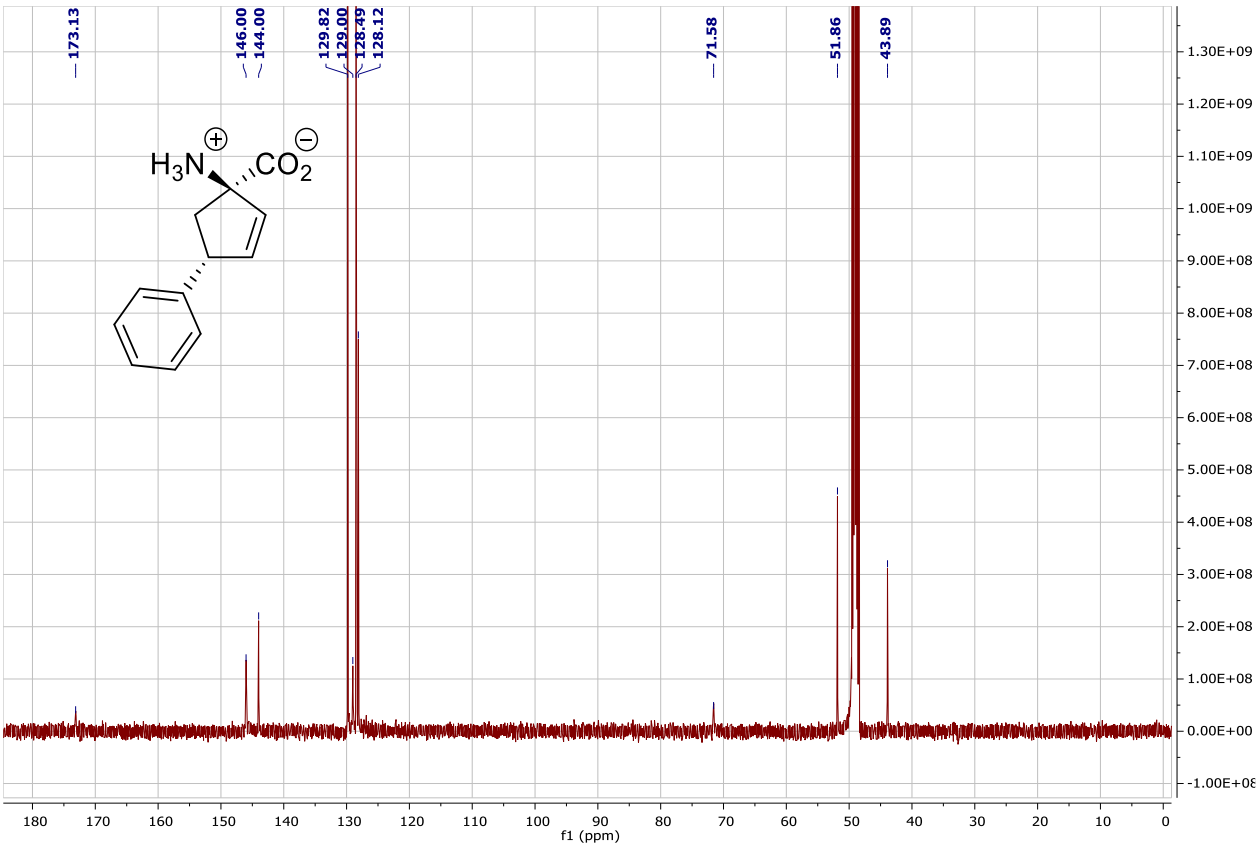
173.13
146.00
144.00
129.82
129.00
128.49
128.12
71.58
51.86
43.89
f1 (ppm)

HPLC traces

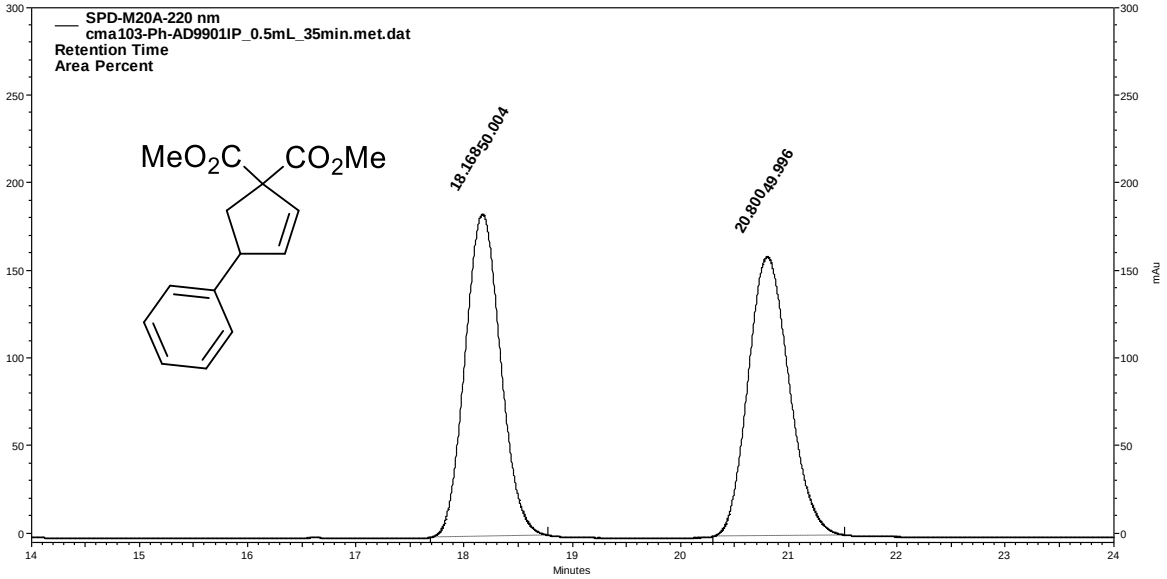
SPD-M20A-220 nm
cma103-Ph-AD9901IP_0.5mL_35min.met.dat
Retention Time
Area Percent
MeO2C
CO2Me
18.16850.004
20.80049.996
mAu
Minutes

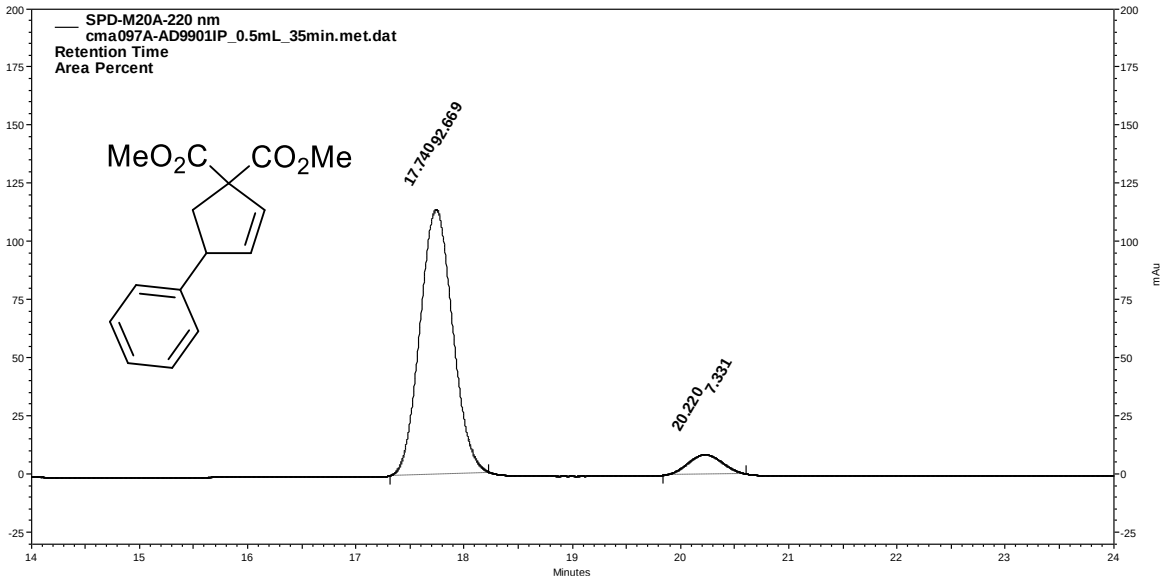
SPD-M20A-220 nm
cma097A-AD9901IP_0.5mL_35min.met.dat
Retention Time
Area Percent
MeO2C
CO2Me
17.74092.669
20.220 7.331
mAu
Minutes

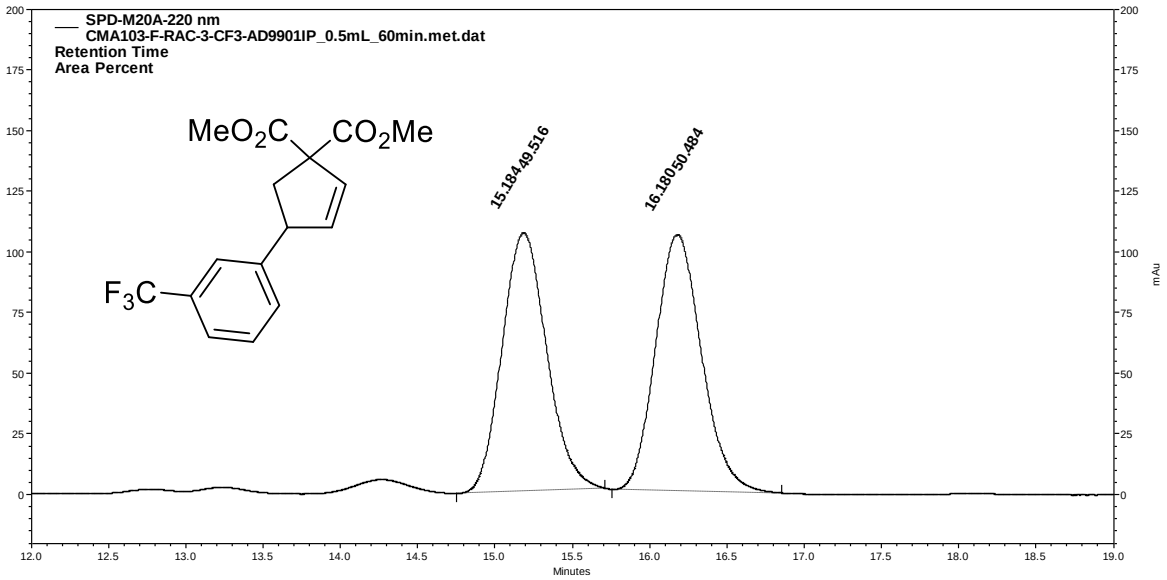
SPD-M20A-220 nm
CMA103-F-RAC-3-CF3-AD9901IP_0.5mL_60min.met.dat
Retention Time
Area Percent
MeO2C
CO2Me
F3C
15.18449.516
16.18050.484
mAu
Minutes

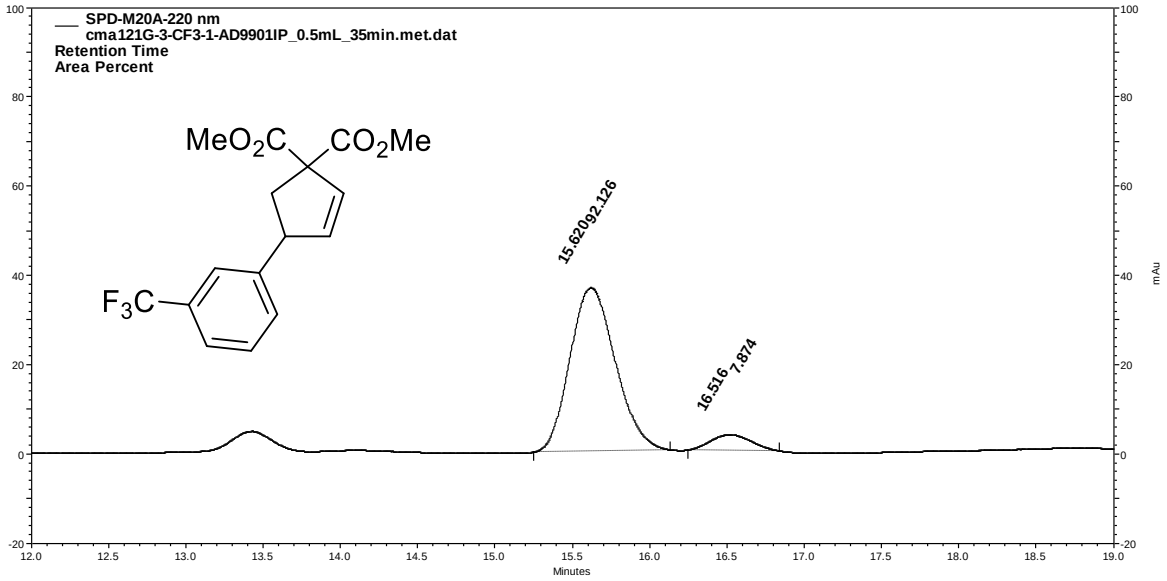
SPD-M20A-220 nm
cma121G-3-CF3-1-AD9901IP_0.5mL_35min.met.dat
Retention Time
Area Percent
MeO2C
CO2Me
F3C
15.62092.126
16.516 7.874
mAu
Minutes

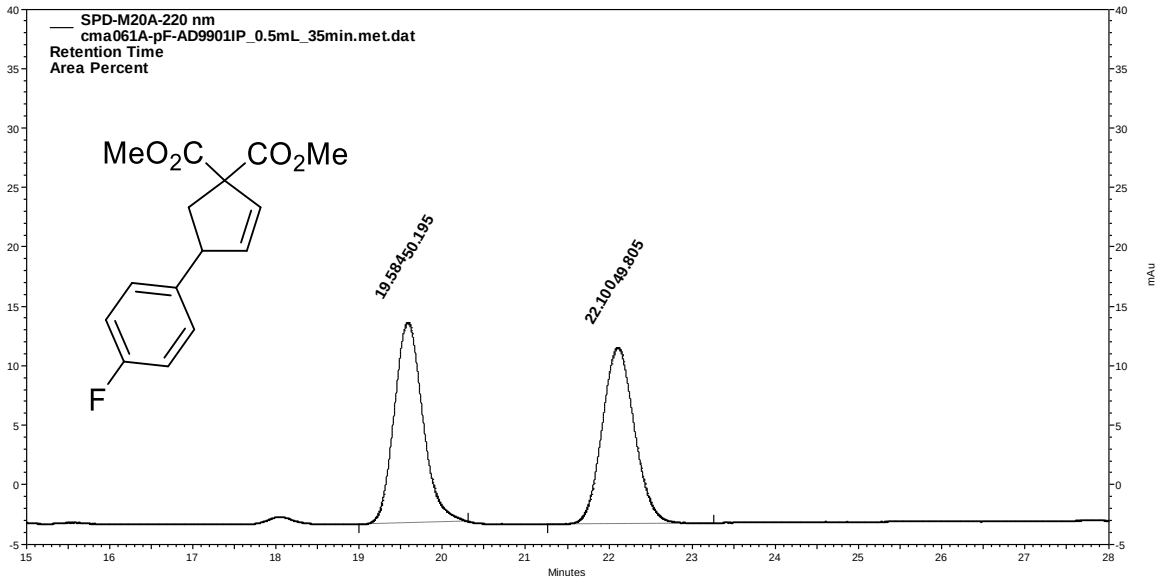
SPD-M20A-220 nm
cma061A-pF-AD9901IP_0.5mL_35min.met.dat
Retention Time
Area Percent
MeO2C
CO2Me
F
19.58450.195
22.10049.805
mAu
Minutes

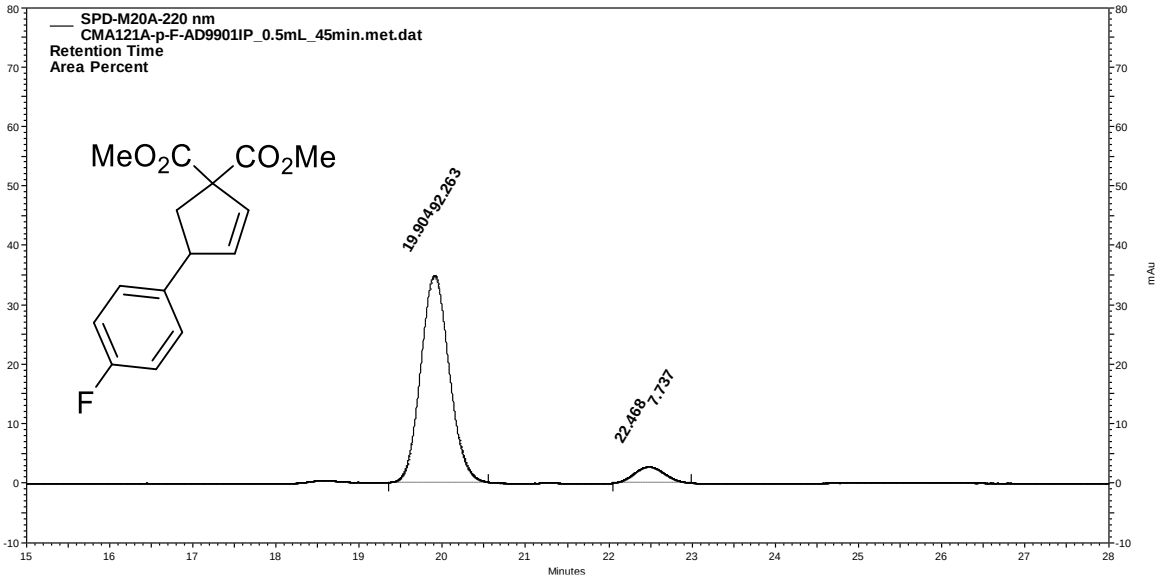
SPD-M20A-220 nm
CMA121A-p-F-AD9901IP_0.5mL_45min.met.dat
Retention Time
Area Percent
MeO2C
CO2Me
F
19.90492.263
22.468 1.737
mAu
Minutes

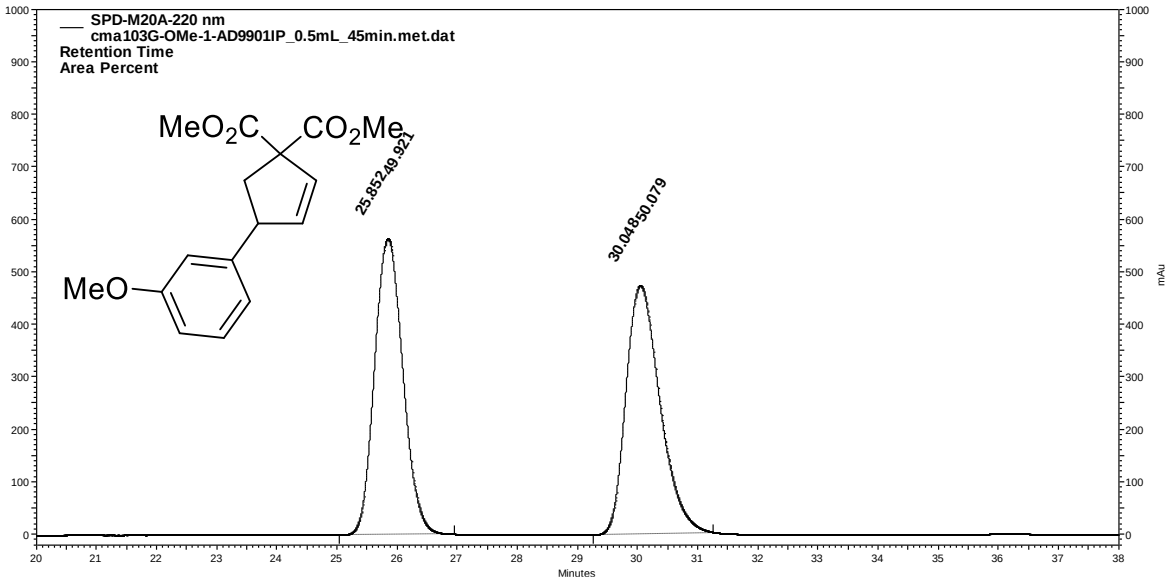
SPD-M20A-220 nm
cma103G-OMe-1-AD9901IP_0.5mL_45min.met.dat
Retention Time
Area Percent
MeO2C
CO2Me
MeO
25.85249.921
30.04850.079
mAu
Minutes

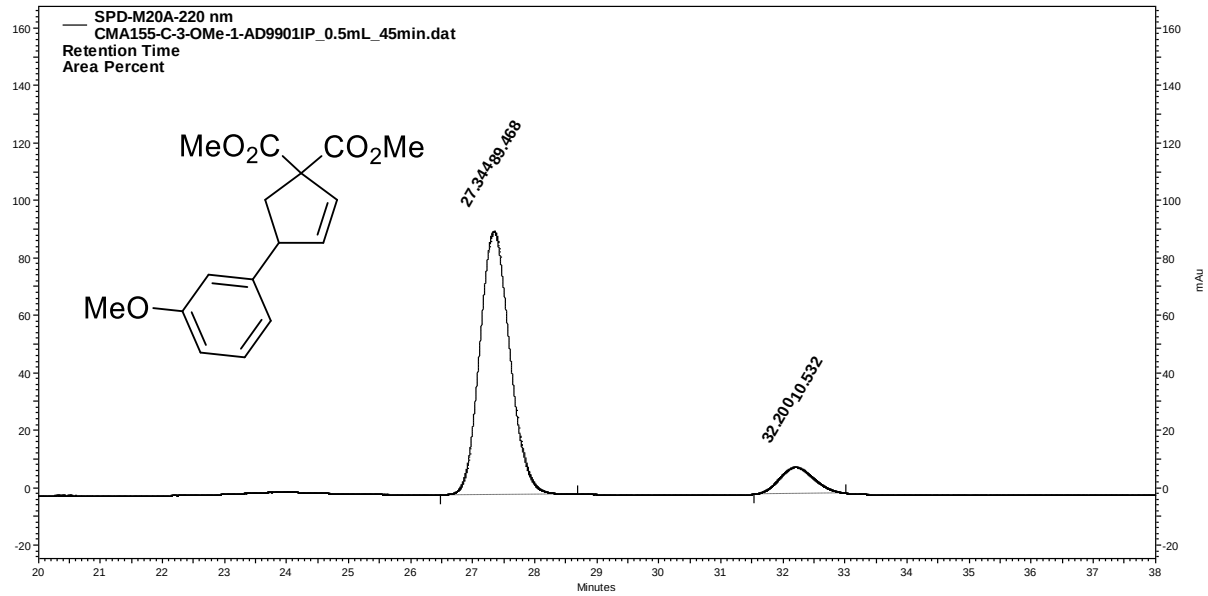
SPD-M20A-220 nm
CMA155-C-3-OMe-1-AD9901IP_0.5mL_45min.dat
Retention Time
Area Percent
MeO2C
CO2Me
MeO
27.34489.468
32.20010.532
mAu
Minutes

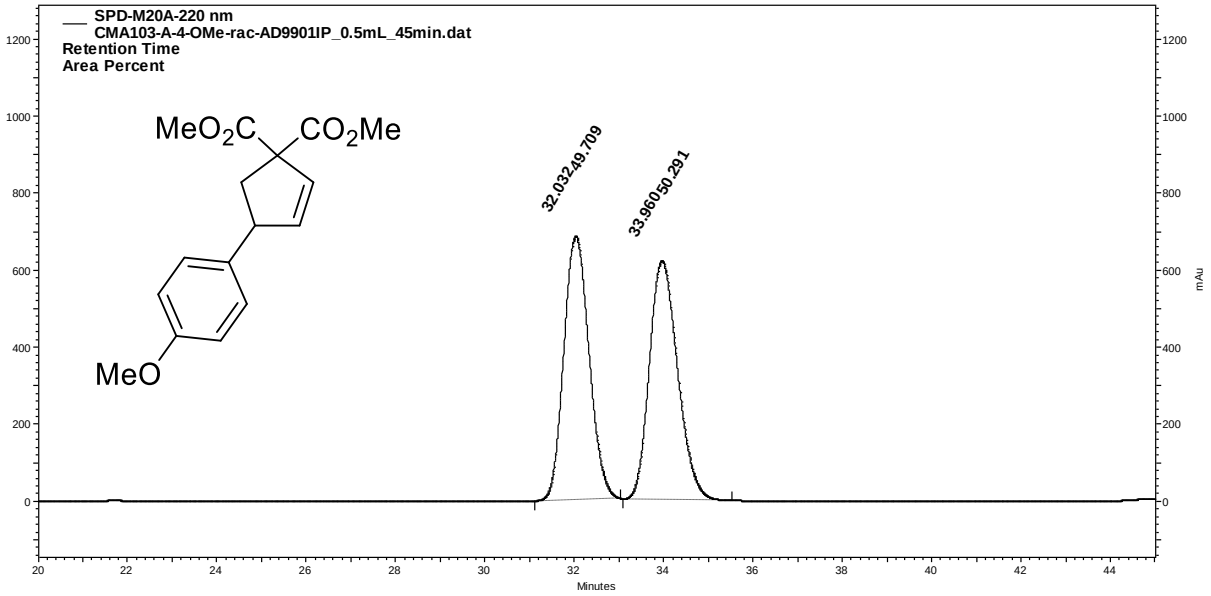
SPD-M20A-220 nm
CMA103-A-4-OMe-rac-AD9901IP_0.5mL_45min.dat
Retention Time
Area Percent
MeO2C
CO2Me
MeO
32.03249.709
33.96050.291
mAu
Minutes

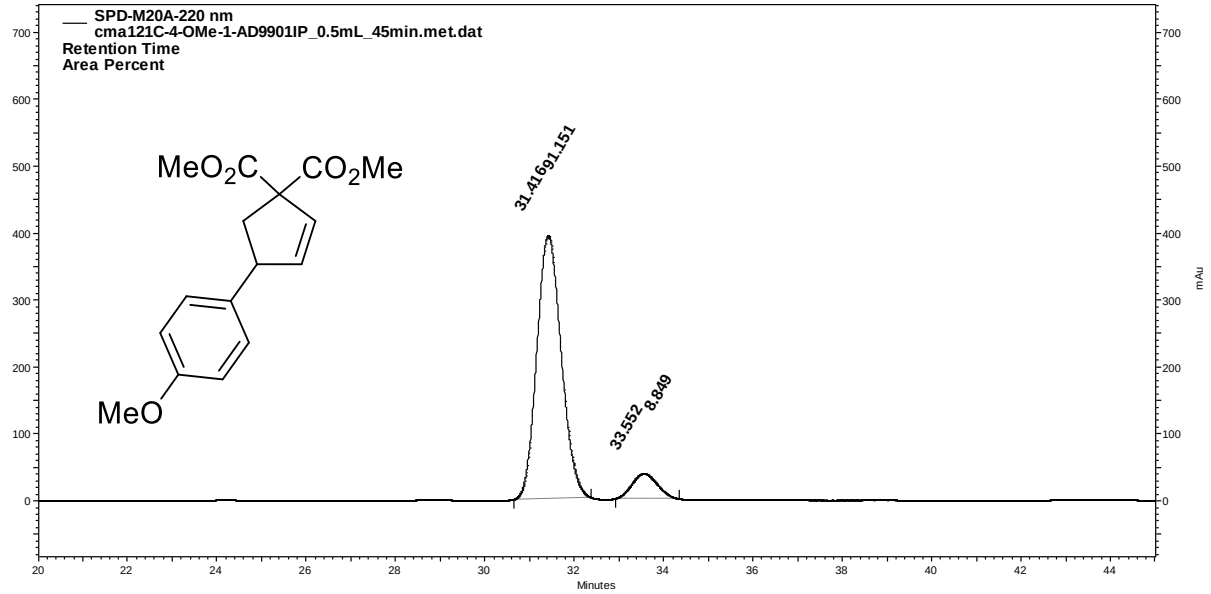
SPD-M20A-220 nm
cma121C-4-OMe-1-AD9901IP_0.5mL_45min.met.dat
Retention Time
Area Percent
MeO2C
CO2Me
MeO
31.41691.151
33.552 8.849
mAu
Minutes

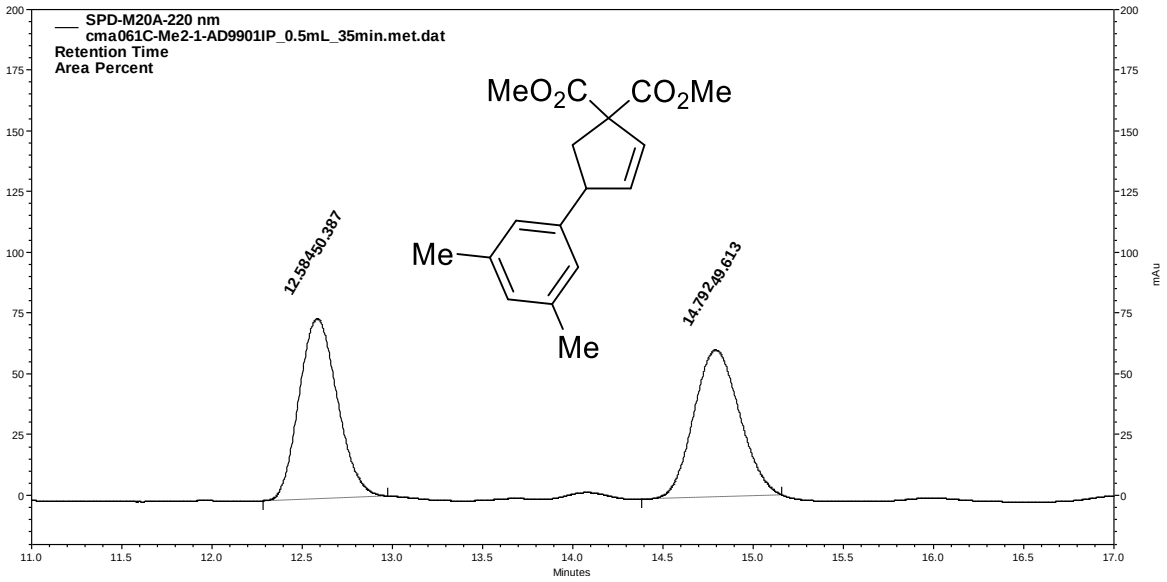
SPD-M20A-220 nm
cma061C-Me2-1-AD9901IP_0.5mL_35min.met.dat
Retention Time
Area Percent
12.58450.387
14.792 49.613
MeO2C
CO2Me
Me
Me
mAu
Minutes

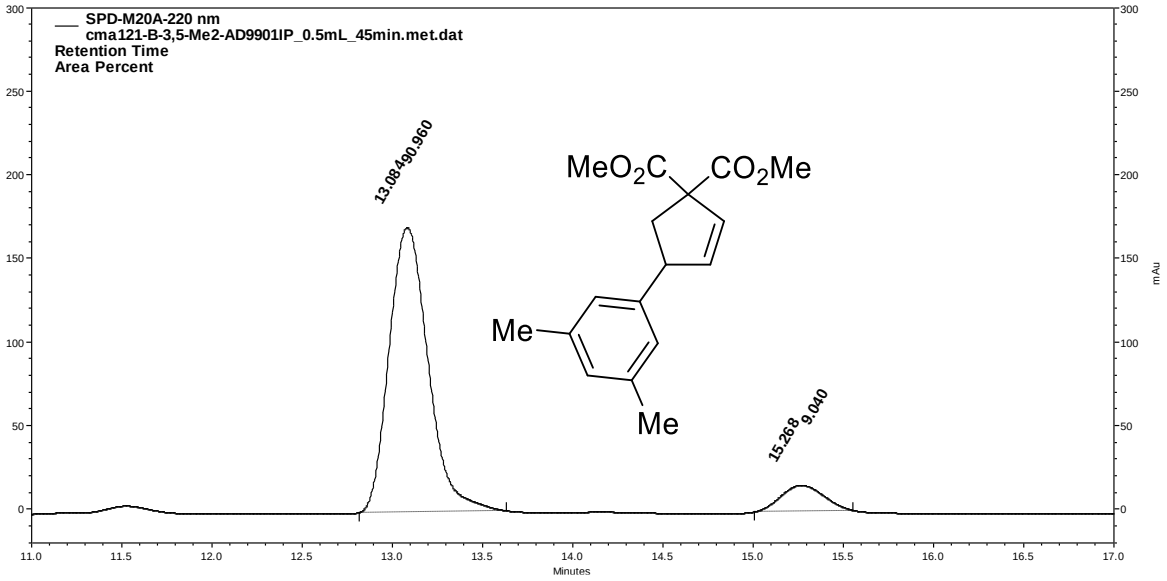
SPD-M20A-220 nm
cma121-B-3,5-Me2-AD9901IP_0.5mL_45min.met.dat
Retention Time
Area Percent
13.08490.960
15.268 9.040
MeO2C
CO2Me
Me
Me
mAu
Minutes

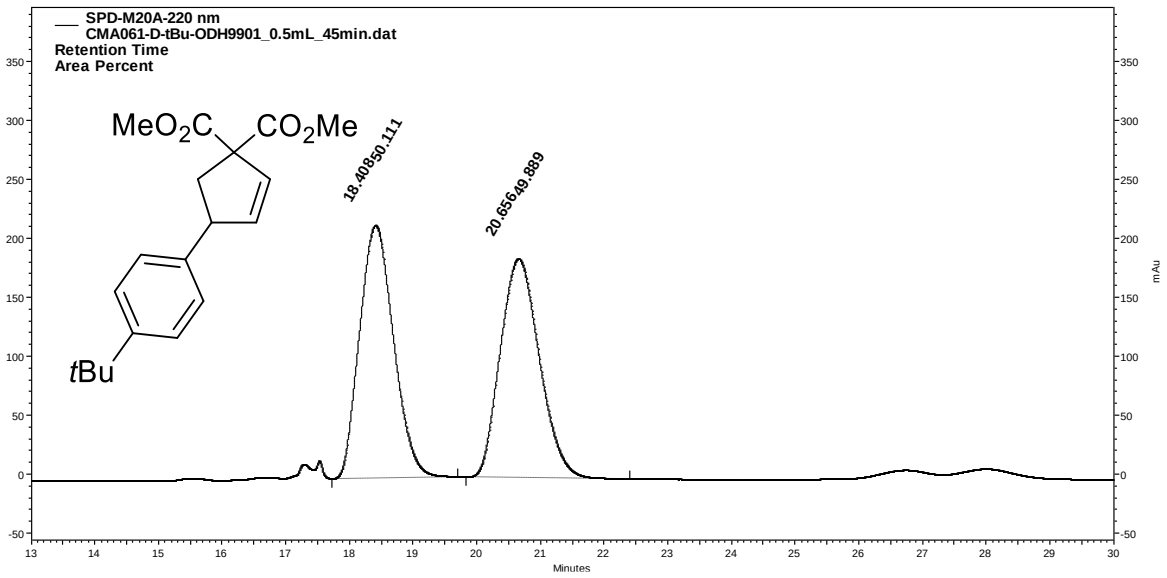
SPD-M20A-220 nm
CMA061-D-tBu-ODH9901_0.5mL_45min.dat
Retention Time
Area Percent
MeO2C
CO2Me
tBu
18.40850.111
20.65649.889
mAu
Minutes

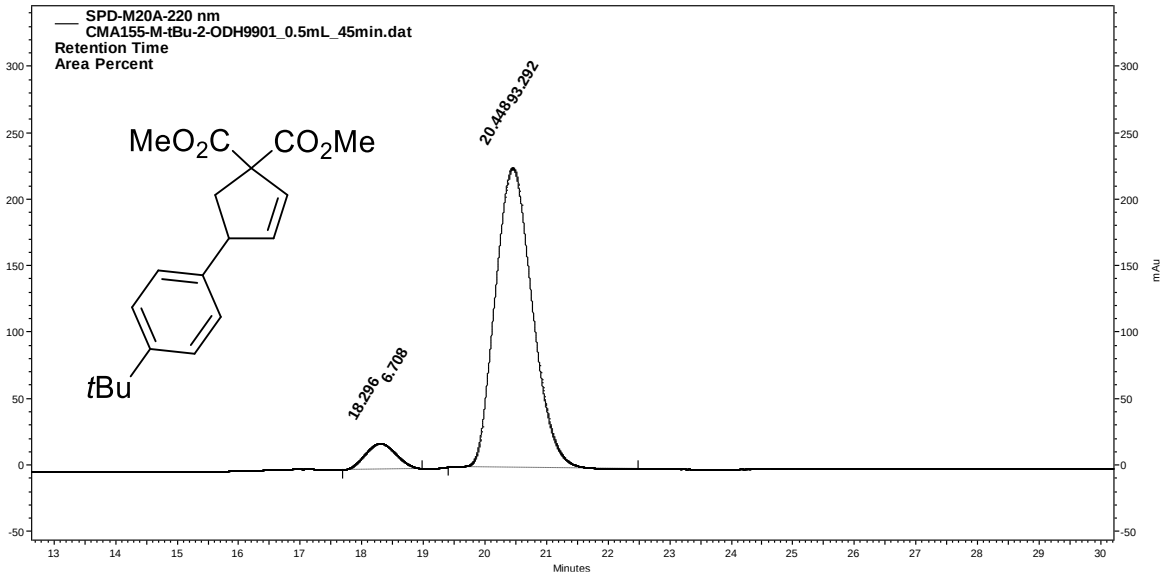
SPD-M20A-220 nm
CMA155-M-tBu-2-ODH9901_0.5mL_45min.dat
Retention Time
Area Percent
MeO2C
CO2Me
tBu
18.296 6.708
20.44893.292
mAu
Minutes

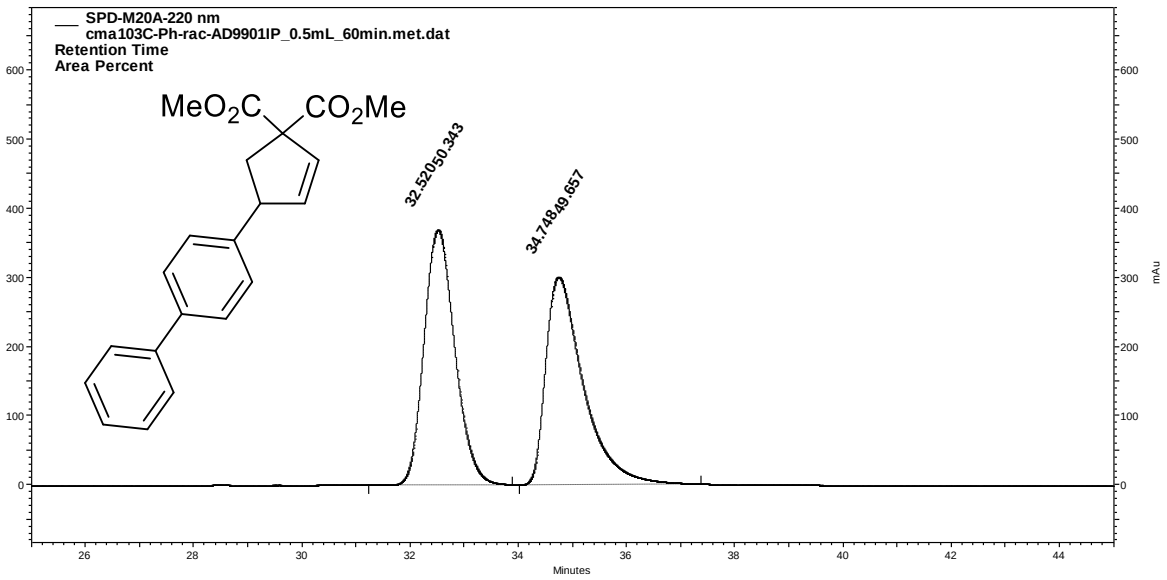
SPD-M20A-220 nm
cma103C-Ph-rac-AD9901IP_0.5mL_60min.met.dat
Retention Time
Area Percent
MeO2C
CO2Me
32.52050.343
34.74849.657
mAu
Minutes

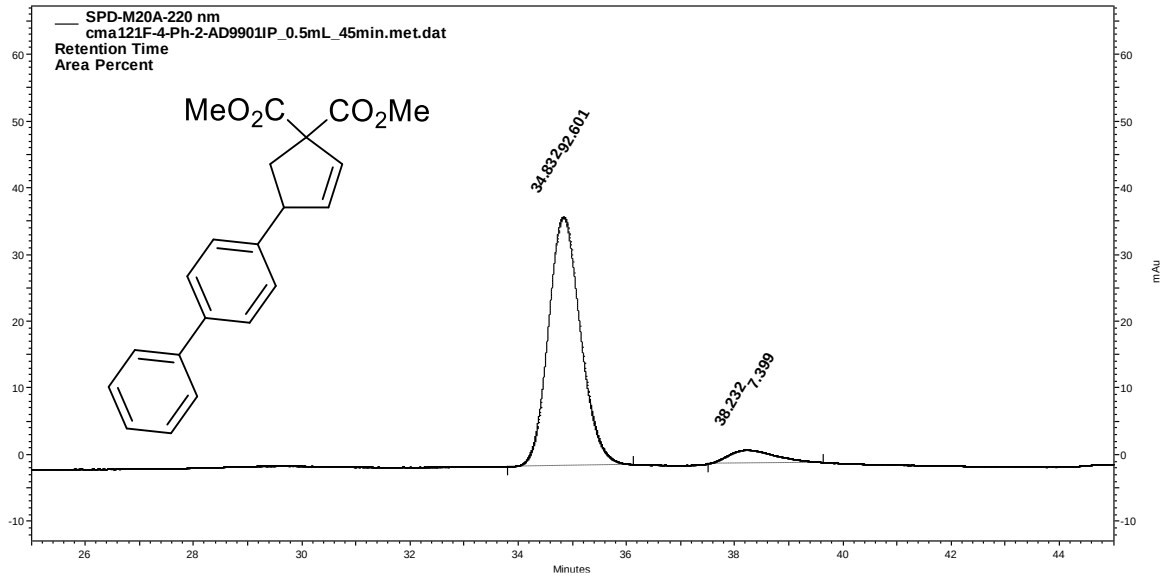
SPD-M20A-220 nm
cma121F-4-Ph-2-AD9901IP_0.5mL_45min.met.dat
Retention Time
Area Percent
MeO2C
CO2Me
34.83292.601
38.2327.399
mAu
Minutes

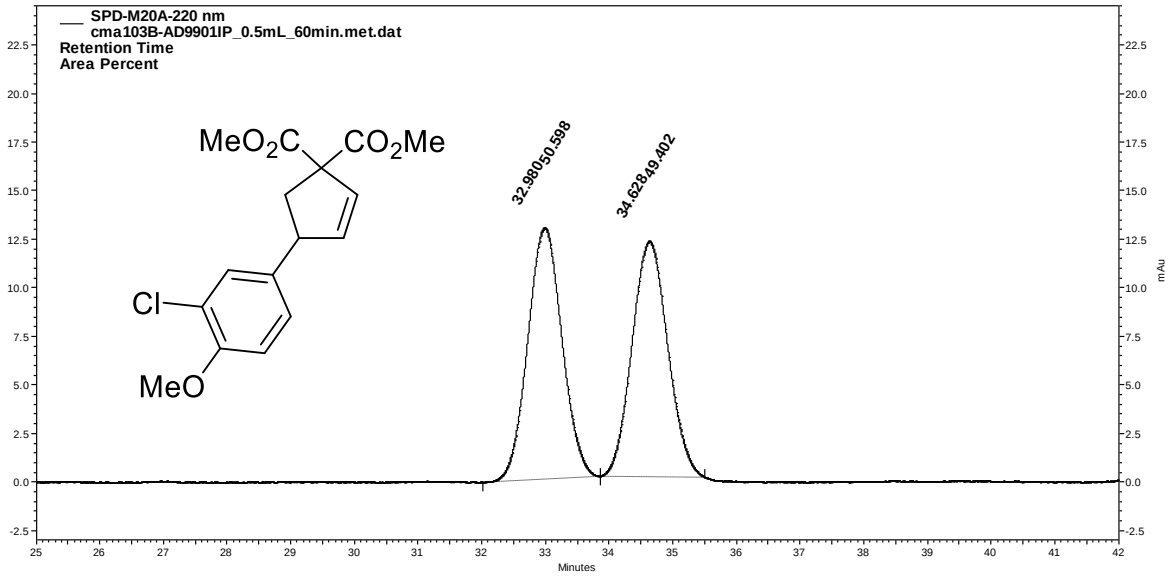
SPD-M20A-220 nm
cma103B-AD9901IP_0.5mL_60min.met.dat
Retention Time
Area Percent
MeO2C
CO2Me
Cl
MeO
32.98050.598
34.62849.402
mAu
Minutes

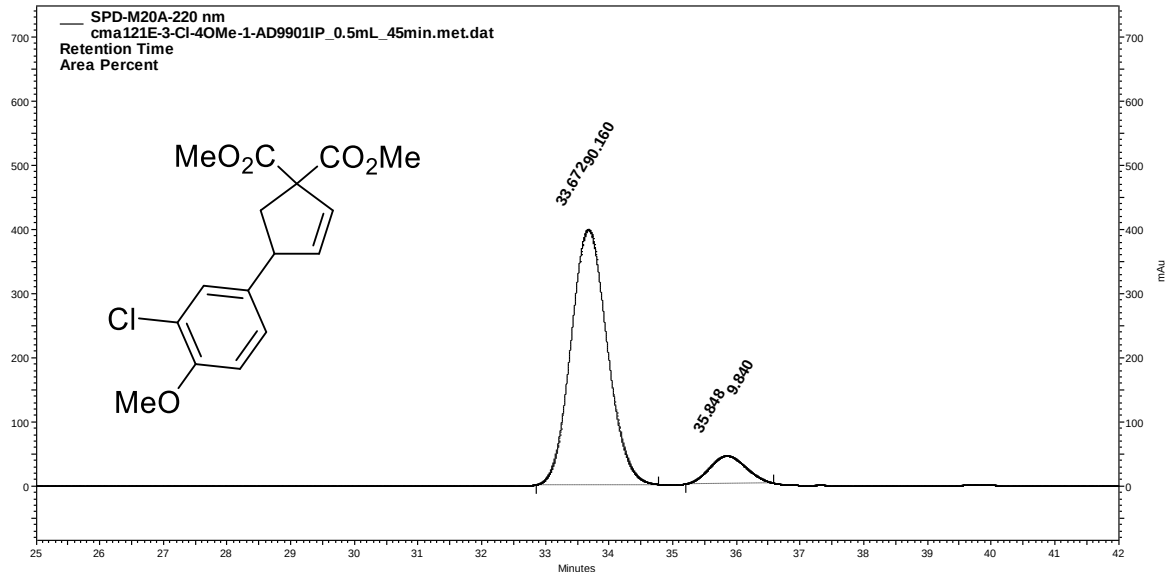
SPD-M20A-220 nm
cma121E-3-Cl-4OMe-1-AD9901IP_0.5mL_45min.met.dat
Retention Time
Area Percent
MeO2C
CO2Me
Cl
MeO
33.67290.160
35.848 9.840
mAu
Minutes

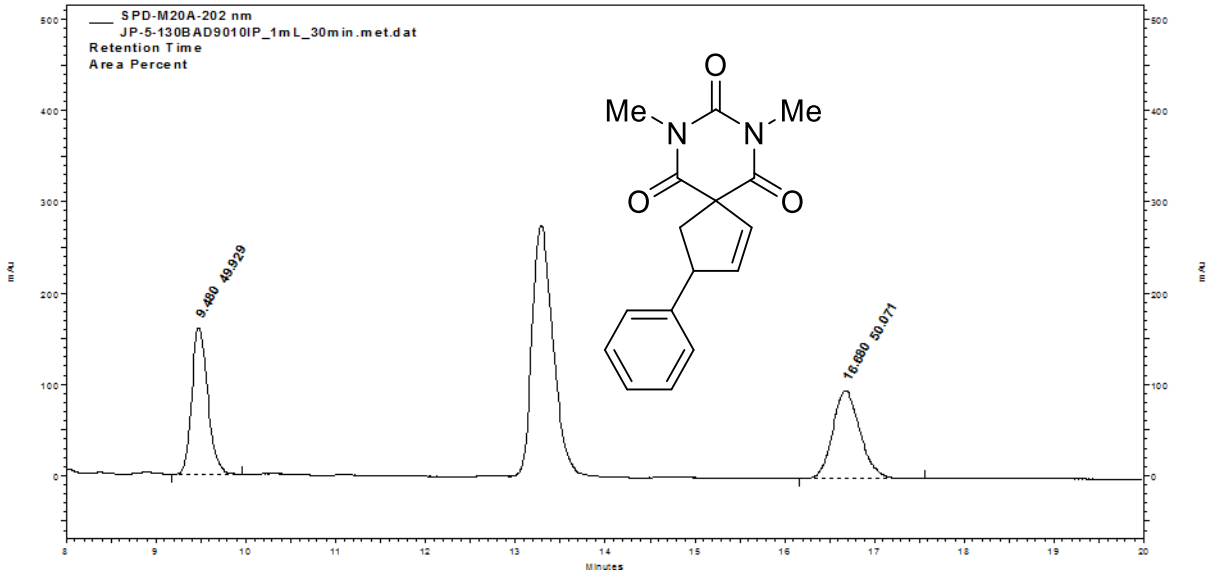
SPD-M20A-202 nm
JP-5-130BAD9010IP_1mL_30min.met.dat
Retention Time
Area Percent
9.480 49.929
16.680 50.071
Minutes
mAU

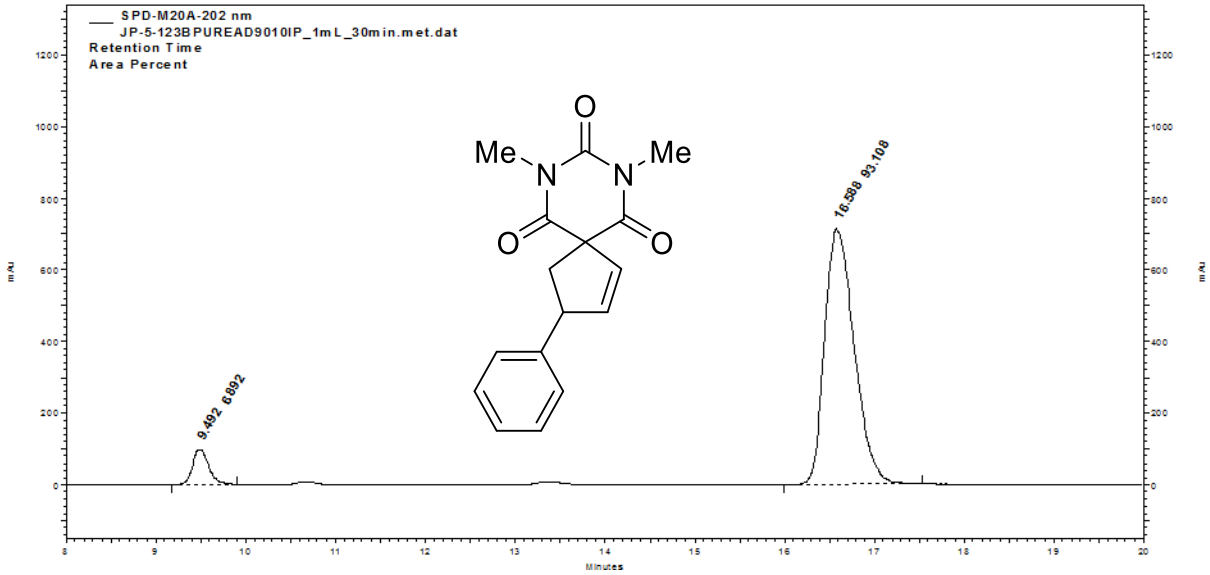
SPD-M20A-202 nm
JP-5-123BPUREAD9010IP_1mL_30min.met.dat
Retention Time
Area Percent
9.492 6.892
16.588 93.108
Minutes
mAU

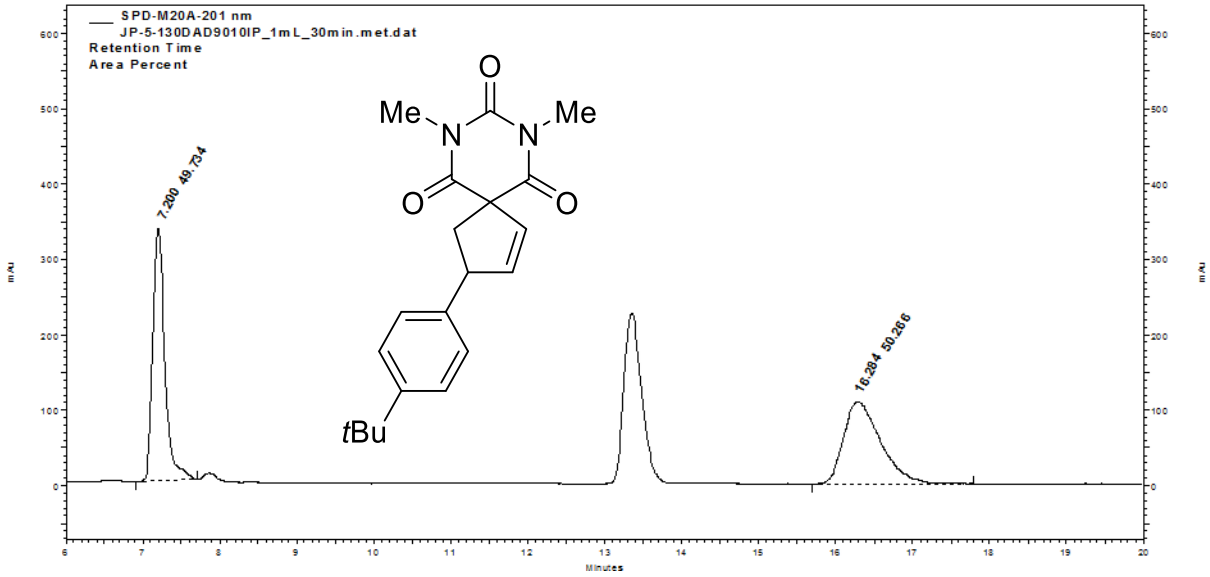
SPD-M20A-201 nm
JP-5-130DAD9010IP_1mL_30min.met.dat
Retention Time
Area Percent
7.200 49.734
16.284 50.266
Me
N
N
Me
O
O
O
tBu
mAu
Minutes

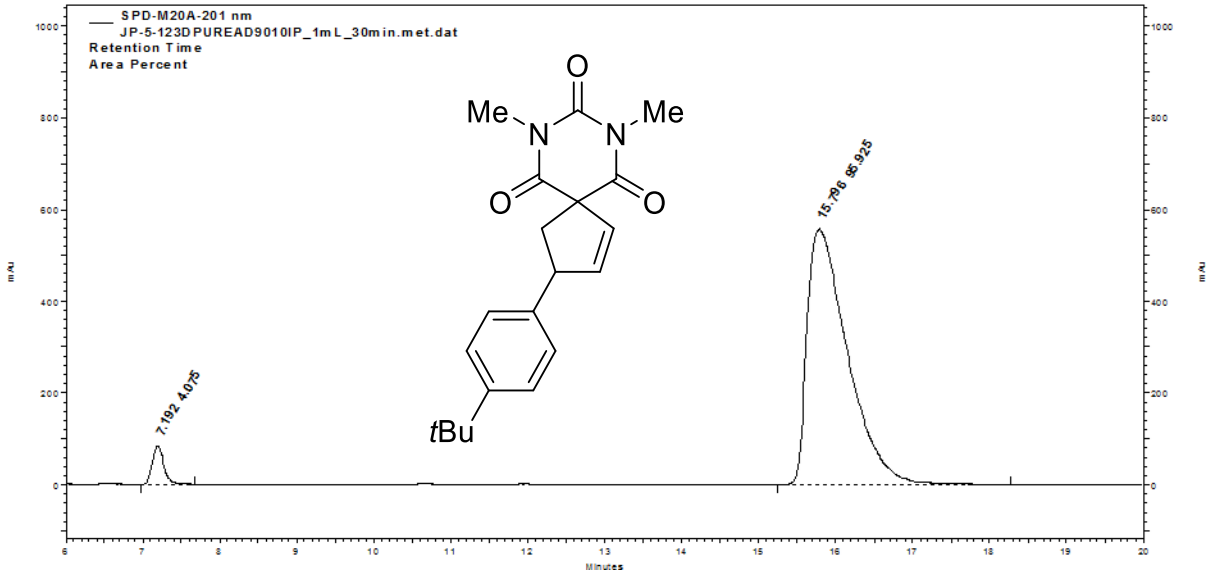
SPD-M20A-201 nm
JP-5-123DPUREAD9010IP_1mL_30min.met.dat
Retention Time
Area Percent
7.192 4.075
15.796 95.925
Me
N
N
Me
O
O
O
tBu
mAu
Minutes

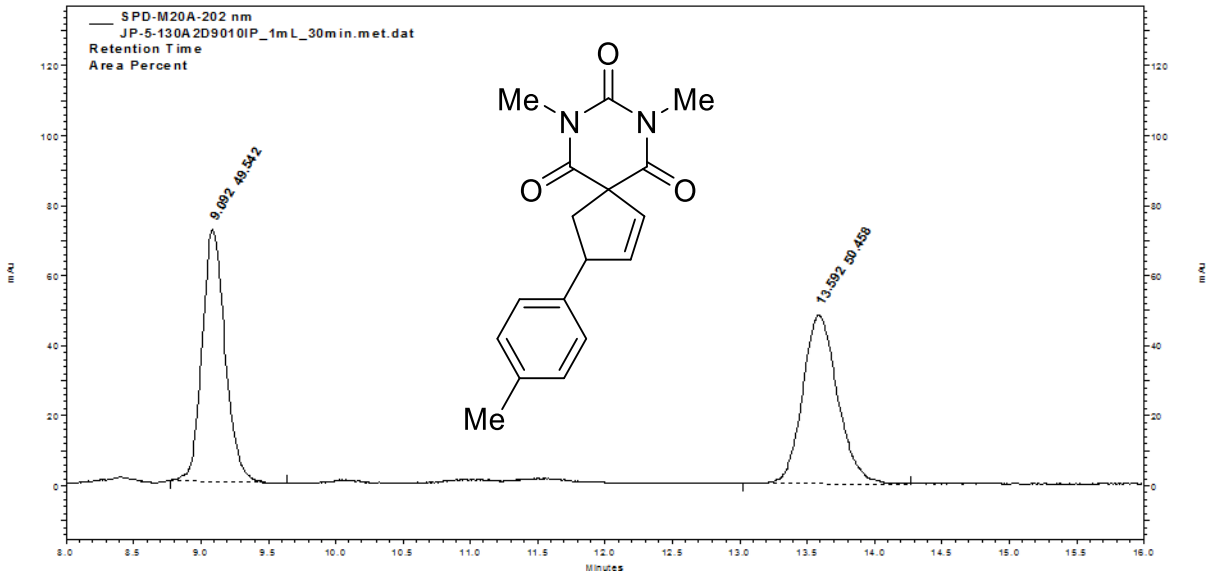
SPD-M20A-202 nm
JP-5-130A2D9010IP_1mL_30min.met.dat
Retention Time
Area Percent
9.092 49.542
13.592 50.458
Me
N
O
Minutes
mAU

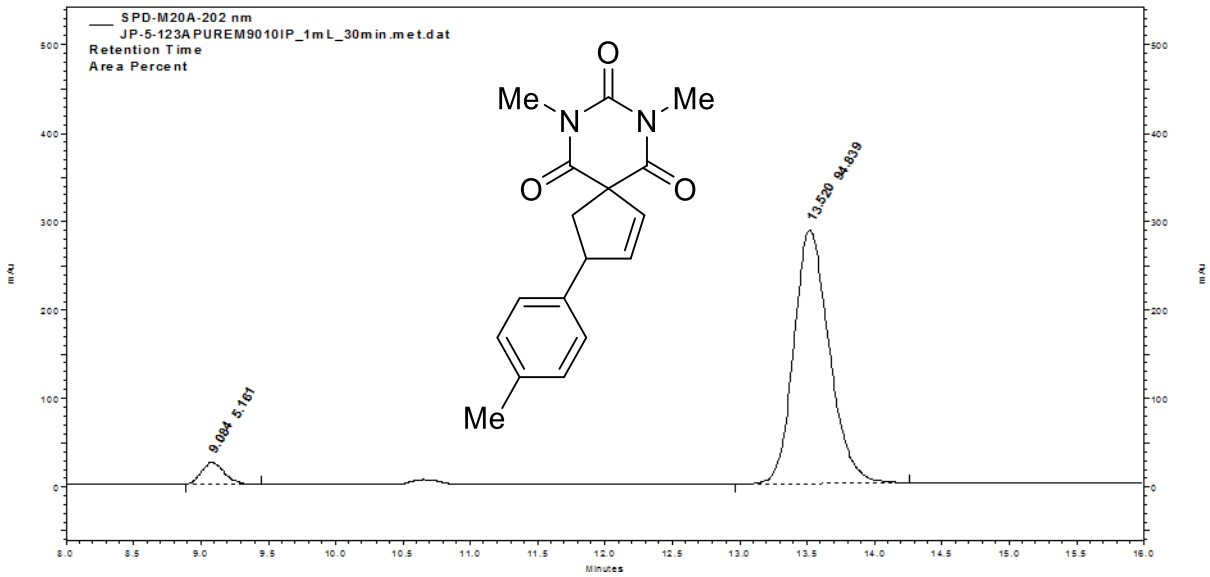
SPD-M20A-202 nm
JP-5-123APUREM9010IP_1mL_30min.met.dat
Retention Time
Area Percent
9.084 5.161
13.520 94.839
Me
N
O
Minutes
mAU

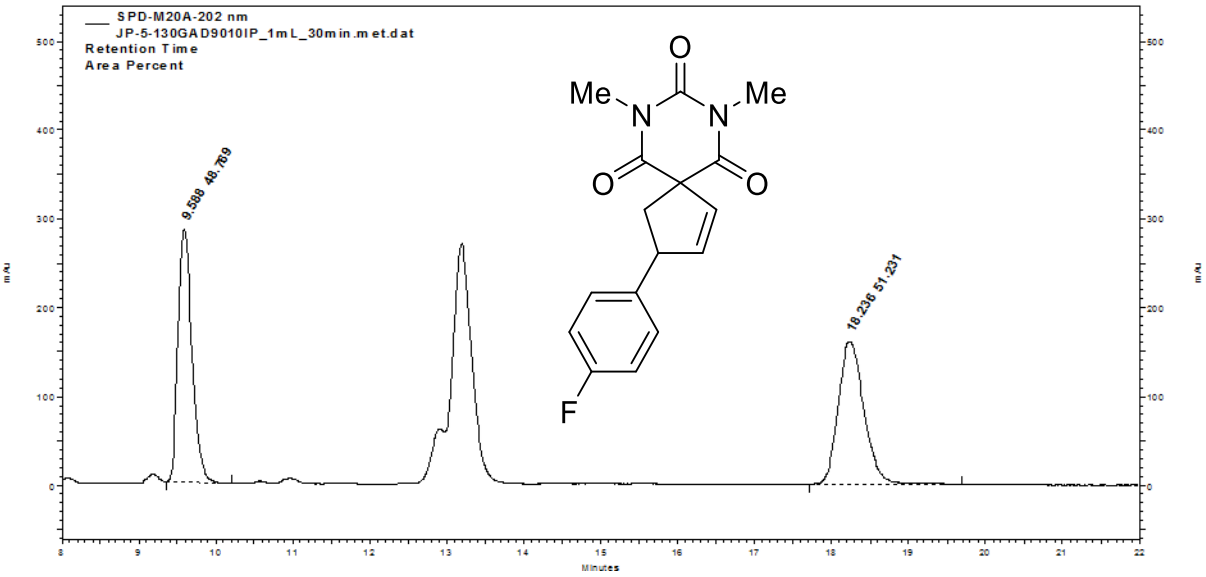
SPD-M20A-202 nm
JP-5-130GAD9010IP_1mL_30min.met.dat
Retention Time
Area Percent
9.588 48.769
18.236 51.231
Me
N
O
F
m AU
Minutes

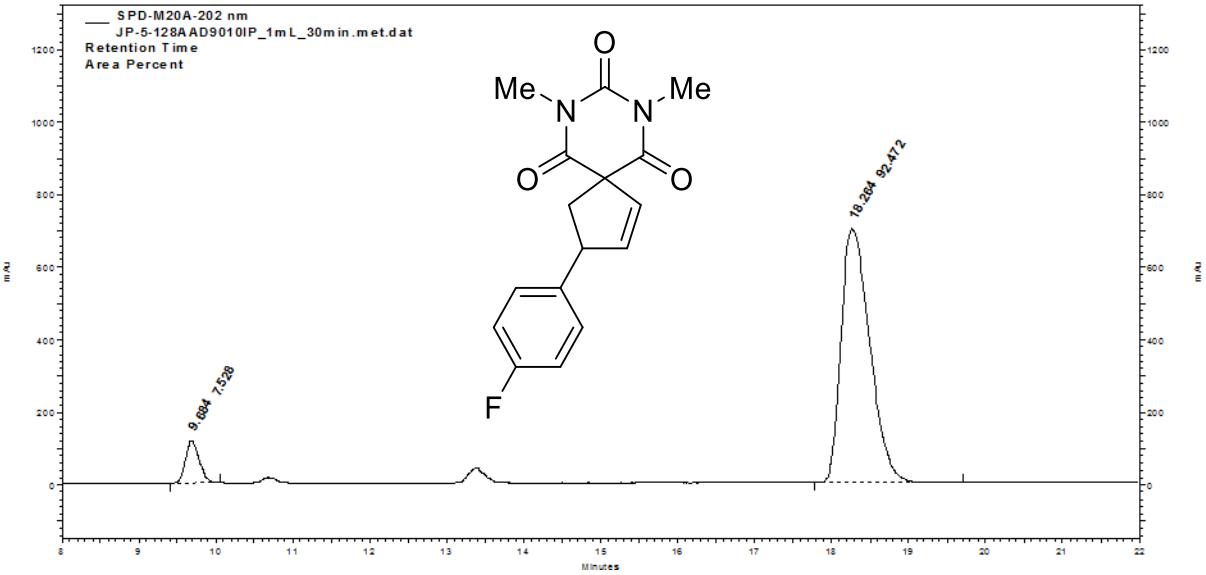
SPD-M20A-202 nm
JP-5-128AAD9010IP_1mL_30min.met.dat
Retention Time
Area Percent
9.684 7.528
18.264 92.472
Me
N
O
F
m AU
Minutes

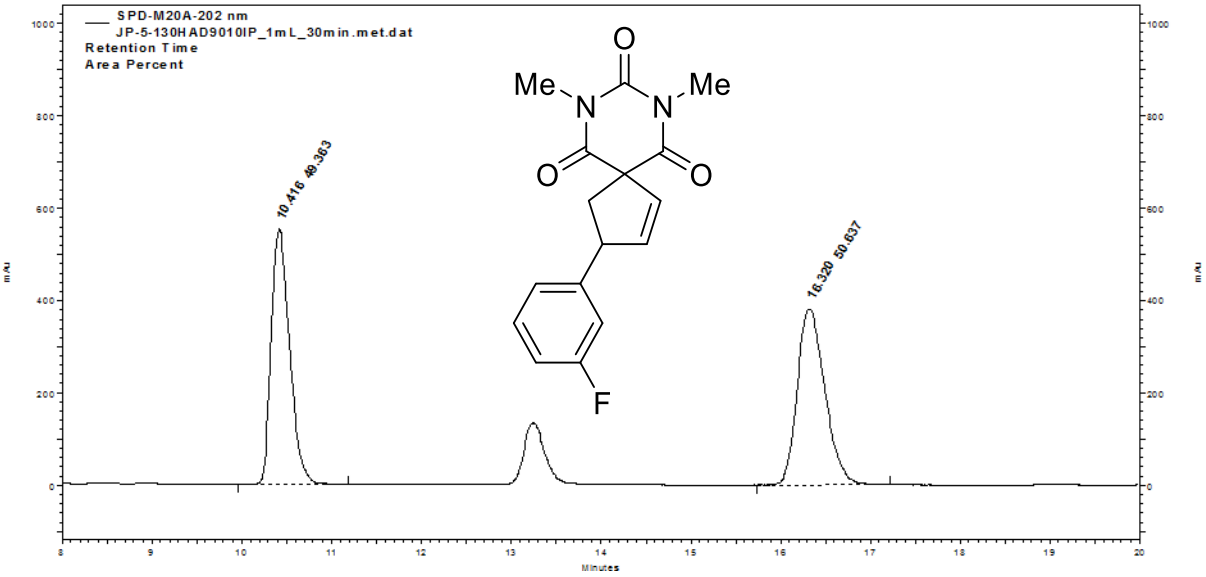
SPD-M20A-202 nm
JP-5-130HAD9010IP_1mL_30min.met.dat
Retention Time
Area Percent
10.416 49.363
16.320 50.637
Me
N
O
F
m AU
Minutes

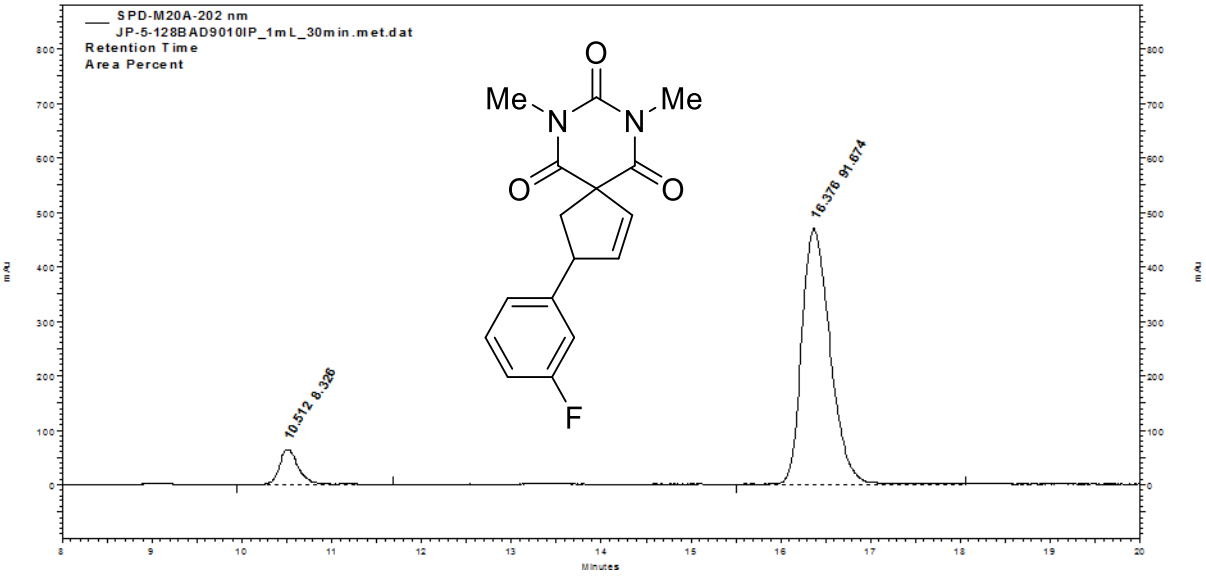
SPD-M20A-202 nm
JP-5-128BAD9010IP_1mL_30min.met.dat
Retention Time
Area Percent
10.512 8.326
16.376 91.674
Me
N
O
F
m AU
Minutes

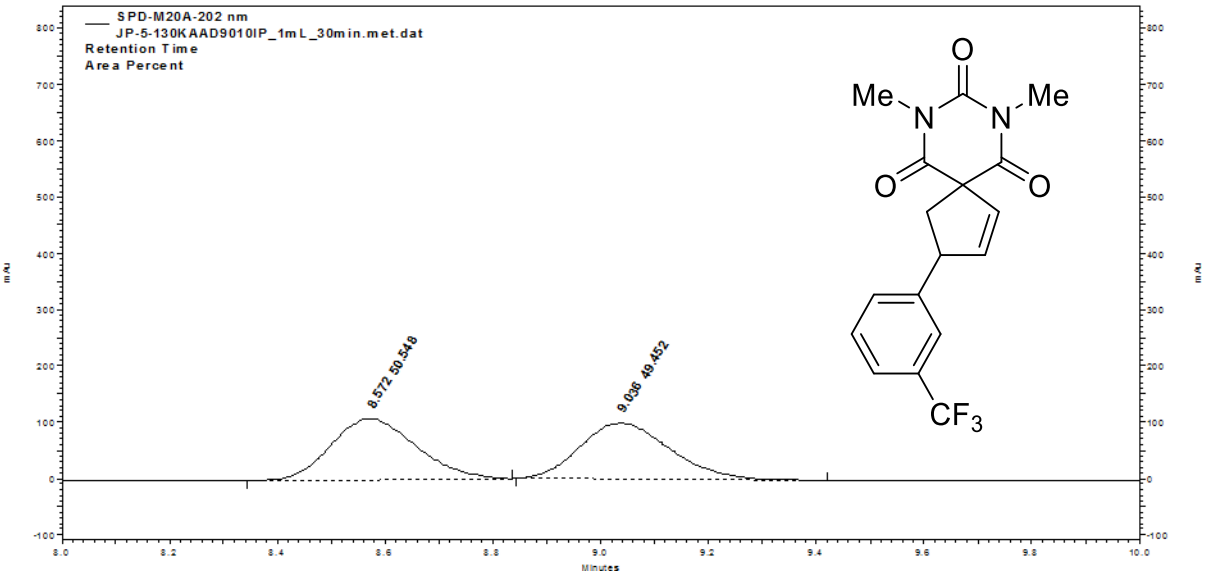
SPD-M20A-202 nm
JP-5-130KAAD9010IP_1mL_30min.met.dat
Retention Time
Area Percent
8.572 50.548
9.036 49.452
Me
N
O
CF3
m/Au
Minutes

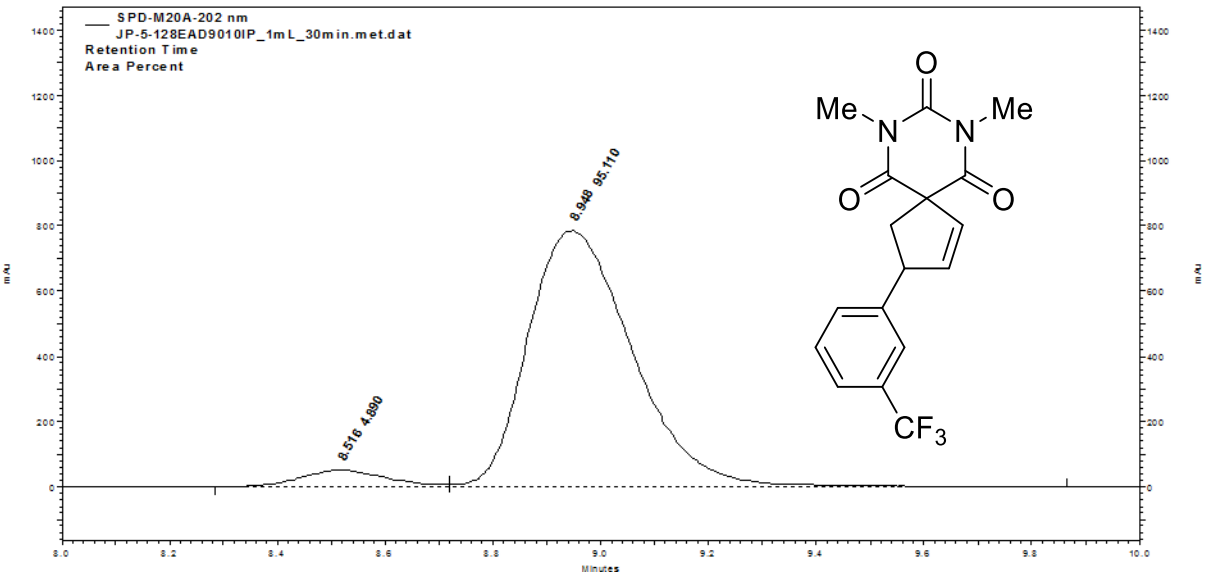
SPD-M20A-202 nm
JP-5-128EAD9010IP_1mL_30min.met.dat
Retention Time
Area Percent
8.516 4.890
8.948 95.110
Me
N
O
CF3
m/Au
Minutes

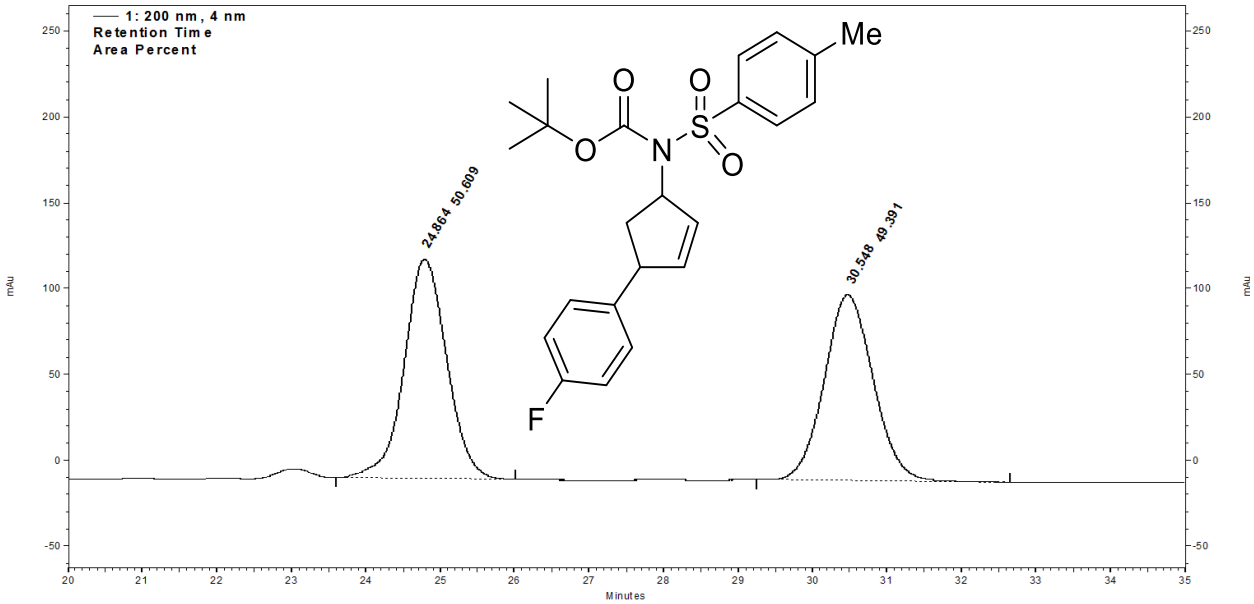
1: 200 nm, 4 nm
Retention Time
Area Percent
24.864 50.609
30.548 49.391
Me
O
O
O
N
S
O
F
mAu
Minutes

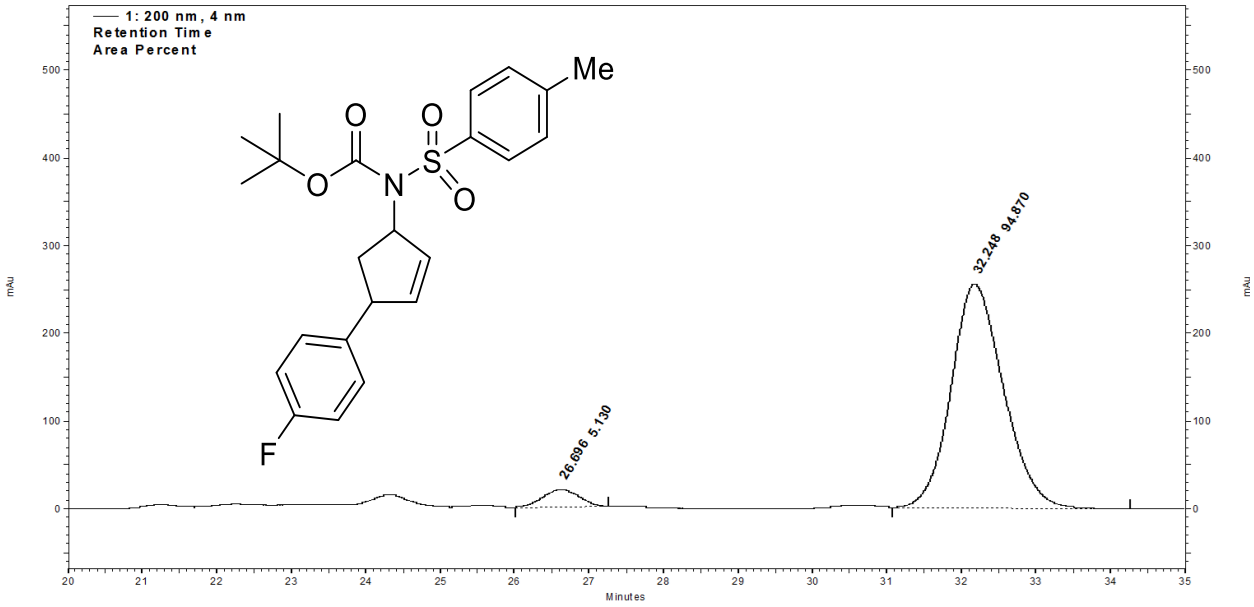
1: 200 nm, 4 nm
Retention Time
Area Percent
26.696 5.130
32.248 94.870
Me
O
O
O
N
S
O
F
mAu
Minutes

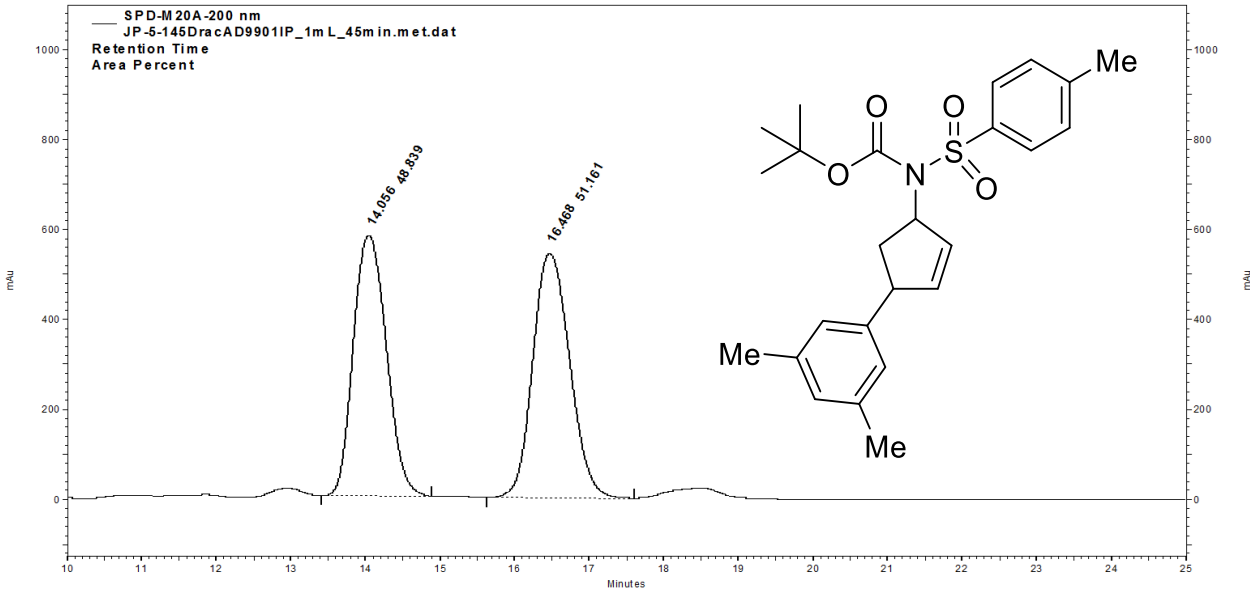
SPD-M20A-200 nm
JP-5-145DracAD9901IP_1mL_45min.met.dat
Retention Time
Area Percent
14.056 48.839
16.468 51.161
mAu
Minutes
Me
O
O
O
N
S
O
Me
Me

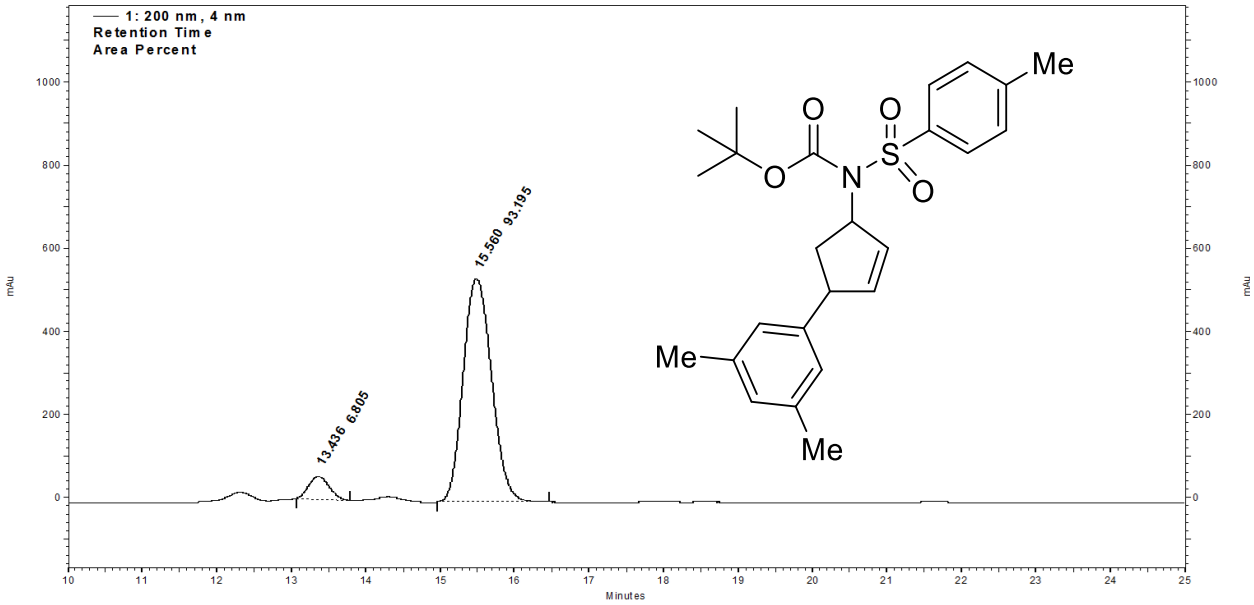
1: 200 nm, 4 nm
Retention Time
Area Percent
13.436 6.805
15.560 93.195
mAu
Minutes
Me
O
O
O
N
S
O
Me
Me

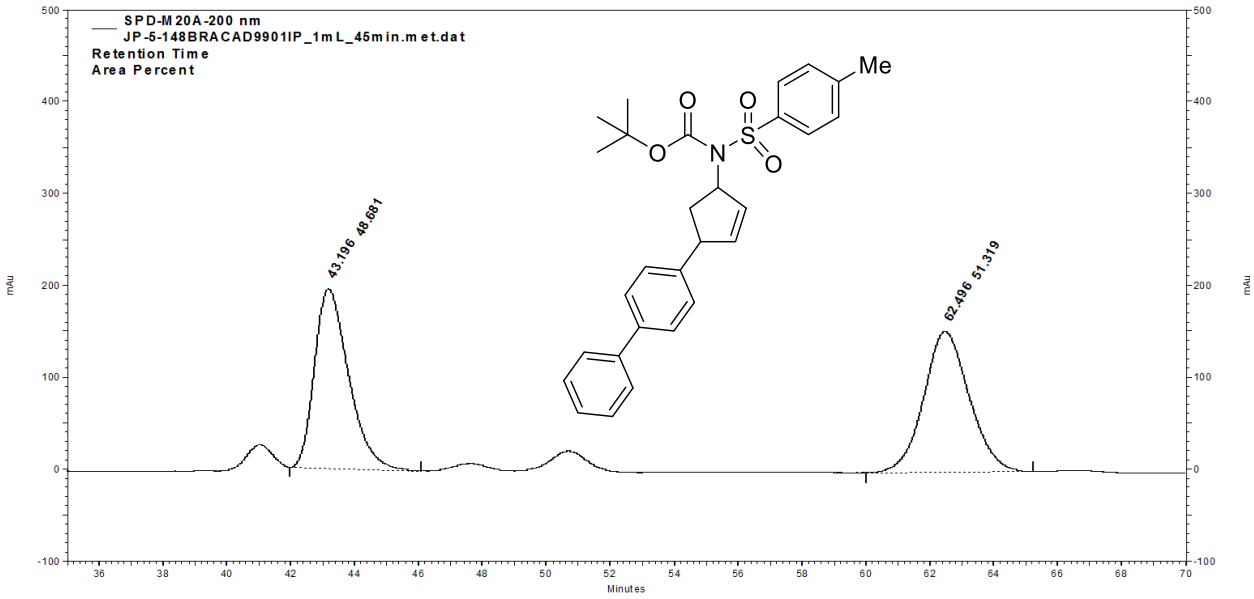
SPD-M20A-200 nm
JP-5-148BRACAD9901IP_1mL_45min.met.dat
Retention Time
Area Percent
43.196 48.681
62.496 51.319
Me
mAu
Minutes

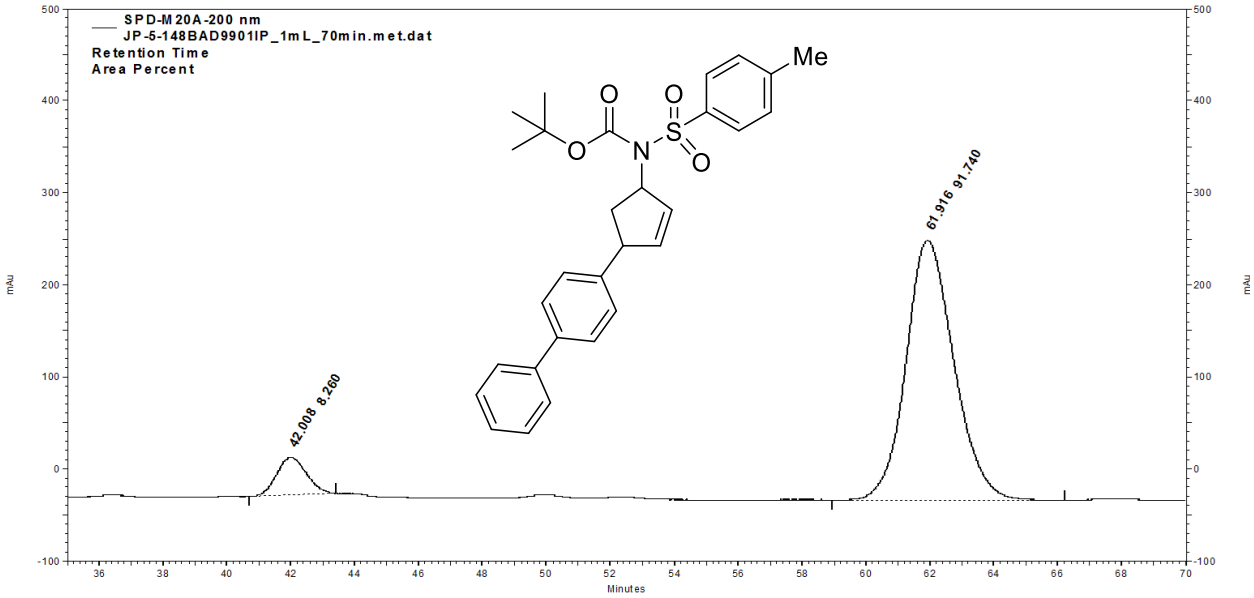
SPD-M20A-200 nm
JP-5-148BAD9901IP_1mL_70min.met.dat
Retention Time
Area Percent
42.008 8.260
61.916 91.740
Me
mAu
Minutes

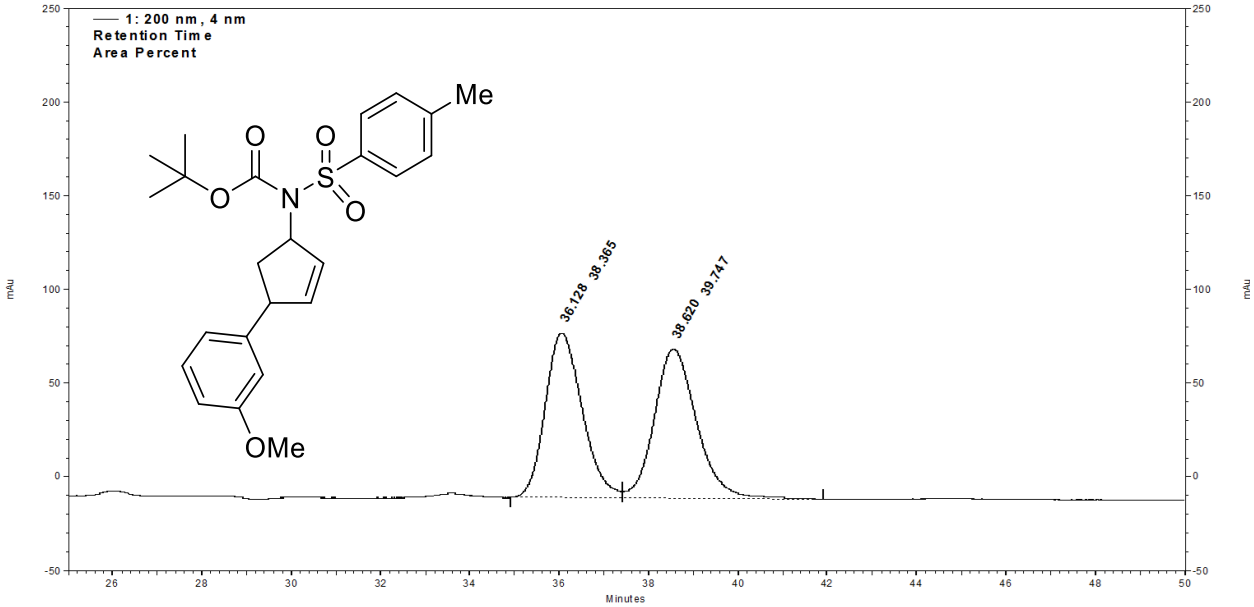
1: 200 nm, 4 nm
Retention Time
Area Percent
Me
O
O
O
S
O
N
O
OMe
36.128 38.365
38.620 39.747
mAu
Minutes

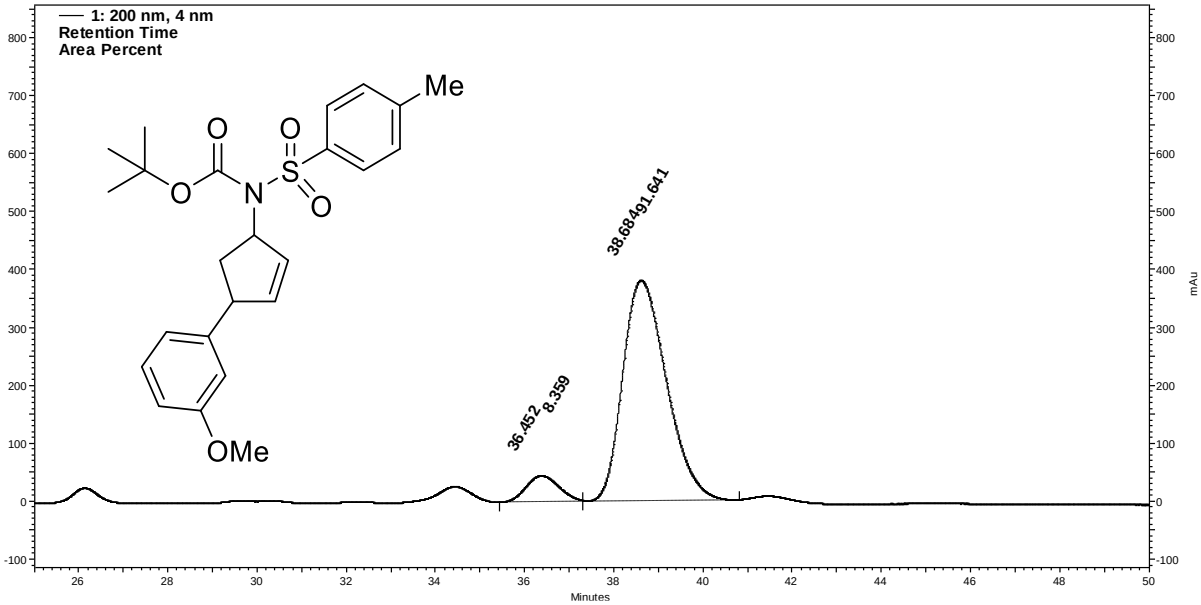
1: 200 nm, 4 nm
Retention Time
Area Percent
Me
O
O
O
S
O
N
O
OMe
36.452 8.359
38.684 91.641
mAu
Minutes

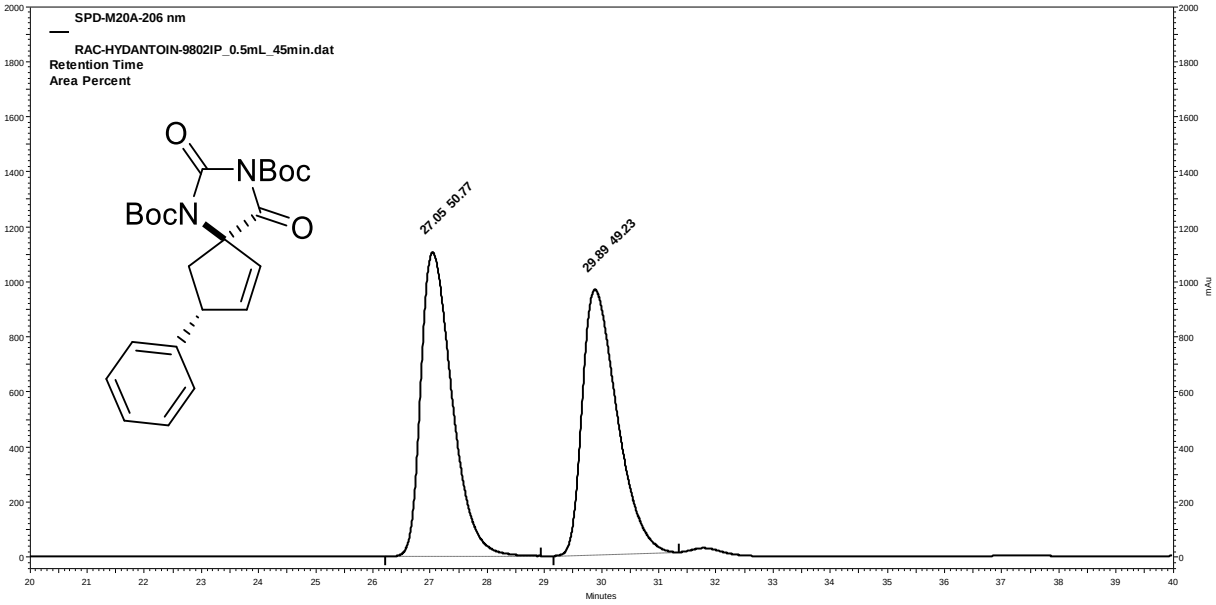
SPD-M20A-206 nm
RAC-HYDANTOIN-9802IP_0.5mL_45min.dat
Retention Time
Area Percent
O
NBoc
BocN
O
27.05 50.77
29.89 49.23
mAu
Minutes

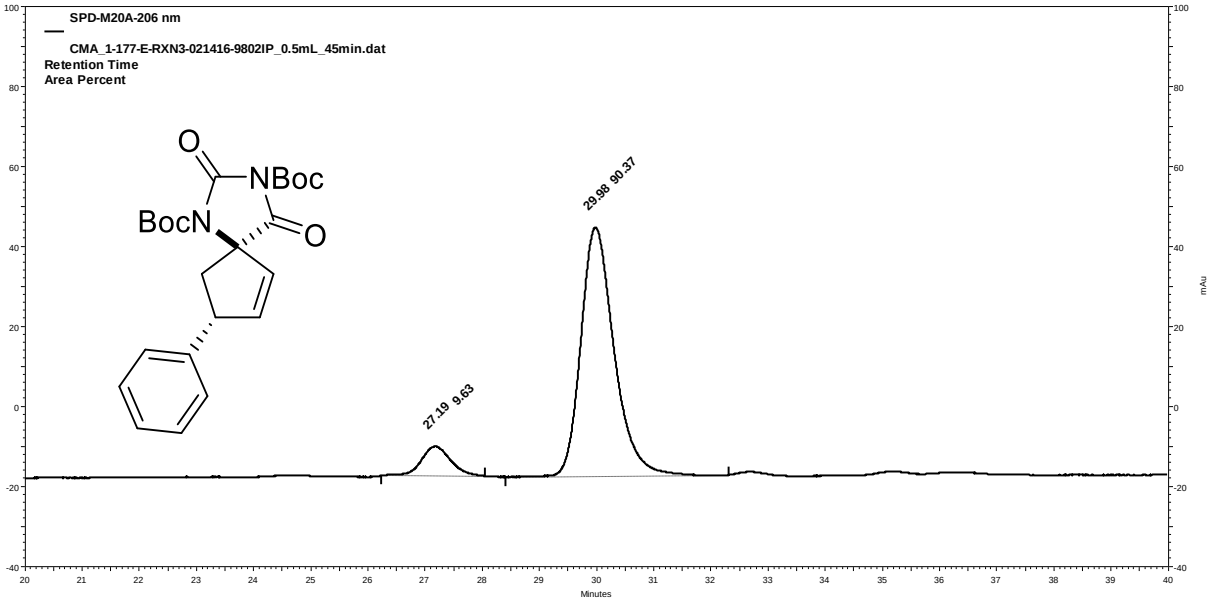
SPD-M20A-206 nm
CMA_1-177-E-RXN3-021416-9802IP_0.5mL_45min.dat
Retention Time
Area Percent
O
NBoc
BocN
O
27.19 9.63
29.98 90.37
mAu
Minutes

After crystallization: